

LIBRARY
COPY

LIQUID-SIDE RESISTANCE IN GAS ABSORPTION
WITH AND WITHOUT CHEMICAL REACTION

by

DONALD WILLIAM PEACEMAN

B.Ch.E., College of The City of New York
(1947)

SUBMITTED IN PARTIAL FULFILLMENT OF THE
REQUIREMENTS FOR THE DEGREE OF
DOCTOR OF SCIENCE

at the

MASSACHUSETTS INSTITUTE OF TECHNOLOGY
(1951)

Signature of Author:

Signature redacted

Department of Chemical Engineering
August 24, 1951

Signature of Professor
in Charge of Research:

J. Edward Vivian

Signature of Chairman,
Departmental Committee on
Graduate Students:

Glenn C. Williams

LIQUID-SIDE RESISTANCE IN GAS ABSORPTION
WITH AND WITHOUT CHEMICAL REACTION

by

DONALD WILLIAM PEACEMAN

Submitted for the degree of Doctor of Science in the
Department of Chemical Engineering, August 24, 1951.

ABSTRACT

This thesis was undertaken to obtain a better understanding of the mechanism of absorption with reversible chemical reaction, with particular reference to the chlorine-water system. Several lines of investigation were pursued: (1) a study of the nature of the liquid-side resistance in the absence of chemical reaction; (2) a mathematical and experimental study of the effect of chemical reaction; (3) measurements of diffusivities.

The film theory, embodying the assumption of a thin stagnant liquid film adjacent to the interface in which steady-state diffusion occurs, has long been open to question, particularly in packed columns. Higbie's penetration theory*, believed to be more reasonable, pictures the liquid flowing over a piece of packing for a very short period of time before being mixed as it flows to the next piece of packing. Absorption occurs during a series of brief contacts, and unsteady-state mass transfer conditions prevail in the liquid.

Short glass wetted-wall columns of length 1.9 to 4.3 cm., were constructed to simulate the assumptions of the penetration theory. Because of the short length, ripples were absent at gas rates below $Re_G = 2200$. The desorption of carbon dioxide from water, of chlorine from dilute HCl (0.16-0.18 N) and of chlorine from water were studied. The desorption rate of carbon dioxide was unaffected gas velocity up to $Re_G = 2200$ and increased 1.1 per cent per °C. over the temperature range 22° to 31°C. All the data on the CO_2-H_2O and $Cl_2-HCl-H_2O$ systems, at 25°C. were correlated by the equation $k_L^* \sqrt{h/D} = 7.13 \Gamma^{0.4}$, where k_L^* is the physical coefficient of desorption, h is length, D is diffusivity, and Γ is liquid flow rate per unit

* Higbie, R., Trans. Am. Inst. Chem. Engrs. 31, 365-89 (1935)

perimeter (all quantities in g., cm., and sec.), with an average deviation of 7.7%. A theoretical equation derived from the penetration and streamline flow theories, $k_L^* = 2\sqrt{D/(\pi h)} \left[(9/8) g \Gamma^2 / (\mu \rho) \right]^{1/6}$, agrees with the experimental equation within 30% at the lowest liquid rate measured ($\Gamma = 7$ g./cm.)(min.) and within 10% at the highest liquid rate ($\Gamma = 90$). For the desorption of chlorine from water at 25°C., the psuedo-coefficient, based on an unhydrolyzed chlorine driving force, was found to be independent of concentration over the range 0.005 to 0.04 mole/l., and to increase linearly with concentration over the range 0.04 to 0.07 mole/l. The normal coefficient, based on a total chlorine driving force, was found to increase with concentration and, at concentrations above about 0.06 mole/l., exceeded the physical coefficient for chlorine in water. These results are in contradiction with the mathematical theory of absorption with reversible chemical reaction developed in this thesis; the theory predicts that the pseudo-coefficient should decrease with concentration and that the normal coefficient cannot be greater than the physical coefficient. No explanation for the anomaly could be found.

In addition, an experimental program of measuring diffusivities was carried out. Using a diaphragm cell, the diffusivities of chlorine through dilute hydrochloric acid, of chlorine through water, of sulfur dioxide through dilute sulfuric acid, and of sulfur dioxide in water were measured.

Department of Chemical Engineering
Massachusetts Institute of Technology
Cambridge 39, Massachusetts

August 24, 1951

Professor Joseph S. Newell
Secretary of the Faculty
Massachusetts Institute of Technology
Cambridge 39, Massachusetts

Dear Sir:

In accordance with the regulations of the Faculty, I herewith submit a thesis, entitled "Liquid-Side Resistance in Gas Absorption with and without Chemical Reaction", in partial fulfillment of the requirements for the degree of Doctor of Science in Chemical Engineering from the Massachusetts Institute of Technology.

Respectfully submitted,
Signature redacted
Donald W. Peaceman

ACKNOWLEDGMENT

I should like to express my appreciation to Professor J. Edward Vivian for stimulating my interest in the field of absorption, and for the continued guidance and encouragement that he supplied during the course of this work.

I am very grateful to the Kimberly-Clark Corporation for their generous financial assistance which made this work possible.

Many students, whose thesis work was undertaken in collaboration with this thesis, contributed materially to it. They are Marshall E. Baker, Peter A. Guercio, George H. Costomiris, Arturo M. de Nicolas, Robert F. Abbanat, Paul A. Lobo, Ross R. Quincy, and James A. Miller. In particular, I am indebted to Harry W. Lambe, for his skill in constructing the short wetted-wall column and in collecting data on it was largely responsible for the successful results obtained in this thesis.

Finally, I should like to thank Miss Roberta M. Bruce and Miss Margaret E. Norton for their aid in typing the thesis.

TABLE OF CONTENTS

	<u>Page</u>
<u>Chapter 1.</u> SUMMARY	1
<u>Chapter 2.</u> INTRODUCTION	11
<u>Chapter 3.</u> APPARATUS AND PROCEDURE	37
<u>Chapter 4.</u> RESULTS	45
4.1 Physical Coefficients in Short Wetted-Wall Column	45
4.2 Description of Chlorine in Short Wetted- Wall Column	51
4.3 Interfacial Velocity in Short Wetted-Wall Column	56
4.4 Measurement of Diffusivities in Liquids	56
4.5 Mathematical Theory of Absorption with Chemical Reaction	57
<u>Chapter 5.</u> DISCUSSION OF RESULTS	72
A. General Aspects of Experimental Procedure	
5.1 Effect of Air Rate	72
5.2 Material Balance	75
5.3 Sampling Procedure	76
5.4 Effect of Slot Width and Type	79
B. Physical Coefficients	
5.5 Absence of Chemical Reaction	81
5.6 Effect of Temperature	82
5.7 Effect of Water Rate	82
5.8 Effect of Length of Column	84
5.9 Effect of Diffusivity	86
5.10 Correlation Using Penetration Theory	87
5.11 Attempted Correlation Using Film Theory	93
5.12 Dimensionless Correlation	97
5.13 Comparison with Data on Long Wetted-Wall Columns	99
C. Desorption of Chlorine from Water	
5.14 Correction for Temperature	106
5.15 Method of Calculating Coefficients	106
5.16 Empirical Correlation of Psuedo-Coefficients	107

	<u>Page</u>
5.17 Effect of Concentration on Total Co-efficient	111
5.18 Comparison of Experimental Results with Theory	112
D. Application of Results to the Study of Packed Columns	
5.19 Effect of Temperature	126
5.20 Comparison of Physical Coefficients	127
5.21 Comparison of Data on Chlorine-Water System	129
<u>Chapter 6.</u> CONCLUSIONS	134
<u>Chapter 7.</u> RECOMMENDATIONS	137

APPENDIX

<u>Chapter 8.</u> MATHEMATICAL THEORY OF ABSORPTION WITH CHEMICAL REACTION	140
Outline	140
<u>Chapter 9.</u> APPLICATION OF MATHEMATICAL THEORY OF ABSORPTION WITH CHEMICAL REACTION TO EXPERIMENT	234
Outline	234
<u>Chapter 10.</u> DETAILS OF APPARATUS AND PROCEDURE; SHORT WETTED-WALL COLUMN	280
10.1 Construction of Column Assembly	280
10.2 Auxiliary Apparatus for Carbon Dioxide-Water Runs	282
10.3 Auxiliary Apparatus for Chlorine Runs	287
10.4 Analytical Procedure for Carbon Dioxide-Water Runs	291
10.5 Analytical Procedure for Chlorine Runs	293
10.6 Sources of Water and of Gases Used	294
<u>Chapter 11.</u> MEASUREMENT OF DIFFUSIVITIES IN LIQUIDS	295
Outline	295
<u>Chapter 12.</u> EFFECT OF DIFFUSIVITY ON LIQUID-SIDE RESISTANCE IN PACKED COLUMNS	354

	<u>Page</u>
<u>Chapter 13.</u> INTERFACIAL LIQUID VELOCITY IN SHORT WETTED-WALL COLUMNS	361
13.1 Introduction	361
13.2 Flow Down a Plane Surface	361
13.3 Effect of Gas Rate	363
13.4 Effect of Acceleration	366
13.5 Previous Work in Long Wetted-Wall Columns	367
13.6 Procedure	368
13.7 Results and Discussion	371
13.8 Conclusions	373
 <u>Chapter 14.</u> APPLICATION OF ELECTRONIC ANALOG COMPUTER	 374
 <u>Chapter 15.</u> SAMPLE CALCULATIONS	 384
15.1 Desorption of Carbon Dioxide from Water in the Short Wetted- Wall Column	384
15.2 Desorption of Chlorine from Dilute Hydrochloric Acid in the Short Wetted- Wall Column	385
15.3 Desorption of Chlorine from Water in the Short Wetted-Wall Column	386
 <u>Chapter 16.</u> SUMMARY OF DATA AND CALCULATED RESULTS FOR DESORPTION IN SHORT WETTED-WALL COLUMNS	 389
 <u>Chapter 17.</u> RECALCULATION OF PSEUDO-COEFFICIENT FROM DATA OF VIVIAN AND WHITNEY	 408
 <u>Chapter 18.</u> LOCATION OF ORIGINAL DATA	 413
 <u>Chapter 19.</u> NOMENCLATURE	 414
 <u>Chapter 20.</u> LITERATURE CITATIONS	 419
 <u>Chapter 21.</u> BIOGRAPHICAL NOTE	 426

LIST OF FIGURES

<u>Fig. No.</u>		<u>Page</u>
2.1	Data of Vivian and Whitney on Chlorine and Oxygen In a Packed Column	16
2.2	Effect of Liquor Rate on Pseudo-Coefficients for Chlorine in Water	23
3.1	Assembly of Short Wetted-Wall Column	38
3.2	Assembly of Short Wetted-Wall Column	39
Desorption of Carbon Dioxide from Water;		
4.1	Effect of Temperature	46
4.2	Effect of Air Rate	46
4.3	Effect of Entrance Slot Width	47
4.4	Effect of Entrance Slot Width	47
4.5	Effect of Water Rate	48
4.6	" " " "	48
4.7	" " " "	49
4.8	" " " "	49
4.9	" " " "	50
4.10	Desorption of Chlorine from Dilute Hydrochloric Acid; Effect of Water Rate	50
Desorption of Chlorine from Water;		
4.11	Effect of Concentration	52
4.12	Effect of Water Rate	55
5.1	Effect of Length on Physical Coefficient in Short Wetted-Wall Column	85
5.2	Correlation, Using Penetration Theory, of Physical Coefficients Obtained on Short Wetted- Wall Column	88
5.3	Attempted Correlation, Using Film Theory, of Physical Coefficients Obtained on Short Wetted-Wall Column	96
5.4	Comparison of Physical Coefficients Measured in Various Wetted-Wall Columns	100
5.5	Experimental Values of ϕ for Desorption of Chlorine from Water in a Short Wetted-Wall Column	109
5.6	Effect of Inlet Concentration on Total Coefficient of Desorption of Chlorine from Water in a Short Wetted-Wall Column	113
5.7	Desorption of Chlorine from Water; Comparison of Theory with Experiment	116
5.8	Desorption of Chlorine from Water; Comparison of Theory with Experiment	117
5.9	Desorption of Chlorine from Water in a Stirred Flask	121
5.10	Desorption of Chlorine from Water in a Stirred Flask	121

<u>Fig. No.</u>		<u>Page</u>
5.11	Effect of Liquor Rate on Interfacial Area in a Packed Column	131
8.1	Sketch of Concentration Gradients in a Film	145
8.2	Sketch of Gradients in an Infinite Body of Liquid at Time t	148
8.3	Sketch of Streamlines in Liquid Flowing Down a Wall	150
8.4	Distortion of an Element of Fluid During Acceleration of Fluid	151
8.5	Correction Factor for Holdup; Film Theory	156
8.6	Correction Factor for Holdup; Penetration Theory	174
8.7	Theoretical Values of ϕ for Absorption with First Order Chemical Reaction	200
8.8	Theoretical Values of ϕ for Absorption with First Order Chemical Reaction	203-4
8.9	Comparison of Eq. (8.161) with Eq. (8.168)	206
8.10	Sketch of Concentration of B in Film for Second Order Reaction	214
8.11	Theoretical Values of ϕ for Absorption with Second Order Chemical Reaction (Film Theory)	217
8.12	Comparison of Eqs. (8.227) and (8.228) with Eq. (8.231)	223
9.1	ϕ -Plots for Chlorine-Water System at 70°F.	244
9.2	Effect of Liquor Rate on Physical Coefficient for Absorption of Chlorine in a Packed Column	246
9.3	Effect of Liquor Rate on Effective Interfacial Area for Absorption of Chlorine in a Packed Column	246
9.4	Comparison of Desorption of Chlorine from Water with Absorption of Chlorine in Dilute HCl in a Packed Column	248
9.5	Correlation of Data on Desorption of Chlorine in a Packed Column	249
9.6	Equilibrium Constant for the Hydrolysis of Chlorine in Water vs. $1/T$	253
9.7	Effect of Equilibrium Constant and Reaction Mechanism on ϕ	255
9.8	Effect of Temperature on the ϕ -Plots	257
9.9	Effect of Temperature on the ϕ -Plots	257
9.10	ϕ -Plots for Sulfur Dioxide-Water System at 70°F.	265
9.11	Absorption of Carbon Dioxide in Sodium Hydroxide Solution in a Short Wetted-Wall Column; Effect of Liquor Rate	272
9.12	Absorption of Carbon Dioxide in Sodium Hydroxide Solution in a Short Wetted-Wall Column; Effect of Hydroxide Concentration	273

<u>Fig. No.</u>		<u>Page</u>
10.1	Assembly of Short Wetted-Wall Column	281
10.2	Glass Sections Used in Short Wetted-Wall Columns	281
10.3	Cell Used to Measure Liquid Diffusivities	281
10.4	Schematic Diagram of Apparatus; Runs 1-78	283
10.5	Schematic Diagram of Apparatus; Runs 79-99	286
10.6	Schematic Diagram of Apparatus; Runs 100-198	288
10.7	Diagram of Chlorine-Water Sampling Apparatus	290
11.1	Integral Diffusivity of Potassium Chloride	318
11.2	Effect of Concentrations on Diffusivity of Chlorine in Dilute Hydrochloric Acid at 25°C.	332
11.3	Effect of Time on Diffusion of Chlorine through Water in a Diaphragm Cell at 25°C.	334
11.4	Effect of Temperature on Diffusivity of "Total" Chlorine in Water	338
11.5	Effect of Temperature on Diffusivity of "Total" Chlorine in Water	338
11.6	Effect of Concentration on Diffusivity of Sulfur Dioxide in Dilute Sulfuric Acid at 30°C.	340
11.7	Effect of Time on Diffusion of Sulfur Dioxide through Water in a Diaphragm Cell at 30°C.	344
11.8	Effect of Temperature on Diffusivity of "Total" Sulfur Dioxide in Water	347
11.9	Effect of Temperature on Diffusivity of "Total" Sulfur Dioxide in Water	347
11.10	Comparison of Data on Diffusivity of Carbon Dioxide in Water	350
11.11	Comparison of Data on Diffusivity of Oxygen in Water	351
12.1	Desorption in Packed Column	355
12.2	Effect of Schmidt Number in Packed Columns	356
12.3	Physical Coefficients in Packed Columns	358
12.4	Effect of Diffusivity on Physical Coefficients in Packed Columns	359
13.1	Profile of Liquid Layer	361
13.2	Effect of Gas Rate on Interfacial Velocity of Liquid	365
13.3	Interfacial Velocity in Long Wetted-Wall Columns	369
13.4	Cross-section of Top of Wetted-Wall Column	370
13.5	Schematic of Dye-Pulse System	371
13.6	Interfacial Velocity in Short Wetted-Wall Column	373
14.1	Hook-up of Electronic Analog Computer	376
14.2	Screen of Oscilloscope Showing Solution Obtained on Electronic Computer	379
14.3	Theoretical Values of ϕ for Absorption with Second Order Irreversible Chemical Reac- tion Solution by Electronic Analog Com- puter	381

LIST OF TABLES

	<u>Page</u>
5.1 Calculation of Interfacial Area in Packed Column	131
8.1 Fraction of Material Diffusing through Film Unreacted for First Order Irreversible Reaction	157
8.2 Comparison of Eqs. (8.102) and (8.104)	176
8.3 Calculation of ϕ for Absorption with First Order Chemical Reaction	200
8.4 Theoretical Values of ϕ for Absorption with Second- Order Reaction, Calculated by Eq. (8.203)	216
8.5 Theoretical Values of ϕ for Absorption with Second-Order Reaction Calculated by Eqs. (8.214)-(8.216)	216
9.1 Calculated Values of ϕ for Absorption of Chlorine in Water	258
9.2 Rate of Hydrolysis of Sulfur Dioxide	263
11.1 Diffusivity of Potassium Chloride in Water at 25°C; (34, 35)	303
11.2 Diffusivity of Hydrochloric Acid in Water; (49)	304
11.3 Average Diffusivity of Hydrochloric Acid in Water at 16°C.; (24)	305
11.4 Diffusivity of Oxygen in Water	306
11.5 Diffusivity of Carbon Dioxide in Water	307
11.6 Computation of γ	318
11.7 Computation of Integral Diffusivities of KCl in Standardization Runs	318
11.8 Calibration of Diaphragm Cells	327
11.9 Calibration of Diaphragm Cells; Results	328
11.10 Diffusion of Chlorine Through Dilute Hydrochloric Acid at 25°C.	330
11.11 Diffusion of Chlorine Through Water at 25°C.	333
11.12 Effect of Temperature on Diffusion of Chlorine Through Water	337
11.13 Diffusion of Sulfur Dioxide Through Dilute Sulfuric Acid at 30°C.	341
11.14 Diffusion of Sulfur Dioxide Through Water at 30°C.	343
11.15 Effect of Temperature on Diffusion of Sulfur Dioxide Through Water	346
11.16 Miscellaneous Diffusion Measurements	349
12.1 Diffusivities of Several Gases in Water	354
16.1 Column Dimensions	389
16.2 Desorption of Carbon Dioxide from Water; Effect of Temperature; Column 3U	390
16.3 Desorption of Carbon Dioxide from Water; Effect of Air Rate; Column 3U	391
16.4 Desorption of Carbon Dioxide from Water; Effect of Slot Width; Column 3U	392

	<u>Page</u>
16.5 Desorption of Carbon Dioxide from Water; Effect of Water Rate; Column 3U	393
16.6 Desorption of Carbon Dioxide from Water; Effect of Water Rate; Column 2U	395
16.7 Desorption of Carbon Dioxide from Water; Effect of Water Rate; Column 3D	397
16.8 Desorption of Carbon Dioxide from Water; Effect of Slot Width; Column 3D	398
16.9 Desorption of Carbon Dioxide from Water; Effect of Water Rate; Column 2D	399
16.10 Desorption of Carbon Dioxide from Water; Effect of Water Rate; Column 1U	400
16.11 Desorption of Chlorine from Dilute Hydrochloric Acid; Column 3D	401
16.12 Desorption of Chlorine from Water Column 3D	402
17.1 Absorption of Chlorine in Water in Packed Column -- Recalculation of Pseudo-Coefficient	411

CHAPTER 1

SUMMARY

The only systematic study of the liquid-side resistance to absorption or desorption in packed columns was performed by Sherwood and Holloway (93), who found the liquid-side coefficients to vary as the 0.75 power of the liquor rate and the half power of the diffusivity. When Vivian and Whitney (101) measured the absorption of chlorine in water in a packed column, it was found to be liquid-side controlled, but it did not fit the Sherwood and Holloway correlation. The coefficients varied as the 0.6 power of the liquor rate and fell 25 to 70 per cent lower than those predicted by the correlation. Vivian and Whitney explained the discrepancy as due to the reaction of chlorine with water, but their explanation was only qualitative.

The thesis was undertaken to obtain a better understanding of the mechanism of absorption with reversible chemical reaction, with particular reference to the chlorine-water system. To this end, several lines of investigation were pursued: (1) a study of the nature of the liquid-side resistance where no chemical reaction is present; (2) a mathematical study and experimental study of the effect of the chemical reaction; (3) measurements of diffusivities.

Two theories have been proposed for the mechanism of the liquid-side resistance. The first is the film theory, which assumes the existence of a thin stagnant liquid film adjoining the interface while the rest of the liquid is well mixed. The film is considered to be sufficiently thin that steady-state mass transfer conditions exist within it. These assumptions lead to the equation for the liquid-side coefficient:

$$k_L^* = \frac{D}{x_f} \quad (1.1)$$

where k_L^* is the physical coefficient, obtained in the absence of chemical reaction. While two concepts of the two-film theory, equilibrium at the interface, and additivity of the resistances of the two phases, have proven very useful in absorption work, the concept of the thin stagnant liquid film adjacent to the interface with steady-state diffusion has long been open to question, particularly in packed columns.

Higbie (37), in 1935, proposed another theory of the liquid-side resistance, which he called the penetration theory. As the liquid flows over the packing, it is pictured as flowing over each piece in laminar flow. It is then partially or wholly mixed in going from one piece of packing to the next. Absorption is considered to take place during a series of brief contacts between the liquid and the gas, in which the solute diffuses only a short distance into

the liquid before the liquid is mixed. Unsteady-state mass transfer conditions prevail in the liquid. Since the dissolved gas penetrates a short distance compared with the total depth of the liquid during ordinary exposure times, it makes little difference whether it is assumed that the depth of the liquid is the actual depth or that it is infinite. To facilitate the mathematics, infinite depth is assumed. The penetration theory then yields the equation for the coefficient:

$$k_L^* = 2\sqrt{\frac{D}{\pi t}} \quad (1.2)$$

where t is the time of exposure of the liquid to the gas between mixings. The driving force for this coefficient is the difference between the interfacial concentration and the concentration in the liquid at the beginning of the short absorption period. Since the concentration change in the liquid in each absorption period is small compared with the overall change in a packed column, this coefficient is practically equivalent to that based on the continuously changing driving force used in the film theory.

While the assumptions of the penetration theory may be an oversimplification of the conditions in a packed column, they are certainly more reasonable than those of the film theory. Furthermore, the conclusion of Sherwood and Holloway that k_L^*a varies as D to the half power is in agreement with

the prediction of the penetration theory.

In studying the mechanism of the liquid-side resistance, the packed column has the disadvantage of unknown interfacial area. The usual wetted-wall columns are not suitable, either, because they are so long that the time of exposure of the liquid to the gas is much greater than that on an individual piece of packing. The result is that the solute is able to penetrate well into the liquid layer and the assumption of infinite depth of liquid is no longer valid. By reducing the length of the wetted-wall column to the order of 1/2 to 2 inches, times of exposure are obtained which approximate those for the liquid on commercial packing. Under such conditions, the assumption of infinite depth of liquid is justified. A further advantage of the short wetted-wall column is the absence of ripples in the falling layer which increase the interfacial area and bring about mixing in the liquid, since in the ordinary wetted-wall column ripples do not form until the layer has fallen several inches from the top of the column.

Such a short wetted wall column was constructed. The wetted-wall section was made of glass, while the tubes leading the gas stream into and out of the column were made of Teflon. By having the liquid enter and leave the column through thin slots between the glass and Teflon which were maintained completely full of liquid, end effects were avoided

in the sense that the only contact between liquid and gas was in the wetted-wall section itself. The diameter of the column was one inch. Three different lengths were used, roughly $5/8$, $1-1/8$ and $1-5/8$ inches long. The width of the entrance slot could be varied, and two types of entrance slots were used, one in which the slot sloped upward, and one in which it sloped downward.

The short column was used to study the desorption of carbon dioxide from water by air, of chlorine from dilute hydrochloric acid by air, and of chlorine from water by air. In the first two systems, the equilibrium is such that hydrolysis of the solutes was negligible, so that physical coefficients were obtained. For the chlorine-water system, in which desorption was accompanied by a reversible chemical reaction, two types of coefficients were calculated. The first, called normal, or "total", coefficient, k_L , is based on a driving force equal to the difference between the total chlorine concentration which would be in equilibrium with the gas and the total chlorine concentration in the inlet liquid. The second type, called the pseudo-coefficient, k_L' , is based on a driving force equal to the difference between the concentration of unreacted chlorine in equilibrium with the gas at the interface and the concentration of unreacted chlorine in the inlet liquid.

Using the carbon dioxide-water system, the effects of liquid flow rate, temperature, gas rate, slot width, slot type, and length of column were investigated. Gas rate was found to have no significant effect up to a Reynolds number in the gas stream of 2200. At higher gas rates ripples were produced which caused an increase in the desorption rate. The absence of an effect of gas rate below $Re_g = 2200$ showed that the gas-side resistance was negligible. Slot width and slot type were found to have no significant effect. Over the range 22° to 31°C ., the coefficient increased 1.1 per cent for each centigrade degree rise in temperature. The coefficient was found to vary as the 0.40 power of the liquid flow rate over the range 7 to 90 g./((cm.)(min.)). Over the range of length of 1.88 to 4.25 cm., it was found to vary inversely as the square root of the column length.

Using the chlorine-dilute hydrochloric acid system, the effects of liquid rate and of chlorine concentration were measured. The concentration of the hydrochloric acid was between 0.16 and 0.18 normal. Over the range 0.011 to 0.040 moles/l., chlorine concentration was found to have no significant effect. The coefficient varied as the 0.40 power of the water rate. Comparison with the carbon dioxide data for the same column length showed that the coefficient varied as the square root of the diffusivity. All of the carbon dioxide-water and chlorine-HCl data were

correlated by the equation

$$k_L^* \sqrt{\frac{h}{D}} = 7.13 \Gamma^{0.4} \quad (1.3)$$

where all quantities are expressed in g., cm., and sec. The average deviation from the data was 7.7%.

A theoretical equation for the physical coefficient was derived by combining the penetration theory with streamline flow theory:

$$k_L^* = 2 \sqrt{\frac{D}{\pi h}} \left(\frac{9}{8} \frac{g \Gamma^2}{\mu \rho} \right)^{1/6} \quad (1.4)$$

Comparison with eq. (1.3) shows that the theory predicts coefficients 30% too high at the lowest liquid flow rates, and only 10% too high at the highest flow rate. The discrepancy may be attributed to uncertainties in the liquid flow pattern. The agreement is good, considering that the mass transfer rate has been predicted solely from theoretical considerations, using only such physical constants as diffusivity, viscosity and density, without recourse to any empirical quantities as film thickness or eddy diffusivity.

In the desorption of chlorine from water, the effects of liquid rate and of chlorine concentration were studied. At each liquid flow rate, the pseudo-coefficient was found to be independent of concentration over the range 0.005 to 0.04 moles/l., and to vary linearly with concentration over the range 0.04 to 0.07 moles/l. The data were correlated with

an average deviation of 4.2% by two equations, one for each of the two concentration ranges:

$$k_L^{\circ} = (k_L^{\circ})' \quad C_1 < 0.040 \quad (1.5)$$

$$k_L^{\circ} = (k_L^{\circ})' + 2.9 \Gamma^{0.40} (C_1 - 0.040) \quad C_1 > 0.040 \quad (1.6)$$

where $(k_L^{\circ})'$ is a function of the liquid rate. At the high flow rates, it approaches the physical coefficient, calculated by eq. (1.3), while at the low flow rates, the ratio of $(k_L^{\circ})'$ to k_L^* approaches a constant value, equal to 1.6.

The normal, or "total", coefficients were also calculated. For each liquid rate, it was found to increase with concentration; at high concentrations (above about 0.06 moles/l.), they were found to exceed the physical coefficient corresponding to that liquid rate. There appeared to be no tendency of the "total" coefficients to level off with increasing concentration.

These results are in direct contradiction with theoretical results obtained by a mathematical study of absorption with reversible chemical reaction. The theory predicts that the pseudo-coefficient should decrease uniformly with concentration. Furthermore, the theory predicts, for infinite rate of hydrolysis and infinite diffusivity of the HCl component in the chlorine-water system, that the "total" coefficient should equal the physical coefficient. For finite hydrolysis rate and finite diffusivity of HCl, the "total" coefficient must

be lower, so that the physical coefficient represents an upper limit which theoretically cannot be exceeded. This is reasonable from the physical point of view, for physically it means that for a given concentration of chlorine in the liquid, the rate of desorption would be greater if the chlorine were uncombined with the water than if some of the chlorine is combined with the water and has to undergo a reaction of finite rate in order to be desorbed. No explanation for this anomalous behavior of the chlorine-water system can be offered at this time.

In addition, an experimental program of measuring diffusivities was carried out. Using a diaphragm cell, the diffusion of chlorine through dilute hydrochloric acid, of chlorine through water, of sulfur dioxide through dilute sulfuric acid, and of sulfur dioxide through water were measured. The following diffusivities were calculated from the results:

Unhydrolyzed chlorine in water at 25°C.	1.48×10^{-5} cm. ² /sec.
Hypochlorous acid in water at 25°C.	1.54
Unhydrolyzed sulfur dioxide at 30°C.	
Concentration: 0.05 moles/l.	1.92
0.10	1.95
0.15	1.97
0.20	1.99
0.30	2.00
0.40	2.01
0.50	2.02
Hydrolyzed sulfur dioxide in water at 30°C.	1.99
Concentration 0.03 to 0.10 moles/l.	

The Stokes-Einstein relationship, that D is proportional to T/μ , was found to hold for chlorine in water over the range 10 to 30°C., and for sulfur dioxide in water over the range 20 to 40°C.

By comparing the data obtained on the short wetted-wall column with data obtained by previous investigators on packed columns, it was possible to calculate the effective interfacial area in the packed column in several ways. For one-inch Raschig rings, it was found that the interfacial area varies as the liquor rate raised to a power between 0.4 and 0.6, and that it equals the total dry area of the packing at a liquor rate of 20,000 lb./((hr.)(ft.²)), which is just below the loading point.

It is concluded that the mechanism of the liquid-side resistance in the short wetted-wall column is that of unsteady-state diffusion as postulated by the penetration theory. The short wetted-wall column was found to be well suited for liquid-phase mass transfer studies, and it is recommended that it be used as a tool for the study of liquid-side resistance for other systems of absorption or desorption with chemical reaction, because of the similarity of the liquid flow conditions to those existing in a packed column.

CHAPTER 2

INTRODUCTION

When a gas and a liquid are brought into contact, a transfer of matter takes place between the two phases until thermodynamic equilibrium is reached. While thermodynamics will predict the direction of mass transfer, it cannot supply any information about the rate. It is necessary, therefore, to resort to experiment to discover the laws governing the rate of mass transfer between gas and liquid phases.

Early studies of the absorption of one component of a gaseous mixture by water and of desorption of a gas from water showed (16) that the rate of these processes is proportional to the "distance from equilibrium." One group of workers, including Coste (16), van Arsdel (4) and Donnan and Masson (21), expressed the distance from equilibrium as the difference between the concentration in equilibrium with the bulk of the gas and the bulk concentration of the liquid; while another group of workers, including Lewis (64), used the difference between the partial pressure in the gas of the component being absorbed and the partial pressure in equilibrium with the bulk of the liquid. The former group conceived the mass transfer process as a diffusion through a stagnant liquid layer at the interface, while the latter

looked on it as a diffusion through a stagnant gaseous layer at the interface. It was realized (5, 104) that though these two views are equivalent when Henry's law is obeyed, since the driving forces are then proportional, they conflict when the equilibrium relationship is non-linear. Actually the choice between the two was made by selecting the one which gave the most consistent results.

That the resistance to mass transfer might be split into a gas-film and a liquid-film resistance was first advanced by Whitman and Keats (105), but it was not until two later papers by Whitman (104) and Lewis and Whitman (65) that the idea was proposed of also splitting the driving force into two parts, the driving force across the gas film alone and that across the liquid film alone. This was expressed mathematically by

$$N_A = k_g (P_g - P_i) = k_L (C_i - C_o) \quad (2.1)$$

where P_g is partial pressure in bulk of gas

P_i is partial pressure at the interface

C_i is concentration in liquid at the interface

C_o is concentration in bulk of liquid

k_g is gas-film coefficient

k_L is liquid film coefficient

Assuming equilibrium at the interface and the validity of Henry's law, we have

$$C_1 = HP_1 \quad (2.2)$$

which may be combined with eq. (2.1) to give

$$N_A = \frac{1}{\frac{1}{k_g} + \frac{1}{Hk_L}} (P_g - C_o/H) = \frac{1}{\frac{H}{k_g} + \frac{1}{k_L}} (HP_g - C_o) \quad (2.3)$$

These equations show the very important role played by solubility in determining the relative importance of the two resistances. When the gas is very soluble, H is large, and eq. (2.3) becomes

$$N_A = k_g(P_g - C_o/H) \quad (2.4)$$

If the gas is slightly soluble, H is small, and eq. (2.3) becomes

$$N_A = k_L(HP_g - C_o) \quad (2.5)$$

This thesis is concerned only with the liquid-side resistance. In practically all the cases considered, the solubility is sufficiently low that the gas-side resistance is negligible compared with the liquid-side resistance. Thus there is no appreciable partial pressure gradient in the gas, so that $P_g = P_1$. Eq. (2.5) becomes

$$N_A = k_L(HP_1 - C_o) \quad (2.6)$$

which is applicable when Henry's law is valid. In any event, we may use

$$N_A = k_L(C_i - C_o) \quad (2.7)$$

where C_i , the interfacial concentration, is in equilibrium with the gas. Eq. (2.7) may be regarded as the defining equation for the liquid-side coefficient, k_L .

The packed column has found wide application in the chemical industry as a device for contacting a liquid and a gas stream continuously. Its chief advantages are large interfacial area per unit volume and comparatively low pressure drop in the gas stream. But, because of uncertainties in the interfacial area and in the flow pattern of the liquid and the gas, little success has been achieved in predicting mass transfer rates. Coefficients obtained on one type of packing are of little value in predicting coefficients on a different type. However, for a given packing, it has been possible to correlate different liquid-gas systems with some success.

The only systematic investigation of liquid-side coefficients in packed columns was performed by Sherwood and Holloway (93). They studied the desorption from water of the slightly soluble gases hydrogen, oxygen and water, using air for the gas stream. The influence of temperature, liquid rate and gas rate were examined. Data were obtained on 0.5, 1.0, 1.5 and 2.0 inch Raschig rings, 0.5, 1.0 and 1.5 inch Berl saddles and 3 inch spiral tile. They correlated their results with the equation

$$\frac{k_L a}{D} = \alpha \left(\frac{L}{\mu}\right)^{1-n} \left(\frac{\mu}{\rho D}\right)^{1-s} \quad (2.8)$$

The value of s was found to be 0.47 while the values of α and n were found to be dependent on the packing. In particular, n was found to be 0.25 for one-inch Raschig rings. A critical review of Sherwood and Holloway's data and of the conclusions which they drew is presented in Chapter 12 in the APPENDIX.

When Vivian and Whitney (101) undertook the study of absorption of chlorine in water in a column packed with one-inch Raschig rings, they expected that the liquid-side resistance would be controlling because of the comparatively low solubility of chlorine in water, and hence that the Sherwood and Holloway correlation would be applicable. The absence of any appreciable effect of gas rate did indeed show that the gas-side resistance was negligible, but the coefficients obtained failed to agree with the Sherwood and Holloway correlation. To make sure that the discrepancy was not due to differences in equipment, Vivian and Whitney also desorbed oxygen from water in their apparatus. The oxygen coefficients agreed very well with those of Sherwood and Holloway. The oxygen and chlorine coefficients are shown in Fig. 2.1.

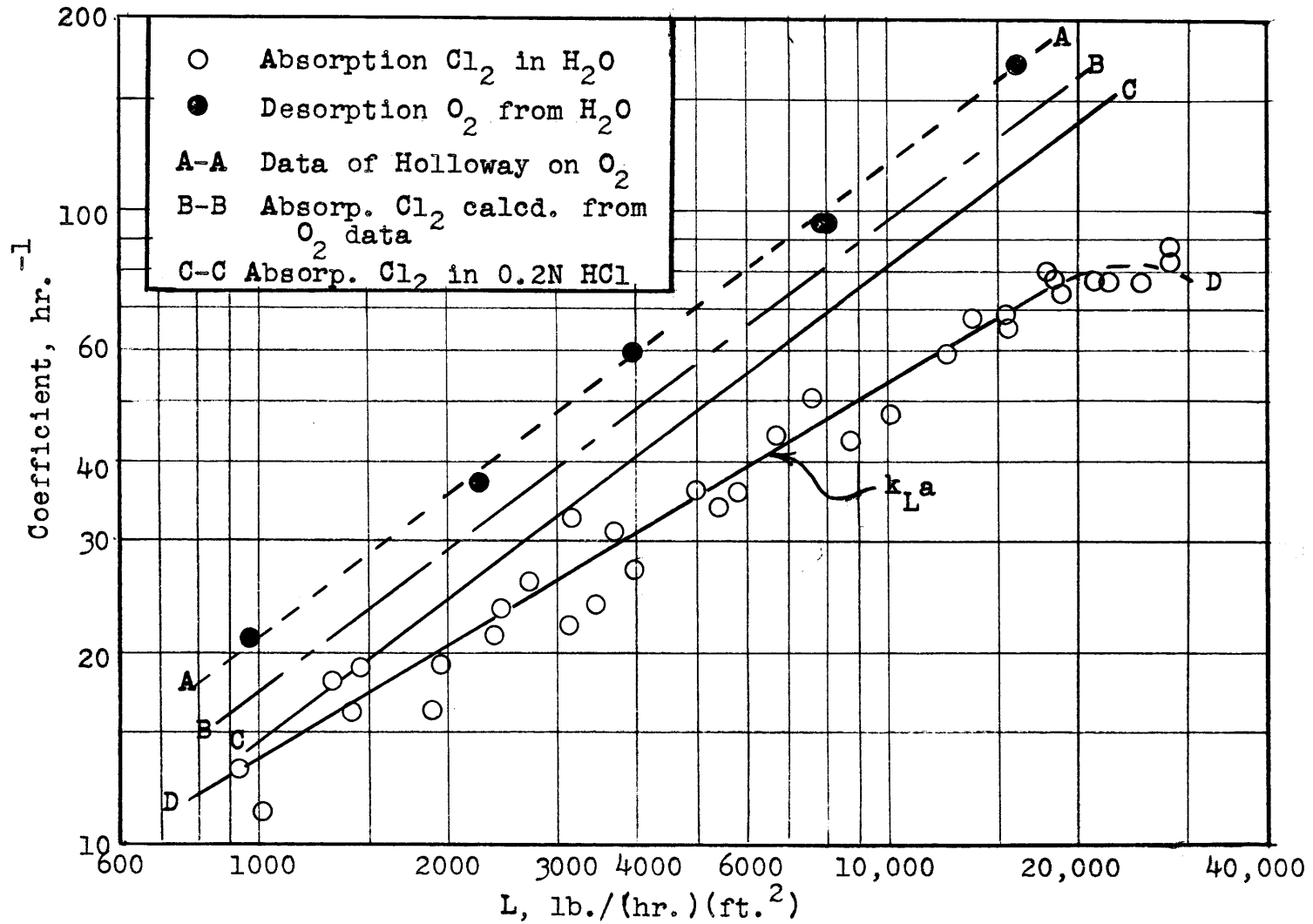
Also plotted in Fig. 2.1 is the line B-B representing the predicted coefficients for chlorine. This line was cal-

Fig. 2.1

Data of Vivian and Whitney on Chlorine and Oxygen in a Packed Column

Temp. = 70°F.

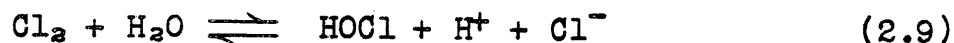
1 inch Raschig Rings



culated from the oxygen data by multiplying the square root of the ratio of the diffusivity of chlorine in water to the diffusivity of oxygen in water, using the best available values of diffusivities at that time. Thus it can be seen that the chlorine coefficients fall 20 to 50% below the predicted values and, even more important, vary as the 0.6 power of the liquid rate while the predicted coefficients vary as the 0.75 power.

As pointed out by Vivian and Whitney, the explanation for the discrepancy lies in the fact that chlorine reacts with water, while the Sherwood and Holloway correlation was made for gases which dissolve in water without reacting. It had been assumed that the rate of hydrolysis of chlorine is so rapid compared to the rate of absorption that it would have no appreciable effect on the absorption, but the results of Vivian and Whitney indicated that this is not true.

Chlorine reacts with water according to the equation



The dissociation constant of hypochlorous acid is of the order of 10^{-6} or lower (41, 81), so that it may be assumed to be undissociated. Because the solution must always be electrically neutral, the concentration of hydrogen ions must everywhere equal that of chloride ions. Letting

A = concentration of Cl_2

E = concentration of HOCl

F = concentration of H^+ and of Cl^-

the equilibrium relation is

$$K_c = EF^2/A \quad (2.10)$$

At the interface, the gas is in equilibrium with the unhydrolyzed, or molecular, chlorine.

$$A_1 = HP \quad (2.11)$$

If, during absorption, the hydrolysis reaction were instantaneous, so that equilibrium existed everywhere in the liquid, and if the diffusivities of each of the three components Cl_2 , HOCl and HCl were equal, then, and only then, would all the chlorine diffuse through the water as if it were a single substance, and only then would the rate of absorption be unaffected by the chemical reaction.

The customary analysis for chlorine in water determines the total chlorine, which is the sum of molecular chlorine plus hypochlorous acid. Let this total chlorine concentration be C.

$$C = A + E \quad (2.12)$$

The coefficients first presented by Vivian and Whitney, which they called the "normal" coefficient, and which are plotted on Fig. 2.1, are calculated from the rate of absorption by the equation

$$N_A = k_L(C_1 - C_0) \quad (2.13)$$

In this thesis, the normal coefficient will be referred to as the "total" coefficient, since it is based on a driving force which is the difference between the total chlorine which would be in equilibrium with the gas, and the total chlorine which is in the bulk of the liquid.

To avoid confusion, it is necessary to distinguish between the coefficients obtained with and obtained without chemical reaction. When absorption takes place without chemical reaction, the coefficient obtained will be referred to as the "physical" coefficient, k_L^* . Since $A = C$ when there is no reaction, the defining equation of k_L^* may be written

$$N_A = k_L^* (C_1 - C_0) = k_L^* (A_1 - A_0) \quad (\text{when } A=C) \quad (2.14)$$

Then, under the conditions of infinite hydrolysis rate and equal diffusivities discussed above, k_L would be equal to k_L^* . The fact that they are different indicates that these conditions are not fulfilled.

There are two ways of determining the physical coefficient for chlorine in water. One method is to use the oxygen data and correct for the lower diffusivity of chlorine, as discussed above. Another method is to suppress the reaction between the chlorine and the water by absorbing the chlorine in dilute hydrochloric acid. Craig (17) absorbed chlorine in 0.2 normal HCl in a column packed with one-inch Raschig rings. His data are plotted in Fig. 12.3 in the

APPENDIX, and the best line through his data is reproduced as line C-C in Fig. 2.1. This line should, of course, coincide with line B-B predicted from the oxygen data. Both lines have a slope of 0.75, but Craig's line is about 17 percent lower. As pointed out in Chapter 12 of the APPENDIX, this difference might be explained by uncertainties in the values of diffusivities of oxygen and chlorine used to calculate B-B, and also by some doubt as to the Sherwood and Holloway correlation itself. It is believed that line C-C, representing Craig's data, is the more reliable. Hence line C-C will be taken as the physical coefficient, k_L^* , for chlorine in water.

Comparing lines C-C and D-D in Fig. 2.1 still gives the conclusion that k_L is not equal to k_L^* and that the conditions of infinite hydrolysis rate and equal diffusivities are not fulfilled. However, the two lines do converge at the low liquor rates, indicating that such a picture is not far from wrong at those liquor rates.

If, on the other hand, the rate of hydrolysis were sufficiently slow relative to the rate of diffusion, the molecular chlorine entering the liquid phase would have time to diffuse into the bulk of the liquid before an appreciable amount would have been hydrolyzed. Then, the proper driving force would be the difference between the concentration of molecular chlorine in equilibrium with the gas and the concentration of molecular chlorine actually present in the bulk of the liquid. Thus,

$$N_A = k_L^0 (A_1 - A_0) \quad (2.15)$$

This equation defines k_L^0 , which Vivian and Whitney called the "pseudo-coefficient." They were the first to propose the use of such a coefficient for absorption in which a reversible chemical reaction is taking place. $(A_1 - A_0)$ is sometimes called the "pseudo-driving force."

Now, to use eq. (2.15), values of A_1 and A_0 must be determined. A_1 is calculated from P by eq. (2.11). A_0 is calculated from C_0 by assuming that equilibrium exists in the bulk of the liquid. Since the hydrolysis reaction produces equal amounts of hypochlorous and hydrochloric acids, $E_0 = F_0$, and eq. (2.10) may be written $K = E_0^3 / A_0$. (It must be remembered that E is not equal to F everywhere in the liquid, since the diffusivities of HOCl and HCl are not the same.) Since $E_0 = C_0 - A_0$, we have

$$K_C = (C_0 - A_0)^3 / A_0 \quad (2.16)$$

which is used to calculate A_0 from C_0 . Values of K and H at various temperatures were determined by Vivian and Whitney (101) from their solubility data.

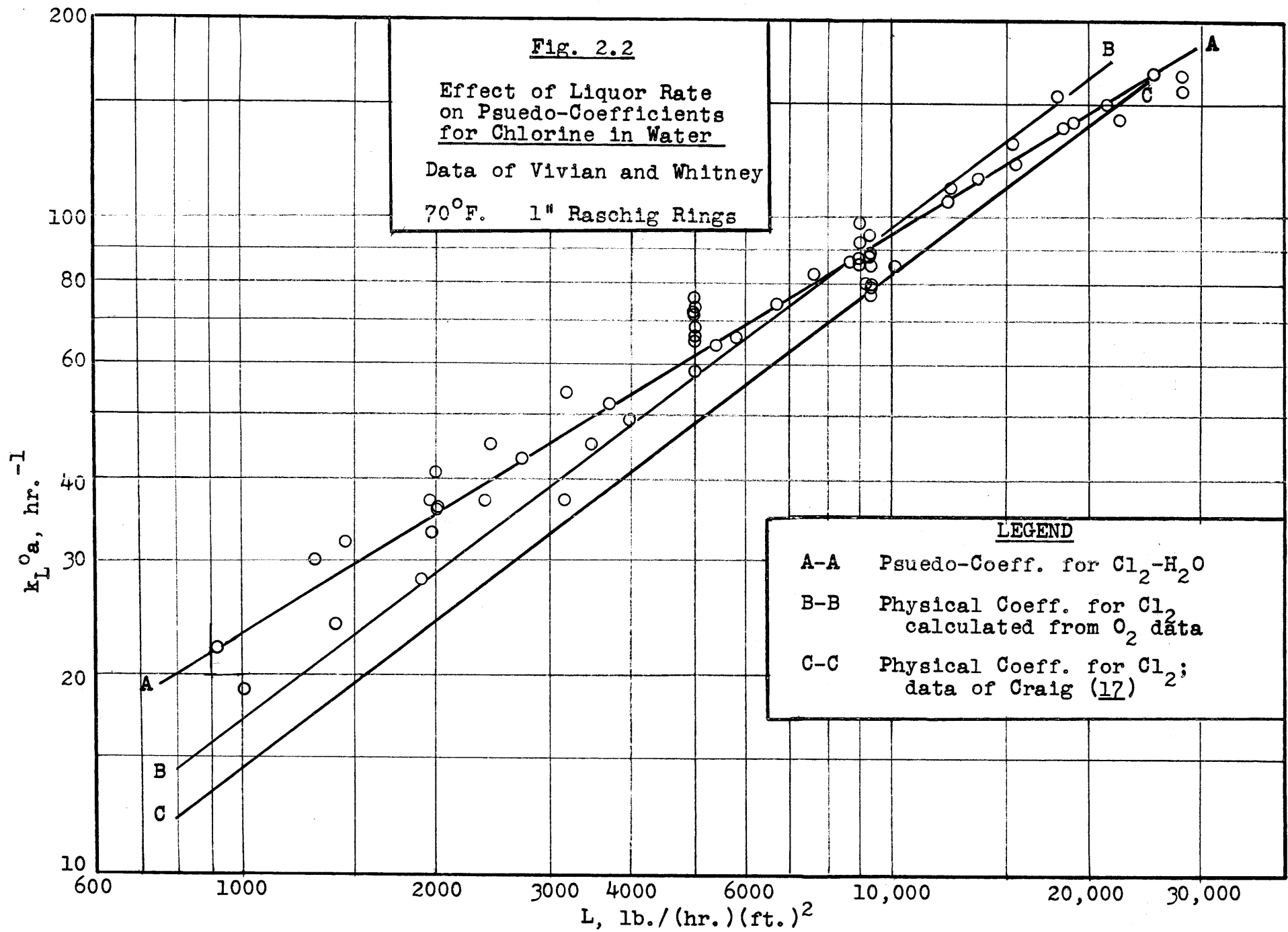
Now, if the hydrolysis reaction were very slow, then k_L^0 would be equal to k_L^* . To test this hypothesis Vivian and Whitney calculated the pseudo-coefficients for their data and compared them with the Sherwood and Holloway correlation. Unfortunately, they used a logarithmic mean "pseudo-driving

force" which is not correct. These have been recalculated using numerical integration (see Chapter 17 of the APPENDIX) and are plotted on Fig. 2.2. For comparison lines B-B and C-C from Fig. 2.1 are reproduced here.

The best line for the pseudo-coefficient, line A-A, has a slope of 0.6. It crosses line B-B, and lies above line C-C, converging to line C-C at the higher liquor rates. But the pseudo-coefficient cannot be less than the physical coefficient. This serves as another indication that line C-C represents more reliable values of the physical coefficient than line B-B.

Since the pseudo-coefficient is, in general, not equal to the physical coefficient, the picture of the hydrolysis rate being slow compared to the diffusion rate is not applicable, except at the higher liquor rates. Actually, the true picture lies between the two extremes presented above. The rate of reaction and the rates of diffusion are of comparable magnitude and both must be taken into account.

The absorption of sulfur dioxide in water is another case of absorption with reversible chemical reaction. Whitney and Vivian (107) studied the absorption of sulfur dioxide in water in a column packed with one-inch Raschig rings. Because of a higher solubility than chlorine, the gas-side resistance was appreciable, amounting to as much as 50 percent of the total resistance. After subtracting the



gas-side resistance, the liquid-side resistance was found to be such that the pseudo-coefficient was equal to the physical coefficient for all liquor rates measured. For this case, then, the picture of the hydrolysis being slow compared to the diffusion rate apparently is valid.

It is the purpose of this thesis to study the mechanism of absorption with reversible chemical reaction from a more fundamental and quantitative point of view with the object, if possible, of being able to predict the rates of absorption from equilibrium constants, rate constants and diffusivities, as well as from the factors which determine the physical coefficients. To this end several lines of investigation have been pursued. A study has been made of liquid-side resistance where no chemical reaction is present, and experimental absorption equipment was devised to simulate liquid flow conditions in a packed column in order to study the physical coefficients. Secondly, the coefficients for the chlorine-water system were studied in this equipment. Thirdly, a mathematical study was made of absorption with chemical reaction in order to develop the theory sufficiently to handle reversible reactions. Finally, the diffusivities of chlorine in water and of sulfur dioxide in water were measured.

Before absorption with chemical reaction can be investigated, the mechanism of the liquid-side resistance in

absorption without chemical reaction must be understood. The mathematical model which has been in chief use to describe the liquid-side resistance is the film theory. The assumptions involved in this theory are: a) there exists a stagnant liquid film next to the interface; b) the remainder of the liquid is sufficiently well-mixed that the concentration gradient in the liquid is localized completely within the stagnant film; c) the film is sufficiently thin that the amount of solute contained in the film is negligible compared with the amount of solute transferred through it; then the rate of diffusion into the film is equal to the rate of diffusion out of it, and steady state may be assumed. These assumptions are stated mathematically by the differential equation

$$D_A \frac{d^2 A}{dx^2} = 0 \quad (2.17)$$

with the boundary conditions

$$\text{At } x = 0, \quad A = A_1 \quad (2.18)$$

$$\text{At } x = x_f, \quad A = A_0 \quad (2.19)$$

These equations lead to the familiar expression

$$k_L^* = D_A/x_f \quad (2.20)$$

Now, the main contributions made by the Lewis and Whitman two-film theory (65, 104) are the concepts of additivity of gas-side and liquid-side resistances and of equilibrium at the interface. These concepts have proved extremely valuable

to the theory of absorption. The concept of the stagnant film, which came before the two-film theory, has proved less useful. There is no way of predicting the film thickness, x_f , or of even measuring it, so that it is a completely empirical quantity. The film theory can predict only one thing, the effect of liquid diffusivity on the physical coefficient. Here it fails miserably, for while it predicts that the coefficient varies as the first power of diffusivity, Sherwood and Holloway (93) report that it varies as the 0.47 power in a packed column.

It should not be surprising that the film theory does not hold in a packed column. Considering the liquid flow conditions existing on the packing, it is difficult to conceive of the existence of a stagnant liquid film at the interface. As the liquid flows over a piece of packing, the stagnant portion of the liquid would be at the interface between the solid packing and the liquid, while the liquid at the gas-liquid interface should be the most rapidly moving portion.

At this point, it is necessary to make a distinction between film and layer. Both the terms film and layer have been applied both to the stagnant film at the interface referred to above and to the whole of the liquid layer running down a surface (as, for example, "falling-film evaporator"). In order to avoid confusion, the term film should be reserved

for the former, while the latter should be called a layer. This nomenclature is used throughout this thesis.

While the film theory might be applicable to some kinds of equipment (as, perhaps, batch absorption in a beaker or flask where both phases are stirred), it has been realized for a long time by some workers that it is too simplified a picture for a packed column. Higbie (37), in 1935, proposed another theory of the liquid-side resistance, which he called the penetration theory. As the liquid flows over the packing, he pictured it as flowing over each piece in laminar flow. It is then partially or wholly mixed in going from one piece of packing to the next. Absorption is considered to take place during a series of brief contacts between the liquid and the gas, in which the dissolved gas diffuses (or "penetrates") only a short distance into the liquid before the liquid is mixed.

Since unsteady state conditions prevail in the liquid, the equation used is

$$D_A \frac{\partial^2 A}{\partial x^2} = \frac{\partial A}{\partial t} \quad (2.21)$$

Since the dissolved gas penetrates only a short distance compared with the total depth of the liquid layer, it makes little difference to the shape of the concentration vs. distance curve whether it is assumed that the depth of

the liquid layer is the actual depth, or whether it is assumed to be infinite. To facilitate the mathematics, it is assumed that there is no relative motion of the liquid and that the liquid layer is of infinite extent away from the interface. As long as the relative motion with the actual "penetration zone" is small, these assumptions are satisfactory. Then, at the interface,

$$\text{At } x = 0, t > 0, \quad A = A_1 \quad (2.22)$$

Just after each mixing, defining A_0 as the average concentration,

$$\text{At } t = 0, x > 0, \quad A = A_0 \quad (2.23)$$

Finally, since infinitely far from the interface the concentration undergoes no change in a finite time,

$$\text{At } x = \infty, t \geq 0, \quad A = A_0 \quad (2.24)$$

This mathematical problem is identical with that involved in finding the temperature distribution of an infinitely long insulated rod which is initially at a uniform temperature where, at time $t = 0$, one end is suddenly raised to another temperature and maintained at that temperature.

Integration of eq. (2.21) with the boundary conditions (2.22)-(2.24) yields (for details see Sec. 8.13 in the APPENDIX)

$$(A - A_0) / (A_1 - A_0) = 1 - \text{erf}(x / 2\sqrt{Dt}) \quad (2.25)$$

The instantaneous rate of absorption varies with time.

$$N_A = -D_A (\partial A / \partial x)_{x=0} \quad (2.26)$$

Differentiating eq. (2.25) to obtain $\partial A / \partial x$, setting $x=0$ and substituting into eq. (2.26) gives

$$N_A = (A_1 - A_0) \sqrt{D_A / \pi t} \quad (2.27)$$

The total amount absorbed in each absorption period of time t is

$$\int_0^t N_A dt = 2(A_1 - A_0) \sqrt{D_A / \pi t} \quad (2.28)$$

The coefficient measured in the packed column would be defined by

$$\int_0^t N_A dt = k_L^* (A_1 - A_0) t \quad (2.29)$$

so that

$$k_L^* = 2 \sqrt{D_A / \pi t} \quad (2.30)$$

Note that as k_L^* is defined here, the driving force, $(A_1 - A_0)$, remains constant for each absorption period and then changes to a new value for the next absorption period depending on the new value of A_0 . (This assumes that the change of A_1 is very small during each absorption period). Since the change in $(A_1 - A_0)$ in each absorption period is small compared with the overall change in a packed column, the coefficient k_L^* is equivalent to the k_L^* defined on the basis of the continuously changing driving force used in the film theory.

Now, it may be that the assumptions of the penetration theory are also an oversimplification of the conditions existing in a packed column. Nevertheless its assumptions are certainly more reasonable than those of the film theory. Furthermore, the conclusion of Sherwood and Holloway (93) that $k_L^* a$ varies as D_A to the 0.47 power is in remarkable agreement with the prediction of the penetration theory that it varies as D_A to the 0.5 power (see eq. (2.30)). Actually, Sherwood and Holloway recommended that 0.5 be used as the exponent on $(\mu\rho D)$ in eq. (2.8).

In making a fundamental study of the mechanism of the liquid-side resistance to absorption, the packed column suffers the severe disadvantage of unknown interfacial area. Two types of equipment have chiefly been used in the laboratory for the fundamental study of absorption and their main advantage has been that their interfacial area can be measured; the first is batch absorption in a flask or beaker where the two phases are stirred; the second is the wetted-wall column. It is quite clear that the liquid flow conditions in the batch absorption system bear no resemblance to those in the packed column. That the liquid flow conditions in the wetted-wall column are different from those in a packed column is not so obvious. The usual wetted-wall columns are of the order of a foot or so in length, with the result that the time of exposure of the liquid to the gas is much longer than is the case on an individual piece of packing,

which may run in size from $1/2$ to 2 or at most 4 inches. The result is that in the wetted-wall column the solute is able to penetrate well into the liquid layer and the concentration at the wall itself is able to change an appreciable amount. In this case the assumption of infinite depth of liquid made in eq. (2.24) is no longer valid and eq. (2.30) can no longer be expected to hold. Another disadvantage of the usual wetted-wall column is the occurrence of ripples. Thus the area for mass transfer, while assumed to be constant and known, actually varies somewhat with the liquid rate. Also, the presence of ripples may either cause or be an indication of some mixing in the liquid, which would cause the mass transfer rate to be higher than it would be otherwise.

These disadvantages of the wetted-wall column may be overcome by reducing its length to the order of $1/2$ to 2 inches. Observation of the longer wetted-wall columns shows that the ripples do not form until several inches down from the top. In a short wetted-wall column we should expect the absence of ripples and hence be more confident that the area for mass transfer is constant and known. Secondly, the time of exposure in such a short wetted-wall column will be of the same order of magnitude as that for the liquid on an individual piece of packing, and this time of exposure will be sufficiently short that the assumption of infinite depth of liquid will be justified. Data obtained in such an

apparatus should be valuable in understanding the liquid-side resistance in a packed column.

The question arises of how to determine the time of exposure, t . Since one is concerned with the time which an element of the surface of the liquid is exposed to the gas, a knowledge of the interfacial velocity of the liquid and of the length of the column should supply this information. If the interfacial velocity, v_i , is uniform,

$$t = h/v_i \quad (2.31)$$

where h is the length of the column. If the liquid layer is in streamline flow, theory (see Chapter 13 for derivation) predicts that the interfacial velocity is

$$v_i = \left(\frac{9}{8} \frac{g\Gamma^2}{\mu\rho} \right)^{1/3} \quad (2.32)$$

Combining eqs. (2.31) and (2.32) with (2.30) gives a theoretical equation for the physical coefficient,

$$k_L^* = 2 \sqrt{\frac{D}{\pi h}} \left(\frac{9}{8} \frac{g\Gamma^2}{\mu\rho} \right)^{1/6} \quad (2.33)$$

This equation may be tested by varying not only liquid rate, but also column length and the solute gas. How well the data for absorption or desorption without chemical reaction in the short wetted-wall column fit the equation would be a measure of the applicability of Higbie's penetration theory in the case where the liquid flow conditions are similar to those existing in a packed column.

There is, however, some uncertainty concerning the interfacial liquid velocity. Measurements in long wetted-wall columns by Friedman and Miller (27) and by Grimley (31) indicate that the interfacial velocity of the liquid is considerably greater than that predicted by eq. (2.32). Furthermore, there is some question as to whether the velocity of the liquid is constant with distance down the column, or whether there is some acceleration of the liquid. Consequently, there is a need for measuring the interfacial velocity in the short wetted-wall column itself.

After measuring physical coefficients in the short wetted-wall column, coefficients for the chlorine-water system were determined. These coefficients may be compared with the physical coefficients for the purpose of experimentally determining the effect of the hydrolysis of the chlorine in a system where the interfacial area is known. This information should be valuable for interpreting the data of Vivian and Whitney (101) in packed columns. Furthermore, the results may be compared with the coefficients predicted by the mathematical theory developed in this thesis.

In studying the mechanism of absorption of chlorine in water and of sulfur dioxide in water, accurate values of their diffusivities are necessary. No direct measurements of the diffusivity of sulfur dioxide in water have been reported at all. Only two measurements have been made on the diffusivi-

ty of chlorine in water, and these do not appear to be reliable (see Sec. 11.5 in APPENDIX). Therefore, it was decided to measure the diffusivities of these two substances in water. Since chlorine reacts with water, its diffusion involves the diffusion not only of molecular chlorine but also of hypochlorous and hydrochloric acids. Similarly the diffusion of sulfur dioxide in water also involves the diffusion of sulfurous acid. These complicating effects should be taken into account in the experimental study.

Thus, the experimental program may be divided into four parts: 1) measurement of physical coefficients in the short wetted-wall column; 2) measurements on the chlorine-water system in the short wetted-wall column; 3) a study of the interfacial liquid velocity in the short wetted-wall column, and 4) measurement of the diffusivity of chlorine and of sulfur dioxide in water. The first two items constitute the main line of investigation of this thesis, while the last two items are to be regarded as supplementary. For this reason the experimental studies in the short wetted-wall column are treated fully in the main body of the thesis, while the measurements of diffusivities and of interfacial velocity are relegated completely to the APPENDIX, in Chapters 11 and 13, respectively. Only the conclusions regarding diffusivities and interfacial velocity are presented in the main body.

In addition to these experimental studies, a mathematical study of absorption with chemical reaction has been carried out. The subject of absorption with chemical reaction is an extremely important one industrially. Outside of the petroleum industry there are relatively few absorptions being carried out which do not involve chemical reaction. The manufacture of nitric acid, the preparation of bleach solutions in the pulp and paper industry, the lead chamber process for sulfuric acid, the removal of carbon monoxide from the feed gas to ammonia converters, and the Solvay process are but a few examples where simultaneous absorption and chemical reaction play a major part. The theory, however, has lagged far behind practice. There are several reasons for this: inadequate knowledge concerning the mechanism of the liquid-side resistance even without chemical reaction; inadequate knowledge concerning the mechanism of the chemical reaction itself; even when the mechanism of the liquid-side resistance and of the chemical reaction are known or assumed, mathematical difficulties may prevent solving the problem, particularly when the order of the chemical reaction is higher than first order.

When this thesis was started, all the theory of absorption with chemical reaction found in the literature was based on the film theory. This theory, which is very satisfactorily reviewed by Sherwood (92), has been developed for

the cases where the chemical reaction is first order irreversible, and where the reaction is second order, irreversible and instantaneous. No theory at all had been developed based on the penetration theory, although during the course of the thesis some work on this phase of the theory had been published by Danckwerts (18, 19).

Practically all the experimental systems which have been used to study absorption with chemical reaction have involved irreversible reactions, that is, reactions in which the reverse reaction does not exist or can be neglected. However, the absorption of chlorine and of sulfur dioxide in water is very different in that the reverse reaction must be taken into account. No information was available in the literature on the theory of absorption with reversible reaction.

The mathematical investigation was undertaken to extend the theory to include, if possible, the assumptions of the penetration theory, and to include the cases of reversible reaction. The mathematical theory is developed in detail in Chapter 8 in the APPENDIX; the theory is then applied to various experimental systems in Chapter 9 in the APPENDIX. The results of these mathematical studies are summarized and discussed in the main body of the thesis.

CHAPTER 3

APPARATUS AND PROCEDURE

The long wetted-wall columns used by previous investigators had appreciable end effects, since there was considerable area of contact between liquid and gas phases at the entrance and exit of the liquid to and from the column, apart from the area of contact on the wetted wall itself. Such end effects have usually been ignored. However, as the length of the column is reduced to the dimensions used here, the end effects could easily outweigh the mass transfer in the column itself. The primary requirement of the design of a short wetted-wall column, then, is that the liquid be brought into and out of the column without there being any gas-liquid contact other than on the wetted wall. This was done by having the liquid enter and leave through thin slots maintained completely full of liquid. In addition, all chambers and tubes through which the liquid passed in its journey to and from the column were kept completely full of liquid.

The assembly of the column is shown in full scale in Figs. 3.1 and 3.2. The materials used were chosen primarily for their corrosion resistance, in order to avoid attack by the chlorine solutions. Glass was used for the wetted-wall section itself because of the ease with which it is wet by water and because of its transparency, which permitted visual observation of the operation of the column. Teflon was chosen for the gas inlet and outlet tubes for its machineability and because it does not wet by water.

Fig. 3.1

Assembly of Short Wetted-Wall Column
(Up-Flow Slot)

Scale: Full Size

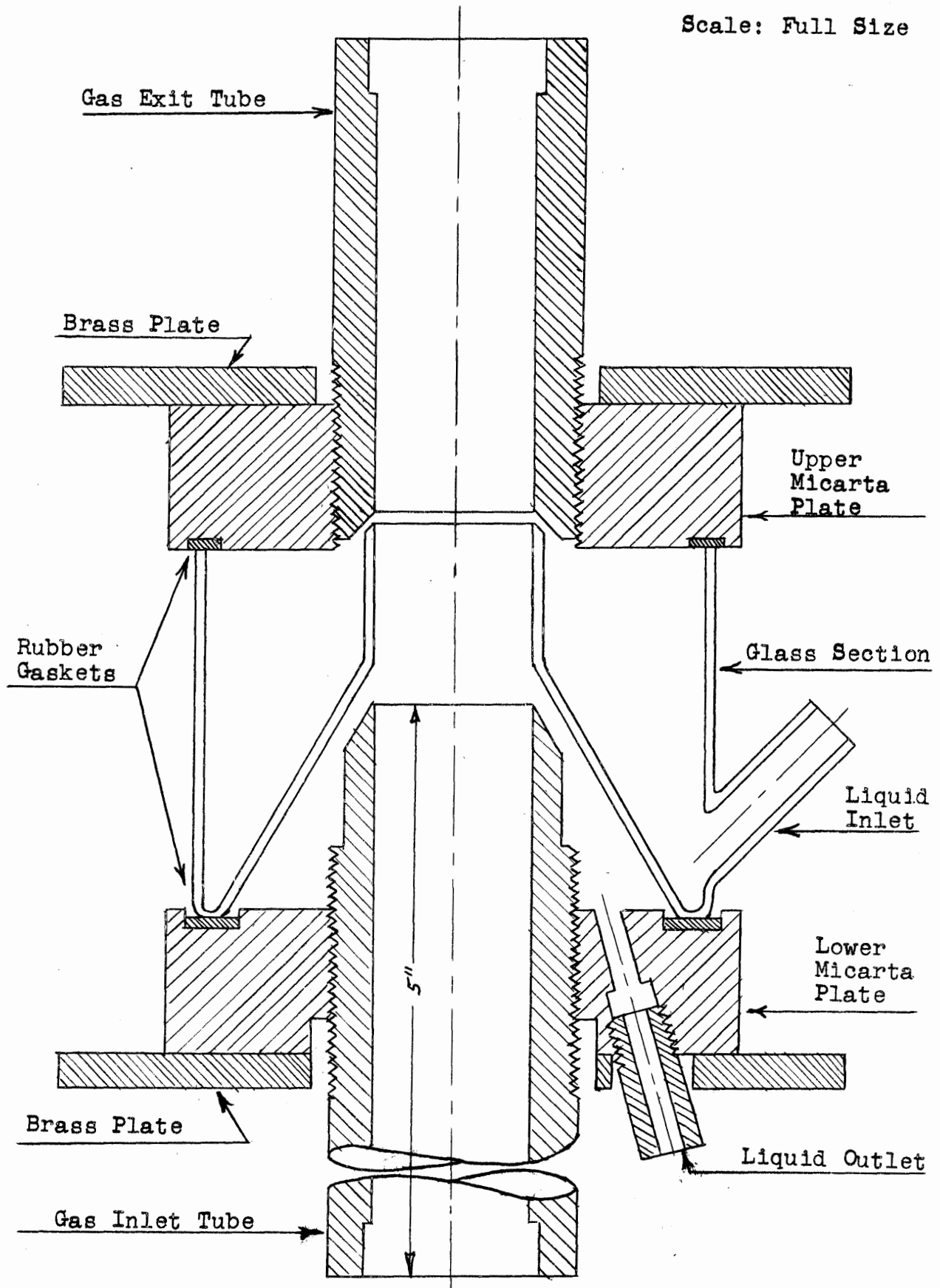
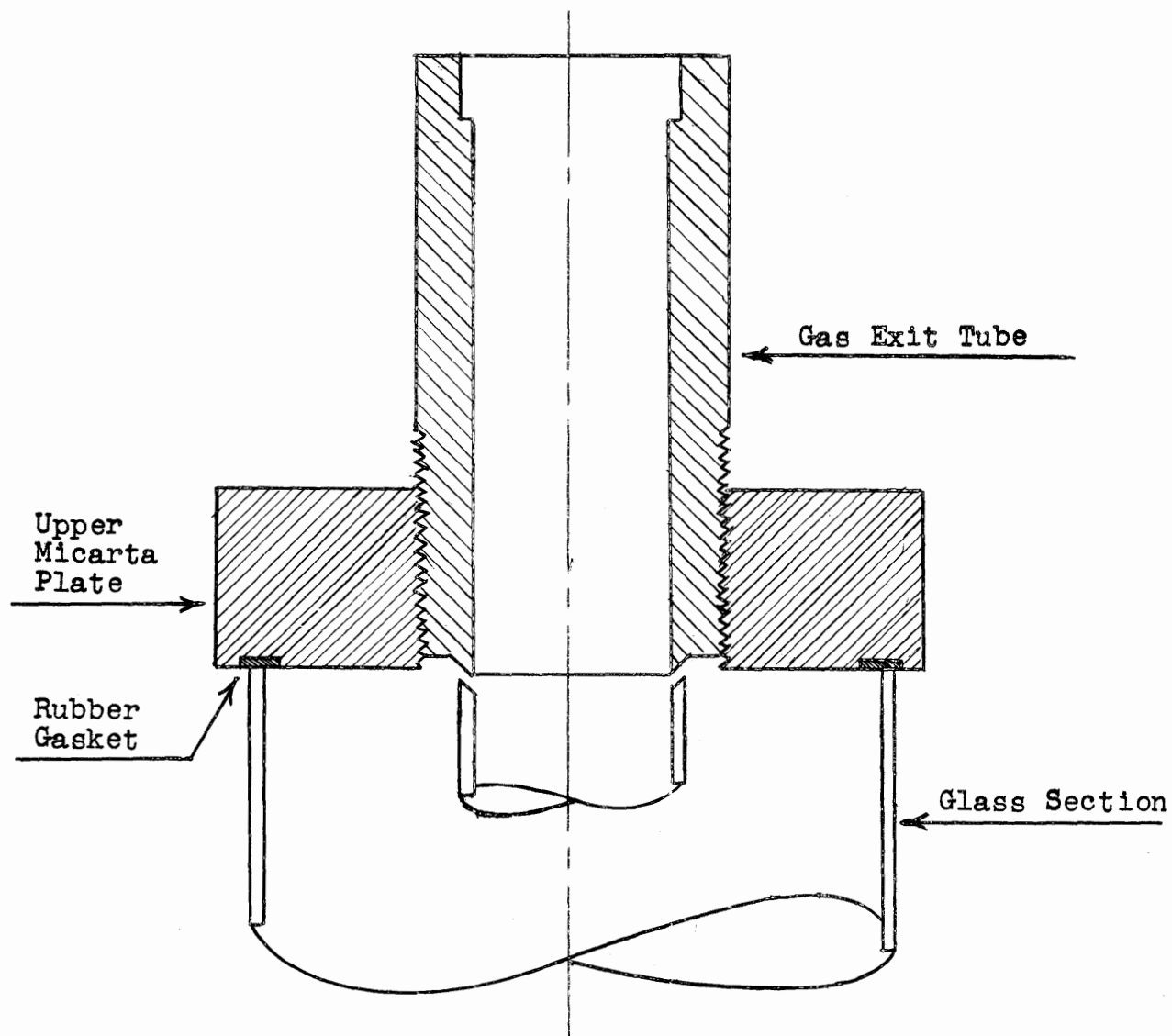


Fig. 3.2

Assembly of Short Wetted-Wall Column
(Down-Flow Slot)



The latter property was valuable since it constrained the liquid flowing through the slots to flow along the glass and not to creep along the Teflon tubes. Micarta was used for the upper and lower supporting plates because it is strong, inexpensive and easy to machine.

Two different types of entrance slots were used: upflow and downflow (compare Figs. 3.1 and 3.2.). The width of the entrance and exit slots could be varied by turning the Teflon tubes, which were threaded into the Micarta plates. The wetted-wall section itself was the inner glass tube, approximately one-inch in diameter, with the upper edge beveled. Three column lengths were used, such that the straight sections of the inner glass tubes were approximately $1/2$, 1 and $1\ 1/2$ inches long. Six glass sections were made, both slot types being used for each length. These columns were designated as follows:

<u>Column Designation</u>	<u>Slot Type</u>	<u>Approximate Length</u>
1D	Downflow	$1/2$ inch
1U	Upflow	$1/2$ inch
2D	Downflow	1 inch
2U	Upflow	1 inch
3D	Downflow	$1\ 1/2$ inches
3U	Upflow	$1\ 1/2$ inches

Rubber gaskets were used as seals. Brass plates and tie-rods served to clamp the assembly together.

The decision to study desorption rather than absorption was based on the following factors. The physical coefficients should

be the same, in view of the results of Carlson (10), who found the coefficients of absorption and desorption to be the same for oxygen and carbon dioxide in water in a stirred flask, and of Allen, who found them to be the same for carbon dioxide in a packed column (93). Secondly, theory predicts (see Secs. 9.3 and 9.5 in the APPENDIX) that the difference between the pseudo-coefficient for chlorine in water and the physical coefficient is greater for desorption than for absorption. Therefore, desorption should provide a more severe test of the theory. Finally, desorption uses up much less solute gas than absorption, unless the gas is recirculated, which would add to the complication of the apparatus.

Two systems were used to study the physical coefficients: carbon dioxide-water and chlorine-dilute hydrochloric acid. They have the advantages of ease of analysis and of having diffusivities known with comparative accuracy. Furthermore, the chlorine-HCl system provides physical coefficients which may be compared directly with the chlorine-water data without a significant correction for diffusivity. The experimental program thus may be divided into three parts: desorption of carbon dioxide from water by air; desorption of chlorine from dilute hydrochloric acid by air; and desorption of chlorine from water by air. The auxiliary apparatus used with the column differed somewhat for the three systems.

Lambe (63), whose S.M. thesis consisted of building the apparatus and of making most of the runs with carbon dioxide reported in this thesis, described the procedure for the carbon

dioxide runs. (Brackets indicate changes in the text made by the author.)

"The liquid feed for the column came from a constant-head tank where distilled water was [practically] saturated with carbon dioxide by bubbling the gas [in considerable excess] through the liquid. A glass cooling coil in the tank allowed the temperature of the water feed to be controlled and maintained at a given value. From the glass head-tank the liquid passed through a calibrated orifice into the column. The temperature of the feed was indicated by a thermometer in a "tee" connection in the feed line just before it entered the column.

"The air was blown through a packed tower to saturate it with water and control its temperature. A calibrated orifice was used to meter the air before it entered the calming section. A thermometer was placed inside the glass tube which formed the calming section, and at the bottom, to indicate the air temperature. Any liquid spill-over from the column was caught in a trap just below the point at which the air entered the calming section. The liquid in this trap was maintained at a high pH with sodium hydroxide to prevent any carbon dioxide from entering the air stream. This was necessary for it was assumed that the concentration of carbon dioxide in the air was negligible when the expression for the theoretical coefficient was derived.

"Samples were taken of the inlet and outlet streams by allowing a portion of the streams to pass continuously through 25 ml. pipets. The rate was such that a volume of liquid equal to six times the pipet volume passed through the pipet per minute. [The sample in the pipet was added to a known volume of standard barium hydroxide, and the residual hydroxide was determined by a conductometric technique.]

"When making a run, the air was saturated and brought to within one degree centigrade of the liquid temperature in order to minimize any mass transfer of water which would affect the diffusion of carbon dioxide in the wetted-wall column and thus give a false value for the measured coefficient. After all the variables had been adjusted to their desired values a minimum of five minutes was allowed for the apparatus to reach steady-state conditions before the samples were taken."

Several changes in the auxiliary apparatus were made when the solute gas was changed to chlorine. For the chlorine-water runs, two constant-head tanks were used. Chlorine gas was injected

at a steady rate into distilled water flowing from the first glass head-tank, the rate being adjusted to give a solution of the desired concentration. This solution flowed into a second glass head-tank, thence to a calibrated flowmeter and into the column.

Instead of using a blower, the air was sucked through the system. As before, the air flowed through a packed column and through the calming section into the wetted-wall column. The exit gas was bubbled through a solution of sodium hydroxide, then passed through a calibrated flowmeter and finally into the laboratory vacuum line.

Liquid-stream samples were taken by allowing a portion of the liquid to flow directly into the titration flask, the volume of sample being determined by weighing the flask before and after sampling. Samples of the inlet liquid were taken for each run, but only a few outlet liquid samples were taken, for the purpose of checking a material balance. The exit gas stream was analyzed by bubbling it for a definite length of time through sodium hydroxide and measuring the amount of chlorine taken up.

For the chlorine-dilute hydrochloric acid runs the only additional change made was in the inlet liquid system. In addition to injecting the chlorine gas into the distilled water flowing from the first head-tank, strong hydrochloric acid was added continuously at a steady rate, such that the concentration of HCl

was between 0.15 and 0.2 normal. The resulting solution of chlorine and hydrochloric acid then flowed into the second glass head-tank, through the flowmeter and into the column.

The effects of the following variables were studied:

Carbon dioxide-water runs:

Temperature, liquid rate, gas rate, entrance slot width, column length.

Chlorine-water runs:

Concentration, liquid rate.

Chlorine-hydrochloric acid runs:

Concentration (of Cl_2), liquid rate.

The following quantities were measured for all runs: liquid rate, air rate, inlet liquid temperature, inlet air temperature, entrance slot width, column length. In addition, the following were measured:

Carbon dioxide-water runs:

Inlet liquid concentration, outlet liquid concentration.

Chlorine-water runs:

Inlet liquid concentration, time of run, amount of chlorine desorbed.

Chlorine-hydrochloric acid runs:

Inlet liquid concentration, time of run, amount of chlorine desorbed, concentration of HCl.

The apparatus, procedure and analytical methods are described in detail in Chapter 10 in the APPENDIX.

CHAPTER 4

RESULTS

4.1. Physical Coefficients in Short Wetted-Wall Column.

Data obtained on desorption without chemical reaction in the short wetted-wall column are shown in Figs. 4.1 to 4.10. The lines drawn in Figs. 4.1 to 4.4 are the best lines through the data for each plot. The dashed lines drawn in Figs. 4.5 to 4.10 are the best lines through the data shown in each of those figures. The solid lines in these figures are obtained from the correlation of all the data shown in these six figures (Eq. (5.4)).

The coefficients plotted in these figures are based on a driving force equal to the initial concentration of solute minus the interfacial concentration of solute. The interfacial concentration is taken to be zero.

Desorption of Carbon Dioxide from Water

- Fig. 4.1 Effect of Temperature
- Fig. 4.2 Effect of Air Rate
- Fig. 4.3 Effect of Entrance Slot Width -- Upflow Slot
- Fig. 4.4 Effect of Entrance Slot Width -- Downflow Slot
- Fig. 4.5 Effect of Water Rate -- Column 3U
- Fig. 4.6 " " " " -- Column 3D
- Fig. 4.7 " " " " -- Column 2U
- Fig. 4.8 " " " " -- Column 2D
- Fig. 4.9 " " " " -- Column 1U

Fig. 4.1

Desorption of Carbon Dioxide from Water
Effect of Temperature

Data of Lambe (63)

Column 3U

Slot Width = 0.05 in.

 $\Gamma = 21.8 \text{ g./}(\text{cm.})(\text{min.})$

Length = 4.25 cm.

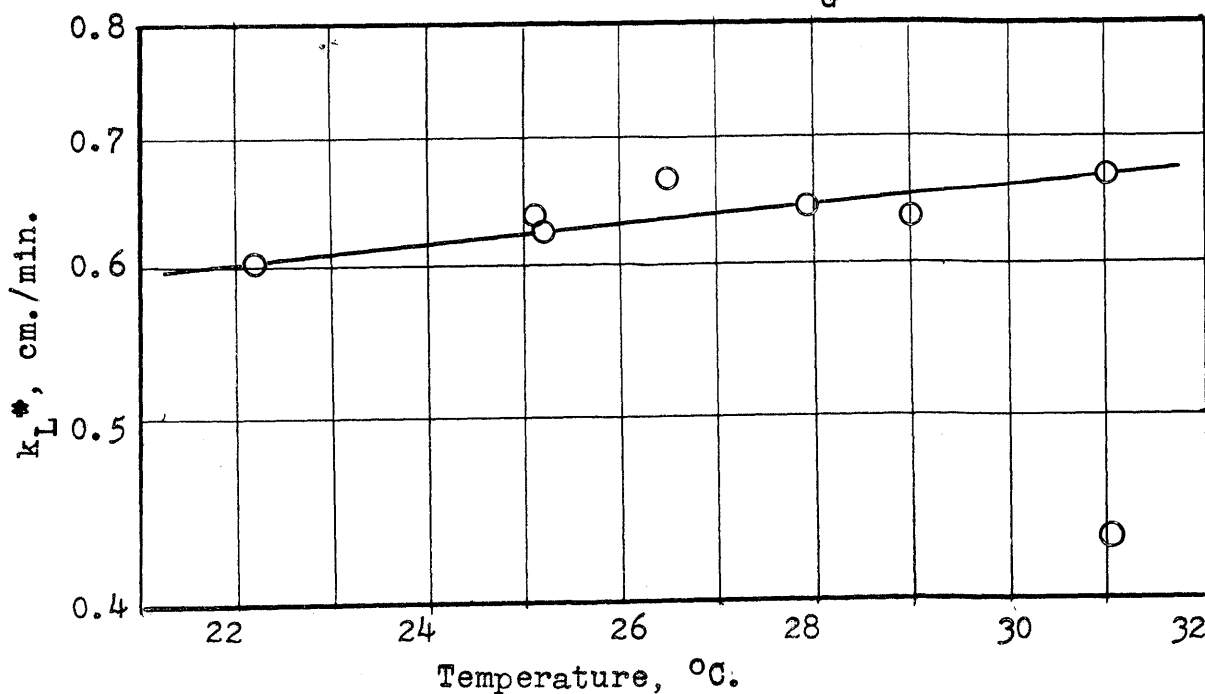
 $Re_G = 2350$ 

Fig. 4.2

Desorption of Carbon Dioxide from Water
Effect of Air Rate

Data of Lambe (63)

Column 3U

Slot Width = 0.05 in.

 $\Gamma = 21.9 \text{ g./}(\text{cm.})(\text{min.})$

Length = 4.25 cm.

Temp. = 25°C.

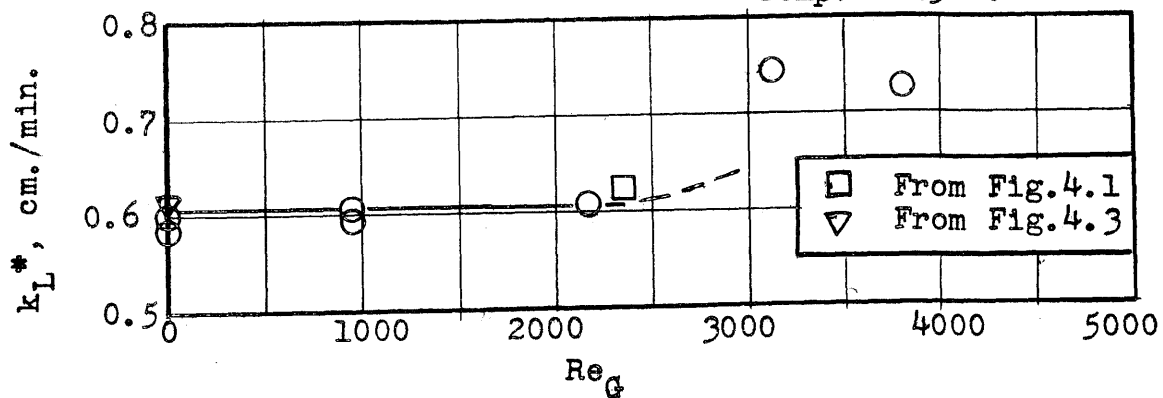


Fig. 4.3

Desorption of Carbon Dioxide from Water
Effect of Entrance Slot Width

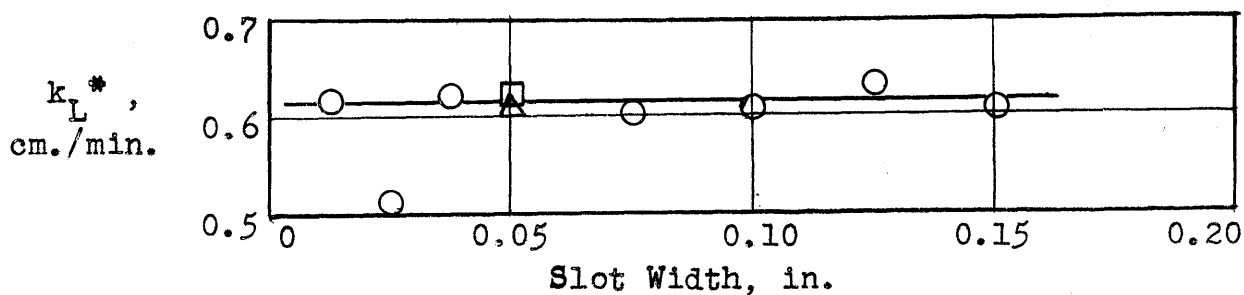
Data of Lambe (63)

Column 3U

 $Re_G = 0$ $\Gamma = 22.0 \text{ g./}(\text{cm.})(\text{min.})$

Length = 4.25 cm.

Temp. = 25°C.



□ From Fig. 4.1

△ From Fig. 4.2

Fig. 4.4

Desorption of Carbon Dioxide from Water
Effect of Entrance Slot Width

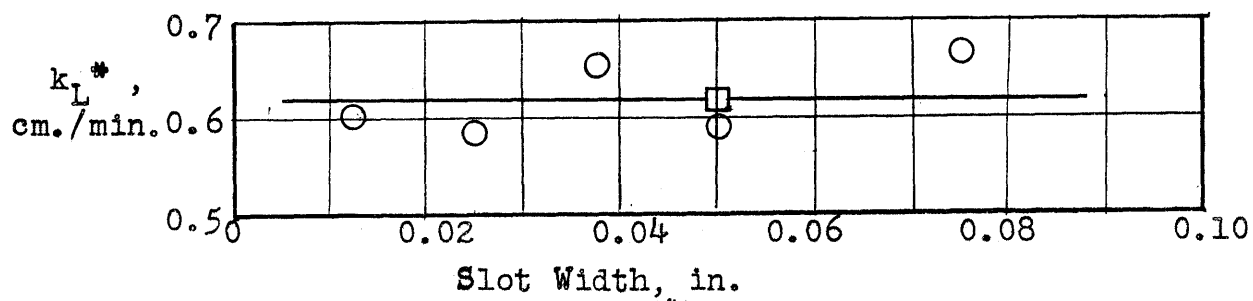
Data of Lambe (63)

Column 3D

 $Re_G = 0$ $\Gamma = 22.2 \text{ g./}(\text{cm.})(\text{min.})$

Length = 4.21 cm.

Temp. = 25°C.



□ From Fig. 4.6

Fig. 4.5

Desorption of Carbon Dioxide from Water
Effect of Water Rate

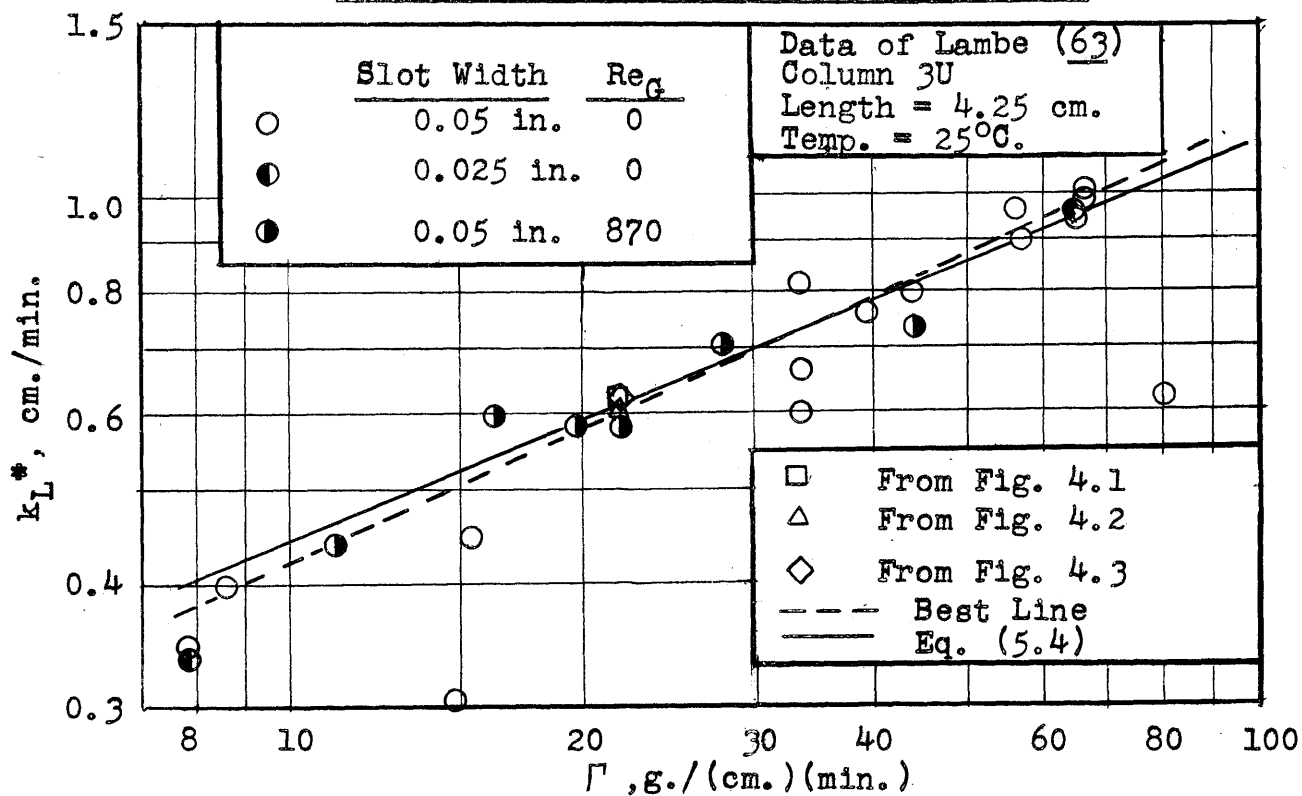


Fig. 4.6

Desorption of Carbon Dioxide from Water
Effect of Water Rate

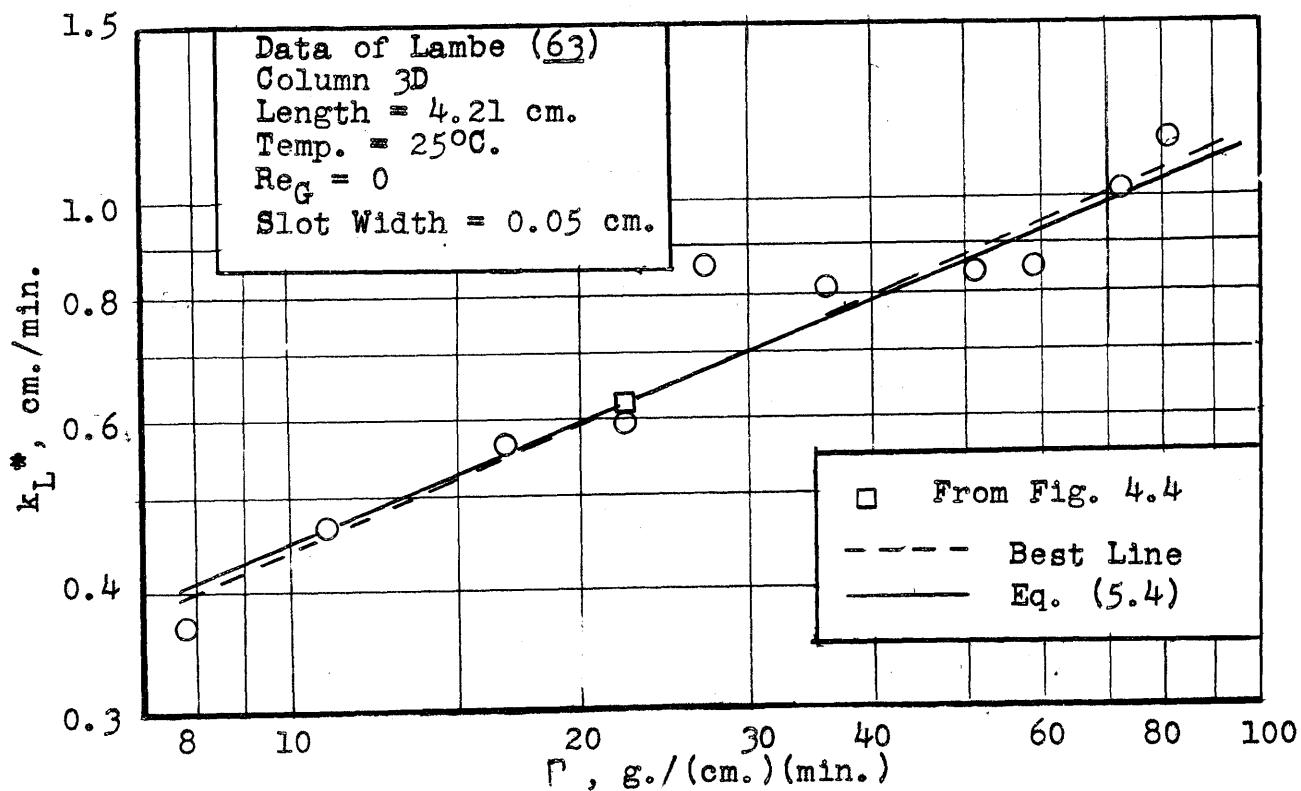


Fig. 4.7

Desorption of Carbon Dioxide from Water
Effect of Water Rate

Data of Lambe (63)

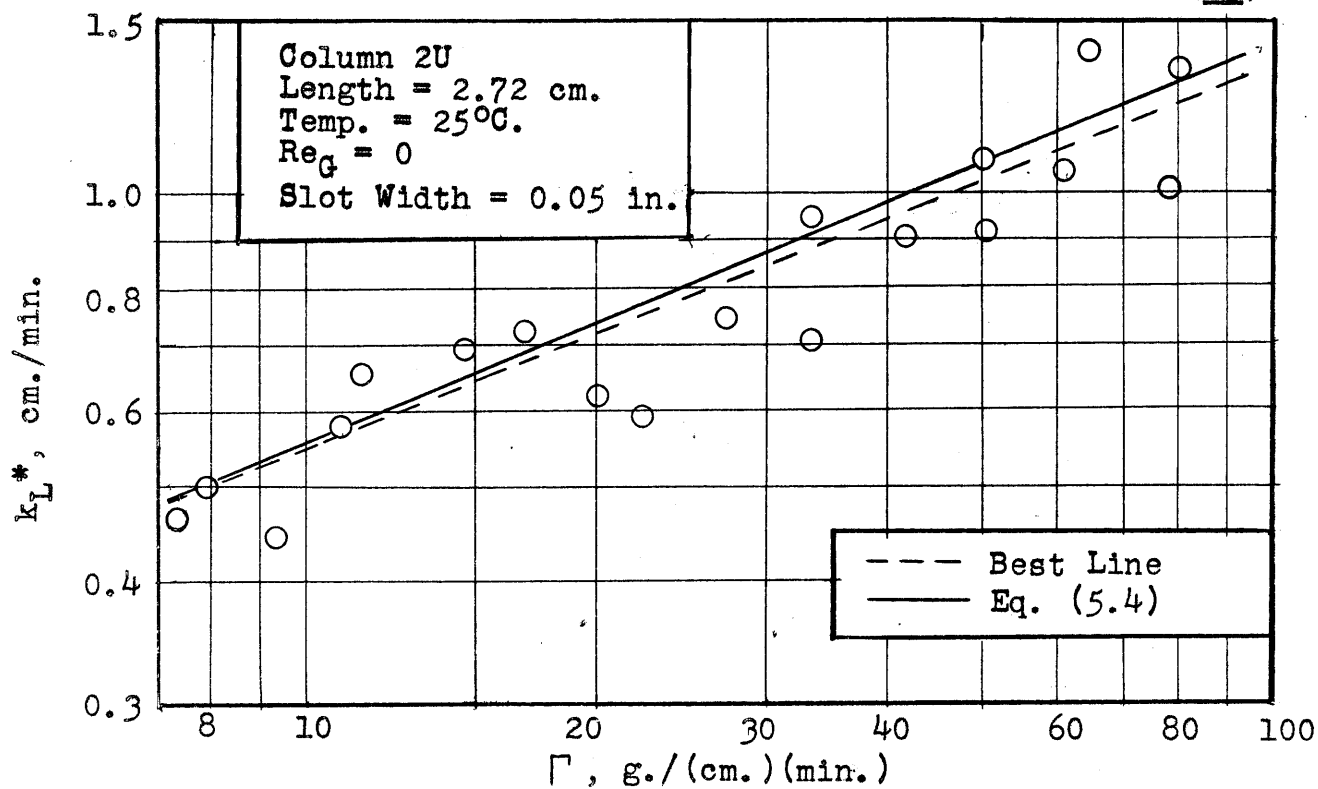


Fig. 4.8

Desorption of Carbon Dioxide from Water
Effect of Water Rate

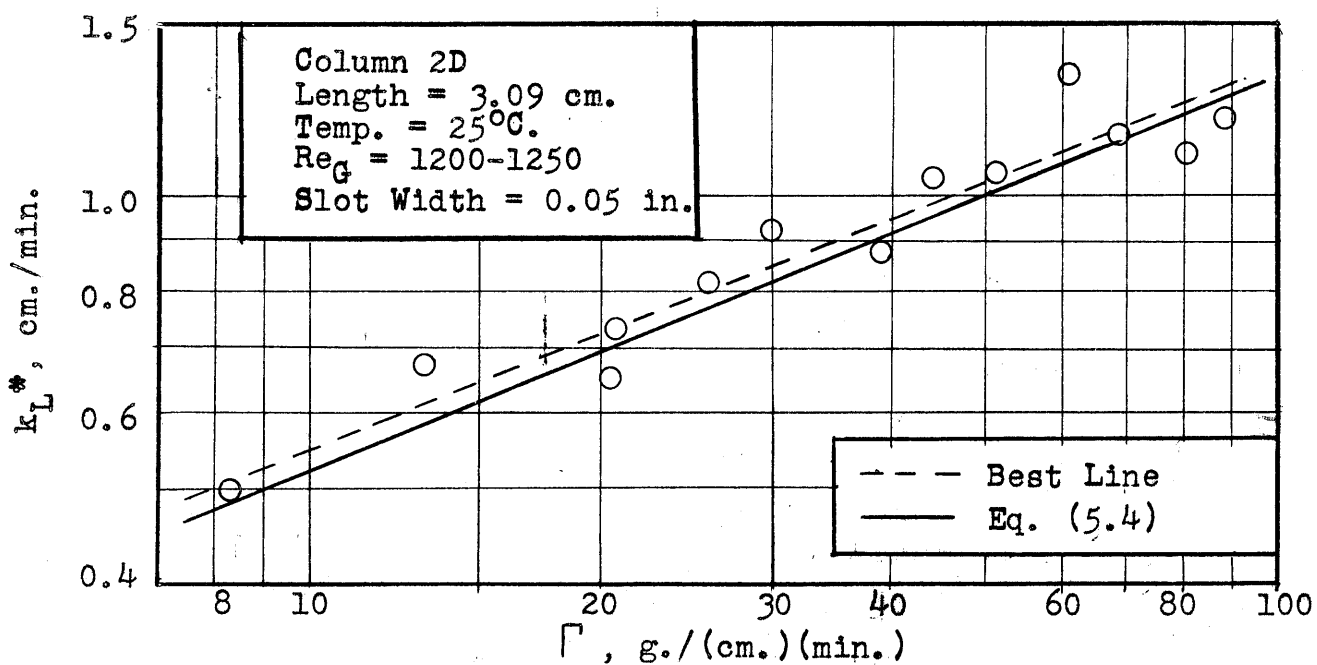


Fig. 4.9

Desorption of Carbon Dioxide from Water
Effect of Water Rate

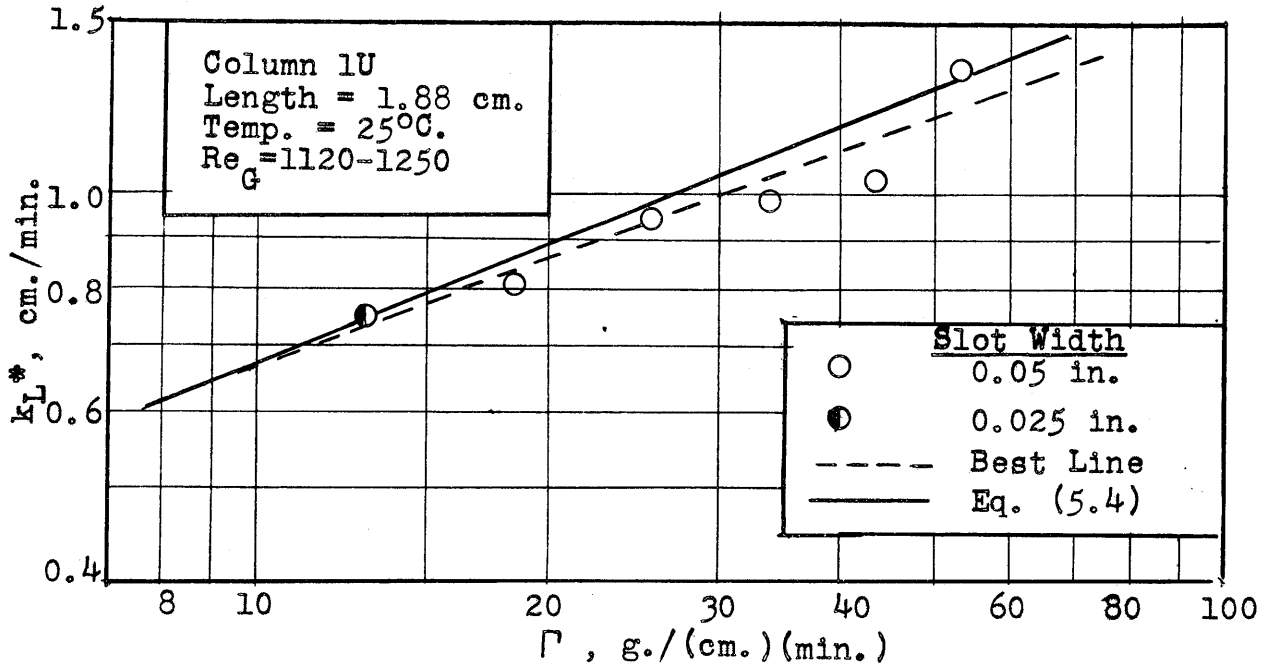
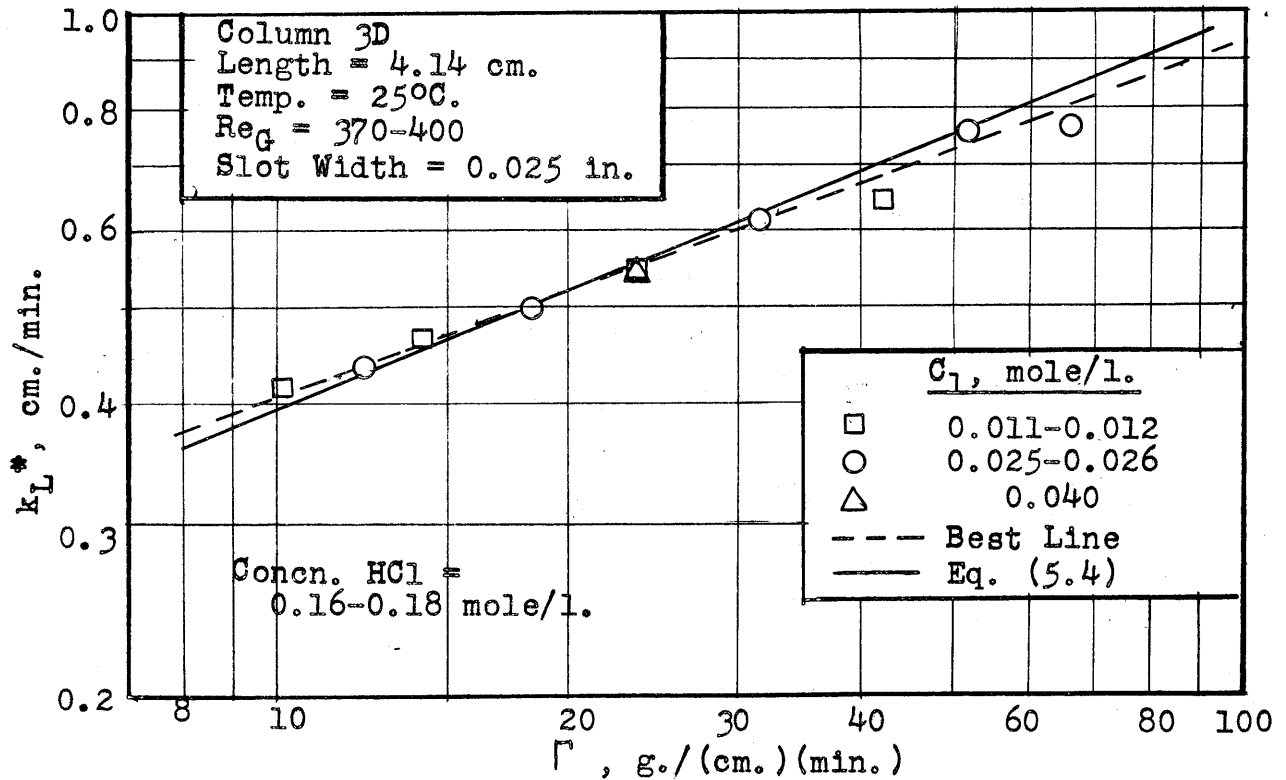


Fig. 4.10

Desorption of Chlorine from Dilute Hydrochloric Acid
Effect of Water Rate



Desorption of Chlorine from Dilute Hydrochloric Acid

Fig. 4.10 Effect of Water Rate -- Column 3D

4.2. Desorption of Chlorine from Water in Short Wetted-Wall Column. The data on desorption of chlorine from water in the short wetted-wall column are presented in terms of the psuedo-coefficient in Figs. 4.11 and 4.12. This coefficient is based on a driving force equal to the initial concentration of unhydrolyzed chlorine minus the interfacial concentration of unhydrolyzed chlorine. The interfacial concentration is taken to be zero. The initial concentration of unhydrolyzed chlorine is calculated from the initial concentration of "total" chlorine using the value of the equilibrium constant measured by Vivian and Whitney (101).

Fig. 4.11 shows the effect of concentration on the psuedo-coefficient for nine values of the water rate.

The psuedo-coefficient is found to be independent of concentration for C_1 below 0.040 moles/l. For this range of concentrations, the psuedo-coefficients are plotted against water rate in Fig. 4.12. The solid line represents the best curve through the points.

The lines in Fig. 4.11 represent an empirical correlation of the data. This correlation may be expressed as

Fig. 4.11

Desorption of Chlorine from Water
 Effect of Concentration

Column 3D

Length = 4.14 cm.

Temp. = 25°C.

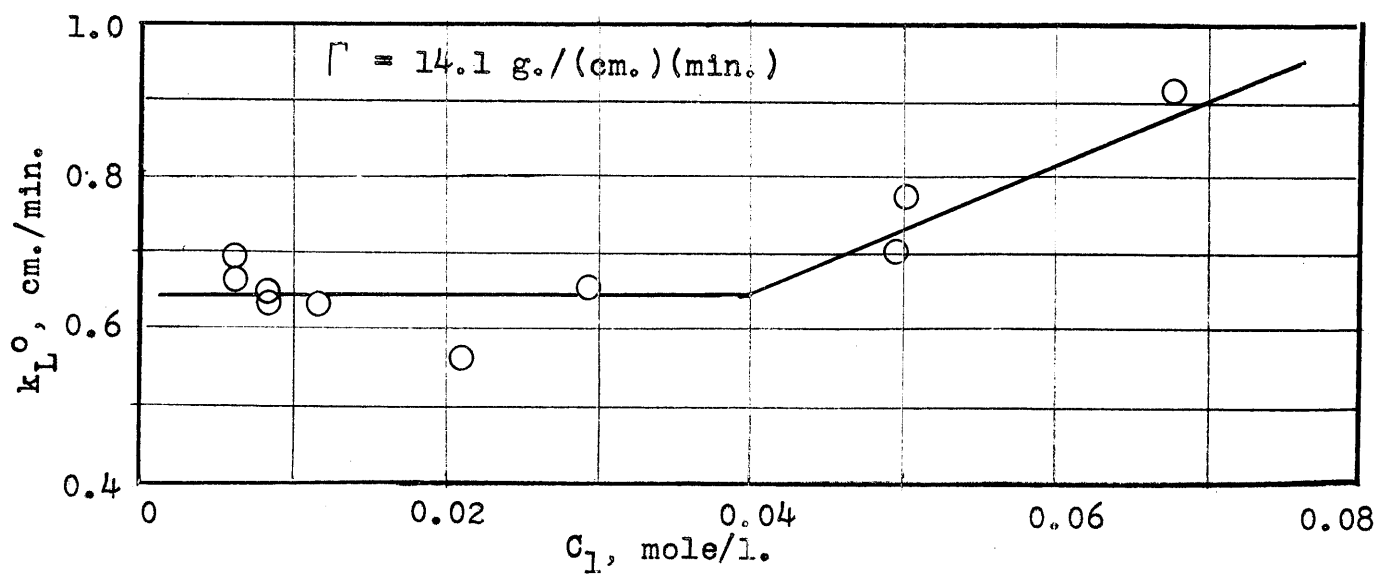
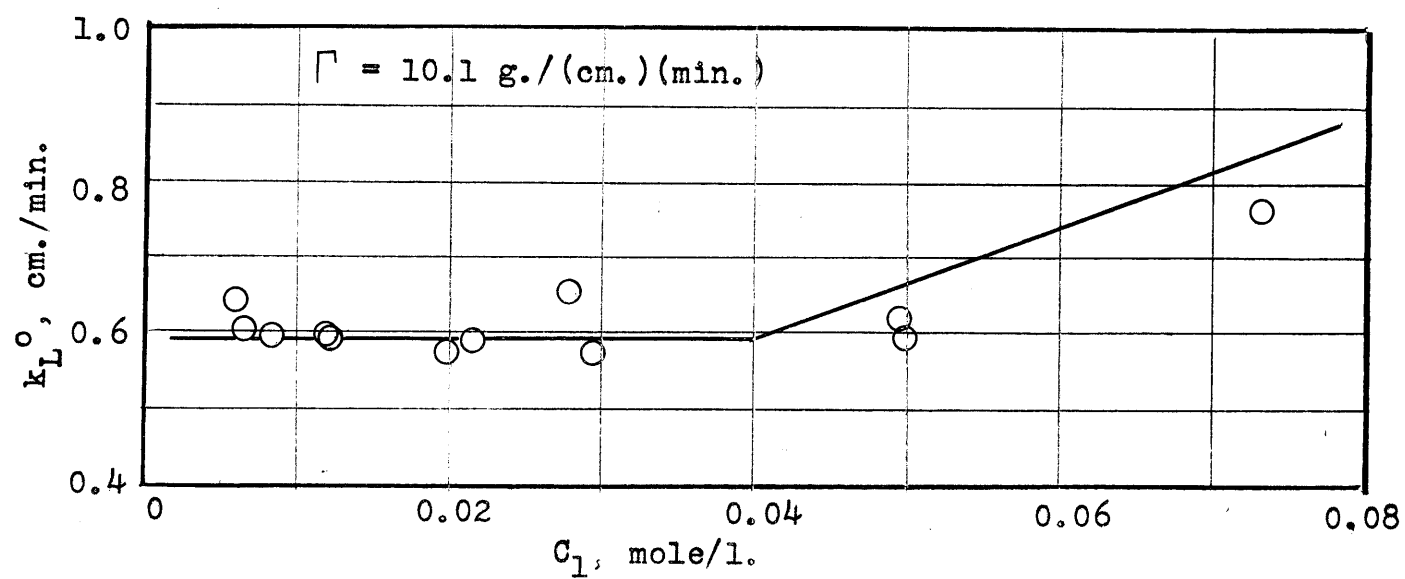
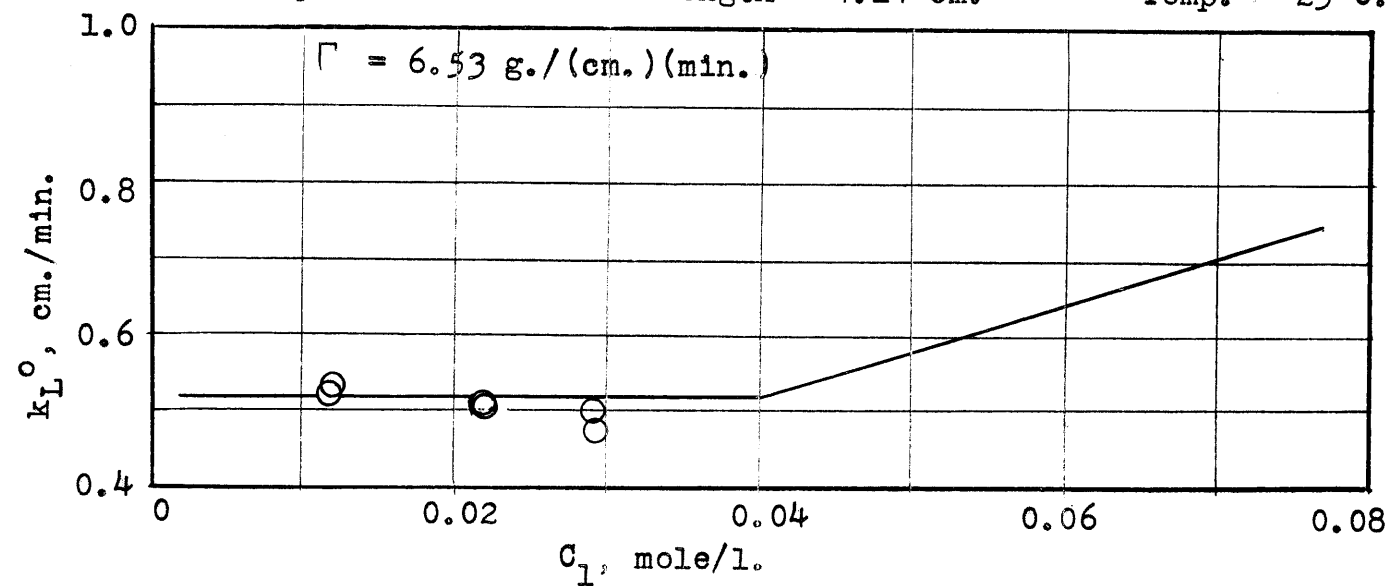


Fig. 4.11 (contd.)

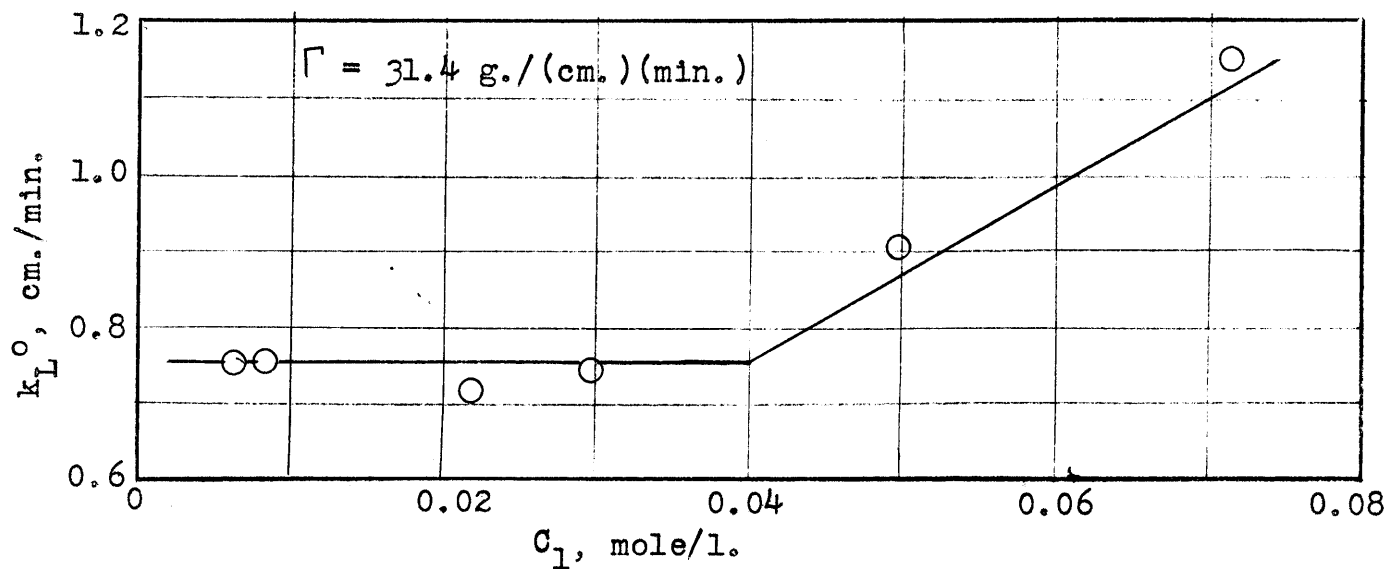
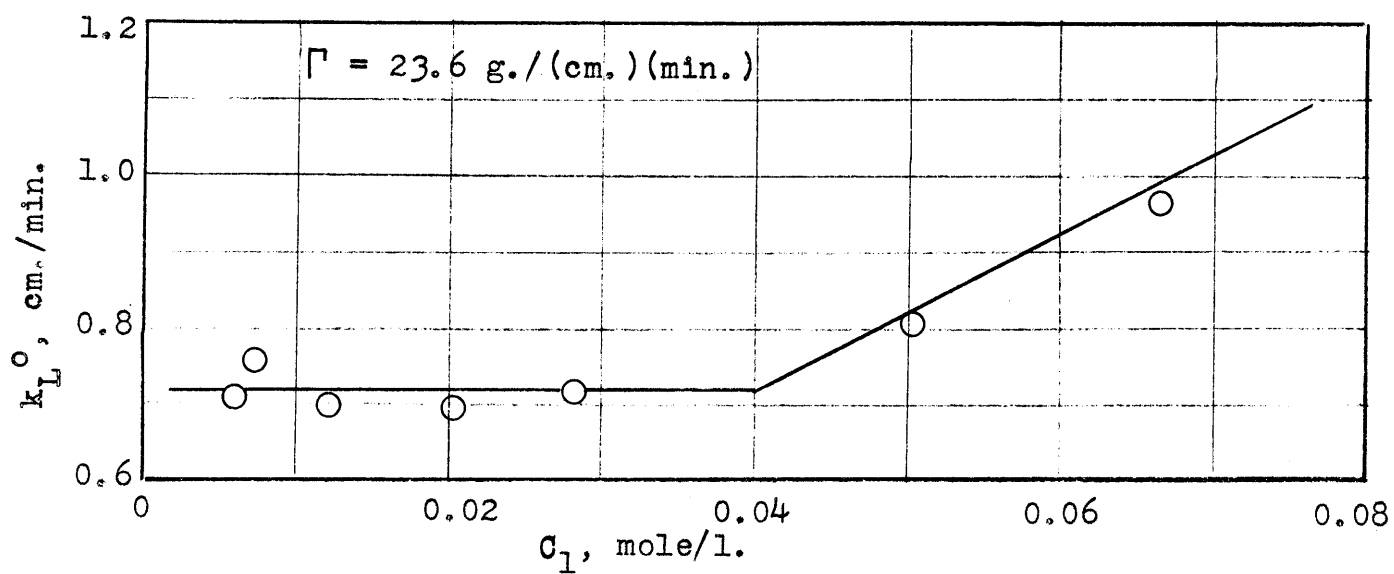
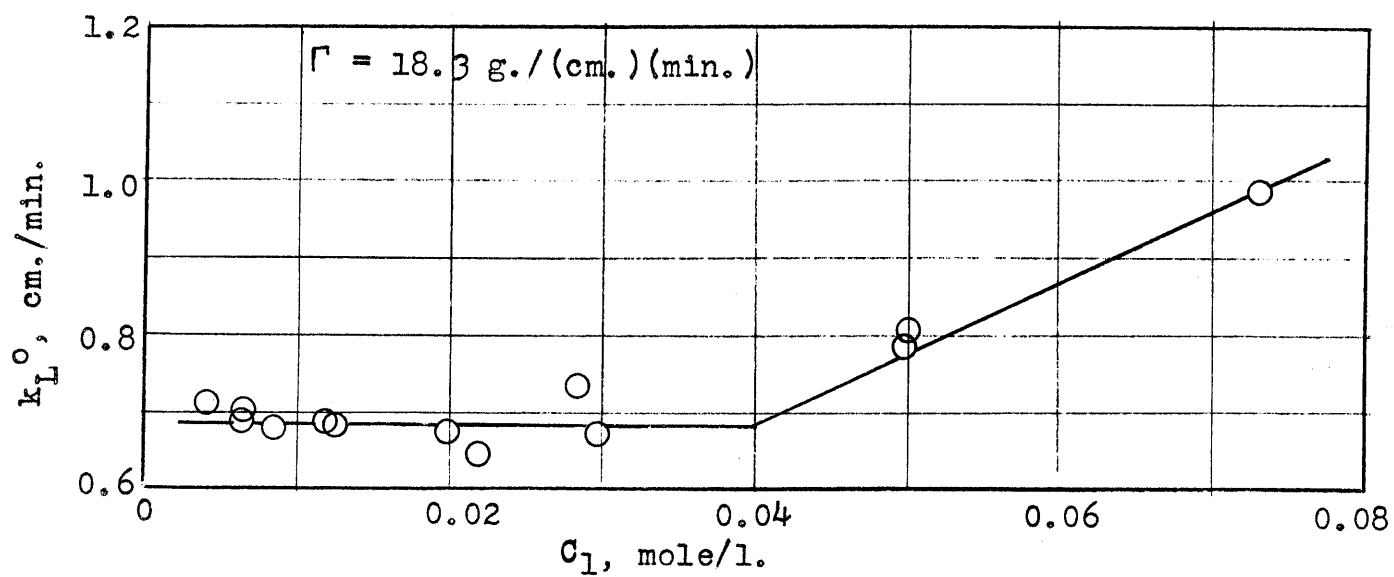


Fig. 4.11 (contd.)

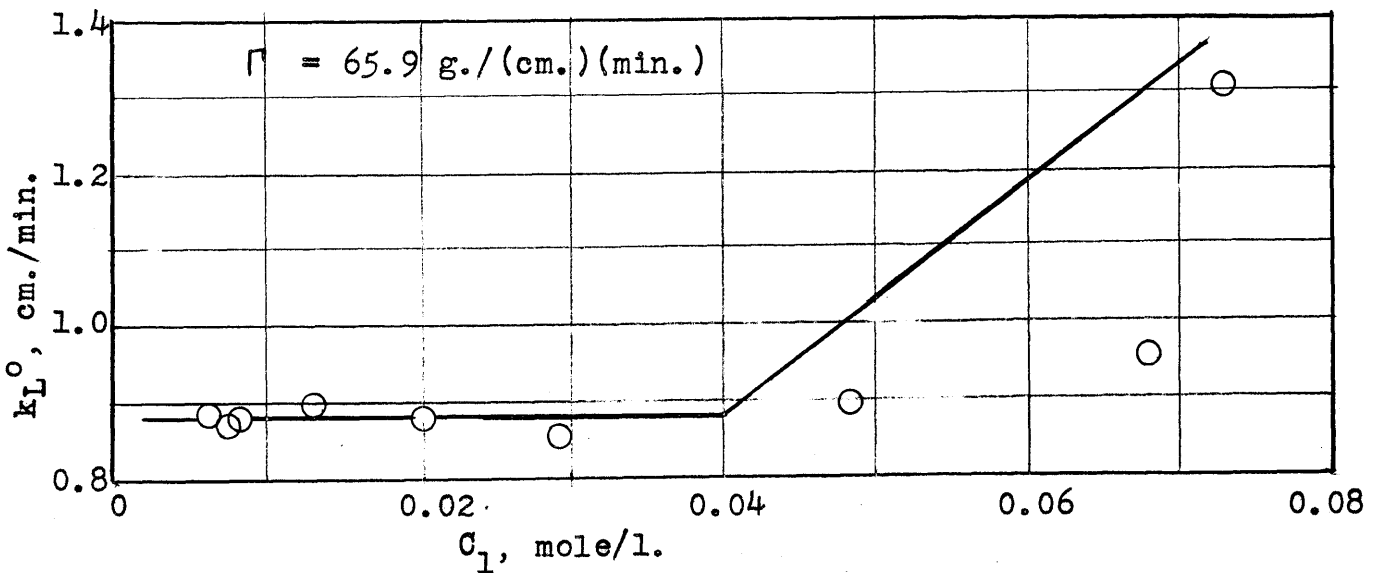
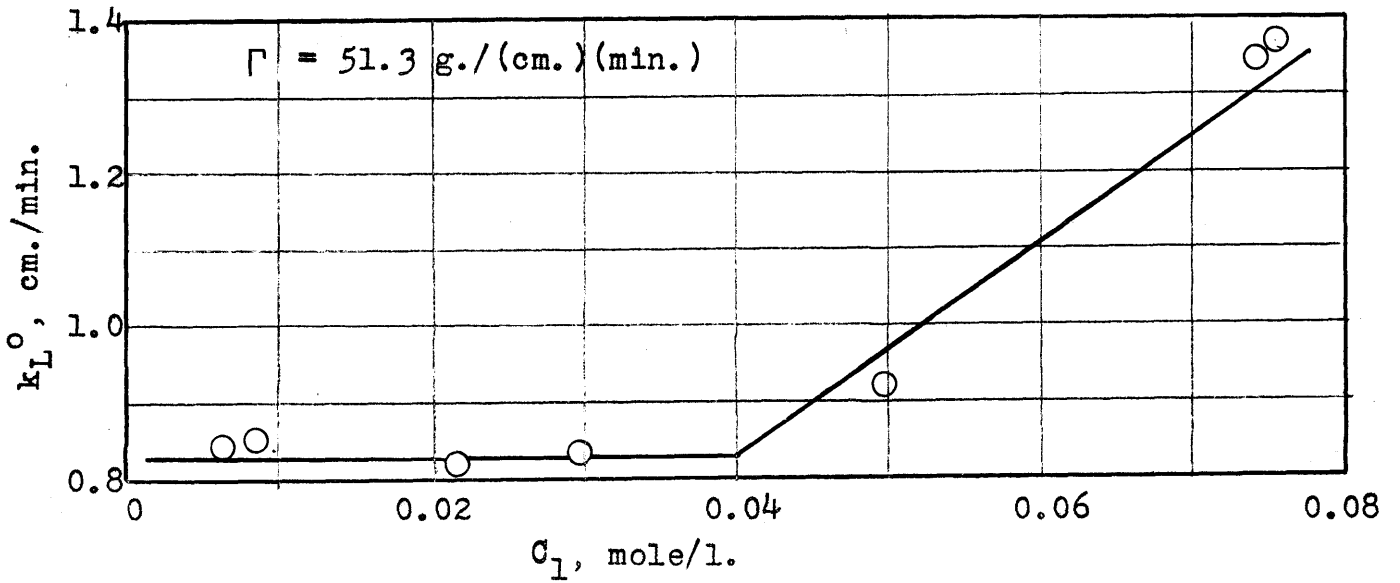
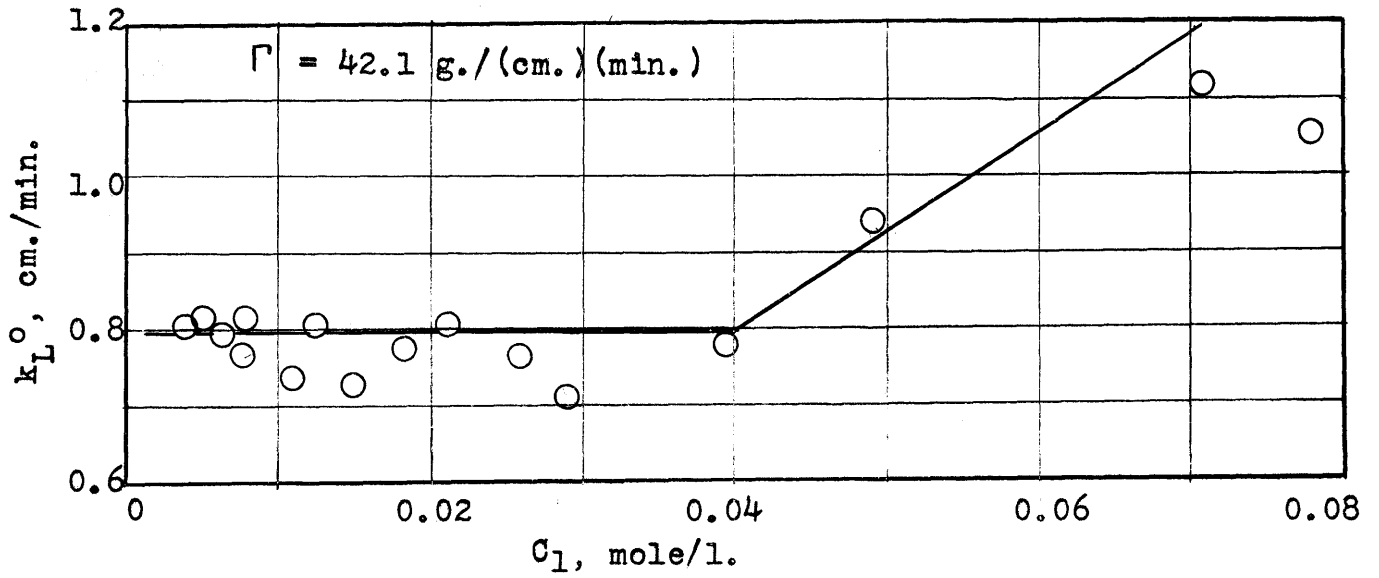
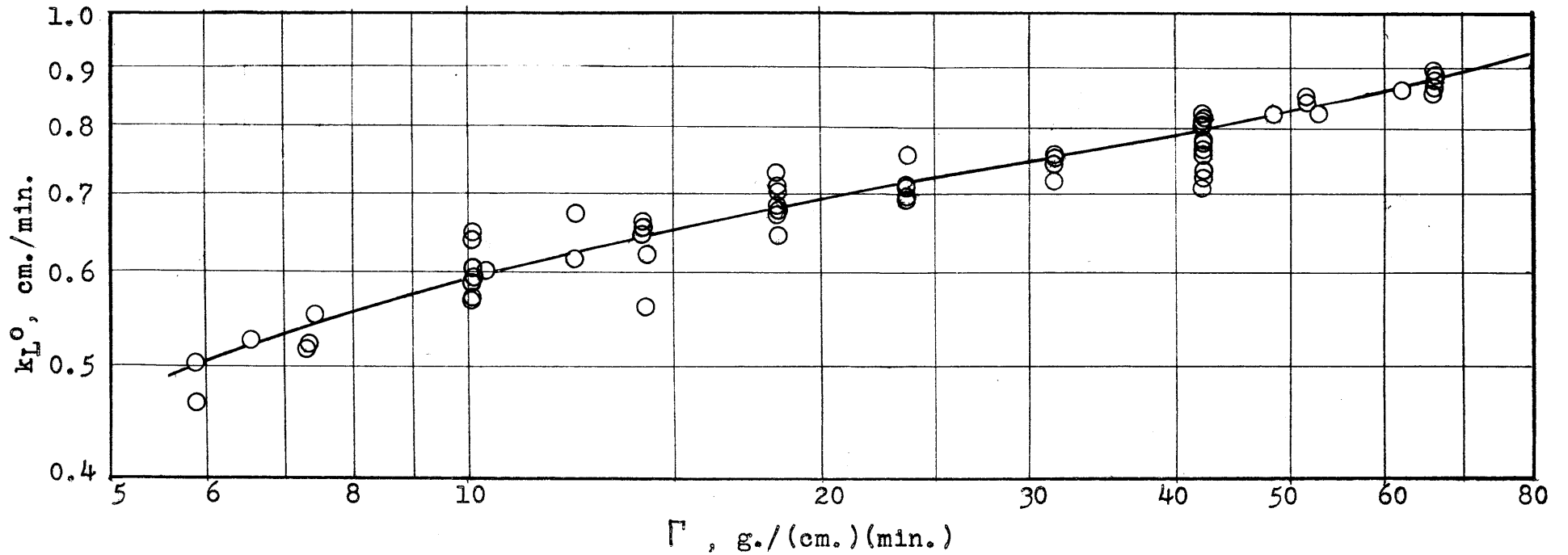


Fig. 4.12

Desorption of Chlorine from Water;
Effect of Water Rate

Initial Concentration of Chlorine
Less than 0.040 mole/l.

Column 3D
Length = 4.14 cm.
Temp. = 25°C.



$$\begin{aligned}
 k_L^{\circ} &= (k_L^{\circ})' & C_1 < 0.040 \\
 k_L^{\circ} &= (k_L^{\circ})' + 2.9 \Gamma^{0.4} (C_1 - 0.040) & C_1 > 0.040
 \end{aligned}
 \tag{4.1}$$

where k_L° is psuedo-coefficient, cm./min.

$(k_L^{\circ})'$ is coefficient given by the line in Fig. 4.12, cm./min.

Γ is water rate, g./ (cm.) (min.)

C_1 is initial concentration of chlorine, moles/l.

4.3. Interfacial Velocity in Short Wetted-Wall Column.

It is concluded from a stroboscopic measurement of the interfacial velocity that, under the conditions existing during desorption runs in the short wetted-wall column, the theoretical equation

$$v_1 = \left(\frac{9}{8} \frac{g \Gamma^3}{\mu \rho} \right)^{1/3} \tag{4.2}$$

is correct. See Chapter 13 in the APPENDIX for details.

4.4. Measurement of Diffusivities in Liquids.

Using the diaphragm cell method, the following diffusivities were measured:

Unhydrolyzed chlorine in water at 25°C. $(1.48 \pm 0.01) \times 10^{-5}$ cm²/sec.
(concn. 0.004 to 0.025 moles/l.)

Hypochlorous acid in water at 25°C. $(1.54 \pm 0.02) \times 10^{-5}$ cm²/sec.
(concn. 0.006 to 0.012 moles/l.)

The Stokes-Einstein relationship (i.e., diffusivity is proportional to absolute temperature divided by viscosity)

was found to hold for chlorine in water over the range 10°C. to 30°C.

Unhydrolyzed sulfur dioxide in water at 30°C.; the diffusivity varies with concentration.

Concn., moles/l.	$D \times 10^5$, cm. ² /sec.
0.05	1.92±0.01
0.10	1.95 "
0.15	1.97 "
0.20	1.99 "
0.30	2.00 "
0.40	2.01 "
0.50	2.02 "

Hydrolyzed sulfur dioxide in water at 30°C. $(1.99 \pm 0.03) \times 10^{-5}$
(concn. 0.03 to 0.10 moles/l.) cm.²/sec.

The Stokes-Einstein relationship was found to hold for sulfur dioxide in water over the range 20°C. to 40°C.

See Chapter 11 in the APPENDIX for details.

4.5. Mathematical Theory of Absorption with Chemical Reaction. A mathematical study of various cases of absorption with chemical reaction was carried out. The derivations are presented in detail in Chapters 8 and 9 of the APPENDIX. In this section the main results obtained, and the assumptions leading to them, are presented.

In applying the film theory to absorption with chemical reaction, the assumption that chemical equilibrium exists between the various components present in the main body of the liquid was investigated by studying the case of absorption with first order irreversible reaction. The

validity of the assumption was found to depend upon the holdup of liquid on the packing. For all practical cases encountered in a packed column, the assumption of equilibrium in the main body of the liquid was found to be satisfactory (See Sec. 8.11).

In applying the penetration theory to absorption with chemical reaction in a packed column, the assumption that chemical equilibrium exists between the various components present in the liquid at the beginning of each absorption period just after mixing has occurred at the end of the previous absorption period was investigated by studying the case of absorption with first order irreversible reaction. The validity of the assumption was found to be dependent upon the holdup, also, and for practical cases encountered in a packed column, it was found to be satisfactorily valid (see Sec. 8.16).

The cases of absorption with first order reversible reaction were studied using both the film and penetration theories. Suppose substance A in the gas is absorbed and reacts in the liquid reversibly to form substance E.



Let K be the equilibrium constant for the reaction, k_1 be the rate constant for the forward reaction, k_2 be the rate constant for the reverse reaction, D_A and D_E be the respective diffusivities of A and E and, finally, let

$$R = \sqrt{\frac{k_1}{D_A} + \frac{k_2}{D_E}} \quad (4.4)$$

In the introduction two types of coefficients were defined: k_L^* , the physical coefficient, obtained when no chemical reaction is present, and k_{L0} , the pseudo-coefficient, obtained for the case where chemical reaction is present and based upon a driving force equal to $A_1 - A_0$. A quantity ϕ is defined as the ratio k_{L0}/k_L^* , which expressed the effect that the chemical reaction has upon the rate of absorption. It is always greater than one.

For the film theory, the following equations express mathematically the assumptions made for the case of first order reversible reaction:

$$D_A \frac{d^2 A}{dx^2} = - D_E \frac{d^2 E}{dx^2} = k_1 A - k_2 E \quad (4.5)$$

The boundary conditions are

$$\text{At } x = 0, \quad A = A_1, \quad dE/dx = 0 \quad (4.6)$$

$$\text{At } x = x_f, \quad A = A_0, \quad E = E_0, \quad K = E_0/A_0 \quad (4.7)$$

The solution obtained (see Secs. 8.12 and 8.20) is

$$\phi = \frac{1 + \frac{KD_E}{D_A}}{1 + \frac{KD_E}{D_A} \frac{\tanh(Rx_f)}{Rx_f}} \quad (4.8)$$

The film thickness, x_f , is an empirical quantity which may be evaluated only by determining the physical coefficient, k_L^* .

$$x_f = D_A/k_L^* \quad (4.9)$$

It is preferable to express eq. (4.8) in terms of k_L^* rather than x_f .

$$\phi = \frac{1 + \frac{KD_E}{D_A}}{1 + \frac{KD_E}{D_A} \frac{\tanh(RD_A/k_L^*)}{(RD_A/k_L^*)}} \quad (4.10)$$

For the penetration theory, the assumptions made for absorption with first order reversible reaction are expressed mathematically as:

$$D_A \frac{\partial^2 A}{\partial x^2} - \frac{\partial A}{\partial t} = \frac{\partial E}{\partial t} - D_E \frac{\partial^2 E}{\partial x^2} = k_1 A - k_2 E \quad (4.11)$$

The boundary conditions are

$$\text{At } x = 0, t > 0, \quad A = A_1, \quad \partial E / \partial t = 0 \quad (4.12)$$

$$\text{At } t = 0, x > 0, \quad A = A_0, \quad E = E_0, \quad K = E_0/A_0 \quad (4.13)$$

$$\text{At } x = \infty, t \geq 0, \quad A = A_0, \quad E = E_0 \quad (4.14)$$

It was not possible to obtain a solution for D_A not equal to D_E . It was necessary to assume

$$D_A = D_E = D \quad (4.15)$$

The solution obtained (see Secs. 8.17 and 8.20) is

$$\phi = \frac{\sqrt{\pi}(K+1)}{2\sqrt{R^2Dt}} \left[\frac{K^2}{\sqrt{K^2-1}} \exp\left(\frac{R^2Dt}{K^2-1}\right) \left(\operatorname{erf} \sqrt{\frac{K^2 R^2Dt}{K^2-1}} - \operatorname{erf} \sqrt{\frac{R^2Dt}{K^2-1}} \right) - K \operatorname{erf} \sqrt{R^2Dt} \right] + (K+1) \quad (4.16)$$

In the packed column, the time of exposure, t , must be evaluated from the physical coefficient, k_L^* .

$$\sqrt{t} = \frac{2\sqrt{D/\pi}}{k_L^*} \quad (4.17)$$

Then eq. (4.16) may be written in terms of k_L^* rather than t .

$$\begin{aligned} \phi = \frac{\pi}{4} \frac{K+1}{(RD/k_L^*)^2} & \left\{ \frac{K^2}{\sqrt{K^2-1}} \exp \left[\frac{4}{\pi} \frac{(RD/k_L^*)^2}{K^2-1} \right] \left[\operatorname{erf} \frac{2K(RD/k_L^*)}{\sqrt{\pi(K^2-1)}} - \right. \right. \\ & \left. \left. - \operatorname{erf} \frac{2(RD/k_L^*)}{\sqrt{\pi(K^2-1)}} \right] - K \operatorname{erf} \frac{2(RD/k_L^*)}{\sqrt{\pi}} \right\} + (K+1) \end{aligned} \quad (4.18)$$

Thus the two theories give two methods of calculating ϕ from k_L^* , K , k_1 , k_2 and D (assuming $D_A = D_B$). The two equations (4.10) and (4.18) have been compared by plotting ϕ versus RD/k_L^* for various values of K (see Figs. 8.7 and 8.8). The comparison shows that the penetration theory gives somewhat higher values of ϕ ; that the two sets of curves approach each other asymptotically for small and large values of RD/k_L^* , while the greatest difference occurs at a value of RD/k_L^* of about 1.5; that this difference increases for increasing values of K , reaching a maximum at $K = \infty$ (which corresponds to irreversible reaction), for which case the maximum difference is about 6%. It is concluded therefore that for first order reaction, the film theory and the penetration theory give, for practical purposes, the same answer in predicting ϕ from k_L^* and the constants of the reaction.

It has not been possible to obtain solutions for the penetration theory for the cases of second order reactions. It has been possible to obtain approximate solutions for ϕ in terms of k_L^* and the constants of the reaction, using the film theory. For second order reactions, then, it has been necessary in the absence of a solution based on the penetration theory to assume that the use of the film theory to predict ϕ will give reasonable results, but the sole justification for this assumption are the results of the analysis of the first order case.

The case of absorption with second order irreversible reaction was next considered. Substance A, in the gas, is absorbed into a liquid containing B, and reacts with B irreversibly.



The film theory yields the non-linear simultaneous differential equation

$$D_A \frac{d^2 A}{dx^2} = D_B \frac{d^2 B}{dx^2} = k_1 AB \quad (4.20)$$

with the boundary conditions

$$\text{At } x = 0, \quad A = A_1, \quad dB/dx = 0 \quad (4.21)$$

$$\text{At } x = x_f, \quad A = 0, \quad B = B_0 \quad (4.22)$$

where k_1 is the rate constant, A_1 is the interfacial concentration of A, and B_0 is the concentration of B in the main body of the liquid. There is no known analytical solution

to eq. (4.20). However, a certain amount of information can be obtained from the first equality

$$D_A \frac{d^2 A}{dx^2} = D_B \frac{d^2 B}{dx^2} \quad (4.23)$$

Integrating this equation and substituting the boundary conditions (see Sec. 8.25) gives a relationship between B_1 (the interfacial concentration of B) and ϕ :

$$\frac{B_1}{B_0} = 1 - \frac{D_A A_1}{D_B B_0} (\phi - 1) \quad (4.24)$$

It then remains to solve the equation

$$D_A \frac{d^2 A}{dx^2} = k_1 A B \quad (4.25)$$

Two approximate solutions were carried out. The first, originally proposed by van Krevelen and Hoftijzer (60), assumes that B is constant throughout the film at the value of B_1 given by eq. (4.24). This leads to the equation (see Sec. 8.26)

$$\phi = \frac{\sqrt{M [1 - q(\phi - 1)]}}{\tanh \sqrt{M [1 - q(\phi - 1)]}} \quad (4.26)$$

$$\text{where } M = k_1 B_0 x_f^2 / D_A \quad (4.27)$$

$$\text{and } q = (D_A A_1) / (D_B B_0) \quad (4.28)$$

The quantity M may be expressed directly in terms of k_L^* by substituting eq. (4.9) into eq. (4.27).

$$M = k_1 B_0 D_A / (k_L^*)^2 \quad (4.29)$$

Using eqs. (4.26), (4.28) and (4.29), ϕ may be obtained from k_L^* and the constants of the reaction by trial and error. It can be shown that this method gives values of ϕ lower than the true value.

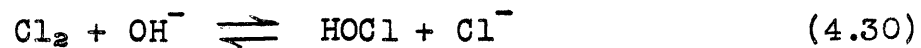
A second approximate solution of eq. (4.25) was obtained by assuming B varies linearly with x in the film, from B_1 at $x = 0$ to B_0 at $x = x_f$. This assumption converts eq. (4.25) into a linear differential equation, which was solved in terms of the Airy integral (see Sec. 8.27) to give another, quite complicated, expression for ϕ as a function of M and q. It can be shown that this method must give a value of ϕ which is greater than the true value.

Thus, the two approximations bracket the true solution between them. The two approximate solutions were compared graphically (see Fig. 8.11), and were found to differ by never more than 8%, though over most of the range the difference is much smaller. It is concluded that eq. (4.26) is slightly in error on the conservative side.

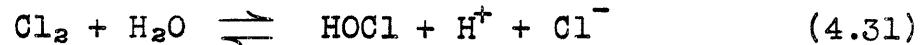
Next, three cases of absorption with second order reversible reactions were studied. The first two cases were absorption of chlorine in water, in which two mechanisms for the reaction of chlorine with water were considered; the third was absorption of sulfur dioxide in water. Three main assumptions were made. First, it was assumed that the film theory could be used to evaluate ϕ from k_L^* and the

constants of the reaction; second, that equilibrium exists in the main body of the liquid; third, that the concentration of hydrogen ions may be assumed constant throughout the film at the interfacial value. The last assumption is analagous to the assumption that B is constant at B_1 for the second order irreversible case discussed above, and was made in order to linearize the differential equations so that they could be solved.

There is some controversy as to whether chlorine reacts with water according to the mechanism



or by the mechanism



Accordingly, derivations have been made using both mechanisms (see Sec. 9.1).

Using A for the concentration of unhydrolyzed chlorine, B for the concentration of hydroxyl ion, E for the concentration of hypochlorous acid and F for the concentration of hydrogen and chloride ions, the equilibrium for the chlorine water system may be expressed by

$$K_c = \frac{EF^2}{A} \quad (4.32)$$

Assuming that the reaction



is infinitely rapid,

$$B = K_w/F \quad (4.34)$$

where K_w is the dissociation constant for water.

Using mechanism (4.30) for the hydrolysis, the differential equation is

$$D_A \frac{d^2 A}{dx^2} = -D_E \frac{d^2 E}{dx^2} = -D_F \frac{d^2 F}{dx^2} = k_1 AB - k_2 EF \quad (4.35)$$

Substituting eq. (4.34), and setting F constant at F_1 gives

$$D_A \frac{d^2 A}{dx^2} = k_1 K_w A / F_1 - k_2 E F_1 \quad (4.36)$$

The boundary conditions are

$$\text{At } x = 0, \quad A = A_1, \quad dE/dx = dF/dx = 0 \quad (4.37)$$

$$\text{At } x = x_f, \quad A = A_0, \quad E = E_0, \quad F = F_0, \quad \text{with } E_0 = F_0 \text{ and } K_c = F_0^3 / A \quad (4.38)$$

Solving the two equations

$$D_A \frac{d^2 A}{dx^2} + D_E \frac{d^2 E}{dx^2} = 0 \quad (4.39)$$

and

$$D_A \frac{d^2 A}{dx^2} + D_F \frac{d^2 F}{dx^2} = 0 \quad (4.40)$$

in turn, and substituting the boundary conditions yields the relations

$$\phi = 1 + \frac{D_E (E_1 - E_0)}{D_A (A_1 - A_0)} \quad (4.41)$$

$$\phi = 1 + \frac{D_F (F_1 - F_0)}{D_A (A_1 - A_0)} \quad (4.42)$$

Integration of eq. (4.36) yields the equation

$$\phi - 1 = \frac{K_c D_E}{F_0^2 D_A} \left(1 - \frac{\tanh U x_f}{U x_f} \right) \quad (4.43)$$

$$\frac{F_1}{F_0} + \frac{K_c D_E}{F_0^2 D_A} \frac{\tanh U x_f}{U x_f} + \left(1 + \frac{F_1}{F_0} \right) \frac{D_E}{D_F} \left(1 - \frac{1}{\cosh U x_f} \right)$$

where

$$U^2 = \frac{k_1 K_W}{D_A F_1} + \frac{k_2 F_1}{D_E} \quad (4.44)$$

Rearrangement of eq. (4.44) and substitution of eq. (4.9) yields

$$k_L^* = \frac{\sqrt{k_2 D_A F_0 / D_E} \sqrt{F_1 / F_0} \sqrt{1 + (K_C D_E / D_A F_0^2) (F_0 / F_1)^2}}{U x_f} \quad (4.45)$$

The system of equations (4.42), (4.43) and (4.45) constitutes the solution to the problem, enabling one to calculate ϕ from A_1 , k_L^* and C_0 (total chlorine concentration). ^{It has not been} possible to rearrange the equations in any way as to reduce the number of independent parameters.

Using the second mechanism (4.31) for the hydrolysis, the differential equation is

$$D_A \frac{d^2 A}{dx^2} = -D_E \frac{d^2 E}{dx^2} = -D_F \frac{d^2 F}{dx^2} = mA - nEF^2 \quad (4.46)$$

where m and n are the forward and reverse rate constants for this mechanism. The boundary conditions are the same as (4.37) and (4.38). Assuming F is constant at F_1 linearizes eq. (4.46):

$$D_A \frac{d^2 A}{dx^2} = mA - nF_1^2 E \quad (4.47)$$

The solution was obtained in a manner similar to that for the first mechanism, and a system of three equations was obtained.

$$\phi - 1 = \frac{\frac{K_C D_E}{F_0^2 D_A} \left(1 - \frac{\tanh Ix_f}{Ix_f}\right)}{\left(\frac{F_1}{F_0}\right)^2 + \frac{K_C D_E}{F_0^2 D_A} \frac{\tanh Ix_f}{Ix_f} + \left(1 + \frac{F_1}{F_0}\right) \frac{D_E}{D_F} \left(1 - \frac{1}{\cosh Ix_f}\right)} \quad (4.48)$$

where

$$I^2 = \frac{m}{D_A} + \frac{nF_1^2}{D_E} \quad (4.49)$$

Eq. (4.42) is still applicable.

$$\phi = 1 + \frac{D_F}{D_A} \frac{(F_1 - F_0)}{(A_1 - A_0)} \quad (4.42)$$

Finally, rearrangement of eq. (4.49) gives

$$k_L^* = \frac{\sqrt{nD_A F_0^2 / D_E} (F_1 / F_0) \sqrt{1 + (K_C D_E / D_A F_0^2) (F_0 / F_1)^2}}{I x_f} \quad (4.50)$$

Eqs. (4.48), (4.42) and (4.50) constitute the solution.

The absorption of sulfur dioxide in water was treated in the same manner (see Sec. 9.6). Letting A be the concentration of unreacted SO₂, B the concentration of hydroxyl ion, and E the concentration of hydrogen and bisulfite ions, and assuming the mechanism of hydrolysis to be



the differential equation is

$$D_A \frac{d^2 A}{dx^2} = -D_E \frac{d^2 E}{dx^2} = k_1 AB - k_2 E \quad (4.52)$$

Assuming the water dissociation is infinitely rapid, so that $B = K_W/E$, and assuming that B is constant throughout the film at its interfacial value, K_W/E_1 , eq. (4.52) becomes

$$D_A \frac{d^2 A}{dx^2} = (k_1 K_W / E_1) A - k_2 E \quad (4.53)$$

with the boundary conditions

$$\text{At } x = 0, \quad A = A_1, \quad dE/dx = 0 \quad (4.54)$$

$$\text{At } x = x_f, \quad A = A_0, \quad E = E_0, \quad K_S = E_0^2/A_0 \quad (4.55)$$

The solution was found to be

$$\phi - 1 = \frac{\frac{K_S D_E}{E_0 D_A} \left(1 - \frac{\tanh Y x_f}{Y x_f}\right)}{\frac{E_1}{E_0} + \frac{K_S D_E}{E_0 D_A} \frac{\tanh Y x_f}{Y x_f} + 1 - \frac{1}{\cosh Y x_f}} \quad (4.56)$$

$$\text{where } Y^2 = \frac{k_1 K_W}{D_A E_1} + \frac{k_2}{D_E} \quad (4.57)$$

Also

$$\phi = 1 + \frac{D_E}{D_A} \frac{(E_1 - E_0)}{(A_1 - A_0)} \quad (4.58)$$

Rearrangement of eq. (4.57) yields

$$k_L^* = \frac{\sqrt{k_2 D_A^2 / D_E} \sqrt{1 + (K_S D_E / E_0 D_A)(E_0 / E_1)}}{Y x_f} \quad (4.59)$$

The system of equations (4.56), (4.58) and (4.58) constitute the solution whereby it is possible to calculate ϕ from k_L^* , A_1 and C_0 . Again it has not been possible to reduce the number of independent parameters.

Putting in the constants for the reaction for 70°F., the equations for the three cases were solved by indirect techniques and graphs were prepared showing ϕ vs. k_L^* for various values of A_1 and C_0 for chlorine (for both mechanisms) and for sulfur dioxide. These graphs show that for all three cases ϕ decreases with increasing k_L^* , increasing A_1 , and increasing C_0 .

Comparison of the two sets of graphs for the chlorine-water system shows that the mechanism $\text{Cl}_2 + \text{H}_2\text{O} \rightleftharpoons \text{HOCl} + \text{H}^+ + \text{Cl}^-$ predicts a lower value of ϕ than does the mechanism $\text{Cl}_2 + \text{OH}^- \rightleftharpoons \text{HOCl} + \text{Cl}^-$ at low values of C_0 ; the first mechanism predicts a slightly higher value of ϕ than the second at high values of C_0 . (See Fig. (9.7)). Both indicate that for the range of k_L^* encountered in a packed column, ϕ is significantly greater than one, and hence that the chlorine water system is one in which the rate of reaction and the rate of diffusion are of comparable magnitude so that both must be taken into account in studying the absorption of chlorine in water.

The graphs for the sulfur dioxide-water system, on the other hand, show that for the range of k_L^* encountered in a packed column, the values of ϕ are much closer to one, being less than 1.2 for extreme cases, and being less than 1.1 for most cases encountered in the packed column. Thus, for practical purposes, for the absorption of sulfur dioxide in water, the psuedo-coefficient may be taken as equal to the physical coefficient.

Finally, a theoretical upper limit for ϕ for the absorption or desorption of chlorine in water was derived (see Sec. 9.11). By assuming that the rate of hydrolysis is infinite, that D_F is infinite, and that $D_A = D_E$, it was shown, using both the film and penetration theory without any further assumptions that

$$\phi < C_0/A_0 \quad (4.60)$$

For any finite values of hydrolysis rate and of D_F , the value of ϕ must be lower than this upper limit.

CHAPTER 5

DISCUSSION OF RESULTS

A. General Aspects of the Experimental Procedure

5.1. Effect of Air Rate. In calculating the coefficients for all three systems investigated, namely $\text{CO}_2\text{-H}_2\text{O}$, $\text{Cl}_2\text{-HCl-H}_2\text{O}$, $\text{Cl}_2\text{-H}_2\text{O}$, the assumption of zero interfacial concentration of solute was made. Whether this assumption is true depends on whether the concentration of solute in the gas is negligible (relative to the concentration which would be in equilibrium with the liquid) and on whether the gas-side resistance is negligible relative to the liquid-side resistance. In order to test the assumption of negligible interfacial concentration, then, it is sufficient to show experimentally the absence of an effect of gas rate, because both these conditions must be satisfied in order for the effect of gas rate to be negligible.

Fig. 4.2 shows that there is no significant effect of gas rate on the desorption of carbon dioxide between a Reynolds number in the gas of 0 and 2200. At higher values of the Reynolds number, ripples were observed in the liquid layer. These would increase the area for mass transfer over that used for calculations, thus giving the apparently higher coefficients observed at the higher gas rates. These same results were noted by Hurlburt (44), who desorbed CO_2 from water in a

long wetted-wall column and found no effect of gas rate up to a Reynolds number of 3500 and an increase in coefficient for further increase in gas rate, and by Sherwood and Holloway (93) who desorbed CO_2 from water in a packed column, and found the coefficient independent of gas rate up to about the loading point.

The fact that the coefficient is unaffected by gas rate down to zero gas rate may be explained by convection currents set up in the gas by the moving liquid layer, which sweep away the carbon dioxide from the gas-liquid interface. Because of this, all but 19 of the first 78 carbon dioxide desorption runs, which were made by Lambe, were taken with zero gas rate in order to reduce the operating difficulties. Before each run was started, the blower was turned on for a short while to sweep out any accumulated carbon dioxide. For these runs, it is not possible to calculate the interfacial concentration of carbon dioxide and to show it to be negligible; it is necessary to rely on the experimental evidence.

For the remaining carbon dioxide runs, because of improvements in the apparatus, it was not inconvenient to blow air through the column. For these runs, it is possible to calculate the interfacial concentration. The inlet air came from the atmosphere, in which the mole fraction of CO_2 is about 0.0003. The maximum mole fraction of CO_2 in the outlet gas stream was 0.0047 obtained in Run No. 90. The inlet water was

usually about 90% saturated with carbon dioxide at one atmosphere, and was never less than 74% saturated, so that the mole fraction of carbon dioxide in equilibrium with the inlet water was 0.74 or greater. Relative to this quantity, the maximum mole fraction of CO_2 in the gas is about 1/2%, a negligible amount.

For the chlorine runs, the maximum ratio of gas outlet concentration to water inlet concentration was obtained in Run No. 193. The concentration of chlorine in the inlet liquid was 0.074 moles/l., and the mole fraction in the gas in equilibrium with that is 0.78. The mole fraction in the exit gas was 0.0073, which can be neglected.

The lowest gas rate used (other than zero) for the carbon dioxide runs was $\text{Re}_G=870$. Using the correlation presented by Gilliland and Sherwood (28) for vaporization data in a wetted-wall column, where the gas-side resistance is controlling, and the gas is in streamline flow, the gas-side coefficient k_G calculated for a length of 4.14 cm. is 6.5×10^{-5} moles/(cm.²)(atm.)(sec.). The overall coefficients for carbon dioxide rarely exceeded 1 cm./min. which, when converted to gas-phase units by multiplying by Henry's law constant for carbon dioxide, gives an overall coefficient of 5.7×10^{-5} moles/(cm.²)(atm.)(sec.). Thus the gas-side resistance is less than a percent, and can be neglected.

The lowest gas rate used for the chlorine runs was $Re_G = 370$. For this case, k_G was calculated to be 3.2×10^{-5} moles/(cm.²)(atm.)(sec.). Pseudo-coefficients for chlorine rarely exceeded 1.0 cm./min. which, when multiplied by Henry's law constant for unhydrolyzed chlorine, gives an "overall pseudo-coefficient" of 1.04×10^{-6} moles/(cm.)(atm.)(sec.). The gas-side resistance for this case, then, is about 3% of the total. Since the scatter of the data is greater than this, the gas-side resistance has been neglected for the chlorine runs also.

A third way in which the gas rate might affect the measured coefficient is by changing the interfacial velocity of the liquid. This in turn would change the time of exposure and hence the value of the coefficient. In Sec. 13.3, the drag effect of the gas on the liquid is calculated and it is shown that for Re_G below 2100, the error in the interfacial velocity of the liquid due to assuming the absence of the drag effect is less than one percent.

5.2. Material Balance. For the carbon dioxide runs, because only the inlet liquid and outlet liquid streams were analyzed, it was not possible to make a material balance.

For the chlorine runs, in general, only the inlet liquid and outlet gas streams were analyzed. In three runs, however, the outlet liquid stream was also sampled in order to

check the material balance. The error of closure, that is, the difference between the chlorine entering the column and the chlorine leaving the column divided by the chlorine entering, was found to be 2.2%, 0.4% and 0.1% for Runs 110, 121 and 173, respectively. Run 110, however, was the first run made with chlorine, and had to be rejected because of poor control. The other two material balances are very good, and indicate that the analytical procedure for the chlorine runs was highly satisfactory.

5.3. Sampling Procedure. For the carbon dioxide runs, the inlet and outlet liquid streams were sampled by allowing a portion of these streams to pass continuously through 25 ml. pipettes at a rate between 100 and 200 ml./min. After the apparatus had reached steady state, it was the practice to wait at least five minutes before taking the samples, though for low water rates twenty minutes was allowed.

It was not until after the completion of the carbon dioxide runs that some experiments were made which showed that volumetric pipettes are not very satisfactory devices for sampling liquids containing slightly soluble gases. When the liquid first enters the pipette, it comes in contact with the air there and desorbs some of the gas. The liquid first contained in the pipette, then, has a lower concentration of solute than the liquid being sampled. The subsequent portions of the liquid sample which flow through the

pipette do not displace the liquid contained in the bulb but, rather, flow in a jet through the middle of the bulb, while the outside part of the bulb still contains the lean liquid. The mixing between the two liquids is slow. The time it takes for the pipette to be filled completely with liquid of the concentration of the sample may be determined by a simple experiment. First the pipette is filled with liquid containing a dye, such as methyl orange. Then water is passed through the pipette at the desired rate and the time noted for the color of the dye to disappear from the bulb. From such experiments it was found that about ten minutes were required to remove completely the original liquid.

Actually, for practically all runs, ten or fifteen minutes, and often half an hour elapsed between the time the pipettes were connected and the sample liquid started flowing, and the time the samples were taken, since considerable time was required to establish steady temperatures and satisfactory flow conditions in the column, and then at least five more minutes would be allowed. Whenever some spillover of liquid into the gas inlet line occurred, it was the practice to wait ten minutes more before taking the sample. This was to allow enough time for the carbon dioxide in the spilled-over liquid which adhered to the walls of the calming section to desorb into the gas stream and pass through the column, so that during the run itself, the inlet gas would not contain any extra carbon dioxide.

Thus, because ample time was allowed, the effect of the jet flow through the pipette was probably not serious, but it is not possible to evaluate the effect exactly. Since both the inlet and outlet samples were subject to this same error, there should be little effect on the average results, though it would increase the scatter of the data.

For the chlorine runs, this trouble was avoided, for the liquid samples were taken by allowing a portion of the liquid to flow directly below the surface of the liquid contained in a titration flask, and weighing the flask before and after sampling to determine the sample weight. Such a procedure is far superior to the use of pipettes, and is strongly recommended for use whenever a liquid containing a volatile solute is to be sampled. The one disadvantage which ruled out this method for the carbon dioxide runs is that a sample of predetermined volume cannot be taken. This predetermined volume was necessary, for it was desired to add the inlet sample to as slight an excess of barium hydroxide as possible, in order that the conductometric measurement of the residual hydroxide concentration be sufficiently precise. (This point is discussed further in Sec. 10.4).

For further work on the carbon dioxide-water system, more precise results could be obtained by changing the procedure. One method would be to study absorption, using pure

carbon dioxide for the gas stream and distilled water for the inlet liquid stream. It would be necessary to analyze only the exit liquid stream, and this analysis could be satisfactorily performed by running some liquid into a flask containing a known amount of $\text{Ba}(\text{OH})_2$, weighing the flask before and after sampling, and titrating the residual hydroxide with HCl . Another method would be to study desorption in a manner similar to that used for the chlorine runs -- that is, to determine the rate of desorption by analysis of the gas stream. It would be necessary, then, to remove all the CO_2 from the inlet air, or to analyze the inlet air and measure its rate accurately.

5.4. Effect of Slot Width and Type. Before the start of this work, it had been expected that the interfacial velocity of the liquid would not be constant with distance down the column but, rather, would increase from the velocity at which the liquid entered the column through the inlet slot to some final velocity which would depend on the water rate. Since the inlet velocity of the liquid would depend on whether the inlet slot was upflow or downflow, and on the width of the inlet slot, it was expected that these variables would have an effect on the coefficients measured.

The results shown in Fig. 4.3 and 4.4 show that slot width has no effect within the normal scatter of the data. Comparison of the two figures shows that the coefficient is practically the same for both upflow and downflow slots.

To check further the fact that the type of slot is immaterial, runs were made to determine the effect of water rate using five columns, three of which were upflow and two downflow. These runs will be discussed later, but it may be pointed out here that the data for the two types of slots fit equally well the correlation developed for these runs, in spite of the fact that the correlation does not take into account the entrance slot at all.

In view of these facts, it appears that acceleration does not occur in the column, but rather that the interfacial velocity is uniform. This is further confirmed by the fact that the correlation just mentioned is developed on the assumption of uniform interfacial velocity. As final supporting evidence may be cited the measurements of interfacial velocity described in the APPENDIX in Chapter 13. By using a stroboscopic technique, it was found that the interfacial velocity is uniform and equal to that predicted by streamline flow theory. Taken by itself, the method used is not sufficiently reliable to be accepted as proof of uniform velocity. Taking all three pieces of evidence together, however, it must be concluded that the liquid interfacial velocity is independent of distance, and depends only on the water rate.

B. Physical Coefficients

5.5. Absence of Chemical Reaction. In the desorption of carbon dioxide from water and of chlorine from dilute hydrochloric acid, some hydrolysis of the solute occurs. It is necessary, then, to show that the extent of this hydrolysis is negligible in order that the coefficients obtained can be interpreted as physical coefficients.

In the carbon dioxide-water system at equilibrium, the percentage of solute which is hydrolyzed decreases as the concentration increases. At the lowest inlet concentration encountered, where the solution was 74% saturated, the carbon dioxide was only 0.4% dissociated.

In the chlorine-dilute hydrochloric acid system at equilibrium, the presence of the hydrochloric acid represses the hydrolysis, so that the percentage of chlorine hydrolyzed decreases as the HCl concentration is increased. In the chlorine-HCl runs, the concentration of HCl varied somewhat from run to run, but the lowest concentration was 0.157 moles/l. For this case, the chlorine was only 1.3% hydrolyzed.

Further evidence of the absence of chemical reaction is the lack of any significant effect of concentration of chlorine on the coefficients obtained, as can be seen on Fig. 4.10, which shows the effect of water rate for several different chlorine concentrations. The chlorine concentration

was varied from 0.011 to 0.040 moles/l.

5.6. Effect of Temperature. In Fig. 4.1, the coefficient for the desorption of carbon dioxide from water is shown as a function of the water temperature. In making these runs, the air was within one degree centigrade of the water temperature in each case, and saturated with water, so that the effects of any mass transfer of water would be eliminated. The best line through the experimental values on semilogarithmic coordinates gives a temperature relationship of the form

$$k_L^* = \psi e^{wt} \quad (5.1)$$

where $w = 0.011$ and t is the liquid temperature, degree centigrade. The coefficients measured for the other runs have been corrected to a standard temperature of 25°C . by the use of eq. (5.1). The significance of the value of the temperature coefficient will be discussed in Sec. 5.12.

No attempt was made to determine experimentally the effect of temperature on the chlorine coefficients. Eq. (5.1), with $w = 0.019$, was used to correct the coefficients for chlorine in dilute HCl to the standard temperature of 25°C . The reason for using this value of w will be discussed in Sec. 5.14.

5.7. Effect of Water Rate. The variation of the physical coefficient with water rate is shown in Figs. 4.5

to 4.10. Figures 4.5 to 4.9 show the data for desorption of carbon dioxide from water in each of five columns. The sixth column, about 5/8" long with downflow slot, was broken before any data could be taken on it. Fig. 4.10 shows the data for desorption of chlorine from dilute hydrochloric acid, all of which were taken on one column.

The dashed line in each figure represents the best line through the data shown in that figure. These lines may be expressed by the equation

$$k_L^* = b \Gamma^n \quad (5.2)$$

where b and n have the values shown in the following table. The units of k_L^* and Γ to be used with these constants are cm./min. and g./(cm.)(min.), respectively.

<u>Fig. No.</u>	<u>b</u>	<u>n</u>	
4.5	0.150	0.45	
4.6	0.167	0.42	<u>Units</u>
4.7	0.224	0.39	
4.8	0.224	0.39	k_L^* , cm./min.
4.9	0.292	0.36	
4.10	0.177	0.36	Γ , g./(cm.)(min.)

Although there appears to be a trend in the exponent, it is not believed that this trend is significant, especially since the data shown in Figs. 4.5 and 4.10 were taken on the same column, though with different solutes. Considering the precision of the data, the second figure of the exponent n cannot be considered significant. Consequently,

it was decided to choose an average value for n of 0.40.

Using this exponent, eq. (5.2) becomes

$$k_L^* / \Gamma^{0.4} = \text{const.} \quad (5.3)$$

This quantity $k_L^* / \Gamma^{0.4}$ was evaluated for each run, and the average value computed for each series of runs. These are summarized in the following table.

Fig. No.	Number of Runs	System	Length, cm.	Average $k_L^* / \Gamma^{0.4}$
4.5	43	CO ₂ -H ₂ O	4.25	0.174
4.6	13	"	4.21	0.180
4.7	19	"	2.72	0.212
4.8	13	"	3.09	0.218
4.9	6	"	1.88	0.255
4.10	10	Cl ₂ -HCl-H ₂ O	4.14	0.155

Units

k_L^* , cm./min.

Γ , g./(cm.)(min.)

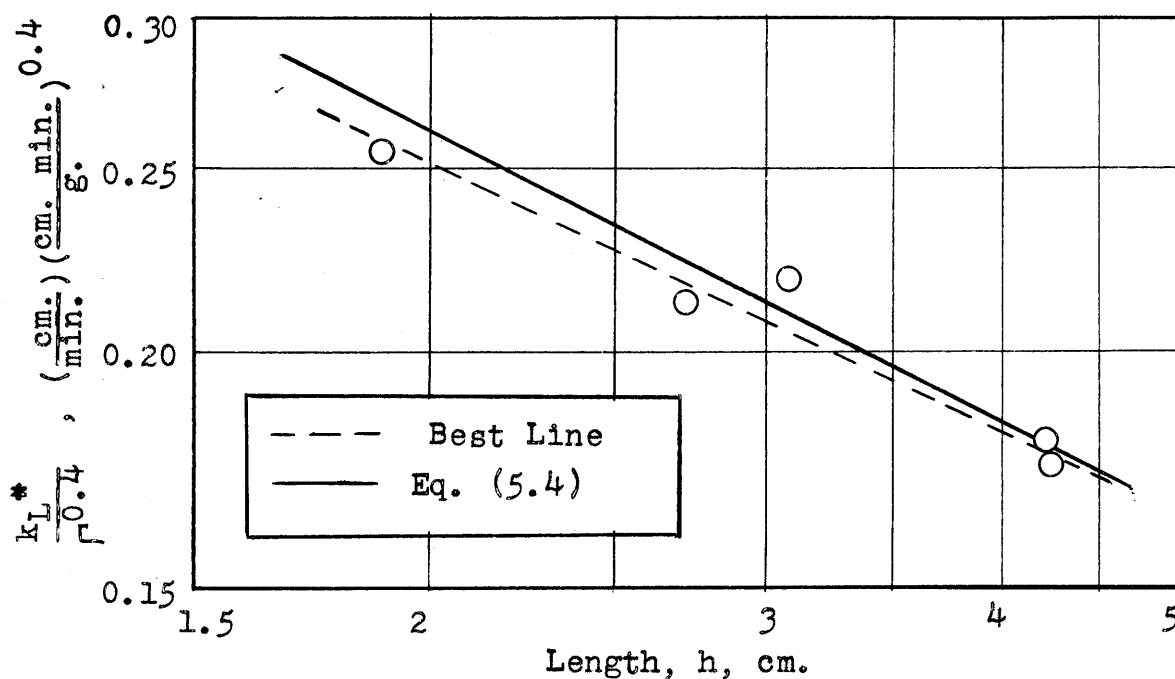
5.8. Effect of Length of Column. In order to determine the effect of length, the average values of $k_L^* / \Gamma^{0.4}$ presented in the above table are plotted versus length on logarithmic coordinates in Fig. 5.1. The circles represent the carbon dioxide data, the square the chlorine runs. The best line through the circles was calculated by the method of least squares, where each circle was weighted by the number of runs that it represents. This best line, shown as a dashed line on the figure, has a slope of -0.46. Considering the

Fig. 5.1

**Effect of Length on Physical Coefficient
in Short Wetted-Wall Column**

System: CO₂-water

Temp. = 25°C.



precision of the data, this is in excellent agreement with the penetration theory. As can be seen from eq. (2.33) in the Introduction,

$$k_L^* = 2 \sqrt{\frac{D}{\pi h}} \left(\frac{9}{8} \frac{g\Gamma^2}{\mu\rho} \right)^{1/6} \quad (2.33)$$

the theory predicts that k_L^* varies inversely as the square root of the length, h . One of the chief assumptions in the derivation of eq. (2.33) from the penetration theory is that the interfacial velocity be constant with distance down the column, and the agreement between experiment and theory con-

cerning the effect of length is one more piece of evidence to be added to those already presented in Sec. 5.4, that acceleration of the liquid does not occur in the column.

5.9. Effect of Diffusivity. By comparing the data on the desorption of chlorine from dilute hydrochloric acid with the data on desorption of carbon dioxide from water at the same column length, the effect of diffusivity can be determined. For the chlorine runs, in which the length of the column was 4.14 cm., the average value of $k_L^*/\Gamma^{0.4}$ is 0.155. From Fig. 5.1, for the length, the value of $k_L^*/\Gamma^{0.4}$ for carbon dioxide is 0.178. The ratio of k_L^* for CO_2 to k_L^* for Cl_2 , then, is $0.178/0.155 = 1.15$.

The diffusivity of unhydrolyzed chlorine in water at 25°C . is $1.48 \times 10^{-5} \text{ cm.}^2/\text{sec}$. (see Sec. 4.4), while carbon dioxide has a diffusivity in water of $1.97 \times 10^{-5} \text{ cm.}^2/\text{sec}$. at 25°C . (obtained from Fig. 11.10). The ratio of the diffusivity of carbon dioxide to that of chlorine is 1.33. The penetration theory predicts that k_L^* varies as the square root of the diffusivity. It predicts, then, that the ratio of k_L^* for the two solutes is $\sqrt{1.33} = 1.15$, in excellent agreement with the experimentally determined ratio of 1.15. If the ratios are evaluated to one more place, which cannot be considered significant, they are, for the experimental, 1.148; for the theoretical, $\sqrt{1.331} = 1.154$. Theory and experiment agree, then, to 1/2%.

In order to confirm further this effect of diffusivity, it is recommended that the desorption of hydrogen from water be studied; since the diffusivity of hydrogen is more than twice that of carbon dioxide. Because there is considerable disagreement in the literature regarding the value of the diffusivity of hydrogen in water, it would be necessary also to supplement the desorption studies with measurements of the diffusivity of hydrogen.

5.10. Correlation Using Penetration Theory. So far, it has been shown that the physical coefficient varies as the square root of the diffusivity and inversely as the square root of length, in agreement with eq. (2.33). The combination of the penetration and streamline flow theory predicts that k_L^* varies as the 1/3 power of the water rate, but it has been found that it actually varies as a higher power. Consequently, to correlate all the data on a single graph, $k_L^* \sqrt{h/D}$ is plotted versus Γ on logarithmic coordinates in Fig. 5.2.

The best line through the data is expressed by the equation

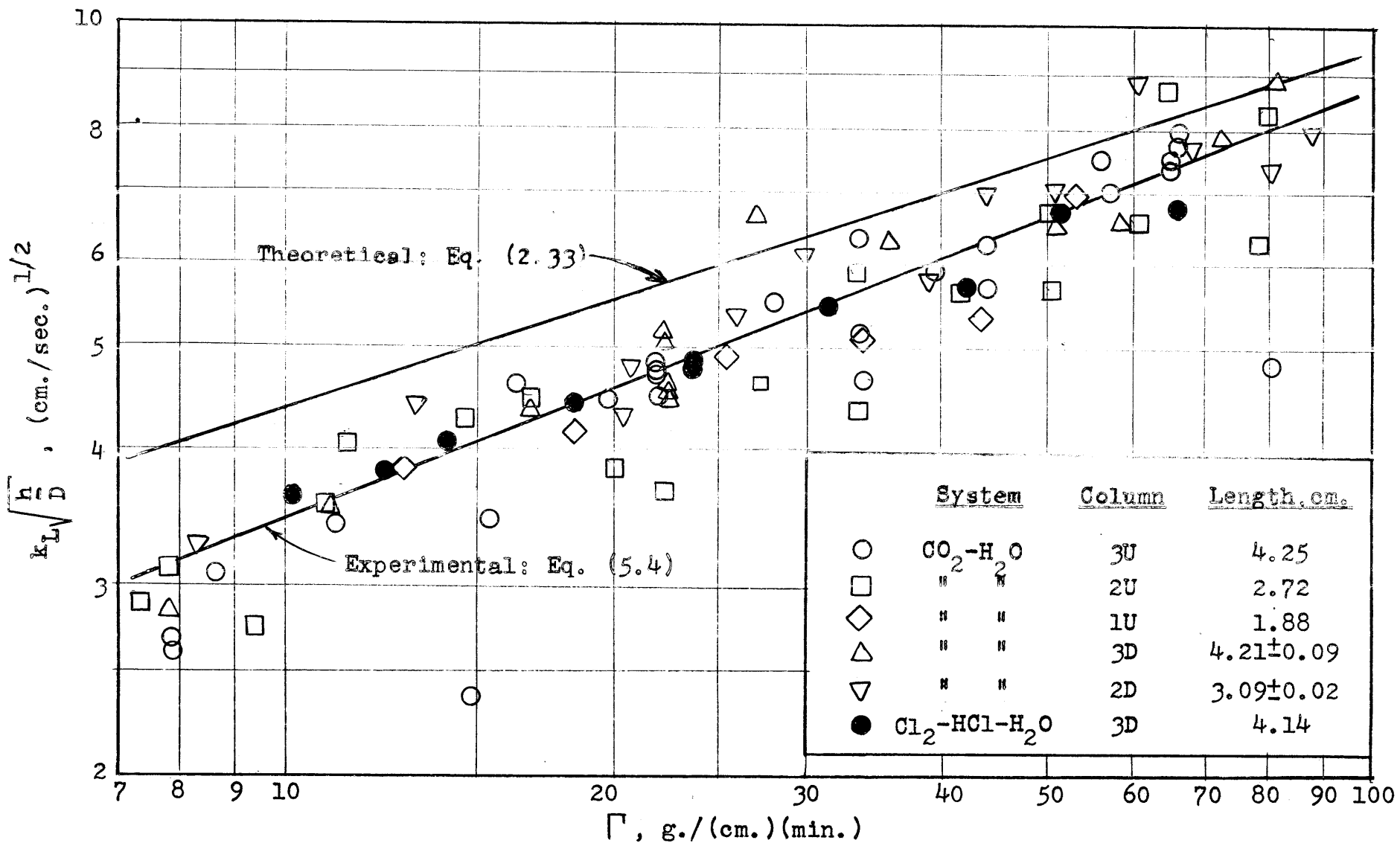
$$k_L^* \sqrt{\frac{h}{D}} = 7.13 \Gamma^{0.40} \quad (\text{at } 25^\circ\text{C.}) \quad (5.4)$$

where all quantities are expressed in units of grams, centimeters and seconds. Since it is common to use minutes rather than seconds for k_L^* and Γ in absorption work and in wetted-

Fig. 5.2

Correlation, Using Penetration Theory, of Physical Coefficients
Obtained on Short Wetted-Wall Column

Temp. = 25°C.



wall column work, it is convenient to rewrite eq. (5.4) as

$$k_L^* \sqrt{\frac{h}{D}} = 83.2 \Gamma^{0.40} \quad (\text{at } 25^\circ\text{C.}) \quad (5.4a)$$

where the units are: k_L^* , cm./min.

Γ , g./(cm.)(min.)

h , cm.

D , cm.²/sec.

Because of the great many points shown in Fig. 5.2, it is difficult to see how well eq. (5.4) fits the data for the separate columns. For this purpose, eq. (5.4) is plotted on Figs. 4.5 to 4.10, and a comparison can be made for each figure. In addition, eq. (5.4) is plotted on Fig. 5.1, which shows the effect of length. In that figure, of course, the line has a slope of -0.5, and the two points on the right of the graph have the greatest influence on the position of the line because they represent over half of the runs.

The deviation of $k_L^* \sqrt{h/D}$ from the value given by eq. (5.4) was calculated for each run, and the following statistics were determined: the average deviation is 7.7%, the standard deviation is 11.0%, 44% of the points lie within 5% of the line, and 78% of the points lie within 10% of the line.

Eq. (2.33), which was derived from the penetration and streamline flow theories, is also plotted on Fig. 5.2, with the values for ρ and μ at 25°C. substituted. It can be seen that the experimental line falls below the theoretical line, the deviation being about 30% at the lowest flow rate and about 10% at the highest flow rate.

One possible explanation for this discrepancy could be the fact that in deriving eq. (2.33), it was assumed that the dissolved gas penetrates such a short distance into the liquid that, in the "zone of penetration", the velocity of the liquid may be assumed uniform. Actually, there exist a parabolic velocity profile in the liquid, so that there is some variation of velocity in this zone; the lower the flow rate, the higher the diffusivity and the longer the column, the less accurate this assumption will be. Johnstone and Pigford (53) solved the mathematical problem of diffusion into a finite liquid layer with parabolic velocity gradient. Assuming negligible diffusion in the vertical direction, and constant interfacial and initial concentrations, the fundamental differential equation reduces to

$$\left[1 - \left(\frac{x}{\delta}\right)^2 \right] \frac{\partial C}{\partial y} = \frac{D}{v_1} \frac{\partial^2 C}{\partial x^2} \quad (5.5)$$

They obtained the following solution:

$$\begin{aligned} \frac{C_2 - C_1}{C_1 - C_i} = & 0.7857 \exp(-5.1213 \theta) + 0.1001 \exp(-39.318 \theta) \\ & + 0.03599 \exp(-105.64 \theta) + 0.01811 \exp(-204.75 \theta) \\ & + \dots \end{aligned} \quad (5.6)$$

where

$$\theta = \frac{Dh}{\delta^2 v_1} \quad (5.7)$$

The thickness of the layer, δ , and the interfacial velocity, v_1 , are found from streamline flow theory (see Sec. 13.2 in the APPENDIX). Substituting eqs. (13.7) and (13.8) into eq. (5.7) gives

$$\theta = \frac{2Dh}{3} \left(\frac{\rho^5 g}{3\mu \Gamma^4} \right)^{1/3} \quad (5.8)$$

The largest deviation from the penetration theory will occur for the largest values of D and h , and the lowest value of Γ , i.e., for the largest value of θ . This most extreme case occurs for $D = 1.97 \times 10^{-5}$ cm.²/sec. (for CO₂ in water); $h = 4.25$ cm.; $\Gamma = 7.4$ g./(cm.)(min.). This gives a maximum value of θ of 0.030. Substitution into eq. (5.6) gives $(C_2 - C_1)/(C_1 - C_1) = 0.706$. Now, from the definition of k_L^* and a material balance, we get

$$k_L^* (C_1 - C_1) = \frac{\Gamma}{\rho h} (C_2 - C_1) \quad (5.9)$$

or

$$k_L^* = \frac{\Gamma}{\rho h} \left(1 - \frac{C_2 - C_1}{C_1 - C_1} \right) \quad (5.10)$$

Substitution gives $k_L^* = 0.512$ cm./min. The value found by use of eq. (2.33), which neglects the parabolic velocity gradient, is also 0.512. Therefore, the error due to this assumption of uniform velocity in the "penetration zone" is negligible.

A more likely explanation of the discrepancy between theory and experiment lies in nature of the liquid flow. It is difficult to conceive of the liquid entering through the slot and immediately assuming the velocity as given by the streamline flow theory. From physical considerations it is clear that it must take a finite time for the liquid to accelerate from the entrance velocity to the final velocity. Earlier in this chapter, it was shown that the lack of an effect of entrance slot width or type on the desorption coefficients indicates that such an acceleration period is absent. It may well be that there is some effect of slot width or type which could not be detected because the experimental procedure was not sufficiently precise. The presence of an acceleration period would explain the low coefficients, because then the time of exposure would be longer than that calculated by assuming that the liquid interface is always at its final value.

In any event, the 10 to 30% difference between the theoretical and experimental coefficients should not be considered very serious. Actually, it is an achievement in absorption work to be able to predict absolute values of mass transfer rates solely from theoretical considerations, using only such physical constants as diffusivity, viscosity, and density with no recourse whatever to any empirical quantities as film thickness or eddy diffusivity, which can

be obtained only by studying some similar mass transfer process. Considering the many assumptions made regarding the desorption process and the nature of the flow of the liquid, the agreement is considered quite good.

5.11. Attempted Correlation Using Film Theory.

In calculating the coefficients so far presented and discussed, the driving force used was the difference between initial and interfacial concentration of solute.

$$N_A = k_L^* (C_0 - C_1) \quad (5.11)$$

since this is the proper driving force according to the penetration theory. A material balance on the liquid layer gives

$$N_A = \frac{\Gamma}{\rho h} (C_1 - C_2) \quad (5.12)$$

where C_1 is the concentration of entering liquid and C_2 is the concentration of the exit liquid. C_0 then is identical with C_1 . Setting $C_1 = 0$, and combining eqs. (5.11) and (5.12), we have

$$k_L^* = \frac{\Gamma}{\rho h} \frac{C_1 - C_2}{C_1} \quad (5.13)$$

If the film theory were to be used, eq. (5.11) could still be used, but C_0 would have to be interpreted as the bulk concentration of solute in the liquid at any time. The material balance on the liquid would have to be written in differential form:

$$N_A dh = - \frac{\Gamma}{\rho} dC_0 \quad (5.14)$$

Combining eqs. (5.11) and (5.14), and setting $C_1 = 0$, we have

$$k_L^* dh = - \frac{\Gamma}{\rho} \frac{dC_0}{C_0} \quad (5.15)$$

Integrating:

$$k_L^* h = - \frac{\Gamma}{\rho} \int_1^2 \frac{dC_0}{C_0} = \frac{\Gamma}{\rho} \ln \frac{C_1}{C_2}$$

or

$$k_L^* = \frac{\Gamma}{\rho h} \ln \frac{C_1}{C_2} \quad (5.16)$$

Eq. (5.16) is the proper formula to be used for calculating k_L^* if it is to be examined from the point of view of the film theory.

Now, $(C_1 - C_2)/C_1$ is always smaller than $\ln(C_1/C_2)$ for $C_1 > C_2$, so that the coefficient calculated by eq. (5.13) (penetration theory) is always smaller than that calculated by eq. (5.16) (film theory). This is to be expected, since the penetration theory bases the coefficient on the initial driving force, while the film theory bases the coefficient on a logarithmic mean driving force which is always less than the initial driving force. The longer is the column, the greater is the deviation between the two coefficients. It could be argued by a proponent of the film theory that this is the reason for the decrease in the coefficient, as calculated by eq. (5.13), rather than the increase in the time of exposure. Consequently, it is necessary to examine the physical

coefficients completely from the point of view of the film theory.

First, the coefficients, which were obtained by use of eq. (5.13), were multiplied by the quantity

$$\frac{\ln (C_1/C_2)}{(C_1-C_2)/C_1}$$

in order to have them agree with eq. (5.16). Secondly, the film theory predicts that the physical coefficient is proportional to diffusivity and inversely proportional to the film thickness.

$$k_L^* = \frac{D}{x_f} \quad (2.20)$$

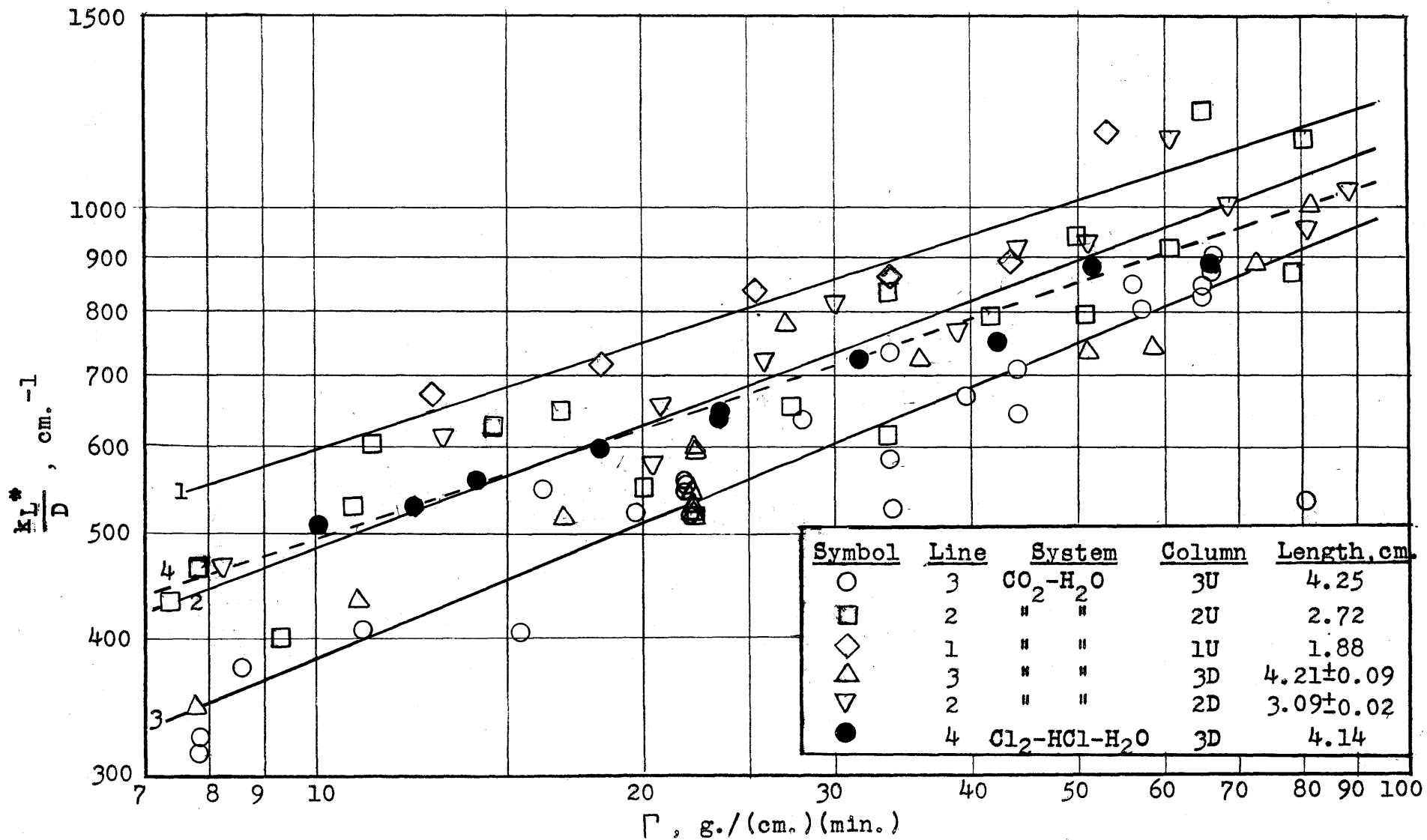
The film thickness should be a function only of the liquid rate and should be independent of solute or of length of column. Consequently, the quantity k_L^*/D has been plotted versus water rate in Fig. 5.3.

The best straight line through the CO_2 data on columns 3U and 3D is labeled 3; through the CO_2 data on columns 2U and 2D is labeled 2,; through the CO_2 data on column 1U is labeled 1; and through the Cl_2 data on column 3D is labeled 4. Comparison of lines 1, 2 and 3 shows that there is still a very definite effect of length, while comparison of lines 3 and 4 shows a marked effect of diffusivity. These effects of length and diffusivity on k_L^*/D are contrary to the predictions of the film theory, and show rather convincingly that the film theory does not apply in the short wetted-wall column.

Fig. 5.3

Attempted Correlation, Using Film Theory, of Physical Coefficients Obtained on Short Wetted-Wall Column

Temp. = 25°C.



5.12. Dimensionless Correlation. The equation which has been developed to correlate the data on physical coefficients, eq. (5.4), is dimensional in form. It is desirable for some purposes to express this equation in dimensionless form. To develop a dimensionless equation, it is necessary to list all the variables which are expected to affect k_L^* ; these are: diffusivity, D ; length, h ; liquid flow rate, Γ ; viscosity of liquid, μ ; density of liquid, ρ ; and acceleration due to gravity, g . Dimensional analysis shows that these variables can be arranged in four dimensionless groups, which may be taken as

$$\frac{k_L^* h}{D}; \quad \frac{\mu}{\rho D}; \quad \frac{\Gamma}{\mu}; \quad \frac{\rho^2 g h^3}{\mu^2}$$

Comparison with eq. (5.4) shows that the dimensionless equation should take the form

$$\frac{k_L^* h}{D} \propto \left(\frac{\mu}{\rho D}\right)^{1/2} \left(\frac{\rho^2 g h^3}{\mu^2}\right)^{1/6} \left(\frac{\Gamma}{\mu}\right)^{0.40} \quad (5.17)$$

The Reynolds' number of the liquid layer is $4\Gamma/\mu$. (See eq. (13.10) in Sec. 13.2 in the APPENDIX). It is convenient then, to use this quantity in the dimensionless equation. Since eq. (5.4) applies at 25°C., the values of μ and ρ at 25°C. are substituted, as well as g , to give

$$\frac{k_L^* h}{D} = 0.433 \left(\frac{\mu}{\rho D}\right)^{1/2} \left(\frac{\rho^2 g h^3}{\mu^2}\right)^{1/6} \left(\frac{4\Gamma}{\mu}\right)^{0.40} \quad (5.18)$$

With the use of eq. (5.18) it is possible to predict k_L^* for systems where the viscosity and density are different from those of water at 25°C. It should be remembered, however, that eq. (5.18) predicts the effect of these variables solely on the basis of dimensional analysis and that there is no experimental evidence regarding these effects. Therefore, it should be used for this purpose with caution.

The effect of temperature on the desorption of carbon dioxide and of chlorine can be calculated by use of eq. (5.18). Only the diffusivity and viscosity will change significantly with temperature, so one may write from eq. (5.18):

$$\frac{dk_L^*}{k_L^* dt} = \frac{1}{2} \frac{dD}{D dt} - 0.23 \frac{d\mu}{\mu dt} \quad (5.19)$$

where t is temperature, °C. From a table of viscosity of water at different temperatures, one can calculate the temperature coefficient of viscosity, $d\mu/\mu dt$, to be -0.023. From Fig. 11.10, which is a plot of $\log D$ versus $1/T$ for carbon dioxide in water, the temperature coefficient of diffusivity, $dD/D dt$, for carbon dioxide in water is calculated to be 0.022. Substituting into eq. (5.19) gives $dk_L^*/k_L^* dt = 0.5(0.022) - 0.23(-0.023) = 0.016$ for the desorption of carbon dioxide in water. As pointed out in Sec. 5.6, the temperature coefficient was found to be 0.011. The range of temperatures over which measurements were made was only nine degrees centigrade, so that the precision of the

experimental value of the temperature coefficient is not very good. As a matter of fact, a line of slope 0.016 could be put through the data shown on Fig. 4.1 which would differ no more than 5% from the experimental points. This agreement is better than the agreement between eq. (5.4) and all the CO₂ data. Consequently, the data on temperature effect is insufficient to permit a definite decision as to the proper value of the temperature coefficient. Comparison of the temperature effect with that obtained in long wetted-wall columns and in packed columns is discussed further in Secs. 5.13 and 5.19.

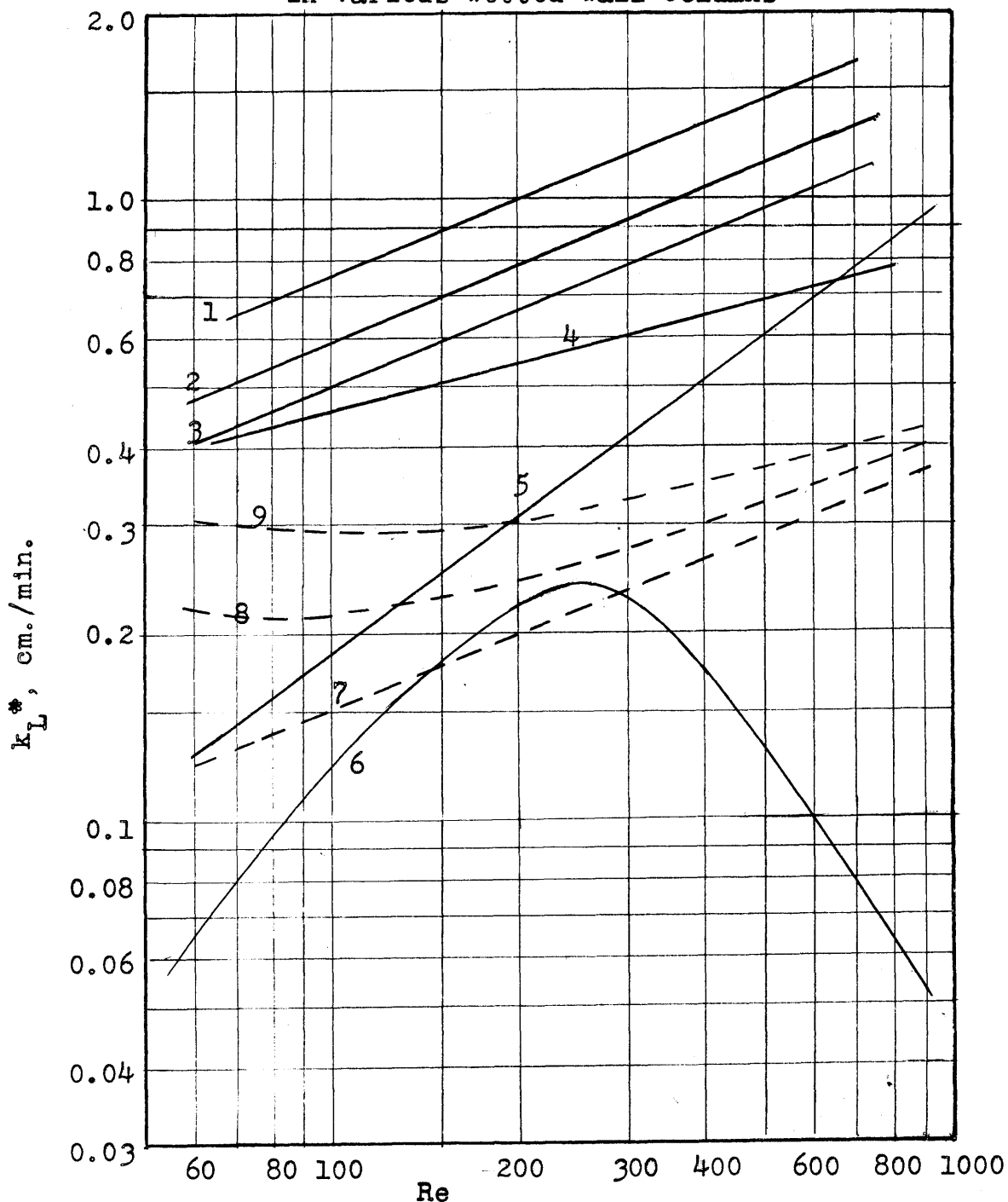
Further study of physical coefficients in the short wetted-wall column could well include a more extensive study of the effect of temperature. A further study of the effect of viscosity, for the purpose of checking eq. (5.19), could be carried out by desorbing carbon dioxide from solutions of glycerine, or by absorbing carbon dioxide in these solutions. It would be necessary, of course, to supplement these experiments by measurements of the diffusivity of carbon dioxide in glycerine solutions of various concentrations, since it is unadvisable to assume that diffusivity is inversely proportional to viscosity without experimental verification.

5.13. Comparison with Data on Long Wetted-Wall Columns.

In Fig. 5.4, physical coefficients calculated by eq. (5.4) for the desorption of CO₂ from water are plotted for three

Fig. 5.4

Comparison of Physical Coefficients Measured in Various Wetted-Wall Columns



Line	Solute	Length of Col. cm.	Source	Driving Force
1	CO ₂	1.88	Eq. (5.4)	initial
2	CO ₂	3.09	"	"
3	CO ₂	4.25	"	"
4	CO ₂	47	Hurlburt (44)	log mean
5	CO ₂	47	Miller (73)	log mean
6	CO ₂	?	Grimley (31)	?
7	CO ₂	47	Eq. (5.4)	initial
8	CO ₂	47	"	log mean
9	CO ₂	47	Eq. (5.6)	log mean

lengths. Lines 1, 2 and 3 then, represent data obtained in this thesis for three columns of length 1.88, 3.09 and 4.25 cm., respectively. These coefficients are based on the initial driving force; since they are to be compared with coefficients obtained on long wetted-wall columns which are based on logarithmic mean driving forces, they should properly be corrected for the difference in driving force, but for these short columns the difference is only a few per cent.

Hurlburt (44) studied the desorption of carbon dioxide in water in a wetted-wall column 18 1/2 inches (47 cm.) long. His coefficients, based upon a log mean driving force are plotted as line 4 in Fig. 5.4. They fall somewhat below the results obtained on the 4.25 cm. column, but more important the slope of the line is only half that obtained for the short columns. Hurlburt reports some data of Miller (73) on absorption of oxygen in water. Miller used column lengths of 46 inches and 28 1/4 inches, and found the coefficients obtained differed by a factor equal to the square root of the ratio of the lengths. Hurlburt corrected Miller's data to the length he used, 18 1/2 inches, and the resulting line is shown as line 5 on Fig. 5.4. Since the diffusivities of oxygen and carbon dioxide are only about 10% different, this line may be compared with the other lines, which are for carbon dioxide. The very large effect of liquid rate is in marked contrast to the effect obtained by Hurlburt

and in this thesis.

Grimley (31) obtained some data on the absorption of carbon dioxide in water in a wetted-wall column. Unfortunately, Grimley did not describe the apparatus, so that the length is not known, and his method of calculation is not presented, so one cannot be sure that he used a log mean driving force. He presented his results in the form of a graph of HTU vs. Re, which has been recalculated by the equation

$$k_L^* = \frac{\Gamma}{\rho (\text{HTU})} \quad (5.26)$$

and plotted as curve 6 in Fig. (5.4). At Reynolds number below 200, he too gets the very large effect of water rate obtained by Miller, but at higher rates of flow, the slope becomes negative, an effect not obtained by any other investigator.

Johnstone and Pigford (53) and Pigford (85) report that Childress (12) obtained data for the absorption of pure SO₂, Cl₂, CO₂ and O₂ by water in a small glass wetted-wall tower and found that the HTU based on an arithmetic mean driving force is independent of water rate for values of Re ranging from 100 to 500. From eq. (5.20), it can be seen that this means that k_L^{*} varies directly as the first power of the water rate for this range.

In order to compare these results with the experimental results of this thesis, coefficients were calculated by means

of eq. (5.4), using a length of 47 cm., which is the length used by Hurlburt. This is shown as line 7. These coefficients are based on the initial driving force, and hence are not directly comparable with Hurlburt's and Miller's data. Consequently, from eq. (5.13), the quantity $(C_1 - C_2)/C_1$ was calculated, then the ratio C_1/C_2 computed and substituted into eq. (5.16) to obtain a coefficient based on a log mean driving force. These are plotted as curve 8 in Fig. 5.4. This curve goes through a minimum because, at the lower liquid rates, as the liquid rate decreases, the logarithmic mean driving force decreases faster than the rate of transfer decreases.

Finally, curve 9 is calculated using the theoretical equation of Johnstone and Pigford (53) for diffusion into a finite layer with a parabolic velocity gradient. In addition to eq. (5.6), the coefficient was calculated by eq. (5.16) in order to be based on a logarithmic mean driving force.

Comparison of lines 4, 5 and 6 shows, then, that there is very serious disagreement concerning the absolute magnitudes of the coefficients and the effect of water rate on the coefficients. Furthermore, none of them show any agreement with the theoretical curve 9. The reason probably lies in the flow pattern of the liquid in long wetted-wall columns. At very low flow rates, the flow of liquid is smooth; ripples begin to occur at a Reynolds number of 25 (27), (31). Friedman and Miller (27) found the interfacial velocity of the liquid

to be abnormally high above $Re = 25$, while Grimley (31) found it to be high above $Re = 12$. True turbulence sets in at $Re = 1500$ to 2000 . Friedman and Miller (27) proposed that the region between $Re = 25$ and $Re = 1500$ be called the "pseudo-streamline" region. Probably this region is characterized by an instability in the flow and some turbulence in the outer part of the liquid layer, which is manifested by the ripples. This would account for the high coefficients (compared with theory) obtained by Hurlburt and Miller, and in particular, one could explain the high effect of water rate on the coefficients obtained by some of the investigators as due to the increasing intensity of rippling with liquid rate. Further evidence for this hypothesis is supplied by van Krevelen and Hoftijzer (61), who flowed liquid along a flat gutter placed inside a sloping glass tube through which the gas flowed; the coefficients they obtained for the absorption of carbon dioxide into water and into mixtures of water and glycerol agreed with theory as long as the Reynolds number was lower than about 25; at higher Reynolds numbers, the coefficients were greater than predicted from theory. Johnstone and Pigford (53) studied distillation in a wetted-wall column. They found the liquid phase resistance to be small compared with the overall resistance, amounting to less than ten per cent, but they were able to show that this resistance was only one-half to one-quarter as great as predicted by theory, which they attributed to the effect of surface ripples.

The occurrence of ripples can be used to explain the difference in the effect of temperature on the desorption of carbon dioxide carried out in the two types of columns. As pointed out in Sec. 5.12, the temperature coefficient for k_L^* for desorption of CO_2 from water in the short column was found experimentally to be 0.011, while eq. (5.18) predicts a value of 0.016. Hodson (39), using Hurlburt's wetted-wall column, desorbed oxygen from water, and found the temperature coefficient to be 0.023, which is significantly greater than the effect found here for short wetted-wall columns. The increase in effect may be explained by an increase in intensity of rippling with temperature, due to the decrease in viscosity which increases the Reynolds number.

The unstable flow could very easily be affected by differences in the manner in which the liquid enters the column, and perhaps by vibration in the column caused by pumps or other moving equipment. This would account for the wide differences between the coefficients measured by the various investigators.

By operating with the short column, it appears that many of these difficulties can be eliminated. The absence of ripples and the good agreement with theory indicate that these results could be duplicated by other workers. These provide more arguments for the use of the short wetted-wall column instead of the long one, as a device for studying liquid-

side controlled mass transfer.

C. Description of Chlorine from Water

5.14. Correction for Temperature. As stated in Sec. 5.6, no experimental determination of the effect of temperature on the coefficient of desorption of chlorine was made. All runs were made within the temperature range 24.7 to 26.4°C., so that only a small correction was required to bring the coefficients to the standard temperature of 25°C. The correction factor was calculated by eq. (5.19). As before, $d\mu/\mu dt = -0.023$. From Fig. 11.5, which is a plot of $\log D$ versus $1/T$ for chlorine in water, the temperature coefficient of diffusivity for chlorine in water is calculated to be 0.028. Substituting into eq. (5.19) gives $dk_L^*/k_L^* dt = 0.5 (0.028) - (0.23)(-0.023) = 0.019$. Thus all runs have been corrected by multiplying the coefficient by a factor

$$e^{0.019(25 - t^\circ\text{C})}$$

The correction was never greater than 2.6%; for all but seven of the 98 chlorine runs, the correction was less than 1%.

5.15. Method of Calculating Coefficients. In the chlorine runs, the rate of desorption is measured directly by collecting in an absorption train the chlorine desorbed in a given length of time. By dividing by the interfacial area, the rate of desorption per unit area, $-N_A$, is determined. The driving force for the normal, or "total" coefficient, k_L , is $(C_0 - C_1)$ where, since the penetration theory is considered

valid, C_0 equals the inlet concentration, C_1 , and where the interfacial concentration, C_i is maintained essentially equal to zero. Then, from eq. (2.13),

$$k_L = -N_A/C_1 \quad (5.21)$$

In calculating the pseudo-coefficient, the driving force is $A_0 - A_1$. Just as C_i is zero, so also is A_i . A_0 is the concentration of molecular chlorine present in the inlet liquid stream, so that $A_0 = A_1$. Then, from eq. (2.15),

$$k_{L0} = -N_A/A_1 \quad (5.22)$$

k_{L0} may be calculated from k_L by the equation

$$k_{L0} = k_L C_1/A_1 \quad (5.23)$$

A_1 is calculated from C_1 by the use of the equilibrium relationship given by eq. (2.16):

$$K_c = \frac{(C_1 - A_1)^3}{A_1} \quad (5.24)$$

The value of K_c at 25°, measured by Vivian and Whitney (101) is 3.29×10^{-4} (g. moles/l.)³. Both coefficients, k_L and k_{L0} , were corrected for temperature as described in Sec. 5.14.

5.16. Empirical Correlation of Pseudo-Coefficients.

Fig. 4.11 shows the effect of inlet concentration of chlorine on the pseudo-coefficient for nine values of the water rate. Of the 86 runs presented, all but 16 were taken at one of these nine water rates. The remaining 16 runs are corrected to the nearest of the nine values of Γ by assuming the pseudo-coefficient is proportional to $\Gamma^{0.2}$. The corrections

are less than 3%. The justification for the exponent of 0.2 will be discussed below.

Over the range of C_1 below 0.040 moles/l., the pseudo-coefficient is found to be independent of the inlet concentration. For this range of concentrations, the pseudo-coefficients are plotted against water rate in Fig. 4.12.

For these runs, the value of ϕ is calculated, using the definition

$$\phi = k_{L0}/k_L^* \quad (5.25)$$

For each run, k_L^* is calculated from eq. (5.4) using the diffusivity of molecular chlorine. ϕ is plotted against water rate in Fig. 5.5. A smooth curve is drawn through the data, which tends to flatten out for low values of Γ , and which approaches one as an asymptote for large values of Γ . Using this smooth curve for ϕ , and the values of k_L^* from eq. (5.4), the curve for k_{L0} shown in Fig. 4.12 is calculated.

If a straight line were put through the points of Fig. 4.12, it would have a slope of approximately 0.2. Thus, as pointed out at the beginning of this section, the pseudo-coefficient was assumed to vary as $\Gamma^{0.2}$ for the purpose of correcting the pseudo-coefficient for water rate. Since the corrections were so small, a more refined procedure would not have been justified.

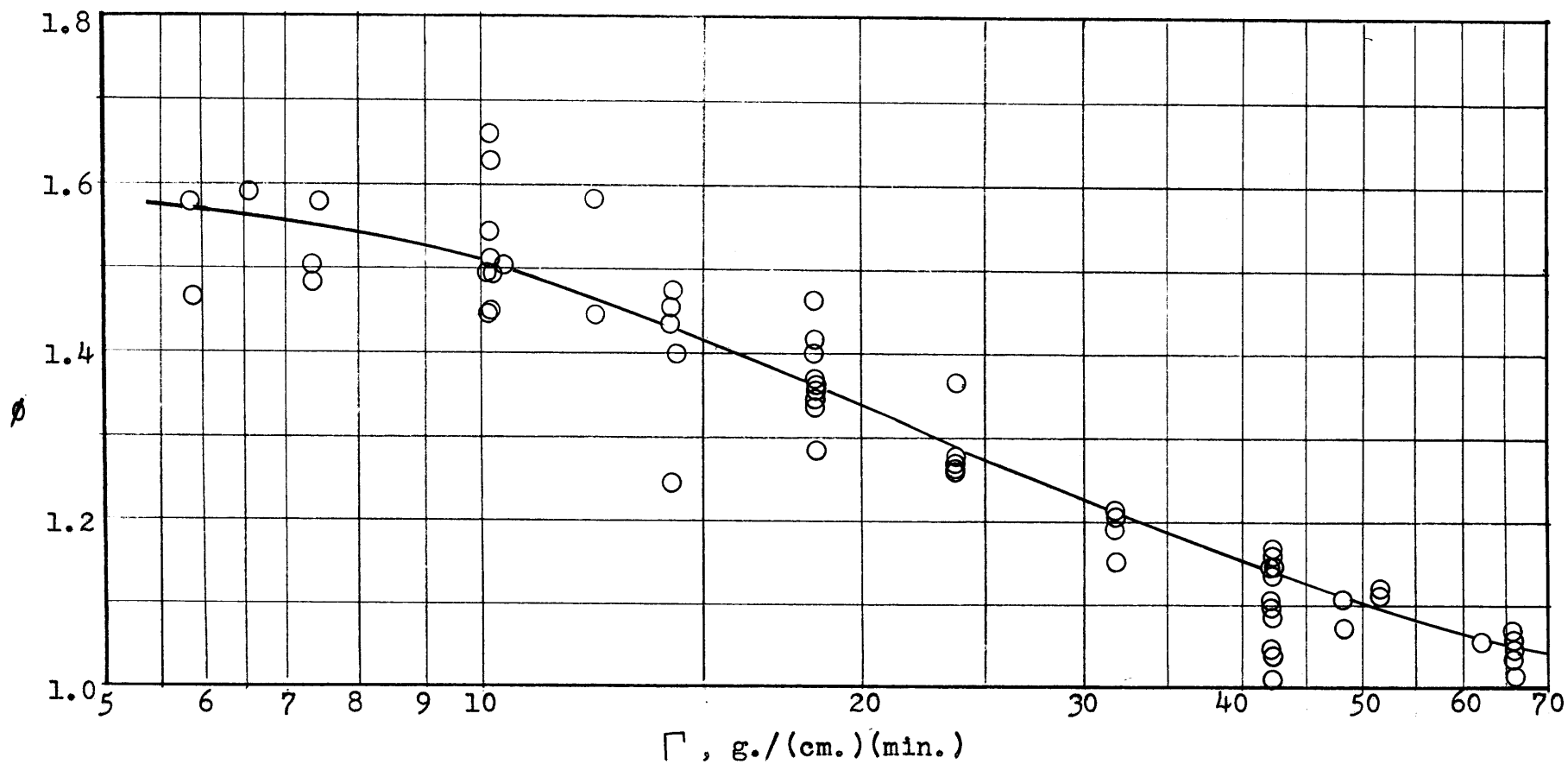
Examination of Fig. 4.11 shows that at constant water rate, for C_1 greater than 0.040 moles/l., the pseudo-coefficient increases with increasing inlet concentration. As

Fig. 5.5

Experimental Values of ϕ for Desorption of Chlorine from Water
in a Short Wetted-Wall Column

Inlet Concentration Less than 0.040 mole/l.

Temp. = 25°C.



far as can be seen from these data, no tendency exists for the pseudo-coefficient to level off at the high concentrations. It was decided, quite arbitrarily, to represent these data by two straight lines on the graph of pseudo-coefficient versus inlet concentration, one horizontal and one sloping. Because of the lack of sufficient data to warrant a more complex correlation, it was decided, also quite arbitrarily, to have the intersection of the two lines be constant, independent of water rate. Finally, since inspection of the graphs shows that the slope of the inclined line should increase with increasing water rate, it was decided to have the slope be a power function of Γ .

It is quite clear that the ordinate of the horizontal lines must be the value of the pseudo-coefficient given by the smooth curve of Fig. 4.12. Let this value be $(k_L^\circ)'$, which is a function only of Γ . Let the concentration at which the lines intersect be C_1' . Then, the empirical correlation may be expressed in two parts:

$$k_L^\circ = (k_L^\circ)' \quad C_1 < C_1' \quad (5.26)$$

$$k_L^\circ = (k_L^\circ)' + \sigma(C_1 - C_1') \Gamma^\nu \quad C_1 > C_1' \quad (5.27)$$

It remains to evaluate the constants σ , C_1' and ν . Inspection of Fig. 4.11 shows that C_1' will lie between 0.030 and 0.050 moles/l. Plots of $[k_L^\circ - (k_L^\circ)'] / (C_1 - C_1')$ versus Γ were made on logarithmic coordinates for each of the values of C_1 of 0.030, 0.035, 0.040, 0.045 and 0.050 moles/l. The

least scatter was obtained for $C_1 = 0.040$. The best straight line was drawn for this plot, with the most weight being given to the runs made at concentrations above 0.060 moles/l. The slope of this line gave $\nu = 0.4$, and the intercept gave $\sigma = 2.9$. The final form of the empirical correlation, valid over the range $0.005 < C_1 < 0.075$ moles/l., is

$$k_L^\circ = (k_L^\circ)^\dagger \quad C_1 < 0.040 \quad (5.28)$$

$$k_L^\circ = (k_L^\circ)^\dagger + 2.9(C_1 - 0.040) \Gamma^{0.40} \quad C_1 > 0.040 \quad (5.29)$$

where the coefficients are expressed in cm./min., and in g./((cm.)(min.)).

Some statistics concerning the agreement of this correlation with the data are as follows: The average deviation is 4.2%; the standard deviation is 6.7%. Of the 86 runs made, 75% have deviations less than 5%. Runs No. 175 and 181 have deviations of 22.5 and 36.6%, respectively. Since these are more than four times the average deviation, they may be rejected. If these two runs are excluded, the average deviation is 3.6% and the standard deviation is 4.9%. Comparison with similar statistics for the physical coefficients show that the precision of the $\text{Cl}_2\text{-H}_2\text{O}$ coefficients is almost twice as good as that of the physical coefficients, a reflection of the superiority of the analytical procedure for the chlorine runs to the procedure for the carbon dioxide runs.

5.17. Effect of Concentration on Total Coefficient.

Because the pseudo-coefficients were found to vary in a simple manner with the concentration, compared with the manner

in which the "total" coefficient varies, the pseudo-coefficients were presented in the Results Section, and were discussed first. In Fig. 5.6, the "total" coefficient, k_L is plotted against inlet concentration of chlorine for each of nine water rates. For the 16 runs which were taken at other than these nine rates, the "total" coefficient was corrected by assuming it to be proportional to $\Gamma^{0.2}$, just as for the pseudo-coefficient.

The curves in Fig. 5.6 are calculated from the empirical correlation, eqs. (5.28) and (5.29). The values of k_L° calculated from these equations are multiplied by A_1/C_1 to obtain k_L , as indicated by eq. (5.23). The agreement between the curves and the points is naturally the same as that obtained in Fig. 4.11 for the pseudo-coefficients.

On each graph in Fig. 5.6, a horizontal line representing the physical coefficient, calculated from eq. (5.4), is drawn. The significance of the comparison of the normal with the physical coefficient is discussed in the next section.

5.18. Comparison of Experimental Results with Theory.

In the Results Section, it was pointed out that two sets of equations have been derived for the absorption of chlorine in water (these equations also apply to the desorption of chlorine from water), whereby ϕ can be calculated from k_L^* , C_0 and A_1 . The assumptions leading to these equations were also presented in the Results Section. One set of equations assumes, among other things, that the mechanism of the hydrolysis of chlorine is

Fig. 5.6

Effect of Inlet Concentration on "Total" Coefficient of Desorption of Chlorine from Water in a Short Wetted-Wall Column

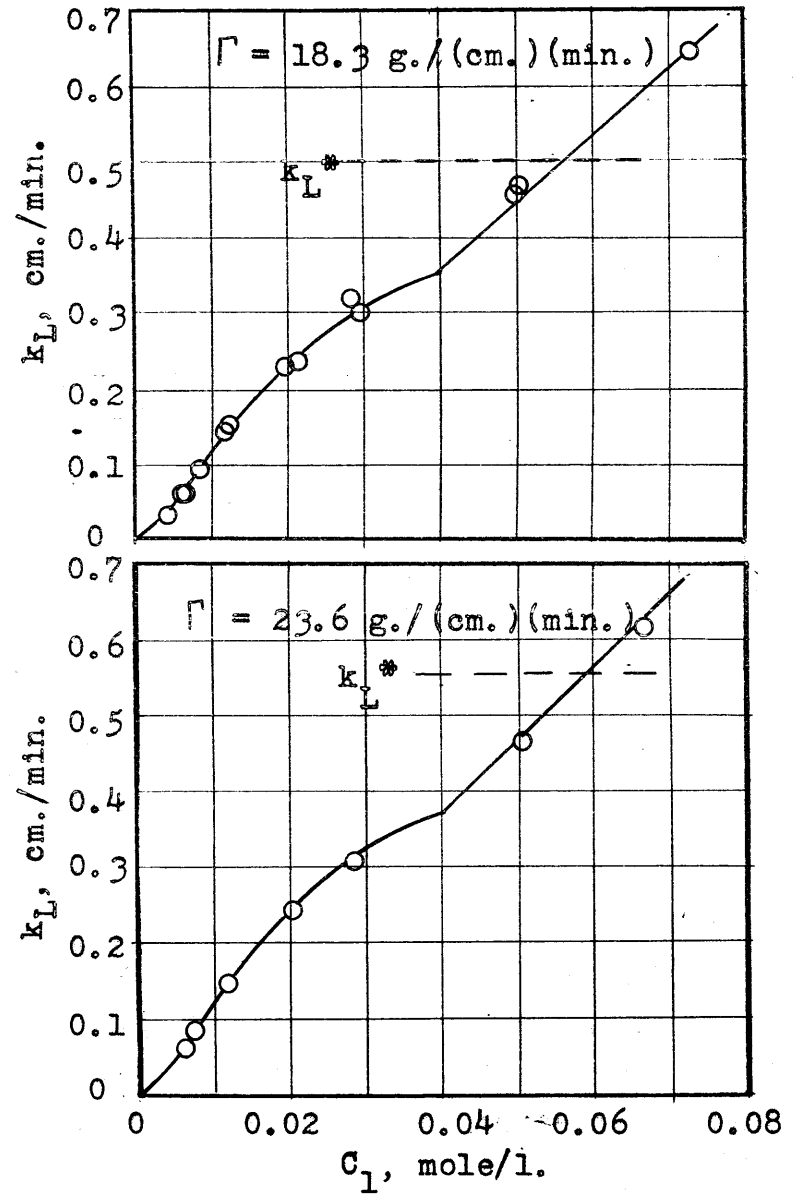
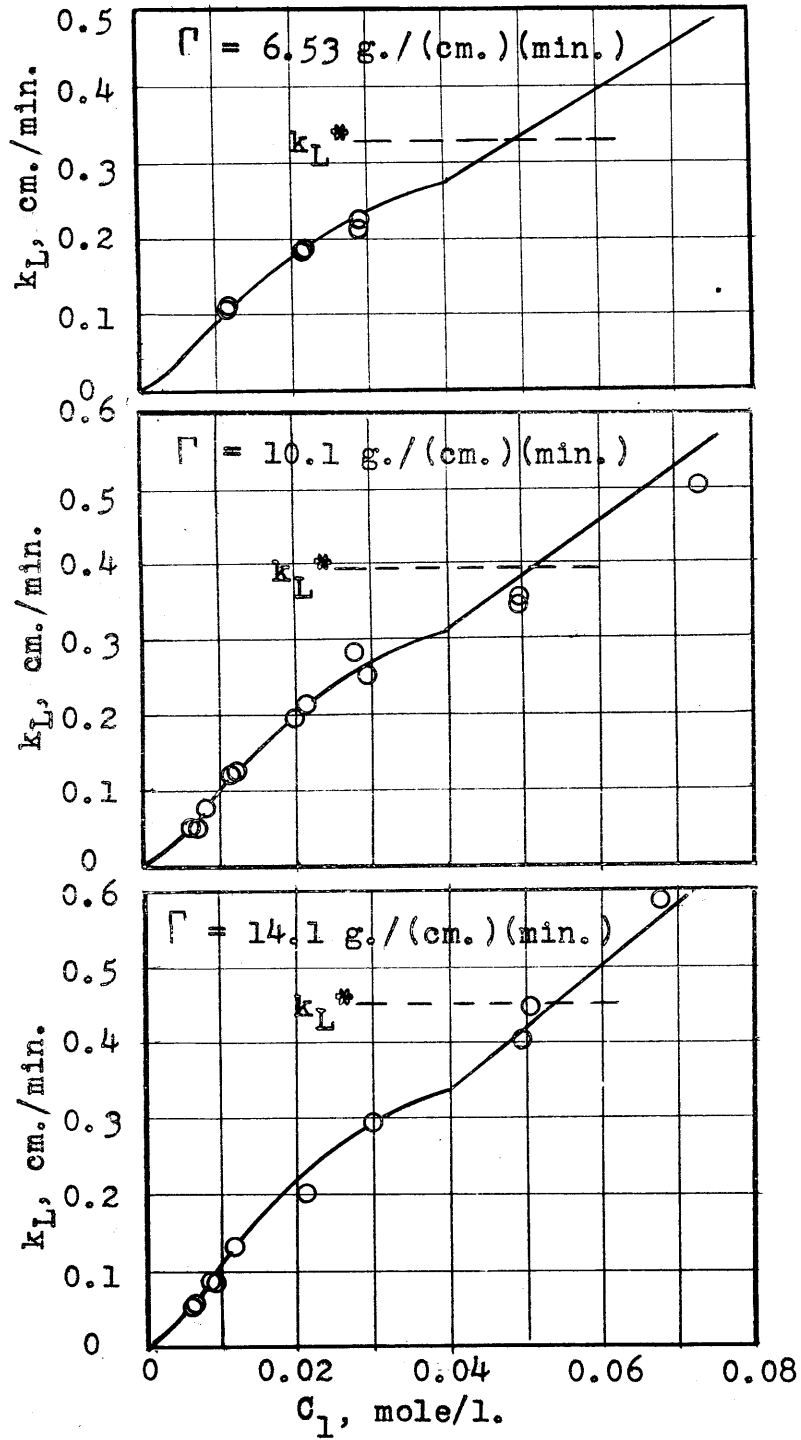
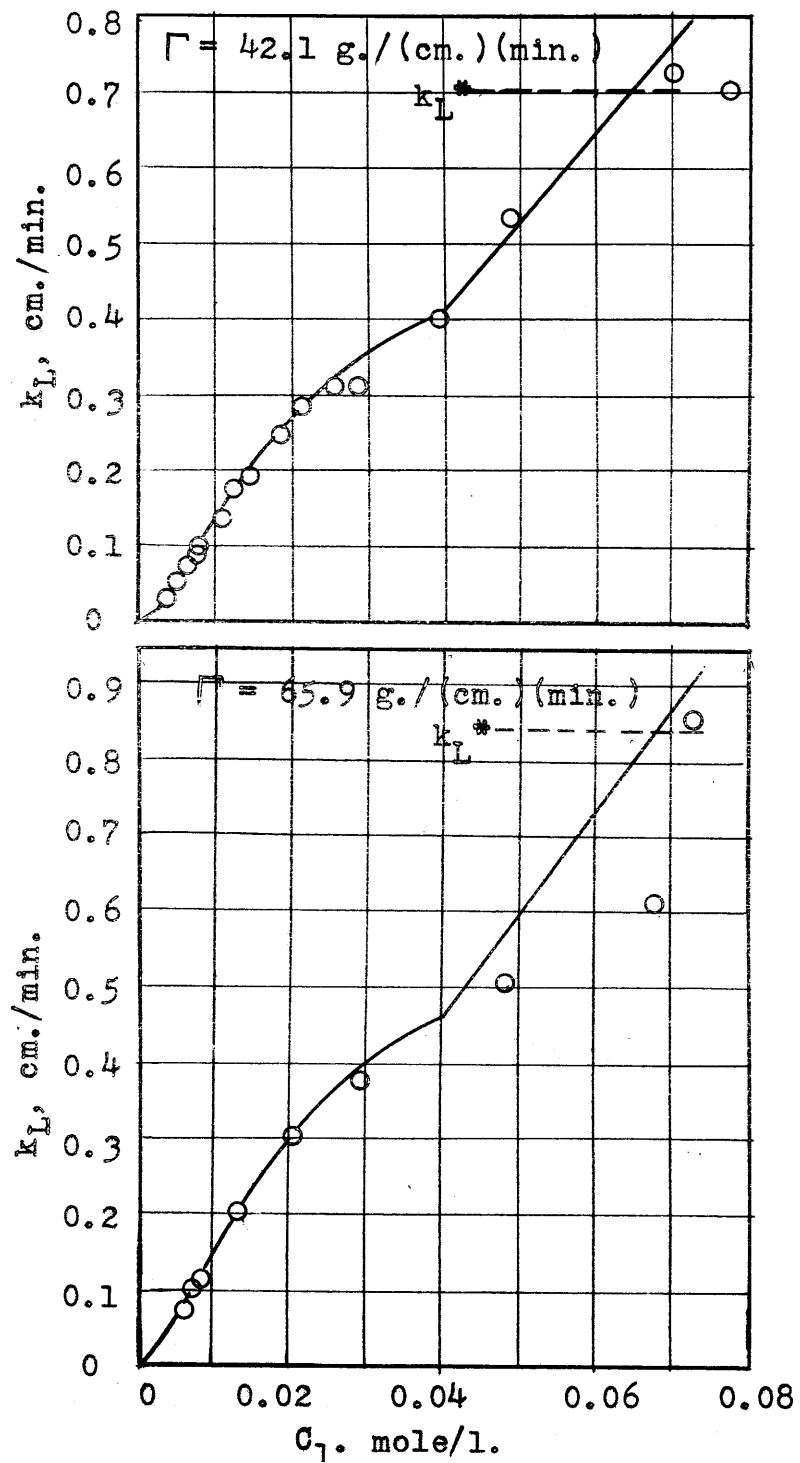
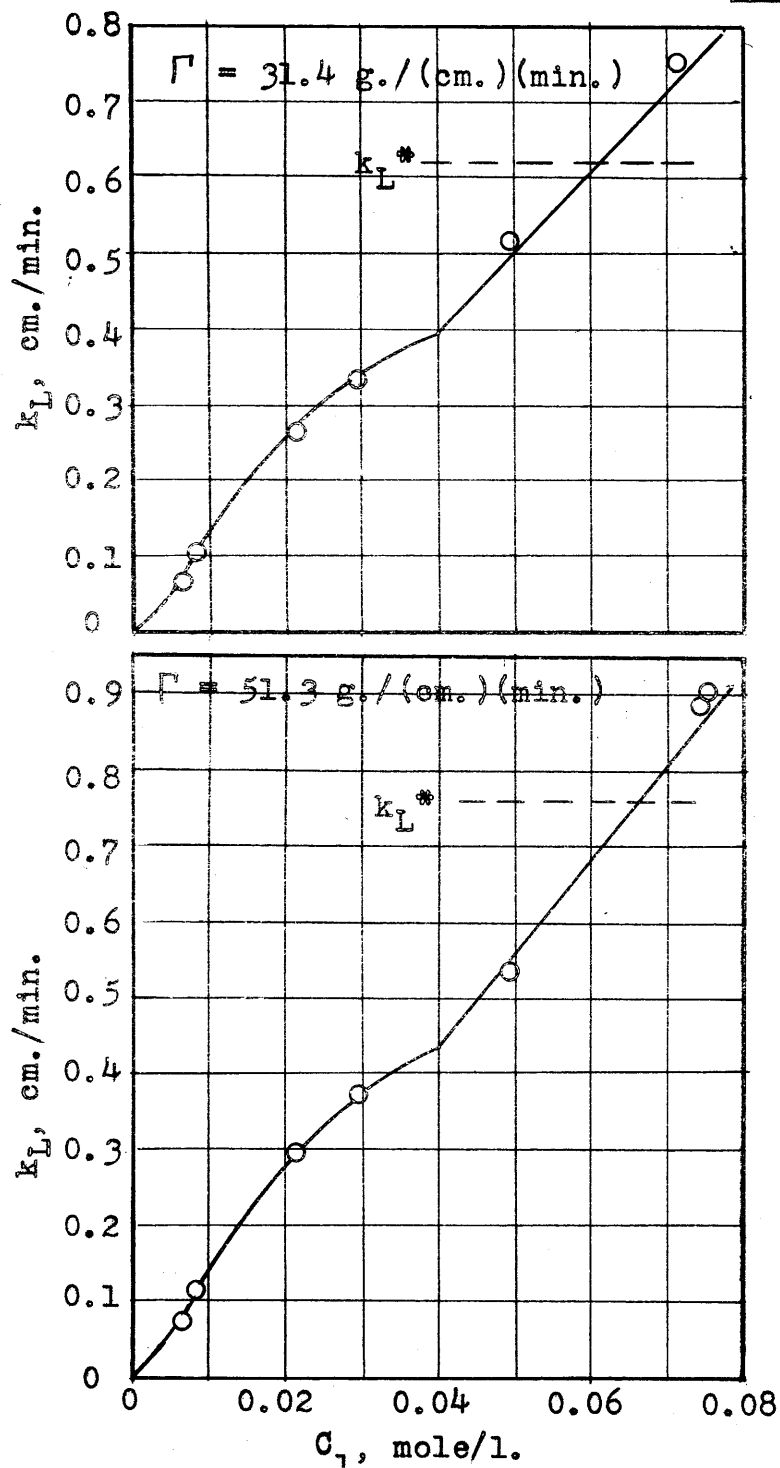
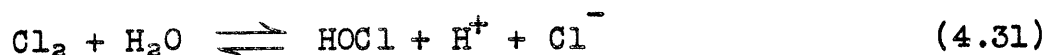


Fig. 5.6 (contd.)





The other set of equations assumes that the mechanism is



The available rate data on the hydrolysis of chlorine were analyzed in terms of both mechanisms by Quincy (86), and rate constants calculated. These along with the equilibrium constants and the diffusivity were substituted into the derived equations to calculate ϕ as a function of k_L^* for various values of C_0 and A_1 for both mechanisms. These calculations are described more fully in Chapter 9 in the APPENDIX.

Since desorption of chlorine from water is under consideration, A_1 is equal to zero. For this value of A_1 , the results of the calculations for the range of k_L^* encountered in the wetted-wall column are plotted as dotted curves in Figs. 5.7 and 5.8 for various values of C_0 . The curves in Fig. 5.7 are based on mechanism (4.30), while those in Fig. 5.8 are based on mechanism (4.31). Comparison of the two figures shows that for the range of C_0 and k_L^* encountered in this experimental work, the two mechanisms give values of ϕ within about 10%.

On these two figures, solid curves are presented, which represent the empirical correlation for desorption of chlorine from water in the short wetted-wall column. ϕ was obtained by dividing the pseudo-coefficient calculated by eqs. (5.28) and (5.29) by the value of k_L^* calculated from Γ by means of eq. (5.4).

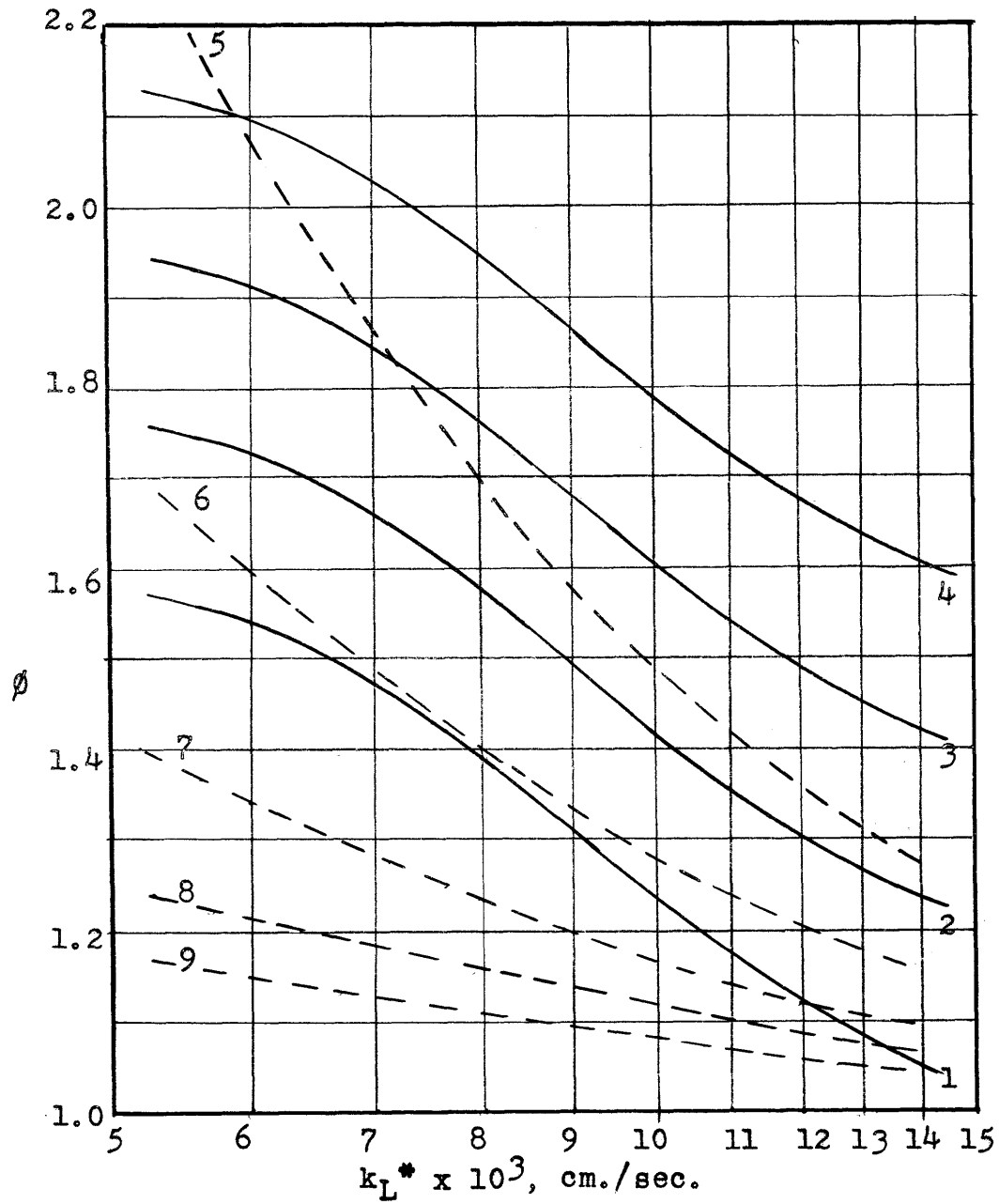


Fig. 5.7
Desorption of Chlorine from
Water; Comparison of Theory
with Experiment

LEGEND

<u>Line</u>	<u>C₁, mole/l.</u>	<u>Note</u>
1	0.005-0.04	Exptl.
2		
3		
4		
5	0.005	Theor.:
6		
7		
8		
9		
		Based on
		$\text{Cl}_2 + \text{OH}^- \rightleftharpoons$
		$\text{HOCl} + \text{Cl}^-$

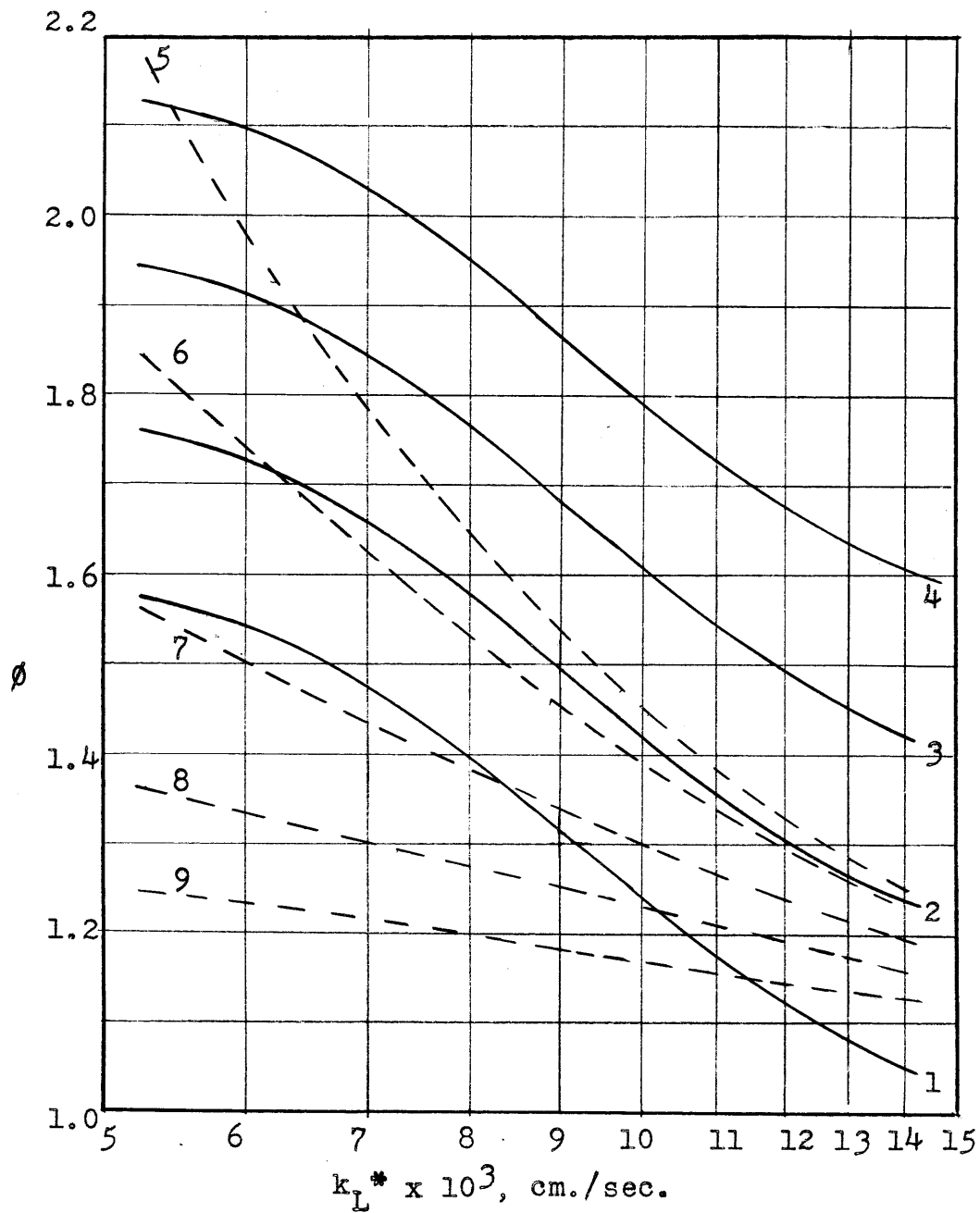


Fig. 5.8

Desorption of Chlorine from Water; Comparison of Theory with Experiment

LEGEND

<u>Line</u>	<u>C₁, mole/l.</u>	<u>Note</u>
1	0.005-0.04	} Exptl.
2	0.05	
3	0.06	
4	0.07	
5	0.005	} Theor.: Based on $\text{Cl}_2 + \text{H}_2\text{O} \rightleftharpoons \text{HOCl} + \text{H}^+ + \text{Cl}^-$
6	0.01	
7	0.02	
8	0.04	
9	0.07	

Comparison of the solid and dotted curves in Figs. 5.8 and 5.9 show that the theory fails very badly in predicting the experimental results. The most significant aspect of the failure is that the theory predicts that ϕ decreases with increasing concentration of chlorine, while it was found experimentally that the pseudo-coefficient, and hence ϕ , remains constant with concentration over the range 0.005 to 0.040 moles/l., and then increases sharply with concentration.

As pointed out in the Results Section, in deriving the theoretical equations it was not possible to obtain a solution based on the penetration theory. It was necessary to assume, in calculating ϕ from k_L^* , C_0 , A_1 , and the constants of the reaction, that both the film theory and penetration theory give approximately the same answer. Because the physical pictures represented by the two theories are so different, there is no reason to expect that they should give the same answer, yet this assumption was shown (in Chapt. 8 in the APPENDIX) to be valid for first order reversible reactions. Furthermore, although one might expect this assumption to lead to an error in the magnitude of ϕ , it is not unreasonable to suppose that both the film and penetration theories should predict the same effect of concentration on ϕ .

In Sec. 9.11 in the APPENDIX, it is shown that there exists an upper limit on ϕ :

$$\phi < C_0/A_0 \quad (4.60)$$

This equation can be derived using either the film theory or the penetration theory. The assumptions made are that the hydrolysis reaction is infinitely rapid, that the diffusivity of hydrochloric acid is infinitely rapid and that the diffusivity of molecular chlorine, Cl_2 , is equal to the diffusivity of hypochlorous acid, HOCl . The last assumption is not a serious one, since they actually differ by only 5% (see Sec. 4.4). It is shown that for finite values of the hydrolysis rate and of the diffusivity of HCl , the value of ϕ must be less than that given by eq. (4.60).

From the definition of ϕ (eq. (5.25)) and from eq. (5.23),

$$k_L = k_L^\circ A_1/C_1 = k_L^* \phi A_1/C_1.$$

Combining with eq. (4.60) gives an upper limit to k_L (noting that $A_0 = A_1$, $C_0 = C_1$),

$$k_L < k_L^* \quad (5.30)$$

This is a conclusion that can be arrived at solely from physical considerations. It should be expected that for a given concentration of chlorine in the liquid, and zero interfacial concentrations, the rate of desorption would be greater if the chlorine were uncombined with the water than if some of the chlorine is combined with the water and has to undergo a reaction of finite rate in order to be desorbed. Although this conclusion has been shown mathematically to be valid for the film and penetration theories,

it is reasonable to suppose that it could be proven mathematically for any other mechanism of the liquid side resistance that might be proposed.

Yet, the experimental results violate this conclusion. Fig. 5.6, where k_L is plotted versus C_1 , and where k_L^* is presented for comparison, shows that at high values of C_1 the "total" coefficient exceeds the physical coefficient. There are sufficient data in the high concentration region to prove definitely that the physical coefficient has been exceeded. Furthermore, the data do not indicate any tendency of the "total" coefficient to level off with increasing concentration, but, rather, indicate that it will keep right on increasing for higher values of C_1 .

That this behavior is a property of the chlorine-water system, and not of the apparatus is indicated by some experiments of Kniel (56). He studied desorption in a batch system, in which air was blown over a stirred water surface in a flask. He measured rates of desorption for hydrogen sulfide from water, carbon dioxide from water and chlorine from dilute hydrochloric acid at different rates of stirring of the liquid. The coefficients of desorption were found to be independent of time, and hence independent of concentration, and therefore were physical coefficients. They were found to vary as the 0.67 power of the stirring rate. In addition, one run on the desorption of chlorine from water was made. The concentration versus time data are shown on Fig. 5.9. The coefficient of desorption, based on the total chlorine driving force, was found

Fig. 5.9

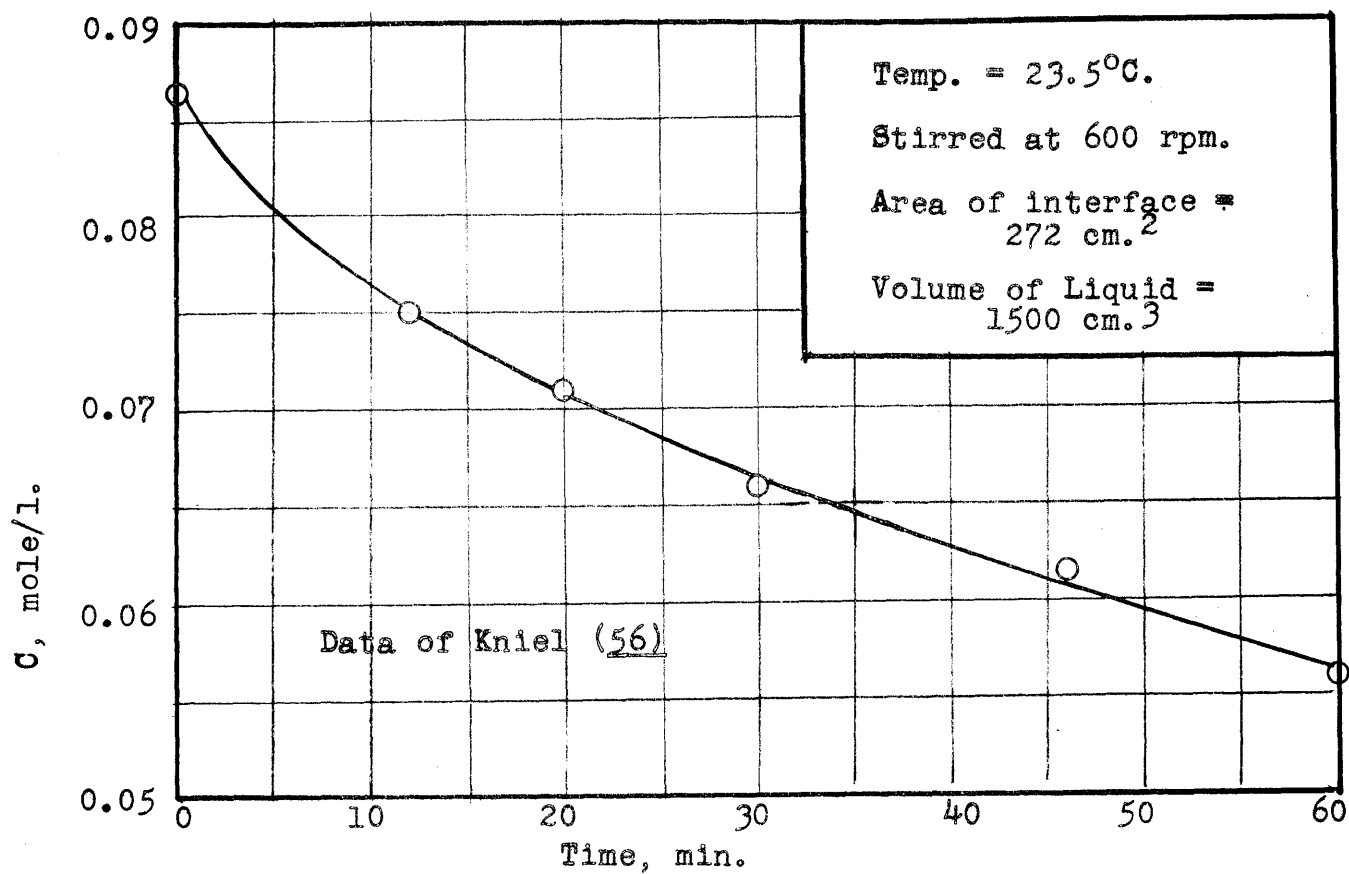
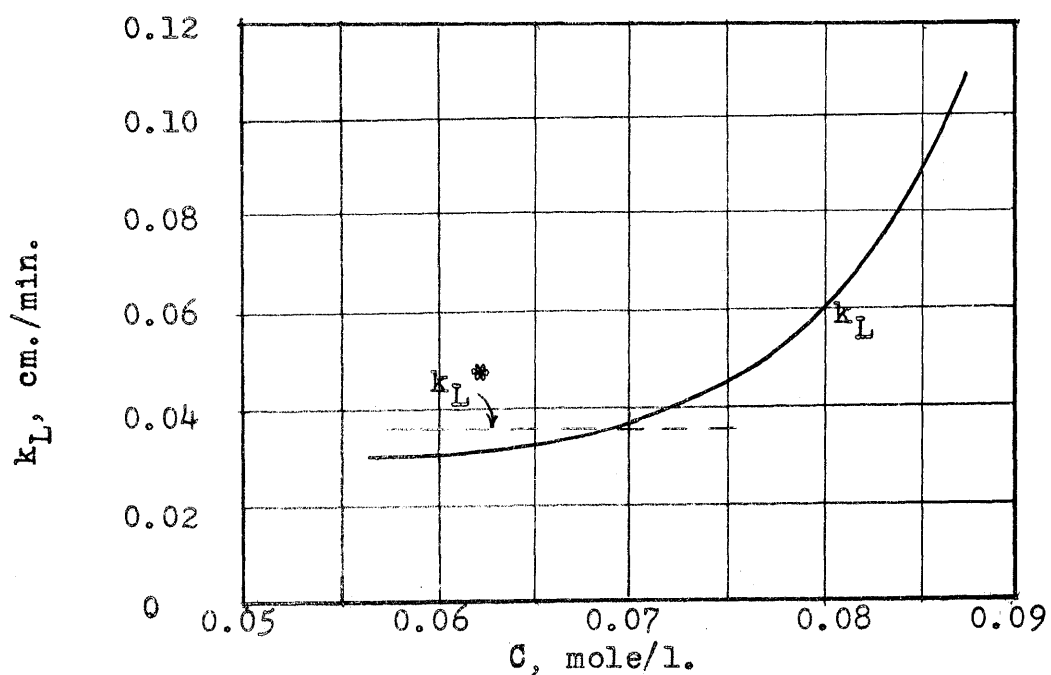
Desorption of Chlorine from Water in a Stirred Flask

Fig. 5.10

Desorption of Chlorine from Water in a Stirred Flask

to vary with time and, hence, with concentration, as shown in Fig. 5.10. On this figure is shown also the physical coefficient for the desorption of chlorine from 0.2N hydrochloric acid at the same stirring rate. Here, again, the "total" coefficient exceeds the physical coefficient at high concentrations of chlorine, and increases rapidly with concentration, showing no tendency to level off at high concentrations.

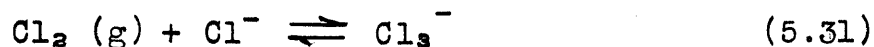
There are, then, two major contradictions between experiment and theory: the effect of concentration on k_L° , and the fact that at high concentrations k_L exceeds k_L^* . Obviously, one or more of the assumptions made in deriving the theoretical relations must be invalid, particularly at high concentrations of chlorine. It is easier to examine the second contradiction since fewer assumptions are involved. Probably when it is explained, the first contradiction will also be explained. In deriving the upper limit for the coefficient, the assumptions made include those involved in the film or penetration theory itself, which were discussed in the Introduction. That the penetration theory is valid in the short wetted-wall column has been shown in the discussion of the physical coefficients. It is further assumed that the hydrolysis reaction rate is infinite and that the diffusivity of HCl is infinite. The fact that they are finite has been shown to cause the rate of desorption to be lower than this upper limit, and hence need not be discussed here. It is not necessary to make any assumption regarding the mechanism of the reaction, since the assumption of

infinite rate means that equilibrium exists throughout the liquid. A very important assumption is the nature of the equilibrium. It is assumed that

$$K_c = \frac{EF^2}{A} \quad (2.10)$$

where A is the concentration of molecular chlorine, E the concentration of HOCl, and F the concentration of HCl. Vivian and Whitney's (101) solubility data, from which K_c was calculated assuming an equilibrium of this type, were obtained up to one atmosphere partial pressure of chlorine, and the data indicate no anomalous behavior at the high chlorine concentrations. Judging from these data, there is no reason to suspect the validity of this equilibrium relationship.

One possibility remains. What is taken for the physical coefficient is perhaps not the physical coefficient at all. Perhaps the solution of chlorine in hydrochloric acid contains a hydrate of chlorine or some compound of chlorine and hydrochloric acid. Sherrill and Izard (91) studied the solubility of chlorine in solutions of hydrochloric acid and found that the solubility of chlorine in water is decreased by small additions of HCl, but is increased by larger additions of acid. The initial decrease in solubility is readily explained by the depression of the hydrolysis of the chlorine by the added acid. At higher concentrations of HCl, however, where the percentage hydrolysis is reduced to an extremely small value, the increased solubility indicates the existence of a complex ion, probably the trichloride ion. From their data, they computed the equilibrium constant for the reaction



and found it to be

$$\frac{[\text{Cl}_3^-]}{[\text{Cl}^-] P_{\text{Cl}_2}} = 0.01 \quad (5.32)$$

at 25°C. Substituting Henry's law for molecular chlorine,

$$[\text{Cl}_2] = A = HP \quad (5.33)$$

into eq. (5.32) gives

$$[\text{Cl}_3^-] / [\text{Cl}_2] = 0.01 [\text{Cl}^-] / H \quad (5.34)$$

The highest concentration of HCl used was 0.18 moles/l. H is equal to 0.0625 g.moles/(1.)(atm.). The maximum percentage of chlorine as trichloride, then, is 2.9% which may be neglected. If chlorine did form some compound to an appreciable extent in the dilute HCl solution, desorption of chlorine from dilute hydrochloric acid would then be accompanied by chemical reaction, and the coefficient measured would be lower than the true physical coefficient. That this is unlikely is indicated by two facts. First, no significant effect of concentration of chlorine was noted in studying the desorption of chlorine from dilute HCl, as can be seen from Fig. 4.10, over the range of chlorine concentration from 0.011 to 0.040 moles/l. Secondly, the coefficients obtained for the desorption of chlorine from dilute HCl agreed very well with those obtained for the desorption of carbon dioxide from water, suitable correction being made for diffusivity, and there is no reason to doubt that the carbon dioxide coefficients are true physical

coefficients.

Several possible explanations for these contradictions between theory and experiment have been considered and rejected. Thus far, it has not been possible to arrive at any explanation of this very puzzling behavior of the chlorine-water system.

An experimental program for solving this anomaly should involve studying the chlorine-water system at still higher concentrations, in order to see if there develop any serious deviations in the various assumptions that are made in deriving the upper limit for the desorption rate. The diffusivity of chlorine in water should be studied at higher concentrations than used in this thesis (reported in Chap. 11 in the APPENDIX) and solubility data should be taken at higher concentrations than those used by Vivian and Whitney (101) to see if there exist any peculiar behavior at the higher concentrations which might give a clue as to what is happening here. Data on desorption of chlorine from water should be taken at still higher concentrations to see if k_L^* continues to increase with C_1 or whether it eventually levels off. The data on desorption of chlorine from dilute hydrochloric acid should be extended to higher concentrations of chlorine. All of these experiments would involve working at superatmospheric pressure, which would make the equipment required much more complicated than has been necessary so far.

D. Application of Results to the Study of Packed Columns

Although no data on packed columns were obtained in this thesis, it is possible to combine some of the results obtained on the short wetted-wall column with packed column data and thereby gain some information concerning packed columns. It should be recognized that the following discussion lies in the realm of conjecture; the conclusions reached, while interesting, should not be regarded as having as much significance as more direct experimental evidence.

5.19. Effect of Temperature. For the desorption of carbon dioxide in the short wetted-wall column, k_L^* was found experimentally to vary as $e^{0.011t}$, where t is in degrees centigrade, while the dimensionless equation (5.18) led to the relation that k_L^* is proportional to $e^{0.016t}$ (Sec. 5.12). Sherwood and Holloway (93) found for the desorption of carbon dioxide in a packed column that k_L^*a varies as $e^{0.023t}$. This may be written

$$\frac{d k_L^*a}{k_L^*a dt} = \frac{dk_L^*}{k_L^*dt} + \frac{da}{a dt} \quad (5.35)$$

Using the figure for the temperature coefficient of k_L^* obtained from the dimensionless correlation, 0.016, we obtain

$$\frac{da}{adt} = 0.023 - 0.016 = 0.007$$

In Sec. 5.12, it was shown that $d\mu/\mu dt$ equals -0.023 , whence it is calculated that

$$\frac{d \ln a}{d \ln \mu} = - \frac{0.007}{0.023} = - 0.3$$

That is, a varies inversely as the 0.3 power of viscosity.

Qualitatively, it is reasonable to expect that the wetting of the packing should improve as the viscosity decreases. The figure of 0.3 found here has little significance, because of the poor precision of the data and of the calculations upon which it is based. It would be possible to determine more precisely the variation of wetted area with viscosity by studying the desorption of carbon dioxide from glycerine solutions of various concentrations in both the short wetted-wall column and the packed column.

5.20. Comparison of Physical Coefficients. Some information may be obtained by comparing the physical coefficients obtained in a short wetted-wall column with physical coefficients measured in a packed column. As pointed out in the Introduction, Craig (17) absorbed chlorine in 0.2 normal HCl in a column packed with one-inch Raschig rings. His data are plotted in Fig. 12.3 in the APPENDIX, and as line C-C in Fig. 2.1. The equation representing his data is

$$k_L^* a = 0.082 L^{0.075} \quad (5.36)$$

where $k_L^* a$ is expressed in reciprocal hours, and L in lbs./hr. (ft.²). For length of 1 inch, and $D = 1.48 \times 10^{-5}$ cm.²/sec. (the diffusivity of molecular chlorine), eq. (5.4) becomes

$$k_L^* = 0.202 \Gamma^{0.40} \quad (5.37)$$

where k_L^* is expressed in cm./min., and Γ in g./cm.(min.).

Also,

$$k_L^* = 0.227 \Gamma^{0.40} \quad (5.38)$$

where k_L^* is expressed in ft./hr., and Γ in lb./(ft.)(hr.).

Consider a cube of packing, one foot on each edge. L lb./hr. of liquid pass through this cube. The wetted area in the cube is a ft.². Assuming that the wetted perimeter is constant at each cross-section, the wetted perimeter available for flow is a ft. Then, the flow rate per unit perimeter is $\Gamma = L/a$ lb./(ft.)(hr.). Substituting into eq. (5.38) gives

$$k_L^* = 0.227 (L/a)^{0.40} \quad (5.39)$$

Eliminating k_L^* between eqs. (5.36) and (5.39) gives

$$0.227 a(L/a)^{0.40} = 0.082 L^{0.75}$$

or

$$a^{0.60} = 0.361 L^{0.35}$$

Finally,

$$a = 0.184 L^{0.58} \quad (5.40)$$

Using this equation, the liquid rate at which the packing becomes completely wet can be calculated. The dry surface area of one-inch Raschig rings is given in a table in Sherwood (92) as 58 ft.²/ft.³. Using this value for a gives $L = 20,000$ lb./(hr.)(ft.²). This is in remarkable agreement with the results of Sherwood and Holloway (93) who, in desorbing oxygen from water in one-inch Raschig rings, found that as the water rate was increased, k_L^*a increased, up to $L = 20,000$ lb./(hr.)(ft.²), after which k_L^* leveled off and

decreased for further increase in water rate. Quoting from Sherwood and Holloway (93):

"These results are typical of those obtained with other packings Contrary to the first supposition the point at which the data break away from the linear relation is not the loading point, but corresponds to a considerably smaller value of L than that at which loading occurs. It is believed that at this "break-away" point the liquid in the packing is beginning to bridge over the free spaces formerly filled with air, and cause much of the free space of the packing to be filled with water. Such a phenomenon would cause a marked decrease in the effective interfacial area, and account for the abnormal changes in $k_L a$ and $(H.T.U.)_L$ at high liquid rates. "

It would be expected that at this "break-away" point, the packing is completely wetted.

5.21. Comparison of Data on Chlorine-Water System.

Finally, by comparing the data on desorption of chlorine in the short wetted-wall column with data on absorption of chlorine in water in a packed column, another estimate of the interfacial area in a packed column may be obtained.

Vivian and Whitney's (101) data on absorption of chlorine in water in one-inch Raschig rings may be compared with Craig's (17) data on absorption of chlorine in 0.2 N HCl in one-inch Raschig rings to obtain average values of ϕ . Since, at corresponding liquor rates, the value of a should be the same in both experiments, we may write, from the definition of ϕ ,

$$\phi = \frac{k_L^\circ}{k_L^*} = \frac{k_L^\circ a}{k_L^* a}$$

This ratio may be calculated from lines A-A and C-C drawn in Fig. 2.2.

Now, it was found experimentally in the short wetted-wall column that for the range of concentration of chlorine in the liquid below 0.040 moles/l., ϕ is independent of concentration. Assuming that it is also independent of the interfacial concentration, ϕ is then a unique function of k_L^* . In Figs. 5.7 and 5.8, line No. 1 gives this functional relationship between ϕ and k_L^* . In calculating \underline{a} in the packed column, the procedure is as follows: At each value of L , read off the values of $k_L^* \underline{a}$ and k_L^* from Fig. 2.2 and divide to obtain ϕ . Using this value of ϕ , using line 1 in Fig. 5.7, k_L^* may be obtained. Finally, \underline{a} is computed by dividing $k_L^* \underline{a}$ by k_L^* . These calculations are summarized in Table 5.1.

The results are plotted as line No. 1 on Fig. 5.11. For comparison, eq. (5.40), which was obtained by the comparison of physical coefficients, is shown as line No. 2. De Nicolas (79) calculated values of \underline{a} from Vivian and Whitney's (101) data on absorption of chlorine in water in a packed column, using theoretical values of ϕ (see Sec. 9.3 in the APPENDIX). His results are shown as line No. 3 on Fig. 5.11. Finally, a horizontal dotted line representing the total dry area of the packing is shown.

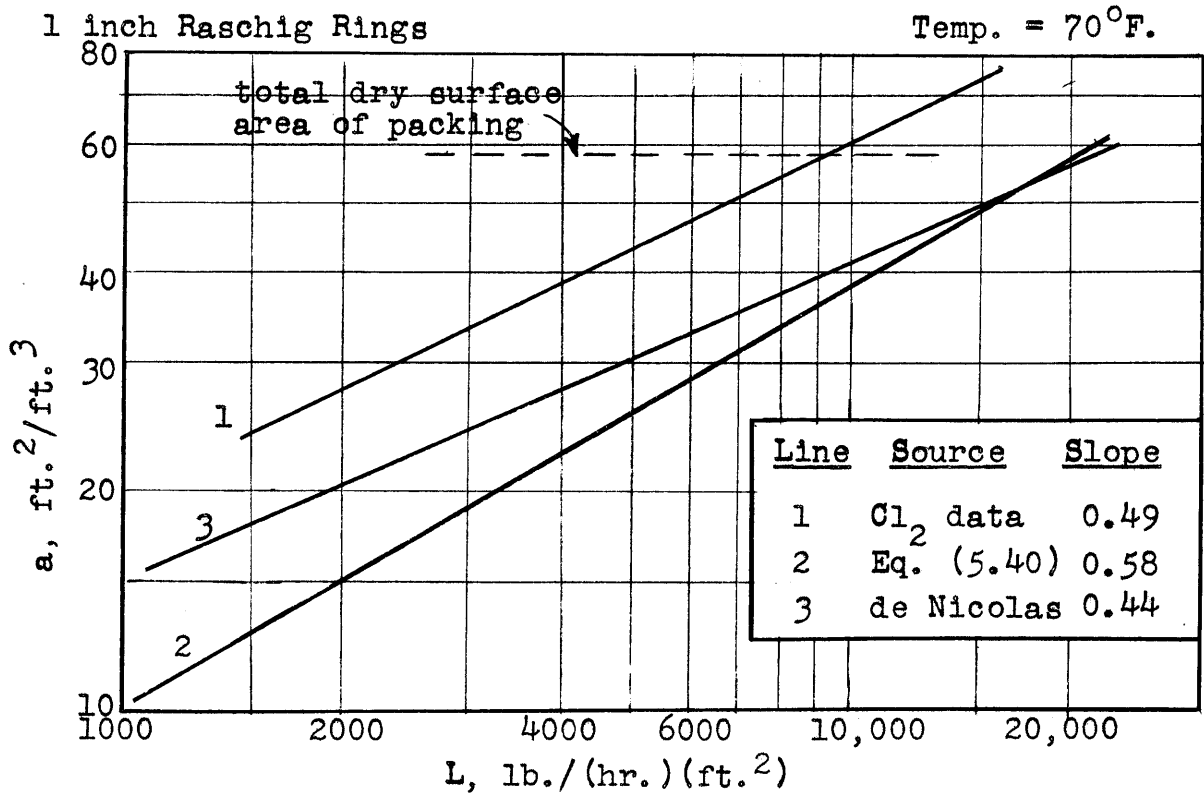
Two of these methods of calculating \underline{a} agree that the packing is completely wetted at a liquor rate of about 20,000 lb./hr. (ft.²), while the third method indicates that the interfacial area at high values of L is even greater than the dry surface area of the packing. Such an increase in inter-

TABLE 5.1

Calculation of Interfacial Area in Packed Column

L lb. (hr.)(ft. ²)	$k_L^* a$ hr. ⁻¹	$k_L^{\circ} a$ hr. ⁻¹	ϕ	$k_L^* \times 10^3$ cm. sec.	a ft. ² / ft. ³
1,500	19.7	29.7	1.51	6.99	24.3
2,000	24.4	35.4	1.45	7.57	27.4
3,000	33.0	45.5	1.38	8.27	33.8
4,000	41.1	54.0	1.314	9.00	38.8
5,000	48.7	61.7	1.268	9.54	43.3
6,000	56.0	69.0	1.232	10.04	47.2
8,000	69.5	82.4	1.184	10.8	54.5
10,000	82.0	94.8	1.155	11.35	61.3
15,000	110.5	121.2	1.097	12.5	75.0

Fig. 5.11

Effect of Liquor Rate on Interfacial Area
in a Packed Column

facial area, if it actually exists, might be attributed to splashing of the liquid between the packing.

From these results, it cannot be concluded definitely what the effect of liquor rate on the interfacial area is, except that it varies as L raised to a power between 0.4 and 0.6. The lack of agreement between the three methods can be attributed to the many assumptions involved, the most serious of which is that the time of exposure is uniform throughout the packing.

Several attempts to measure wetted area of tower packings are described in the literature, but there have been no previous attempts to measure the effective interfacial area under conditions where the liquid-side resistance is controlling, as was done here. Mayo, Hunter and Nash (72) used 1/2- and 1-inch paper Rashchig rings and dissolved dye in the water. They found the wetted area proportional to $L^{0.45}$. This method should be expected to give high results because fluctuations in the liquid path would dye more area than that wetted at any moment and because the interfacial area at points of contact would be much smaller than the wetted packing area (103). Grimley (31) measured wetted area of 3/8-inch stoneware ring packing by measuring its electrical resistance. He found the percentage of area wetted to be 11% for L from 22 to 300; to increase proportional to $L^{0.63}$ for L from 500 to 15,000, and thereafter to remain constant at 103%. However, the electrical resistance does not correctly average the stream cross-section but rather its reciprocal (103). These two methods are attempts to measure wetted area

directly, rather than effective interfacial area.

Van Krevelen, Hoftijzer and van Hooren (62), and Weisman and Bonilla (103) have calculated the effective interfacial area under conditions where the gas-side resistance is controlling. Weisman and Bonilla (103) state that it might be expected that the effective interfacial area for the process in which liquid-side resistance is controlling should be about the same as when gas-side resistance controls. This is not necessarily the case, because of the presence of stagnant portions of liquid and gas. Stagnant pockets of gas would reduce the effective interfacial area when gas-side resistance controls, but not when liquid-side resistance controls; conversely, stagnant portions of liquid would reduce the effective interfacial area when liquid-side controls, but not when gas-side controls. Since the relative amounts of stagnant gas and stagnant liquid would not be expected to be the same, the effective interfacial areas for the two processes should be different. Consequently, the results presented here cannot properly be compared with any previous attempts in the literature to measure interfacial area.

CHAPTER 6CONCLUSIONS

From the results of this thesis, it is concluded that in the short wetted-wall column:

1. The mechanism of the liquid-side resistance is that of unsteady-state diffusion as postulated by the penetration theory.
2. For physical desorption, the penetration theory combined with streamline flow theory predicts from physical constants alone rates which are 30% too high at low liquid flow rates ($\Gamma = 7 \text{ g./}(\text{cm.})(\text{min.})$), and only 10% too high at high liquid flow rates ($\Gamma = 90 \text{ g./}(\text{cm.})(\text{min.})$).
3. The physical coefficient of desorption varies as the 0.40 power of the water rate over the range of water rate of 7 to 90 g./(\text{cm.})(\text{min.}).
4. The physical coefficient of desorption varies inversely as the square root of the length of the column.
5. The physical coefficient varies as the square root of the diffusivity.
6. The physical coefficient of desorption of carbon dioxide from water increases 1.1 per cent for each centigrade degree rise in temperature.

7. There is no significant effect of gas flow rate on the desorption rate up to a Reynolds number in the gas stream of 2200. At higher flow rates, ripples are produced which cause an increase in the desorption rate.
8. In the desorption of carbon dioxide from water, the interfacial concentration of carbon dioxide in the liquid is negligible compared with the average concentration in the liquid.
9. There is no significant effect of entrance slot width or type on the desorption rate. From this and approximate direct measurements it is concluded that the interfacial velocity of the liquid is uniform with distance down the column.
10. In the desorption of chlorine from dilute hydrochloric acid solution, there is no significant effect of concentration of chlorine on the physical desorption coefficient.
11. In the desorption of chlorine from water, the psuedo-coefficient is independent of chlorine concentration over the range of concentration of 0.005 to 0.04 moles/l. At higher concentrations, the psuedo-coefficient increases linearly with concentration up to the highest concentration used, 0.07 moles/l.

12. In the desorption of chlorine from water, the "total", or normal, coefficient increases with concentration and, at high concentrations (above about 0.06 moles/l.) it exceeds the physical coefficient. There appears to be no tendency of the "total" coefficient to level off with increasing concentration.

13. From theoretical considerations, it can be shown that the "total" coefficient cannot exceed the physical coefficient. No explanation for this anomaly can be offered at this time.

It is further concluded, from a comparison of data obtained on the short wetted-wall column with data obtained by other investigators on packed columns that in a column packed with one-inch Raschig rings, when the liquid-side resistance is controlling, the effective interfacial area varies as the liquor rate raised to a power between 0.4 and 0.6, and that it equals the total dry surface area of the packing at a liquor rate of about 20,000 lb./hr. (ft.²).

CHAPTER 7

RECOMMENDATIONS

On the basis of the results of this thesis, it is recommended that:

1. The short wetted-wall column be used to study other systems of absorption or desorption with chemical reaction.

2. A further study of physical coefficients in the short wetted-wall column be made by

a) Absorbing or desorbing oxygen in or from water.

b) Absorbing or desorbing hydrogen in or from water.

c) Absorbing carbon dioxide in water using a pure CO_2 gas stream with pure water inlet, or desorbing carbon dioxide from water and analyzing the gas stream. Either of these methods should give better precision than that obtained on carbon dioxide in this thesis.

d) Absorbing or desorbing carbon dioxide in or from solutions of glycerol in order to determine the effect of viscosity.

e) Absorb or desorb carbon dioxide in or from water over a wider temperature range in order to determine the effect of temperature with greater precision.

3. A further study of the chlorine-water system be made by

studying absorption of chlorine in water at various concentrations of chlorine in the gas and liquid. Higher concentrations of chlorine than those used in this thesis should be investigated.

4. The diffusivity of oxygen, hydrogen and carbon dioxide in water and of carbon dioxide in glycerol solutions be studied. The diffusivity of chlorine at higher concentrations than those used in this thesis should also be measured.

5. The equilibrium of the chlorine-water system be studied at partial pressures of chlorine above one atmosphere.

6. Whenever possible, samples of a liquid containing a volatile solute be taken by introducing the liquid directly below the surface of the liquid in a titration flask, the size of the sample being determined by weighing the flask before and after sampling. The use of pipettes for sampling such liquids is discouraged.

APPENDIX

CHAPTER 8MATHEMATICAL THEORY OF ABSORPTION WITH CHEMICAL REACTIONOutline

	<u>Page</u>
A. Introduction	
8.1 Preliminary Remarks	142
8.2 Nomenclature	142
8.3 Procedure	144
B. The Basic Differential Equations	
8.4 Assumptions of the Film Theory	144
8.5 Basic Equations of the Film Theory	145
8.6 Assumptions of the Penetration Theory	147
8.7 Basic Equations of the Penetration Theory	148
8.8 Effect of Acceleration of the Liquid on the Basic Differential Equation of the Penetration Theory	150
C. The Film Theory of Absorption with First Order Chemical Reaction	
8.9 Physical Absorption or Desorption	152
8.10 First Order Irreversible Reaction	153
8.11 The Effect of Holdup	154
8.12 First Order Reversible Reaction	158
D. The Penetration Theory of Absorption with First Order Chemical Reaction	
8.13 Physical Absorption or Desorption	163
8.14 The Effect of Vertical Diffusion	166
8.15 First Order Irreversible Reaction	168
8.16 The Effect of Holdup	172
8.17 First Order Reversible Reaction	177
8.18 First Order, Infinitely Rapid, Reversible Reaction	189
E. Comparison of the Film and Penetration Theories for Absorption with First Order Chemical Reaction	
8.19 Definition of Absorption Coefficients	192
8.20 The Definition of ϕ	194
8.21 The Scheme for Comparing the Film and Pene- tration Theories	197
8.22 Calculated Values of ϕ	199
8.23 Significance of the Comparison	199
8.24 The Effect of Unequal Diffusivities	205

	<u>Page</u>
F. The Film Theory of Absorption with Second Order Irreversible Reaction	
8.25 Introduction	206
8.26 First Approximate Solution	208
8.27 Second Approximate Solution	211
8.28 Comparison of the Two Approximate Solutions	214
G. The Penetration Theory of Absorption with Second Order Irreversible Reaction	
8.29 The General Case	218
8.30 The Case of Infinitely Rapid Reaction . . .	218
8.31 The Effect of Unequal Diffusivities	220
H. The Film Theory of Absorption with Second Order Reversible Reaction	
8.32 General Solution	224
8.33 The Case of Second Order Forward, First Order Reverse, Reaction	230
I. Citations - 834	232

A. INTRODUCTION

8.1 Preliminary Remarks. The theory of absorption with chemical reaction has not been developed sufficiently by previous investigators to handle the cases of absorption of chlorine or sulfur dioxide in water, and little work has been done in examining absorption with chemical reaction from the point of view of the penetration theory. Thus, it was felt necessary in this thesis to make a further mathematical study of absorption with chemical reaction. The results of this investigation are presented in this chapter.

An examination of the literature on the mathematical theory of absorption with chemical reaction is apt to prove confusing, because the various authors approach the subject in different manners, and because some authors have a tendency to make distinctions between the cases of slow reactions, moderately fast reactions and very rapid reactions. They consider that these cases have different mechanisms, when, in fact, they are merely special cases of a more general picture.

In order to avoid this confusion, this chapter is written with the object of presenting the theory as a unified and consistent whole, with no regard for whether the material is original with this investigation. Although a great portion of the theory presented here is original, much of it has been developed by previous workers, and some of it has been derived independently by both the author and other workers. The proper assignment of credit will be made at the very end of this chapter.

8.2 Nomenclature. Consider a system in which a gas, containing substance A, is in contact with a liquid which contains substance B. A is absorbed into the liquid, and reacts reversibly with B to form substances E and F according to the equation



Let A = concentration of A in the liquid at any pt,
moles/cm.³

B = concentration of B

E = concentration of E

F = concentration of F

C = total concentration of absorbed substance; i.e., total of reacted plus unreacted forms = A + E

N_A = rate of absorption per unit area, moles/(cm²)(sec).

Reaction(8.1) proceeds according to a rate equation

$$-dA/dt = -dB/dt = dE/dt = dF/dt = k_1 AB - k_2 EF \quad (8.2)$$

Thus, we let

k_1 = forward rate constant

k_2 = reverse rate constant

and K = equilibrium constant = k_1/k_2 .

There will exist concentration gradients of all the components in the liquid bringing about transfer of these components by diffusion. Throughout this work Fick's law is assumed. This states that the rate of transfer of material across a plane by diffusion is proportional to the concentration gradient. The proportionality factor is the diffusivity, which is assumed to be constant.

Let x = distance in the liquid from the interface, cm.

$N_{x,A}$ = rate of transfer of A across a plane parallel to the interface, and at a distance x from it, moles/(cm²)(sec).

$N_{x,B}$ = rate of transfer of B across the same plane

$N_{x,E}$ and $N_{x,F}$ are similarly defined.

D_A, D_B, D_E, D_F = diffusivities of A, B, E and F, respectively, cm²/sec.

Since there is no bulk motion of the fluid perpendicular to the interface (with one exception. See Sec. 8.8), material will be transferred across a plane parallel to the interface solely by diffusion. Thus,

$$N_{x,A} = -D_A \left(\frac{\partial A}{\partial x} \right) \quad (8.3)$$

$$N_{x,B} = -D_B \left(\frac{\partial B}{\partial x} \right) \quad (8.4)$$

$$N_{x,E} = -D_E \left(\frac{\partial E}{\partial x} \right) \quad (8.5)$$

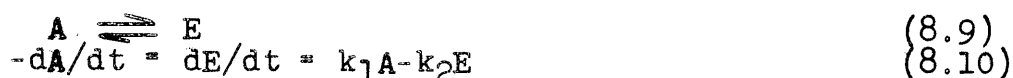
$$N_{x,F} = -D_F \left(\frac{\partial F}{\partial x} \right) \quad (8.6)$$

8.3. Procedure. The theory of absorption with chemical reaction will be developed from two viewpoints, the film theory and the penetration theory. First, the fundamental assumptions of the two theories will be presented, and the basic differential equations will be derived. The differential equations will be solved for various cases, starting first with the simplest case of physical absorption or desorption (i.e., with no chemical reaction), and considering in turn the various chemical reactions in order of complexity until the type represented by eq. (8.1) is reached. The several types of chemical reaction are listed below, together with the appropriate reaction rate equation.

First order irreversible



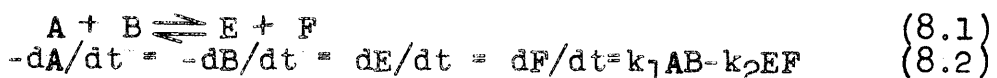
First order reversible



Second order irreversible



Second order reversible



In analyzing the simpler cases of absorption with chemical reaction, certain approximations will be demonstrated to be valid. These approximations will then be used as additional assumptions for the more complex cases which follow.

B. The Basic Differential Equations

8.4 Assumptions of the Film Theory. The film theory postulates:

- 1) the existence of a thin stagnant film of liquid next to the gas-liquid interface.
- 2) that all the resistance to mass transfer which resides in the liquid phase is confined to the film. This is equivalent to saying that the bulk of the fluid is well mixed.

- 3) that the film is sufficiently thin that the amount of material which is being transferred that can reside within the film is negligible compared with the total amount of material which is transferred. This is equivalent to the statement that accumulation or depletion within the film is negligible, so that steady state may be assumed.
- 4) that the gas and liquid are in equilibrium at the gas-liquid interface.

8.5. Basic Equations of the Film Theory. Consider a film of thickness x_f , in which components A, B, E and F are present, as shown in Fig. 8.1. The region to the left of $x = 0$ represents the gas, so that the line $x = 0$ corresponds to the gas-liquid interface. A_i is the concentration of unreacted A in the liquid in equilibrium with the gas at the interface. The region to the right of $x = x_f$ corresponds to the bulk of the liquid, in which all concentrations are constant at A_o , B_o , E_o and F_o . Consider a slab of infinitesimal thickness parallel to the interface, with

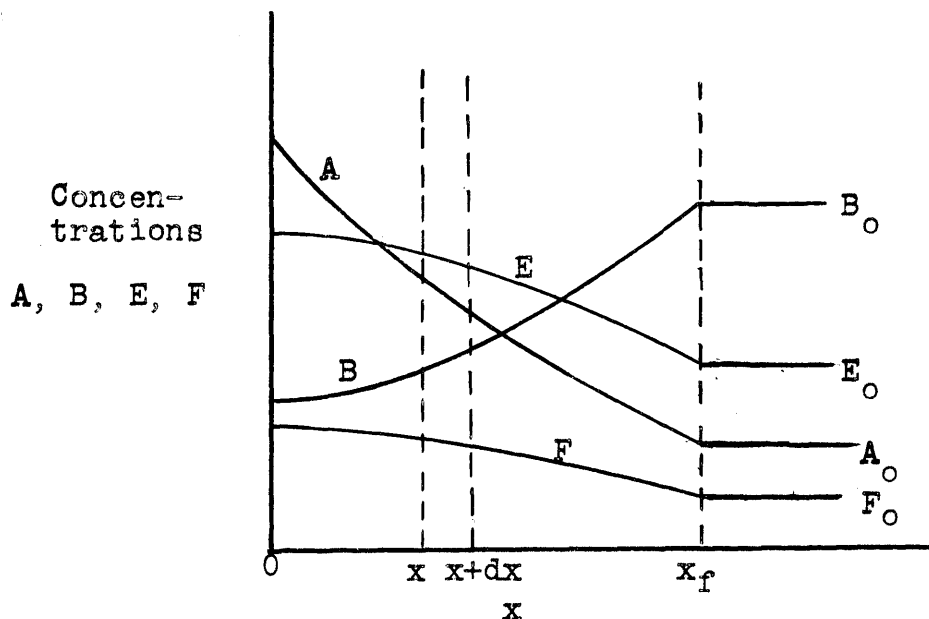


Fig. 8.1
Sketch of Concentration Gradients in a Film

faces at x and $x + dx$. The rate of transfer of component A from left to right across the plane at x is as follows:

$$N_{x,A} = -D_A \frac{dA}{dx} \quad (8.13)$$

(Since steady state exists, concentrations are independent of time and are functions only of x , so that total derivatives may be used). The rate of transfer of component A from left to right across the plane at $x + dx$ is given by

$$N_{x+dx,A} = -D_A \left(\frac{dA}{dx} + \frac{d^2A}{dx^2} dx \right) \quad (8.14)$$

Since we are considering unit area, the volume of the slab is dx . Rate equation (8.2) gives the rate of disappearance of A in a unit volume, moles/(cm³)(sec.), so that the rate at which A is disappearing in the slab is given by $(k_1AB - k_2EF)dx$. Now, the amount of A diffusing into the slab from the left is equal to the amount of A leaving the slab by diffusion to the right, plus the amount of A that disappears within the slab because of the reaction. Thus,

$$-D_A \frac{dA}{dx} = -D_A \left(\frac{dA}{dx} + \frac{d^2A}{dx^2} dx \right) + (k_1AB - k_2EF)dx \quad (8.15)$$

This simplifies to

$$D_A \frac{d^2A}{dx^2} = k_1AB - k_2EF \quad (8.16)$$

By precisely the same considerations, we may arrive at a similar equation for component B.

$$D_B \frac{d^2B}{dx^2} = k_1AB - k_2EF \quad (8.17)$$

Similar considerations hold for components E and F, except that it must be remembered that eq. (8.2) gives $k_1AB - k_2EF$ as the rates of appearance of E and F in the unit volume, so that the rates of disappearance of E and F in the slab would be given by $(k_2EF - k_1AB)dx$

Then

$$D_E \frac{d^2E}{dx^2} = k_2EF - k_1AB \quad (8.18)$$

$$D_F \frac{d^2F}{dx^2} = k_2EF - k_1AB \quad (8.19)$$

Eqs. (8.16) - (8.19) may be combined to form the basic differential equation for the film theory:

$$D_A \frac{d^2 A}{dx^2} = D_B \frac{d^2 B}{dx^2} = -D_E \frac{d^2 E}{dx^2} = -D_F \frac{d^2 F}{dx^2} = k_1 AB - k_2 EF \quad (8.20)$$

The boundary conditions for these equations are as follows:

$$\begin{aligned} \text{At } x = 0, \quad A &= A_i \\ \frac{dB}{dx} &= \frac{dE}{dx} = \frac{dF}{dx} = 0 \end{aligned} \quad (8.21)$$

The last set of equations follows from the assumption (which was not previously stated, but was implied by the fact that we confine our attention to transfer only of A across the interface) that components B, E and F are non-volatile, so that there is no diffusion of these components across the interface:

$$\text{At } x = x_f, \quad A = A_o, \quad B = B_o, \quad E = E_o, \quad F = F_o \quad (8.22)$$

8.6. Assumptions of the Penetration Theory. The postulates of the penetration theory are:

- 1) There is no relative motion within the fluid (with one exception. See Sec. 8.8)
- 2) Unsteady state prevails in the liquid.
- 3) At the beginning of the period of exposure of the liquid to the gas, the liquid is well mixed, and the concentrations are uniform.
- 4) At any time during the exposure period, the maximum depth of liquid at which any appreciable concentration changes have occurred is small compared with the total depth of liquid. Thus, it makes little difference in determining the shape of the concentration-distance curves whether we assume that the depth of the liquid is the actual depth or assume that it is infinite. To facilitate the mathematics, then, we shall assume that the liquid is of infinite extent away from the interface. (The one exception to this assumption will be during the discussion of the effect of holdup in Sec. 8.16).
- 5) The gas and liquid are in equilibrium at the gas-liquid interface.

8.7. Basic Equations of the Penetration Theory. Consider a body of liquid of infinite depth in which components A, B, E and F are present, as shown in Fig. 8.2. The region to the left of $x = 0$ represents the gas, so that the line $x = 0$ corresponds to the gas-liquid interface. A_1 is the concentration of unreacted A in the liquid in equilibrium with the gas at the interface. At time

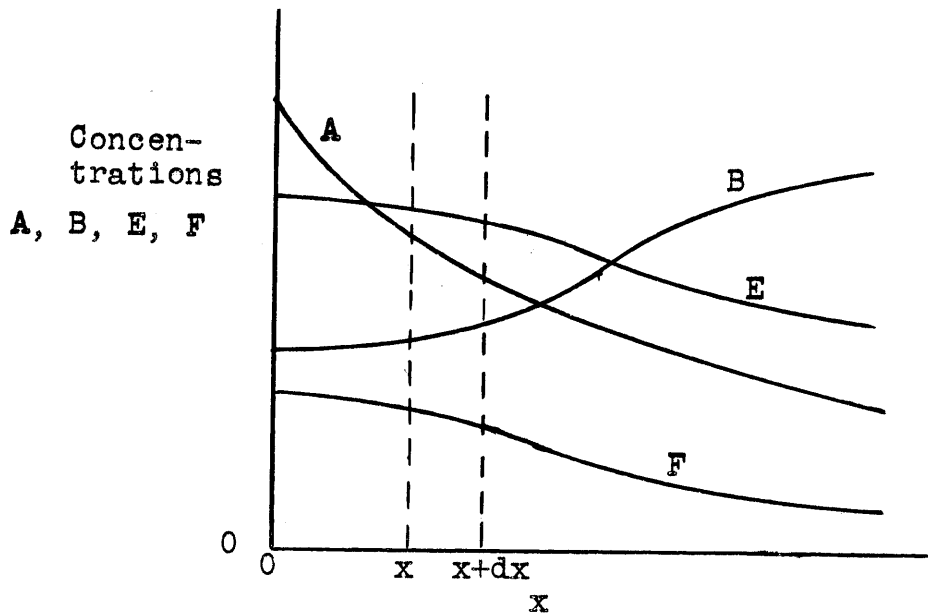


Fig. 8.2.

Sketch of Gradients in an Infinite Body of Liquid at Time t

$t = 0$, the concentrations are all uniform at the values A_0 , B_0 , E_0 and F_0 , respectively. Consider a slab of infinitesimal thickness parallel to the interface, with faces at x and $x + dx$. At time t , the rate of transfer of component A from left to right across the plane at x is

$$N_{x,A} = -D_A \frac{\partial A}{\partial x} \quad (8.23)$$

That across the plane at $x + dx$ is

$$N_{x+dx,A} = -D_A \left(\frac{\partial A}{\partial x} + \frac{\partial^2 A}{\partial x^2} dx \right) \quad (8.24)$$

Again, the rate at which A is disappearing in the slab is given by $(k_1AB - k_2EF)dx$. Further, there is an accumulation of A in the slab. Since the volume of the slab (for unit area) is dx , the amount of A present in the slab is $A dx$. The rate at which A accumulates in the slab is $\partial(A dx)/\partial t$ or $(\partial A/\partial t)dx$. Now, the rate at which A diffuses into the slab from the left is equal to the rate at which A leaves the slab by diffusion to the right plus the rate at which A disappears within the slab because of the chemical reaction plus the rate at which A accumulates within the slab. Thus,

$$-D_A \frac{\partial A}{\partial x} = -D_A \left(\frac{\partial A}{\partial x} + \frac{\partial^2 A}{\partial x^2} dx \right) + (k_1AB - k_2EF)dx + \frac{\partial A}{\partial t} dx \quad (8.25)$$

This simplifies to

$$D_A \frac{\partial^2 A}{\partial x^2} - \frac{\partial A}{\partial t} = k_1AB - k_2EF \quad (8.26)$$

Similarly,

$$D_B \frac{\partial^2 B}{\partial x^2} - \frac{\partial B}{\partial t} = k_1AB - k_2EF \quad (8.27)$$

And since the rate of disappearance, due to chemical reaction, of E and F are given by $(k_2EF - k_1AB)dx$, we obtain

$$D_E \frac{\partial^2 E}{\partial x^2} - \frac{\partial E}{\partial t} = k_2EF - k_1AB \quad (8.28)$$

$$D_F \frac{\partial^2 F}{\partial x^2} - \frac{\partial F}{\partial t} = k_2EF - k_1AB \quad (8.29)$$

Eqs. (8.26) - (8.29) may be combined to form the basic differential equation for the penetration theory:

$$\begin{aligned} D_A \frac{\partial^2 A}{\partial x^2} - \frac{\partial A}{\partial t} &= D_B \frac{\partial^2 B}{\partial x^2} - \frac{\partial B}{\partial t} = \frac{\partial E}{\partial t} - D_E \frac{\partial^2 E}{\partial x^2} \\ &= \frac{\partial F}{\partial t} - D_F \frac{\partial^2 F}{\partial x^2} = k_1AB - k_2EF \end{aligned} \quad (8.30)$$

The boundary conditions for these equations are as follows:

$$\text{At } x = 0, t > 0, \quad A = A_1, \quad \frac{\partial B}{\partial x} = \frac{\partial E}{\partial x} = \frac{\partial F}{\partial x} = 0 \quad (8.31)$$

As in eq. (8.21), the last set of equations follows from the assumption that B, E and F are non-volatile.

$$\text{At } t = 0, x > 0, \quad A = A_0, B = B_0, E = E_0, F = F_0 \quad (8.32)$$

$$\text{At } x = \infty, t \geq 0, \quad A = A_0, B = B_0, E = E_0, F = F_0 \quad (8.33)$$

The last set of equations represents the condition that there be no change of concentration at a distance infinitely far from the interface in any finite time t .

It will be noted that the extreme right-hand side of eqs. (8.20) and (8.30) are identical with the right-hand side of rate eq. (8.2). It should be clear that for the simpler types of chemical reaction, these right-hand sides should be replaced by the right-hand side of the appropriate rate equation for that type, either eq. (8.8), (8.10) or (8.12).

8.8. Effect of Acceleration of the Liquid on the Basic Differential Equation of the Penetration Theory. When a layer of fluid flows down a wall, it may undergo an acceleration for the first few inches of travel. During the period of acceleration the layer becomes thinner, so that each element of fluid must be distorted, becoming thinner in the direction perpendicular to the interface and longer in the direction parallel to the interface.

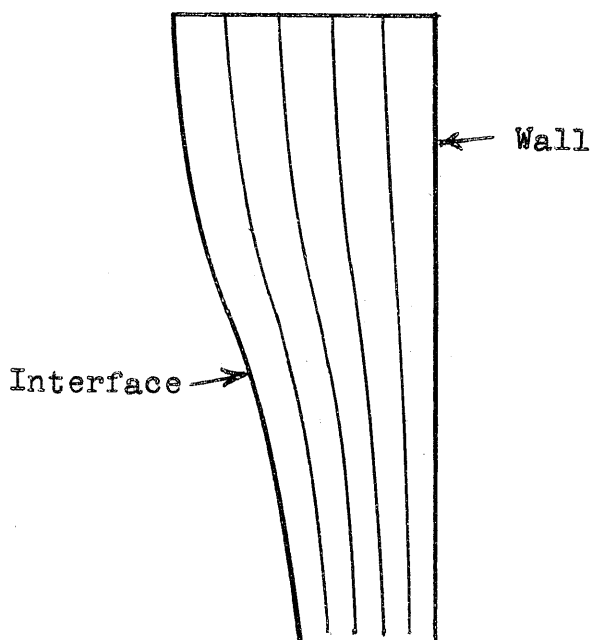


Fig. 8.3.
Sketch of Streamlines in Liquid Flowing Down a Wall

Fig. 8.3 illustrates what the streamlines of flow might look like. Let x be the distance from the interface in a direction perpendicular to the interface, y be the distance down from the top of the wall and v be the downward velocity of an element of fluid. If we consider that the depth of penetration (i.e., the depth of the region in which any appreciable concentration change occurs) is small compared with the total depth, then over this region we may assume that v is independent of x , but is a function only of y .

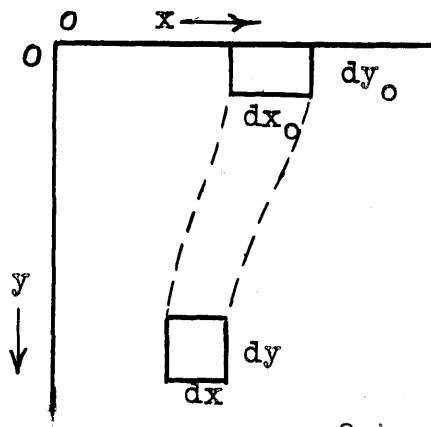


Fig. 8.4.

Distortion of an Element of Fluid During Acceleration of Fluid

Fig. 8.4 shows a plot of y vs. x . Consider an element of fluid having the shape of a rectangular parallelepiped with unit length in direction perpendicular to the x - and y - axes, and originally having depth dx_0 , and length dy_0 . Also, the element has an original downward velocity v_0 . At any time, the element will have dimensions dx and dy , and a velocity v . The element will flow between the streamlines shown by the dotted lines, and its volume will remain unchanged during flow, having the value $dx dy = dx_0 dy_0$. Since v is assumed independent of x , the element will remain a rectangular parallelepiped.

The rate of transfer of component A into the element from the left is

$$-D_A \frac{\partial A}{\partial x} dy.$$

The rate of transfer of A out of the element to the right is

$-D_A \left(\frac{\partial A}{\partial x} + \frac{\partial^2 A}{\partial x^2} dx \right) dy$. The rate of disappearance of A due to chemical

reaction is $(k_1 AB - k_2 EF) dx dy$. The rate of accumulation of A in the element is

$$\frac{\partial A}{\partial t} dx dy.$$

Then,

$$-D_A \frac{\partial A}{\partial x} dy = -D_A \left(\frac{\partial A}{\partial x} + \frac{\partial^2 A}{\partial x^2} dx \right) dy + (k_1 AB - k_2 EF) dx dy + \frac{\partial A}{\partial t} dx dy \quad (8.34)$$

This reduces to

$$D_A \frac{\partial^2 A}{\partial x^2} - \frac{\partial A}{\partial t} = k_1 AB - k_2 EF \quad (8.35)$$

This equation is identical with eq. (8.26). The same result would be obtained with all the other components.

The conclusion may then be made that the differential equations for the penetration theory remain unchanged by the fact that the liquid may be undergoing distortion due to acceleration as it flows down a wall. Furthermore, an examination of the boundary conditions shows that they will not be affected either. Thus, the mathematical problem remains the same as for the simpler case in which the fluid flows downward with uniform velocity.

C. The Film Theory of Absorption with First-order Chemical Reaction

8.9. Physical Absorption or Desorption (No Chemical Reaction).
For the simple case where there is no chemical reaction, eq.(8.20) reduces to

$$D_A \frac{d^2 A}{dx^2} = 0 \quad (8.36)$$

with the boundary conditions

$$\text{At } x = 0, \quad A = A_1 \quad (8.37)$$

$$\text{At } x = x_f, \quad A = A_0 \quad (8.38)$$

The solution of (8.36) is

$$A = C_1 x + C_2 \quad (8.39)$$

Substituting B.C. (8.37) yields

$$C_2 = A_1$$

$$A = C_1 x + A_1$$

Substituting B.C. (8.38) gives

$$\begin{aligned} A_0 &= C_1 x_f + A_1 \\ C_1 &= \frac{A_0 - A_1}{x_f} \end{aligned}$$

whence
$$A = (A_0 - A_1) \frac{x}{x_f} + A_1 \quad (8.40)$$

Differentiating once,

$$\frac{dA}{dx} = \frac{A_0 - A_1}{x_f} \quad (8.41)$$

Since $N_A = -D_A \left(\frac{dA}{dx} \right)_x = 0$, then

$$N_A = \frac{D_A}{x_f} (A_i - A_0) \quad (8.42)$$

8.10. First Order Irreversible Reaction. For this case, eq. (8.20) reduces to

$$D_A \frac{d^2 A}{dx^2} = k_1 A \quad (8.43)$$

with the boundary conditions

$$\text{at } x = 0, \quad A = A_1 \quad (8.44)$$

$$x = x_f \quad A = A_0 \quad (8.45)$$

Two independent solutions of eq. (8.43) are $\sinh \left(\sqrt{k_1/D_A} x \right)$ and $\sinh \left(\sqrt{k_1/D_A} [x_f - x] \right)$. Thus, the general solution of eq. (8.43) may be written

$$A = C_1 \sinh \sqrt{\frac{k_1}{D_A}} x + C_2 \sinh \sqrt{\frac{k_1}{D_A}} (x_f - x) \quad (8.46)$$

Substituting B.C. (8.44) yields

$$C_2 = \frac{A_1}{\sinh \sqrt{k_1/D_A} x_f}$$

Substituting B.C. (8.45) gives

$$C_1 = \frac{A_0}{\sinh(\sqrt{k_1/D_A} x_f)}$$

$$\text{Let } R = \sqrt{k_1/D_A}$$

$$\text{Then } A = \frac{A_0 \sinh Rx + A_1 \sinh R(x_f - x)}{\sinh R x_f} \quad (8.47)$$

Differentiating once,

$$\frac{dA}{dx} = R \left[\frac{A_0 \cosh Rx - A_1 \cosh R(x_f - x)}{\sinh R x_f} \right] \quad (8.48)$$

Substituting $x = 0$ gives (since $\cosh 0 = 1$)

$$\left(\frac{dA}{dx}\right)_{x=0} = R \left[\frac{A_0}{\sinh R x_f} - \frac{A_1}{\tanh R x_f} \right] \quad (8.49)$$

Now,

$$N_A = -D_A \left(\frac{dA}{dx}\right)_{x=0} = 0$$

$$N_A = R D_A \left[\frac{A_1}{\tanh R x_f} - \frac{A_0}{\sinh R x_f} \right] \quad (8.50)$$

8.11. The Effect of Holdup. The magnitude of A_0 may be obtained in terms of other variables by writing a material balance on the bulk of the fluid. Let δ be the thickness of the liquid layer, which is equal to the volume of holdup per unit interfacial area. Then, the volume of the bulk of the fluid corresponding to unit area of interface is $\delta - x_f$. The rate of transfer of A into this volume of the bulk of the fluid by diffusion is

$$-D_A \left(\frac{dA}{dx}\right)_x = x_f$$

The rate at which A disappears by chemical reaction in this volume is

$$(k_1 A_0)(\delta - x_f)$$

Since no A leaves the bulk of the fluid by diffusion, we have

$$-D_A \left(\frac{dA}{dx} \right)_{x=x_f} = k_1 A_0 (\delta - x_f) \quad (8.51)$$

Substituting $x = x_f$ into eq. (8.48) gives

$$\left(\frac{dA}{dx} \right)_{x=x_f} = R \left[\frac{A_0}{\tanh R x_f} - \frac{A_1}{\sinh R x_f} \right] \quad (8.52)$$

Combining with eq. (8.51) gives

$$RD_A \left[\frac{A_1}{\sinh R x_f} - \frac{A_0}{\tanh R x_f} \right] = k_1 A_0 (\delta - x_f)$$

Solving for A_0 ,

$$A_0 = \frac{A_1}{R(\delta - x_f) \sinh R x_f + \cosh R x_f} \quad (8.53)$$

Substituting for A_0 in eq. (8.50) yields

$$N_A = RD_A \left[\frac{A_1}{\tanh R x_f} - \frac{A_1}{R(\delta - x_f) \sinh^2 R x_f + \sinh R x_f \cosh R x_f} \right]$$

$$N_A = \frac{RD_A A_1}{\tanh R x_f} \left[1 - \frac{\tanh R x_f}{R(\delta - x_f) \sinh^2 R x_f + \sinh R x_f \cosh R x_f} \right]$$

$$N_A = \frac{RD_A A_1}{\tanh R x_f} \left[1 - \frac{1}{\left(\frac{\delta}{x_f} - 1 \right) R x_f \sinh R x_f \cosh R x_f + \cosh^2 R x_f} \right] \quad (8.54)$$

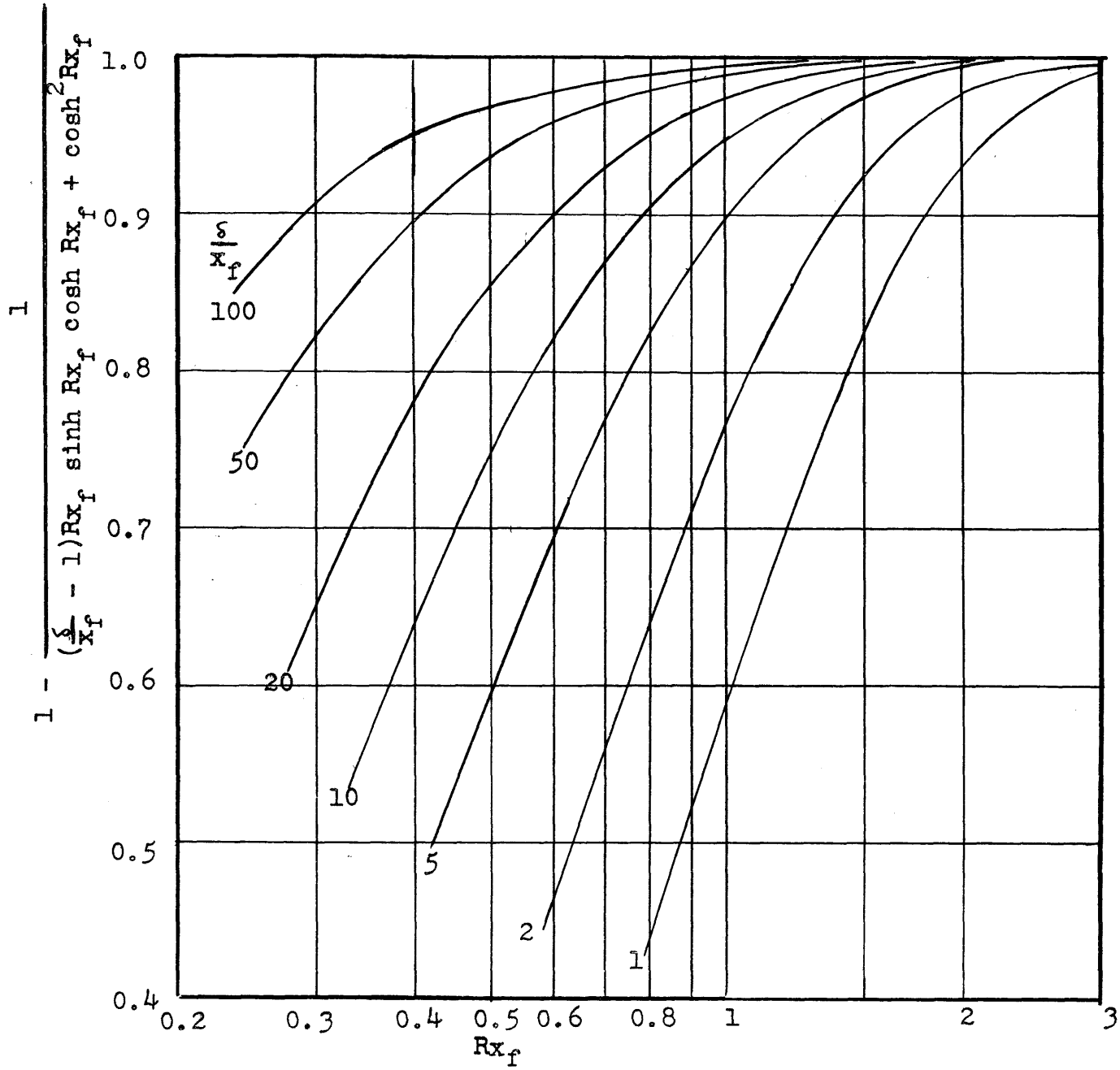
If the holdup is infinite, the term in the brackets becomes unity, and

$$N_A = \frac{R D_A A_1}{\tanh R x_f} \quad (8.55)$$

The term in the brackets may be regarded as a correction factor to allow for the finite holdup. This correction factor has been plotted as a function of $R x_f$ for various values of δ/x_f in Fig. 8.5.

Fig. 8.5

Correction Factor for Holdup -- Film Theory



If we reconsider one of the fundamental assumptions of the film theory, that the film is sufficiently thin that accumulation in it may be neglected, then clearly any values of δ/x_f lower than 10 or 20 would be in contradiction with that assumption. Therefore, as long as we consider the subject of absorption with chemical reaction from the point of view of the film theory, we may consider that δ/x_f is greater than 10 or 20. The question of the actual values of δ that might be expected in a packed tower or other equipment will be deferred until the discussion of the case of first order irreversible reaction from the point of view of the penetration theory (see Sec. 8.16).

From Fig. 8.5, it can be seen that for $\delta/x_f = 20$ and $Rx_f = 0.5$ the correction factor is 0.855, and that the correction factor rapidly increases to unity as δ/x_f or Rx_f is increased. The question arises as to what happens as Rx_f decreases. To investigate this, consider the ratio obtained by dividing eq. (8.52) by eq. (8.49). This ratio becomes

$$\frac{\left(\frac{dA}{dx}\right)_{x=x_f}}{\left(\frac{dA}{dx}\right)_{x=0}} = \frac{A_0 \cosh Rx_f - A_1}{A_0 - A_1 \cosh Rx_f} \quad (8.56)$$

This ratio is that fraction of A entering the film at the interface which diffuses through the film unreacted, enters the bulk of the fluid and reacts there. Substituting $\delta/x_f = 20$ and $Rx_f = 0.5$ into eq. (8.53), we find $A_0 = 0.165 A_1$. Substituting this relationship, plus $Rx_f = 0.5$ into eq. (8.56) yields the ratio 0.845 as the fraction of A which diffuses through the film unreacted. The calculations were repeated for lower values of Rx_f at the same value of δ/x_f , and the results are tabulated in Table 8.1.

TABLE 8.1

Fraction of Material Diffusing through Film
Unreacted for First Order Irreversible Reaction

$\delta/x_f = 20$	
Rx_f	$(dA/dx)_{x=x_f} / (dA/dx)_{x=0}$
0.1	0.944
0.2	0.933
0.3	0.912
0.4	0.880
0.5	0.845

Thus, for lower values of Rx_f , even more of the material diffuses through the film unreacted. Physically, the reason why this fraction is so close to unity is that for a low reaction rate constant or for small thickness of film, there is not much opportunity for reaction to take place within the film.

The conclusions to be drawn from the above discussion are that for values of Rx_f below 0.5, the process of absorption of A is essentially a diffusion of A through the film followed by reaction within the bulk of the fluid, while for values of Rx_f greater than 0.5, where simultaneous diffusion and chemical reaction take place within the film (which is the case, after all, for which the theory of absorption with chemical reaction needs to be developed), the holdup may be considered sufficiently large that the correction factor of eq. (8.54) is near to unity. Eq. (8.55) is then valid for the latter case.

The purpose of the above has been to justify a further assumption for the film theory that will be used for the more complex cases of absorption with chemical reaction. This assumption may be stated in either of two ways: either the holdup is infinite, or equilibrium exists in the bulk of the fluid. Infinite holdup does imply equilibrium in the bulk of the fluid.

If the assumption of equilibrium had been made at the beginning of this section, the boundary condition at $x = x_f$ would have become $A_0 = 0$, since the reaction is assumed irreversible. Then, instead of eq. (50), eq. (55) would have been obtained directly.

8.12. First Order Reversible Reaction. For this case the appropriate differential equation is

$$D_A \frac{d^2 A}{dx^2} = -D_E \frac{d^2 E}{dx^2} = k_1 A - k_2 E \quad (8.57)$$

with the boundary conditions

$$\text{at } x = 0,$$

$$A = A_1, \quad \frac{dE}{dx} = 0 \quad (8.58)$$

$$\text{at } x = x_f \quad A = A_0, \quad E = E_0, \quad K = \frac{E_0}{A_0} \quad (8.59)$$

The last equation follows from the assumption of equilibrium in the bulk of the fluid. Since $K = k_1/k_2$, and since $k_1 A - k_2 E = 0$ at equilibrium, it follows that $K = E_0/A_0$.

Eq. (8.57) may be rewritten

$$D_A \frac{d^2(A-A_0)}{dx^2} = -D_E \frac{d^2(E-E_0)}{dx^2} = k_1(A-A_0) - k_2(B-B_0) + k_1A_0 - k_2B_0 \quad (8.60)$$

But $k_1A_0 = k_2B_0$, since A_0 and B_0 are in equilibrium with each other. Eq. (8.60) becomes

$$D_A \frac{d^2(A-A_0)}{dx^2} = -D_E \frac{d^2(E-E_0)}{dx^2} = k_1(A-A_0) - k_2(B-B_0) \quad (8.61)$$

The first part of eq. (8.61) may be rewritten

$$D_A \frac{d^2(A-A_0)}{dx^2} + D_E \frac{d^2(E-E_0)}{dx^2} = 0 \quad (8.62)$$

Integrating eq. (8.62) once,

$$D_A \frac{d(A-A_0)}{dx} + D_E \frac{d(E-E_0)}{dx} = c_1 \quad (8.63)$$

$$\text{At } x = 0, N_A = -D_A \frac{dA}{dx} = -D_A \frac{d(A-A_0)}{dx}$$

$$\text{and } \frac{dE}{dx} = \frac{d(E-E_0)}{dx} = 0$$

whence $c_1 = -N_A$

Substituting for c_1 in eq. (8.63) and integrating once more,

$$D_A (A-A_0) + D_E (E-E_0) = -N_A x + c_2 \quad (8.64)$$

Substituting B.C. (8.59) gives

$$0 = -N_A x_f + c_2, \text{ or } c_2 = N_A x_f$$

$$D_A (A-A_0) + D_E (E-E_0) = N_A (x_f - x) \quad (8.65)$$

Substituting for $(E-E_0)$ in eq. (8.61) gives

$$D_A \frac{d^2(A-A_0)}{dx^2} = k_1 (A-A_0) - k_2 \left[\frac{N_A}{D_E} (x_f - x) - \frac{D_A}{D_E} (A-A_0) \right] \quad (8.66)$$

Rearranging:

$$\frac{d^2(A-A_0)}{dx^2} = \left(\frac{k_1}{D_A} + \frac{k_2}{D_E}\right) (A-A_0) - \frac{NAk_2}{DADE} (x_f-x) \quad (8.67)$$

Let $R = \sqrt{\frac{k_1}{D_A} + \frac{k_2}{D_E}}$. (This is equivalent to letting $R = \sqrt{\frac{k_1}{D_A}}$

for the irreversible case. In that case, $k_2 = 0$). Two independent homogeneous solutions of eq. (8.67) are $\cosh Rx$ and $\cosh R(x_f-x)$. By inspection, it can be seen that one particular solution is

$$(A-A_0) = \frac{NAk_2}{R^2 D_A D_E} (x_f-x)$$

Then the complete general solution of (8.67) is

$$(A-A_0) = c_3 \cosh Rx + c_4 \cosh R(x_f-x) + \frac{NAk_2}{R^2 D_A D_E} (x_f-x) \quad (8.68)$$

From B.C. (8.59),

$$0 = c_3 \cosh Rx_f + c_4 \quad (8.69)$$

Differentiating eq. (8.68) once,

$$\frac{d(A-A_0)}{dx} = c_3 R \sinh Rx - c_4 R \sinh R(x_f-x) - \frac{NAk_2}{R^2 D_A D_E}$$

From B.C. at $x = 0$,

$$-\frac{NA}{D_A} = -c_4 R \sinh Rx_f - \frac{NAk_2}{R^2 D_A D_E}$$

Whence

$$c_4 = \frac{\frac{NA}{D_A} \left(1 - \frac{k_2}{R^2 D_E}\right)}{R \sinh Rx_f} \quad (8.70)$$

Then

$$c_3 = \frac{-\frac{NA}{D_A} \left(1 - \frac{k_2}{R^2 D_E}\right)}{R \sinh Rx_f \cosh Rx_f} \quad (8.71)$$

Combining eqs. (8.68), (8.70) and (8.71), and substituting $x = 0$, $A = A_1$ gives

$$(A_1 - A_0) = \frac{-\frac{N_A}{D_A} \left(1 - \frac{k_2}{R^2 D_E}\right)}{R \sinh R x_f \cosh R x_f} + \frac{\frac{N_A}{D_A} \left(1 - \frac{k_2}{R^2 D_E}\right)}{R \tanh R x_f} + \frac{N_A k_2 x_f}{R^2 D_A D_E}$$

Now

$$\frac{1}{\tanh R x_f} - \frac{1}{\sinh R x_f \cosh R x_f} = \tanh R x_f (\coth^2 R x_f - \operatorname{csch}^2 R x_f) = \tanh R x_f$$

Then

$$(A_1 - A_0) = \frac{N_A}{R D_A} \left[\left(1 - \frac{k_2}{R^2 D_E}\right) \tanh R x_f + \frac{k_2 x_f}{R D_E} \right]$$

$$(A_1 - A_0) = \frac{N_A x_f}{D_A} \left[\left(1 - \frac{k_2}{R^2 D_E}\right) \frac{\tanh R x_f}{R x_f} + \frac{k_2}{R^2 D_E} \right]$$

Now

$$R^2 = \frac{k_1}{D_A} + \frac{k_2}{D_E} = k_2 \left[\frac{K}{D_A} + \frac{1}{D_E} \right]$$

$$\frac{k_2}{R^2 D_E} = \frac{D_A}{K D_E + D_A} = \frac{1}{1 + K D_E / D_A}$$

$$1 - \frac{k_2}{R^2 D_E} = \frac{K D_E / D_A}{1 + K D_E / D_A}$$

$$(A_1 - A_0) = \frac{N_A x_f}{D_A} \left[\frac{K D_E / D_A}{1 + K D_E / D_A} \frac{\tanh R x_f}{R x_f} + \frac{1}{1 + K D_E / D_A} \right]$$

$$N_A = \frac{D_A (A_1 - A_0)}{x_f} \cdot \frac{1 + \frac{K D_E}{D_A}}{1 + \frac{K D_E}{D_A} \frac{\tanh R x_f}{R x_f}} \quad (8.72)$$

An examination of certain limiting forms of eq. (8.72) will be instructive.

$$(1) K \rightarrow \infty$$

Rearrange eq. (8.72) to:

$$N_A = \frac{D_A(A_1 - A_0)}{x_f} \frac{\frac{D_A}{KD_E} + 1}{\frac{D_A}{KD_E} + \frac{\tanh Rx_f}{Rx_f}}$$

$$\lim_{K \rightarrow \infty} N_A = \frac{D_A(A_1 - A_0)}{x_f} \frac{1}{\frac{\tanh Rx_f}{Rx_f}}$$

Since $A_0 \rightarrow 0$, this eq. is identical with eq. (8.55).

(2) $Rx_f \rightarrow 0$

$$\text{Noting that } \lim_{Rx_f \rightarrow 0} \frac{\tanh Rx_f}{Rx_f} = 1,$$

eq. (8.72) becomes

$$N_A = \frac{D_A(A_1 - A_0)}{x_f}$$

which is identical with eq. (8.42)

(3) $Rx_f \rightarrow \infty$

Note that $\lim_{Rx_f \rightarrow \infty} \tanh Rx_f = 1$, and hence,

$$\lim_{Rx_f \rightarrow \infty} \frac{\tanh Rx_f}{Rx_f} = 0, \text{ eq. (8.72) becomes}$$

$$N_A = \frac{D_A(A_1 - A_0)}{x_f} \left(1 + \frac{KD_E}{D_A}\right)$$

If we let C_1 = total concentration of A + E in equilibrium with the gas at the interface, and C_0 = total concentration of A + E in the bulk of the liq, we have

$$C_1 = A_1 + A_1K = A_1(1+K)$$

$$C_0 = A_0 + B_0 = A_0 + A_0K = A_0(1+K)$$

Then, if $D_A = D_E$,

$$N_A = \frac{D_A(C_1 - C_0)}{x_f} \quad (8.73)$$

Thus, if the diffusivities are equal, and the reaction is infinitely rapid, a "total" driving force, $(C_1 - C_0)$, may be used. Such a driving force is very commonly used in the treatment of absorption with chemical reaction, but the assumptions inherent in its use, namely infinitely rapid reaction and equal diffusivities, are not so commonly recognized.

D. The Penetration Theory of Absorption with First Order Chemical Reaction.

8.13. Physical Absorption or Desorption (No Chemical Reaction).

For the case where there is no reaction, eq. (8.30) reduces to

$$D_A \frac{\partial^2 A}{\partial x^2} - \frac{\partial A}{\partial t} = 0 \quad (8.74)$$

with the boundary conditions

$$\begin{array}{ll} \text{At } x = 0, & t > 0, & A = A_1 \\ t = 0, & x > 0, & A = A_0 \\ x = \infty, & t \geq 0, & A = A_0 \end{array} \quad (8.75)$$

Make the substitution $\alpha = \frac{A - A_0}{A_1 - A_0}$

Then, the differential equation and the boundary conditions become

$$D_A \frac{\partial^2 \alpha}{\partial x^2} - \frac{\partial \alpha}{\partial t} = 0 \quad (8.76)$$

$$\begin{array}{ll} \text{At } x = 0, & t > 0, & \alpha = 1 \\ t = 0, & x > 0, & \alpha = 0 \\ x = \infty, & t \geq 0, & \alpha = 0 \end{array} \quad (8.77)$$

The solution of linear partial differential equations with initial time conditions are most easily carried out by Laplace transforms. A brief review of the subject of Laplace transforms and of some properties most useful in solving these equations will be presented here. For a more complete presentation of the subject, the reader is referred to Hildebrand (38) and to Marshall and Pigford (71).

The Laplace transform of α will be represented by either of two symbols, $\mathcal{L}(\alpha)$ or $\bar{\alpha}$, and is defined as

$$\mathcal{L}(\alpha) = \bar{\alpha} = \int_0^{\infty} e^{-pt} \alpha \, dt \quad (8.78)$$

Multiplying α by e^{-pt} and integrating with respect to t from zero to infinity is a linear operation which transforms α from a function of x and t to a function of x and p . Some properties of interest are

$$\mathcal{L}\left(\frac{\partial \alpha}{\partial x}\right) = \frac{\partial}{\partial x} \mathcal{L}(\alpha) = \frac{\partial \bar{\alpha}}{\partial x}$$

$$\mathcal{L}\left(\frac{\partial \alpha}{\partial t}\right) = p \bar{\alpha} - (\alpha)_{t=0}$$

$$\mathcal{L}\int_0^t \alpha \, dt = \frac{\bar{\alpha}}{p}$$

The procedure in solving a partial differential equation is to operate on both the differential equation and the boundary conditions with the Laplace transform. This reduces the equations to a differential equation in which p may be regarded as constant. Thus, the equations involve only total derivatives of $\bar{\alpha}$ with respect to x . These equations are then integrated, using the transformed boundary conditions, to yield $\bar{\alpha}$ as a function of x and p . By using tables of inverse transforms, the function may then be transformed back to give α as a function of x and t . The inverse operation will be designated by the symbol \mathcal{L}^{-1} . Thus $\mathcal{L}^{-1}(\bar{\alpha}) = \alpha$. Perhaps the most extensive tables of inverse transforms are those of Campbell and Foster (7).

In this work we desire not to know α as a function of x and t , but rather to find $(\partial \alpha / \partial x)_{x=0}$, which is used to obtain the rate of absorption. Therefore, rather than find $\bar{\alpha}$ as a function of x and p , we shall usually find $(\partial \bar{\alpha} / \partial x)_{x=0}$ as a function of p , the inverse transform of which is the desired $(\partial \alpha / \partial x)_{x=0}$ as a function of t .

Operating on eq. (8.76) yields

$$D_A \frac{d \bar{\alpha}}{dx^2} - (p\bar{\alpha} - 0) = 0 \quad (8.79)$$

The boundary conditions become

$$\text{At } x = 0, \quad \bar{\alpha} = 1/p \quad (8.80)$$

$$\text{At } x = \infty, \quad \bar{\alpha} = 0 \quad (8.81)$$

Note that the initial condition, $t = 0$, $\alpha = 0$, has been used in obtaining eq. (8.79).

The general solution of eq. (8.79) is

$$\bar{\alpha} = c_1 \exp\left(\sqrt{\frac{p}{D_A}} x\right) + c_2 \exp\left(-\sqrt{\frac{p}{D_A}} x\right)$$

Using B.C. (8.81) gives $c_1 = 0$. B.C. (8.80) yields $c_2 = 1/p$.
Then

$$\bar{\alpha} = 1/p \exp\left(-\sqrt{\frac{p}{D_A}} x\right) \quad (8.82)$$

$$\frac{d\bar{\alpha}}{dx} = -\frac{1}{\sqrt{pD_A}} \exp\left(-\sqrt{\frac{p}{D_A}} x\right)$$

$$\left(\frac{d\bar{\alpha}}{dx}\right)_{x=0} = -\frac{1}{\sqrt{pD_A}}$$

Using pair 522, page 50 of Campbell and Foster (7), $\left(\frac{\partial \alpha}{\partial x}\right)_{x=0} = -\frac{1}{\sqrt{D_A \pi t}}$
Now,

$$N_A = -D_A \left(\frac{\partial \alpha}{\partial x}\right)_{x=0} = -D_A (A_1 - A_0) \left(\frac{\partial \alpha}{\partial x}\right)_{x=0}$$

Then

$$N_A = \sqrt{\frac{D_A}{\pi t}} (A_1 - A_0) \quad (8.83)$$

This gives the instantaneous rate of absorption at any time t .
For the case where there is no acceleration of the fluid, the total amount absorbed in time t will be given by

$$\begin{aligned} \int_0^t N_A dt &= \sqrt{\frac{D_A}{\pi}} (A_1 - A_0) \int_0^t t^{-1/2} dt \\ &= 2 \sqrt{\frac{D_A t}{\pi}} (A_1 - A_0) \end{aligned} \quad (8.84)$$

It will be of interest to determine the concentration as a function of distance and time. This may be found by obtaining the inverse transform of eq. (8.82). Using pair 805.3, page 92 of Campbell and Foster, where $\sqrt{\sigma} = x/\sqrt{D_A}$, and $\gamma = 0$,

$$\alpha = 1/2 \left[\operatorname{erfc} \left(\frac{x}{\sqrt{D_A}} \frac{1}{2\sqrt{t}} \right) + \operatorname{erfc} \left(\frac{x}{\sqrt{D_A}} \frac{1}{2\sqrt{t}} \right) \right]$$

$$\alpha = \operatorname{erfc} \left(\frac{x}{2\sqrt{D_A t}} \right)$$

$$\frac{A-A_0}{A_1-A_0} = 1 - \operatorname{erf} \frac{x}{2\sqrt{D_A t}} \quad (8.85)$$

8.14. The Effect of Vertical Diffusion. At this point it is advisable to consider the effect of vertical diffusion. Actually, the differential eq. (8.74) should be

$$D_A \frac{\partial^2 A}{\partial x^2} + D_A \frac{\partial^2 A}{\partial y^2} - \frac{\partial A}{\partial t} = 0 \quad (8.86)$$

where y is the vertical distance through which a liquid layer has fallen. It is necessary to show that $D_A \partial^2 A / \partial y^2$ is small compared with $\partial A / \partial t$, or, alternatively, that $D_A (\partial^2 A / \partial y^2)$ divided by $\partial A / \partial t$ is small compared to unity.

Now,

$$\frac{\partial A}{\partial y} = \frac{\partial A}{\partial t} \frac{\partial t}{\partial y} = \frac{1}{v} \frac{\partial A}{\partial t}$$

$$\frac{\partial^2 A}{\partial y^2} = \frac{1}{v} \frac{\partial^2 A}{\partial t^2} \frac{\partial t}{\partial y} - \frac{1}{v^2} \frac{\partial A}{\partial t} \frac{\partial v}{\partial y}$$

$$= \frac{1}{v^2} \left(\frac{\partial^2 A}{\partial t^2} - \frac{\partial A}{\partial t} \frac{\partial v}{\partial y} \right)$$

$$D_A \frac{\partial^2 A / \partial y^2}{\partial A / \partial t} = \frac{D_A}{v^2} \frac{\frac{\partial^2 A}{\partial t^2} - \frac{\partial A}{\partial t} \frac{\partial v}{\partial y}}{\frac{\partial A}{\partial t}}$$

$$= \frac{D_A}{v^2} \left[\frac{\partial^2 A / \partial t^2}{\partial A / \partial t} - \partial v / \partial y \right]$$

If we assume for the moment that $\partial^2 A / \partial y^2 = 0$, we have from eq. (8.85) that

$$A = A_0 + (A_1 - A_0) \left(1 - \operatorname{erf} \frac{x}{2\sqrt{D_A t}} \right)$$

Differentiating once, and then again with respect to time gives:

$$\frac{\partial A}{\partial t} = (A_1 - A_0) \frac{x}{2t\sqrt{\pi D_A t}} \exp\left(-\frac{x^2}{4D_A t}\right)$$

$$\frac{\partial^2 A}{\partial t^2} = (A_1 - A_0) \frac{x}{2t\sqrt{\pi D_A t}} \exp\left(-\frac{x^2}{4D_A t}\right) \left[\frac{x^2}{4D_A t^2} - \frac{3}{2t} \right]$$

$$\frac{\partial^2 A / \partial t^2}{\partial A / \partial t} = \frac{x^2}{4D_A t^2} - \frac{3}{2t}$$

$$D_A \frac{\partial^2 A / \partial y^2}{\partial A / \partial t} = \frac{D_A}{v^2} \left[\frac{x^2}{4D_A t^2} - \frac{3}{2t} - \frac{\partial v}{\partial y} \right]$$

Now, we run into trouble at the point $t = 0$ (or $y = 0$) and presumably it would then be necessary to take the vertical diffusion into account. However, let us neglect the region within 0.01 cm. of the origin, since a very small percentage of the total absorption occurs there, and concern ourselves with the region $y \geq 0.01$ cm. Then, recognizing that for small y , $v = v_0$, the initial velocity, and $y = v_0 t$,

$$D_A \frac{\partial^2 A / \partial y^2}{\partial A / \partial t} = \frac{x^2}{4y^2} - \frac{3D_A}{2v_0 y} - \frac{D_A}{v_0^2} \frac{\partial v}{\partial y}$$

If we arbitrarily define the depth of penetration as that region in which concentration change is greater than 1%, the depth of penetration is given by

$$1 - \operatorname{erf} \left(\frac{x}{2\sqrt{D_A t}} \right) = 0.01$$

whence

$$\frac{x}{2\sqrt{D_A t}} = 1.821$$

$$x^2 = 13.27 D_A t$$

$$\frac{x^2}{4y^2} = \frac{3.320 D_A}{y v_0}$$

$$D_A \frac{\partial^2 A / \partial y^2}{\partial A / \partial t} = 1.820 \frac{D_A}{v_0 y} - \frac{D_A}{v_0^2} \frac{\partial v}{\partial y}$$

The maximum value that $\partial v / \partial y$ can have is when acceleration of the fluid is a maximum, and this acceleration could not conceivably exceed the acceleration due to gravity.

$$\frac{\partial v}{\partial y} = \frac{\partial v}{\partial t} \frac{\partial t}{\partial y} = \frac{g}{v_0}$$

$$D \frac{\partial^2 A / \partial y^2}{\partial A / \partial t} = 1.820 \frac{D_A}{v_0 y} - \frac{D_A g}{v_0^3}$$

The lowest values of v_0 encountered in the short wetted-wall columns were about 0.9 cm./sec. Using $D_A = 2 \times 10^{-5}$ cm./sec., $y = 0.01$ cm., the first term is

$$1.820 \frac{2 \times 10^{-5}}{(0.9)(0.01)} = 4 \times 10^{-3}$$

The second term is

$$\frac{2 \times 10^{-5}(980)}{(0.9)^3} = 2.7 \times 10^{-2}$$

Both terms may be considered small compared with 1. Usually v_0 runs considerably higher, so that the magnitude of the second term would generally be much lower. Thus, it may be concluded that the effect of vertical diffusion is negligible, except at very low liquor rates, in which case the effect is still a small one.

8.15. First Order Irreversible Reaction. For this case, eq. (8.30) reduces to

$$D_A \frac{\partial^2 A}{\partial x^2} - \frac{\partial A}{\partial t} = k_1 A \quad (8.87)$$

with the boundary conditions

$$\begin{aligned} \text{At } x = 0, \quad t > 0, & \quad A = A_1 \\ t = 0, \quad x > 0, & \quad A = A_0 \\ x = \infty, \quad t \geq 0, & \quad A = A_0 \exp(-k_1 t) \end{aligned} \quad (8.88)$$

The last boundary condition follows from the fact that at a distance infinitely far from the interface, the concentration will change with time. The change results, however, not from diffusion, but from the chemical reaction. In this region, differential eq. (8.8) will hold:

$$- \frac{dA}{dt} = k_1 A \quad (8.8)$$

Integrating

$$\int_{A_0}^A \frac{dA}{A} = -k_1 \int_0^t dt$$

$$\ln \frac{A}{A_0} = -k_1 t$$

$$A = A_0 \exp(-k_1 t)$$

Taking the transform of eqs. (8.87), (8.88) and (8.8), we have

$$D_A \frac{d^2 \bar{A}}{dx^2} - (p \bar{A} - A_0) = k_1 \bar{A} \quad (8.89)$$

$$\text{At } x = 0, \quad \bar{A} = \frac{A_1}{p} \quad (8.90)$$

$$x = \infty, \quad \bar{A} = \frac{A_0}{p+k_1} \quad (8.91)$$

Rearranging (8.89)

$$\frac{d^2 \bar{A}}{dx^2} - \frac{(p+k_1)}{D_A} \bar{A} = - \frac{A_0}{D_A}$$

The homogeneous solution is

$$\bar{A} = c_1 \exp\left(\sqrt{\frac{p+k_1}{D_A}} x\right) + c_2 \exp\left(-\sqrt{\frac{p+k_1}{D_A}} x\right)$$

A particular solution is $\bar{A} = \frac{A_0}{p+k_1}$

The complete solution is

$$\bar{A} = c_1 \exp\left(\sqrt{\frac{p+k_1}{D_A}} x\right) + c_2 \exp\left(-\sqrt{\frac{p+k_1}{D_A}} x\right) + \frac{A_0}{p+k_1}$$

Substituting B.C. (8.91) gives $c_1 = 0$. Substituting B.C. (8.90) gives

$$\begin{aligned} \frac{A_1}{p} &= c_2 + \frac{A_0}{p+k_1} \\ c_2 &= \frac{A_1}{p} - \frac{A_0}{p+k_1} \\ \bar{A} &= \left(\frac{A_1}{p} - \frac{A_0}{p+k_1}\right) \exp\left(-\sqrt{\frac{p+k_1}{D_A}} x\right) + \frac{A_0}{p+k_1} \end{aligned} \quad (8.92)$$

$$\begin{aligned} \frac{d\bar{A}}{dx} &= -\left(\frac{A_1}{p} - \frac{A_0}{p+k_1}\right) \sqrt{\frac{p+k_1}{D_A}} \exp\left(-\sqrt{\frac{p+k_1}{D_A}} x\right) \\ \left(\frac{d\bar{A}}{dx}\right)_{x=0} &= -\frac{A_1}{D_A} \frac{\sqrt{p+k_1}}{p} + \frac{A_0}{\sqrt{D_A} \sqrt{p+k_1}} \\ \left(\frac{d\bar{A}}{dx}\right)_{x=0} &= \frac{1}{\sqrt{D_A}} \left[\frac{-A_1(p+k_1) + A_0 p}{p \sqrt{p+k_1}} \right] \\ \left(\frac{d\bar{A}}{dx}\right)_{x=0} &= \frac{1}{\sqrt{D_A}} \left[\frac{A_0 - A_1}{\sqrt{p+k_1}} - \frac{A_1 k_1}{p \sqrt{p+k_1}} \right] \end{aligned} \quad (8.93)$$

Pair 526, page 53, of Campbell and Foster (7) gives

$$\mathcal{L}^{-1} \left(\frac{1}{\sqrt{p+k_1}} \right) = \frac{1}{\sqrt{\pi t}} \exp(-k_1 t) \quad (8.94)$$

Pair 546, page 57, of Campbell and Foster gives

$$\mathcal{L}^{-1} \left(\frac{1}{p \sqrt{p+k_1}} \right) = \frac{1}{\sqrt{k_1}} \operatorname{erf} \sqrt{k_1 t} \quad (8.95)$$

Then

$$\left(\frac{\partial A}{\partial x}\right)_{x=0} = \frac{1}{\sqrt{D_A}} \left[\frac{A_0 - A_1}{\sqrt{\pi t}} \exp(-k_1 t) - \frac{A_1 \cdot k_1}{\sqrt{k_1}} \operatorname{erf} \sqrt{k_1 t} \right]$$

$$N_A = -D_A \left(\frac{\partial A}{\partial x}\right)_{x=0}$$

$$N_A = \sqrt{D_A} \left[\frac{A_1 - A_0}{\sqrt{\pi t}} \exp(-k_1 t) + A_1 \sqrt{k_1} \operatorname{erf} \sqrt{k_1 t} \right] \quad (8.96)$$

To find the total absorbed in time t , write

$$\int_0^t N_A dt = -D_A \int_0^t \left(\frac{\partial A}{\partial x}\right)_{x=0} dt$$

From eq. (8.93), we obtain

$$\mathcal{L}\left(\int_0^t \left(\frac{\partial A}{\partial x}\right)_{x=0} dt\right) = \frac{1}{\sqrt{D_A}} \left[\frac{A_0 - A_1}{p \sqrt{p+k_1}} - \frac{A_1 k_1}{p^2 \sqrt{p+k_1}} \right] \quad (8.97)$$

Now, $\mathcal{L}^{-1}\left(\frac{1}{p^2 \sqrt{p+k_1}}\right)$ cannot be found in Campbell and Foster.

One way to proceed is to consider eq. (8.95). Multiplying the right hand function by $(-t)$ is equivalent to differentiating the left hand function of p with respect to p . (For proof, see Hildebrand (38), page 62.) Then

$$\mathcal{L}\left(\frac{t}{\sqrt{k_1}} \operatorname{erf} \sqrt{k_1 t}\right) = -\frac{d}{dp} \left(\frac{1}{p \sqrt{p+k_1}}\right) = \frac{1}{p^2 \sqrt{p+k_1}} + \frac{1}{2p(p+k_1)^{3/2}}$$

From pair 565.4, page 61 of Campbell and Foster, we have

$$\frac{1}{p(p+k_1)^{3/2}} = \frac{1}{k_1^{3/2}} \operatorname{erf} \sqrt{k_1 t} - \frac{2\sqrt{t}}{k_1 \sqrt{\pi}} \exp(-k_1 t) \quad (8.98)$$

Thus,

$$\frac{1}{p^2 \sqrt{p+k_1}} = \mathcal{L}\left[\frac{t}{\sqrt{k_1}} \operatorname{erf} \sqrt{k_1 t} - \frac{1}{2k_1^{3/2}} \operatorname{erf} \sqrt{k_1 t} + \frac{\sqrt{t}}{k_1 \sqrt{\pi}} \exp(-k_1 t)\right] \quad (8.99)$$

Taking the inverse transform of eq. (8.97), using eqs. (8.95) and (8.99), we get

$$\int_0^t \left(\frac{\partial A}{\partial x} \right)_{x=0} dt = \frac{1}{\sqrt{D_A}} \left[\frac{A_0 - A_1}{\sqrt{k_1}} \operatorname{erf} \sqrt{k_1 t} - A_1 t \sqrt{k_1} \operatorname{erf} \sqrt{k_1 t} + \frac{A_1}{2\sqrt{k_1}} \operatorname{erf} \sqrt{k_1 t} - A_1 \sqrt{\frac{t}{\pi}} \exp(-k_1 t) \right]$$

Finally,

$$\int_0^t N_A dt = A_1 \sqrt{\frac{D_A}{k_1}} \left[\left(\frac{1}{2} - \frac{A_0}{A_1} + k_1 t \right) \operatorname{erf} \sqrt{k_1 t} + \sqrt{\frac{k_1 t}{\pi}} \exp(-k_1 t) \right] \quad (8.100)$$

8.16. The Effect of Holdup. The question of the value of A_0/A_1 now arises. In the case of a short wetted-wall column, the liquid will obviously enter with all its components in equilibrium which, in this case, implies that $A_0=0$. In the case of a packed column, where the liquid becomes mixed as it flows from one piece of packing to another and undergoes a short period of exposure to the gas between mixings, A_0 will be a function of the holdup. If the holdup is infinite, at the end of a finite absorption time, the concentration change will be zero throughout practically all the liquid, and will be appreciable only in a small zone near the interface. The volume of the "penetration zone" will be infinitesimal compared to the total volume of the liquid. Hence, after mixing, A_0 for the following period of absorption will still be zero.

For a finite holdup, however, A_0 will be greater than zero. After the liquid has flowed down over several pieces of packing, a sort of steady state will be reached, in which A_0 will remain constant, that is, the concentration after mixing will not change. (This argument assumes constant A_1 , of course). Then, the amount of absorption that occurs in one period of absorption will be equal to the amount of A which reacts in that same period:

$$\int_0^t N_A dt = \int_0^t \int_0^{\delta} k_1 A dx dt$$

At any time t there will be an average concentration:

$$A_{av} = \frac{1}{\delta} \int_0^{\delta} A dx$$

Then

$$\int_0^t N_A dt = k_1 \delta \int_0^t A_{av} dt$$

A fair approximation is that A_{av} is constant over t . Since at $t=0$, $A_{av} = A_0$, and at the end of the absorption period $A_{av} = A_0$, we have

$$\int_0^t N_A dt = k_1 \delta A_0 t$$

Then

$$\frac{A_0}{A_1} = \frac{1}{A_1 \delta k_1 t} \int_0^t N_A dt \quad (8.101)$$

Substituting eq. (8.101) into eq. (8.100) and rearranging:

$$\int_0^t N_A dt + \frac{1}{\delta k_1 t} \sqrt{\frac{D_A}{k_1}} \operatorname{erf} \sqrt{k_1 t} \int_0^t N_A dt = A_1 \sqrt{\frac{D_A}{k_1}} \left[\left(\frac{1}{2} + k_1 t \right) \operatorname{erf} \sqrt{k_1 t} + \sqrt{\frac{k_1 t}{\pi}} \exp(-k_1 t) \right]$$

$$\int_0^t N_A dt = \frac{A_1 \sqrt{\frac{D_A}{k_1}} \left[\left(\frac{1}{2} + k_1 t \right) \operatorname{erf} \sqrt{k_1 t} + \sqrt{\frac{k_1 t}{\pi}} \exp(-k_1 t) \right]}{1 + \sqrt{\frac{D_A}{k_1}} \frac{\operatorname{erf} \sqrt{k_1 t}}{\delta k_1 t}} \quad (8.102)$$

The quantity

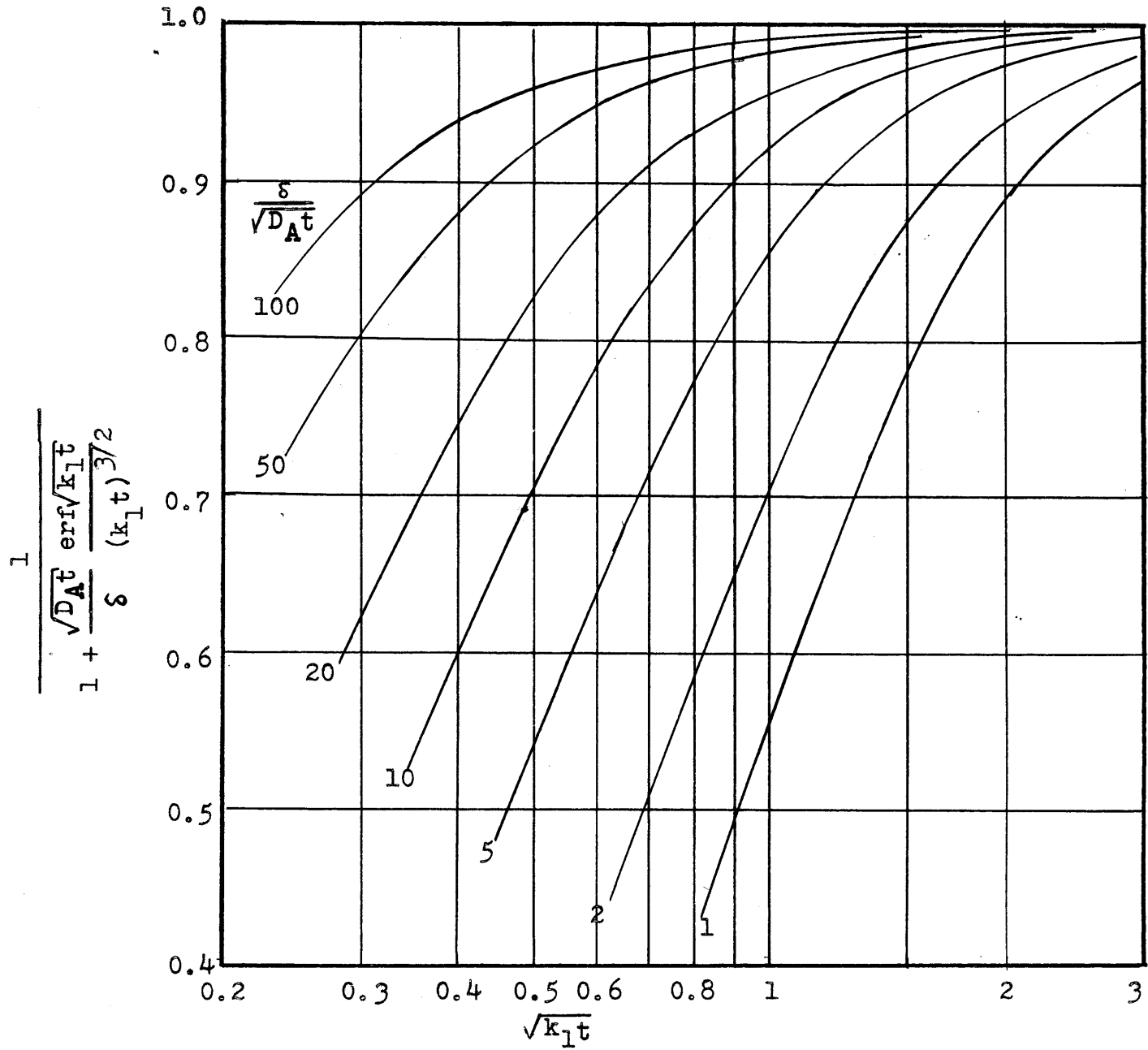
$$\frac{1}{1 + \sqrt{\frac{D_A}{k_1}} \frac{\operatorname{erf} \sqrt{k_1 t}}{\delta k_1 t}}$$

may be regarded as a correction factor to allow for the finite holdup. This quantity, which may be written

$$\frac{1}{1 + \frac{\sqrt{D_A t}}{\delta} \frac{\operatorname{erf} \sqrt{k_1 t}}{(k_1 t)^{3/2}}} \quad (8.103)$$

Fig. 8.6

Correction Factor for Holdup -- Penetration Theory



has been plotted as a function of $\sqrt{k_1 t}$ for various values of $\delta / \sqrt{D_A t}$ in Fig. 8.6. Note the remarkable similarity between Figs. 8.5 and 8.6.

In order to determine whether the effect of holdup may be disregarded, it is necessary to determine the lowest values of $\delta / \sqrt{D_A t}$ which might be expected in a packed column. The lowest value would occur at the lowest flow rate. The lowest flow rate used by Vivian and Whitney (101) was 900 lb./hr. (ft²). Perhaps the most comprehensive data on holdup in packed columns were obtained by Jesser and Elgin (52). At 900 lb./hr. (ft²) they found that 1/2-inch Raschig rings had a holdup of 0.029 ft³ per ft³ of packing. They also presented a correlation of holdup vs packing size which indicated that 1-inch Raschig rings should have a holdup 82% that of 1/2-inch rings, or 0.024 ft³/ft³. The work of deNicolas, which is described in Sec. 9.3, indicates that at this flow rate, the effective wetted area of the packing is $a = 0.48 \text{ cm}^2/\text{cm}^3$ (see Fig. 9.3). δ will then be $0.024/0.48 = 0.05 \text{ cm}$. For oxygen the diffusivity is about $2 \times 10^{-5} \text{ cm}^2/\text{sec}$. The time of exposure in flowing one inch is about 0.1 sec. or less. Then

$$\delta / \sqrt{D_A t} = 0.05 / \sqrt{(2 \times 10^{-5})(0.1)} = 35$$

Fig. 8.6 shows that at $\sqrt{k_1 t}$ above 0.5, for values of $\delta / \sqrt{D_A t}$ above 35, the correction factor is 0.85 or greater.

At low values of $\sqrt{k_1 t}$, the reaction is sufficiently slow that, aside from the effect on A_0 , the reaction will have little effect on the shape of the concentration-distance curve, and hence little effect on the rate of absorption. To show that this is true, we proceed as follows. Rewrite eq. (8.102)

$$\frac{\int_0^t N_A dt}{A_1 \sqrt{D_A t}} = \frac{\frac{1}{\sqrt{k_1 t}} \left[\left(\frac{1}{2} + k_1 t \right) \text{erf} \sqrt{k_1 t} + \sqrt{\frac{k_1 t}{\pi}} \exp(-k_1 t) \right]}{1 + \frac{\sqrt{D_A t}}{\delta} \frac{\text{erf} \sqrt{k_1 t}}{(k_1 t)^{3/2}}} \quad (8.104)$$

Rewrite eq. (8.101)

$$\frac{A_0}{A_1} = \frac{\sqrt{D_A t}}{\delta} \frac{1}{k_1 t} \frac{\int_0^t N_A dt}{A_1 \sqrt{D_A t}} \quad (8.105)$$

Rewrite eq. (8.84)

$$\frac{\int_0^t N_A dt}{A_1 \sqrt{D_A t}} = \frac{2}{\sqrt{\pi}} \left(1 - \frac{A_0}{A_1}\right) \quad (8.106)$$

At $\delta / \sqrt{D_A t} = 35$, substitute various values of $k_1 t$ into eq. (8.104). The result is substituted into eq. (8.105) to give A_0/A_1 . This value of A_0/A_1 is then substituted into eq. (8.106) to obtain the value of $\int_0^t N_A dt / (A \sqrt{D_A t})$ which would be obtained if the value of A_0 were the same, but there was no chemical reaction. The calculations are summarized in Table 8.2. The last column is the ratio of the result from eq. (8.106) divided by the result obtained from eq. (8.104).

TABLE 8.2

Comparison of Eqs. (8.102) and (8.104)

$\sqrt{k_1 t}$	A_0/A_1	$\frac{\int_0^t N_A dt}{A_1 \sqrt{D_A t}}$		Ratio $\frac{\text{eq. (8.106)}}{\text{eq. (8.104)}}$
		From eq. (8.104)	From eq. (8.106)	
0.1	0.768	0.2689	0.2615	0.972
0.2	0.455	0.637	0.615	0.967
0.3	0.274	0.862	0.820	0.950
0.4	0.178	0.996	0.928	0.931
0.5	0.125	1.090	0.988	0.906

What has been done was to calculate the value of A_0/A_1 which would actually exist using eqs. (8.101) and (8.102). Eq. (8.104) allows one to calculate the actual rate of absorption. Eq. (8.106) tells the rate of absorption if the same value of A_0/A_1 existed, but if there were no chemical reaction. The last column in Table 8.2, then, gives the ratio of the rate of absorption without chemical reaction to the rate of absorption with chemical reaction, A_0/A_1 being the same for both. We see then that at $\sqrt{k_1 t} = 0.5$, the error of neglecting the chemical reaction during the diffusion process is only 9%, and decreases for lower values of $\sqrt{k_1 t}$. Larger values of $\delta / \sqrt{k_1 t}$ would also decrease this error. Physically, the reason for the small difference is that the reaction is so

slow that very little of it occurs during the diffusion process, but rather takes place after the fluid is mixed at the end of the absorption period.

To summarize, in the region $\sqrt{k_1 t} < 0.5$, the absorption process may be regarded as straight physical diffusion followed by chemical reaction after mixing with little error, while for $\sqrt{k_1 t} > 0.5$, where chemical reaction is occurring simultaneously with the diffusion, the holdup may be considered sufficiently large that the error of assuming infinite holdup is small.

Thus, for the case of first order irreversible reaction in packed columns, we have justified the assumption of infinite holdup or, equivalently, equilibrium in the fluid at the beginning of the short absorption period (i.e., just after mixing). Of course, in the experiments on short wetted-wall columns, such an assumption is obviously justified. In further work on the more complicated cases of absorption with chemical reaction, we shall, therefore, make the assumption that at $t = 0$, the concentrations of the various components in the liquid, in addition to being uniform, are at equilibrium.

With that assumption, since $A_0 = 0$ at equilibrium, eq. (8.96) becomes

$$N_A = A_1 \sqrt{D_A} \left[\frac{1}{\sqrt{\pi t}} \exp(-k_1 t) + \sqrt{k_1} \operatorname{erf} \sqrt{k_1 t} \right] \quad (8.107)$$

and eq. (8.100) becomes

$$\int_0^t N_A dt = A_1 \sqrt{\frac{D_A}{k_1}} \left[\left(\frac{1}{2} + k_1 t \right) \operatorname{erf} \sqrt{k_1 t} + \frac{\sqrt{k_1 t}}{\pi} \exp(-k_1 t) \right] \quad (8.108)$$

8.17. First Order Reversible Reaction. For this case the differential equation is

$$D_A \frac{\partial^2 A}{\partial x^2} - \frac{\partial A}{\partial t} = \frac{\partial E}{\partial t} - D_E \frac{\partial^2 E}{\partial x^2} = k_1 A - k_2 E \quad (8.109)$$

with the boundary conditions

$$\begin{aligned} \text{At } x = 0, t > 0, & \quad A = A_1, \quad \frac{\partial E}{\partial x} = 0 \\ \text{At } t = 0, x > 0, & \quad A = A_0, \quad E = E_0, \quad K = \frac{E_0}{A_0} \\ \text{At } x = \infty, t \geq 0, & \quad A = A_0, \quad E = E_0 \end{aligned} \quad (8.110)$$

In addition, we have

$$K = \frac{E_0}{A_0} = \frac{k_1}{k_2} \quad (8.111)$$

Equation (8.109) may be rewritten

$$D_A \frac{\partial^2 (A-A_0)}{\partial x^2} - \frac{\partial (A-A_0)}{\partial t} = \frac{\partial (E-E_0)}{\partial t} - D_E \frac{\partial^2 (E-E_0)}{\partial x^2} \\ = k_1 (A-A_0) - k_2 (E-E_0) + k_1 A_0 - k_2 E_0 \quad (8.112)$$

From eq. (8.111), $k_1 A_0 - k_2 E_0 = 0$, so the last two terms of eq. (8.112) may be cancelled out.

Unfortunately, it has not been possible to solve this problem for the case of unequal diffusivities. It is necessary to assume

$$D_A = D_B = D \quad (8.113)$$

Again, let $\alpha = \frac{A-A_0}{A_1-A_0}$

Let

$$\epsilon = \frac{E-E_0}{A_1-A_0}$$

With these substitutions, eq. (8.112) and the boundary conditions become

$$D \frac{\partial^2 \alpha}{\partial x^2} - \frac{\partial \alpha}{\partial t} = \frac{\partial \epsilon}{\partial t} - D \frac{\partial^2 \epsilon}{\partial x^2} = k_1 \alpha = k_2 \epsilon \quad (8.114)$$

$$\text{At } x = 0, \quad t > 0, \quad \alpha = 1, \quad \frac{\partial \epsilon}{\partial x} = 0$$

$$\text{At } t = 0, \quad x > 0, \quad \alpha = 0, \quad \epsilon = 0 \quad (8.115)$$

$$\text{At } x = \infty, \quad t \geq 0, \quad \alpha = 0, \quad \epsilon = 0$$

We take the Laplace transforms of eqs. (8.114) and (8.115).

$$D \frac{d^2 \bar{\alpha}}{dx^2} - p \bar{\alpha} = p \bar{\epsilon} - D \frac{d^2 \bar{\epsilon}}{dx^2} = k_1 \bar{\alpha} - k_2 \bar{\epsilon} \quad (8.116)$$

$$\text{At } x = 0, \quad \bar{\alpha} = 1/p, \quad \frac{d\bar{\epsilon}}{dx} = 0 \quad (8.117)$$

$$\text{At } x = \infty, \quad \bar{\alpha} = 0, \quad \bar{\epsilon} = 0 \quad (8.118)$$

The first equation of (8.116) may be rewritten

$$\frac{d^2(\bar{\alpha} + \bar{\epsilon})}{dx^2} - \frac{p}{D} (\bar{\alpha} + \bar{\epsilon}) = 0 \quad (8.119)$$

The complete general solution of eq. (8.119) is

$$(\bar{\alpha} + \bar{\epsilon}) = c_1 \exp\left(\sqrt{\frac{p}{D}}x\right) + c_2 \exp\left(-\sqrt{\frac{p}{D}}x\right) \quad (8.120)$$

From B.C. (8.118), we have $c_1 = 0$. Differentiate eq. (8.120) once with respect to x .

$$\frac{d\bar{\alpha}}{dx} + \frac{d\bar{\epsilon}}{dx} = -c_2 \sqrt{\frac{p}{D}} \exp\left(-\sqrt{\frac{p}{D}}x\right)$$

Using B.C. (8.117) and defining $Q = \left(\frac{d\bar{\alpha}}{dx}\right)_{x=0}$, we have

$$Q = -c_2 \sqrt{\frac{p}{D}}, \text{ or } c_2 = -Q \sqrt{\frac{D}{p}}$$

Substituting into eq. (8.120), and solving for $-\bar{\epsilon}$:

$$-\bar{\epsilon} = \bar{\alpha} + Q \sqrt{\frac{D}{p}} \exp\left(-\sqrt{\frac{p}{D}}x\right)$$

This result is then substituted into eq. (8.116):

$$D \frac{d^2\bar{\alpha}}{dx^2} - p\bar{\alpha} = k_1\bar{\alpha} + k_2\left(\bar{\alpha} + Q \sqrt{\frac{D}{p}} \exp\left(-\sqrt{\frac{p}{D}}x\right)\right)$$

Rearranging:

$$\frac{d^2\bar{\alpha}}{dx^2} = \left(\frac{k_1+k_2+p}{D}\right) \bar{\alpha} + \frac{k_2Q}{\sqrt{Dp}} \exp\left(-\sqrt{\frac{p}{D}}x\right) \quad (8.121)$$

As in the case for the film theory, we let

$$R = \sqrt{\frac{k_1+k_2}{D}}$$

To facilitate the manipulations which follow, we define

$$s = \sqrt{\frac{k_1 + k_2 + p}{D}}, \quad T = \sqrt{\frac{p}{D}}$$

Then eq. (8.121) becomes

$$\frac{d^2 \bar{u}}{dx^2} = s^2 \bar{u} + \frac{k_2 Q}{D T} \exp(-Tx) \quad (8.122)$$

The homogeneous solution of eq. (8.122) is

$$\bar{u}_H = c_3 \exp(Sx) + c_4 \exp(-Sx)$$

A particular solution is obtained by the method of undetermined coefficients. Let $\bar{u}_p = c_5 \exp(-Tx)$, where c_5 is the undetermined coefficient. Substituting into eq. (8.122) gives

$$T^2 c_5 \exp(-Tx) = s^2 c_5 \exp(-Tx) + \frac{k_2 Q}{DT} \exp(-Tx)$$

whence

$$c_5 = \frac{k_2 Q}{DT(T^2 - s^2)} = -\frac{k_2 Q}{DTR^2}$$

The complete general solution of eq. (8.122) is then

$$\bar{u} = c_3 \exp(Sx) + c_4 \exp(-Sx) - \frac{k_2 Q}{DTR^2} \exp(-Tx) \quad (8.123)$$

Using B.C. (8.118) once again, we have $c_3 = 0$.

Differentiating eq. (8.123) once, we have

$$\frac{d\bar{u}}{dx} = -Sc_4 \exp(-Sx) + \frac{k_2 Q}{DR^2} \exp(-Tx)$$

Using the definition of Q :

$$Q = -Sc_4 + \frac{k_2 Q}{DR^2}$$

$$c_4 = \frac{Q}{S} \left(\frac{k_2}{DR^2} - 1 \right)$$

Substituting into eq. (8.123) gives

$$\bar{u} = \frac{Q}{S} \left(\frac{k_2}{DR^2} - 1 \right) \exp(-Sx) - \frac{k_2 Q}{DTR^2} \exp(-Tx)$$

Using B.C. (8.117), we have

$$\frac{1}{p} = \frac{Q}{S} \left(\frac{k_2}{DR^2} - 1 \right) - \frac{k_2 Q}{DTR^2}$$

Since $DR^2 = k_1 + k_2$

$$\frac{k_2}{DR^2} = \frac{k_2}{k_1 + k_2} = \frac{1}{\frac{k_1}{k_2} + 1} = \frac{1}{K+1}$$

$$\frac{k_2}{DR^2} - 1 = \frac{1}{K+1} - 1 = -\frac{K}{K+1}$$

Then $\frac{1}{p} = \frac{Q}{S} \left(-\frac{K}{K+1} \right) - \frac{Q}{T} \left(\frac{1}{K+1} \right)$

$$Q = -\frac{K+1}{p} \frac{1}{\left(\frac{K}{S} + \frac{1}{T} \right)}$$

$$Q = -\frac{K+1}{p} \frac{1}{\left(\frac{K}{\sqrt{R^2 + \frac{p}{D}}} + \frac{1}{\sqrt{\frac{p}{D}}} \right)}$$

$$Q = -\frac{K+1}{\sqrt{Dp}} \frac{\sqrt{R^2 D + p}}{K \sqrt{p} + \sqrt{R^2 D + p}}$$

(8.124)

Multiply numerator and denominator by $K\sqrt{p} - \sqrt{R^2 D + p}$

$$Q = -\frac{K+1}{\sqrt{D}} \frac{1}{\sqrt{p}} \frac{K\sqrt{p} \sqrt{R^2 D + p} - (R^2 D + p)}{K^2 p - (R^2 D + p)}$$

$$Q = -\frac{K+1}{\sqrt{D}} \left[\frac{K \sqrt{R^2 D + p}}{(K^2-1)p - R^2 D} - \frac{R^2 D + p}{\sqrt{p} [(K^2-1)p - R^2 D]} \right]$$

$$Q = -\frac{1}{\sqrt{D}(K-1)} \left[\frac{K \sqrt{p + R^2 D}}{p - \frac{R^2 D}{K^2-1}} - \frac{R^2 D}{\sqrt{p} (p - \frac{R^2 D}{K^2-1})} - \frac{\sqrt{p}}{p - \frac{R^2 D}{K^2-1}} \right] \quad (8.125)$$

Using pairs 549, 542 and 541 on pages 57, 55 and 55, respectively, of Campbell and Foster (7), we have

$$\begin{aligned} \mathcal{L}^{-1}(Q) = & -\frac{1}{\sqrt{D}(K-1)} \left\{ K \left[\frac{1}{\sqrt{\pi t}} \exp(-R^2 D t) + \sqrt{\frac{R^2 D + \frac{R^2 D}{K^2-1}}{K^2-1}} \exp\left(\frac{R^2 D t}{K^2-1}\right) \operatorname{erf} \sqrt{R^2 D t + \frac{R^2 D t}{K^2-1}} \right] \right. \\ & - R^2 D \left[\frac{1}{\sqrt{\frac{R^2 D}{K^2-1}}} \exp\left(\frac{R^2 D t}{K^2-1}\right) \operatorname{erf} \sqrt{\frac{R^2 D t}{K^2-1}} \right] \\ & \left. - \left[\frac{1}{\sqrt{\pi t}} + \sqrt{\frac{R^2 D}{K^2-1}} \exp\left(\frac{R^2 D t}{K^2-1}\right) \operatorname{erf} \sqrt{\frac{R^2 D t}{K^2-1}} \right] \right\} \end{aligned}$$

$$\begin{aligned} \mathcal{L}^{-1}(Q) = & -\frac{1}{\sqrt{D}(K-1)} \left[\frac{K}{\sqrt{\pi t}} \exp(-R^2 D t) + \frac{K^2 \sqrt{R^2 D}}{K^2-1} \exp\left(\frac{R^2 D t}{K^2-1}\right) \operatorname{erf} \sqrt{\frac{K^2 R^2 D t}{K^2-1}} \right. \\ & \left. - \frac{K^2 \sqrt{R^2 D}}{\sqrt{K^2-1}} \exp\left(\frac{R^2 D t}{K^2-1}\right) \left(\operatorname{erf} \sqrt{\frac{R^2 D t}{K^2-1}} - \frac{1}{\sqrt{\pi t}} \right) \right] \end{aligned}$$

$$\begin{aligned} \mathcal{L}^{-1}(Q) = & -\frac{1}{\sqrt{D}(K-1)} \left[\frac{K \exp(-R^2 D t) - 1}{\sqrt{\pi t}} \right. \\ & \left. + \frac{K^2 \sqrt{R^2 D}}{\sqrt{K^2-1}} \exp\left(\frac{R^2 D t}{K^2-1}\right) \left(\operatorname{erf} \sqrt{\frac{K^2 R^2 D t}{K^2-1}} - \operatorname{erf} \sqrt{\frac{R^2 D t}{K^2-1}} \right) \right] \end{aligned}$$

$$\begin{aligned} \text{Now, } N_A &= -D_A \left(\frac{\partial A}{\partial x} \right)_{x=0} = -D_A (A_1 - A_0) \left(\frac{\partial a}{\partial x} \right)_{x=0} \\ &= -D_A (A_1 - A_0) \mathcal{L}^{-1}(Q) \end{aligned}$$

$$\begin{aligned} N_A &= \frac{(A_1 - A_0) \sqrt{D}}{K-1} \left[\frac{K \exp(-R^2 Dt) - 1}{\sqrt{\pi t}} \right. \\ &\quad \left. + \frac{K^2 \sqrt{R^2 D}}{\sqrt{K^2 - 1}} \exp\left(\frac{R^2 Dt}{K^2 - 1}\right) \left(\operatorname{erf} \sqrt{\frac{K^2 R^2 Dt}{K^2 - 1}} - \operatorname{erf} \sqrt{\frac{R^2 Dt}{K^2 - 1}} \right) \right] \quad (8.126) \end{aligned}$$

When $K = 1$, this formula is indeterminate. For this special case, we go back to eq. (8.124). This becomes

$$Q = - \frac{2}{\sqrt{Dp}} \frac{\sqrt{R^2 D + p}}{\sqrt{p} + \sqrt{R^2 D + p}}$$

Multiply numerator and denominator by $\sqrt{p} - \sqrt{R^2 D + p}$

$$\begin{aligned} Q &= - \frac{2}{\sqrt{D}} \frac{1}{\sqrt{p}} \frac{\sqrt{p} \sqrt{R^2 D + p} - (R^2 D + p)}{p - (R^2 D + p)} \\ Q &= \frac{2}{R^2 D \sqrt{D}} \left[\sqrt{p + R^2 D} - \frac{R^2 D}{\sqrt{p}} - \sqrt{p} \right] \quad (8.127) \end{aligned}$$

Using pairs 506, 522 and 503, pages 49, 50 and 49, respectively, of Campbell and Foster (?), we have

$$\mathcal{L}^{-1}(Q) = \frac{2}{R^2 D \sqrt{D}} \left[- \frac{1}{2t \sqrt{\pi t}} \exp(-R^2 Dt) - \frac{R^2 D}{\sqrt{\pi t}} + \frac{1}{2t \sqrt{\pi t}} \right]$$

This rearranges to:

$$\mathcal{L}^{-1}(Q) = \frac{-1}{\sqrt{\pi D t}} \left[2 + \frac{\exp(-R^2 Dt) - 1}{R^2 Dt} \right]$$

Then

$$N_A = (A_1 - A_0) \sqrt{\frac{D}{\pi t}} \left[2 + \frac{\exp(-R^2 Dt) - 1}{R^2 Dt} \right] \quad (8.128)$$

Now, we shall investigate various limiting forms of the instantaneous rate of absorption.

$$(1) R^2Dt \rightarrow 0$$

As the argument becomes smaller, $\exp(-R^2Dt)$ approaches unity, and the error function vanishes. The second term in the bracket of eq. (8.126) vanishes, and eq. (8.126) becomes

$$\lim_{R^2Dt \rightarrow 0} N_A = \frac{(A_1 - A_0)\sqrt{D}}{K-1} \frac{K-1}{\sqrt{\pi t}} = (A_1 - A_0) \sqrt{\frac{D}{\pi t}}$$

This equation is the same as eq. (8.83).

$$(2) R^2Dt \rightarrow \infty$$

The error function may be represented by the following series (Pierce (84), page 120).

$$\operatorname{erf}(x) = 1 - \frac{\exp(-x^2)}{x\sqrt{\pi}} \left(1 - \frac{1}{2x^2} + \frac{1.3}{(2x^2)^2} + \frac{1.3.5}{(2x^2)^3} + \dots \right).$$

Hence, for large values of x , we may replace

$\operatorname{erf}(x)$ by $1 - \frac{\exp(-x^2)}{x\sqrt{\pi}}$. Then eq. (8.126) becomes

$$\lim_{R^2Dt \rightarrow \infty} N_A = \frac{(A_1 - A_0)\sqrt{D}}{K-1} \left[-\frac{1}{\sqrt{\pi t}} + \frac{K^2\sqrt{R^2D}}{\sqrt{K^2-1}} \exp\left(\frac{R^2Dt}{K^2-1}\right) \left(1 - \frac{\exp\left(-\frac{K^2R^2Dt}{K^2-1}\right)}{\sqrt{\pi} \sqrt{\frac{K^2R^2Dt}{K^2-1}}} - 1 + \frac{\exp\left(-\frac{R^2Dt}{K^2-1}\right)}{\sqrt{\pi} \sqrt{\frac{R^2Dt}{K^2-1}}} \right) \right]$$

Upon rearrangement, this becomes

$$\begin{aligned} \lim_{R^2Dt \rightarrow \infty} N_A &= \frac{(A_1 - A_0)}{K-1} \sqrt{\frac{D}{\pi t}} \left[-1 + K^2 \left(-\frac{\exp(-R^2Dt)}{K} + 1 \right) \right] \\ &= \frac{(A_1 - A_0)}{K-1} \sqrt{\frac{D}{\pi t}} [K^2 - 1] \\ &= (A_1 - A_0) \sqrt{\frac{D}{\pi t}} (K + 1) \end{aligned} \tag{8.129}$$

(3) $K \rightarrow 0$

For values of K less than one, the values of the arguments of the error function in eq. (8.126) are imaginary. However, when the argument goes to zero, the error function will still vanish, as can be seen by recourse to its definition. Thus, eq. (8.126) will become

$$\begin{aligned} \lim_{K \rightarrow 0} N_A &= \frac{(A_1 - A_0) \sqrt{D}}{-1} \left[-\frac{1}{\sqrt{\pi t}} \right] \\ &= (A_1 - A_0) \sqrt{\frac{D}{\pi t}} \end{aligned} \quad (8.130)$$

It now is necessary to evaluate the total amount absorbed during the absorption period.

$$\begin{aligned} \int_0^t N_A dt &= -D \int_0^t \left(\frac{\partial A}{\partial x} \right)_{x=0} = -D (A_1 - A_0) \int_0^t \left(\frac{\partial q}{\partial x} \right)_{x=0} \\ &= -D (A_1 - A_0) \int_0^t \mathcal{L}^{-1}(Q) \\ &= -D (A_1 - A_0) \mathcal{L}^{-1} \left(\frac{Q}{p} \right) \end{aligned} \quad (8.131)$$

Thus, it is necessary to find Q/p and obtain the inverse transform of it. Equation (8.125) becomes:

$$\frac{Q}{p} = -\frac{1}{\sqrt{D}(K-1)} \left[\frac{K \sqrt{p + R^2 D}}{p(p - \frac{R^2 D}{K^2 - 1})} - \frac{R^2 D}{p \sqrt{p(p - \frac{R^2 D}{K^2 - 1})}} - \frac{1}{\sqrt{p(p - \frac{R^2 D}{K^2 - 1})}} \right]$$

Using the method of partial fractions, the first two fractions in the brackets may be further separated.

$$\begin{aligned} \frac{Q}{p} &= -\frac{1}{\sqrt{D}(K-1)} \left[\frac{K(K^2-1) \sqrt{p + R^2 D}}{R^2 D} \frac{1}{p - \frac{R^2 D}{K^2-1}} - \frac{K(K^2-1) \sqrt{p + R^2 D}}{R^2 D} \frac{1}{p} \right. \\ &\quad \left. - \frac{(K^2-1)}{\sqrt{p} (p - \frac{R^2 D}{K^2-1})} + \frac{(K^2-1)}{\sqrt{p} p} - \frac{1}{\sqrt{p} (p - \frac{R^2 D}{K^2-1})} \right] \end{aligned}$$

Some simplification may be accomplished:

$$\frac{Q}{p} = - \frac{1}{\sqrt{D}(K-1)} \left[\frac{K(K^2-1)}{R^2D} \left(\frac{\sqrt{p+R^2D}}{p - \frac{R^2D}{K^2-1}} - \frac{\sqrt{p+R^2D}}{p} \right) - \frac{K^2}{\sqrt{p(p - \frac{R^2D}{K^2-1})}} \right. \\ \left. + \frac{K^2-1}{p^{3/2}} \right]$$

Using pairs 549, 549, 542 and 520, pages 57, 57, 55 and 50, Campbell and Foster (2), we have

$$\mathcal{L}^{-1}\left(\frac{Q}{p}\right) = - \frac{1}{\sqrt{D}(K-1)} \left[\frac{K(K^2-1)}{R^2D} \left(\frac{\exp(-R^2Dt)}{\sqrt{\pi t}} + \sqrt{R^2D + \frac{R^2D}{K^2-1}} \exp\left(\frac{R^2Dt}{K^2-1}\right) \cdot \right. \right. \\ \left. \left. \operatorname{erf} \sqrt{\left(R^2D + \frac{R^2D}{K^2-1}\right)t} - \frac{\exp(-R^2Dt)}{\sqrt{\pi t}} - \sqrt{R^2D} \operatorname{erf} \sqrt{R^2Dt} \right) \right. \\ \left. - \frac{K^2}{\sqrt{\frac{R^2D}{K^2-1}}} \exp\left(\frac{R^2Dt}{K^2-1}\right) \operatorname{erf} \sqrt{\frac{R^2Dt}{K^2-1}} + \frac{2(K^2-1)\sqrt{t}}{\sqrt{\pi}} \right]$$

This reduces to

$$\mathcal{L}^{-1}\left(\frac{Q}{p}\right) = - \frac{1}{\sqrt{D}(K-1)} \left[\frac{K(K^2-1)}{R^2D} \left(\sqrt{\frac{K^2R^2D}{K^2-1}} \exp\left(\frac{R^2Dt}{K^2-1}\right) \operatorname{erf} \sqrt{\frac{K^2R^2Dt}{K^2-1}} \right. \right. \\ \left. \left. - \sqrt{R^2D} \operatorname{erf} \sqrt{R^2Dt} \right) \right. \\ \left. - \frac{K^2\sqrt{K^2-1}}{\sqrt{R^2D}} \exp\left(\frac{R^2Dt}{K^2-1}\right) \operatorname{erf} \sqrt{\frac{R^2Dt}{K^2-1}} + \frac{2(K^2-1)\sqrt{t}}{\sqrt{\pi}} \right]$$

$$\mathcal{L}^{-1}\left(\frac{Q}{p}\right) = - \frac{K+1}{RD} \left[\frac{K^2}{\sqrt{K^2-1}} \exp\left(\frac{R^2Dt}{K^2-1}\right) \left(\operatorname{erf} \sqrt{\frac{K^2R^2Dt}{K^2-1}} - \operatorname{erf} \sqrt{\frac{R^2Dt}{K^2-1}} \right) \right. \\ \left. - K \operatorname{erf} \sqrt{R^2Dt} \right] + 2(K+1) \sqrt{\frac{t}{\pi D}}$$

Substituting into eq. (8.131), we have

$$\int_0^t N_A dt = (A_1 - A_0) \frac{K+1}{R} \left[\frac{K^2}{\sqrt{K^2-1}} \exp\left(\frac{R^2Dt}{K^2-1}\right) \left(\operatorname{erf} \sqrt{\frac{K^2R^2Dt}{K^2-1}} - \operatorname{erf} \sqrt{\frac{R^2Dt}{K^2-1}} \right) - K \operatorname{erf} \sqrt{R^2Dt} + 2 \sqrt{\frac{R^2Dt}{\pi}} \right] \quad (8.132)$$

Again, the special case of $K = 1$ must be solved separately. Equation (8.127) becomes

$$\frac{Q}{p} = \frac{2}{R^2D \sqrt{D}} \left[\frac{\sqrt{p + R^2D}}{p} - \frac{R^2D}{p^{3/2}} - \frac{1}{\sqrt{p}} \right]$$

Using pairs 549, 520 and 522, pages 57, 50 and 50 of Campbell and Foster, we get

$$\mathcal{L}^{-1}(Q/p) = \frac{2}{R^2D \sqrt{D}} \left[\frac{\exp(-R^2Dt)}{\sqrt{\pi t}} + \sqrt{R^2D} \operatorname{erf} \sqrt{R^2Dt} - \frac{2R^2D \sqrt{t}}{\sqrt{\pi}} - \frac{1}{\sqrt{\pi t}} \right]$$

Substituting into eq. (8.131):

$$\int_0^t N_A dt = 2(A_1 - A_0) \sqrt{\frac{Dt}{\pi}} \left[2 + \frac{1 - \exp(-R^2Dt)}{R^2Dt} - \frac{\sqrt{\pi} \operatorname{erf} \sqrt{R^2Dt}}{\sqrt{R^2Dt}} \right] \quad (8.133)$$

Again, we shall investigate the limiting forms of the total amount absorbed.

(1) $R^2Dt \rightarrow 0$

Since, for small values of x , $\operatorname{erf}(x)$ may be replaced by $2x/\sqrt{\pi}$, eq. (8.132) may be written

$$\lim_{R^2Dt \rightarrow 0} \int_0^t N_A dt = (A_1 - A_0) \frac{(K+1)}{R} \left[\frac{K^2}{\sqrt{K^2-1}} \frac{2}{\sqrt{\pi}} \left(\sqrt{\frac{K^2R^2Dt}{K^2-1}} - \sqrt{\frac{R^2Dt}{K^2-1}} \right) - \frac{2}{\sqrt{\pi}} K \sqrt{R^2Dt} + \frac{2}{\sqrt{\pi}} \sqrt{R^2Dt} \right]$$

$$\lim_{R^2Dt \rightarrow 0} \int_0^t N_A dt = (A_1 - A_0) 2\sqrt{\frac{Dt}{\pi}} (K+1) \left[\frac{K^2}{\sqrt{K^2-1}} \frac{K-1}{\sqrt{K^2-1}} - K + 1 \right]$$

$$= 2(A_1 - A_0) \sqrt{\frac{Dt}{\pi}}$$

This equation is identical with eq. (8.84).

(2) $R^2Dt \rightarrow \infty$

Proceeding the same way as for the corresponding limit of the instantaneous coefficient, eq. (8.132) becomes

$$\lim_{R^2Dt \rightarrow \infty} \int_0^t N_A dt = (A_1 - A_0) \frac{K+1}{R} \left[\frac{K^2}{\sqrt{K^2-1}} \exp\left(\frac{R^2Dt}{K^2-1}\right) \left(1 - \frac{\exp\left(-\frac{K^2 R^2Dt}{K^2-1}\right)}{\sqrt{\pi} \sqrt{\frac{K^2 R^2Dt}{K^2-1}}}\right) - 1 + \frac{\exp\left(-\frac{R^2Dt}{K^2-1}\right)}{\sqrt{\pi} \sqrt{\frac{R^2Dt}{K^2-1}}}\right] - K + 2\sqrt{\frac{R^2Dt}{\pi}}$$

$$\lim_{R^2Dt \rightarrow \infty} \int_0^t N_A dt = (A_1 - A_0) \frac{K+1}{R} \left[\frac{K^2}{\sqrt{K^2-1}} \left(-\frac{\exp(-R^2Dt)}{\sqrt{\pi} \sqrt{\frac{K^2 R^2Dt}{K^2-1}}} + \frac{1}{\sqrt{\pi} \sqrt{\frac{R^2Dt}{K^2-1}}}\right) - K + 2\sqrt{\frac{R^2Dt}{\pi}} \right]$$

$$\lim_{R^2Dt \rightarrow \infty} \int_0^t N_A dt = (A_1 - A_0)(K+1) \sqrt{\frac{Dt}{\pi}} \left[-\frac{K}{R^2Dt} + 2 \right]$$

$$= 2(A_1 - A_0) \sqrt{\frac{Dt}{\pi}} (K+1) \quad (8.134)$$

As with the corresponding case for the film theory, we may write $C_1 = A_1 + KA_1 = A_1(K+1)$, and $C_0 = A_1 + E_0 = A_1(K+1)$. Then

$$\lim_{R^2Dt \rightarrow \infty} \int_0^t N_A dt = 2(C_1 - C_0) \sqrt{\frac{Dt}{\pi}} \quad (8.135)$$

(3) $K \rightarrow 0$

Eq. (8.132) becomes

$$\begin{aligned} \lim_{K \rightarrow 0} \int_0^t N_A dt &= (A_1 - A_0)(1/R) \left[2 \sqrt{\frac{R^2Dt}{\pi}} \right] \\ &= 2(A_1 - A_0) \sqrt{\frac{Dt}{\pi}} \end{aligned} \quad (8.136)$$

8.18. First Order, Infinitely Rapid, Reversible Reaction.

For this case of reversible reaction, it is possible to solve the problem when the diffusivities are not equal. Eq. (8.109) may be written

$$D_A \frac{\partial^2 A}{\partial x^2} - \frac{\partial A}{\partial t} + D_E \frac{\partial^2 E}{\partial x^2} - \frac{\partial E}{\partial t} = 0 \quad (8.137)$$

At any point within the liquid, equilibrium exists between A and E. Thus, $E = KA$ at any x and t . If this is true, however, since the slope of A is finite at $x = 0$, it must follow that the slope of E is also finite there, in contradiction with the boundary condition $(\partial E / \partial x)_{x=0} = 0$, which comes from the assumption that E is non-volatile. The paradox is resolved by realizing that at the interface there exists an infinitesimal zone in which a finite amount of reaction is taking place. As A dissolves into the liquid at the interface, it undergoes instantaneous reaction in this infinitesimal reaction zone to form the equilibrium quantity of E. This quantity of E must then diffuse from the reaction zone into the body of the liquid, so that the gradient of E must be greater than zero in all parts of the liquid, including the region adjacent to the interface.

The boundary conditions, then, are

$$\begin{array}{lll} x = 0, & t > 0, & A = A_1, \quad E = KA_1 \\ t = 0, & x > 0, & A = A_0, \quad E = E_0 = KA_0 \\ x = \infty, & t \geq 0, & A = A_0, \quad E = E_0 = KA_0 \end{array} \quad (8.138)$$

Eq. (8.137) may be rewritten

$$(D_A + KD_E) \frac{\partial^2 A}{\partial x^2} - (K + 1) \frac{\partial A}{\partial t} = 0 \quad (8.139)$$

The Laplace transform of eq. (8.139) is

$$(D_A + KD_E) \frac{d^2 \bar{A}}{dx^2} - (K + 1)(p\bar{A} - A_0) = 0 \quad (8.140)$$

The transformed boundary conditions are

$$x = 0, \quad \bar{A} = A_1/p \quad (8.141)$$

$$x = \infty, \quad \bar{A} = A_0/p \quad (8.142)$$

Let

$$J = \frac{K+1}{D_A + KD_E} \quad (8.143)$$

Eq. (8.140) becomes

$$\frac{d^2 \bar{A}}{dx^2} - Jp\bar{A} = -JA_0 \quad (8.144)$$

The complete general solution is

$$\bar{A} = c_1 \exp(\sqrt{Jp}x) + c_2 \exp(-\sqrt{Jp}x) + \frac{A_0}{p}$$

B.C. (8.142) gives $c_1 = 0$. B.C. (8.141) gives

$$c_2 = \frac{A_1 - A_0}{p}$$

Whence

$$\bar{A} = \frac{A_1 - A_0}{p} \exp(-\sqrt{Jp}x) + \frac{A_0}{p}$$

$$\frac{d\bar{A}}{dx} = -\sqrt{Jp} \frac{A_1 - A_0}{p} \exp(-\sqrt{Jp}x)$$

$$\left(\frac{dA}{dx}\right)_{x=0} = -(A_1 - A_0) \sqrt{\frac{J}{p}} \quad (8.145)$$

Taking the inverse transform, we get

$$\left(\frac{\partial A}{\partial x}\right)_{x=0} = -(A_1 - A_0) \sqrt{\frac{J}{\pi t}} \quad (8.146)$$

Because of the instantaneous reaction occurring at the interface, the rate of absorption is given not by the rate of diffusion of A from the interface into the body of the liquid, but rather by the rates of diffusion of both A and E from the interface into the body of the liquid. Thus

$$N_A = -D_A \left(\frac{\partial A}{\partial x}\right)_{x=0} - D_E \left(\frac{\partial E}{\partial x}\right)_{x=0}$$

$$N_A = -D_A \left(\frac{\partial A}{\partial x}\right)_{x=0} - K D_E \left(\frac{\partial A}{\partial x}\right)_{x=0}$$

$$N_A = -(D_A + K D_E) \left(\frac{\partial A}{\partial x}\right)_{x=0}$$

Substituting eq. (8.146) and eq. (8.143)

$$N_A = (A_1 - A_0) (D_A + K D_E) \sqrt{\frac{K+1}{\pi t (D_A + K D_E)}}$$

$$N_A = (A_1 - A_0) \sqrt{\frac{D_A}{\pi t}} \sqrt{(K+1) (1 + K D_E / D_A)}$$

To obtain the total amount absorbed we integrate N_A .

$$\int_0^t N_A dt = -(D_A + K D_E) \int_0^t \left(\frac{\partial A}{\partial x}\right)_{x=0} dt$$

From eq. (8.145), we obtain

$$\mathcal{L} \left[\int_0^t \left(\frac{\partial A}{\partial x}\right)_{x=0} dt \right] = -(A_1 - A_0) \frac{\sqrt{J}}{p^{3/2}}$$

The inverse transformation yields

$$\int_0^t \left(\frac{\partial A}{\partial x} \right)_{x=0} dt = -2(A_1 - A_0) \sqrt{\frac{Jt}{\pi}}$$

Then

$$\int_0^t N_A dt = 2(A_1 - A_0)(D_A + KD_E) \sqrt{\frac{(K+1)t}{\pi(D_A + KD_E)}}$$

$$\int_0^t N_A dt = 2(A_1 - A_0) \sqrt{\frac{D_A t}{\pi}} \sqrt{(K+1)(1 + KD_E/D_A)} \quad (8.148)$$

E. COMPARISON OF THE FILM AND PENETRATION THEORIES FOR ABSORPTION WITH FIRST ORDER CHEMICAL REACTION.

8.19. Definition of Absorption Coefficients. It is customary in absorption work to express the rate of absorption as a product of an absorption coefficient and a driving force. For the liquid side of a gas-liquid system, a "total" coefficient, k_L , may be defined on the basis of a "total" driving force:

$$N_A = k_L (C_1 - C_0) \quad (8.149)$$

where C_1 is the total concentration of the material being absorbed in equilibrium with the gas at the interface and C_0 is the total concentration in the bulk of the liquid.

For the case where chemical reaction is present, Vivian and Whitney (101) introduced the concept of a pseudo-coefficient (k_L^0), which they based on a "pseudo-driving force." This pseudo-driving force is the difference between the concentration of the unreacted species of the substance being absorbed which would be in equilibrium with the gas at the interface and the concentration of the unreacted species of the substance being absorbed which is present in the bulk of the liquid.

$$N_A = k_L^0 (A_1 - A_0) \quad (8.150)$$

Where there is no chemical reaction, one may define the ratio of the rate of absorption to the driving force as the "physical" coefficient, k_L^* . Then, since $A = C$,

$$N_A = k_L^* (C_1 - C_0) = k_L^* (A_1 - A_0) \quad (8.151)$$

The above discussion has been presented from the point of view of the film theory. The same driving forces may be used for the penetration theory, provided that the subscript 0 refers to the concentration at the beginning of the absorption period. However,

there are two types of rates involved. One may base the coefficients on the instantaneous rate of absorption, leading to the following types of coefficients:

Instantaneous "total" coefficient

$$N_A = k_{L \text{ inst}} (C_1 - C_0) \quad (8.152)$$

Instantaneous pseudo-coefficient

$$N_A = k_{L \text{ inst}}^{\circ} (A_1 - A_0) \quad (8.153)$$

Instantaneous physical coefficient (in absence of chemical reaction)

$$N_A = k_{L \text{ inst}}^* (C_1 - C_0) = k_{L \text{ inst}} (A_1 - A_0) \quad (8.154)$$

One may likewise base the coefficients on the average rate of absorption, the average being taken over the whole period of absorption.

Average "total" coefficient

$$\frac{\int_0^t N_A dt}{t} = k_{L \text{ av}} (C_1 - C_0) \quad (8.155)$$

Average pseudo-coefficient

$$\frac{\int_0^t N_A dt}{t} = k_{L \text{ av}}^{\circ} (A_1 - A_0) \quad (8.156)$$

Average physical coefficient (in absence of chemical reaction)

$$\frac{\int_0^t N_A dt}{t} = k_{L \text{ av}}^* (C_1 - C_0) = k_{L \text{ av}} (A_1 - A_0) \quad (8.157)$$

Since average rates of absorption are obtained in any type of absorption experiment so far performed, the data are reported in terms of average coefficients. It will be convenient, then, to omit the subscript *av*, and to recognize when the penetration theory is being used, that k_L , k_L° and k_L^* are the average coefficients.

8.20. The Definition of ϕ . In practically all the cases of absorption with chemical reaction so far considered, rate of absorption is equal to the pseudo-driving force multiplied by a term which is completely independent of concentration. In only two cases so far considered has any other driving force been encountered. Eqs. (8.73) and (8.135) show that a total driving force may be used for the special case of first order infinitely rapid reaction with equal diffusivities. The utility of the pseudo-coefficient concept in the field of absorption with chemical reaction should be readily apparent.

It is convenient to express the effect of the chemical reaction upon the rate of absorption in terms of a quantity ϕ , defined as the ratio of the pseudo-coefficient to the physical coefficient. Thus,

$$\phi = \frac{k_L^\circ}{k_L^*} \quad (8.158)$$

ϕ may also be defined, more clumsily perhaps, as the ratio of the rate of absorption with chemical reaction to the rate of absorption if chemical reaction were absent but if the same pseudo-driving force existed.

For the case of the film theory, we may rewrite eq. (8.42):

$$k_L^* = \frac{D_A}{x_f} \quad (8.159)$$

Then

$$\phi = \frac{k_L^\circ x_f}{D_A} = \frac{N_A x_f}{(A_1 - A_0) D_A} \quad (8.160)$$

For the penetration theory, eq. (8.84) may be rewritten:

$$k_L^* = \frac{\int_0^t N_A dt}{(A_1 - A_0) t} = 2 \sqrt{\frac{D_A}{\pi t}} \quad (8.161)$$

Then

$$\phi = \frac{k_L^\circ \sqrt{\pi t}}{2 \sqrt{D_A}} = \frac{\int_0^t N_A dt}{2(A_1 - A_0) \sqrt{D_A t}} \quad (8.162)$$

Eq. (8.162) defines an average value for ϕ . One may also obtain an instantaneous value of ϕ from eq. (8.83).

$$k_L^* \text{ inst} = \sqrt{\frac{D_A}{\pi t}} \quad (8.163)$$

$$\phi \text{ inst} = k_L^\circ \sqrt{\frac{\pi t}{D_A}} = \frac{N_A}{(A_1 - A_0)} \sqrt{\frac{\pi t}{D_A}} \quad (8.164)$$

With the aid of eqs. (8.160), (8.162) and (8.164), we shall now write the equations for ϕ for each of the cases of absorption with chemical reaction so far investigated. Note that in every case ϕ is independent of concentration.

Film Theory. First Order Chemical Reaction.

Irreversible Reaction (from eq. (8.55))

$$\phi = \frac{R x_f}{\tanh R x_f} \quad (8.165)$$

Reversible Reaction (from eq. (8.72))

$$\phi = \frac{1 + \frac{K D_E}{D_A}}{1 + \frac{K D_E}{D_A} \frac{\tanh R x_f}{R x_f}} \quad (8.166)$$

The limiting forms for ϕ are

$$\lim_{K \rightarrow \infty} \phi = \frac{R x_f}{\tanh R x_f} \quad (\text{identical with eq. (8.165)})$$

$$\lim_{R x_f \rightarrow 0} \phi = 1 \quad (8.167)$$

$$\lim_{R x_f \rightarrow \infty} \phi = 1 + \frac{K D_E}{D_A} \quad (8.168)$$

Penetration Theory. First Order Chemical Reaction.

Irreversible Reaction (from eqs. (8.107) and (8.108)).

$$\phi_{\text{inst}} = \exp(-R^2 Dt) + \sqrt{\pi R^2 Dt} \operatorname{erf} \sqrt{R^2 Dt} \quad (8.169)$$

$$\phi = \frac{\sqrt{\pi}}{2} \left(\frac{1}{2 \sqrt{R^2 Dt}} + \sqrt{R^2 Dt} \operatorname{erf} \sqrt{R^2 Dt} + (1/2) \exp(-R^2 Dt) \right) \quad (8.170)$$

Reversible Reaction (from eqs. (8.126) and (8.132)).

$$\begin{aligned} \phi_{\text{inst}} = & \frac{1}{K-1} \left[K \exp(-R^2 Dt) - 1 \right. \\ & \left. + \sqrt{\pi} \frac{K^2 \sqrt{R^2 Dt}}{\sqrt{K^2-1}} \exp\left(\frac{R^2 Dt}{K^2-1}\right) \left(\operatorname{erf} \sqrt{\frac{K^2 R^2 Dt}{K^2-1}} - \operatorname{erf} \sqrt{\frac{R^2 Dt}{K^2-1}} \right) \right] \end{aligned} \quad (8.171)$$

$$\phi = \frac{\sqrt{\pi}}{2\sqrt{R^2Dt}} \left[\frac{K^2}{\sqrt{K^2-1}} \exp\left(\frac{R^2Dt}{K^2-1}\right) \left(\operatorname{erf} \sqrt{\frac{K^2R^2Dt}{K^2-1}} - \operatorname{erf} \sqrt{\frac{R^2Dt}{K^2-1}} \right) - K \operatorname{erf} \sqrt{R^2Dt} \right] + K + 1 \quad (8.172)$$

For the special case of $K = 1$ (from eqs. (8.128) and (8.133))

$$\phi_{\text{inst}} = 2 + \frac{\exp(-R^2Dt) - 1}{R^2Dt} \quad (8.173)$$

$$\phi = 2 + \frac{1 - \exp(-R^2Dt)}{R^2Dt} - \frac{\sqrt{\pi} \operatorname{erf} \sqrt{R^2Dt}}{\sqrt{R^2Dt}} \quad (8.174)$$

The limiting forms for ϕ are:

$$\lim_{R^2Dt \rightarrow 0} \phi_{\text{inst}} = 1 \quad (8.175)$$

$$\lim_{R^2Dt \rightarrow 0} \phi = 1 \quad (8.176)$$

$$\lim_{R^2Dt \rightarrow \infty} \phi_{\text{inst}} = K + 1 \quad (\text{from eq. (8.129)}) \quad (8.177)$$

$$\lim_{R^2Dt \rightarrow \infty} \phi = K + 1 \quad (\text{from eq. (8.134)}) \quad (8.178)$$

$$\lim_{K \rightarrow 0} \phi_{\text{inst}} = 1 \quad (\text{from eq. (8.130)}) \quad (8.179)$$

$$\lim_{K \rightarrow 0} \phi = 1 \quad (\text{from eq. (8.136)}) \quad (8.180)$$

For the limit $K \rightarrow \infty$, eqs. (8.169) and (8.170) are applicable.

For the case of infinitely rapid, reversible reaction with unequal diffusivities, eqs. (8.147) and (8.148) lead to

$$\phi = \phi_{\text{inst}} = \sqrt{(K+1)(1+KD_E/D_A)} \quad (8.181)$$

8.21. The Scheme for Comparing the Film and Penetration Theories. In the application of the film theory to the packed column, it has never been possible to measure directly the film thickness, x_f . Similarly, in applying the penetration theory to the packed column, it has not been possible to assign a definite value to the time of exposure of the liquid to the gas between mixings. Even with the short wetted-wall column, there is some uncertainty as to the time of exposure. If the area for mass transfer is known, however, it is possible to estimate these quantities by measuring rates of absorption in the absence of chemical reaction and calculating from them the physical coefficients. Then, if the film theory were to be used, one could evaluate the film thickness by recourse to eq. (8.159).

$$x_f = \frac{D_A}{k_L^*} \quad (8.182)$$

If the penetration theory were to be used, the time of exposure could be obtained from the instantaneous physical coefficient at the end of the absorption period by using eq. (8.163).

$$\sqrt{t} = \frac{\sqrt{D_A/\pi}}{k_L^* \text{inst.}} \quad (8.183)$$

It is more likely that the average physical coefficient would be determined from experiment, in which case eq. (8.162) could be used.

$$\sqrt{t} = \frac{2\sqrt{D_A/\pi}}{k_L^*} \quad (8.184)$$

It is now possible to calculate ϕ , as well as the pseudo-coefficient $k_L^\circ = \phi k_L^*$, for the cases of absorption accompanied by first-order chemical reaction, given only the physical coefficient and certain constants of the system (i.e., diffusivities, reaction rate constants, equilibrium constants). Such a calculation may be performed using either the film or penetration theory, and permits us to compare the two theories. It should be borne in mind that we will not compare the abilities of the two theories to predict the physical coefficients. Rather, given the physical coefficient and the constants of the system, we shall compare the abilities of the two theories to predict the effect of the chemical reaction on the pseudo-coefficient.

A glance at eqs. (8.165)-(8.168) will show that, for the film theory of absorption with first-order chemical reaction, ϕ is a function of two dimensionless parameters, KD_E/D_A and Rx_f . The latter parameter may be expressed in terms of k_L^* by use of

eq. (8.182) to give

$$R_{x_f} = \frac{RD_A}{k_L^*} = \frac{D_A}{k_L^*} \sqrt{\frac{k_1}{D_A} + \frac{k_2}{D_E}} \quad (8.185)$$

Likewise, eqs. (8.169) - (8.180) show that, for the penetration theory of absorption with first-order reaction ϕ is a function of the dimensionless quantities K and $\sqrt{R^2Dt}$. The latter may be expressed in terms of either the instantaneous or average physical coefficient by means of eq. (8.183) or (8.184). Thus

$$\sqrt{R^2Dt} = \frac{1}{\sqrt{\pi}} \frac{RD}{k_L^* \text{inst}} = \frac{\sqrt{(k_1+k_2)D}}{\sqrt{\pi} k_L^* \text{inst}} \quad (8.186)$$

$$\sqrt{R^2Dt} = \frac{2}{\sqrt{\pi}} \frac{RD}{k_L^*} = \frac{2}{\sqrt{\pi}} \frac{\sqrt{(k_1+k_2)D}}{k_L^*} \quad (8.187)$$

For the purposes of the comparison, we shall calculate ϕ as a function of K and RD/k_L^* , assuming that $D_A = D_E$.

In calculating ϕ for the penetration theory, values of the error function are obtained from page 116 of Pierce (84). However, when K lies between 0 and 1, the arguments of the error function become imaginary (see eqs. (8.171) and (8.172)), and the table in Pierce cannot be used. For an imaginary argument we may write, from the definition of erf x ,

$$\text{erf}(ix) = \frac{2}{\sqrt{\pi}} \int_0^{ix} \exp(-u^2) du$$

Substituting $u = iz$ gives

$$\text{erf}(ix) = \frac{2i}{\sqrt{\pi}} \int_0^x \exp(z^2) dz$$

The integral $\int_0^x \exp(z^2) dz$ is tabulated on page 32 of Jahnke and

Emde (48). A more extensive tabulation is presented by Terill and Sweeney (98).

8.22. Calculated Values of ϕ . The results of the calculations of ϕ for various values of K and RD/k_L^* , using eqs. (8.165)-(8.180), are presented in Table 8.3. Round numbers were used for RD/k_L^* for the film theory; the values of RD/k_L^* used for the penetration theory were chosen so that the values of the arguments of the exponential and error functions which appear in eqs. (8.171) and (8.172) would be round numbers, in order to facilitate looking up these numbers in the tables.

The results have been plotted in Figs. 8.7 and 8.8. The values for $K = 0.5, 2$ and 10 have been placed on Fig. 8.7, while those for $K = 1, 5$ and ∞ were put on Fig. 8.8. Two separate graphs were used to avoid too much overlapping of curves.

8.23. Significance of the Comparison. Figs. 8.7 and 8.8 show that the difference between the values of ϕ predicted by the film theory and by the penetration theory using average coefficients is never greater than 6%; that this difference increases with increasing K , becoming a maximum for infinite K ; and that the difference is a maximum for values of RD/k_L^* about 1.5, decreasing for smaller and larger values of RD/k_L^* . The value for the penetration theory is always larger than that for the film theory.

The curves also show that the deviations between the value of ϕ_{inst} predicted by the penetration theory and of ϕ predicted by the film theory show no such neat behavior, varying quite widely, and being as much as 17%.

Thus, it has been demonstrated that for absorption with first-order chemical reaction, one may use the film theory to calculate ϕ (average value) from RD/k_L^* and K with an error of not more than 6%. Since the film theory always gives somewhat lower values of ϕ , its use in design would be conservative practice, affording a small margin of safety.

In later sections of this chapter, it will be shown that it has not been possible to use the penetration theory to any appreciable extent for absorption with second-order chemical reactions. It has been possible, however, to arrive at solutions for the second-order cases from the point of view of the film theory. It is proposed, then, in view of the agreement between the film and penetration theories for the first-order cases, that the film theory will provide a good approximate method for calculating ϕ from k_L^* and the physical constants of the system for the second-order cases as well.

TABLE 8.3

Calculation of ϕ for Absorption with First-Order Chemical Reaction

Film Theory		Penetration Theory (Instantaneous Coeffs.)		Penetration Theory (Average Coefficients)	
RD/k_L^*	ϕ	$RD/k_L^* \text{ inst}$	ϕ_{inst}	RD/k_L^*	ϕ
K = 0					
0 - ∞	1.000	0 - ∞	1.000	0 - ∞	1.000
K = 0.5					
0.0	1.000	0.0000	1.000	0.0000	1.000
0.2	1.005	0.1842	1.004	0.0921	1.001
0.3	1.010	0.3684	1.014	0.1842	1.005
0.4	1.017	0.5526	1.031	0.2763	1.011
0.5	1.030	0.9210	1.081	0.4605	1.028
0.7	1.048	1.2280	1.134	0.6140	1.048
1.0	1.086	1.7806	1.235	0.8903	1.090
1.5	1.152	2.671	1.364	1.335	1.162
2.0	1.209	3.53	1.431	1.765	1.220
2.5	1.253	4.45	1.463	2.226	1.267
3.0	1.287	5.37	1.476	2.686	1.302
4.0	1.334	7.09	1.487	3.545	1.346
5.0	1.364	8.86	1.492	4.431	1.375
7.0	1.400	12.41	1.496	6.204	1.409
10.0	1.429	17.73	1.498	8.862	1.435
∞	1.500	∞	1.500	∞	1.500
K = 1					
0.0	1.000	0.0000	1.000	0.0000	1.000
0.2	1.007	0.3545	1.020	0.1772	1.007
0.3	1.015	0.5317	1.044	0.2659	1.015
0.4	1.026	0.7090	1.076	0.3545	1.026
0.5	1.039	0.8662	1.115	0.4431	1.040
0.7	1.073	1.2407	1.209	0.6204	1.074
1.0	1.135	1.7725	1.368	0.8862	1.139
1.5	1.247	2.659	1.602	1.3293	1.256
2.0	1.350	3.545	1.755	1.772	1.363
2.5	1.434	4.431	1.840	2.216	1.451
3.0	1.502	5.317	1.889	2.659	1.520
4.0	1.600	7.090	1.938	3.545	1.619
5.0	1.667	8.862	1.960	4.431	1.686
7.0	1.750	12.407	1.980	6.204	1.767
10.0	1.818	17.725	1.990	8.862	1.833
∞	2.000	∞	2.000	∞	2.000

TABLE 8.3 (Contd)

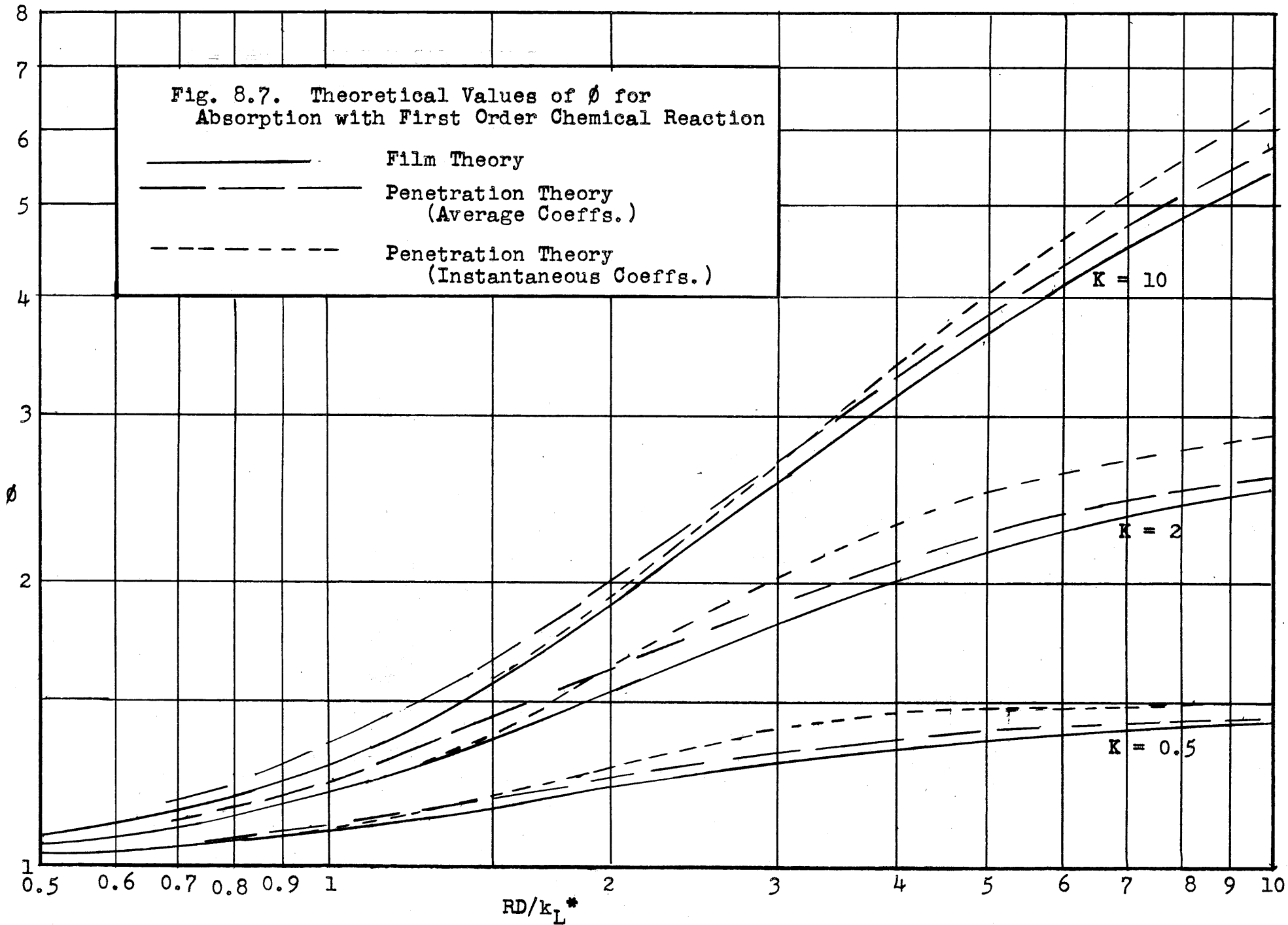
<u>Film Theory</u>		<u>Penetration Theory (Instantaneous Coeffs.)</u>		<u>Penetration Theory (Average Coeffs.)</u>	
<u>RD/k_L</u>	<u>ϕ</u>	<u>RD/k_L inst</u>	<u>ϕ_{inst}</u>	<u>RD/k_L</u>	<u>ϕ</u>
K = 2					
0.0	1.000	0.0000	1.000	0.000	1.000
0.2	1.009	0.1842	1.007	0.0921	1.003
0.3	1.020	0.3070	1.020	0.1535	1.007
0.4	1.035	0.6140	1.077	0.3070	1.026
0.5	1.053	0.9210	1.167	0.4605	1.058
0.7	1.100	1.2280	1.282	0.6140	1.099
1.0	1.189	1.8420	1.548	0.9210	1.203
1.5	1.359	2.763	1.933	1.3815	1.384
2.0	1.528	3.684	2.222	1.8420	1.560
2.5	1.677	4.605	2.420	2.3025	1.713
3.0	1.804	6.140	2.621	3.070	1.918
4.0	2.001	10.745	2.853	5.373	2.280
5.0	2.143	15.35	2.924	7.675	2.465
7.0	2.333	∞	3.000	∞	3.000
10.0	2.500				
∞	3.000				
K = 5					
0.0	1.000	0.0000	1.000	0.0000	1.000
0.2	1.011	0.3473	1.032	0.1737	1.005
0.3	1.025	0.5210	1.071	0.2605	1.027
0.4	1.044	0.6947	1.124	0.3473	1.043
0.5	1.067	0.8683	1.190	0.4342	1.065
0.7	1.129	1.3025	1.402	0.6512	1.125
1.0	1.248	1.7366	1.658	0.8683	1.237
1.5	1.494	2.605	2.213	1.3025	1.470
2.0	1.760	3.473	2.726	1.7366	1.722
2.5	2.018	4.342	3.160	2.171	1.966
3.0	2.257	5.210	3.524	2.605	2.196
4.0	2.668	6.947	4.084	3.473	2.603
5.0	3.000	8.683	4.487	4.342	2.941
7.0	3.500	13.025	5.093	6.512	3.569
10.00	4.000	17.366	5.408	8.683	3.994
∞	6.000	∞	6.000	∞	6.000

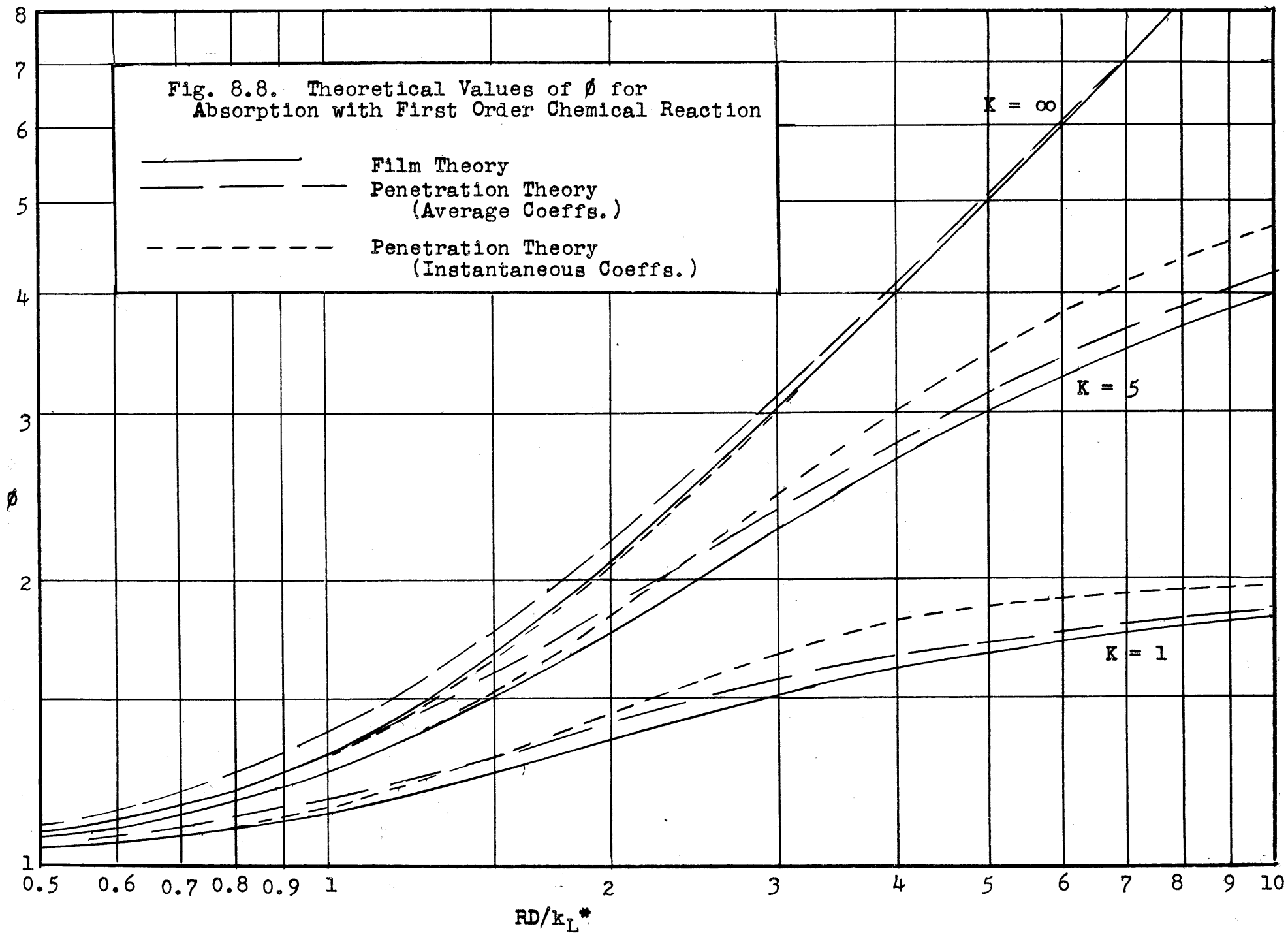
TABLE 8.3 (Contd)

Film Theory		Penetration Theory (Instantaneous Coeffs.)		Penetration Theory (Average Coeffs.)	
RD/k_L^*	ϕ	RD/k_L^* inst	ϕ inst	RD/k_L^*	ϕ
$K = 10$					
0.0	1.000	0.0000	1.000	0.000	1.000
0.2	1.012	0.3527	1.040	0.1764	1.011
0.3	1.027	0.5291	1.080	0.2645	1.028
0.4	1.048	0.7054	1.140	0.3527	1.045
0.5	1.074	0.8818	1.215	0.4409	1.072
0.7	1.142	1.2345	1.403	0.6172	1.139
1.0	1.277	1.7636	1.754	0.8818	1.270
1.5	1.564	2.6454	2.420	1.3227	1.541
2.0	1.890	3.527	3.077	1.7636	1.843
2.5	2.224	4.409	3.681	2.2045	2.150
3.0	2.548	5.291	4.229	2.6454	2.454
4.0	3.145	7.054	5.173	3.527	3.019
5.0	3.667	8.818	5.952	4.409	3.530
7.0	4.529	12.345	7.139	6.172	4.402
10.0	5.500	17.64	8.310	8.818	5.413
∞	11.000	∞	11.000	∞	11.000
$K = \infty$					
0.0	1.000	0.0000	1.000	0.0000	1.000
0.2	1.013	0.3545	1.040	0.1772	1.013
0.3	1.030	0.5317	1.089	0.2659	1.030
0.4	1.053	0.7090	1.156	0.3545	1.053
0.5	1.082	0.8862	1.240	0.4431	1.081
0.7	1.158	1.2407	1.454	0.6204	1.156
1.0	1.313	1.7725	1.862	0.8862	1.304
1.5	1.657	2.659	2.674	1.3293	1.622
2.0	2.075	3.545	3.547	1.7725	1.994
2.5	2.534	4.431	4.431	2.216	2.393
3.0	3.015	5.317	5.317	2.659	2.806
4.0	4.003	7.090	7.090	3.545	3.656
5.0	5.001	8.862	8.862	4.431	4.520
7.0	7.000	12.407	12.407	6.204	6.267
10.0	10.000	17.725	17.725	8.862	8.907

Fig. 8.7. Theoretical Values of ϕ for Absorption with First Order Chemical Reaction

————— Film Theory
 - - - - - Penetration Theory (Average Coeffs.)
 - - - - - Penetration Theory (Instantaneous Coeffs.)





8.24 The Effect of Unequal Diffusivities. So far, the film and penetration theories have been compared for the cases where the diffusivities of A and E were assumed equal. While the assumption of equal diffusivities was not necessary in using the film theory, it could be avoided in using the penetration theory only for the case of infinitely rapid reaction. To compare the two theories while taking into account the effect of unequal diffusivities, we must, therefore, restrict ourselves to infinitely rapid reaction.

For the film theory, eq. (8.168) applies:

$$\phi = 1 + KD_E/D_A \quad (8.168)$$

For the penetration theory, eq. (8.181) applies:

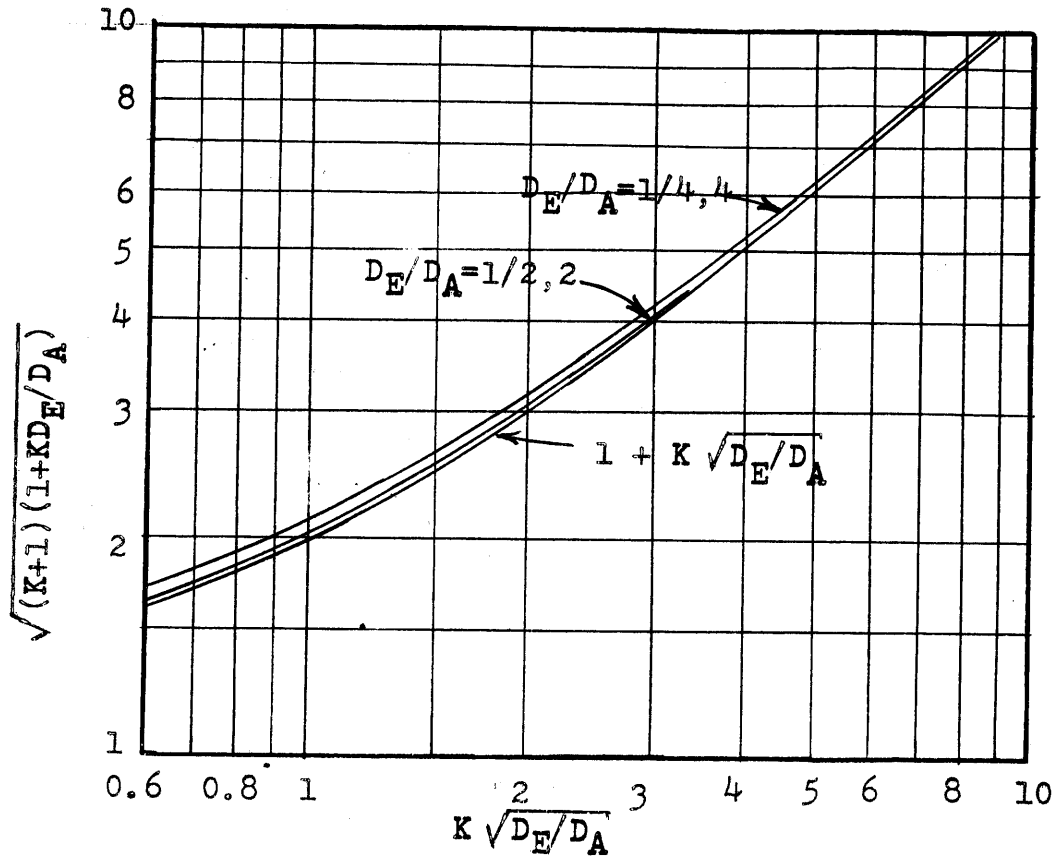
$$\phi = \phi_{inst} = \sqrt{(K+1)(1+KD_E/D_A)} \quad (8.181)$$

It should be noted that film thickness or time of exposure are not involved in these expressions, so that the two theories may be compared directly. It is quite clear that they do not give the same values of ϕ when the ratio of diffusivities differs appreciably from one.

It turns out that eq. (8.181) may be approximated by

$$\phi = \phi_{inst} \approx 1 + K \sqrt{D_E/D_A} \quad (8.188)$$

To show that this is true, Fig. 8.9 shows a plot of $\sqrt{(K+1)(1+KD_E/D_A)}$ vs. $K \sqrt{D_E/D_A}$ for the ratios of diffusivities $D_E/D_A = 1/4, 1/2, 2$ and 4 . On this plot a line for a given ratio of D_E/D_A coincides with a line for the reciprocal ratio. It can be seen that the approximation represented by eq. (8.188) is good to 2% for $D_E/D_A = 1/2$ or 2 , and good to 7% for $D_E/D_A = 1/4$ or 4 . Diffusivities in liquids do not vary over a wide range. For example, a table of representative liquid diffusivities presented by Sherwood (92) lists twenty systems and the diffusivities in all but three lie within a four-fold range; in half of the systems they lie within a two-fold range. In general, then, eq. (8.188) represents a good approximation.



For the film theory of absorption with first-order reversible reaction, it was shown that only two dimensionless parameters were needed, and that these were KD_E/D_A and RD_A/k_L^* . For the penetration theory, for equal diffusivities, K and RD/k_L^* were shown to be sufficient parameters to determine ϕ . A comparison of eqs. (8.168) and (8.188) suggests that the parameter associated with the equilibrium constant and the ratio of diffusivities for the penetration theory might well be $K\sqrt{D_E/D_A}$. The parameter involving the rate constant and the physical coefficient may well be RD_A/k_L^* , just as for the film theory. These ideas are only conjecture, it is realized, but they do suggest, for the purposes of using the film theory to predict ϕ from k_L^* and the constants of the system even where the assumptions of the penetration theory are believed valid, that wherever the quantity KD_E/D_A appears, it should be replaced by $K\sqrt{D_E/D_A}$.

F. The Film Theory of Absorption with Second-Order Irreversible Reaction

8.25. Introduction. For this case, eq. (8.20) becomes

$$D_A \frac{d^2A}{dx^2} = D_B \frac{d^2B}{dx^2} = k_1 AB \quad (8.189)$$

with the boundary conditions

$$\text{At } x = 0, \quad A = A_1, \quad \frac{dB}{dx} = 0 \quad (8.190)$$

$$\text{At } x = x_f, \quad A = 0, \quad B = B_0 \quad (8.191)$$

The statement that $A = 0$ at $x = x_f$ results from the assumption of equilibrium in the bulk of the fluid.

The first part of eq. (8.189) may be rewritten

$$\frac{d^2}{dx^2} (D_A A - D_B B) = 0 \quad (8.192)$$

Integrating once gives

$$\frac{d}{dx} (D_A A - D_B B) = c_1$$

Noting that at $x = 0$, $\frac{dB}{dx} = 0$, $\frac{dA}{dx} = -\frac{N_A}{D_A}$, we have $c_1 = -N_A$

Integrating once again gives

$$D_A A - D_B B = -N_A x + c_2$$

Substituting B.C. (8.191) yields

$$c_2 = -D_B B_0 + N_A x_f$$

Then

$$D_A A - D_B (B - B_0) = N_A (x_f - x) \quad (8.193)$$

If we let $B_1 =$ concentration of B at the interface, and substitute $x = 0$, $A = A_1$, we obtain

$$D_A A_1 - D_B (B_1 - B_0) = N_A x_f$$

Now, since

$$\phi = \frac{k_L^\circ}{k_L^*} = \frac{N_A/A_1}{D_A/x_f} = \frac{N_A x_f}{D_A A_1} \quad (8.194)$$

we obtain

$$1 - \frac{D_B}{D_A} \frac{B_1 - B_0}{A_1} = \phi$$

$$\text{Let } q = \frac{D_A A_1}{D_B B_0} \quad (8.195)$$

Then

$$\frac{B_1}{B_0} = 1 - q(\phi - 1) \quad (8.196)$$

Eq. (8.196) gives us a relationship between B_1/B_0 and ϕ in terms of the dimensionless parameter q , but as yet we cannot determine either B_1/B_0 or ϕ explicitly.

Letting $R^2 = k_1/D_A$, eq. (8.189) may now be written

$$\frac{d^2 A}{dx^2} = R^2 AB \quad (8.197)$$

Eq. (8.193) gives B as a function of A and x . This function could be substituted in eq. (8.197) giving a non-linear differential equation in A , for which no known analytical solution exists. In the next two sections approximations are made which convert eq. (8.197) into linear equations which can be solved.

8.26. First Approximate Solution. The first approximation, first used by van Krevelen and Hoftijzer (60), consists of assuming that B is constant throughout the film at B_1 , which is related to ϕ by eq. (8.196). Then eq. (8.197) becomes

$$\frac{d^2 A}{dx^2} = (B_1 R^2) A \quad (8.198)$$

A complete general solution of eq. (8.198) is

$$A = c_1 \sinh(\sqrt{B_1} R x) + c_2 \sinh(\sqrt{B_1} R [x_f - x])$$

Substituting B.C. (8.191) gives $c_1 = 0$. Substituting B.C. (8.190) gives

$$c_2 = \frac{A_1}{\sinh(\sqrt{B_1} R x_f)}$$

whence

$$A = A_1 \frac{\sinh(\sqrt{B_1} R [x_f - x])}{\sinh(\sqrt{B_1} R x_f)}$$

Differentiating once,

$$\frac{dA}{dx} = -\sqrt{B_1} R A_1 \frac{\cosh \sqrt{B_1} R [x_f - x]}{\sinh(\sqrt{B_1} R x_f)} \quad (8.199)$$

Now, at $x = 0$, using eq. (8.194),

$$\frac{dA}{dx} = -\frac{N_A}{D_A} = \frac{A_1}{x_f} \phi$$

Then, letting $x = 0$, eq. (8.199) becomes

$$\phi = -\frac{\sqrt{B_1} R x_f}{\tanh(\sqrt{B_1} R x_f)} \quad (8.200)$$

Substituting eq. (8.196) into eq. (8.200), we have

$$\phi = \frac{\sqrt{B_0 R^2 x_f^2 [1 - q(\phi - 1)]}}{\tanh \sqrt{B_0 R^2 x_f^2 [1 - q(\phi - 1)]}} \quad (8.201)$$

It is convenient to define a new dimensionless parameter

$$M = B_0 R^2 x_f^2 = k_1 B_0 x_f^2 / D_A \quad (8.202)$$

Then eq. (8.201) becomes

$$\phi = \frac{\sqrt{M [1 - q(\phi - 1)]}}{\tanh \sqrt{M [1 - q(\phi - 1)]}} \quad (8.203)$$

Van Krevelen and Hofstijzer (60) presented an "ideal concentration diagram" which embodies the assumption that B is constant at B_1 , and they presented a plot of ϕ vs. \sqrt{M} for various values of q , based on their version of eq. (8.203). It should be noted that their nomenclature is considerably different from the one used here. They expressed their constants in terms of the limiting rates of absorption which arise under various limiting conditions. This nomenclature seems to be a very confusing one. Furthermore, Van Krevelen and Hofstijzer never actually presented eq. (8.203) or any rearrangement of it, but rather presented an equation which is the equivalent of (8.203) with the right-hand side multiplied by a correction factor to allow for the fact that A is not equal to zero in the bulk of the liquid. Then they stated the assumption that (in their terminology) $R_2/M_1 > R_1 > M_1$ which is equivalent to the assumption that the holdup of the liquid in the column is very large. Apparently they set the correction factor equal to unity when they constructed the plot of ϕ vs. \sqrt{M} , though they never said so explicitly. It is believed that the derivation of eq. (8.203) presented here is considerably easier to understand than that of Van Krevelen and Hofstijzer and, furthermore, that the assumptions involved are stated more explicitly here.

The various limiting forms of eq. (8.203) are of interest.

$$(1) \quad M \rightarrow 0$$

$$\text{Since } \lim_{x \rightarrow 0} \frac{\tanh x}{x} = 1,$$

$$\lim_{M \rightarrow 0} \phi = 1$$

$$(2) \quad M \rightarrow \infty$$

Noting that $\lim_{x \rightarrow \infty} \tanh x = 1$, eq. (8.203) becomes

$$\phi = \sqrt{M [1 - q(\phi - 1)]}$$

$$\phi^2 = M [1 - q(\phi - 1)] \quad (8.204)$$

Now, ϕ cannot become infinite; in fact, it has a definite upper limit. From eq. (8.196), we get

$$\phi = 1 + (1/q) \left(1 - \frac{B_1}{B_0}\right)$$

from which we see that the smaller B_1/B_0 becomes, the larger is ϕ . However, it is physically absurd for B_1/B_0 to become negative, so that the largest value ϕ can have is $1 + 1/q$. Going back to eq. (8.204), since ϕ^2 cannot become infinite, then $1 - q(\phi-1)$ must become zero. Whence

$$\lim_{M \rightarrow \infty} \phi = 1 + 1/q \quad (8.205)$$

$$(3) \quad q = 0$$

Eq. (8.203) becomes

$$\lim_{q \rightarrow 0} \phi = \frac{\sqrt{M}}{\tanh \sqrt{M}} \quad (8.206)$$

This equation is similar to eq. (8.165), which was derived for the first order irreversible case. Eq. (8.165) may be rewritten

$$\phi = \frac{\sqrt{k_1/D_A} x_f}{\tanh(\sqrt{k_1/D_A} x_f)}$$

Eq. (8.206) may be written

$$\phi = \frac{\sqrt{k_1 B_0/D_A} x_f}{\tanh(\sqrt{k_1 B_0/D_A} x_f)}$$

The significance of this similarity is that for small values of the ratio A_1/B_0 , the concentration of B throughout the film is practically constant, so that the reaction becomes first-order.

8.27. Second Approximate Solution. Instead of assuming that B is constant throughout the film, one may linearize eq. (8.197) by assuming that B varies linearly with x, going from $B = B_1$ (which again is related to ϕ by eq. (8.196)) at $x = 0$ to $B = B_0$ at $x = x_f$. Then

$$B = B_1 + (B_0 - B_1) \frac{x}{x_f} \quad (8.207)$$

Eq. (8.197) then becomes

$$\frac{d^2A}{dx^2} = R^2 \left[B_1 + (B_0 - B_1) \frac{x}{x_f} \right] A \quad (8.208)$$

If we let

$$b = \frac{B_1}{B_0}$$

and define new variables

$$\alpha = \frac{A}{A_1}$$

$$\lambda = k \left[b + (1-b) \frac{x}{x_f} \right]$$

where k is a constant to be determined later, we have

$$\frac{d\lambda}{dx} = \frac{k(1-b)}{x_f}$$

$$\frac{d^2A}{dx^2} = \frac{d^2A}{d\lambda^2} \left(\frac{d\lambda}{dx} \right)^2 = \frac{k^2(1-b)^2}{x_f^2} \frac{d^2A}{d\lambda^2}$$

Eq. (8.208) becomes

$$\frac{k^2(1-b)^2}{x_f^2} \frac{d^2A}{d\lambda^2} = R^2 B_0 \frac{\lambda}{k} A \quad (8.209)$$

If we define

$$k^3 = \frac{R^2 x_f^2 B_0}{(1-b)^2} = \frac{M}{(1-b)^2}$$

eq. (8.209) becomes

$$\frac{d^2\alpha}{d\lambda^2} = \lambda \alpha \quad (8.210)$$

This equation has undergone considerable investigation in the past by Airy and others. Two independent solutions, $Ai(\lambda)$ and $Bi(\lambda)$, known as the Airy integrals, have been tabulated. The most recent and complete tabulation was brought out by Miller (75). He tabulates $Ai(\lambda)$, $Bi(\lambda)$, their first derivatives $Ai'(\lambda)$, $Bi'(\lambda)$, as well as various combinations, such as $Ai'(\lambda)/Ai(\lambda)$, $Ai(\lambda)/Bi(\lambda)$, and $\log Ai(\lambda)$.

The solution of eq. (8.210) is then

$$\alpha = c_1 Ai(\lambda) + c_2 Bi(\lambda) \quad (8.211)$$

The boundary conditions associated with eq. (8.210) derived from eqs. (8.190) and (8.191), are

$$\text{At } \lambda = kb, \quad \alpha = 1 \quad (8.212)$$

$$\text{At } \lambda = k, \quad \alpha = 0 \quad (8.213)$$

Substituting these boundary conditions into eq. (8.211) gives, respectively,

$$1 = c_1 Ai(kb) + c_2 Bi(kb)$$

$$0 = c_1 Ai(k) + c_2 Bi(k)$$

Then

$$c_2 = -c_1 \frac{Ai(k)}{Bi(k)}$$

$$c_1 = \frac{1}{Ai(kb) - \frac{Ai(k)}{Bi(k)} Bi(kb)}$$

Differentiating eq. (8.211) once, we get

$$\frac{d\alpha}{d\lambda} = c_1 Ai'(\lambda) + c_2 Bi'(\lambda)$$

At $x = 0$, (or $\lambda = kb$),

$$\frac{d\alpha}{d\lambda} = \frac{d\alpha}{dA} \frac{dA}{dx} \frac{dx}{d\lambda} = \frac{1}{Ai} \left(-\frac{N_A}{D_A} \right) \frac{x_f}{k(1-b)} = -\frac{\phi}{k(1-b)}$$

$$\text{Then } -\frac{\phi}{k(1-b)} = \frac{A_1'(kb) - \frac{A_1(k)}{B_1(k)} B_1'(kb)}{A_1(kb) - \frac{A_1(k)}{B_1(k)} B_1(kb)}$$

For convenience in using Miller's tables, this equation is rearranged.

$$\frac{\phi}{1-b} = k \frac{\frac{A_1(k) B_1'(kb)}{B_1(k) B_1(kb)} - \frac{A_1'(kb) A_1(kb)}{A_1(kb) B_1(kb)}}{\frac{A_1(kb)}{B_1(kb)} - \frac{A_1(k)}{B_1(k)}} \quad (8.214)$$

Eq. (8.214), combined with

$$k = \frac{M^{1/3}}{(1-b)^{2/3}} \quad (8.215)$$

and

$$b = 1 - q(\phi - 1) \quad (8.216)$$

constitutes a system of equations which approximates the solution to the problem, giving ϕ as a function of the dimensionless parameters q and M .

8.28. Comparison of the Two Approximate Solutions. Referring back to eq. (8.189), since A and B are both positive quantities, d^2B/dx^2 is positive. Therefore the plot of B vs. x must be concave upward. Since the slope of B vs. x is zero at $x=0$, the slope must always be greater than zero at any point $x > 0$. Thus Fig. 8.10 shows a typical plot of B vs. x . The first approximation uses the assumption that B is constant as shown by the dashed line; the second

approximation uses the assumption that B varies linearly with x , as shown by the dotted lines. Thus, the first approximation assumes a value of B which is always too low, while the second one assumes a value which is always too high. Physically, one can see that assuming too low a value for B would lead to too small a rate of absorption, while too high a value should predict too high a rate.

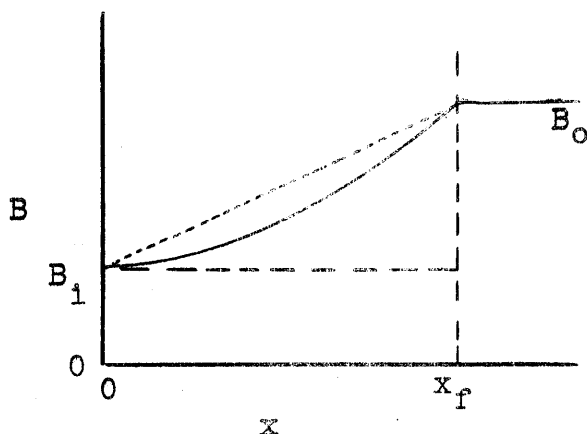


Fig. 8.10. Sketch of Concentration of B in Film for Second Order Reaction.

Therefore, we should expect that the values of ϕ obtained from the first approximation will be too low; those obtained from the second will be too high. The true value of ϕ must be in between.

Values of ϕ calculated by the first approximation are tabulated in Table 8.4. These values were calculated from eq. (8.203) for each value of q and \sqrt{M} by trial and error.

Values of ϕ calculated from eqs. (8.214)-(8.216) are tabulated in Table 8.5. An indirect graphical technique was used to obtain ϕ as a function of q and M . A graph was constructed with k as the abscissa, and the right-hand side of eq. (8.214) as the ordinate, for the value of $b = 0, 0.1, 0.2, 0.3, \dots, 0.8$. Then for each value of q and b , ϕ was calculated by means of eq. (8.216). $\phi/(1-b)$ was then computed and, referring to the graph, using the line corresponding to the value of b in question, the value of k was obtained. Then M was calculated from eq. (8.215).

From the physical situation, one may expect that, for infinite reaction rate, B is zero at the interface; thus $b = 0$ when $M \rightarrow \infty$. One would also expect that b would be greater than zero for any finite value of M . This condition is met by the first approximation. The second approximation, however, gives a finite value to M for $b = 0$, as seen from Table 8.5, and the corresponding value of ϕ is the maximum value that ϕ can have for a particular value of q (i.e., $\phi = 1 + 1/q$). For larger values of M , we may say that the second approximation predicts that ϕ is constant at $\phi = 1 + 1/q$, and still satisfy the requirement that the second approximation predict a value of ϕ larger than the true value.

The two approximations are compared graphically in Fig. 8.11. The solid lines represent the first approximation, while the dashed lines represent the second approximation. The agreement between the two is quite remarkable. The largest difference is about 8%, occurring at $q = 1$, and decreases as q decreases. Since they bracket the true solution, we may say that both approximations are correct to within 8% at low values of q , and become more correct as q decreases.

For subsequent use it is preferable to employ the first approximate method because it is simpler to derive and to calculate, and because it gives a slightly conservative value of ϕ for use in design.

TABLE 8.4

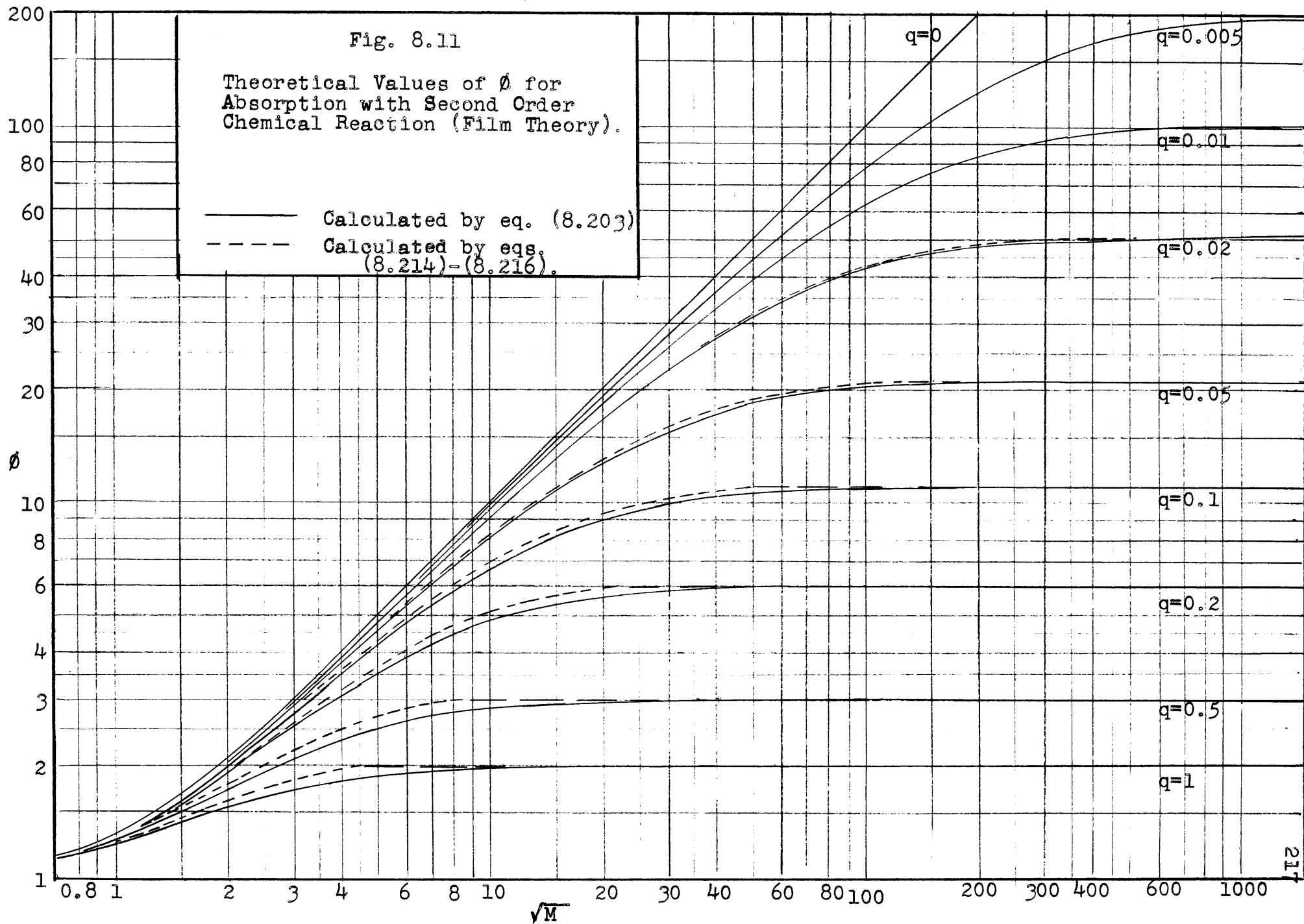
THEORETICAL VALUES OF ϕ FOR ABSORPTION WITH
SECOND-ORDER REACTION, CALCULATED BY EQ. (8.203).

\sqrt{M}	ϕ								
	q=1	q=0.5	q=0.2	q=0.1	q=0.05	q=0.02	q=0.01	q=0.005	q=0
0.2	1.013	1.013	1.013	1.013	1.013	1.013	1.013	1.013	1.013
0.3	1.029	1.029	1.030	1.030	1.030	1.030	1.030	1.030	1.030
0.5	1.076	1.079	1.081	1.081	1.082	1.082	1.082	1.082	1.082
0.7	1.137	1.147	1.154	1.156	1.157	1.158	1.158	1.158	1.158
1.0	1.241	1.273	1.296	1.304	1.308	1.311	1.312	1.313	1.313
1.5	1.409	1.506	1.588	1.621	1.639	1.650	1.654	1.655	1.657
2	1.544	1.731	1.909	1.986	2.029	2.056	2.065	2.070	2.074
3	1.722	2.093	2.532	2.749	2.875	2.957	2.986	3.000	3.015
5	1.875	2.510	3.524	4.143	4.537	4.807	4.902	4.951	5.000
7	1.931	2.707	4.201	5.290	6.052	6.597	6.794	6.896	7.000
10	1.965	2.841	4.833	6.619	8.048	9.149	9.562	9.778	10.00
15	1.984	2.925	5.361	8.091	10.74	13.07	13.99	14.49	15.00
20	1.991	2.957	5.607	8.983	12.80	16.59	18.20	19.08	20.00
30	1.996	2.980	5.812	9.909	15.60	22.61	25.98	27.91	30.00
50	1.999	2.993	5.930	10.554	18.32	33.35	39.28	44.26	50.00
70	1.999	2.996	5.964	10.764	19.46	37.02	49.99	58.99	70.00
100		2.998	5.982	10.882	20.19	42.13	62.25	78.32	100.00
150		2.999	5.992	10.947	20.62	46.25	75.62	104.3	150.0
200		3.000	5.996	10.970	20.78	48.11	83.55	124.1	200.0
300			5.998	10.987	20.90	49.63	91.66	150.6	300.0
500			5.999	10.995	20.97	50.49	97.22	176.1	500.0
700			6.000	10.998	20.98	50.74	98.97	186.8	700.0
1,000				10.999	20.99	50.87	100.00	193.5	1,000.
1,500					21.00	50.94	100.55	197.5	1,500.
2,000						50.97	100.75	199.0	2,000.
3,000						50.99	100.89	200.1	3,000.
5,000						50.99	100.96	200.7	5,000.
7,000						51.00	100.98	200.8	7,000.
10,000							100.99	200.9	10,000.

TABLE 8.5

THEORETICAL VALUES OF ϕ FOR ABSORPTION WITH
SECOND-ORDER REACTION, CALCULATED BY EQS. (8.214)-(8.216)

b	q=1		q=0.5		q=0.2		q=0.1		q=0.05		q=0.02	
	\sqrt{M}	ϕ	\sqrt{M}	ϕ	\sqrt{M}	ϕ	\sqrt{M}	ϕ	\sqrt{M}	ϕ	\sqrt{M}	ϕ
0.8	0.80	1.20	1.18	1.40	2.08	2.0	3.20	3.0	5.48	5.0	12.2	11.0
0.7	1.08	1.30	1.59	1.60	2.83	2.5	4.60	4.0	8.21	7.0	18.9	16.0
0.6	1.343	1.40	2.02	1.80	3.70	3.0	6.10	5.0	11.43	9.0	27.2	21.0
0.5	1.63	1.50	2.50	2.00	4.69	3.5	7.96	6.0	15.25	11.0	36.4	26.0
0.4	1.91	1.60	2.85	2.20	5.85	4.0	10.25	7.0	19.9	13.0	49.1	31.0
0.3	2.31	1.70	3.64	2.40	7.31	4.5	13.4	8.0	25.9	15.0	64.1	36.0
0.2	2.77	1.80	4.45	2.60	9.5	5.0	17.8	9.0	35.8	17.0	89.5	41.0
0.1	3.48	1.90	5.7	2.80	12.9	5.5	26.4	10.0	54.5	19.0	139	46.0
0.0	4.47	2.00	8.36	3.00	23.2	6.0	57.	11.0	152.	21.0	600	51.0



G. The Penetration Theory of Absorption with Second-Order Irreversible Reaction.

8.29 The General Case. Eq. (8.30) becomes

$$D_A \frac{\partial^2 A}{\partial x^2} - \frac{\partial A}{\partial t} = D_B \frac{\partial^2 B}{\partial x^2} - \frac{\partial B}{\partial t} = k_1 AB \quad (8.217)$$

with the boundary conditions

$$\begin{aligned} \text{At } x = 0, t > 0, & \quad A = A_1, \quad \frac{\partial B}{\partial x} = 0 \\ \text{At } t = 0, x > 0, & \quad A = 0, \quad B = B_0 \\ \text{At } x = \infty, t \geq 0, & \quad A = 0, \quad B = B_0 \end{aligned} \quad (8.218)$$

The conditions that $A = 0$ for $t = 0$ and $x = \infty$ follow from the assumption of equilibrium at those boundaries.

Even with the assumption of equal diffusivities, this case cannot be solved because eq. (8.217) is non-linear.

8.30 The Case of Infinitely Rapid Reaction. When the reaction rate is infinite, A and B cannot exist together at finite concentrations. Since A is present in finite quantity at the interface at the value A_1 , the concentration of B at the interface must be zero. For this case, a solution may be obtained by the use of Laplace transforms, provided the assumption of equal diffusivities is made.

The Laplace transform of the first part of eq. (8.217) is:

$$D \frac{d^2 \bar{A}}{dx^2} - p\bar{A} = D \frac{d^2 \bar{B}}{dx^2} - (p\bar{B} - B_0) \quad (8.219)$$

The transform of the boundary conditions are:

$$\text{At } x = 0, \quad \bar{A} = A_1/p, \quad \bar{B} = 0, \quad \frac{d\bar{B}}{dx} = 0 \quad (8.220)$$

$$x = \infty, \quad \bar{A} = 0, \quad \bar{B} = B_0/p \quad (8.221)$$

Eq. (8.219) may be rearranged.

$$D \frac{d^2}{dx^2} (\bar{A} - \bar{B}) = p (\bar{A} - \bar{B}) + B_0 \quad (8.222)$$

The complete general solution of eq. (8.222) is

$$(\bar{A}-\bar{B}) = c_1 \exp(\sqrt{p/D} x) + c_2 \exp(-\sqrt{p/D} x) - \frac{B_0}{p}$$

Using B.C. (8.221) gives

$$-\frac{B_0}{p} = c_1 \exp(\infty) - \frac{B_0}{p}$$

Whence $c_1 = 0$. B.C. (8.220) gives

$$\frac{A_1}{p} = c_2 - \frac{B_0}{p}$$

Whence $c_2 = (A_1 + B_0)/p$

$$\bar{A}-\bar{B} = \frac{A_1+B_0}{p} \exp(-\sqrt{p/D} x) - \frac{B_0}{p}$$

Differentiating once, we obtain

$$\frac{d\bar{A}}{dx} - \frac{d\bar{B}}{dx} = -\sqrt{\frac{p}{D}} \frac{A_1+B_0}{p} \exp(-\sqrt{p/D} x)$$

B.C. (8.220) leads to

$$\left(\frac{d\bar{A}}{dx}\right)_{x=0} = -\sqrt{\frac{p}{D}} \frac{A_1+B_0}{p} = -\frac{A_1+B_0}{\sqrt{D}} \frac{1}{\sqrt{p}} \quad (8.223)$$

Taking the inverse transform,

$$\left(\frac{\partial A}{\partial x}\right)_{x=0} = -\frac{A_1+B_0}{\sqrt{D}} \frac{1}{\sqrt{\pi t}}$$

$$N_A = -D \left(\frac{\partial A}{\partial x}\right)_{x=0} = (A_1+B_0) \sqrt{\frac{D}{\pi t}}$$

Substituting into eq. (8.164), noting $A_0 = 0$, gives

$$\phi_{inst} = 1 + \frac{B_0}{A_1} = 1 + \frac{1}{q} \quad (8.224)$$

To get the average value we first divide eq. (8.223) by p .

$$\mathcal{L} \left[\int_0^t \left(\frac{\partial A}{\partial x} \right)_{x=0} dt \right] = - \frac{A_1 + B_0}{\sqrt{D}} \frac{1}{p^{3/2}}$$

The inverse transform is

$$\int_0^t \left(\frac{\partial A}{\partial x} \right)_{x=0} dt = - \frac{A_1 + B_0}{\sqrt{D}} \frac{2\sqrt{t}}{\sqrt{\pi}}$$

$$\int_0^t N_A dt = -D \int_0^t \left(\frac{\partial A}{\partial x} \right)_{x=0} dt = 2(A_1 + B_0) \sqrt{\frac{Dt}{\pi}}$$

Substituting into eq. (8.162) gives

$$\phi = 1 + \frac{B_0}{A_1} = 1 + \frac{1}{q} \quad (8.225)$$

Note that eqs. (8.224) and (8.225) are identical with eq. (8.205), which was obtained for the film theory for the limit $M \rightarrow \infty$ (i.e., infinitely rapid reaction). Thus, for this case, the film and penetration theories agree exactly.

8.31 The Effect of Unequal Diffusivities. An exact solution for the case of infinitely rapid reaction with unequal diffusivities has been performed by Danckwerts (19), who arrived at a general method of solution for this class of problems which involve unsteady-state diffusion or heat conduction with a moving boundary. In this case the moving boundary is the boundary between the region containing A and that containing B. He showed that

$$\int_0^t N_A dt = \frac{2 A_1}{\operatorname{erf}(\omega / \sqrt{D_A})} \sqrt{\frac{D_A t}{\pi}} \quad (8.226)$$

where ω is defined by the equation

$$\frac{A_1}{\sqrt{D_B}} \exp\left(\frac{\omega^2}{D_B}\right) \operatorname{erfc}\left(\frac{\omega}{\sqrt{D_B}}\right) = \frac{B_0}{\sqrt{D_A}} \exp\left(\frac{\omega^2}{D_A}\right) \operatorname{erf}\left(\frac{\omega}{\sqrt{D_A}}\right) \quad (8.227)$$

Eq. (8.226) may be combined with eq. (8.162) to give

$$\phi = \frac{1}{\operatorname{erf}\left(\omega/\sqrt{D_A}\right)} \quad (8.228)$$

According to another article by Danckwerts (18)

$$N_A = \frac{A_1}{\operatorname{erf}\left(\omega/\sqrt{D_A}\right)} \sqrt{\frac{D_A}{\pi t}}$$

(where ω is again defined by eq. (8.227), so that

$$\phi_{\text{inst}} = \frac{1}{\operatorname{erf}\left(\omega/\sqrt{D_A}\right)} \quad (8.229)$$

Some idea of the significance of eqs. (8.227)-(8.229) may be obtained by considering small values of ω (i.e., $\omega/\sqrt{D_A} < 0.1$). Then $\exp(\omega^2/D_B) = \exp(\omega^2/D_A) = 1$, $\operatorname{erf}\left(\omega/\sqrt{D_A}\right) = 2\omega/\sqrt{\pi D_A}$, and $\operatorname{erfc}\left(\omega/\sqrt{D_B}\right) = 1 - 2\omega/\sqrt{\pi D_B}$. Eq. (8.227) then becomes

$$\frac{A_1}{B_0} \sqrt{\frac{D_A}{D_B}} = \frac{2\omega/\sqrt{\pi D_A}}{1 - 2\omega/\sqrt{\pi D_B}}$$

Multiply both sides by $\sqrt{D_A/D_B}$.

$$\frac{A_1}{B_0} \frac{D_A}{D_B} = \frac{2\omega/\sqrt{\pi D_B}}{1 - 2\omega/\sqrt{\pi D_B}}$$

Taking the reciprocal of each side and rearranging,

$$\frac{1}{2\omega/\sqrt{\pi D_B}} = 1 + \frac{B_0 D_B}{A_1 D_A} .$$

Multiply both sides by $\sqrt{D_A/D_B}$.

$$\frac{1}{2\omega/\sqrt{\pi D_A}} = \sqrt{\frac{D_A}{D_B}} + \frac{B_0}{A_1} \sqrt{\frac{D_B}{D_A}}$$

Since we are considering the case of small ω , this quantity is large compared with one. It may be approximated by

$$\frac{1}{2\omega/\sqrt{\pi D_A}} \approx 1 + \frac{B_0}{A_1} \sqrt{\frac{D_B}{D_A}} \quad (8.230)$$

with an error of $1 - \sqrt{D_A/D_B}$. Since values of D_A/D_B will very seldom exceed four, this error will be less than one.

Substitution of eq. (8.230) into eqs. (8.228) and (8.229) yields

$$\phi = \phi_{\text{inst.}} \approx 1 + \frac{1}{\frac{A_1}{B_0} \sqrt{\frac{D_A}{D_B}}} \quad (8.231)$$

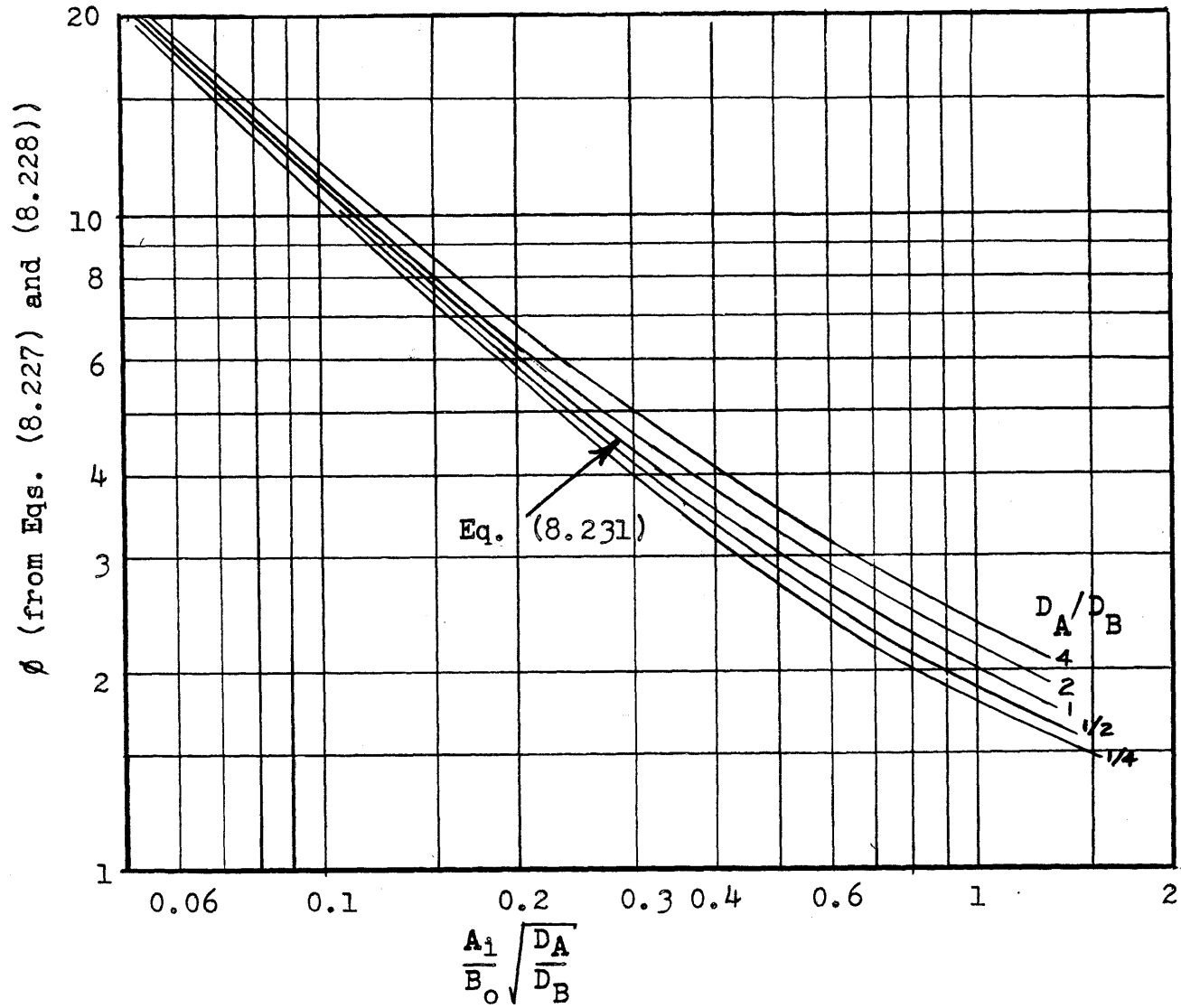
To test this equation at higher values of ω , which corresponds to higher values of $(A_1/B_0)\sqrt{D_A/D_B}$, ϕ has been calculated using eqs. (8.227) and (8.228), and plotted in Fig. 8.12 as a function of $(A_1/B_0)\sqrt{D_A/D_B}$ for various values of D_A/D_B . The line for $D_A=D_B$ coincides with eq. (8.231). One can see from the graph that if ϕ had been plotted as a function of A_1/B_0 , or as a function of $A_1 D_A / B_0 D_B$, that the lines would be spread apart much more than they are on this plot. Thus, the error of assuming that ϕ is a unique function of A_1/B_0 , or of $A_1 D_A / B_0 D_B$ is much greater than if it is assumed to be a unique function of $(A_1/B_0)\sqrt{D_A/D_B}$. From the graph, we see that the latter assumption leads to an error which is less than 10% for values of $(A_1/B_0)\sqrt{D_A/D_B}$ less than 0.1 when $D_A/D_B = 4$, and that the error decreases for decreasing values of A_1/B_0 , and for decreasing values of D_A/D_B . In practice, values of A_1/B_0 generally do run below 0.1, so that eq. (8.231) is a good approximation to use.

For the film theory of the case of infinitely rapid reaction, eq. (8.205) applies:

$$\phi = 1 + \frac{1}{\frac{A_1}{B_0} \frac{D_A}{D_B}} \quad (8.205)$$

Fig. 8.12

Comparison of Eqs. (8.227) and (8.228) with Eq. (8.231)



The comparison of eq. (8.205) with eq. (8.231) suggests the same idea that arose in connection with unequal diffusivities in first order reversible reaction. When the film theory is used to predict ϕ from k_1 and the constants of the system even where the assumptions of the penetration theory are believed valid, it is suggested that wherever the ratio $q = A_1 D_A / B_0 D_B$ arises, it be replaced by the quantity $(A_1 / B_0) \sqrt{D_A / D_B}$.

H. The Film Theory of Absorption with Second-Order Reversible Reaction.

8.32 General Solution. Eq. (8.20) is applicable.

$$D_A \frac{d^2 A}{dx^2} = D_B \frac{d^2 B}{dx^2} = -D_E \frac{d^2 E}{dx^2} = -D_F \frac{d^2 F}{dx^2} = k_1 AB - k_2 EF \quad (8.20)$$

The boundary conditions are

$$\text{At } x = 0, \quad A = A_1, \quad \frac{dB}{dx} = \frac{dE}{dx} = \frac{dF}{dx} = 0 \quad (8.21)$$

$$\text{At } x = x_f, \quad A = A_0, \quad B = B_0, \quad E = E_0, \quad F = F_0 \quad (8.22)$$

The assumption of equilibrium in the bulk of the liquid gives

$$K = \frac{k_1}{k_2} = \frac{E_0 F_0}{A_0 B_0} \quad (8.232)$$

From eq. (8.20) we have

$$D_A \frac{d^2 A}{dx^2} = D_B \frac{d^2 B}{dx^2}$$

Integrating once:

$$D_A \frac{dA}{dx} = D_B \frac{dB}{dx} + c_1$$

Using $N_A = -D_A (dA/dx)_{x=0}$, and $(dB/dx)_{x=0} = 0$, we get

$$c_1 = -N_A$$

Integrating once more:

$$D_A A = D_B B - N_A x + c_2$$

Letting the concentration of B at the interface be B_1 , and using B.C. (8.21) we get

$$c_2 = D_A A_1 - D_B B_1$$

Then

$$D_A (A - A_1) = D_B (B - B_1) - N_A x$$

Substituting B.C. (8.22) gives

$$D_A (A_0 - A_1) = D_B (B_0 - B_1) - N_A x_f$$

or

$$\frac{N_A x_f}{D_A (A_1 - A_0)} = 1 - \frac{D_B}{D_A} \frac{(B_1 - B_0)}{(A_1 - A_0)}$$

Substituting eq. (8.160) gives

$$\phi = 1 - \frac{D_B}{D_A} \frac{(B_1 - B_0)}{(A_1 - A_0)} \quad (8.233)$$

From eq. (8.20), we have

$$\frac{d^2}{dx^2} (D_A A + D_E E) = 0$$

The complete general solution is

$$D_A A + D_E E = c_1 x + c_2$$

From B.C. (8.21), $c_2 = D_A A_1 + D_E E_1$. From B.C. (8.22),

$$D_A A_0 + D_E E_0 = c_1 x_f + D_A A_1 + D_E E_1$$

$$c_1 = \frac{D_A (A_0 - A_1) + D_E (E_0 - E_1)}{x_f}$$

Then

$$D_A A + D_E E = \left[D_A (A_0 - A_1) + D_E (E_0 - E_1) \right] \frac{x}{x_f} + D_A A_1 + D_E E_1 \quad (8.234)$$

Differentiating once

$$D_A \frac{dA}{dx} + D_E \frac{dE}{dx} = \frac{D_A(A_0 - A_1) + D_E(E_0 - E_1)}{x_f}$$

Substituting $N_A = -D_A(dA/dx)_{x=0}$, and $(dE/dx)_{x=0} = 0$, we get

$$-N_A = \frac{D_A(A_0 - A_1) + D_E(E_0 - E_1)}{x_f}$$

Substituting eq. (8.160) gives

$$\phi = 1 + \frac{D_E}{D_A} \frac{(E_1 - E_0)}{(A_1 - A_0)} \quad (8.235)$$

The expression for F_1 will be exactly analogous to that for E_1 :

$$\phi = 1 + \frac{D_F}{D_A} \frac{(F_1 - F_0)}{(A_1 - A_0)} \quad (8.236)$$

Eqs. (8.233), (8.235) and (8.236) relate the interfacial concentrations of B, E and F to ϕ .

Now consider the following part of eq. (8.20):

$$D_A \frac{d^2A}{dx^2} = k_1 AB - k_2 EF \quad (8.237)$$

Eq. (8.237) is non-linear, and cannot be solved analytically. An approximate solution may be obtained by linearizing it, just as we did for the second-order irreversible case. We shall employ here the same procedure used in the first approximate solution for the irreversible case, and assume that some of the concentrations are constant at their interfacial values.

Assume that B is constant throughout the film at B_1 , which is related to ϕ by eq. (8.233), and that F is constant throughout the film at F_1 , which is related to ϕ by eq. (8.236). Then eq. (8.237) becomes

$$D_A \frac{d^2A}{dx^2} = (k_1 B_1) A - (k_2 F_1) E \quad (8.238)$$

We may solve eq. (8.234) for E and substitute into eq. (8.238).

$$D_A \frac{d^2 A}{dx^2} = (k_1 B_1) A - (k_2 F_1) \left\{ \left[\frac{D_A}{D_E} (A_0 - A_1) + (E_0 - E_1) \right] \frac{x}{x_f} + \frac{D_A}{D_E} A_1 + E_1 - \frac{D_A}{D_E} A \right\} \quad (8.239)$$

To facilitate the algebra, we make the following substitutions. Let

$$U^2 = \frac{k_1 B_1}{D_A} + \frac{k_2 F_1}{D_E} \quad (8.240)$$

$$U^2 W = k_2 F_1 \left(\frac{A_0 - A_1}{D_E} + \frac{E_0 - E_1}{D_A} \right) \quad (8.241)$$

$$U^2 Z = k_2 F_1 \left(\frac{A_1}{D_E} + \frac{E_1}{D_A} \right) \quad (8.242)$$

Then eq. (8.239) may be rearranged to give

$$\frac{d^2 A}{dx^2} = U^2 A - U^2 Wx/x_f - U^2 Z \quad (8.243)$$

The general homogeneous solution of eq. (8.243) is

$$A = c_1 \sinh Ux + c_2 \sinh U(x_f - x)$$

A particular solution is

$$A = Wx/x_f + Z$$

The complete general solution is the sum of the homogeneous and particular solutions, or

$$A = c_1 \sinh Ux + c_2 \sinh U(x_f - x) + Wx/x_f + Z \quad (8.244)$$

Using B.C. (8.21),

$$A_1 = c_2 \sinh Ux_f + Z$$

$$c_2 = \frac{A_1 - Z}{\sinh Ux_f}$$

From B.C. (8.22),

$$A_0 = c_1 \sinh Ux_f + W + Z$$

$$c_1 = \frac{A_0 - W - Z}{\sinh Ux_f}$$

Differentiating eq. (8.244) once:

$$\frac{dA}{dx} = c_1 U \cosh Ux - c_2 U \cosh U(x_f - x) + W/x_f$$

Substituting for c_1 and c_2 , and setting $x=0$ gives

$$-\frac{N_A}{D_A} = \frac{(A_0 - W - Z)U - (A_1 - Z)U \cosh Ux_f}{\sinh Ux_f} + \frac{W}{x_f}$$

Noting that $N_A/D_A = \phi (A_1 - A_0)/x_f$, we get

$$\frac{\phi(A_0 - A_1)}{Ux_f} = \frac{(A_0 - W - Z)(1/\cosh Ux_f) - (A_1 - Z)}{\tanh Ux_f} + \frac{W}{Ux_f} \quad (8.245)$$

Now, let us go back to eqs. (8.240)-(8.242). Eq. (8.240) may be rearranged to give

$$U^2 = \frac{k_2 F_1}{D_E} \left(1 + \frac{k_1 B_1 D_E}{k_2 F_1 D_A}\right) = \frac{k_2 F_1}{D_E} \left(1 + \frac{K B_1 D_E}{F_1 D_A}\right) \quad (8.246)$$

Substituting eq. (8.246) into eq. (8.241) and rearranging gives

$$\frac{k_2 F_1}{D_E} \left(1 + \frac{K B_1 D_E}{F_1 D_A}\right) W = \frac{k_2 F_1 (A_0 - A_1)}{D_E} \left[1 + \frac{D_E}{D_A} \frac{E_0 - E_1}{A_0 - A_1}\right]$$

This may be combined with eq. (8.235), and rearranged:

$$W = \frac{(A_0 - A_1) \phi}{1 + \frac{KB_1 D_E}{F_1 D_A}} \quad (8.247)$$

Adding eq. (8.241) to (8.242) gives

$$U^2 (W+Z) = k_2 F_1 \left(\frac{A_0}{D_E} + \frac{E_0}{D_A} \right)$$

Substituting eq. (8.246):

$$\frac{k_2 F_1}{D_E} \left(1 + \frac{KB_1 D_E}{F_1 D_A} \right) (W+Z) = \frac{k_2 F_1}{D_E} (A_0 + E_0 D_E / D_A)$$

Note that $E_0 = KA_0 B_0 / F_0$

Then

$$W+Z = \frac{A_0 \left(1 + \frac{K B_0 D_E}{F_0 D_A} \right)}{1 + \frac{K B_1 D_E}{F_1 D_A}} \quad (8.248)$$

whence

$$A_0 - W - Z = \frac{\frac{KA_0 D_E}{D_A} \left(\frac{B_1}{F_1} - \frac{B_0}{F_0} \right)}{1 + \frac{KB_1 D_E}{F_1 D_A}} \quad (8.249)$$

Subtracting eq. (8.247) from eq. (8.248):

$$Z = \frac{A_0 - A_0 \phi + A_1 \phi + \frac{K A_0 B_0 D_E}{F_0 D_A} \phi}{1 + \frac{K B_1 D_E}{F_1 D_A}}$$

Then

$$A_1 - Z = \frac{(A_0 - A_1)(\phi - 1) + \frac{K D_E}{D_A} \left(\frac{A_1 B_1}{F_1} - \frac{A_0 B_0}{F_0} \right)}{1 + \frac{K B_1 D_E}{F_1 D_A}}$$

$$A_1 - Z = \frac{(A_0 - A_1)(\phi - 1) + \frac{K A_0 D_E}{D_A} \left(\frac{B_1}{F_1} - \frac{B_0}{F_0} \right) - \frac{K B_1 D_E}{F_1 D_A} (A_0 - A_1)}{1 + \frac{K B_1 D_E}{F_1 D_A}} \quad (8.250)$$

Substituting eqs. (8.247), (8.249) and (8.250) into eq. (8.245), and multiplying through by $(1 + \frac{K B_1 D_E}{F_1 D_A}) \tanh U_{x_f}$ gives

$$\begin{aligned} \frac{\phi(A_0 - A_1)}{U_{x_f}} \left(1 + \frac{K B_1 D_E}{F_1 D_A} \right) \tanh U_{x_f} &= \frac{K A_0 D_E}{D_A} \left(\frac{B_1}{F_1} - \frac{B_0}{F_0} \right) \left(\frac{1}{\cosh U_{x_f}} \right) \\ &- (A_0 - A_1)(\phi - 1) - \frac{K A_0 D_E}{D_A} \left(\frac{B_1}{F_1} - \frac{B_0}{F_0} \right) + \frac{K B_1 D_E}{F_1 D_A} (A_0 - A_1) \\ &+ \frac{\phi (A_0 - A_1)}{U_{x_f}} \tanh U_{x_f} \end{aligned}$$

Rearrangement yields

$$\phi \left(1 + \frac{K B_1 D_E}{F_1 D_A} \frac{\tanh U_{x_f}}{U_{x_f}} \right) = 1 + \frac{K B_1 D_E}{F_1 D_A} + \frac{A_0}{A_1 - A_0} \frac{K D_E}{D_A} \left(\frac{B_1}{F_1} - \frac{B_0}{F_0} \right) \left(1 - \frac{1}{\cosh U_{x_f}} \right) \quad (8.251)$$

Eq. (8.251), combined with eqs. (8.233), (8.236), and (8.240) constitutes the solution.

8.33. The Case of Second-Order Forward, First-Order Reverse Reaction. For the use of the reaction of the type



the form of eq. (8.20) which applies is

$$D_A \frac{d^2A}{dx^2} = D_B \frac{d^2B}{dx^2} = -D_E \frac{d^2E}{dx^2} = k_1 AB - k_2 E \quad (8.253)$$

The boundary conditions are

$$\text{At } x = 0, \quad A = A_1, \quad \frac{dB}{dx} = \frac{dE}{dx} = 0 \quad (8.254)$$

$$\text{At } x = x_f, \quad A = A_0, \quad B = B_0, \quad E = E_0 \quad (8.255)$$

The assumption of equilibrium in the bulk of the liquid gives

$$K = \frac{k_1}{k_2} = \frac{E_0}{A_0 B_0} \quad (8.256)$$

The following results obtained previously will still apply:

$$\phi = 1 - \frac{D_B}{D_A} \frac{(B_1 - B_0)}{(A_1 - A_0)} \quad (8.233)$$

$$\phi = 1 + \frac{D_E}{D_A} \frac{(E_1 - E_0)}{(A_1 - A_0)} \quad (8.235)$$

The derivation proceeds in the same way as for the case where both the forward and reverse reactions are second order. Eq. (8.253) is written

$$D_A \frac{d^2A}{dx^2} = k_1 AB - k_2 E \quad (8.257)$$

This equation is linearized by assuming that B is constant at its interfacial value B_1 . If we define

$$Y^2 = \frac{k_1 B_1}{D_A} + \frac{k_2}{D_E} \quad (8.258)$$

by looking at eq. (8.251) and recognizing that the F terms will disappear, we obtain

$$\phi \left(1 + \frac{KB_1 D_E}{D_A} \frac{\tanh Yx_f}{Yx_f} \right) = 1 + \frac{KB_1 D_E}{D_A} + \frac{A_0}{A_1 - A_0} \frac{KD_E}{D_A} (B_1 - B_0) \left(1 - \frac{1}{\cosh Yx_f} \right) \quad (8.259)$$

Eq. (8.259), combined with eqs. (8.233) and (8.258) constitutes the solution.

I. Citations

8.34 As pointed out at the beginning of this chapter, not all of the material presented in this chapter is original with this investigation. In this section, the various derivations will be considered with the object of pointing out the previous and contemporary literature where similar derivations have been found.

The basic differential equations, being quite straightforward, have been presented by many authors in many different forms. Juttner (54) presented an unusually complete collection of these equations for both the steady-state and unsteady state cases, including the cases where the molecules react in other than one-to-one ratios.

The film theory of absorption with first order irreversible reaction was derived by Hatta, and an excellent review of this subject is presented by Sherwood (92), who also takes into account the gas-side resistance.

The film theory of second-order infinitely rapid irreversible reaction was derived here as a limiting case of the second-order reaction, but it has been considered in the literature chiefly from the point of view of the so-called double liquid film concept. Sherwood (92) has also reviewed this case in considerable detail.

Jenny (51) considered the film theory of second-order irreversible reaction with finite rate, but could not solve the differential equation by straightforward methods. Van Krevelan and Hofstijzer (60) derived an approximate solution to this problem, which was presented in the treatment here.

Chou (13) considered the film theory for reversible, first order forward, third order backward, reaction with particular reference to the chlorine-water system. He obtained a series solution to the differential equation which, while rigorous, is extremely difficult and tedious to use.

All of the work on the penetration theory of absorption with chemical reaction presented here was derived without recourse to the literature, with the exception of the second order, infinitely rapid, irreversible case. This case was studied by Adair (2) who presented the results in a form not convenient for calculation of rates of absorption. Danckwerts (19) derived a general solution to the problem of unsteady-state diffusion with a moving boundary, and presented as a specific example the solution for this case. His result was in a more convenient form than Adair's, and has been included in this chapter. The rest of the development is the author's, but a considerable portion of it has later been found to duplicate work done about the same time by some other investigators. Danckwerts (18) derived the penetration theory of first-order irreversible reaction. The author had the

opportunity to read the manuscript of the chapter on "Absorption with Chemical Reaction" which will appear in the forthcoming edition of "Absorption and Extraction" by Sherwood and Pigford. This manuscript shows that R. L. Pigford has derived the penetration theory for first order, both reversible and irreversible reactions.

Contributions which are claimed to be new are as follows:

Consideration of the effect of holdup and the justification of the assumption of equilibrium in the bulk of the liquid (or at the beginning of the time of exposure) for the film and penetration theories; the effect of acceleration of the liquid and of vertical diffusion on the penetration theory; the penetration theory of first order infinitely rapid reversible reaction with unequal diffusivities; the comparison of the film and penetration theories for first order chemical reaction; the film theory of absorption with second order irreversible reaction, using the Airy integral (also, showing the accuracy of van Krevelen's approximation for this case); and the film theory of absorption with second order reversible reaction.

CHAPTER 9

APPLICATION OF MATHEMATICAL THEORY OF ABSORPTION WITH
CHEMICAL REACTION TO EXPERIMENT

Outline

	<u>Page</u>
A. Absorption of Chlorine in Water	
9.1 Development of Theory	235
9.2 Procedure for Calculating ϕ -Plots	242
9.3 Application of Theory to Data on Absorption of Chlorine in Water in a Packed Column . . .	243
9.4 Application of Theory to Data on Desorption of Chlorine from Water in a Packed Column ..	247
9.5 A Study of the Effect of Certain Variables on the Theoretical Values of ϕ	250
B. Absorption of Sulfur Dioxide in Water	
9.6 Development of Theory	259
9.7 The Rate of Hydrolysis of Sulfur Dioxide. . .	261
9.8 Calculation of ϕ	264
9.9 Application to Packed Column Data	264
C. Absorption of Carbon Dioxide in Sodium Hydroxide Solution: 9.10	268
D. Theoretical Upper Limit for Absorption of Chlorine in Water: 9.11	275

A. Absorption of Chlorine in Water

9.1. Development of Theory

The assumptions made are:

1. The water is originally pure before any chlorine is dissolved in it.
2. Hypochlorous acid does not dissociate.
3. The reaction $\text{H}_2\text{O} \rightleftharpoons \text{H}^+ + \text{OH}^-$ is instantaneous.
4. Diffusivities are independent of concentration.
5. HOCl and HCl are non-volatile.
6. The film theory may be used to calculate ϕ from k_L^* , and the constants of the reaction.

It is first desired to prove that at every point in the liquid, the approximation

$$[\text{OH}^-] = \frac{K_w}{[\text{Cl}^-]} \quad (9.1)$$

is valid. Since, because of assumptions 1 and 2, the only ions present are OH^- , H^+ , and Cl^- , and since electrical neutrality must exist every where,

$$[\text{H}^+] = [\text{OH}^-] + [\text{Cl}^-] \quad (9.2)$$

Because of assumption 3, water dissociation equilibrium exists every where

$$[\text{H}^+][\text{OH}^-] = K_w \quad (9.3)$$

The validity of eq. (9.1) depends on whether $[\text{OH}^-]$ is negligible compared with $[\text{H}^+]$. Since $[\text{H}^+]$ decreases with decreasing chlorine concentration, the test should be made at the lowest concentration of chlorine encountered. Assume that the chlorine concentration is 0.01% of saturation, i.e., $C = 9 \times 10^{-6}$ moles/l. At this low concentration, the chlorine would be practically completely dissociated at equilibrium. Even if conditions in the liquid were such that the hydrolysis reaction had time to proceed only 10% toward

equilibrium, $[H^+]$ would equal 9×10^{-7} moles/l. Then, from eq. (9.3), $[OH^-] = 10^{-14}/9 \times 10^{-7} = 1.1 \times 10^{-8}$, which is only 1% of $[H^+]$. Thus, for this very extreme case, eq. (9.1) is good to 1%; for higher concentrations or closer approach to equilibrium the accuracy is much greater.

Thus, we may adopt the following nomenclature:

$$A = [Cl_2]$$

$$B = [OH^-] = K_w/F$$

$$E = [HOCl]$$

$$F = [H^+] = [Cl^-]$$

$$D_A = \text{diffusivity of } Cl_2$$

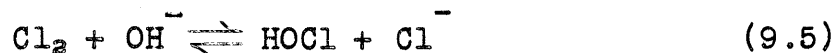
$$D_E = \text{diffusivity of } HOCl$$

$$D_F = \text{diffusivity of } HCl$$

Two expressions for the rate of hydrolysis of chlorine have been proposed in the literature. Shilov and Solodushenkov (95) examined their rate data on the basis of the mechanism



while Morris (76) proposed that the mechanism of the hydrolysis is



The theory will now be derived assuming first the second mechanism and then the first.

Assuming the mechanism of eq. (9.5), i.e., second order forward and second order reverse, the appropriate differential equation is

$$D_A \frac{d^2A}{dx^2} = D_B \frac{d^2B}{dx^2} = -D_E \frac{d^2E}{dx^2} = -D_F \frac{d^2F}{dx^2} = k_1AB - k_2EF \quad (9.6)$$

which was treated in Sec. 8.32. The solution was found to be

$$\phi \left(1 + \frac{KB_1 D_E}{F_1 D_A} \frac{\tanh Ux_f}{Ux_f} \right) = 1 + \frac{KB_1 D_E}{F_1 D_A} + \frac{A_0}{A_1 - A_0} \frac{K D_E}{D_A} \left(\frac{B_1}{F_1} - \frac{B_0}{F_0} \right) \left(1 - \frac{1}{\cosh Ux_f} \right) \quad (8.251)$$

together with

$$\phi = 1 - \frac{D_E (B_1 - B_0)}{D_A (A_1 - A_0)} \quad (8.233)$$

$$\phi = 1 + \frac{D_F (F_1 - F_0)}{D_A (A_1 - A_0)} \quad (8.236)$$

$$U^2 = \frac{k_1 B_1}{D_A} + \frac{k_2 F_1}{D_E} \quad (8.240)$$

Note that

$$K = k_1/k_2 = E_0 F_0 / A_0 B_0 \quad (8.232)$$

Usually the equilibrium of the chlorine-water system is expressed in terms of reaction (9.4). Thus,

$$K_c = E_0 F_0^2 / A_0 \quad (9.7)$$

From eq. (9.3) we have

$$B = K_w / F \quad (9.8)$$

The two equilibrium constants, K and K_c , then, are related by

$$K = K_c / K_w \quad (9.9)$$

In eq. (8.235) K occur several times multiplied by B_1 or B_0 . Since $K B_1 = K K_w / F_1 = K_c / F_1$

and

$$K B_0 = K_c / F_0$$

eq. (8.251) becomes

$$\phi \left(1 + \frac{K_c D_E \tanh U x_f}{F_1^2 D_A U x_f} \right) = 1 + \frac{K_c D_E}{F_1^2 D_A} + \frac{A_0}{A_1 - A_0} \frac{K_c D_E}{F_0^2 D_A} \left(\frac{F_0^2}{F_1^2} - 1 \right) \left(1 - \frac{1}{\cosh U x_f} \right) \quad (9.10)$$

term Included in the right-hand side of eq. (9.10) is the

$$\frac{A_0}{A_1 - A_0} \left(\frac{F_0^2}{F_1^2} - 1 \right)$$

This may be rearranged, and eq. (8.236) substituted.

$$\frac{A_0(F_0^2 - F_1^2)}{(A_1 - A_0)F_1^2} = \frac{A_0(F_0 + F_1)}{F_1^2} \frac{(F_0 - F_1)}{(A_1 - A_0)} = \frac{A_0(F_0 + F_1)}{F_1^2} \frac{D_A}{D_F} (1 - \phi)$$

Substituting into eq. (9.10).

$$\phi \left(1 + \frac{K_c D_E}{F_1^2 D_A} \frac{\tanh Ux_f}{Ux_f} \right) = 1 + \frac{K_c D_E}{F_1^2 D_A} - \frac{K_c}{F_0^2} \frac{D_E}{D_F} \frac{A_0(F_0 + F_1)}{F_1^2} (\phi - 1) \left(1 - \frac{1}{\cosh Ux_f} \right) \quad (9.11)$$

Noting that $K_c A_0 / F_0^2 = E_0$ and that $E_0 = F_0$, and subtracting from both sides the quantity

$$1 + \frac{K_c D_E}{F_1^2 D_A} \frac{\tanh Ux_f}{Ux_f}$$

$$\begin{aligned} (\phi - 1) \left(1 + \frac{K_c D_E}{F_1^2 D_A} \frac{\tanh Ux_f}{Ux_f} \right) &= \frac{K_c D_E}{F_1^2 D_A} \left(1 - \frac{\tanh Ux_f}{Ux_f} \right) - \\ &- \frac{D_E}{D_F} \frac{F_0(F_0 + F_1)}{F_1^2} (\phi - 1) \left(1 - \frac{1}{\cosh Ux_f} \right) \end{aligned}$$

This rearranges to

$$\phi - 1 = \frac{\frac{K_c D_E}{F_0^2 D_A} \left(1 - \frac{\tanh Ux_f}{Ux_f} \right)}{\left(\frac{F_1^2}{F_0} \right) + \frac{K_c D_E}{F_0^2 D_A} \frac{\tanh Ux_f}{Ux_f} + \left(1 + \frac{F_1}{F_0} \right) \frac{D_E}{D_F} \left(1 - \frac{1}{\cosh Ux_f} \right)} \quad (9.12)$$

Eq. (8.236) becomes

$$\frac{F_1}{F_0} = 1 + \frac{D_A}{D_F} \frac{A_1 - A_0}{F_0} (\phi - 1) \quad (9.13)$$

Eq. (8.240) becomes

$$U^2 = \frac{k_2 K_C}{D_A F_1} + \frac{k_2 F_1}{D_E} = \frac{k_2 F_1}{D_E} \left(1 + \frac{K_C D_E}{D_A F_1^2} \right)$$

Noting that $k_L^* = D_A/x_f$, this rearranges to

$$U^2 x_f^2 = \frac{k_2 D_A^2 F_1}{k_L^{*2} D_E} \left(1 + \frac{K_C D_E}{D_A F_1^2} \right)$$

Solving for k_L^* :

$$k_L^* = \frac{\sqrt{k_2 D_A^2 F_0 / D_E} \sqrt{F_1 / F_0} \sqrt{1 + (K_C D_E / D_A F_0^2) (F_0 / F_1)^2}}{U x_f} \quad (9.14)$$

Eqs. (9.12), (9.13) and (9.14) constitute a system of equations whereby, by eliminating F_1/F_0 and $U x_f$, one could obtain ϕ as a function of k_L^* , D_A , D_E , D_F , K_C , A_0 , A_1 , F_0 and k_2 . For a given temperature, D_A , D_E , D_F , K_C and k_2 are fixed, and A_0 and F_0 can be calculated from C_0 , so that ϕ then is a function of k_L^* , A_1 and C_0 .

The special case of $C_0 = 0$ must be considered separately. Then $A_0 = F_0 = 0$. Multiplying eq. (9.12) through by $(F_0/F_1)^2$,

$$\phi - 1 = \frac{\frac{K_C D_E}{F_1^2 D_A} (1 - \frac{\tanh U x_f}{U x_f})}{1 + \frac{K_C D_E}{F_1^2 D_A} \frac{\tanh U x_f}{U x_f}}$$

or

$$\phi = \frac{1 + \frac{K_C D_E}{F_1^2 D_A}}{1 + \frac{K_C D_E}{F_1^2 D_A} \frac{\tanh U x_f}{U x_f}}$$

with

$$k_L^* = \frac{\sqrt{k_a D_A^2 F_1 / D_E} \sqrt{1 + K_c D_E / D_A F_1^2}}{U x_f}$$

and

$$F_1 = \frac{D_A A_1}{D_F} (\phi - 1)$$

If the mechanism of eq. (9.4) is assumed, i.e., first order forward and third order reverse, the appropriate differential equation is

$$D_A \frac{d^2 A}{dx^2} = - D_E \frac{d^2 E}{dx^2} = - D_F \frac{d^2 F}{dx^2} = mA - nEF^2 \quad (9.15)$$

where m is the forward rate constant for this mechanism, and n is the reverse rate constant.

This type of chemical reaction is not treated in Chapter 8, but the method of integrating it is very similar to that used for the second order forward, second order reverse mechanism. The following derivation was first made by Quincy (86); the nomenclature used here is somewhat different, however.

Going back to Chapter 8, eqs. (8.234)-(8.236) are still applicable. Thus,

$$D_A A + D_E E = \left[D_A (A_0 - A_1) + D_E (E_0 - E_1) \right] \frac{x}{x_f} + D_A A_1 + D_E E_1 \quad (8.234)$$

$$\phi = 1 + \frac{D_E}{D_A} \frac{(E_1 - E_0)}{(A_1 - A_0)} \quad (8.235)$$

$$\phi = 1 + \frac{D_E}{D_A} \frac{(F_1 - F_0)}{(A_1 - A_0)} \quad (8.236)$$

Eq. (9.15) may be written

$$D_A \frac{d^2 A}{dx^2} = mA - nEF^2 \quad (9.16)$$

In order to obtain an approximate solution, this equation is linearized by assuming F is constant at its interfacial value

F_1 . Solving eq. (8.234) for E and substituting into eq. (9.16) gives

$$D_A \frac{d^2 A}{dx^2} = mA - nF_1^2 \left\{ \left[\frac{D_A}{D_E} (A_0 - A_1) + (E_0 - E_1) \right] \frac{x}{x_f} + \frac{D_A}{D_E} A_1 + E_1 - \frac{D_A}{D_E} A \right\} \quad (9.17)$$

To simplify the algebra, let

$$I^2 = \frac{m}{D_A} + \frac{nF_1^2}{D_E} \quad (9.18)$$

$$I^2 W' = nF_1^2 \left(\frac{A_0 - A_1}{D_E} + \frac{E_0 - E_1}{D_A} \right) \quad (9.19)$$

$$I^2 Z' = nF_1^2 \left(\frac{A_1}{D_E} + \frac{E_1}{D_A} \right) \quad (9.20)$$

Then eq. (9.17) becomes

$$\frac{d^2 A}{dx^2} = I^2 A - I^2 W' \frac{x}{x_f} - I^2 Z' \quad (9.21)$$

which is analogous to eq. (8.243). The integration parallels that between eqs. (8.243) and (8.245) to give

$$\frac{\phi(A_0 - A_1)}{Ix_f} = \frac{(A_0 - W' - Z')(1/\cosh Ix_f) - (A_1 - Z')}{\tanh Ix_f} + \frac{W'}{Ix_f} \quad (9.22)$$

Noting that

$$K_c = m/n \quad (9.23)$$

eq. (9.18) becomes

$$I^2 = \frac{nF_1^2}{D_E} \left(1 + \frac{K_c D_E}{F_1^2 D_A} \right) \quad (9.24)$$

This is analogous to eq. (8.246), where $k_2 F_1 / D_E$ corresponds to nF_1^2 / D_E and $KB_1 D_E / F_1 D_A$ corresponds to $K_c D_E / F_1^2 D_A$. Actually, since $KB_1 = K_c / F_1$ (from eqs. (9.8) and (9.9)), $KB_1 D_E / F_1 D_A$ is

equal to $K_c D_E / F_1^2 D_A$. The remainder of the derivation is similar to that leading to eq. (9.12), and by analogy, we may write

$$\phi - 1 = \frac{\frac{K_c D_E}{F_0 D_A} \left(1 - \frac{\tanh I x_f}{I x_f}\right)}{\left(\frac{F_1}{F_0}\right)^2 + \frac{K_c D_E}{F_0^2 D_A} \frac{\tanh I x_f}{I x_f} + \left(1 + \frac{F_1}{F_0}\right) \frac{D_E}{D_F} \left(1 - \frac{1}{\cosh I x_f}\right)} \quad (9.25)$$

From eq. (9.24),

$$k_L^* = \frac{\sqrt{n D_A^2 F_0^2 / D_E} \left(F_1 / F_0\right) \sqrt{1 + (K_c D_E / D_A F_0^2) (F_0 / F_1)^2}}{I x_f} \quad (9.26)$$

Finally, we have

$$\frac{F_1}{F_0} = 1 + \frac{D_A}{D_F} \frac{A_1 - A_0}{F_0} (\phi - 1) \quad (9.13)$$

Eqs. (9.25), (9.26) and (9.13) constitute the solution. As before, for a given temperature, ϕ is a function of k_L^* , A_1 and C_0 .

9.2. Procedure for Calculating ϕ - Plots. Rather than solve the three simultaneous equations for each case of interest, it is more convenient to construct plots of ϕ vs. k_L^* at constant values of A_1 and C_0 . In constructing these plots, the equations may be solved by an indirect graphical procedure which avoids trial and error. This procedure will now be described, using eqs. (9.12), (9.13) and (9.14).

After picking values for K_c , D_A , D_E , D_F and k_2 , curves were made of $\phi - 1$ vs. F_1 / F_0 at constant values of $U x_f$ (values of $U x_f$ used were 0.2, 0.3, 0.5, 0.8, 1.25, 2.0, 3.0, 5.0, 8.0, 12.5) for each value of C_0 , using eq. (9.12). Also for each value of C_0 , straight lines of $\phi - 1$ vs. F_1 / F_0 as given by eq. (9.13) were plotted for each value of A_1 . From the intersection of the lines with the curves, values of F_1 / F_0 and $\phi - 1$ were obtained for each combination of $U x_f$ and A_1 . From eq. (9.14), it was then possible to calculate k_L^* .

9.3. Application of Theory to Data on Absorption of Chlorine in Water in a Packed Column. Plots of ϕ vs. k_L^* were constructed for the chlorine-water system at 70°F. based on the second-order forward, second-order reverse mechanism for the hydrolysis, using eqs. (9.12), (9.13) and (9.14). These plots are shown in Fig. 9.1.

The decision to use the second-order forward, second-order reverse mechanism was based on the work of Morris (76), who demonstrated that the rate data of Shilov and Solodushenkov (95) was better correlated by that mechanism than by the first-order forward, third-order reverse mechanism. The constants for the chlorine-water system used to calculate the ϕ -plots were: $K_c = 2.88 \times 10^{-4}$ (g.mole/l.)² obtained by interpolation between values determined by Vivian and Whitney (101); $k_1 = 5 \times 10^{-14}$ l./(mole)(min.) calculated by Morris (76), who also found k_1 to be independent of temperature; $K_w = 0.75 \times 10^{-14}$, obtained by interpolation between values given by Harned and Geary (33); $k_2 = k_1 K_w / K_c = 217$ l./(mole)(sec.); $D_A = 1.31 \times 10^{-5}$ cm.²/sec. and $D_E = 1.37 \times 10^{-5}$ cm.²/sec. obtained in this thesis. (These values of diffusivities are about 2% lower than those given in Chapt. 11 because they were based on preliminary calculations; it was not considered worthwhile to revise the plots for the correct values of D_A and D_E); $D_F = 2.85 \times 10^{-5}$ cm.²/sec. obtained by interpolation to a concentration of 0.005 moles/l. and a temperature of 70°F. from the data on hydrochloric acid of James and Gordon (49).

Examination of Fig. 9.1 shows that ϕ is a monotonic function of k_L^* , A_1 and C_0 , decreasing for increasing values of k_L^* , A_1 and C_0 .

In applying the plots to data on the absorption of chlorine in water in a packed column, it is necessary to take into account the variation of A_1 and C_0 with height, which causes a variation of ϕ with height. From a material balance and the concentrations of the inlet and outlet streams, one can relate A_1 (= HP) to C_0 . The differential rate equation for the packed column is

$$\frac{L}{\rho} dC_0 = k_L^0 a (A_1 - A_0) dz \quad (9.27)$$

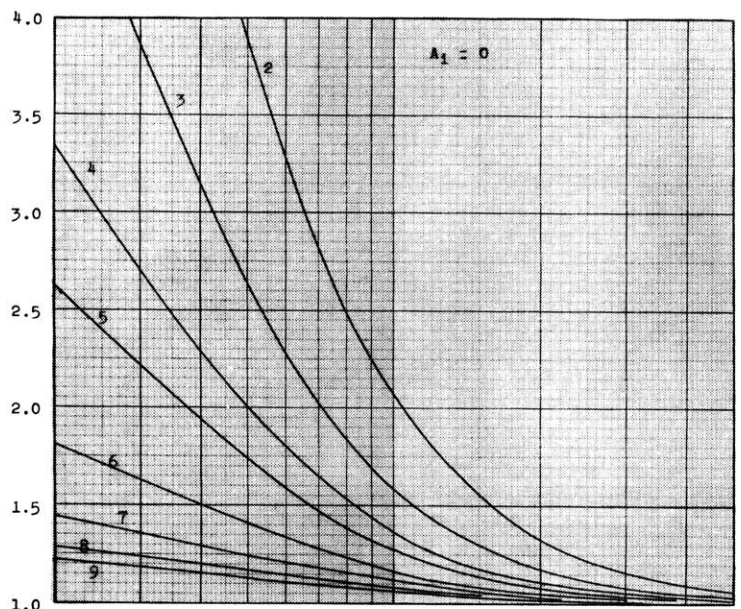
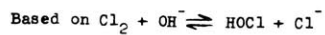
Since $\phi = k_L^0 / k_L^*$, we may write

$$\frac{L}{\rho} dC_0 = k_L^* a \phi (A_1 - A_0) dz \quad (9.28)$$

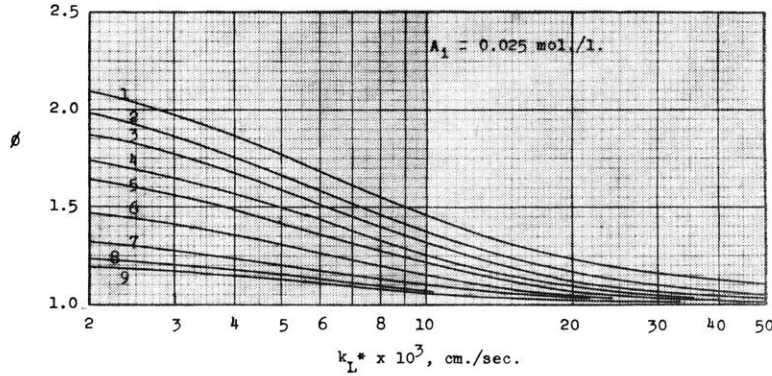
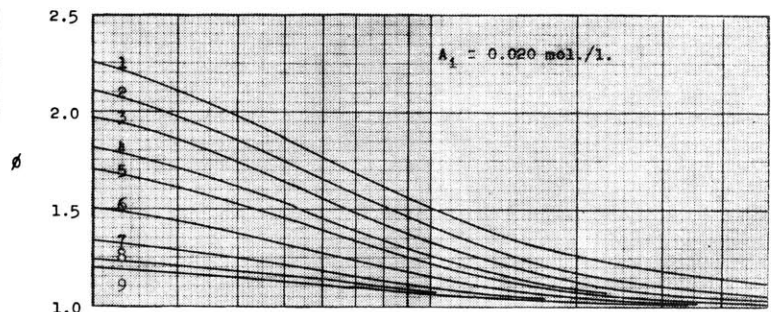
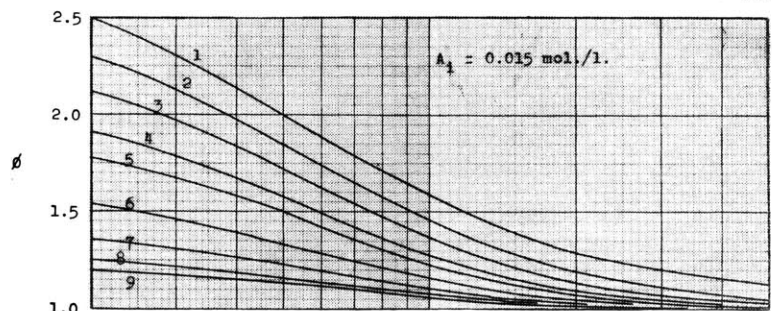
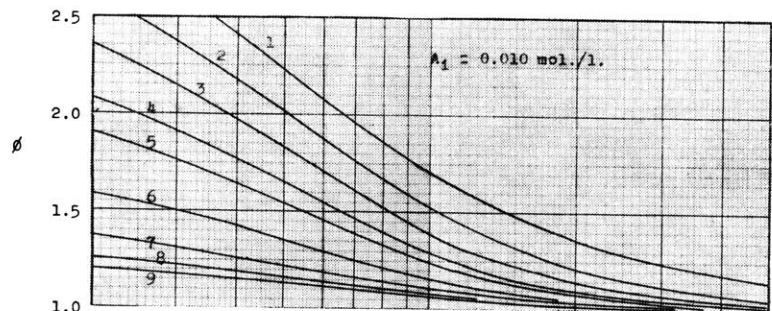
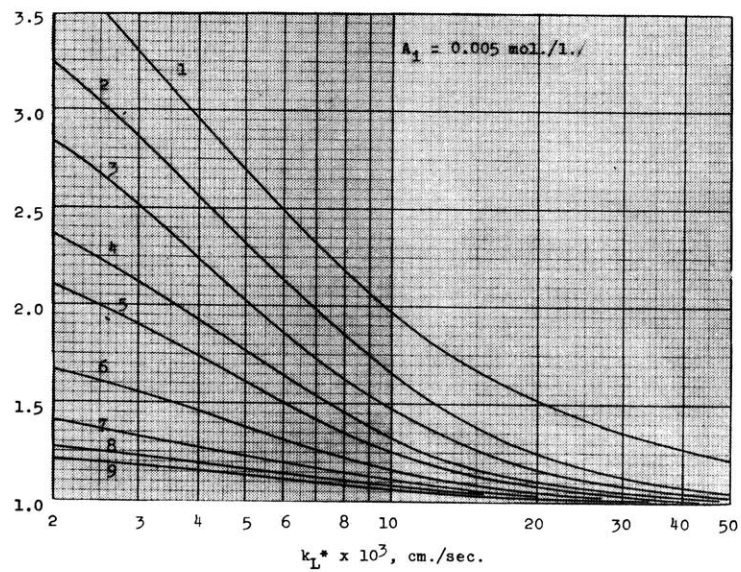
Since $k_L^* a$ is constant with height, this may be integrated to

Fig. 9.1

ϕ -Plots for Chlorine-Water System at 70°F.



Legend	
Line No.	C_0 , mol./l.
1	0
2	0.002
3	0.004
4	0.007
5	0.01
6	0.02
7	0.04
8	0.07
9	0.10



$$k_L^*a = \frac{L}{\rho z} \int \frac{dC_0}{\phi(A_1 - A_0)} \quad (9.29)$$

If the values of k_L^* were known in advance for each run, one could obtain ϕ as well as A_1 as a function of C_0 through the column and integrate eq. (9.29) graphically. This is not the case, however. From the data of Craig (17) on the desorption of chlorine from dilute hydrochloric acid in a packed column, one can obtain the value of k_L^*a for the run. A trial and error solution can be made to determine the value of k_L^* for each run by carrying out the integration of eq. (9.29) for various trial values of k_L^* until the known value of k_L^*a is obtained.

Thus, for each run of Vivian and Whitney (101) on the absorption of chlorine in water in a packed column at 70°F., it is possible to calculate k_L^* . By dividing k_L^*a by this value of k_L^* , one can calculate the value of ϕ for each run. This provides a novel method of calculating the interfacial area in a packed column.

These calculations were carried out by deNicolas (79) on the data of Vivian and Whitney using the ϕ -plots of Fig. 9.1 in an S.M. thesis associated with this thesis. Not all of the runs of Vivian and Whitney were used, but only those in which exit liquor samples were taken just below the base-plate rather than those in which the samples were taken at the trap, since the latter samples include the bottom end effect. It is true that Vivian and Whitney made a correction for this end effect, but it was not felt by deNicolas that this procedure was sufficiently accurate for this type of calculation. The results of the calculations of deNicolas are shown in Figs. 9.2 and 9.3.

The dry surface area of one-inch Raschig rings is given in a table in Sherwood (92) as 58 ft.²/ft.³, or 0.19 cm.²/cm.³. It can be seen that the wetted area as given by this calculation is equal to the total dry surface area of the packing at 20,000 lbs./hr.(ft.²). The loading point for this packing is approximately equal to this liquor rate, so that one may conclude that the packing is completely wet at the loading point. Below the loading point, the interfacial area was found to vary as the 0.44 power of the liquor rate.

Fig. 9.2

Effect of Liquor Rate on Physical Coefficient, k_L^* ,
for Absorption of Chlorine in a Packed Column^{L*}

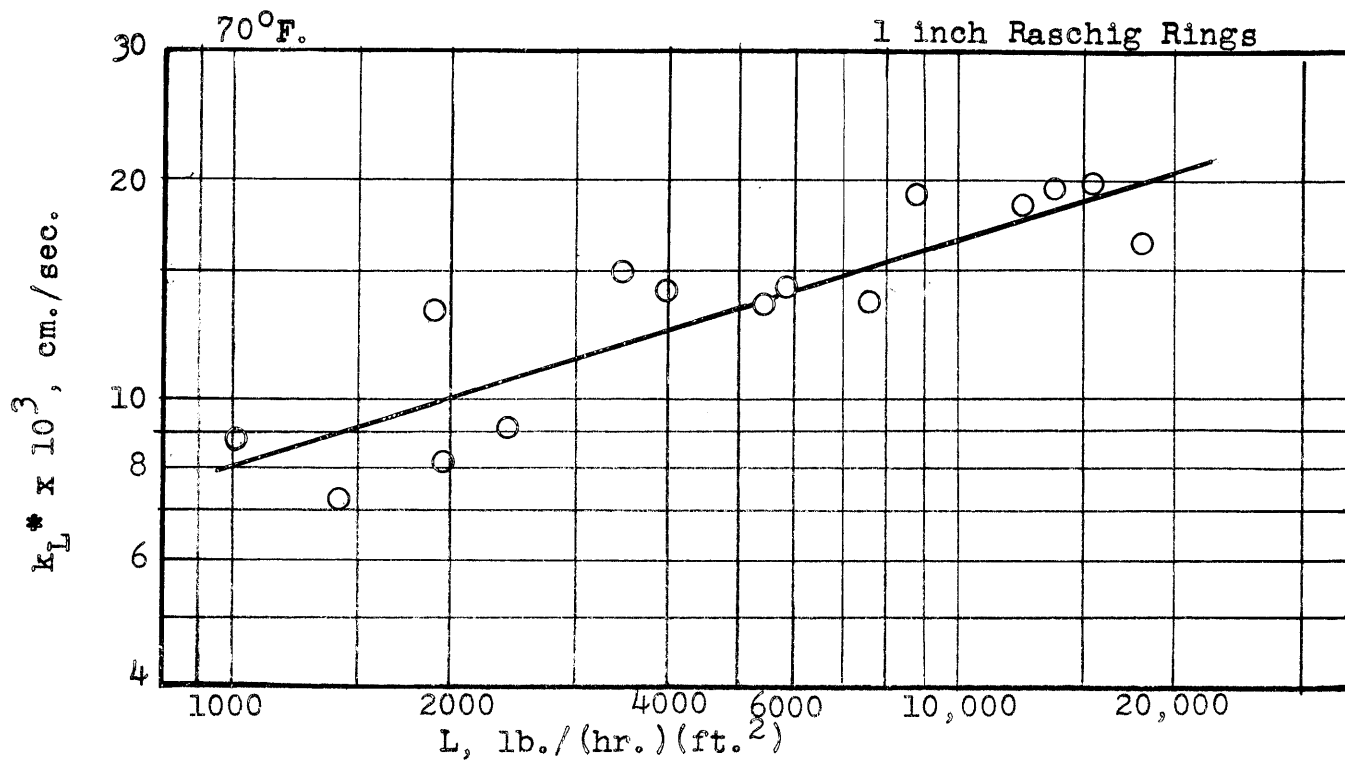
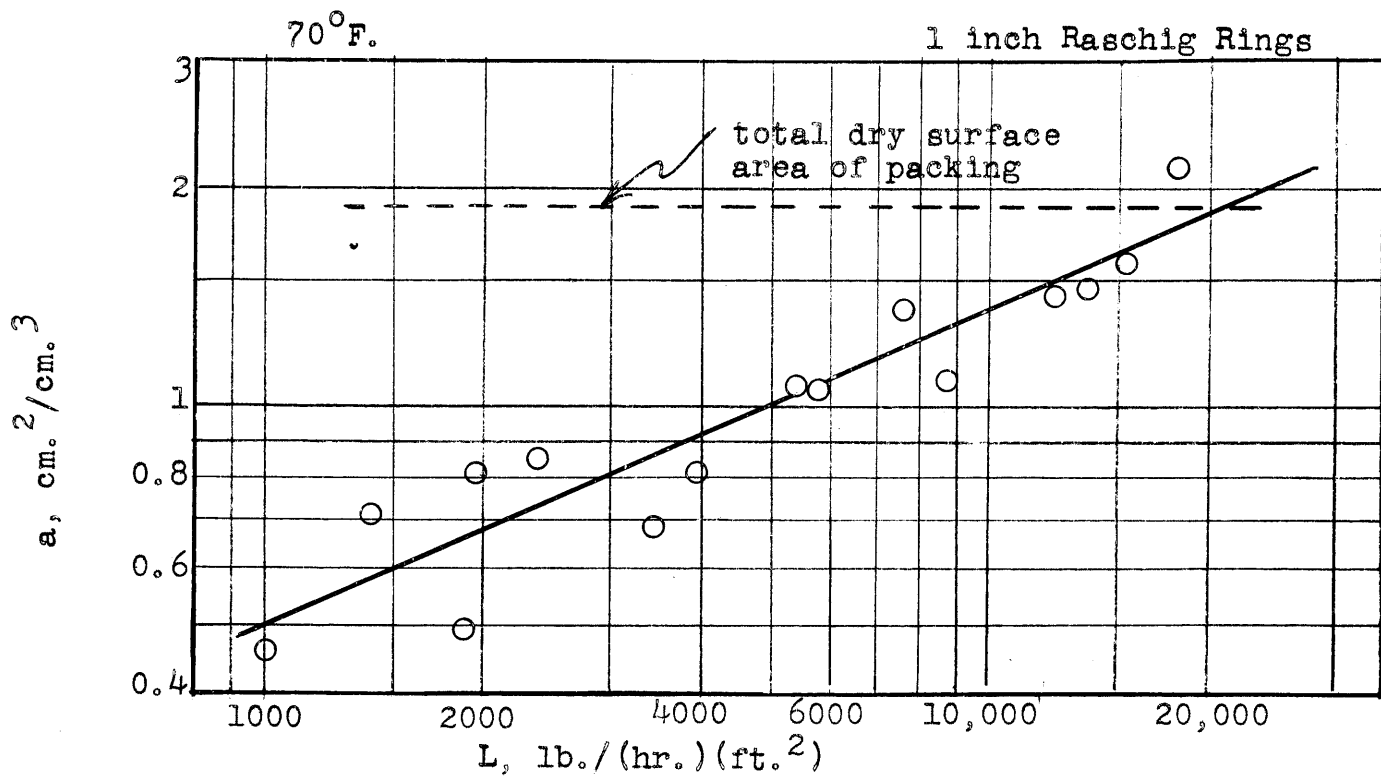


Fig. 9.3

Effect of Liquor Rate on Effective Interfacial Area
for Absorption of Chlorine in a Packed Column



9.4. Application of Theory to Data on Desorption of Chlorine from Water in a Packed Column. Using the same column and packing as did Craig (17), Voorhees (102) studied the desorption of chlorine from water. Because of an error in his choice of Henry's law constant, H , the pseudo-coefficients which Voorhees calculated from his data were incorrect, and the conclusions which he drew from them were erroneous. Miller (74), in another S.M. thesis associated with this thesis, recalculated the coefficients from Voorhees' data and obtained the total coefficients and pseudo-coefficients shown in Fig. 9.4. For comparison the physical coefficients of Craig are also plotted. The results are similar to those obtained by Vivian and Whitney (101) for absorption of chlorine in water in a packed column (see Figs. 2.1 and 2.2). The difference between the pseudo and physical coefficient for desorption is less than for absorption, which would be expected because the values of C_0 for the desorption runs are much higher than for the absorption runs, and the ϕ -plots (Fig. 9.1) show that ϕ is much closer to unity for high values of C_0 .

Miller (74) calculated k_L^*a by means of eq. (9.29).

$$k_L^*a = \frac{L}{\rho z} \int \frac{dC_0}{\phi(A_1 - A_0)} \quad (9.29)$$

using the data of Voorhees and the results of deNicolas (79). For each run, he determined the value of k_L^* from L , using Fig. 9.2. From the original data of Voorhees on the concentrations of the entering and leaving streams and a material balance, he calculated A_1 as a function of C_0 , and from the ϕ -plots (Fig. 9.1) calculated ϕ as a function of C_0 for each run. Graphical integration then yielded k_L^*a . The results are plotted on Fig. 9.5. For comparison the data of Craig for k_L^*a are also plotted.

The agreement is fair. Miller found the average deviation of his calculated values of k_L^*a from Craig's values were 7.6%. The deviations are probably due to three factors: the scatter of the original data, which may be estimated by the failure of closure of material balances, which averaged 5.6%; the range of temperatures of the runs, which was 69 to 87°F; the values of ϕ used in the graphical integration were assumed to be independent of temperature, and the resulting values of k_L^*a were corrected to 70°F. by the Sherwood-Holloway (93) relation that k_L^*a is proportional to $\exp(0.023 t^\circ\text{C})$; some of the deviation must be a result of the many assumptions used to derive the ϕ -plots.

Fig. 9.4

Comparison of Desorption of Chlorine from Water with Absorption of Chlorine in Dilute HCl in a Packed Column

1 inch Raschig Rings 70°F Data of Voorhees (102) recalculated by Miller (74)

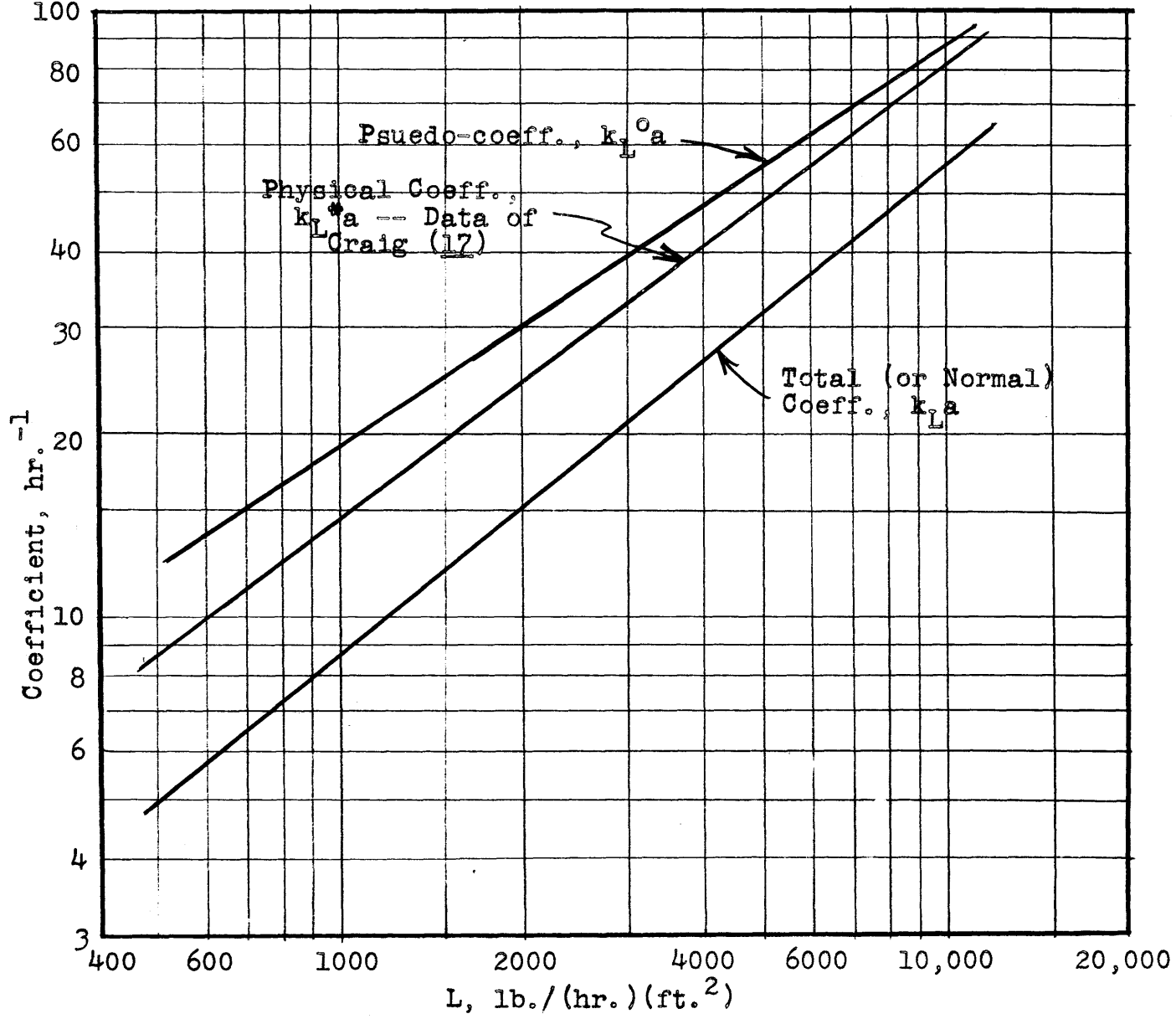
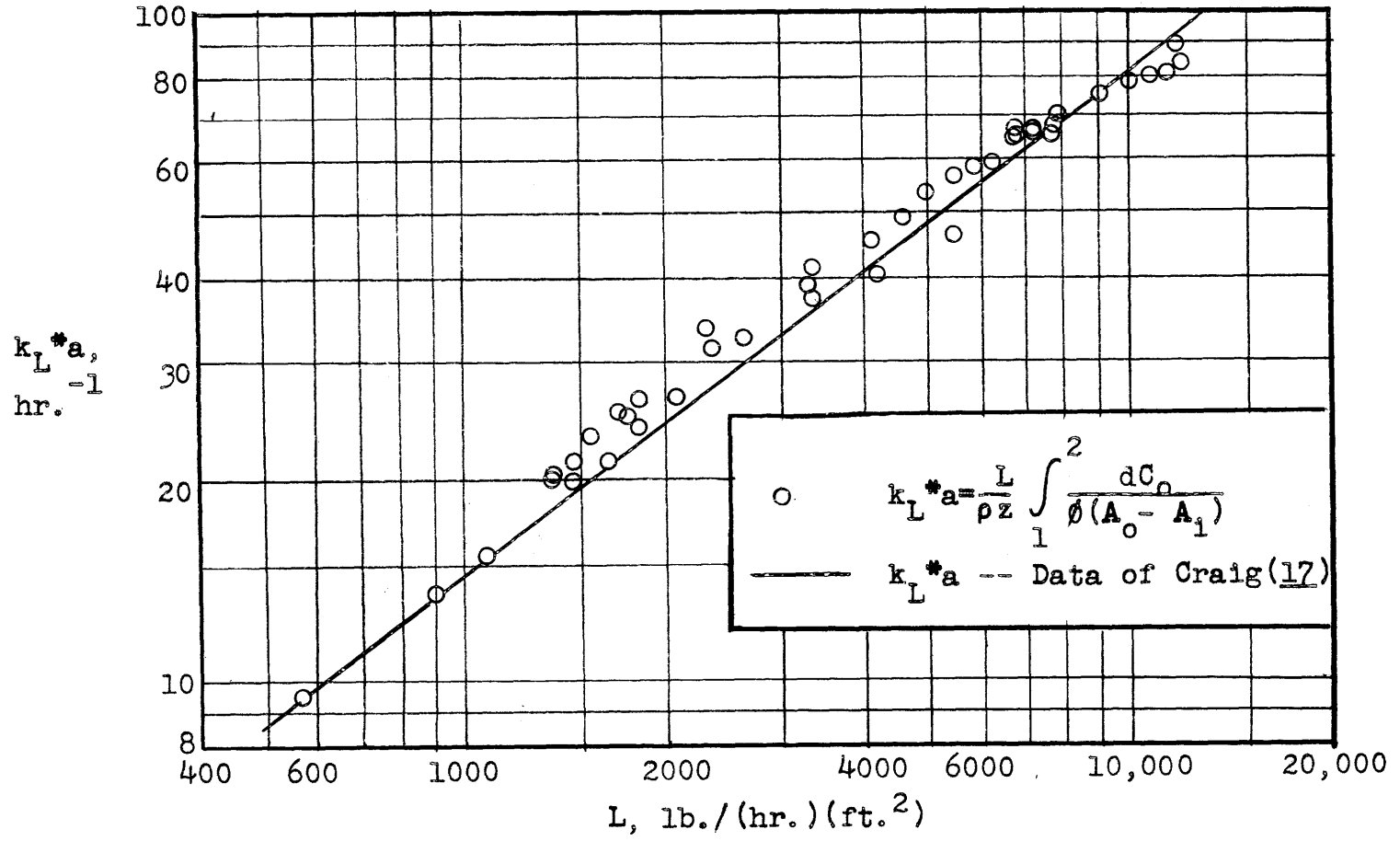


Fig. 9.5

Correlation of Data on Desorption
of Chlorine in a Packed Column



9.5. A Study of the Effect of Certain Variables on the Theoretical Values of ϕ . There are several uncertainties in the calculation of the theoretical values of ϕ , even after assuming that the film theory may be used to calculate ϕ . In the first place, there exists a controversy over the mechanism of the hydrolysis of chlorine; secondly, there is some disagreement over the value of the equilibrium constant K_c ; finally there is some uncertainty regarding the effect of temperature. Quincy (86), in a third S.M. calculational thesis associated with this thesis, examined the controversial issues and studied the effect of reaction mechanism, equilibrium constant and temperature on the theoretical values of ϕ . The remainder of this section is either quoted directly or paraphrased from Quincy's thesis.

The hydrolysis of chlorine is an extremely rapid reaction and requires special techniques to determine the reaction rate constant. In 1936, Shilov and Solodushenkov (95) published some experimental results on the rate of the chlorine hydrolysis. The reaction rate was determined by a stream dilution technique. The concentrations were determined by measuring the electrical conductivity of the solution. The rate constants reported by Shilov and Solodushenkov were far from constant and in 1946, Morris (76) proposed an alternate mechanism for the hydrolysis of chlorine, one which involved the reaction of the hydroxyl ion instead of the water molecule. The rate constants calculated by Morris assuming the proposed mechanism, were more constant than those calculated by Shilov and Solodushenkov, but the constants still varied considerably.

Shilov and Solodushenkov (95) assumed that the hydrolysis proceeded according to the following equations:



The rate expression for this reaction would then be written as

$$-\frac{d[\text{Cl}_2]}{d\theta} = m[\text{Cl}_2] - n[\text{HOCl}][\text{H}^+][\text{Cl}^-] \quad (9.30)$$

The values of m varied about 100% during the run. Only three runs were reported at that time. In 1945, Shilov and Solodushenkov (94) reported more data on the hydrolysis reaction. The values of m reported in the later article were more constant than those reported in 1936.

In an attempt to explain the varying rate constants reported by Shilov and Solodushenkov in 1936, Morris (76) proposed an alternate mechanism which was as follows:

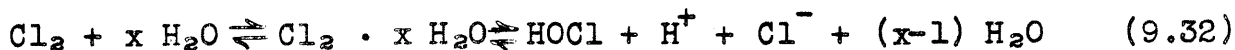


The rate equation would then be written as

$$-\frac{d[\text{Cl}_2]}{dt} = k_1 [\text{Cl}_2][\text{OH}^-] - k_2 [\text{HOCl}][\text{Cl}^-] \quad (9.31)$$

Morris recalculated the data of Shilov and Solodushenkov and determined the constant k_1 . The k_1 value were more constant, varying about 10 to 30% during the run.

Quincy studied the new data of Shilov and Solodushenkov from Morris' point of view and calculated values of k_1 . In addition, he made an attempt to fit the new data to a first order equation, assuming that a hydrate was formed according to the following reaction:



If the formation of the hydrate was the controlling factor, then the equilibrium between the hydrate and the hydrolyzed chlorine could be assumed to exist at all times.

On the basis of the new rate data of Shilov and Solodushenkov (94), Quincy found the first-order forward, third-order reverse mechanism of eq. (9.4) to be the most reasonable of the various mechanisms proposed. The values of m varied less than 5% during the run, while the values of k_1 fluctuated as much as 40%. Furthermore, Quincy found that plotting the logarithm of the rate constant against the reciprocal of the temperature gave consistent results for m , but wide scatter for k_1 . The attempt to fit the rate data to a first order equation gave chaotic results which seemed to have no relation to temperature.

Considering only the earlier rate data that were published by Shilov and Solodushenkov (95), the interpretation given them by Morris seemed valid. However, the data published later (94) seem to contradict the mechanism proposed by Morris and indicate that the mechanism of the reaction is as shown in reaction (9.4). All the data obtained by Shilov and Solodushenkov were not reported, only those data which they considered most reliable. Obviously, one of the criteria used to determine the reliability of the data was the constancy of the reaction rate constant m . It may be that all the data considered together would support the argument of Morris. Until more data are available, however, it seems as if the mechanism proposed by Shilov and Solodushenkov will have to be

assumed correct. More data on the reaction rate is definitely needed before the reaction mechanism can be fully understood.

Just as the reaction mechanism is in doubt, so is the value of the equilibrium constant, K_c . In 1900, Yakovkin (109) reported values for the equilibrium constant, determined by measuring the electrical conductivity of the solution and calculating the concentrations of the separate components, knowing the total concentration of chlorine in the solution. The equilibrium constant was expressed as follows:

$$K_c = \frac{[\text{HOCl}] [\text{H}^+] [\text{Cl}^-]}{[\text{Cl}_2]} \quad (9.33)$$

which may be written

$$K_c = \frac{EF^2}{A} \quad (9.34)$$

From previous measurements on conductivity of hydrochloric acid solutions, F was calculated from the conductivity of the chlorine solutions, and the other concentrations were calculated by $E = F$ and $A = C - F$.

$$K_c = \frac{F^3}{C - F} \quad (9.35)$$

In 1945, Shilov and Solodushenkov (94) reported values for K_c determined from conductivity measurements which agreed with C those reported by Yakovkin. The values of Shilov and Solodushenkov and of Yakovkin are plotted in Fig. 9.6, the line through the points being labeled "Conductivity Method."

In 1945, Vivian (99) determined the equilibrium constant for the hydrolysis by measuring the pressure of chlorine above the water solution and by determining the total concentration of chlorine in the solution. Equilibrium was approached from both directions and the results checked. The total chlorine concentration may be expressed as follows:

$$C = A + E$$

Since $E = F$, from eq. (9.34) we have

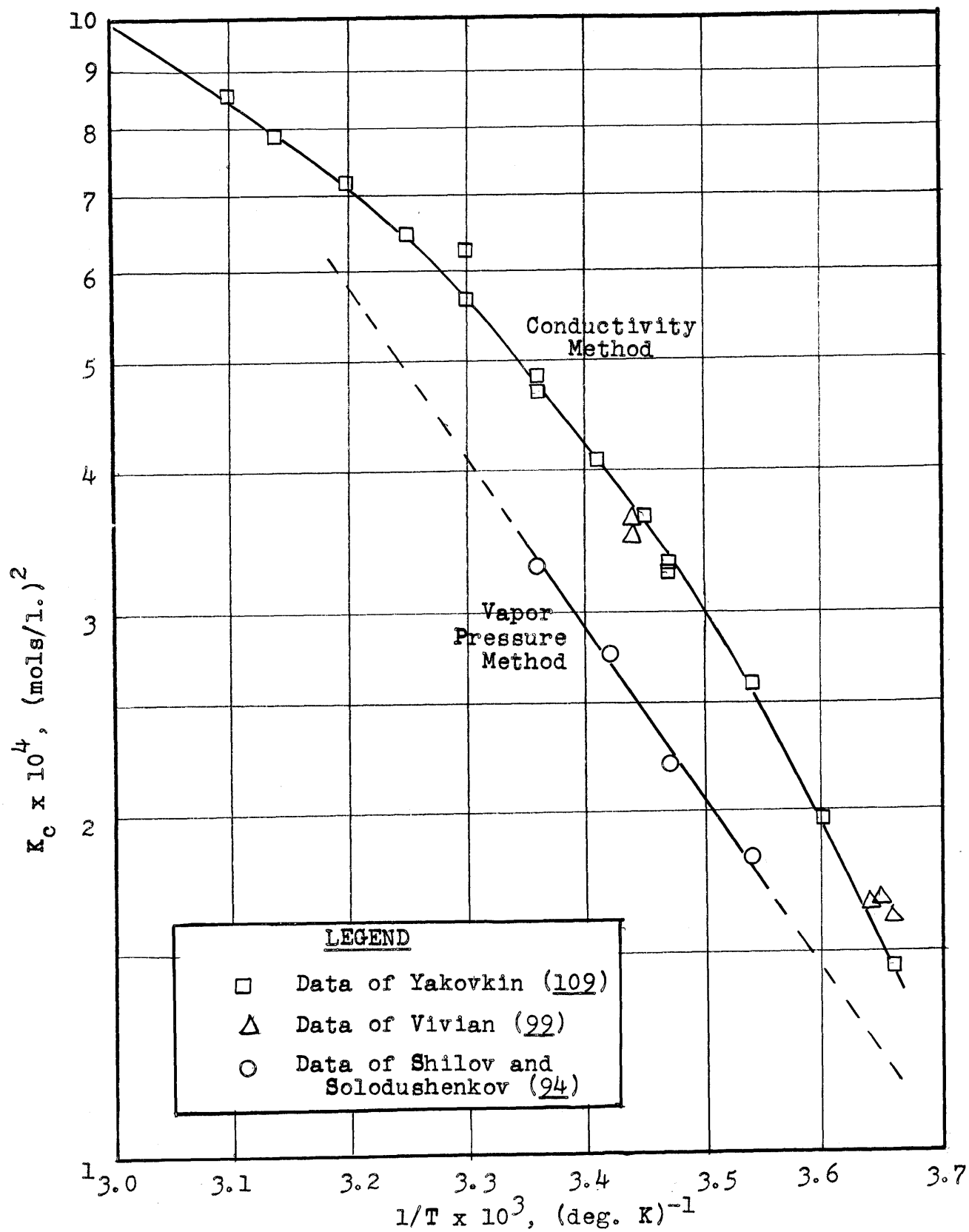
$$K_c = E^3/A$$

Then,

$$C = A + (K_c A)^{1/3} \quad (9.36)$$

Fig. 9.6

Equilibrium Constant for the Hydrolysis of Chlorine in
Water vs. $1/T$



Since $A = HP$,

$$C = HP + (K_c HP)^{1/3} \quad (9.37)$$

or

$$C/P^{1/3} = HP^{2/3} + (K_c H)^{1/3} \quad (9.38)$$

Thus, by plotting $C/P^{1/3}$ vs. $P^{2/3}$, Vivian was able to determine the equilibrium constant. The vapor pressure data plotted as straight lines on this type plot, the slopes being equal to H and the intercept to $(K_c H)^{1/3}$. Vivian's values for K_c are plotted in Fig. 9.6, the line through the points being labeled "Vapor Pressure Method."

An examination of Fig. 9.6 shows that the vapor pressure method yields values approximately 50% lower than the conductivity method. One reason for the discrepancy might be that concentrations were used instead of activities in the expressions for the equilibrium constant. The activity coefficients might have some effect upon the relative values of the equilibrium constants since the constants were obtained by two very different methods. Quincy studied the effect of variation of activity coefficients, assuming that the activity coefficient for the hydrogen ion and for the chloride ion are the same, and the activity coefficient for the chlorine and hypochlorous acid are the same. For both types of experiments he derived an expression relating the equilibrium constant based on activities to the two activity coefficients and to the equilibrium constant based on concentrations. He found, however, that there were no reasonable choice of activity coefficients which would make the equilibrium constants based on activities the same for the two methods.

Quincy also analyzed the precision of the experimental methods and concluded that the discrepancy between the constants could not be accounted for by inaccuracies in the methods of determining the constants. Other factors must be responsible for the discrepancy, but no explanation of it can be offered at this time.

Quincy then made some calculations to determine the effect of choice of mechanism and of equilibrium constant on ϕ . These calculations are summarized in Fig. 9.7. The curves for the reaction mechanism



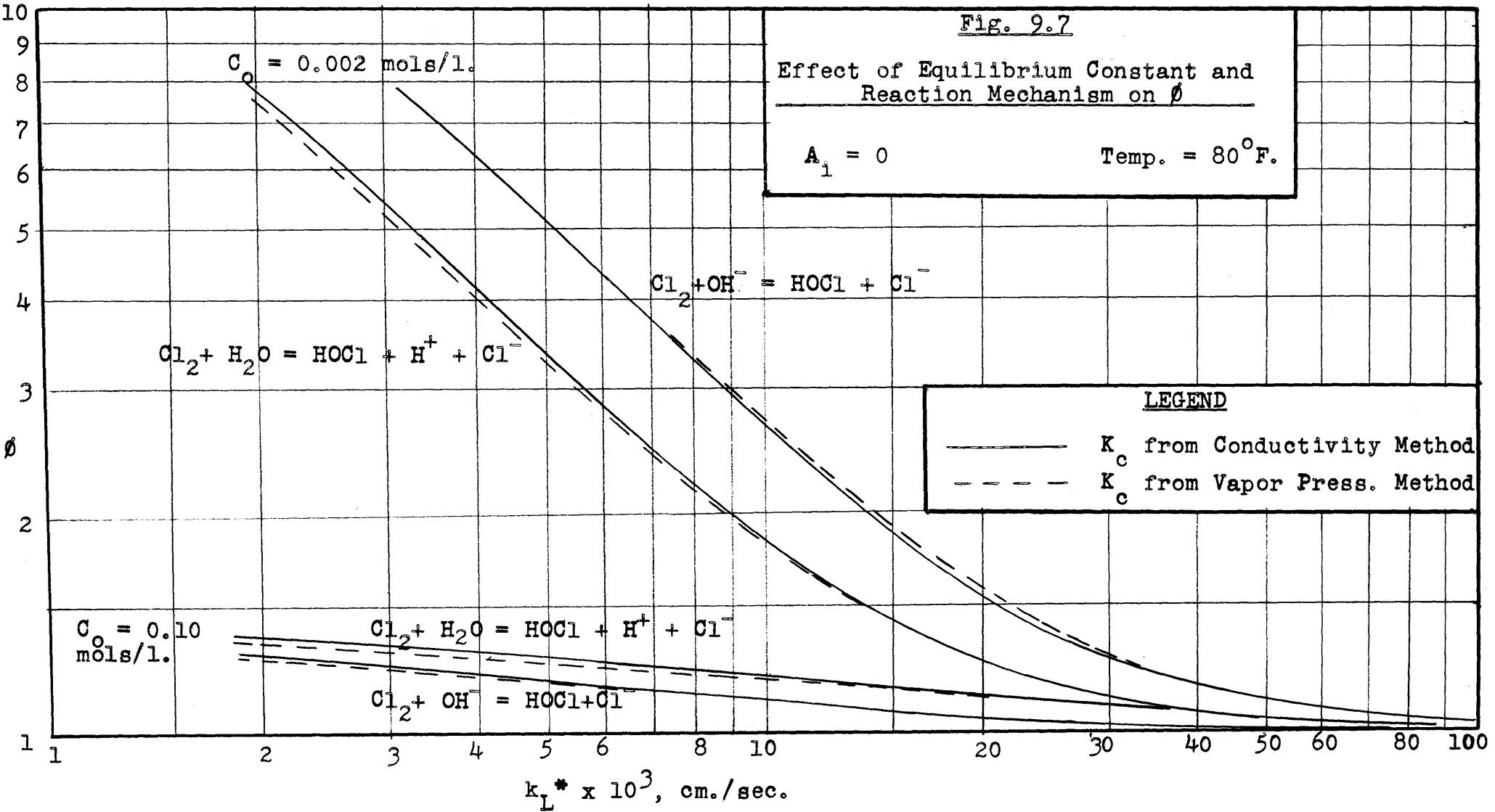
were computed by using equ. (9.12), (9.13) and (9.14), while the curves for the reaction mechanism

Fig. 9.7

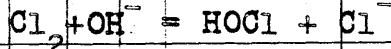
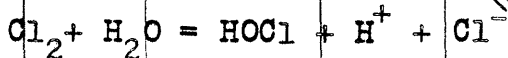
Effect of Equilibrium Constant and Reaction Mechanism on ϕ

$A_1 = 0$

Temp. = 80°F.



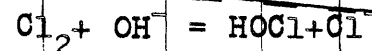
$C_0 = 0.002$ mols/l.



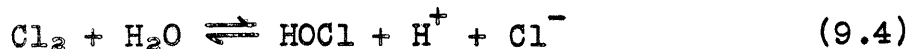
LEGEND

- K_c from Conductivity Method
- - - K_c from Vapor Press. Method

$C_0 = 0.10$ mols/l.



$k_L^* \times 10^3, \text{ cm./sec.}$



were obtained by the use of eqs. (9.25), (9.26) and (9.13). Simultaneous solution of these equations were carried out by the indirect graphical method described in Sec. 9.2. The values used for the diffusivities were $D_A = 1.48 \times 10^{-5}$ cm.²/sec., $D_E = 1.55 \times 10^{-5}$ cm.²/sec., $D_F = 3.12 \times 10^{-5}$ cm.²/sec. at 25°C. These were corrected to 80°F. by the Stokes-Einstein relationship. The values of the rate constants were obtained from the study of the rate data of Shilov and Solodushenkov (94). At 80°F., $K_c = 5.17 \times 10^{-4}$ (g. moles/l.)² from the conductivity method, while $K_c = 3.67 \times 10^{-4}$ (g. moles/l.) from the vapor pressure method. The two extremes of concentration are shown.

An examination of Fig. 9.7 will show that the value of the equilibrium constant has relatively little effect upon ϕ , but the reaction mechanism has a very large effect. Because of the negligible effect of equilibrium constant, it makes little difference which one is chosen, so it was decided to use those based on the vapor pressure method of Vivian in subsequent calculations by Quincy. The choice of reaction mechanism is important, however, and because Quincy concluded that the first-order forward, third-order reverse mechanism was the more reasonable one, he used eqs. (9.25), (9.26) and (9.13) with the rate constants of Shilov and Solodushenkov (94) for the subsequent calculations on the effect of temperature.

Quincy has tabulated ϕ vs. k_L^* for various values of A_1 and C_0 at the four temperatures 60°F., 70°F., 80°F., and 94°F. The values for 70°F., are listed in Table 9.1. The temperature relation was expressed as the ratio of ϕ at the temperature in question to ϕ at a reference temperature. The ratio of ϕ to ϕ_{ref} was found to be a function of A_1 , C_0 , k_L^* , and temperature. A few examples are plotted in Figs. 9.8 and 9.9 to show trends. The reference temperature was taken at 70°F.

A comparison of Figs. 9.8 and 9.9 will show that the temperature correction is most important at low values of C_0 , A_1 , and k_L^* . The temperature correction is due mostly to the change in the reaction rate constant, n , and the diffusivity D_A , with temperature.

It is concluded that the ϕ -plots are significantly affected by the temperature, particularly when ϕ is large compared with unity.

Effect of Temperature on the ϕ -Plots

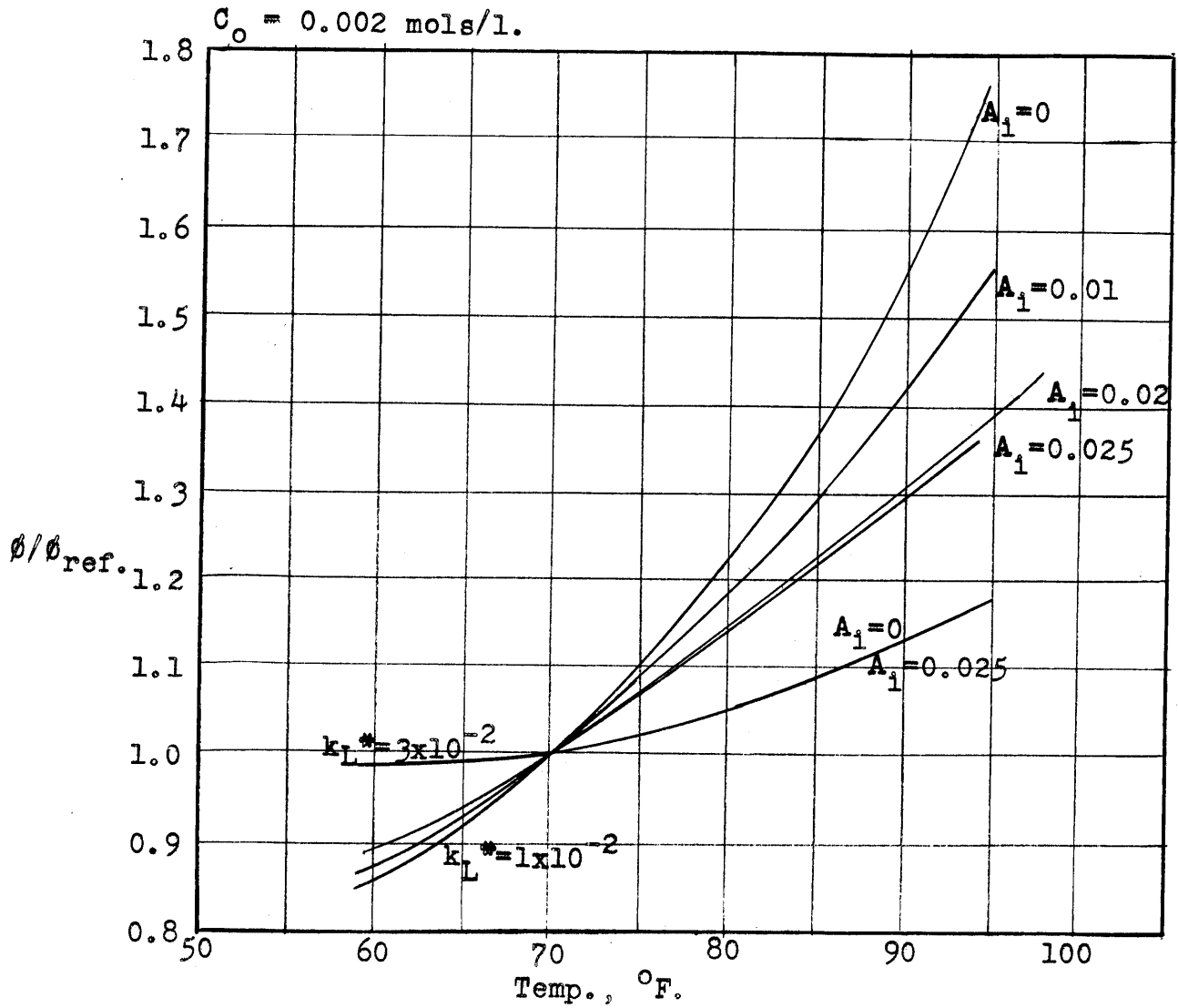


Fig. 9.9

Effect of Temperature on the ϕ -Plots

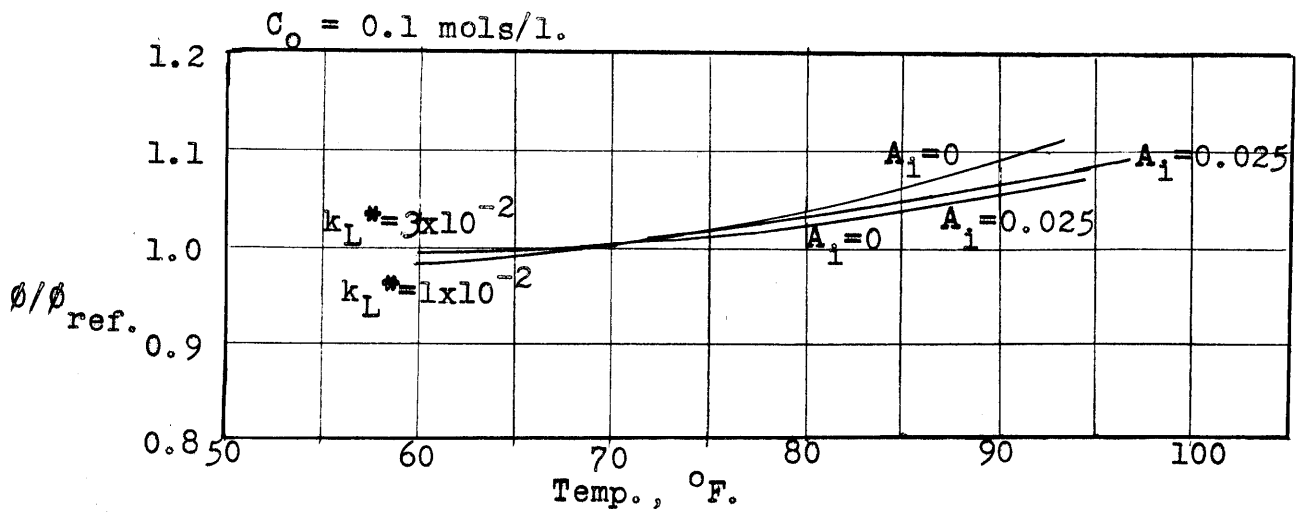


TABLE 9.1

Calculated Values of β for Absorption of Chlorine in Water

Temp. = 70°F.

Equilibrium Constant from Vapor Pressure Method
Reaction Mechanism: $\text{Cl}_2 + \text{H}_2\text{O} \rightleftharpoons \text{HOCl} + \text{H}^+ + \text{Cl}^-$

$A_1 = 0$			$A_1 = 0.005 \text{ mol./l.}$			$A_1 = 0.01 \text{ mol./l.}$			$A_1 = 0.015 \text{ mol./l.}$			$A_1 = 0.02 \text{ mol./l.}$			$A_1 = 0.025 \text{ mol./l.}$		
C_0 mol./l.	$k_L^* \times 10^3$ cm./sec.	β	C_0 mol./l.	$k_L^* \times 10^3$ cm./sec.	β	C_0 mol./l.	$k_L^* \times 10^3$ cm./sec.	β	C_0 mol./l.	$k_L^* \times 10^3$ cm./sec.	β	C_0 mol./l.	$k_L^* \times 10^3$ cm./sec.	β	C_0 mol./l.	$k_L^* \times 10^3$ cm./sec.	β
0.002	1.014	9.83	0.0	1.11	4.34	0.0	1.16	3.20	0.0	1.22	2.70	0.0	1.27	2.42	0.0	1.31	2.233
	1.59	6.88		1.70	4.03		1.80	3.07		1.88	2.63		1.95	2.365		2.02	2.184
	2.54	4.57		2.67	3.54		2.81	2.84		2.91	2.477		3.04	2.250		3.13	2.095
	4.24	2.878		4.34	2.725		4.50	2.413		4.66	2.200		4.81	2.045		4.95	1.923
	6.35	2.027		6.36	2.057		6.55	1.954		6.70	1.862		6.86	1.785		7.00	1.725
	10.15	1.462		10.1	1.472		10.2	1.465		10.5	1.453		10.6	1.438		10.5	1.424
	15.9	1.201		15.6	1.205		15.7	1.204		15.8	1.203		15.8	1.202		15.9	1.201
	25.4	1.081		25.0	1.082		25.0	1.082		25.0	1.082		25.0	1.082		25.1	1.082
	42.4	1.029		41.5	1.030		41.5	1.030		41.6	1.030		41.6	1.030		41.6	1.030
	65.5	1.013		62.2	1.013		62.2	1.013		62.2	1.013		62.2	1.013		62.2	1.013
0.004	1.03	6.77	0.002	1.12	3.74	0.002	1.19	2.88	0.002	1.25	2.482	0.002	1.29	2.253	0.002	1.33	2.097
	1.58	5.13		1.73	3.49		1.83	2.77		1.92	2.410		1.99	2.198		2.05	2.050
	2.51	3.80		2.72	3.09		2.87	2.57		2.94	2.279		3.10	2.101		3.20	1.974
	4.31	2.600		4.43	2.480		4.71	2.235		4.76	2.070		4.92	1.917		5.06	1.825
	6.48	1.920		6.52	1.940		6.68	1.843		6.85	1.764		7.01	1.699		7.20	1.645
	10.4	1.430		10.3	1.448		10.4	1.435		10.5	1.420		10.7	1.403		11.0	1.390
	16.2	1.192		16.0	1.200		16.0	1.197		16.1	1.195		16.2	1.192		16.3	1.190
	26.0	1.078		25.4	1.080		25.5	1.080		25.6	1.080		25.6	1.080		25.7	1.079
	43.4	1.028		42.4	1.029		42.4	1.029		42.5	1.029		42.5	1.029		42.5	1.029
	65.0	1.013		63.5	1.013		63.5	1.013		63.5	1.013		63.5	1.013		63.6	1.013
0.007	1.05	4.44	0.004	1.13	3.23	0.004	1.20	2.60	0.004	1.25	2.294	0.004	1.30	2.107	0.004	1.33	1.977
	1.62	3.65		1.75	3.03		1.85	2.50		1.93	2.227		2.00	2.055		2.06	1.926
	2.66	2.945		2.76	2.74		2.89	2.330		3.02	2.109		3.13	1.965		3.22	1.864
	4.44	2.223		4.51	2.250		4.69	2.040		4.85	1.904		5.08	1.805		5.15	1.781
	6.68	1.765		6.65	1.818		6.82	1.740		7.01	1.674		7.18	1.620		7.35	1.573
	10.7	1.377		10.5	1.412		10.6	1.397		10.8	1.380		10.9	1.365		11.1	1.350
	16.8	1.180		16.4	1.189		16.4	1.185		16.5	1.182		16.6	1.179		16.7	1.177
	26.8	1.073		26.0	1.077		26.0	1.077		26.1	1.076		26.2	1.075		26.2	1.074
	44.8	1.026		43.3	1.028		43.3	1.028		43.3	1.028		43.3	1.028		43.3	1.028
	67.1	1.012		65.0	1.013		65.0	1.013		65.0	1.013		65.0	1.013		65.0	1.013
0.01	1.07	3.37	0.007	1.15	2.73	0.007	1.22	2.30	0.007	1.27	2.073	0.007	1.31	1.940	0.007	1.35	1.840
	1.69	2.92		1.79	2.576		1.89	2.206		1.97	2.015		2.05	1.895		2.09	1.807
	2.72	2.455		2.82	2.336		2.97	2.072		3.10	1.933		3.19	1.833		3.28	1.757
	4.57	1.965		4.64	1.991		4.82	1.845		5.00	1.747		5.15	1.675		5.27	1.620
	6.90	1.628		6.87	1.680		7.06	1.612		7.27	1.561		7.45	1.521		7.61	1.489
	11.1	1.327		10.9	1.360		11.1	1.342		11.2	1.328		11.4	1.315		11.5	1.306
	17.4	1.156		16.9	1.166		17.0	1.165		17.2	1.163		17.3	1.158		17.4	1.156
	27.9	1.065		27.0	1.073		27.0	1.072		27.1	1.071		27.2	1.070		27.3	1.069
	46.5	1.024		44.9	1.026		44.9	1.026		45.0	1.026		45.0	1.026		45.0	1.026
	69.6	1.011		67.2	1.012		67.3	1.012		67.3	1.012		67.4	1.012		67.4	1.012
0.02	1.13	2.165	0.01	1.17	2.40	0.01	1.24	2.09	0.01	1.29	1.92	0.01	1.34	1.820	0.01	1.37	1.745
	1.79	2.00		1.82	2.27		1.92	2.01		2.00	1.87		2.06	1.776		2.12	1.704
	2.92	1.736		2.89	2.075		3.04	1.90		3.16	1.78		3.25	1.703		3.34	1.644
	4.95	1.576		4.78	1.815		4.96	1.708		5.14	1.636		5.28	1.582		5.45	1.540
	7.55	1.406		7.12	1.570		7.31	1.522		7.51	1.484		7.68	1.453		7.85	1.426
	12.3	1.230		11.25	1.313		11.45	1.300		11.6	1.288		11.8	1.287		12.0	1.268
	19.4	1.115		17.5	1.153		17.65	1.150		17.8	1.147		18.1	1.140		18.1	1.143
	31.2	1.050		28.0	1.064		28.0	1.064		28.1	1.063		28.2	1.063		28.3	1.062
	52.2	1.019		46.5	1.024		46.5	1.024		46.6	1.024		46.6	1.024		46.6	1.024
	78.5	1.008		69.6	1.011		69.6	1.011		69.7	1.011		69.7	1.011		69.7	1.011
0.04	1.24	1.625	0.02	1.22	1.877	0.02	1.29	1.743	0.02	1.34	1.656	0.02	1.38	1.594	0.02	1.42	1.550
	1.98	1.547		1.92	1.800		2.01	1.687		2.08	1.612		2.14	1.557		2.20	1.519
	3.25	1.448		3.08	1.677		3.20	1.597		3.31	1.544		3.40	1.503		3.47	1.470
	5.58	1.337		5.15	1.516		5.31	1.475		5.49	1.442		5.58	1.414		5.70	1.390
	8.55	1.252		7.76	1.380		7.94	1.359		8.21	1.340		8.25	1.323		8.39	1.309
	14.1	1.153		12.5	1.223		12.7	1.216		12.8	1.210		13.0	1.204		13.1	1.200
	22.5	1.080		19.6	1.113		19.7	1.111		19.8	1.109		19.9	1.107		20.1	1.105
	36.4	1.054		31.4	1.050		31.4	1.041		31.6	1.049		31.6	1.049		31.7	1.048
	61.0	1.014		52.4	1.019		52.4	1.019		52.5	1.019		52.5	1.019		52.5	1.019
	92.0	1.006		78.5	1.008		78.6	1.008		78.6	1.008		78.6	1.008		78.6	1.008
0.07	1.35	1.392	0.04	1.31	1.535	0.04	1.37	1.480	0.04	1.41	1.441	0.04	1.46	1.412	0.04	1.50	1.386
	2.15	1.350		2.06	1.483		2.15	1.437		2.21	1.407		2.28	1.383		2.34	1.362
	3.58	1.290		3.36	1.410		3.47	1.380		3.56	1.357		3.65	1.339		3.73	1.323
	6.20	1.265		5.1	1.333		5.19	1.309		5.36	1.290		5.65	1.277		6.21	1.267
	9.60	1.172		8.21	1.241		8.85	1.235		9.01	1.224		9.15	1.217		9.30	1.211
	16.0	1.107		14.2	1.149		14.4	1.145		14.6	1.143		14.7	1.140		14.8	1.137
	25.8	1.058		22.6	1.079		22.9	1.077		22.9	1.077		23.0	1.076		23.1	1.076
	42.0	1.026		36.5	1.036		36.6	1.036		36.7	1.035		36.8	1.035		37.0	1.035
	70.8	1.010		61.0	1.014		61.0	1.014		61.1	1.014		61.1	1.014		61.5	1.014
	106.5	1.005		91.8	1.006		91.8	1.006		92.0	1.006		92.0	1.006		92.2	1.006
0.10	1.43	1.297	0.07	1.40	1.360	0.07	1.45	1.335	0.07	1.50	1.315	0.07	1.54	1.299	0.07	1.57	1.285
	2.32	1.260		2.23	1.325		2.30	1.305		2.36	1.290		2.42	1.277		2.48	1.266
	3.88	1.220		3.68	1.274		3.76	1.262		3.86	1.251		3.93	1.243		4.00	1.235
	6.76	1.172		6.34	1.217		6.45	1.210		6.55	1.202		6.65	1.196		6.75	1.191
	10.5	1.123		9.75	1.167		9.85	1.163		10.0	1.160		10.1	1.157		10.25	1.153
	17.6	1.086		16.1	1.105		16.2	1.103		16.4	1.102		16.5	1.101		16.6	1.100
	28.5	1.046		25.9	1.058		26.1	1.057		26.1	1.057		26.2	1.056		26.2	1.056
	46.6	1.021		42.1	1.026		42.2	1.026		42.2	1.026		42.4	1.025		42.5	1.025
	78.4	1.008		70.8	1.010		70.8	1.010		70.8	1.010		71.0	1.010		71.0	1.010
	118.5	1.004		106.5	1.005		106.5	1.005		106.5	1.005		106.8				

B. Absorption of Sulfur Dioxide in Water

It is the purpose of this section to derive theoretically the experimental conclusion of Whitney and Vivian (107) that for the liquid-side resistance in the absorption of sulfur dioxide in water, the pseudo-coefficient may be taken as equal to the physical coefficient. For this purpose, it is necessary to show that $(\phi-1)$ is small compared to unity.

9.6. Development of Theory. In the case of the chlorine-water system, it was shown that for the two mechanisms chosen, the magnitudes of $(\phi-1)$ were within 50% of each other. Thus, for the purpose of calculating the order of magnitude of $(\phi-1)$ for the sulfur dioxide-water system, it should not make much difference what mechanism is chosen, provided that the reaction rate data are analyzed in terms of that mechanism.

The picture that is chosen here is that sulfur dioxide reacts with hydroxyl ion to form bisulfite ion. The assumptions made are:

1. The water is originally pure before any sulfur dioxide is dissolved in it.
2. Sulfurous acid, H_2SO_3 is not present.
3. The second ionization, $\text{HSO}_3^- \rightleftharpoons \text{H}^+ + \text{SO}_3^{2-}$ is negligible.
4. The reaction $\text{H}_2\text{O} \rightleftharpoons \text{H}^+ + \text{OH}^-$ is instantaneous.
5. Diffusivities are independent of concentration.
6. HSO_3^- is non-volatile.
7. The film theory may be used to calculate ϕ from k_L^* , and the constants of the reaction.
8. The reaction rate is

$$-\frac{d[\text{SO}_2]}{dt} = k_1 [\text{SO}_2] [\text{OH}^-] - k_2 [\text{HSO}_3^-] \quad (9.39)$$

$$\text{Let } A = [\text{SO}_2]$$

$$B = [\text{OH}^-]$$

$$E = [\text{HSO}_3^-]$$

$$D_A = \text{diffusivity of } \text{SO}_2$$

$$D_E = \text{diffusivity of } \text{H}^+ + \text{HSO}_3^-$$

The appropriate differential equation is

$$D_A \frac{d^2 A}{dx^2} = - D_E \frac{d^2 E}{dx^2} = k_1 A B - k_2 E \quad (9.40)$$

which was treated in Sec. 9.33. Assuming B is constant at B_1 , the solution was found there to be

$$\phi \left(1 + \frac{K B_1 D_E}{D_A} \frac{\tanh Y x_f}{Y x_f} \right) = 1 + \frac{K B_1 D_E}{D_A} + \frac{A_0}{A_1 - A_0} \frac{K D_E}{D_A} (B_1 - B_0) \left(1 - \frac{1}{\cosh Y x_f} \right) \quad (8.259)$$

together with

$$Y^2 = \frac{k_1 B_1}{D_A} + \frac{k_2}{D_E} \quad (8.258)$$

$$\phi = 1 + \frac{D_E}{D_A} \frac{(E_1 - E_0)}{(A_1 - A_0)} \quad (8.235)$$

As in the chlorine-water system, $[OH^-]$ is assumed negligible compared with $[H^+]$ so that

$$B = K_w / E \quad (9.41)$$

In addition, the equilibrium for the SO_2-H_2O system is generally expressed by

$$K_S = [H^+] [HSO_3^-] / [SO_2] \quad (9.42)$$

sometimes referred to as the apparent equilibrium constant. Since

$$K = [HSO_3^-] / [SO_2] [OH^-], \quad K_S = K K_w. \quad \text{Then } K B = K_S / E.$$

Eq. (8.259) becomes

$$\phi \left(1 + \frac{K_S D_E}{E_1 D_A} \frac{\tanh Y x_f}{Y x_f} \right) = 1 + \frac{K_S D_E}{E_1 D_A} + \frac{A_0}{A_1 - A_0} \frac{K_S D_E}{E_1 E_0 D_A} (E_0 - E_1) \left(1 - \frac{1}{\cosh Y x_f} \right) \quad (9.43)$$

Substituting eq. (8.235), noting that $K_S A_0 / E_0 = E_0$, and subtracting from both sides the quantity

$$1 + \frac{K_S D_E \tanh Y_{x_f}}{E_1 D_A Y_{x_f}}$$

$$(\phi-1) \left(1 + \frac{K_S D_E \tanh Y_{x_f}}{E_1 D_A Y_{x_f}} \right) = \frac{K_S D_E}{E_1 D_A} \left(1 - \frac{\tanh Y_{x_f}}{Y_{x_f}} \right) - \frac{E_0}{E_1} (\phi-1) \left(1 - \frac{1}{\cosh Y_{x_f}} \right) \quad (9.44)$$

This rearranges to

$$\phi-1 = \frac{\frac{K_S D_E}{E_0 D_A} \left(1 - \frac{\tanh Y_{x_f}}{Y_{x_f}} \right)}{\frac{E_1}{E_0} + \frac{K_S D_E}{E_0 D_A} \frac{\tanh Y_{x_f}}{Y_{x_f}} + 1 - \frac{1}{\cosh Y_{x_f}}} \quad (9.45)$$

From eq. (8.235)

$$\frac{E_1}{E_0} = 1 + \frac{D_A}{D_E} \frac{A_1 - A_0}{E_0} (\phi-1) \quad (9.46)$$

Eq. (8.258) may be rewritten

$$Y^2 = \frac{k_2}{D_E} \left(1 + \frac{K_S D_E}{E_1 D_A} \right) \quad (9.47)$$

From $k_L^* = D_A/x_f$, we obtain

$$k_L^* = \frac{\sqrt{k_2 D_A^2 / D_E} \sqrt{1 + (K_S D_E / E_0 D_A) (E_0 / E_1)}}{Y_{x_f}} \quad (9.48)$$

The system of eqs. (9.45), (9.46) and (9.48) constitute the solution.

9.7. The Rate of Hydrolysis of Sulfur Dioxide.

The only data available on the rate of hydrolysis of sulfur dioxide was obtained in an S.B. thesis by Phipps (83). The rate turned out to be higher than he had expected, so that his apparatus was too limited to follow the reaction at room temperature; it was necessary for him to run at lower temperatures in order to measure the rate. Two runs were made, at 12.5°C. and 11.2°C. The procedure consisted of mixing a sulfur dioxide solution with water rapidly, allowing the resulting mixture to flow through a tube, and measuring the conductivity of the solution at various points along the tube.

Phipps analyzed his data in terms of the reaction mechanism



Furthermore, he used wrong values of the equilibrium constant K_S . In order to use the derivation in Sec. 9.6, Phipps' data are recalculated in terms of the mechanism



The rate expression is

$$-dA/dt = k_1AB - k_2E \quad (9.51)$$

Since $B = K_W/[H^+] = K_W/E$,

$$-dA/dt = k_1K_W A/E - k_2E \quad (9.52)$$

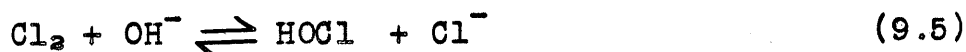
Now $k_1/k_2 = K_S/K_W$, so that

$$-dA/dt = k_1K_W \left(\frac{A}{E} - \frac{E}{K_S} \right) \quad (9.53)$$

$$A_{t=0} - A = k_1K_W \int_0^t \left(\frac{A}{E} - \frac{E}{K_S} \right) dt \quad (9.54)$$

The first run was at 12.5°C. Before dilution, $C = 0.242$ moles/l., after dilution $C = 0.0540$. Thus, the original SO_2 solution was diluted to $0.242/0.0540 = 4.49$ times its volume. By interpolation between values of K_S measured by Campbell and Maass (8), $K_S = 0.0234$. By use of the equation $K_S = E^2/A = E^2/(\bar{C}-E)$, we get $E = 0.0645$ before dilution, $E = 0.0645/4.49 = 0.0144$ just after dilution. Corresponding to the concentration C after dilution, the equilibrium concentration of E is 0.0257. During the runs, the concentrations E were obtained from the conductivity. The graphical integration indicated by eq. (9.55) is then carried out, and k_1K_W calculated. By interpolation of the values of Harned and Geary (33), the values of K_W at 12.5 and 11.2 are respectively 0.37×10^{-14} and 0.33×10^{-14} . Thus, the values of k_1 may be calculated. The data and calculations are summarized in Table 9.2.

The result is that $k_1 = 6 \times 10^{12}$ moles/(l.)(sec.). This compares with Morris' value (76) for k_1 for the reaction



of 8.3×10^{12} , which he found to be invariant with temperature. Because of the similarity between the two reactions,

Table 9.2

Rate of Hydrolysis of Sulfur Dioxide (Data of Phipps (83))Run I temp. = 12.5°C., $K_S = 0.0234$

	<u>C</u>	<u>E</u>	<u>A</u>	<u>$\frac{A}{E} - \frac{E}{K_S} A_{t=0} - A \int_0^t (\frac{A}{E} - \frac{E}{K_S}) dt$</u>	<u>$k_1 K_W$</u>	<u>$k_1 \times 10^{-12}$</u>		
Before dilution	0.242	0.0645	0.1775					
After dilution								
time, sec.								
0	0.0540	0.0144	0.0396	2.135	0	0		
0.179	"	0.0200	0.0340	0.845	0.0056	0.253	0.0221	6.0
0.394	"	0.0230	0.0310	0.366	0.0086	0.372	0.0232	6.3
0.609	"	0.0240	0.0300	0.223	0.0096	0.434	0.0221	6.0
∞	"	0.0257	0.0283	0				

Run II temp. = 11.2°C., $K_S = 0.0243$

	<u>C</u>	<u>E</u>	<u>A</u>	<u>$\frac{A}{E} - \frac{E}{K_S} A_{t=0} - A \int_0^t (\frac{A}{E} - \frac{E}{K_S}) dt$</u>	<u>$k_1 K_W$</u>	<u>$k_1 \times 10^{-12}$</u>		
Before dilution	0.111	0.0412	0.0698					
After dilution								
time, sec.								
0	0.0279	0.01036	0.01754	1.266	0	0		
0.179	"	0.0135	0.0144	0.512	0.00314	0.133	0.0236	7.2
0.356	"	0.0145	0.0134	0.329	0.00414	0.207	0.0200	6.1
0.536	"	0.0155	0.0124	0.162	0.00514	0.251	0.0204	6.2
∞	"	0.0166	0.0113	0				

it is assumed here that k_1 for the SO_2 hydrolysis is also invariant with temperature.

9.8. Calculation of ϕ . The results of Chapter 11 show that the ratio of the diffusivity of ionized sulfurous acid to that of unionized sulfur dioxide is 1.03. That is, $D_E/D_A = 1.03$. At 70°F ., the values of the following constants are obtained:

$$K_S = 0.01915 \quad \text{from Campbell and Maass (8)}$$

$$K_W = 0.76 \times 10^{-14} \quad \text{from Harned and Geary (33)}$$

$$\begin{aligned} k_2 &= k_1 K_W / K_S = (6 \times 10^{12})(0.76 \times 10^{-14}) / (0.01915) = \\ &= 2.38 \text{ sec.}^{-1} \end{aligned}$$

$$\begin{aligned} H &= A_1/P = 0.0885 \text{ lb. moles}/(\text{ft.}^3)(\text{atm.}) \\ &= 1.418 \text{ g. moles}/(1.)(\text{atm.}) \quad \text{from Whitney (106)} \end{aligned}$$

$$\begin{aligned} D_A &= 1.95 \times 10^{-5} \text{ cm.}^2/\text{sec.} \quad \text{at } 30^\circ\text{C. from Fig. 11.6.} \\ &= 1.55 \times 10^{-5} \text{ cm.}^2/\text{sec.} \quad \text{at } 70^\circ\text{F. using Stokes-} \\ &\quad \text{Einstein equation.} \end{aligned}$$

$$\sqrt{k_2 D_A^2 / D_E} = \sqrt{(2.38)(1.55 \times 10^{-5}) / (1.03)} = 6.0 \times 10^{-3} \text{ cm./sec.}$$

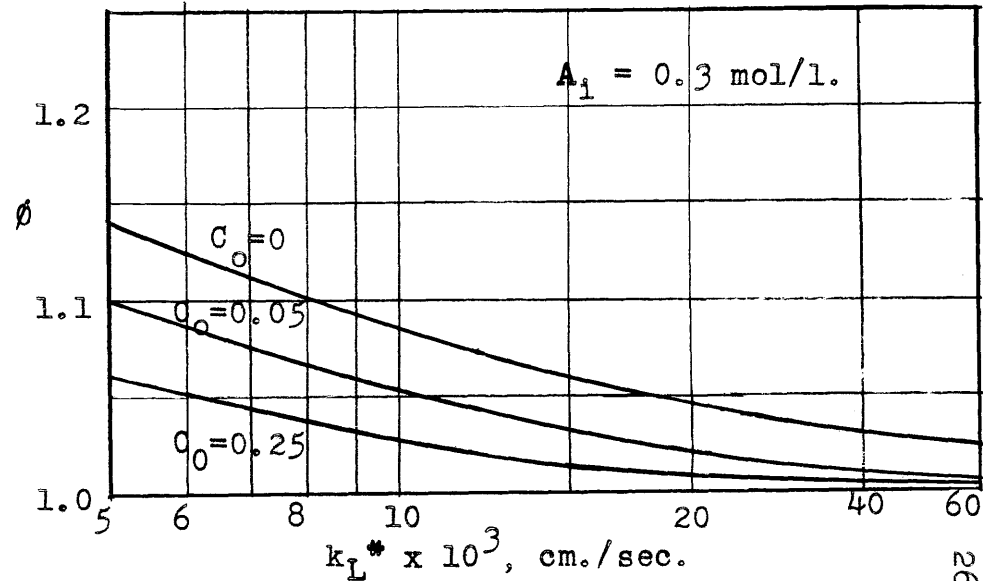
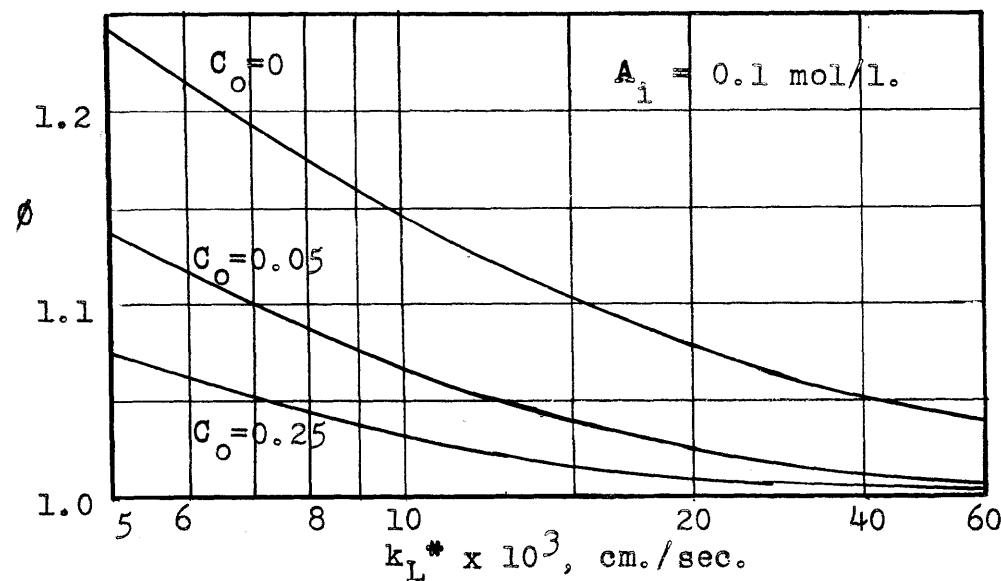
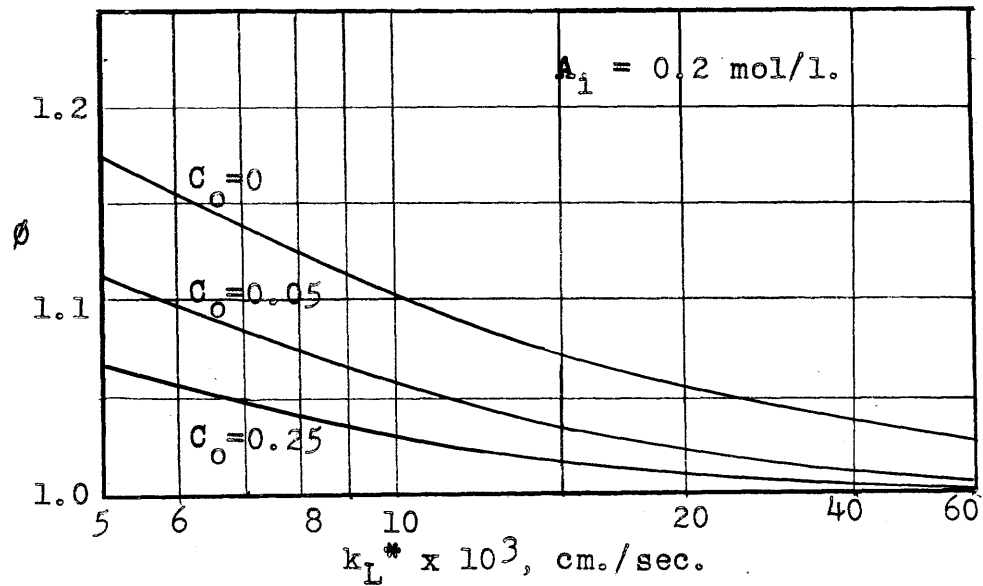
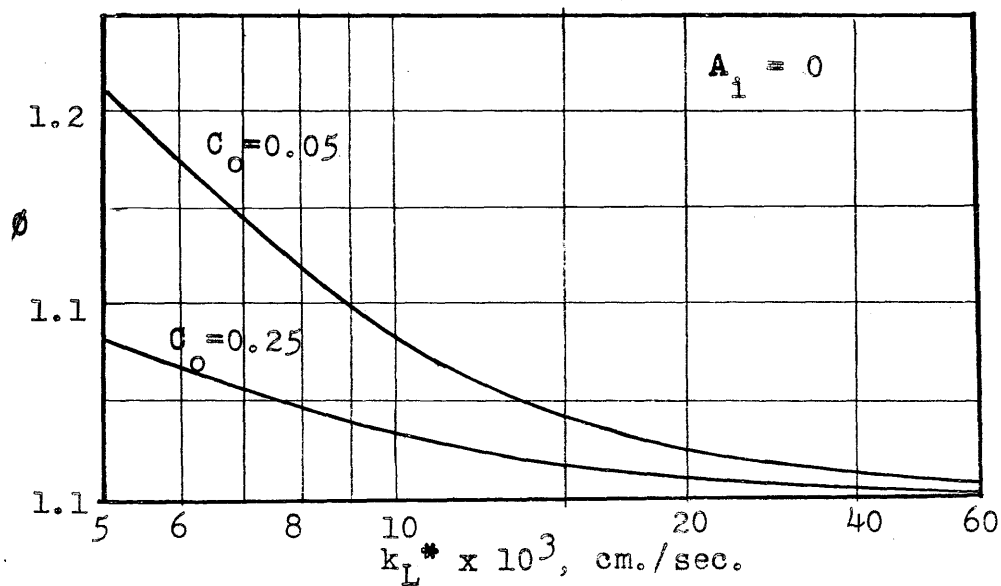
$$K_S D_E / D_A = 0.01915 (1.03) = 0.0197 \text{ g. mole/l.}$$

Some ϕ -plots were constructed, using a procedure similar to that used for the chlorine-water system. For each value of C_0 , plots of $(\phi-1)$ vs. E_1/E_0 was constructed for various values of Y_x (0.2, 0.3, 0.5, 0.8, 1.25, 2.0) using eq. (9.44); on the same graph for each value of A_1 , $(\phi-1)$ was plotted vs. E_1/E_0 , using eq. (9.46). From the intersections were obtained values of $(\phi-1)$ and E_1/E_0 for each combination of C_0 and A_1 . Then eq. (9.48) was used to calculate k_L^* . The results are shown in Fig. 9.10.

9.9. Application to Packed Column Data. Comparison of Fig. 9.10 with Fig. 9.1 shows that the values of ϕ for the sulfur dioxide-water system lie much closer to unity than for the chlorine-water system, in spite of the fact that the forward hydrolysis rate constants are almost the same for the two systems. The reason lies in the fact that at equilibrium, hydrolysis is less complete for sulfur dioxide than for chlorine. For example, in a solution saturated with chlorine at 0.1 atm., the dissolved chlorine is 64% hydrolyzed, while in a solution saturated

Fig. 9.10

ϕ -Plots for Sulfur Dioxide-Water System at 70°F.



with sulfur dioxide at 0.1 atm., the dissolved sulfur dioxide is only 27% hydrolyzed. Thus, the sulfur dioxide-water system behaves more like a physical system, and the pseudo-coefficients are closer to the physical coefficients, than is true for the chlorine-water system.

The lowest liquor rate used by Whitney and Vivian (107) in their study of the absorption of sulfur dioxide in water in a packed column was 910 lbs./hr.(ft.²). From Fig. 9.2, the corresponding value of k_L^* is 7.9×10^{-3} cm./sec. From Fig. 9.10, it can be seen that for this value of k_L^* , ϕ is less than 1.20, and for most of the concentrations encountered in the packed column study, and particularly for the higher liquor rates, ϕ will be less than 1.10. Thus, it can be predicted that the pseudo-coefficients measured by Whitney and Vivian would be equal to the physical coefficient within 10%. This prediction was borne out, for within the scatter of the data, which was greater than 10%, the two coefficients were concluded to be the same.

Unfortunately, the method of calculation of the pseudo-coefficients that Whitney and Vivian used was not completely logical. They first analyzed the data using an overall "total" liquid-side coefficient, that is, one based on a driving force equal to the difference between the total SO₂ concentration in equilibrium with the gas minus the total SO₂ concentration in the bulk of the liquid. By the application of the Wilson plot, they separated the overall resistance into a gas-side and a liquid-side resistance. However, the liquid-side resistance, being based on a total SO₂ driving force, must be a function of the concentration of SO₂ in the liquid, and hence must vary with height in any one run. The gas-side resistance obtained by this technique must be in error. In evaluating the pseudo-coefficient, Whitney (106) used an overall pseudo-driving force, that is, the difference between the unhydrolyzed SO₂ in equilibrium with the gas minus the unhydrolyzed SO₂ in equilibrium with the bulk of the liquid. From the reciprocal of the overall liquid-side coefficient, Whitney then subtracted the gas-side resistance, multiplied by H (equal to A_1/P), the remainder being the reciprocal of the pseudo-coefficient. Such a procedure would have been correct if the gas-side resistance were evaluated correctly. Where the gas-side resistance is small compared with the overall resistance, the error would be unimportant. Indeed, for the lower gas velocities, where the gas-side resistance was the most important, the pseudo-coefficient found by Whitney scattered more widely than for the higher gas velocities.

The correct procedure to use for analysis of data and for design purposes, when the pseudo-coefficient equals the physical coefficient, is to use an overall gas-side coefficient, since it can be expected to be constant

with height during any one run, as shown by the following derivation.

$$N_A a = k_G a (P - P_1) = k_L^* a \phi (A_1 - A_0). \quad (9.55)$$

Since $\phi = 1$, $A_1 = H P_1$, and $P^* = A_0/H$,

$$N_A a = k_G a (P - P_1) = H k_L^* a (P_1 - P^*) \quad (9.56)$$

Eliminating P_1 gives

$$N_A a = \frac{P - P^*}{\frac{1}{H k_L^* a} + \frac{1}{k_G a}} \quad (9.57)$$

Since the overall gas-side coefficient is defined by $N_A a = K_G a (P - P^*)$, we have

$$\frac{1}{K_G a} = \frac{1}{H k_L^* a} + \frac{1}{k_G a} \quad (9.58)$$

Since $k_L^* a$ and $k_G a$ are constant during any one run, and H is constant, $K_G a$ must be constant.

A similar derivation for the overall liquid-side coefficient would be:

$$N_A a = k_G a (P - P_1) = k_L a (C_1 - C) \quad (9.59)$$

Whitney and Vivian (107) observed that for calculating the overall liquid-side coefficient, the equilibrium curve can be approximated by a straight line not passing through the origin. The slope of this line was called H' , so that $C_1 - C = H' (P_1 - P^*)$. Then one obtains

$$\frac{1}{K_L a} = \frac{1}{k_L a} + \frac{H'}{k_G a} \quad (9.60)$$

Since $k_L a$ is not constant in a given run, but varies with concentration in the liquid, then $K_L a$ must also vary.

Thus, it is concluded that an overall gas-side coefficient should be used, whenever the pseudo-coefficient equals the physical coefficient. Even when the gas-side

resistance is negligible, the overall gas-side coefficient can be employed. Furthermore, its use has the advantage of avoiding the necessity of constructing a pseudo-operating line.

C. Absorption of Carbon Dioxide in Sodium Hydroxide Solution

9.10. Because of the lack of agreement between the theoretical and experimental coefficients obtained in this thesis for the desorption of chlorine in water in the short wetted-wall column, it was decided that a simpler case of absorption with chemical reaction should be studied in this column. Accordingly, in an S.M. thesis associated with this thesis, Abbanat and Lobo (1) investigated the absorption of carbon dioxide in sodium hydroxide solutions, using the same short wetted-wall column used for the desorption of carbon dioxide and of chlorine from water.

The auxiliary apparatus was greatly modified in order to carry out absorption, rather than desorption. Pure carbon dioxide gas was used, being first saturated with water and brought to the temperature of the run. A solution of sodium hydroxide was fed into the column at the temperature of the run, and the concentration of carbon dioxide, present as carbonate, was determined for both inlet and outlet liquid streams. For all runs, the temperature was $25 \pm 1^\circ\text{C}.$, while the gas rate was maintained at a constant Reynolds number of 800.

The experimental coefficient was calculated by the equation

$$k_L^o = \frac{V(C_2 - C_1)}{a A_1} \quad (9.61)$$

where V is the volumetric flow rate, $C_2 - C_1$ is the change in carbonate concentration, a is the interfacial area, and A_1 is the concentration of carbon dioxide in the liquid at the interface. The concentration of carbon dioxide in the entering liquid is zero, so that the driving force is $A_1 - 0$. Hence, eq. (9.61) defines a pseudo-coefficient, since the difference in concentrations of unreacted carbon dioxide is used for the driving force. The "total" driving force is meaningless for absorption with irreversible chemical reaction, since the concentration of reacted carbon dioxide in equilibrium with the gas at the interface is infinite. The use of a pseudo-

coefficient is natural for this case, and has always been used, although it has never been given that name.

The value of A_1 is calculated from the solubility of carbon dioxide in pure water, which must be corrected for a salting-out effect. The presence of salts in a solution of a gas in water reduces the solubility of the gas because some of the water which might be used to dissolve the gas is used for the hydration of the salt. Similarly, the presence of sodium hydroxide decreases the solubility of the carbon dioxide, completely apart from the reaction between the two.

Van Krevelen and Hoftijzer (59) have presented the empirical relation

$$A_1 = HP_1 \exp(-0.202 \mu') \quad (9.62)$$

where H is the Henry's law constant for the pure solution, and μ' is the ionic strength of the solution. Van Krevelen and Hoftijzer did not present the actual value of the constant 0.202; they did, however, present some tables of data and calculations, from which Abbanat and Lobo were able to calculate the constant.

The chemical reactions taking place are believed to be



The second reaction is considered to be very rapid compared with the first, so that the first reaction is the rate controlling step. The rate data of Brinkhan *et al* (6) and Saal (88) were considered by Abbanat and Lobo to be the most reliable.

If A is the concentration of carbon dioxide, and B is the concentration of sodium hydroxide, then, using the film theory, a material balance on a differential slice of the film (in the manner used in Sec. 8.5) yields the differential equation

$$D_A \frac{d^2A}{dx^2} = \frac{1}{2} D_B \frac{d^2B}{dx^2} = k_1AB \quad (9.65)$$

The factor $1/2$ arises from the fact that for each molecule of CO_2 which reacts in the differential slice, there must be a net diffusion of one molecule of CO_2 into the slice, but a net diffusion of two molecules of NaOH . This is true

because each molecule of CO_2 reacts with two molecules of NaOH according to eqs. (9.63) and (9.64).

As pointed out in Chap. 8, no solution has been found for the case of absorption with second order irreversible chemical reaction, using the penetration theory. Hence, it is assumed that the film theory may be used to calculate ϕ from k_L^* , k_1 , D_A and D_B . One of the chief purposes of these experiments was to test this assumption under conditions where the penetration theory is known to be valid.

Eq. (9.65) is somewhat different from eq. (8.189), so that the solution given in Sec. 8.26 must be modified for the factor of 1/2 appearing in eq. (9.65). Comparing these two equations shows that the sole difference is that D_B is divided by 2, so that the solution may be obtained from eqs. (8.195), (8.201) and (8.202)

$$\phi = \frac{\sqrt{M [1 - q (\phi - 1)]}}{\tanh \sqrt{M [1 - q (\phi - 1)]}} \quad (8.203)$$

$$M = k_1 B_0 x_f^2 / D_A \quad (8.202)$$

$$q = \frac{D_A A_1}{D_B B_0} \quad (8.195)$$

It is necessary only to change the definition of q .

$$q' = \frac{2 D_A A_1}{D_B B_0} \quad (9.66)$$

and rewrite eq. (8.203)

$$\phi = \frac{\sqrt{M [1 - q' (\phi - 1)]}}{\tanh \sqrt{M [1 - q' (\phi - 1)]}} \quad (9.67)$$

Substituting $k_L^* = D_A / x_f$, eq. (8.202) becomes

$$\sqrt{M} = \frac{\sqrt{k_1 B_0 D_A}}{k_L^*} \quad (9.68)$$

Eqs. (9.66), (9.67) and (9.68) constitute the solution. Eq. (8.203) has been plotted on Fig. 8.11; the same plot may, of course, be used for eq. (9.67).

Since $k_{L0} = k_L^* \phi$, a theoretical value of the pseudo-coefficient may be obtained by evaluating first the physical coefficient and then ϕ , and by multiplying the two together. k_L^* was calculated from eq. (5.18), the actual viscosity and density of the sodium hydroxide solution being used. D_A was obtained from the diffusivity of carbon dioxide in pure water multiplied by the ratio of the viscosity of water to the viscosity of the sodium hydroxide solution. Using this value of k_L^* , M could be calculated. D_B was calculated from the available data on diffusivity of sodium hydroxide in the International Critical Tables (46), and corrected for temperature and viscosity by the Stokes-Einstein equation. q' was then calculated, ϕ read off from Fig. 8.11, and the product $k_L^* \phi$ obtained.

Abbanat and Lobo made two series of runs, one at constant hydroxide concentration and various liquor rates, and one at constant liquor rate and various hydroxide concentrations. The first series, at $B_0 = 0.3$ moles/l., is shown as circles in Fig. 9.11. Abbanat and Lobo drew line No. 2 as the best line through the data, giving more weight to points at higher flow rates. Line No. 1 represents values of k_L^* obtained from eq. (5.18). Line No. 3 represents predicted values of the coefficients, i.e., $k_L^* \phi$. While the experimental line lies about 15% below the theoretical line, they are both of the same slope, within experimental error, and significantly different from the slope of the line for the physical coefficient. The difference between the absolute values may be explained by uncertainties in the values of diffusivities and rate constant used.

The second series of runs, carried out at a liquor rate, Γ , of 19.5 g./((cm.)(min.)), is plotted on Fig. 9.12. Line No. 2 represents the best curve through the data. Line No. 1 is k_L^* . The decrease in k_L^* at the higher concentrations is the result of increased viscosity of the solution, which both increases the time of exposure of the liquid to the gas, and decreases the diffusivity of carbon dioxide. Line No. 3 represents, again, the predicted coefficient, $k_L^* \phi$. The agreement is excellent at 0.1

N NaOH. The experimental coefficient then lies about 30% below theoretical at 1 N NaOH, and continues to increase rapidly with concentration while the theoretical coefficient levels off. The leveling off of the theoretical coefficient is due to the dropping off of k_L^* at high concentrations; apparently the increase in viscosity does not affect the measured coefficients as much as had been expected. The failure of the theory to predict the behavior of the experimental curve at the high concentration of hydroxide is not surprising, in view of the many assumptions concerning

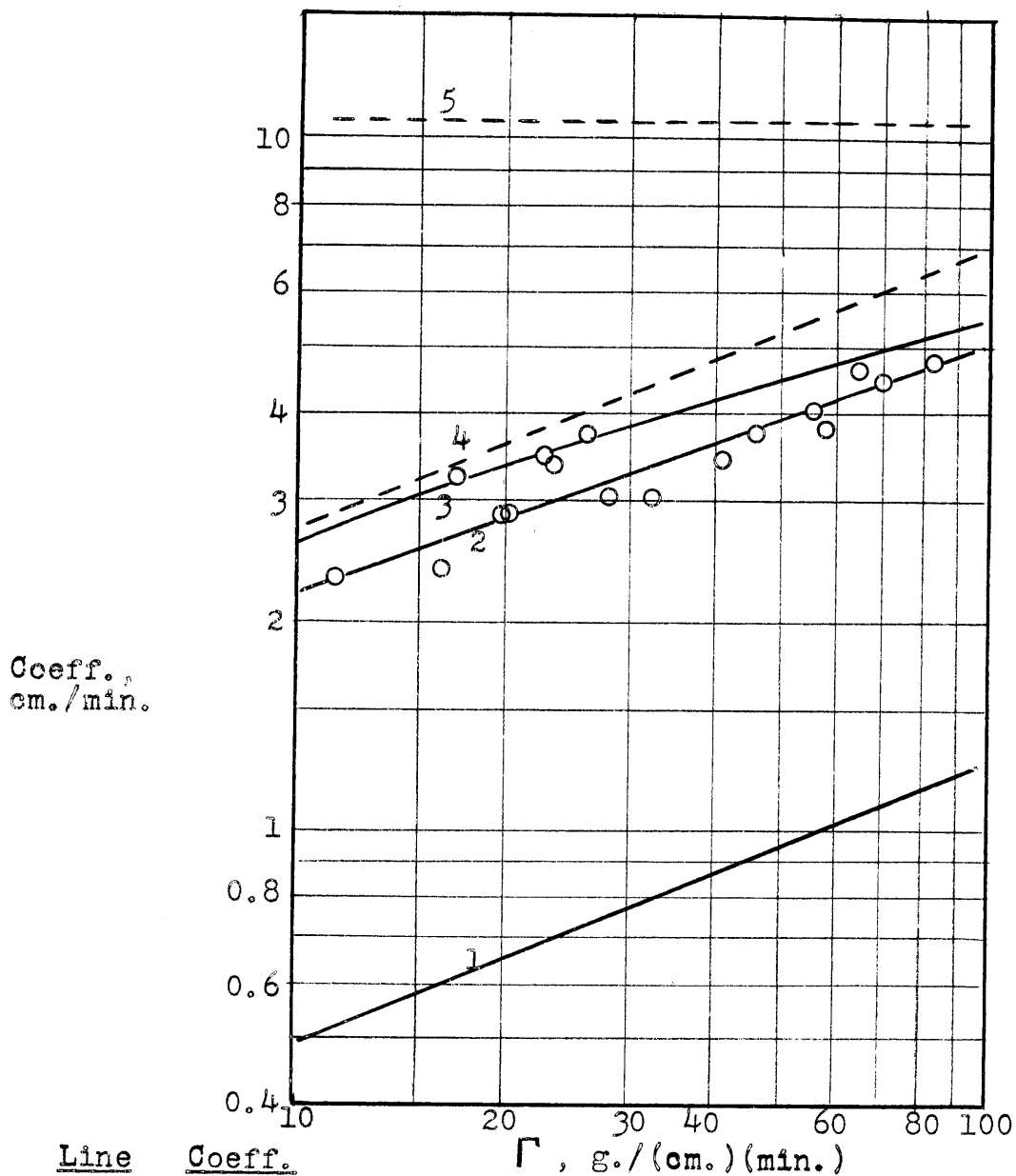
Fig. 9.11

Absorption of Carbon Dioxide in Sodium Hydroxide Solution in a Short Wetted-Wall Column

Effect of Liquor Rate

Data of Abbanat and Lobo (1)

Temp. = 25°C.
 $B_0 = 0.30$
 mols/l.
 $q' = 0.22$



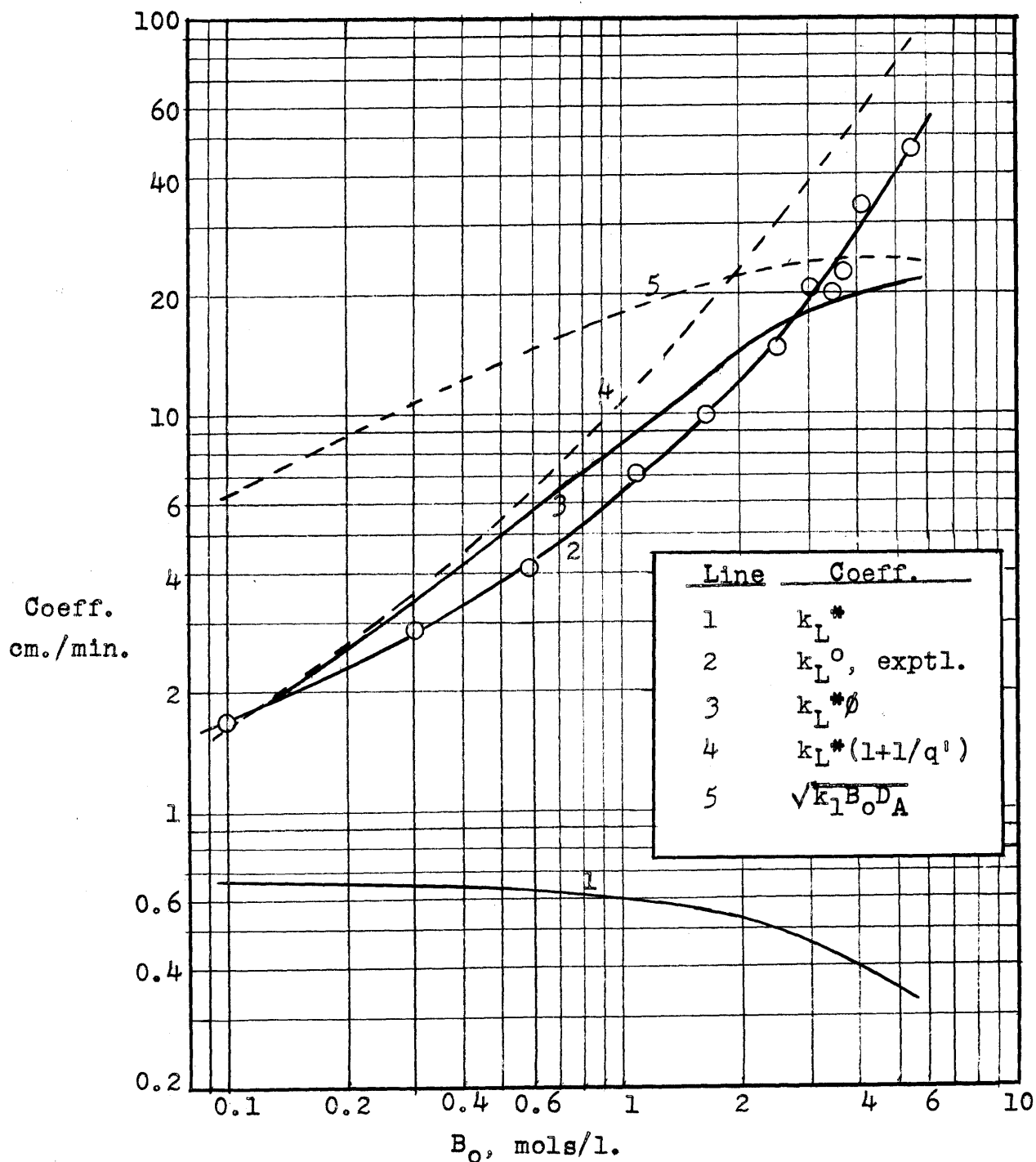
Line	Coeff.
1	k_L^*
2	k_{L_0} exptl.
3	$k_L^* \phi$
4	$k_L^* (1 + 1/q')$
5	$\sqrt{k_1 B_0 D A}$

Fig. 9.12

Absorption of Carbon Dioxide in Sodium Hydroxide
Solution in a Short Wetted-Wall Column
Effect of Hydroxide Concentration

Data of Abbanat and Lobo (1)

Temp. = 25°C.
 $\Gamma = 19.5 \text{ g/(cm.) (min.)}$



the effect of viscosity on k_L^* , D_A , and D_B , which are very uncertain at the higher concentrations. Furthermore, no correction was made to the reaction rate constant for the effect of concentration, since the effect is unknown.

For comparison, two limiting cases are considered. If the reaction rate were infinite, M would be infinite, and eq. (8.189) would be valid:

$$\phi = 1 + 1/q' \quad (9.69)$$

Then the theoretical coefficient would be

$$k_L^* \phi = k_L^* (1 + 1/q') \quad (9.70)$$

This is plotted on Figs. 9.11 and 9.12 as line No. 4.

A second limiting case occurs if the reaction is considered to be first order, that is, if the concentration of sodium hydroxide is assumed to be constant throughout the film at the value B_0 . This is equivalent to assuming $q = 0$, whereupon eq. (9.67) becomes

$$\phi = \sqrt{M} / \tanh \sqrt{M} \quad (9.71)$$

The values of \sqrt{M} encountered here all lie above 8, so that $\tanh \sqrt{M}$ may be taken as unity, and

$$\phi = \sqrt{M} \quad (9.72)$$

Combining (9.68) and (9.72), we have for the theoretical coefficient

$$k_L^* \phi = \sqrt{k_1 B_0 D_A} \quad (9.73)$$

This is plotted on Figs. 9.11 and 9.12 as line No. 5.

It is quite clear, from comparison of the data with line No. 5, that the system does not behave as if the concentration of hydroxide were constant throughout the film; there must indeed be a sharp gradient of hydroxide in the liquid.

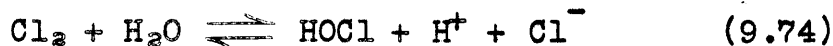
Comparison of the data with line No. 4 in Fig. 9.11 indicates that the reaction rate is not infinite; if anything, the data indicate that the reaction rate is lower than that used to calculate the theoretical coefficients. In Fig. 9.12, however, the shape of the experimental line is remarkably similar to line No. 4, and neither line shows the tendency to level off at the high hydroxide concentration that the theoretical line has.

This might be explained by an increase in the reaction rate constant with hydroxide concentration, or it might be explained, as was suggested above, by the failure to correct the diffusivities and k_L^* properly for viscosity in deriving the theoretical line.

It may be concluded that the short wetted-wall column may be used to study absorption with chemical reaction for the cases where theory cannot be applied. Because of the failure of the experimental coefficients to agree exactly with the predicted coefficients, however, the data cannot be used either to justify the assumption that the film theory may be used instead of the penetration theory to calculate ϕ from k_L^* and the constants of the reaction. Because of the uncertainties in the constants used, the data cannot be used to disprove that assumption, either.

D. Theoretical Upper Limit for Absorption of Chlorine in Water

9.11. In connection with the experimental results obtained on desorption of chlorine from water in the short wetted-wall column, it is necessary to derive a theoretical upper limit for ϕ for the chlorine-water system. From the results obtained earlier, it could be seen that, for a given k_L^* and K , the value of ϕ increases with increasing reaction rate, so that an upper limit should be obtained for infinite reaction rate. Secondly, the existence of a concentration gradient of hydrochloric acid in the liquid results in lowering the value of ϕ . In absorption, the concentration of HCl at the interface is higher than in the bulk of the liquid; this shifts the equilibrium



to the left, thus reducing the extent of the chemical reaction in the region near the interface, and thereby reducing the rate of absorption. In desorption, the reverse is true. The concentration of HCl at the interface is lower than in the bulk of the liquid; the equilibrium is shifted to the right, while the reaction itself is proceeding to the left. Again the extent of the chemical reaction in the region near the interface is reduced, and the rate of desorption is lower. Thus, to obtain an upper limit, the diffusivity of HCl should be assumed to be infinite.

Finally, it may be assumed, to simplify the problem, that the diffusivities of Cl_2 and of HOCl are equal. Actually, they differ by only 5%.

$$D_A = D_E = D \quad (9.75)$$

Because of the assumption of infinite reaction rate, equilibrium exists everywhere in the liquid.

$$K_c = \frac{EF^2}{A} \quad (9.76)$$

Because of the assumption of infinite diffusivity of HCl, the concentration of F is uniform, and equal to the bulk concentration (for film theory) or initial concentration (for penetration theory). Then

$$E = A (K_c/F_0^2) \quad (9.77)$$

This equation is true everywhere in the liquid.

Using the film theory, the differential equation is

$$D \frac{d^2 A}{dx^2} = -D \frac{d^2 E}{dx^2} \quad (9.78)$$

with the boundary conditions

$$\begin{aligned} \text{At } x = 0, \quad A &= A_1, \quad E = E_1 = A_1 (K_c/F_0^2) \\ \text{At } x = x_f, \quad A &= A_0, \quad E = E_0 = A_0 (K_c/F_0^2) \end{aligned} \quad (9.79)$$

Differentiating eq. (9.77) twice gives

$$\frac{d^2 E}{dx^2} = \frac{d^2 A}{dx^2} (K_c/F_0^2)$$

whence eq. (9.78) becomes

$$D \frac{d^2 A}{dx^2} = -D \frac{d^2 A}{dx^2} (K_c/F_0^2)$$

or

$$D \frac{d^2 A}{dx^2} = 0 \quad (9.80)$$

Integration and substitution of the boundary conditions (exactly as in Sec. 8.9) gives

$$A = (A_0 - A_1) \frac{x}{x_f} + A_1 \quad (9.81)$$

Differentiating once gives

$$\frac{dA}{dx} = \frac{A_0 - A_1}{x_f} \quad (9.82)$$

Now, the rate of absorption is given, not by the gradient of A, but by the combined gradient of A and E, because the gradient of E is not zero at the interface. This point is discussed in Sec. 8.18 more completely.

$$N_A = -D \left(\frac{dA}{dx} \right)_{x=0} - D \left(\frac{dE}{dx} \right)_{x=0} \quad (9.83)$$

Differentiating eq. (9.77) once gives

$$\frac{dE}{dx} = \frac{dA}{dx} (K_c/F_0^2) \quad (9.84)$$

Substituting into eq. (9.83),

$$N_A = -D(1+K_c/F_0^2) \left(dA/dx \right)_{x=0} \quad (9.85)$$

Substituting eq. (9.82) yields

$$N_A = \frac{D}{x_f} (A_1 - A_0) (1+K_c/F_0^2) \quad (9.86)$$

But, from eq. (8.160),

$$\phi = \frac{N_A x_f}{(A_1 - A_0) D} \quad (9.87)$$

whence

$$\phi = 1 + K_c/F_0^2 \quad (9.88)$$

The identical result may be obtained from eqs. (9.12), (9.13) and (9.25). From eq. (9.13), we get $F_1/F_0 = 1$. For infinite reaction rate, U and I become infinite, whence both eqs. (9.12) and (9.25) become

$$\phi - 1 = \frac{K_c D_E}{F_0^2 D_A}$$

which is the same as eq. (9.88) for $D_A = D_E = D$.

From eq. (9.77)

$$E_0/A_0 = K_c/F_0^2 \quad (9.89)$$

so that

$$\phi = 1 + E_0/A_0 = C_0/A_0 \quad (9.90)$$

Using the penetration theory, the differential equation is

$$D \frac{\partial^2 A}{\partial x^2} - \frac{\partial A}{\partial t} = \frac{\partial E}{\partial t} - D \frac{\partial^2 E}{\partial x^2} \quad (9.91)$$

with the boundary conditions

$$\begin{aligned} \text{At } t = 0, \quad A &= A_0, \quad E = E_0 = A_0(K_C/F_0^2) \\ \text{At } x = 0, \quad A &= A_1, \quad E = E_1 = A_1(K_C/F_0^2) \\ \text{At } x = \infty, \quad A &= A_0, \quad E = E_0 \end{aligned} \quad (9.92)$$

Differentiating eq. (9.77) gives

$$\frac{\partial E}{\partial x} = \frac{\partial A}{\partial x} (K_C/F_0^2) \quad (9.93)$$

$$\frac{\partial^2 E}{\partial x^2} = \frac{\partial^2 A}{\partial x^2} (K_C/F_0^2) \quad (9.94)$$

$$\frac{\partial E}{\partial t} = \frac{\partial A}{\partial t} (K_C/F_0^2) \quad (9.95)$$

Substituting eqs. (9.94) and (9.95) into eq. (9.91) gives

$$D \frac{\partial^2 A}{\partial x^2} (1 + K_C/F_0^2) = \frac{\partial A}{\partial t} (1 + K_C/F_0^2)$$

or

$$D \frac{\partial^2 A}{\partial x^2} = \frac{\partial A}{\partial t} \quad (9.96)$$

This equation with the same boundary conditions was solved in Sec. 8.13 to give

$$\left(\frac{\partial \alpha}{\partial x} \right)_{x=0} = - \frac{1}{\sqrt{D\pi t}} \quad (9.97)$$

where $\alpha = (A - A_0)/(A_1 - A_0)$

Then

$$\left(\frac{\partial A}{\partial x}\right)_{x=0} = \frac{A_1 - A_0}{\sqrt{D\pi t}} \quad (9.98)$$

$$\text{Now, } N_A = -D \left(\frac{\partial A}{\partial x}\right)_{x=0} - D \left(\frac{\partial E}{\partial x}\right)_{x=0} \quad (9.99)$$

Combining eqs. (9.93), (9.98) and (9.99) gives

$$N_A = \sqrt{\frac{D}{\pi t}} (A_1 - A_0) (1 + K_c/F_0^2) \quad (9.100)$$

Eq. (8.164) gives

$$\phi_{inst} = \frac{N_A}{A_1 - A_0} \sqrt{\frac{\pi t}{D}} \quad (8.164)$$

whence

$$\phi_{inst} = 1 + K_c/F_0^2 \quad (9.101)$$

Integrating eq. (9.100) gives

$$\int_0^t N_A dt = 2 \sqrt{\frac{Dt}{\pi}} (A_1 - A_0) (1 + K_c/F_0^2) \quad (9.102)$$

From eq. (8.162)

$$\phi = \frac{\int_0^t N_A dt}{2 (A_1 - A_0)} \sqrt{\frac{\pi}{Dt}} \quad (8.162)$$

whence

$$\phi = 1 + K_c/F_0^2$$

Substituting eq. (9.89) then gives, for both instantaneous and average values

$$\phi = 1 + E_0/A_0 = C_0/A_0 \quad (9.103)$$

This is identical with the solution obtained by use of the film theory.

CHAPTER 10

Details of Apparatus and Procedure --

Short Wetted-Wall Column

In this chapter details of the short wetted-wall column, the auxiliary equipment, the procedure and of the analytical methods are presented. In connection with the description of apparatus and procedures for the carbon dioxide runs, the author has borrowed freely from the S.M. thesis of Lambe (63), who constructed the apparatus and made the first 78 of the 99 carbon dioxide runs.

10.1 Construction of Column Assembly. A photograph of the wetted-wall column assembly is shown in Fig. 10.1. The glass sections, two of which are shown in Fig. 10.2, were made by the glass blowing firm of Ryan, Velluto and Anderson. Six glass sections were made, one with an upflow slot and one with a downflow slot for each of the three wetted-wall lengths, 1/2 in., 1 in. and 1 1/2 in. The upper and lower edges of the outer glass cylinder were ground flat to form a seal against the rubber gaskets set in the Micarta plates. These were machined from a one-inch slab of Micarta (Grade No. 273), a laminated phenolic plastic manufactured by Westinghouse. A nipple, also machined from Micarta, was threaded into the lower plate to form an exit tube. Two machined brass plates with brass tie-rods connecting them served to clamp the assembly firmly together.

The top of the wetted-wall section itself, the inner glass cylinder, was ground to a 45° bevel, either up or down, as the case may be, by first grinding the surface plane with the base, and then grinding on the bevel. Three brass tools were machined for this purpose, one flat, one with a cone-shaped hollow, and one cone-shaped. The tools could be inserted into a chuck on a drill press, rotated at low speed, and, with a mixture of emery powder and kerosene as the grinding agent, accomplished the work quite rapidly.

The gas entrance and exit tubes were machined from Teflon (polytetrafluoroethylene resin, manufactured by the duPont Plastics Division) tubes. They were threaded with twenty threads per inch so that the slot widths could be easily adjusted. Two exit tubes were made, one with a bevel for the upflow slot and one with a bevel for the downflow slot. The inside of the inlet tube was recessed at the bottom to fit the one-inch glass tubing which formed the calming section.

The water layer formed a very smooth cylinder inside the column with no distortion at the ends. The actual length of the layer was determined by inserting a depth gage down from the top of the column. When the downflow slot was used, the length was taken as the distance from the lowest extremity

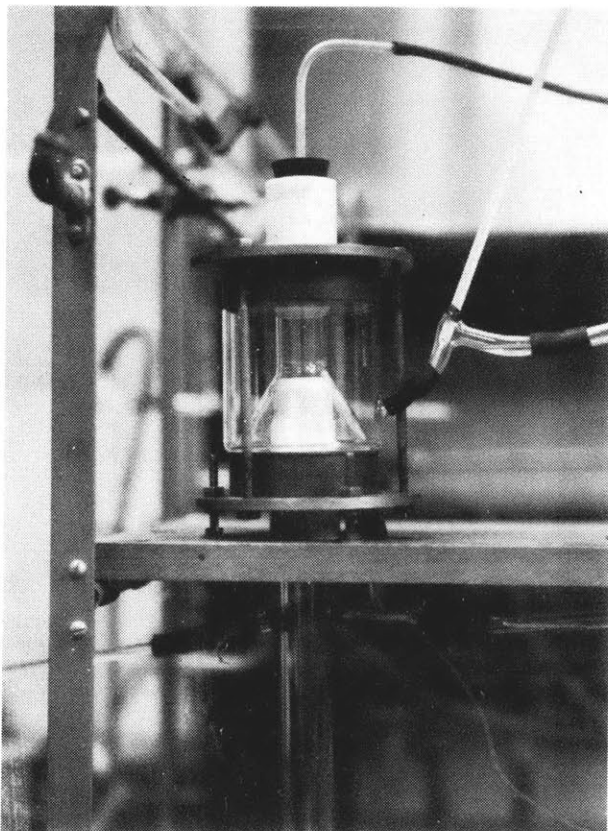


Fig. 10.1
 Assembly of Short
 Wetted-Wall Column

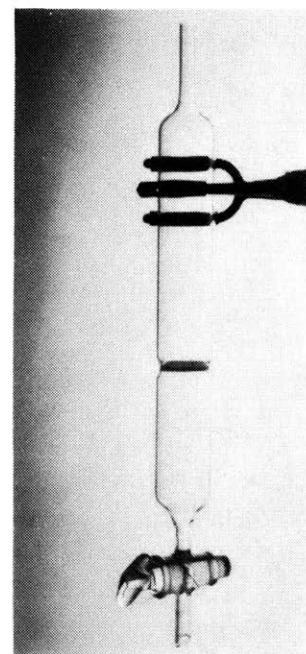


Fig. 10.3
 Cell Used to Measure
 Liquid Diffusivities
 (See Chapter 11)

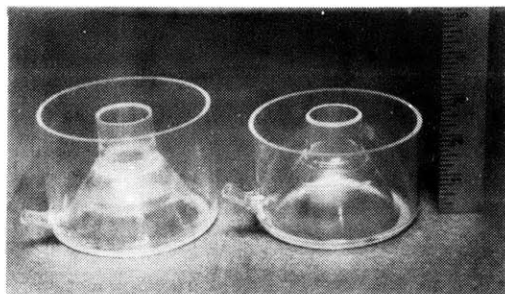


Fig. 10.2
 Glass Sections Used in Short
 Wetted-Wall Columns

of the upper teflon tube to the highest extremity of the lower teflon tube. When the upflow slot was used, it was found that the top of the water layer was always 0.14 cm. above the top extremity of the inner glass cylinder, independent of slot width and of liquid rate. Then the length of the air-water interface was taken as the distance from the top of inner glass cylinder to the top of the lower teflon tube plus 0.14 cm.

It was found that the water wetted the glass more easily if the glass section were boiled in a soap or detergent solution before being used. Chromic acid cleaning solution left a surface that was more difficult to wet than that left by the detergent solution.

When water was first put through the column to start a series of runs, bubbles of air would usually collect at the top of the entrance chamber just below the teflon tube. These could be removed by unscrewing the upper teflon piece so that the entrance slot was about $1/4$ inch and inserting a thin glass tube, bent 135° , through the slot and applying suction to the other end of the tube.

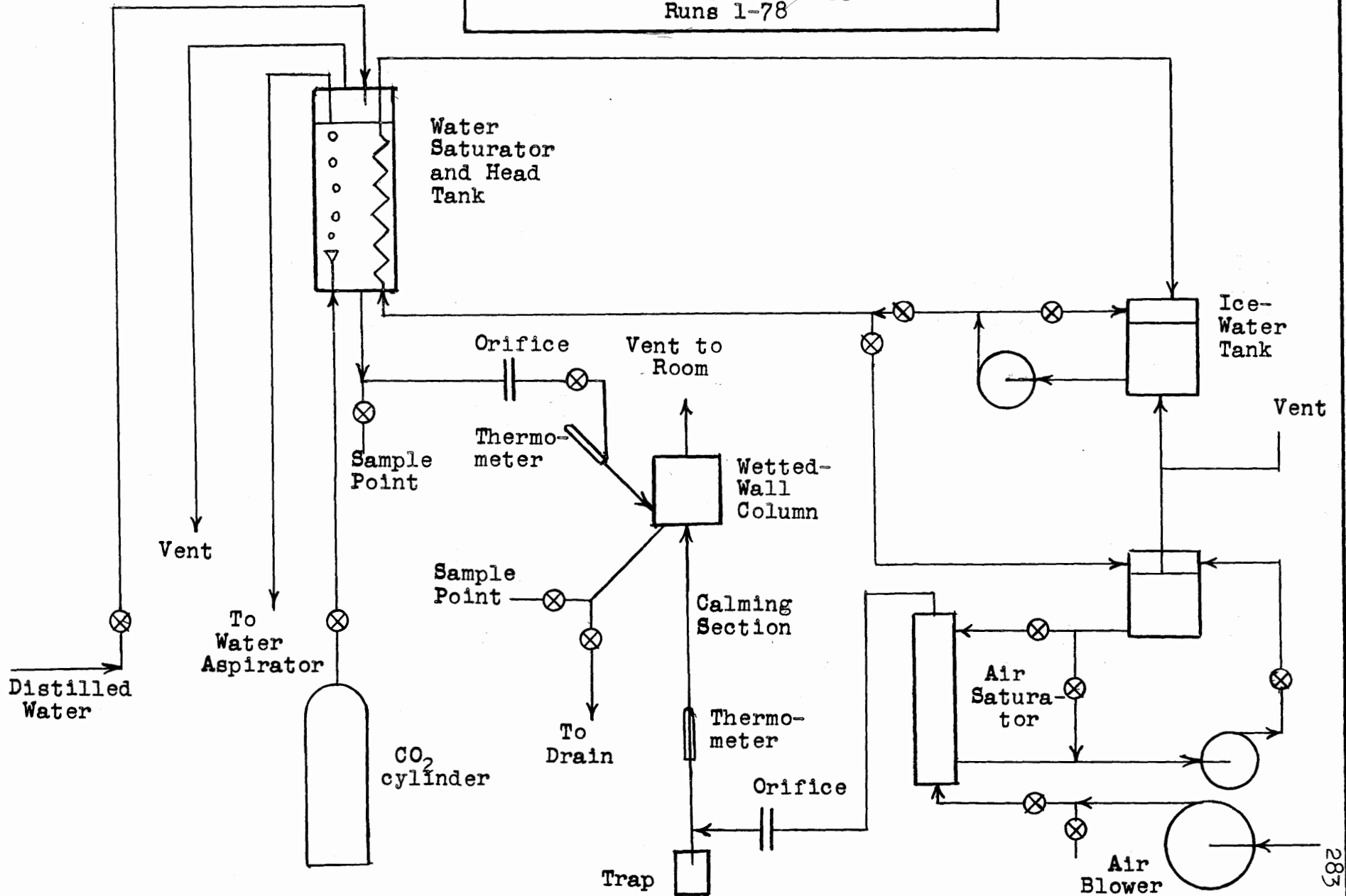
10.2 Auxiliary Apparatus for Carbon Dioxide-Water Runs.

A schematic diagram of the apparatus as used by Lambe is shown in Fig. 10.4. The air was blown into the system by a converted vacuum cleaner blower. A valve in the line and a by-pass valve were used to control the flow. The saturator tower was a four-inch glass tube packed to a depth of 21 inches with three-eighths inch Raschig rings. Water was gravity-fed to the top of the tower and flowed through, countercurrent to the air, into a sump beneath the tower. A centrifugal pump forced the water from the sump back to the reservoir. To prevent the liquid level in the sump from falling so low that air would be drawn back into the pump, a cork float valve was used. A by-pass valve from the reservoir to the inlet side of the pump helped to adjust the flow rate. If this by-pass valve were not slightly open, the cork float valve would not open ^{due} to the high pressure drop across the seat.

The water fed into the saturator was cooled by directly injecting ice-water into the reservoir. A tube leading from the reservoir back to the ice-water tank allowed the surplus water to escape.

The air was metered by a brass-plate orifice calibrated with a dry gas meter. The calibration of the meter was not checked since it was not necessary to know the air flow rate with any great accuracy. The temperature of the air was measured with a thermometer in the lower end of a forty-inch long piece of one-inch glass tubing which served as a calming section for the air entering the column. A one-liter flask placed at the bottom of this calming section was a trap for

Fig. 10.4
Schematic Diagram of Apparatus
Runs 1-78



any spill-over from the column. A sodium hydroxide solution was kept in the flask to prevent any carbon dioxide desorbed from the spill-over from entering the gas stream. The trap was emptied, when full, by applying suction with a water aspirator to an outlet tube provided.

Distilled water was fed into a head tank made of four-inch glass tube two feet long, mounted eight feet above the column. Carbon dioxide was bubbled through the liquid, twenty inches deep, from a commercial cylinder through a sintered glass bubbler (gas diffuser). A glass cooling coil through which ice water was circulated served to control the water temperature.

A constant head was maintained in the tank by connecting a glass tube projecting down from the top to a water aspirator. A gas vent led down from the top of the column to the hood.

A large metal can, about five gallons capacity, filled with cracked ice and water served as a reservoir for cooling water. A centrifugal pump provided with a by-pass and control valves served to force the water through the cooling system. All the cooling water was returned to the ice-water tank.

From the bottom of the head tank, the almost saturated liquid flowed through a brass-plate orifice connected to an inverted water manometer, through the column, and to a drain in the hood. Brass needle valves placed after the orifice and after the column allowed the flow rate and the liquid level in the outlet chamber of the column to be controlled.

Two orifice plates were used to cover the desired flow ranges. These were calibrated on distilled water using a graduated cylinder and a stopwatch.

Glass "tees" were inserted in the liquid line just before the orifice and just after the column to provide sample outlets. A 25 ml. pipet was connected to each outlet with a rubber tube and liquid was allowed to drain through them continuously at a rate about equal to six times the volume of the pipet per minute. To take a sample, the rubber tubes were shut off with a pinch clamp, the one on the exit line first, the pipets were removed and allowed to drain to the graduation mark.

The order in which the apparatus was started up was as follows:

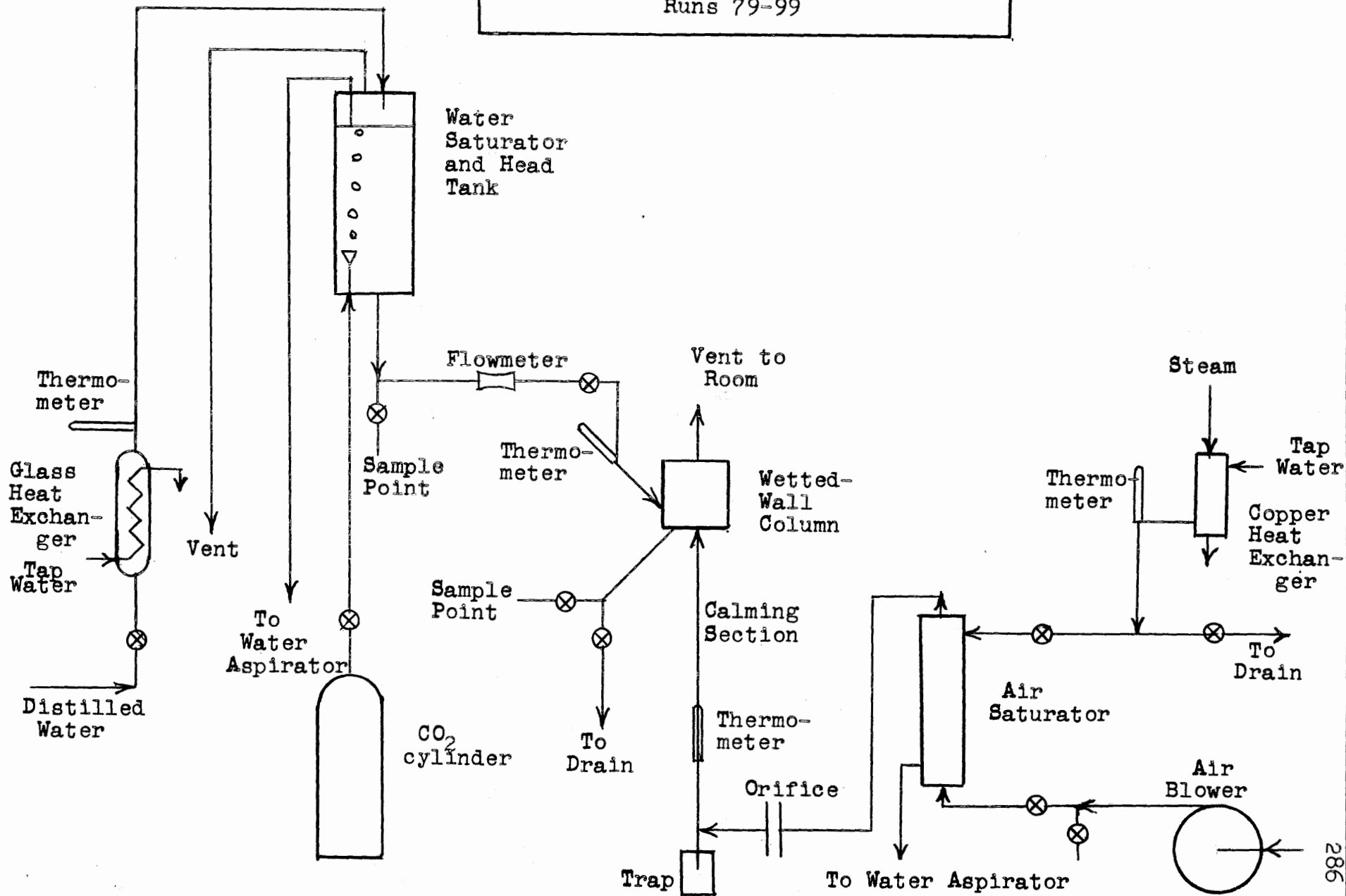
1. The head tank was filled up and the water aspirator was turned on. The gas cylinder valve was opened to admit carbon dioxide to the head tank.

2. The air blower was turned on and the rate adjusted to the desired value.
3. The cooling water pump was started and the valves controlling the flow to the air saturator reservoir and the head tank cooling coil opened.
4. The water was allowed to run into the saturator column by opening the valve half-way. The circulating pump was then started, the by-pass valve opened two or three turns and then the valve in the line leading from the pump back to the saturator reservoir opened about one-half turn. The by-pass valve was then adjusted until the water level in the sump remained constant.
5. Water was then admitted to the column at the desired rate and the flow of distilled water to the head tank was increased until two-phase flow in the line to the water aspirator was obtained. Slugging was to be avoided as it caused fluctuations in the manometer reading.
6. The liquid level in the exit chamber was adjusted by means of the valve in the exit line. At low liquid flow rates it was necessary to restrict the flow through the outlet sampling pipet with a pinchclamp. The exit line had to be kept running full, otherwise it was very difficult to control the level of the liquid in the column since it had a tendency to drift. The level in the exit chamber was kept such that the chamber was completely full and the water layer on the wetted wall ran smoothly into the exit chamber without spilling over into the gas inlet tube.
7. Any necessary corrections in valve settings were made and a minimum of five minutes was allowed for the apparatus to reach steady-state operation before any samples were taken.

The above description applies to the apparatus as used by Lambe for the first 78 runs. Several changes were made by the author before proceeding with the remaining carbon dioxide runs. The apparatus after these changes is pictured schematically in Fig. 10.5.

In the first place, it was decided that the system involving recirculation of the water to the air saturator was more complicated than necessary and required too much attention to keep the level in the sump pump constant, even with the cork float valve. This

Fig. 10.5
Schematic Diagram of Apparatus
Runs 79-99



set-up was replaced by one in which tap water was heated by steam in a copper heat exchanger to the desired temperature and then passed into the saturator. There it flowed counter-current to the air into the sump, from which it was removed by a line connected to a second water aspirator.

Secondly, the ice-water system was dispensed with. While ice-water was necessary for Lambe, who worked in the summer months when the tap water reached 27°C, it was possible during the remainder of the runs to rely on tap water for cooling since they were made during the fall and winter when the tap water was sufficiently cold. Also, it was found possible to control the temperature of the distilled water coming out of the tap by adjusting the water rate in the condenser at the still itself. This was set so that the water coming out of the tap was several degrees warmer than the temperature of the run. The distilled water was then cooled to the desired temperature by tap water in a glass heat exchanger (a distilling condenser with an inner coil).

10.3 Auxiliary Apparatus for Chlorine Runs. Some further changes were made in the apparatus when the solute gas was changed to chlorine. The brass orifice used to meter the liquid entering the column was changed to a glass flowmeter which was also calibrated on distilled water using a graduated cylinder and a stopwatch. In addition, the brass valve used to control the flow into the column was replaced by a combination of a piece of neoprene rubber tubing with a large hosecock. The brass valve was left on the liquid outlet line from the column, since corrosion at that point was immaterial, and the valve was considered expendable.

The water supply system to the air saturator was left unaltered, but the air inlet system was changed. The blower was removed, and suction was used at the gas exit to pull the air through. Also, the orifice was removed from the air line, and a glass flowmeter, calibrated with a dry gas meter, was placed in the gas exit line.

It might be well to note at this point that all the lines (except the air inlet) were constructed of glass connected with ordinary rubber tubing. The use of rubber is permissible with chlorine water since it becomes covered with a coating of "rubber chloride" which protects it from further attack.

The liquid feed system underwent considerable change. It was not found possible to obtain concentrations of chlorine in water lower than saturation which remained constant with time using the same apparatus as for carbon dioxide. This was remedied by the use of a second, smaller constant head tank which was made of a six-inch piece of 2 1/2 inch glass tubing. The first head tank was used to supply a constant flow of distilled water. Chlorine was metered by a Monel regulating

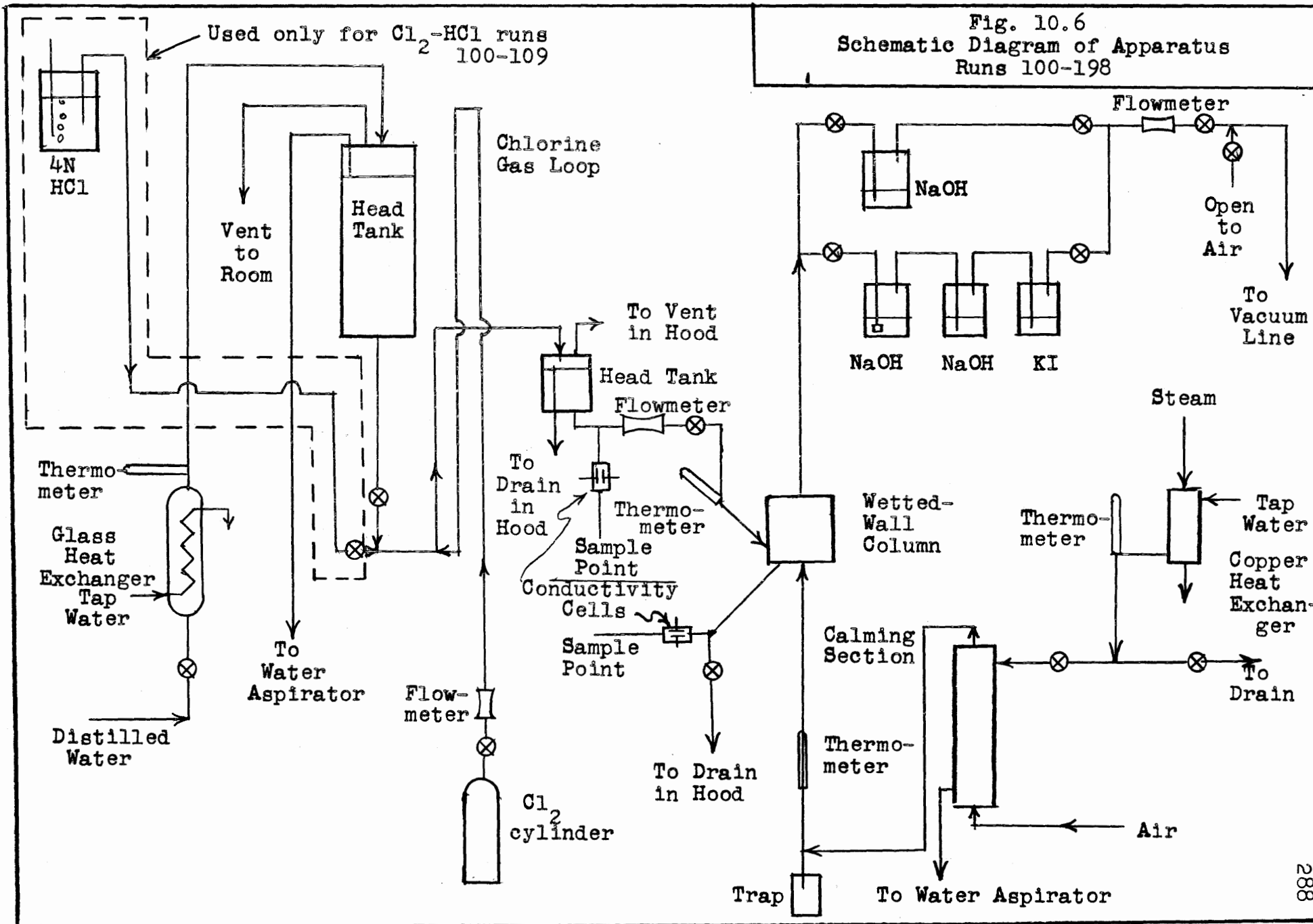


Fig. 10.6
Schematic Diagram of Apparatus
Runs 100-198

valve (obtained from the Matheson Company) through a small glass flowmeter, passed through a loop, the purpose of which was to prevent water from entering the gas inlet line, and then injected into the line carrying distilled water from the first to the second head tank. The chlorine was injected through a drawn out piece of glass tubing in order to form small bubbles. Glass beads were placed in the glass line leading from the point of injection to the second head tank in order to facilitate the solution of the gas. Any undissolved gas escaped from the second head tank by means of a vent line to the hood. Constant head was maintained in the second head tank by means of an overflow pipe which led to a drain in the hood.

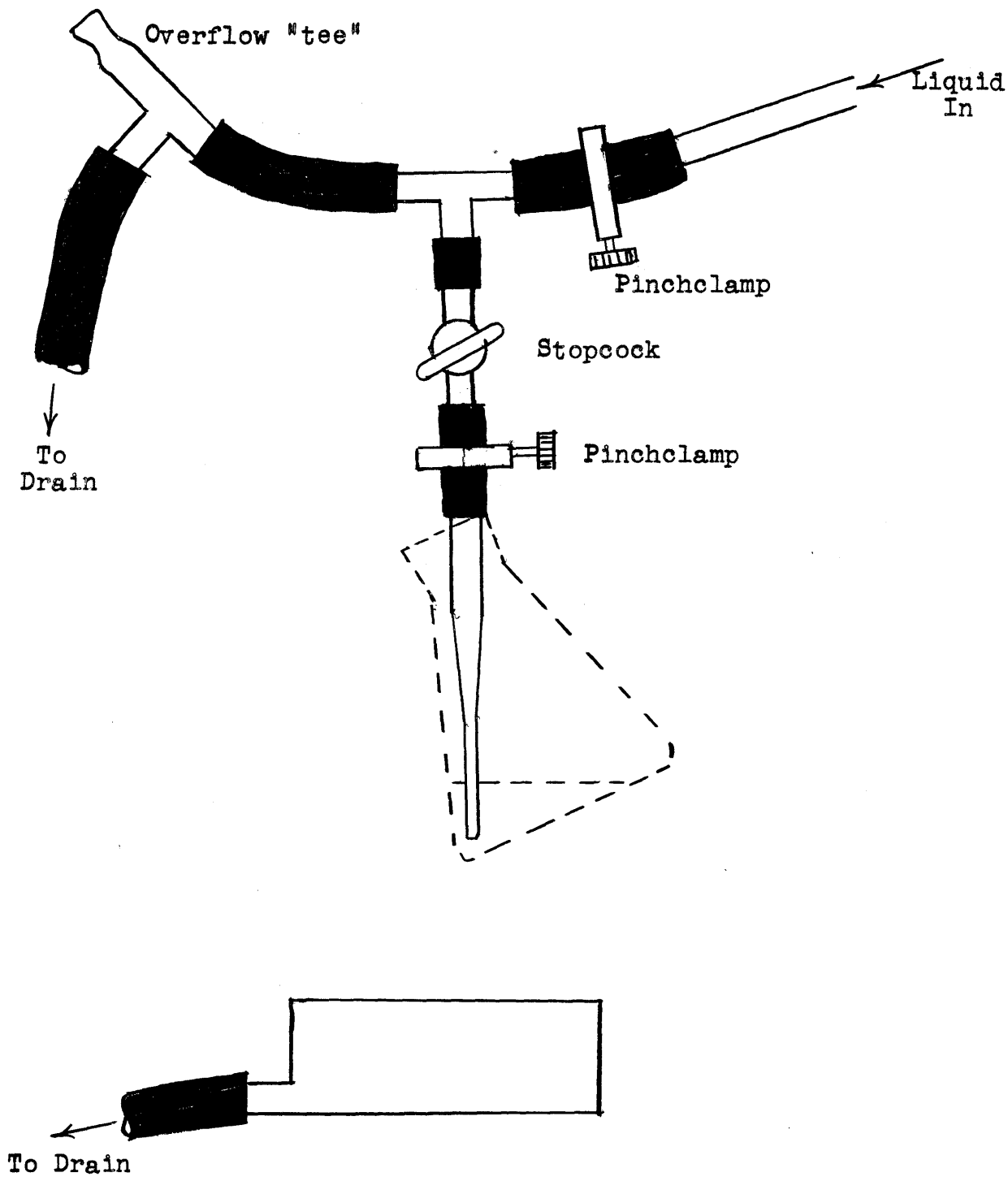
The solution of chlorine in water then passed through the glass flowmeter, through the rubber-tube valve, past the thermometer and into the column. From the column, it passed to a drain in the hood.

The sample points were located at the same positions as before, but the method of sampling was changed greatly. Glass tubes led from the sampling point to two sampling set-ups placed in the hood. One of these set-ups is shown in Fig. 10.7. Normally, the stopcock was open, and the pinch clamps adjusted to divide the flow between the nozzle and the overflow "tee." Just before a sample was taken, the stopcock was closed, the titration flask placed in position so that the nozzle was beneath the surface of the liquid in the flask, and the stopcock was opened. When enough of a sample was taken, the stopcock was closed, the flask withdrawn and stoppered, and the stopcock opened once more. This arrangement had the advantage of not having any desorption occurring from the sample, and the purpose of the overflow "tee" was to prevent the opening and closing of the stopcock from disturbing the flow rates in the apparatus itself. The size of the sample was determined by weighing the flask before and after sampling.

For the purpose of control, that is, to see if the concentrations in the inlet and outlet liquid streams were constant with time, conductivity cells were inserted into sample lines, and the resistance measured periodically on a conductivity bridge.

A further change was the use of an absorption train on the exit gas line. Between runs, the gas coming from the column was passed through a single bottle containing sodium hydroxide solution, thence through the flowmeter and into the laboratory vacuum line. When the concentrations were steady, a run would be started by rapidly switching the gas flow to the absorption train of three bottles in series. In the first bottle, the gas would bubble through a diffuser tube into sodium hydroxide solution; in the second bottle through a piece of drawn-out glass tubing into sodium hydroxide solution; in the third bottle

Fig. 10.7
Diagram of Chlorine-Water Sampling Apparatus



through a piece of drawn-out glass tubing into potassium iodide solution. At the end of the run, a definite period of time ranging from ten to twenty-five minutes, the gas flow would be shut off from the absorption train and shunted through the single bottle again. The liquid sample or samples were taken when the runs were about half over.

All the bottles through which the gas passed were 32 oz. bottles. The single bottle contained about 350 ml. of about 2N NaOH. The first bottle of the absorption train contained about 350 ml of approximately 0.5 N NaOH, while the second bottle, used to collect any chlorine not absorbed in the first bottle, contained about 150 ml of the 0.5N NaOH. The final bottle of the train, used to make sure all the chlorine was collected, contained about 350 ml. of water with a few grams of KI. After each run was over, the contents of the second bottle of the absorption train were poured into the first bottle, and rinsed two times, the rinsings being added to the first bottle. This first bottle was then set aside for analysis. The third bottle of KI was used for all the runs made during a series, usually eight to ten runs, and then titrated for iodine at the end of the series. The amount of chlorine collected in this third bottle was never greater than 0.2% of the total chlorine desorbed, and for most of the runs was less than 0.04%.

The preceding changes were made for the chlorine-water runs. In addition, for the chlorine-0.2N HCl runs, provision was made for the continuous addition of strong hydrochloric acid to the distilled water. This was done by having approximately 4N HCl flow from a constant head bottle (located higher than the distilled water constant head tank) into the line carrying distilled water. It was found that the resistance of the conductivity cells depended only on the HCl concentration and were independent of the Cl₂ concentration, so for these runs the conductivity cells were used to check the constancy of the concentration of HCl.

10.4 Analytical Procedure for Carbon Dioxide-Water Runs.

The general scheme of the analytical method used to analyze the samples for carbon dioxide was to add the sample to a known amount of barium hydroxide, then, by measuring the conductance of the solution, determining the amount of hydroxide left. The difference between the initial and final amounts of barium hydroxide was equivalent to the carbon dioxide in the sample.

Since the percent desorption of carbon dioxide is relatively small, and the difference between the inlet and outlet concentrations was desired, it was necessary to adjust the barium hydroxide concentration so that the sample of the inlet stream precipitated nearly all of the barium as carbonate. Then, since the conductivity is roughly proportional to the concentration

of $\text{Ba}(\text{OH})_2$ and the resistance can be measured to 1%, the difference between the two concentrations could be determined to about 2%. Since the conductivity of a saturated solution of barium carbonate is negligible, it did not interfere with the analysis. It was found that a 25 ml. sample added to 50 ml. of barium hydroxide gave satisfactory concentrations when the column was operating at 25°C and the barium hydroxide was 0.031 normal. For lower temperatures a stronger solution was needed so that a slight surplus of hydroxyl ion was assured. Conversely, for higher temperatures a weaker solution was needed so that the excess hydroxyl ion concentration would not be too high. These values can be calculated by assuming 90% saturation in the saturator. A blank of 25 ml. of boiled distilled water plus 50 ml. of barium hydroxide was used with each series of samples to determine the initial barium hydroxide concentration.

The conductivity bridge used to measure the conductivity was an alternating current impedance bridge with a self-contained 1000 cycle oscillator, manufactured by Industrial Instruments, Inc., Model RC-1B. The bridge was designed to measure resistances of 2 to 250,000 ohms with an error of less than one percent. It was checked with a standard Leeds and Northrup decade box and found to be satisfactory except in the vicinity of the 100 ohm point on the dial. By a suitable choice of multipliers this region could be avoided and caused no difficulty.

The electrodes used were made from platinum foil, each being 15 mm. by 7 mm., 0.25 mm. thick and mounted 8 mm. apart. They were spot-welded to 0.15 mm. platinum wire leads fused into glass tubes. The tubes were held rigid by glass spacers and mounted in a rubber stopper so they could be inserted into the sample bottle. A drop of mercury at the bottom of the tubes provided contact with the leads from the bridge circuit.

A deposit of platinum black was placed on the electrodes, to make them more reversible, in the following manner: They were cleansed in a hot solution of sodium hydroxide, washed, then electroplated in a 3% solution of chloroplatinic acid to which 0.025% of lead acetate had been added. The potential used was four volts, and the polarity was changed frequently to avoid excessive adsorption of chlorine on the platinum black. A satisfactory deposit was obtained in about 10 minutes. The electrodes were then used to electrolyze a dilute solution of sulfuric acid, the potential being changed frequently, to remove the residual chlorine. They were kept in distilled water when not in use to avoid contamination.

The cell constant was determined with a known strength solution of potassium chloride and checked with a standardized solution of hydrochloric acid. The I.C.T. values (47) for the conductivity of barium hydroxide solutions were checked by using the cell constant and diluted samples of standardized barium hydroxide.

Four ounce glass bottles were used for the samples. A number of them were prepared before each run by flushing them with carbon dioxide-free air obtained by passing air from the laboratory through a tube filled with soda lime (for runs 79-99, water pumped prepurified nitrogen from a cylinder was used), and adding 50 ml. of barium hydroxide to each, then stoppering tightly with rubber stoppers. When the samples were taken, the tip of the pipet was placed below the surface of the liquid in the bottle and the contents allowed to drain while filling the pipet with carbon dioxide-free air (or nitrogen). The last drop was blown from the tip with the air (or nitrogen) to sweep any carbon dioxide desorbed in the pipet into the solution of barium hydroxide. The bottles were then stoppered, shaken and allowed to remain in a thermostat bath at 25°C for about four hours until the precipitate had settled before measuring the resistance of the supernatant liquid.

10.5 Analytical Procedure for Chlorine Runs. All the titration flasks used to analyze the liquid samples taken during a series of eight to ten runs were prepared before the series was started. In each 250 ml. glass-stoppered flask were placed about 40 ml. of distilled water, 2 ml. of a strong solution of potassium iodide (50 g. KI per 100 ml.) and 1/2 ml. of glacial acetic acid. Each flask was then weighed. After the sample was taken, the flask was weighed again, and the contents were titrated for iodine with standardized, approximately 0.05N, sodium thiosulfate solution, starch indicator solution being added just before the end-point. The sodium thiosulfate was standardized by titrating weighed samples of potassium iodate according to the procedure outlined by Willard and Furman ().

The purpose of the acetic acid was to ensure that the solution was acid during titration. For the samples of chlorine in dilute hydrochloric acid, the addition of acetic acid was omitted, since the solution was already acid. However, it was then necessary that the titration be performed within several hours after the sampling in order that the oxidation of hydriodic acid, which is very easily oxidized by air, be not excessive.

The solutions of sodium hydroxide in which chlorine was absorbed were analyzed for chlorine as follows. If the amount of chlorine was equivalent to less than 60 or 70 ml. of thiosulfate solution, the solution was titrated right in the 32 oz. bottle. Otherwise, the contents of the bottle were quantitatively transferred to a one-liter volumetric flask, diluted to one liter, and two separate aliquot portions were transferred to titration flasks. In either case, 2 ml. of KI solution (50 g. KI per 100 ml.) was added to the titration solution. Then the solution was acidified by the addition of 2N sulfuric acid. One could tell when the solution became acid by the appearance of the characteristic dark brown color of the iodine. Some excess of acid was added. Then the solution was titrated with the standardized sodium thiosulfate, with addition of starch indicator solution just before the end-point.

10.6 Sources of Water and of Gases Used. The distilled water was obtained from the tap located in the laboratory. Its specific conductance was found to be about $3 \times 10^{-6} \text{ ohm}^{-1} \text{ cm.}^{-1}$.

The carbon dioxide was obtained from commercial cylinders supplied by the Carbonic Corporation. Chlorine was obtained from #4 cylinders supplied by the Matheson Company. The nitrogen was supplied by the Airco Corporation. The sulfur dioxide used in the diffusivity studies was obtained from the Virginia Smelting Company.

CHAPTER 11
MEASUREMENT OF DIFFUSIVITIES IN LIQUIDS

Outline

	<u>Page</u>
A. Introduction: 11.1	297
B. Methods of Measuring Diffusivities in Liquids 11.2	297
C. Previous Measurements of Diffusivities of Various Substances in Water	302
11.3 Potassium Chloride	302
11.4 Hydrochloric Acid	303
11.5 Chlorine	305
11.6 Sulfur Dioxide	305
11.7 Oxygen	306
11.8 Carbon Dioxide	307
D. Apparatus and Procedure	307
11.9 Description of Diaphragm Cell and Thermostat Bath	307
11.10 Cleaning Procedure	309
11.11 Loading Procedure	309
11.12 Sampling Procedure	310
11.13 Analysis of Potassium Chloride	311
11.14 Analysis of Chlorine in Water	311
11.15 Analysis of Chlorine in Dilute Hydrochloric Acid	312
11.16 Analysis of Sulfur Dioxide	312
11.17 Sources of Water and Gases Used	313
E. Equations	313
11.18 Constant Diffusivity; No Chemical Reaction	314
11.19 Diffusivity a Function of Concentration; No Chemical Reaction	315
11.20 Diffusion of Chlorine Through Water	317
11.21 Diffusion of Sulfur Dioxide Through Water	322
11.22 Volume of Pores of Diaphragm	326
F. Results and Discussion	326
11.23 Calibration of Cells	326
11.24 Diffusion of Chlorine Through Dilute Hydro- chloric Acid	329
11.25 Diffusion of Chlorine Through Water at 25°C.	332
11.26 Effect of Temperature on Diffusion of Chlorine Through Water	336
11.27 Diffusion of Sulfur Dioxide Through Dilute Sulfuric Acid	339

	<u>Page</u>
11.28 Diffusion of Sulfur Dioxide Through Water at 30°C.	342
11.29 Effect of Temperature on Diffusion of Sulfur Dioxide in Water	345
11.30 Miscellaneous Measurements	348
11.31 Sources of Error	348
G. Conclusions and Recommendations: 11.32	353

A. Introduction

11.1. In order to understand the mechanism of the liquid-side resistance to mass transfer, and to be able to predict mass transfer rates for new systems on which little or no mass transfer data have been obtained, accurate values of the liquid diffusivities of the various substances involved are required. For the purposes of this thesis, it is necessary to know the diffusivity in water of the following substances: chlorine, hypochlorous acid, hydrochloric acid, sulfur dioxide, sulfurous acid, carbon dioxide and oxygen. Since most of this information is not available in the literature, or conflicting values are reported, an experimental program of measuring liquid diffusivities was undertaken. In this chapter, the methods used by previous workers to measure liquid diffusivities are reviewed and the results they obtained which are of interest to this thesis are tabulated. The procedure used in this investigation to study the diffusion of dissolved gases in water is then described and the results obtained are presented.

B. Methods of Measuring Diffusivities in Liquids

11.2. Diffusion experiments may be classified into three general types: free diffusion, restricted diffusion and steady-state diffusion. Free diffusion refers to diffusion from an initially sharp boundary between two liquid layers of different concentrations, or from an interface between liquid and gas, in an apparatus in which the concentrations at some finite distance from the initial boundary or interface remain unchanged. It is exemplified by an experiment in which pure gas is brought in contact with a column of liquid which is sufficiently long that the concentration at the end of the liquid column away from the interface remains constant for the duration of the experiment. In restricted diffusion, the experiment is allowed to proceed long enough that concentrations will change continuously in all parts of the liquid. Both free and restricted diffusion are unsteady-state experiments. In steady-state diffusion, the concentrations at both ends of a column of liquid are maintained constant; the experiment is allowed to proceed until there is no change in concentration with time within the column, and the rate of transfer is measured.

Because of the slow nature of diffusion in liquids, it is imperative that convection currents be eliminated completely. There have been four general methods of accomplishing this. The first is to conduct the experiment in capillary tubes of diameter sufficiently small that convection currents are prevented. Carlson (9) gives the following review of this method:

"..... Wroblewski (1877) was the first to attempt to ascertain the law in accordance with which CO_2 diffuses in water. His attempt failed because, when he allowed the gas to enter at the top of a column of water, the upper layers were first saturated with it and, hence, became heavier and sank, thus causing turbulence. Soon afterwards, Stefan proved that these currents depend on the width of the test-pipe, and might be entirely prevented if the cross-section of the pipe were made small enough, at most 1 mm. Stefan's experiments were of two kinds; in one, carbonic acid was made to traverse a column of fluid made as long as possible, and assumed to be infinitely long, while in the other the gas had access to the open air through a short column of water. It is evident, however, when experimenting with a gas whose coefficient of absorption [solubility] is relatively small, as oxygen in water, Stefan's method is not very suitable. In order to obtain an accurately measurable diminution in volume of gas, too long a time is necessary, and even supposing the temperature could be kept constant, considerable disturbances are inevitable, due to evaporation of fluid."

Since Stefan's time, only one investigator has used the capillary method. Ringbom (87) used an improved form of apparatus designed to overcome some of the disadvantages and sources of error of Stefan's method. The capillary method suffers the disadvantage that the area of the interface is uncertain.

The second method of avoiding turbulence is to "solidify" the liquid by dissolving some gelatin or agar-agar. This method has several disadvantages: it is restricted to gases which do not react with the solidifying agent; it cannot be used at high temperatures or with organic solvents; the diffusion rates are slower

than for pure water and must be corrected to give the diffusivity in water. The possibility exists that the correction is not the same for all gases.

The third method of preventing convection currents is the layer method, which utilizes the stabilizing influence of gravity. The experiment is arranged so that the heavier solution lies at the bottom and diffusion occurs upward. Because of the slight change in density of the solution with concentration of dissolved gas, this method is not suitable for measuring the diffusivity of gases in liquids. Carlson (9) is the only investigator to report using this method on dissolved gas. He got around the difficulty just mentioned by adding 1% potassium chloride to the liquid originally containing the dissolved gas and forming the lower layer, while the upper layer placed above it originally consisted of pure water. Thus, he achieved the density gradient by the addition of potassium chloride, but at the expense of having simultaneous diffusion of both the gas and the salt, which may have affected the diffusion rate of the gas.

The layer method has been extensively employed to study the diffusion of electrolytes and of macromolecules, using both free diffusion and restricted diffusion. Harned (32) has written an excellent review of this method, and of the diaphragm-cell method described below, as well as of the theory of diffusion of electrolytes. In the diffusion of macromolecules, using the layer method, optical methods have been used with great success. It is possible, by measuring the absorption of light by the solution at various heights, or by measuring the index of refraction at various heights using interferometric or "schlieren scanning" techniques, to determine both the concentration and the concentration gradient as a function of height and of time. The method yields sufficient information to calculate diffusivity as a function of concentration. According to Harned (32), "with

the exception of Clark's researches, very few accurate diffusion coefficients of electrolytes have been determined by optical means. On the other hand, these procedures can be carried out in a short time as compared with that usually required for the study of the slow process of diffusion and for this reason may prove important in future studies." In the study of the diffusion of electrolytes by the layer method, electromotive-force measurements and conductance measurements, as well as direct analysis of the layers, have been applied. By using a method involving the measurement of electrical resistance at the top and bottom of a carefully designed vertical cell, Harned and Nuttall (34, 35) have determined the diffusion coefficient of potassium chloride in water with an accuracy of the order of 0.1 per cent, an accuracy probably unparalleled in this field.

The disadvantages of the layer method lie in the elaborate precautions required to avoid mechanical vibrations, temperature fluctuations and to avoid mixing when the two layers are placed one on top of the other.

The fourth method of avoiding convection (and the one used in this investigation) is to cause the diffusion to take place within the pores of a sintered-glass or an alundum diaphragm. When the volume of solution on either side of the diaphragm is sufficiently large, and is stirred to keep the concentration uniform, the conditions within the diaphragm, for all practical purposes, are steady state. Since the area or the length of the diffusion path cannot be determined by direct measurement, it is necessary that each cell be calibrated, using a solute of known diffusivity. Potassium chloride has almost always been chosen for this purpose; with the new, accurate data on diffusivity of potassium chloride as a function of concentration obtained by Harned and Nuttall (34, 35), it provides an excellent standard for the calibration of diaphragm cells.

The first reported use of the diaphragm cell was by Northrup and Anson (80), who used it to measure the diffusivity of carbon monoxide hemoglobin. No use of this method for measuring the diffusivity of dissolved gases has been reported, but it has found considerable use in studying the diffusion of electrolytes and macromolecules. Quoting further from Harned's review (32):

"The use of sintered-glass diaphragm cells for measuring diffusion coefficients has been shown by McBain (67) and especially by Gordon (14, 29) and Hartley and Runnicles (36) to be convenient and accurate. Since the diffusion process is slow,

measurements in vessels without diaphragms are most sensitive to any factors which, like local gradients of temperatures or initial stirring, may cause convection. In the diaphragm cell, the diffusion is confined to the pores of a sintered-glass or an alundum diaphragm, so that the errors caused by agitation by thermal or mechanical means are reduced to a minimum.

"The apparatus used by McBain and Liu (68) and Gordon (14, 29) consisted of a bell-shaped vessel with a stopcock at the top and a flat diaphragm of sintered glass at the bottom. This (inner) vessel is filled with the more concentrated solution and is suspended in such a way that the diaphragm just touches the surface of a weaker (outer) solution. The diaphragm must be adjusted horizontally and must be in contact with the outer solution over its entire surface. The whole apparatus is placed in an air thermostat. In this form of apparatus, only density stirring can take place.

"Mouquin and Cathcart (77) have described a glass cell containing a sintered-glass diaphragm at the middle, which was stirred by rotating end over end. Hartley and Runnicles (36) obtained stirring by rotation of their cell about its axis at an angle inclined to the vertical. The upper solution was stirred by a glass sphere resting on the diaphragm, and the lower solution by a lighter [i.e., lighter than the solution] glass sphere which pressed against the bottom surface of the diaphragm. The concentration in the inner compartment of the apparatus was measured by conductance."

The use of moving glass spheres to stir the contents of the compartment has the disadvantages of causing mechanical vibrations to occur within the diaphragm, and of causing the diaphragm to wear away, thus necessitating recalibration after every few runs. Stokes (96) also used mechanical stirring, using glass rods which were turned magnetically from outside the cell.

Density-stirring may be brought about by placing the heavy solution in the upper compartment and the light solution in the bottom. The process of diffusion causes a density unbalance in both compartments and thus brings about convection which tends to keep the concentration in them uniform. Gordon (29) has shown that the density-

stirred method yields results which agree with those obtained by mechanical stirring. Stokes (96), however, in measuring the diffusivity of hydrochloric acid in water has found that density stirring gave values several percent lower than did magnetic stirring. He claims that, with density stirring, there exists a stagnant film at both sides of the diaphragm which exerts different effects on different solutes.

The question arises as to whether the pores of the diaphragm are small enough to prevent completely convection and bulk transfer of the solute within the pores. Stokes (96), using magnetic stirring, ran two sets of experiments, one with the heavy solution on top, and one with the light solution on top and found no difference. Hartley and Runnicles (36) used two grades of diaphragms and found that with the fine diaphragm, above a certain stirring rate, increasing the rate had no effect; while for the coarser diaphragm, the rate had a big effect at the high speeds, indicating that some bulk transport was occurring under those conditions. Dawson (20) suggested a simple test to determine whether a diaphragm is coarse enough to permit bulk motion, namely, to run several experiments with the cell tilted at an angle such as 30° . If the pores are too coarse, he says, the transfer may be increased by as much as four-fold, in which case finer diaphragms should be used. In this investigation, several runs were made with the cells tilted about 30° , and the results were found to be consistent with the runs carried out in the vertical position.

C. Previous Measurements of Diffusivities of Various Substances in Water

In this section, values of diffusivities found by previous workers, which are of interest to this thesis, are tabulated.

11.3. Potassium Chloride. Values of the diffusivities of potassium chloride in water at 25°C . for various concentrations are required, since potassium chloride at that temperature was employed to calibrate the diaphragm cells used in this investigation. The most accurate data are those of Harned and Nuttall (34, 35), who obtained them by using a layer method with restricted diffusion and measuring the concentrations continually by means of conductivities.

Table 11.1

Diffusivity of Potassium Chloride in Water at 25°C.

Data of Harned and Nuttall (34, 35)

<u>Concn. moles/l.</u>	<u>D x 10⁵, cm.²/sec.</u>
0.00000	(1.9958) (calc'd. from theory)
.00125	1.961
.00194	1.954
.00325	1.943
.00585	1.931
.00704	1.924
.00980	1.918
.01261	1.908
.02654	1.879
.03992	1.877
.04620	1.872
.05450	1.860
.06074	1.856
.1298	1.838
.3323	1.842
.5276	1.852

11.4. Hydrochloric Acid. It is desirable to know the diffusivity of hydrochloric acid in water because it is one of the components present in the chlorine-water system. Two of the most recent and probably most reliable determinations of the diffusivity at various temperatures and concentrations are presented here.

James and Gordon (49, 50) measured the rate of diffusion by hydrochloric acid by using a diaphragm cell and analyzing the solutions by means of an interferometer. As will be pointed out later, when the diffusivity is a function of concentration, the diaphragm cell yields an average value of the diffusivity. Gordon (30) showed that this average value is a close approximation to the actual diffusivity at a concentration equal to the arithmetic average of the concentrations in the upper and lower compartments. James and Gordon used this rule, and from the smoothed data, calculated the following table.

Table 11.2

Diffusivity of Hydrochloric Acid in Water

Data of James and Gordon (49)

	$D \times 10^5$, cm. ² /sec.			
<u>Temperature:</u>	10°C.	15°C.	25°C.	35°C.
<u>Concn., moles/l.</u>				
0	2.16	2.48	3.14	3.87
0.02	2.05	2.35	2.97	3.66
0.05	2.02	2.33	2.93	3.61
0.10	2.03	2.33	2.92	3.60
0.20	2.05	2.35	2.98	3.65
0.35	2.11	2.40	3.06	3.77
0.50		2.45	3.18	
0.75		2.56	3.37	
1.00		2.68	3.58	

Falinski (24) carried out his measurements using the layer method, with restricted diffusion. As pointed out by Harned (32), methods such as these also yield an average, or integrated, value of the diffusivity, but it is very difficult to compare such results with the average values obtained by the diaphragm cell method.

Table 11.3

Average Diffusivity of Hydrochloric Acid in Water at 16°C.

Data of Falinski (24)

						D x 10 ⁵ , cm. ² /sec.	
HCl	0.01	N	diffusing	into	water	2.60	----
HCl	0.1	N	"	"	"	2.53	2.50
HCl	0.5	N	"	"	"	2.52	2.48
HCl	1	N	"	"	"	2.55	2.51
HCl	2	N	"	"	"	2.66	2.60
HCl	1	N	diffusing	into	HCl 0.5 N	2.77	----
HCl	1.5	N	"	"	HCl 1 N	2.97	----
HCl	2	N	"	"	HCl 1.5 N	3.32	3.17
HCl	5	N	"	"	HCl 4.5 N	4.9	----

In addition, Falinski (25) measured the effect of temperature between 9° and 18°C., and found the diffusivity to be linear with temperature in that range, with dD/dt equal to 0.060×10^{-5} cm.²/(sec.)(°C.) .

11.5. Chlorine. Only two measurements on the diffusion of chlorine in water have been reported. Euler (23), using a layer method, found the diffusivity of 0.1 molar chlorine diffusing into water to be 1.4×10^5 cm.²/day at 12°C. Hufner (42), using the capillary method, with free diffusion and carried out in the dark, obtained a value of 1.27 at 16.3°C. Since diffusivity of gases in liquids have all been noted to increase with temperature, it is clear that both these values cannot be correct. It is the opinion of the editor of the International Critical Tables (46) that Hufner's value is probably too low. It is to be noted that neither of these authors considered the effect of the hydrolysis of the chlorine.

11.6. Sulfur Dioxide. No direct measurements of the rate of diffusion of sulfur dioxide have been reported in the literature. There is one indirect measurement, however, which was reported by Kolthoff and Miller (58). They carried out an electrolytic reduction of sulfur dioxide at a dropping mercury electrode, and found that the diffusion current was proportional to the SO₂ con-

centration. From this diffusion current, they calculated that sulfur dioxide has a diffusivity at 25°C. of 2.04×10^{-5} cm.²/sec.

11.7. Oxygen. Kolthoff and Miller (57) also reported experiments in which they electrolytically reduced oxygen at a dropping mercury electrode. They calculated from the shape of the current versus voltage curve that the diffusivity of dissolved oxygen at 25°C., is 2.6×10^{-5} cm.²/sec.

Another indirectly measured value was reported by Semerano, Riccoboni and Foffani (90), who measured diffusion currents as a function of concentration and calculated the diffusivity of oxygen to be $1.87 \pm .02 \times 10^{-5}$ cm.²/sec. at 25°C.

Directly measured rates of diffusion have been made by Hufner (42, 43), Carlson (9), and Tammann and Jessen (97). According to Tammann and Jessen (97), Hufner used a steady-state method in which oxygen was diffused upward through a hydrophane plate, through a column of water located in a glass tube, and into the atmosphere. Carlson used the layer method, adding 1% potassium chloride to the liquid originally containing the dissolved gas. As pointed out above, this gives rise to simultaneous diffusion of both the KCl and the oxygen. Tammann and Jessen had free diffusion of oxygen into an agar solution. The results are tabulated below:

Table 11.4

Diffusivity of Oxygen in Water

<u>Investigator</u>	<u>Temp. °C.</u>	<u>D x 10⁵, cm.²/sec.</u>
Hufner (43)	16	1.87
Carlson (9)	18.2 ± 0.2	1.97
	"	2.02
	"	1.98
	Average	1.99
Tammann and Jessen (97)	1.0	1.23
	10.0	1.82
	17.5	2.45
	25.0	3.54

11.8. Carbon Dioxide. Hufner, Carlson, and Tammann and Jessen measured the rate of diffusion of carbon dioxide in water in the same manner as for oxygen. Hufner (42) and Arnold (3) refer to two values obtained by Stefan by the use of the capillary method. In addition, Ringbom (87) has measured the diffusivity of carbon dioxide by an improved capillary method. The results are tabulated below:

Table 11.5

Diffusivity of Carbon Dioxide in Water

<u>Investigator</u>	<u>Temp. °C.</u>	<u>D x 10⁵, cm.²/sec.</u>
Stefan (42, 3)	17	1.63
	"	1.57
Hufner (42) " (3)	16	1.59
	10.3	1.46
	15.2	1.60
	20.4	1.78
Carlson (9)	18.2	1.70
	"	1.72
	"	1.69
	Average	1.71
Ringbom (87)	25	1.82
	30	2.08
	40	2.75
	50	3.26

D. Apparatus and Procedure

11.9. Description of Diaphragm Cell and Thermostat Bath. The diaphragm cell method was chosen for this investigation because of its simplicity, and because there were six diaphragm cells available which had been used by Chang (11) in a previous thesis for the determination of the diffusivities of benzoic acid and cinnamic acid in water. It was felt that density stirring would be satisfactory; that the accuracy required would not warrant the comparative complexity which would be involved in any mechanical stirring system.

One of the cells is pictured in Fig. 10.3. Each cell was constructed from a Pyrex sealing tube with a fritted glass plate sealed in its center. One end of the sealing tube was reduced and joined to a pyrex stopcock,

the other end joined to a short length of 35 mm. Pyrex tubing which was reduced and joined to another short length of 10 mm. Pyrex tubing. The six cells were labeled A, B, C, D, E and F. According to Chang (11), cells A, B and C had diaphragms made of medium grade (Designation: Pyrex M) fritted glass, while cells D, E and F had diaphragms made of fine grade (Pyrex F) fritted glass. Laboratory glassware catalogs give the nominal maximum pore size of Pyrex M as 14 microns and that of Pyrex F as 5 microns. These diaphragms may be compared with those of previous workers, most of whom used fritted glass disks obtained from the Jena glass works and designated with porosities G3 and G4. According to Erday-Gruz and coworkers (22), the diameter of the largest pores of diaphragms of type G4 is 9-10 microns, while those of type G3 contain pores with a maximum diameter of 18-20 microns. Gordon (29) states that type G4 have pore diameters 2-5 microns, and type G3 have pore diameters 15-20 microns. Dawson (30), who recommended testing cells for whether the pores were coarse enough to permit bulk motion by tilting the cells 30° and comparing the results with those obtained in the vertical position, reported that cells with type G3 diaphragms were scarcely affected by tilting. In view of the above, it appears that the diaphragms in the cells used in this investigation are sufficiently fine to prevent any bulk motion, and this is borne out by the fact that comparatively consistent results were obtained with all the cells used.

The cells were maintained at constant temperature by a Cenco-type 97100 B constant temperature water bath. Temperature regulation to 0.02°C. was obtained with a Cenco No. 99200 Mercury Thermoregulator which controlled, by means of an electronic relay, electrical knife-type immersion heaters submerged in the bath. For runs where the ambient temperature was ever above the bath temperature, a copper cooling coil was placed in the bath, and a small flow of tap water was maintained through the coil.

For most of the runs, the cells were clamped in a vertical position and submerged in the bath as much as possible. The water bath was not deep enough to submerge the cells completely, so that the top two inches of the cell (in addition to the 10 mm. tube) were above the water level. Since most of the runs were made at somewhat above room temperature, this resulted in increased convection stirring of the upper compartment, which was felt to be desirable. It is important, of course, that the temperature within the diaphragm be the same as the bath temperature, but since the diaphragm was four inches below the surface of the water, it is felt that this

condition was satisfied. For the runs made below room temperature, it was not so desirable to have any part of the upper compartment above the water level, so the cells were clamped in a tilted position in order to submerge them completely.

For the runs made with chlorine, the water bath was covered with a black cloth to prevent the action of light on the chlorine solutions.

11.10. Cleaning Procedure. Before every run, each cell was cleaned in the following manner. The top compartment was rinsed with distilled water three times. By applying suction to the top of the cell, distilled water was sucked through the stopcock into the lower chamber and through the diaphragm into the upper chamber. The water was removed from both compartments and the suction procedure was repeated once more. Then the top compartment was rinsed two more times with distilled water.

11.11. Loading Procedure. The water used for these experiments was drawn from the distilled water tap, boiled, and cooled in a closed container, in order to degas it. The cell was inverted and the lower compartment was filled with water by means of a drawnout piece of glass tubing which was thin enough to go through the open stopcock. When the lower compartment was full, compressed air was applied to force some water through the diaphragm, in order to insure that the diaphragm was completely full of solvent. More water was then added to the lower compartment, and the stopcock closed, making sure that there were absolutely no air bubbles in the lower compartment. The upper chamber was rinsed out three times with the solution to be used, and then filled with that solution. For the calibration runs, the KCl solution was measured out from a burette and a volume equal to that of the lower compartment was put in. For all other runs, the upper compartment was almost completely filled with the solution (prepared by bubbling the gas through boiled distilled water), leaving a small gas space of about 0.3 ml. at the top. With a nonvolatile solute, a gas space above the upper solution was permissible, but when the solute was a slightly soluble gas, it was necessary to have the gas space as small as possible. Some gas space is required, however, to allow for some expansion due to temperature changes. A rubber tube was placed over the top of the cell and closed with a screw clamp. The cell was then placed in the water bath and clamped in position. The time when the solution was first

put into the upper compartment was noted, and taken as the beginning of the run.

For the cases where the diffusivity of chlorine in dilute hydrochloric acid and of sulfur dioxide in dilute sulfuric acid were measured, a slightly different procedure was used. A batch of dilute acid was made up, using boiled distilled water. This solution was used to fill the lower compartments in the same way that water was used, as described in the previous paragraph. The gas being investigated was then bubbled through the remainder of the acid solution until the desired concentration was reached, and this solution of the gas was used to fill the upper compartment.

11.12. Sampling Procedure. Two 10 ml. samples were taken from each compartment by means of a pipette. Since the stem of the pipette was not long enough to reach to the bottom of the upper compartment, nor thin enough to go through the stopcock into the lower compartment, the tip of the pipette was joined by means of a short piece of rubber tubing to a drawn-out piece of glass tubing that was long enough and thin enough to meet the above requirements. For the calibration runs, the pipette was rinsed out three times with each solution, and two samples were taken in the usual manner. For the other runs, because of the volatility of the solute, the procedure had to be altered. Suction was applied to the upper end of the pipette continuously until 20 or 30 ml. of solution flowed through the pipette and then the suction was removed and the top of the pipette closed with a finger. The solution was allowed to run out until the level reached the mark, the tip of the pipette was then placed below the surface of the liquid in a glass-stoppered flask, and the contents of the pipette were allowed to flow out. The pipette was then blown out, with the tip of the pipette still submerged, in order to ensure collecting any solute which had been desorbed from the surface of the liquid in the pipette. The flask was then stoppered, and the contents shaken.

Each sample was analyzed separately, and the results of the two analyses for each compartment were averaged to give the final concentrations. For the calibration runs, the initial solutions were also analyzed. For the cases of the volatile solutes, however, it was not possible to determine the initial concentration of the solutions placed in the upper compartment because these solutions were continuously desorbing solute during the loading process.

The time when the cell was inverted just prior to taking samples from the lower compartment (i.e., when solution of the upper compartment was no longer in contact with the diaphragm) was noted and taken as the end of the run.

11.13. Analysis of Potassium Chloride. The potassium chloride samples were titrated with an approximately 0.1 N solution of silver nitrate, using Mohr's method, as outlined by Willard and Furman (108), which involves potassium dichromate indicator, with an endpoint correction being made to allow for the solubility of silver chromate. The silver nitrate solution was standardized by titrating weighed samples of potassium chloride.

11.14. Analysis of Chlorine in Water. When chlorine is dissolved in pure water, the products of the hydrolysis, HCl and HOCl, are present in equal quantities. Because of the more rapid rate of diffusion of HCl, the two components resulting from the hydrolysis no longer are present in equal concentrations, there being an excess of HCl in the lower compartment (which originally contained pure water) and a deficiency of HCl in the upper compartment. In order to calculate the concentration of each component present in the system (i.e., of Cl_2 , HCl and of HOCl) it was necessary not only to determine total chlorine (i.e., the sum of chlorine plus hypochlorous acid) by iodimetry, but also to determine the excess or deficiency of acid by an alkilmetric titration. The procedure was as follows: Standard solutions of approximately 0.05N sodium thiosulfate, 0.05N HCl and 0.05N NaOH were prepared. The sodium thiosulfate was standardized by titrating weighed samples of potassium iodate according to the procedure outlined by Willard and Furman (108). The hydrochloric acid solution was standardized by titrating weighed samples of sodium carbonate, using methyl red indicator with boiling of the titration solution to drive off the evolved CO_2 . The sodium hydroxide solution was standardized by titrating against the hydrochloric acid solution, using methyl red indicator; the titration solution was boiled when just on the acid side of the end-point and then cooled down, whereupon the titration was completed. The purpose of boiling was to drive off the CO_2 evolved from the carbonate present in the sodium hydroxide solution, in order to prevent the interference of the CO_2 with the methyl red end-point.

For analysis of the samples, 25 ml. of boiled distilled water and 5 ml. of 12% KI was placed in each glass-

stoppered titration flask. For those flasks used for samples taken from the upper compartment (in which there was a deficiency of HCl), a measured volume of standard HCl solution was added, in order to ensure that the solution was always acid during the titration with the thiosulfate. The 10 ml. sample was added in the manner described in the previous section. The iodine liberated was titrated with the standard sodium thiosulfate solution, the addition of starch being omitted. Methyl red indicator was then added, and the titration was continued, with sodium hydroxide solution, the boiling off of CO₂ being omitted (since the comparatively poor precision did not warrant it). In calculating the excess or deficiency of acid in the sample, corrections had to be made for the sodium carbonate which was present in the sodium thiosulfate as a preservative (correction = 0.03515 ml. of NaOH solution per ml. of thiosulfate), and also for the slight amount of base present in the potassium iodide (correction = 0.02 ml. of NaOH).

The procedure outlined above was adapted from the procedure for the determination of hypochlorous acid in the presence of chlorine given by Scott (89).

11.15. Analysis of Chlorine in Dilute Hydrochloric Acid. The concentration of the original hydrochloric acid solution used as the solvent was determined by titration with the sodium hydroxide.

Since titration for acid in the samples was not necessary, the procedure outlined above could be simplified, as follows: 25 ml. of water and 5 ml. of 12% KI were placed in each flask. No preliminary addition of acid was necessary since the samples were already acid. The sample was added and the iodine liberated was titrated with the standard sodium thiosulfate, with starch being added just before the endpoint.

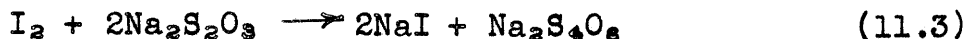
11.16. Analysis of Sulfur Dioxide. In neither of the two cases, sulfur dioxide in water, and sulfur dioxide in dilute sulfuric acid, was the determination of "excess acid" required. The procedure used to determine sulfur dioxide, adapted from that used by Philoon (82) and Whitney (106) involved the reaction of sulfur dioxide with an excess of potassium iodate.



- The solution was then acidified to liberate iodine from the excess iodate.



The liberated iodine was thereupon titrated with thiosulfate.



The detailed procedure follows: Stock solutions of potassium iodate of various concentrations were prepared. Into each flask 25 ml. of water and 5 ml. of 12% KI solutions were placed. A known volume of a stock solution of KIO_3 was pipetted in, the amount and concentration being chosen to provide 10 to 30 per cent excess of iodate. The sample from the cell was pipetted in as described in the section on sampling procedure. Sufficient 2N H_2SO_4 was added to ensure liberation of iodine from all of the remaining potassium iodate, and to ensure that the solution was acid during the titration. The contents of the flask were titrated with the standard sodium thiosulfate solution used for the chlorine determinations, with starch indicator being added just before the endpoint.

11.17. Sources of Water and of Gases Used. See Sec. 10.6.

E. Equations

The following assumptions regarding diaphragm cells have been shown by Gordon (29) to be valid: both solutions are of uniform composition right up to the entrance to the pores; transport from one compartment to the other takes place only by diffusion; steady state exists at all times within the pores. The validity of the last assumption rests on the fact that the volumes of the solutions are very large compared with the volume of the pores, so that the concentration change at both sides of the diaphragm is very slow, with the result that the accumulation term in the differential equation for diffusion within the pores may be neglected. Using these assumptions, the following relations for various cases are derived.

11.18. Constant Diffusivity; No Chemical Reaction

Let s = effective area for diffusion through the pores, cm.^2

L = effective length of the diffusion path, cm.

V' = volume in lower compartment, cm.^3

V'' = volume in upper compartment, cm.^3

C' = concentration of solution in lower compartment at any time, moles./cm.^3

C'' = concentration of solution in upper compartment at any time, moles./cm.^3

t = time, sec.

x = distance in the pore from the lower surface of the diaphragm, cm.

D = diffusivity, $\text{cm.}^2/\text{sec.}$

It follows from the assumption of steady state that the rate at which the upper chamber loses solute equals the rate at which material is diffusing through the pores at any distance x , which equals the rate at which the lower chamber gains solute.

$$-V''(dC''/dt) = sD(dC/dx) = V'(dC'/dt) \quad (11.4)$$

Because D is assumed constant, the gradient (dC/dx) must be independent of x . Then

$$dC/dx = (C''-C')/L \quad (11.5)$$

Eq. (11.4) becomes

$$-V''(dC''/dt) = (s/L)D(C''-C') = V'(dC'/dt) \quad (11.6)$$

Eq. (11.6) may be rewritten

$$dC''/dt = -(1/V'')(s/L)D(C''-C') \quad (11.7)$$

$$dC'/dt = (1/V')(s/L)D(C''-C') \quad (11.8)$$

Subtracting eq. (11.8) from eq. (11.7)

$$d(C''-C')/dt = - \left[(1/V') + (1/V'') \right] (s/L)D(C''-C') \quad (11.9)$$

If we define

$$\Delta C = C'' - C' \quad (11.10)$$

$$\beta = \left[(1/V') + (1/V'') \right] (s/L) \quad (11.11)$$

Eq. (11.9) becomes

$$-d(\Delta C)/\Delta C = D \beta dt \quad (11.12)$$

Integrating over the whole run, letting t be the time of the run,

$$\Delta C_0 = C''_0 - C'_0 = C''_0 \quad (\text{since } C'_0 \text{ always} = 0), \text{ and}$$

$$\Delta C_f = C''_f - C'_f, \text{ we have}$$

$$\ln(\Delta C_0/\Delta C_f) = D \beta t \quad (11.13)$$

11.19. Diffusivity a Function of Concentration; No Chemical Reaction. In making use of potassium chloride for calibrating the diaphragm cells, one must take into account the variation in the diffusivity of KCl with concentration, which variation can be seen by glancing at Table 11.1. It is clear that the diffusivity calculated from eq. (11.13) will be some sort of average value (referred to in the literature as integral diffusivity). Thus we may define the integral diffusivity as follows:

$$\ln(\Delta C_0/\Delta C_f) = D_{int} \beta t \quad (11.14)$$

The following derivation, relating D_{int} to the actual values of D (referred to in the literature as differential diffusivity) and to the conditions of the experiment, is based on Gordon's treatment (29).

From eq. (11.4), which is still valid, we see that at any given time, $D(dC/dx)$ is independent of x . Since C is a function of x , D also varies with x , so that the gradient is no longer constant. We may write, from Fick's law,

$$\frac{d}{dx} \left(D \frac{dC}{dx} \right) = 0 \quad (11.15)$$

Integrating once gives

$$D \frac{dC}{dx} = c_1 \quad (11.16)$$

Integrating over the diaphragm gives

$$\int_{C'}^{C''} D dC = c_1 L \quad (11.17)$$

At any given time, c_1 may be regarded as constant (i.e., independent of x), but it will vary with time as the values of the limits in eq. (11.17) change. Substituting eq. (11.16) into eq. (11.4) gives

$$-V''(dC''/dt) = sc_1 = V'(dC'/dt) \quad (11.18)$$

which may be written

$$dC''/dt = (1/V'')sc_1 \quad (11.19)$$

$$dC'/dt = (1/V')sc_1 \quad (11.20)$$

Subtracting eq. (11.20) from eq. (11.19), and using eqs. (11.10) and (11.11):

$$d(\Delta C)/dt = -\beta c_1 L \quad (11.21)$$

Substituting eq. (11.17) and rearranging:

$$\frac{d(\Delta C)}{\int_{C'}^{C''} D dC} = -\beta dt \quad (11.22)$$

If we define a quantity γ which is a function of C' and C'' such that

$$\frac{D_0 \Delta C}{\int_{C'}^{C''} D dC} = 1 + \gamma \quad (11.23)$$

where D_0 is the diffusivity at zero concentration, eq. (11.22) may be written

$$(1 + \gamma)d(\Delta C)/\Delta C = -\beta D_0 dt \quad (11.24)$$

Integration over the run gives

$$\ln(\Delta C_f/\Delta C_0) + \int_{\Delta C_0}^{\Delta C_f} \gamma d(\Delta C)/\Delta C = -\beta D_0 t \quad (11.25)$$

Eliminating βt between eqs. (11.14) and (11.25) and rearranging yields

$$\left(\frac{D_0}{D_{int}} - 1\right) \ln \frac{\Delta C_0}{\Delta C_f} = \int_{C_f}^{C_0} \gamma d(\Delta C) / \Delta C \quad (11.26)$$

By using eqs. (11.23) and (11.26) it is possible, by numerical integration, for given initial conditions, to evaluate D_{int} as a function of ΔC_f . Since all of the calibration runs were made with C_0'' practically equal to 0.100, and V' practically equal to V'' , calculations were carried out for these initial conditions. These calculations, summarized in Tables 11.6 and 11.7 were carried out as follows. Using the data of Table 11.1, D was plotted as a function of C , and the integral

$$\int_{C'}^{C''} D dC$$

was obtained graphically as a function of ΔC , using the relations

$$C'' = 0.05 + C/2$$

$$C' = 0.05 - C/2$$

Then, with eq. (11.23), γ was obtained as a function of ΔC , taking $D_0 = 1.996$.

Next, the integral

$$\int_{\Delta C_f}^{\Delta C_0} \gamma d(\Delta C) / \Delta C = \int_{\ln(\Delta C_f)}^{\ln(\Delta C_0)} \gamma d \ln(\Delta C)$$

was evaluated by graphically integrating under the curve γ versus $\ln \Delta C$. From this quantity D_{int} was calculated. These values are plotted on Fig. 11.1. Stokes (96), using the same data on the diffusivity of KCl , calculated that when $\Delta C_f = 0.05$, $D_{int} = 1.867 \times 10^{-5}$, which agrees with the value of 1.868×10^{-5} found here.

11.20. Diffusion of Chlorine Through Water. The concentration gradients encountered within the pores of the diaphragm cell are considerably lower than those found in the liquid during absorption or desorption. Thus, while the

TABLE 11.6
Computation of γ

ΔC	$\int_{C^i}^{C^o} D \, dC$	γ
0	0	0.0713
0.02	0.03727	0.0711
0.04	0.07458	0.0705
0.06	0.11197	0.0696
0.08	0.14950	0.0681
0.10	0.18734	0.0654

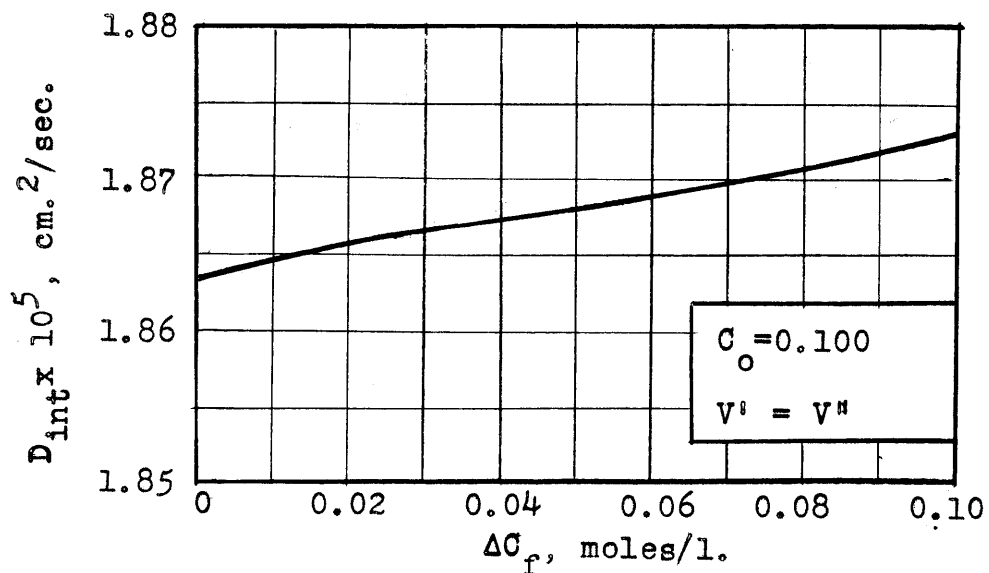
TABLE 11.7
Computation of Integral Diffusivities of KCl
in Standardization Runs

ΔC_f	$\int_{\Delta C_f}^{\Delta C_o} \gamma \, d(\Delta C) / \Delta C$	$(D_o / D_{int}) - 1$	$D_{int} \times 10^5$
0.00	-----	-----	1.863*
0.02	0.1122	0.0697	1.866
0.04	0.0631	0.0689	1.867
0.06	0.0347	0.0679	1.869
0.08	0.0149	0.0668	1.871
0.10	0	0.0654	1.873

*This value is the differential diffusivity at $C = 0.05$

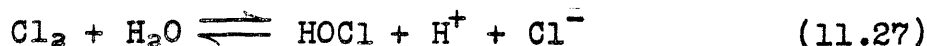
Fig. 11.1

Integral Diffusivity of Potassium Chloride



rate of hydrolysis of chlorine must be taken into account in the theory of absorption of chlorine in water, for the case of diffusion through a diaphragm, the rate of hydrolysis may be considered infinite. This leads to the assumption that equilibrium exists everywhere within the diaphragm cell.

The reaction of interest is



Let A = concentration of Cl_2

E = concentration of HOCl

F = concentration of H^+ = concentration of Cl^-

The diffusivities of Cl_2 and HOCl are, respectively, D_A and D_E . Because electrical neutrality must be maintained everywhere, and because H^+ and Cl^- are the only ions present, they must diffuse together, with the diffusivity of hydrochloric acid in water, D_F . (Actually, D_F may be slightly different from the diffusivity of HCl in water because of the possible influence of the other components). The equilibrium is expressed by the relation

$$K_c = EF^2/A \quad (11.28)$$

At any point in the pores (assuming for the time being that the diffusivities are constant), we have from eq. (8.20)

$$D_A \frac{d^2 A}{dx^2} = -D_E \frac{d^2 E}{dx^2} = -D_F \frac{d^2 F}{dx^2} \quad (11.29)$$

with the boundary conditions

$$x = 0, \quad A = A', \quad E = E', \quad F = F' \quad (11.30)$$

$$x = L, \quad A = A'', \quad E = E'', \quad F = F'' \quad (11.31)$$

Eq. (11.29) may be written:

$$\frac{d^2}{dx^2} (D_A A + D_E E) = 0 \quad (11.32)$$

Integrating twice, we have

$$D_A A + D_E E = c_1 x + c_2 \quad (11.33)$$

Evaluation of the constants of integration from B.C. (11.30) and (11.31) and substitution into eq. (11.33) gives

$$D_A A + D_E E = \left[D_A (A'' - A') + D_E (E'' - E') \right] (x/L) + D_A A' + D_E E' \quad (11.34)$$

Differentiating once,

$$D_A \frac{dA}{dx} + D_E \frac{dE}{dx} = \frac{D_A (A'' - A') + D_E (E'' - E')}{L} \quad (11.35)$$

Consider a material balance on Cl_2 in the lower compartment. Cl_2 is diffusing in at a rate

$$s D_A (dA/dx)_{x=0}$$

Cl_2 is accumulating within the compartment at a rate

$$V' dA'/dt$$

Cl_2 is disappearing due to reaction at a rate which we shall call ρ_A . Then, since the amount diffusing in equals accumulation plus that disappearing due to reaction, we have

$$s D_A (dA/dx)_{x=0} = V' dA'/dt + \rho_A \quad (11.36)$$

We may write exactly the same material balance for HOCl, which gives

$$s D_E (dE/dx)_{x=0} = V' dE'/dt + \rho_E \quad (11.37)$$

From eq. (11.27) we see that

$$\rho_A = -\rho_E \quad (11.38)$$

Eliminating ρ_A and ρ_E from eqs. (11.36), (11.37) and (11.38) and rearranging gives

$$s D_A (dA/dx)_{x=0} + s D_E (dE/dx)_{x=0} = V' dA'/dt + V' dE'/dt \quad (11.39)$$

Substituting eq. (11.35) and dividing by V' yields

$$(1/V')(s/L) \left[D_A (A'' - A') + D_E (E'' - E') \right] = dA'/dt + dE'/dt \quad (11.40)$$

A material balance on Cl_2 in the upper compartment will be similar, except that the rate at which Cl_2 diffuses into

the compartment is given by

$$-s D_A (dA/dx)_{x=L}$$

Thus, we have

$$-s D_A (dA/dx)_{x=L} = V'' dA''/dt + \rho_A \quad (11.41)$$

Exactly the same material balance equation will be found for HOCl.

$$-s D_E (dE/dx)_{x=L} = V'' dE''/dt + \rho_E \quad (11.42)$$

Combining eqs. (11.41), (11.42) and (11.38) and rearranging gives

$$-s D_A (dA/dx)_{x=L} - s D_E (dE/dx)_{x=L} = V'' dA''/dt + V'' dE''/dt \quad (11.43)$$

Substituting eq. (11.35) and dividing by V'' yields

$$-(1/V'')(s/L) [D_A(A''-A') + D_E(E''-E')] = dA''/dt + dE''/dt \quad (11.44)$$

Subtract eq. (11.40) from eq. (11.44):

$$\begin{aligned} - \left[(1/V') + (1/V'') \right] (s/L) [D_A(A''-A') + D_E(E''-E')] &= \\ &= d(A''+E'')/dt - d(A'+E')/dt \end{aligned} \quad (11.45)$$

When the solution is titrated by sodium thiosulfate, the sum of the concentrations of Cl_2 and HOCl are determined, since



and



Thus, the iodimetric titration determines $C = A + E$.

Substituting $C = A + E$, and the definition of ρ , eq. (11.11), we have

$$-\rho [D_A(A''-A') + D_E(E''-E')] = d(C''-C')/dt \quad (11.46)$$

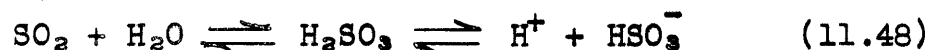
This may be rewritten

$$\begin{aligned}
 -\beta [D_A(A''+E''-A'-E')+ (D_E-D_A)(E''-E')] &= d(\Delta C)/dt \\
 -\beta [D_A(C''-C')+ (D_E-D_A)(E''-E')] &= d(\Delta C)/dt \\
 [D_A + (D_E-D_A)(\Delta E/\Delta C)] &= -d(\ln \Delta C)/d(\beta t) \quad (11.47)
 \end{aligned}$$

One may obtain D_A from runs performed on diffusion of chlorine through dilute hydrochloric acid, in which the hydrolysis is suppressed. Then, from runs on diffusion of chlorine through water of various lengths of time, one may construct a plot of $-\ln(\Delta C_f)$, or better, $\ln(\Delta C_o/\Delta C_f)$ versus βt , and from the slope, and the values of $\Delta E/\Delta C$, evaluate D_E .

11.21. Diffusion of Sulfur Dioxide Through Water.

For the case of diffusion of sulfur dioxide through water in a diaphragm cell, the concentration gradients are also sufficiently small that equilibrium may be assumed to exist throughout. This equilibrium may be said to involve following reactions:



If we let

A = concentration of SO_2 ,

E = concentration of H_2SO_3

F = concentration of H^+ = concentration of HSO_3^- ,

the equilibrium may be expressed in terms of two constants

$$K_1 = E/A \quad (11.49)$$

$$K_2 = F^2/E \quad (11.50)$$

Strictly speaking, the denominator of eq. (11.49) should involve the activity of water, but Campbell and Maass (8) show that at 25°C., over the range they investigated (partial pressure of SO_2 from 0 to 800 mm. Hg) either no H_2SO_3 exists or at least that the proportionality of H_2SO_3 to SO_2 is constant, so that the activity of water, for this range is substantially constant.

We see from eq. (11.48) that SO_2 may exist in solution in any of three forms. Thus, the concentration of

"total" sulfur dioxide, C , is equal to $A + E + F$. Furthermore, the rate at which "total" sulfur dioxide diffuses across a plane of unit area in the x -direction is:

$$-D_A \frac{dA}{dx} - D_E \frac{dE}{dx} - D_F \frac{dF}{dx}$$

A material balance of "total" sulfur dioxide on a differential slice with faces at x and at $x + dx$ yields the differential equation (assuming the diffusivities are constant)

$$D_A \frac{d^2 A}{dx^2} + D_E \frac{d^2 E}{dx^2} + D_F \frac{d^2 F}{dx^2} = 0 \quad (11.51)$$

which may be written

$$\frac{d^2}{dx^2} (D_A A + D_E E + D_F F) = 0 \quad (11.52)$$

The boundary conditions are

$$x = 0, \quad A = A', \quad E = E', \quad F = F' \quad (11.53)$$

$$x = L, \quad A = A'', \quad E = E'', \quad F = F'' \quad (11.54)$$

Just as was done in the previous section, eq. (11.52) may be integrated twice, and the boundary conditions substituted to yield the solution

$$D_A A + D_E E + D_F F = \left[D_A (A'' - A') + D_E (E'' - E') + D_F (F'' - F') \right] (x/L) + D_A A' + D_E E' + D_F F' \quad (11.55)$$

Differentiating once,

$$D_A \frac{dA}{dx} + D_E \frac{dE}{dx} + D_F \frac{dF}{dx} = \frac{D_A (A'' - A') + D_E (E'' - E') + D_F (F'' - F')}{L} \quad (11.56)$$

Consider a material balance of "total" sulfur dioxide on the lower compartment. "Total" sulfur dioxide is diffusing in at a rate

$$s \left[D_A \left(\frac{dA}{dx} \right)_{x=0} + D_E \left(\frac{dE}{dx} \right)_{x=0} + D_F \left(\frac{dF}{dx} \right)_{x=0} \right]$$

"Total" sulfur dioxide is accumulating within the compartment at a rate

$$V' d(A'+E'+F')/dt = V' dC'/dt$$

Since "total" sulfur dioxide includes all the forms in which it can exist, there is no disappearance due to chemical reaction. Then

$$s \left[D_A (dA/dx)_{x=0} + D_E (dE/dx)_{x=0} + D_F (dF/dx)_{x=0} \right] = V' dC'/dt \quad (11.57)$$

Substituting eq. (11.56) and dividing by V' yields

$$(1/V')(s/L) \left[D_A (A''-A') + D_E (E''-E') + D_F (F''-F') \right] = dC'/dt \quad (11.58)$$

The material balance on the upper compartment will be similar, except that the rate at which "total" sulfur dioxide diffuses in is

$$-s \left[D_A (dA/dx)_{x=L} + D_E (dE/dx)_{x=L} + D_F (dF/dx)_{x=L} \right]$$

By equating this to $V'' dC''/dt$, substituting eq. (11.56) and dividing by V'' , we have

$$-(1/V'')(s/L) \left[D_A (A''-A') + D_E (E''-E') + D_F (F''-F') \right] = dC''/dt \quad (11.59)$$

Subtracting eq. (11.58) from eq. (11.59), and substituting the definition of ΔC (eq. (11.10)) and of β (eq. (11.11)),

$$-\beta \left[D_A (A''-A') + D_E (E''-E') + D_F (F''-F') \right] = d(\Delta C)/dt \quad (11.60)$$

From eq. (11.49), we have

$$E = K_1 A$$

Eq. (11.60) may be written

$$-\beta \left[D_A + K_1 D_E \right] (A''-A') + D_F (F''-F') = d(\Delta C)/dt \quad (11.61)$$

Since it is very difficult to distinguish between SO_2 and H_2SO_3 in the solution (the method used takes into account the change in the activity of water for various concentrations of SO_2 , and this change is very small), it is convenient to represent the sum of their concentrations by a single quantity G . Then we have

$$G = A + E = C - F \quad (11.62)$$

Since $G = A(1+K_1)$, eq. (11.61) becomes

$$\begin{aligned} -\beta \left[(D_A + K_1 D_E)(G'' - G') / (1 + K_1) + D_F(F'' - F') \right] = \\ = d(\Delta C / dt) \end{aligned} \quad (11.63)$$

If we write $D_G = (D_A + K_1 D_E) / (1 + K_1)$, we have

$$-\beta \left[D_G(G'' - G') + D_F(F'' - F') \right] = d(\Delta C / dt) \quad (11.64)$$

The significance of the last equation is that the combination of SO_2 and H_2SO_3 diffuses as a single substance, with an apparent diffusivity D_G . Since most equilibrium data on SO_2 -water systems are in terms of an apparent dissociation constant

$$K_S = \frac{F''}{G} \quad (11.65)$$

it is possible to evaluate quite easily the values of F and G . The relationship of K_S to K_1 and K_2 is

$$K_S = \frac{K_2 E}{A + E} = \frac{K_2 K_1 A}{A + K_1 A} = \frac{K_2 K_1}{1 + K_1} \quad (11.66)$$

Eq. (11.64) may be rewritten (in the same manner as eq. (11.46) was rewritten)

$$D_G + (D_F - D_G)(\Delta F / \Delta C) = -d(\ln \Delta C) / d(\beta t) \quad (11.67)$$

One may obtain D_G from runs performed on diffusion of sulfur dioxide through dilute sulfuric acid, in which the ionization to HSO_3 is suppressed so that only SO_2 and H_2SO_3 are present. From runs on diffusion of SO_2 through water of various lengths of time, a plot of $\ln(\Delta C_0 / \Delta C_t)$ versus βt may be constructed, and from the slope and the values of $\Delta F / \Delta C$, D_F may be evaluated.

11.22. Volume of Pores of Diaphragm. In studying the diffusion of gases in water, it was not feasible to measure the initial concentration of the solution of gas, C_0'' . Hence, it was necessary to calculate this initial concentration from the final concentrations and the volumes of the solution. However, an appreciable quantity of solution is contained in the pores, and the volume of the pores must be taken into account in the material balance. Let r be the ratio of the volume of the pores to the volume of the lower compartment. Assuming a linear concentration gradient in the pores, the amount of solute contained within the pores is

$$rV'(C'+C'')/2$$

Since the pores originally are free of solute, the material balance equation is

$$V'' C_0'' = V'' C_f'' + V' C_f' + rV'(C_f'' + C_f')/2 \quad (11.68)$$

Solving for $r/2$,

$$r/2 = \frac{(C_0'' - C_f'')(V''/V') - C_f'}{(C_f'' + C_f')} \quad (11.69)$$

Since the value of C_0'' was known for the calibration runs, r could be calculated for each cell by means of this equation. This value of r was then used to calculate C_0'' for each run by means of the equation

$$C_0'' = C_f'' + (V'/V'')(1+r/2)C_f' + rV'C_f''/(2V'') \quad (11.70)$$

F. Results and Discussion

11.23. Calibration of Cells. Three calibration runs were made on each cell. The data and calculated results for each run are tabulated in Table 11.8.

Using the values of ΔC_f , the values of D_{int} were obtained from Fig. 11.1. β was calculated by the use of eq. (11.14). The values of s/L were calculated by eq. (11.11); those of $r/2$ by eq. (11.69). The three values of s/L and of $r/2$ for each cell were averaged, and listed in Table 11.9.

Table 11.8

Calibration of Diaphragm Cells; Data and Calculated Results

Run No.	Cell	Concentration, moles/l.			Volumes, cm. ³		time, hours	ΔC_f moles/l.
		C_o''	C_f''	C_f'	V'	V''		
1	A	0.09976	0.08716	0.01240	71.3	77.0	47.42	0.07476
2	B	.09976	.08862	.01146	71.6	78.0	46.50	.07716
3	C	.09976	.08929	.01078	73.1	76.0	45.58	.07851
4	D	.09976	.09073	.00894	66.8	70.0	41.17	.08179
5	E	.09976	.09228	.00711	69.2	70.0	40.08	.08517
6	F	.09976	.09128	.00832	66.1	68.0	38.75	.08296
7	A	0.09996	0.08358	0.01578	71.3	71.3	61.67	0.06780
8	B	.09996	.08577	.01357	71.6	71.6	60.67	.07220
9	C	.09996	.08598	.01370	73.1	73.1	59.58	.07228
10	D	.09996	.09028	.00945	66.8	66.8	42.83	.08083
11	E	.09996	.09222	.00722	69.2	69.2	40.92	.08500
12	F	.09996	.09082	.00882	66.1	66.1	39.92	.08200
13	A	0.09996	0.08320	0.01609	71.3	71.3	64.47	0.06711
14	B	.09996	.08450	.01479	71.6	71.6	65.75	.06971
15	C	.09996	.08452	.01494	73.1	73.1	67.33	.06958
16	D	.09996	.08533	.01419	66.8	66.8	68.92	.07114
17	E	.09996	.08765	.01192	69.2	69.2	69.82	.07573
18	F	.09996	.08506	.01445	66.1	66.1	70.63	.07061
Run No.	Cell	$\log_{10} (\Delta C_o / \Delta C_f)$	$D_{int} \times 10^5$ cm ² /sec.	β cm. ⁻²	$(1/V') + (1/V'')$ cm. ⁻³	s/L cm.	r/2	
1	A	0.12529	1.870	0.0904	0.02701	3.35	0.0122	
2	B	.11156	1.871	.0820	.02679	3.06	.0068	
3	C	.10404	1.871	.0780	.02683	2.91	.0010	
4	D	.08625	1.871	.0716	.02925	2.45	.0052	
5	E	.06867	1.871	.0586	.02874	2.04	.0066	
6	F	.08009	1.871	.0707	.02984	2.37	.0040	
7	A	0.16859	1.870	0.0935	0.02805	3.33	0.0060	
8	B	.14129	1.870	.0797	.02793	2.85	.0061	
9	C	.14082	1.870	.0808	.02735	2.96	.0028	
10	D	.09226	1.871	.0736	.02994	2.46	.0023	
11	E	.07041	1.871	.0588	.02890	2.04	.0052	
12	F	.08601	1.871	.0737	.03026	2.43	.0032	
13	A	0.17304	1.870	0.0918	0.02805	3.27	0.0067	
14	B	.15652	1.870	.0814	.02793	2.92	.0067	
15	C	.15734	1.870	.0799	.02735	2.92	.0050	
16	D	.14771	1.870	.0733	.02994	2.45	.0044	
17	E	.12057	1.870	.0591	.02890	2.04	.0039	
18	F	.15097	1.870	.0731	.03026	2.42	.0045	

Table 11.9
Calibration of Diaphragm Cells; Results

Cell	Mean Values		Std. dev. of s/L	Std. error of Mean Value of s/L
	s/L cm.	r		
A	3.32	0.0083	1.2%	0.7%
B	2.94	.0065	3.7	2.0
C	2.93	.0029	0.8	0.5
D	2.45	.0040	0.3	0.2
E	2.04	.0052	0.2	0.1
F	2.41	.0039	1.4	0.8

The precision of the values of r is quite poor because they are obtained by subtracting large numbers from each other, but this uncertainty will contribute a very small error in the calculation of C_0'' because of the relative smallness of r compared with the other terms of eq. (11.70).

The standard deviations of the values of s/L were calculated by the use of the formulas obtained from the statistical theory of small samples:

$$\text{std. dev.} = \sqrt{\frac{\sum(x-x_m)^2}{n-1}} \quad (11.71)$$

where x is one individual value, x_m is the mean value, and n is the number of samples.

$$\text{std. error of the mean} = \frac{\text{std. dev.}}{\sqrt{n}} \quad (11.72)$$

The standard deviations and errors of the values of s/L , expressed as per cent, are also listed in Table 11.9.

The expected error in s/L was calculated from the probable errors encountered in the analytical procedure and was found to be about 1.4 per cent. In the light of this expected error, the precision obtained is quite good

for cells C, D and E, and is satisfactory for cells A and F. Cell B had a comparatively large standard deviation, which is equivalent to saying that a consistent calibration was not obtained. For this reason, Cell B was not used in any of the following runs. This is in line with the experience of Hartley and Runnicles (36) who reported that a few of their diaphragms had to be discarded owing to failure to give reproducible results.

11.24. Diffusion of Chlorine through Dilute Hydrochloric Acid. Twenty-seven runs were made, using three different concentrations of hydrochloric acid, all but five runs being made at 25°C. The last five runs were made at 30°C. because warm weather made it difficult to maintain the thermostat bath at 25°C. The data obtained are listed in Table 11.10 in columns 3 through 8; the remaining columns are derived results. Since the solutions of chlorine in hydrochloric acid are more viscous than solutions in water, a correction must be made for the viscosity in order to yield the diffusivity of molecular (i.e., unhydrolyzed) chlorine in water. The correction was obtained from the Stokes-Einstein relationship, which states that diffusivity is proportional to absolute temperature divided by viscosity. Thus, the correction factor for viscosity is the ratio of the viscosity of the original hydrochloric acid solution to the viscosity of water. This ratio was obtained by interpolation from the values given in the International Critical Tables (45). In addition, the diffusivities measured at 30°C. (Runs 42-45) were corrected to 25°C. by multiplying by 0.865 (see Table 11.12 below - - it is assumed that the diffusivity of molecular chlorine has the same temperature variation as that found for "total" chlorine in water).

Figure 11.2 shows a plot of D (thus corrected for viscosity and temperature) versus C_0 , with different symbols used for the various concentrations of HCl. It can be seen that there is no significant trend of D with the concentration of either chlorine or hydrochloric acid.

The mean value of D for runs 19-44 is 1.48×10^{-5} ; the standard deviation is 2.5%; the standard error of the mean is 0.5%. Run 45 was rejected, because its deviation is about eight times the standard deviation.

Since, in any of the solutions encountered, less than three per cent of the chlorine was hydrolyzed and, since the concentration of hydrochloric acid was found to have no effect, it is concluded that the diffusivity measured here is the diffusivity of molecular chlorine in water, $(1.48 \pm 0.01) \times 10^{-5}$ cm.²/sec.

Table 11.10

Diffusion of Chlorine through Dilute Hydrochloric Acid at 25°C.Data and Calculated Results

Run No.	Cell	Concentrations, moles/l.			Volumes, cm. ³		time, hours	C ₀ " moles per l.	ΔC _r moles per l.
		C _r "	C _r '	HCl	v'	v"			
19	A	0.01533	0.00246	0.23	71.3	125.7	72.28	0.01681	0.01287
20	C	.02693	.00391	0.23	73.1	124.3	72.85	.02929	.02302
21	D	.03805	.00504	0.23	66.8	127.3	72.17	.04079	.03301
22	E	.02670	.00286	0.10	69.2	121.2	70.73	.02842	.02384
23	F	.02681	.00334	0.43	66.1	120.2	69.10	.02871	.02347
24	A	0.03589	0.00894	0.22	71.3	125.7	114.23	0.04118	0.02695
25	C	.02170	.00516	0.22	73.1	124.3	117.35	.02479	.01654
26	D	.02917	.00618	0.22	66.8	127.3	118.37	.03249	.02299
27	E	.03018	.00525	0.22	69.2	121.2	118.78	.03328	.02493
28	F	.02547	.00585	0.22	66.1	120.2	120.87	.02875	.01962
29	A	0.00920	0.00219	0.22	71.3	125.7	111.87	0.01049	0.00701
30	D	.01687	.00341	0.22	66.8	127.3	114.37	.01871	.01346
31	E	.01507	.00251	0.22	69.2	121.2	114.65	.01656	.01256
32	F	.02093	.00430	0.22	66.1	120.2	115.43	.02334	.01663
33	A	0.01302	0.00383	0.11	71.3	125.7	136.40	0.01527	0.00919
34	C	.03787	.01008	0.11	73.1	124.3	136.83	.04388	.02779
35	D	.02072	.00512	0.11	66.8	127.3	130.05	.02346	.01560
36	E	.03893	.00788	0.11	69.2	121.2	138.37	.04357	.03105
37	F	.01333	.00334	0.11	66.1	120.2	140.02	.01520	.00999
38	A	0.04266	0.01075	0.22	71.3	125.7	112.83	0.04901	0.03191
39	D	.04417	.00907	0.22	66.8	127.3	113.32	.04904	.03510
40	E	.04333	.00746	0.22	69.2	121.2	115.48	.04774	.03587
41	F	.03987	.00929	0.22	66.1	120.2	130.83	.04508	.03058
42*	A	0.00692	0.00195	0.10	71.3	125.7	107.75	0.00807	0.00497
43*	D	.01108	.00250	0.10	66.8	127.3	107.98	.01242	.00858
44*	E	.01042	.00199	0.10	69.2	121.2	108.60	.01159	.00843
45*	F	.01640	.00437	0.10	66.1	120.2	108.82	.01884	.01203

* Runs 42-45 were made at 30°C.

Table 11.10 (cont'd.)

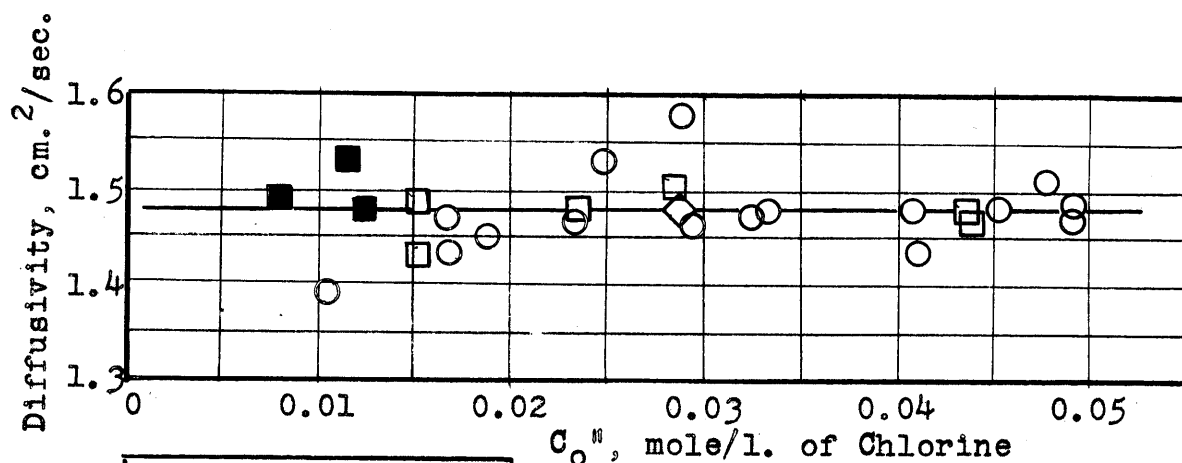
Run No.	Cell	$\log_{10} (\Delta C_o / \Delta C_f)$	β cm. ⁻²	D cm ² /sec.	Correction Factor for Viscosity	Corrected D x 10 ⁵ cm ² /sec.	D x 10 ⁵ cm ² /sec. at 25°C.
19	A	0.1160	0.0729	1.41	1.014	1.43	
20	C	.1046	.0636	1.44	1.014	1.46	
21	D	.0919	.0560	1.46	1.014	1.48	
22	E	.0763	.0463	1.49	1.007	1.50	
23	F	.0875	.0564	1.44	1.027	1.48	
24	A	0.1841	0.0729	1.41	1.014	1.43	
25	C	.1757	.0636	1.51	1.014	1.53	
26	D	.1502	.0560	1.45	1.014	1.47	
27	E	.1255	.0463	1.46	1.014	1.48	
28	F	.1659	.0564	1.56	1.014	1.58	
29	A	0.1751	0.0729	1.37	1.014	1.39	
30	D	.1430	.0560	1.43	1.014	1.45	
31	E	.1201	.0463	1.45	1.014	1.47	
32	F	.1472	.0564	1.45	1.014	1.47	
33	A	0.2205	0.0729	1.42	1.007	1.43	
34	C	.1984	.0636	1.46	1.007	1.47	
35	D	.1772	.0560	1.47	1.007	1.48	
36	E	.1471	.0463	1.47	1.007	1.48	
37	F	.1823	.0564	1.48	1.007	1.49	
38	A	0.1864	0.0729	1.45	1.014	1.47	
39	D	.1453	.0560	1.47	1.014	1.49	
40	E	.1242	.0463	1.49	1.014	1.51	
41	F	.1686	.0564	1.46	1.014	1.48	
42*	A	0.2105	0.0729	1.71	1.007	1.73	1.49
43*	D	.1607	.0560	1.70	1.007	1.71	1.48
44*	E	.1383	.0463	1.76	1.007	1.77	1.53
45*	F	.1948	.0564	2.03	1.007	2.04	1.77

* Runs 42-45 were made at 30°C.

Average D = 1.48×10^{-5} cm.²/sec. (corrected for viscosity and temperature).

Fig. 11.2

Effect of Concentrations on Diffusivity of Chlorine
in Dilute Hydrochloric Acid at 25°C.



Conc. of HCl	
□ ■	0.10±0.01
○	0.22±0.01
◇	0.43
■	Measured at 30°C. and cor- rected to 25°C.

11.25. Diffusion of Chlorine through Water at 25°C. Twelve runs were made, using three different initial concentrations of chlorine. As pointed out in the Procedure section, the titration with sodium thiosulfate yielded values of C , while the titration with acid and base yielded the excess of hydrochloric acid over hypochlorous acid, (F-E). The data obtained are listed in Table 11.11 in columns 3 through 9; the remaining columns are derived results.

In Fig. 11.3, $\log_{10} (\Delta C_0 / \Delta C_f)$ has been plotted against \sqrt{t} , with different symbols used for the various initial concentrations of chlorine. Contrary to expectations, (see eq. (11.47)), the plot is remarkably straight, the slope being independent of time. Furthermore, it is seen that there is no significant effect of concentration of chlorine.

TABLE 11.11

Diffusion of Chlorine through Water at 25°C.
Data and Calculated Results

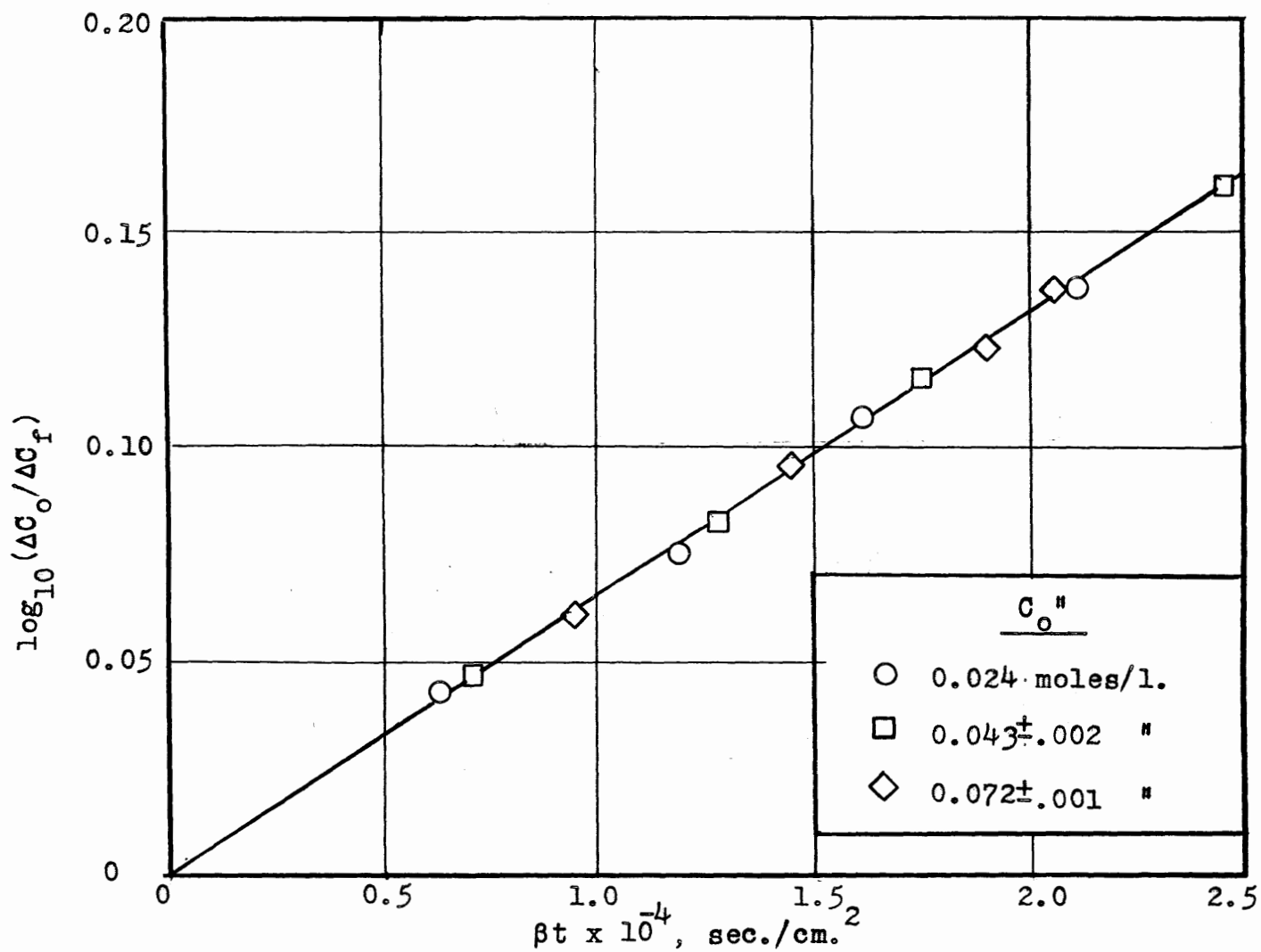
Run No.	Cell	Concentrations, moles/l.				Volumes, cm. ³		Time, hours	C ^o mole/l.	ΔC _f moles/l.
		C _f ^o	C _f ⁱ	E _f ^o -F _f ^o	F _f ⁱ -E _f ⁱ	V ⁱ	V ^o			
46	A	0.02140	0.00402	0.00105	0.00191	71.3	125.7	80.63	0.02380	0.01738
47	C	.02246	.00237	.00058	.00116	73.1	125.8	52.00	.02388	.02009
48	D	.02187	.00334	.00097	.00155	66.8	127.3	80.02	.02368	.01853
49	F	.02296	.00139	.00025	.00097	66.1	120.2	31.18	.02378	.02157
50	A	.04145	.00476	.00089	.00210	71.3	125.7	48.60	.04436	.03669
51	C	.03833	.00838	.00141	.00288	73.1	125.8	107.45	.04329	.02995
52	D	.04184	.00286	.00066	.00127	66.8	127.3	35.50	.04344	.03898
53	F	.03850	.00629	.00066	.00238	66.1	120.2	85.93	.04205	.03221
54	A	.06477	.01103	.00180	.00315	71.3	125.7	72.25	.07138	.05374
55	C	.06452	.01210	.00141	.00318	73.1	125.8	90.15	.07168	.05242
56	D	.06912	.00607	.00119	.00174	66.8	127.3	46.85	.07247	.06305
57	F	.06647	.00903	.00133	.00274	66.1	120.2	71.10	.07160	.05744

Run No.	Cell	log ₁₀ (ΔC _f ^o /ΔC _f)	β cm. ⁻²	βt x 10 ⁻⁵ sec./cm. ²	D _C x 10 ⁵ cm. ² /sec.	Concentrations, moles/l.				ΔE _f	ΔE _o
						E _o ^o	E _f ^o	E _f ⁱ	ΔE _f	ΔC _f	ΔC _o
46	A	0.1365	0.0729	0.2117	1.49	.01451	.01410	.00367	.01043	.600	.610
47	C	.0751	.0633	.1186	1.46	.01454	.01429	.00229	.01200	.597	.609
48	D	.1065	.0560	.1612	1.52	.01447	.01424	.00313	.01111	.600	.611
49	F	.0424	.0564	.0633	1.54	.01455	.01433	.00138	.01295	.600	.612
50	A	.0824	.0729	.1276	1.49	.02001	.01983	.00424	.01559	.425	.451
51	C	.1600	.0633	.2450	1.50	.01978	.01936	.00659	.01277	.426	.457
52	D	.0470	.0560	.0715	1.51	.01981	.01980	.00273	.01707	.438	.456
53	F	.1158	.0564	.1745	1.53	.01950	.01902	.00533	.01369	.425	.464
54	A	.1233	.0729	.1897	1.50	.02484	.02482	.00798	.01684	.313	.348
55	C	.1359	.0633	.2055	1.52	.02488	.02452	.00854	.01598	.305	.347
56	D	.0605	.0560	.0944	1.48	.02500	.02516	.00528	.01988	.315	.345
57	F	.0957	.0564	.1444	1.53	.02486	.02482	.00701	.01781	.310	.347

Average D_C = 1.51 x 10⁻⁵ cm.²/sec.

Fig. 11.3

Effect of Time on Diffusion of Chlorine through Water in a Diaphragm Cell at 25°C.



The significance of these results is that it is permissible to speak of the diffusivity of "total" chlorine, D_C , which may be calculated by

$$D_C = \frac{\ln(\Delta C_O / \Delta C_F)}{\rho t} \quad (11.73)$$

This diffusivity has been calculated for each run. The average value is 1.51×10^{-5} ; the standard deviation is 1.6%; the standard error of the mean is 0.5%. Thus $D_C = (1.51 \pm 0.01) \times 10^{-5}$ cm.²/sec.

In order to calculate D_E , we proceed as follows. From eqs. (11.47) and (11.73), we get

$$D_C = D_A + (D_E - D_A)(\Delta E / \Delta C) \quad (11.74)$$

which may be solved for D_E .

$$D_E = D_A + (D_C - D_A) / (\Delta E / \Delta C) \quad (11.75)$$

Now, it is necessary to calculate the values of E for each compartment at the beginning and end of every run. This has been done by using the values of C and F-E already determined, and the equilibrium relationship

$$K_C = EF^2 / A \quad (11.28)$$

which may be written

$$K = E [(F-E) + E]^2 / (C-E) \quad (11.76)$$

and solved for E by trial and error. The value used for K_C is 3.29×10^{-4} (moles/cm.³)² at 25°C. as measured by Vivian and Whitney (101).

In the last two columns of Table 11.11 are listed values of $\Delta E_F / \Delta C_F$ and $\Delta E_O / \Delta C_O$. (Note that $\Delta E_O / \Delta C_O = E_O'' / C_O''$.) From the table, it can be seen that, for a given value of C_O'' , there is remarkably little variation of $\Delta E / \Delta C$ with time, being practically the same at the beginning and the end of the runs. Thus, for each value of C_O'' , it is possible to assign a value of $\Delta E / \Delta C$; in the following table, for each set of runs, average values of C_O'' and $\Delta E / \Delta C$ were taken.

Runs	C_O''	$\Delta E / \Delta C$
46-49	0.024	0.61
50-53	0.043	0.44
54-57	0.072	0.33

Using these values of $\Delta E/\Delta C$, and the values of D_A and D_C obtained above, D_E may be calculated for each C_0'' by eq. (11.75).

C_0''	D_E
0.024	1.52
0.043	1.54
0.072	1.56

This trend in D_E with C_0'' probably is not significant, since the variation is within the combined experimental error for D_A and D_C . Thus, we conclude that the diffusivity of hypochlorous acid in water at 25°C. is $(1.54 \pm 0.02) \times 10^{-5}$ cm.²/sec.

11.26. Effect of Temperature on Diffusion of Chlorine Through Water. In view of the lack of dependence of D_C on C_0'' or time, it was decided to study the effect of temperature on D_C , rather than on D_A , since the procedure for determining the former is somewhat simpler. Ten runs were made at five different temperatures, in addition to the twelve runs made at 25°C. which were discussed in the previous section. The data and derived results are presented in Table 11.12. The results have been plotted on Fig. 11.4 and Fig. 11.5. The average of the runs at 25° and at 30°C. have been plotted as single points, while the individual runs have plotted at the other temperature.

Figure 11.4 also includes the two values presented in the previous literature. The results of this investigation are significantly lower than either of them. It is to be noted that Euler's value, which is considered more reliable by the International Critical Tables (46), appears to be greater in error than Hufner's value.

Figure 11.4 shows a comparison of the data with the Stokes-Einstein relationship,

$$D \propto T/\mu \quad (11.77)$$

which may be written

$$D = (T/\mu)(\mu_{\text{ref.}}/T_{\text{ref.}}) \quad (11.78)$$

Because most of the runs were made at 25°C., that temperature is chosen as the reference. The agreement between eq. (11.78) and the data is fairly good.

Table 11.12

Effect of Temperature on Diffusion of Chlorine Through WaterData and Calculated Results

Run No.	Cell	Temp. °C.	Concn., moles/l.		Volumes, cm. ³		Time, hours
			C _f ^o	C _f ⁱ	v ⁱ	v ^o	
58	C	20.0	0.04232	0.00540	73.1	125.8	71.42
59	D	20.0	.04305	.00501	66.8	127.3	70.55
60	C	15.0	0.05418	0.00595	73.1	125.8	69.38
61	D	15.0	.05466	.00547	66.8	127.3	69.32
62	C	10.0	0.05640	0.00576	73.1	125.8	75.50
63	F	30.0	0.05120	0.01417	66.1	120.2	129.35
64	A	30.0	0.04697	0.01440	71.3	125.7	119.23
65	D	30.0	.04920	.01237	66.8	127.3	119.83
66	E	30.0	.04902	.01038	69.2	121.2	121.82
67	F	30.0	.04542	.01180	66.1	120.2	122.55

Run No.	Cell	C _o ^o moles per l.	ΔC _f moles per l.	log ₁₀ (ΔC _o /ΔC _f)	β cm. ⁻²	Dx10 ⁵ cm. ² / sec.
58	C	0.04554	0.03692	0.0911	0.0633	1.29
59	D	.04578	.03804	.0804	.0560	1.30
60	C	0.05774	0.04823	0.0782	0.0633	1.138
61	D	.05765	.04919	.0689	.0560	1.136
62	C	0.05986	0.05064	0.0727	0.0633	0.972
63	F	0.05913	0.03703	0.2033	0.0564	1.78
64	A	0.05543	0.03257	0.2309	0.0729	1.70
65	D	.05582	.03683	.1805	.0560	1.72
66	E	.05513	.03864	.1544	.0463	1.75
67	F	.05204	.03362	.1897	.0564	1.76

Average D_c at 30°C. = 1.74 x 10⁻⁵ cm.²/sec.

Average D_c at 25°C. = 1.51 x 10⁻⁵ cm.²/sec.

Ratio (D_c at 25°C.)/(D_c at 30°C.) = 0.865

Fig. 11.4

Effect of Temperature on Diffusivity of "Total" Chlorine in Water

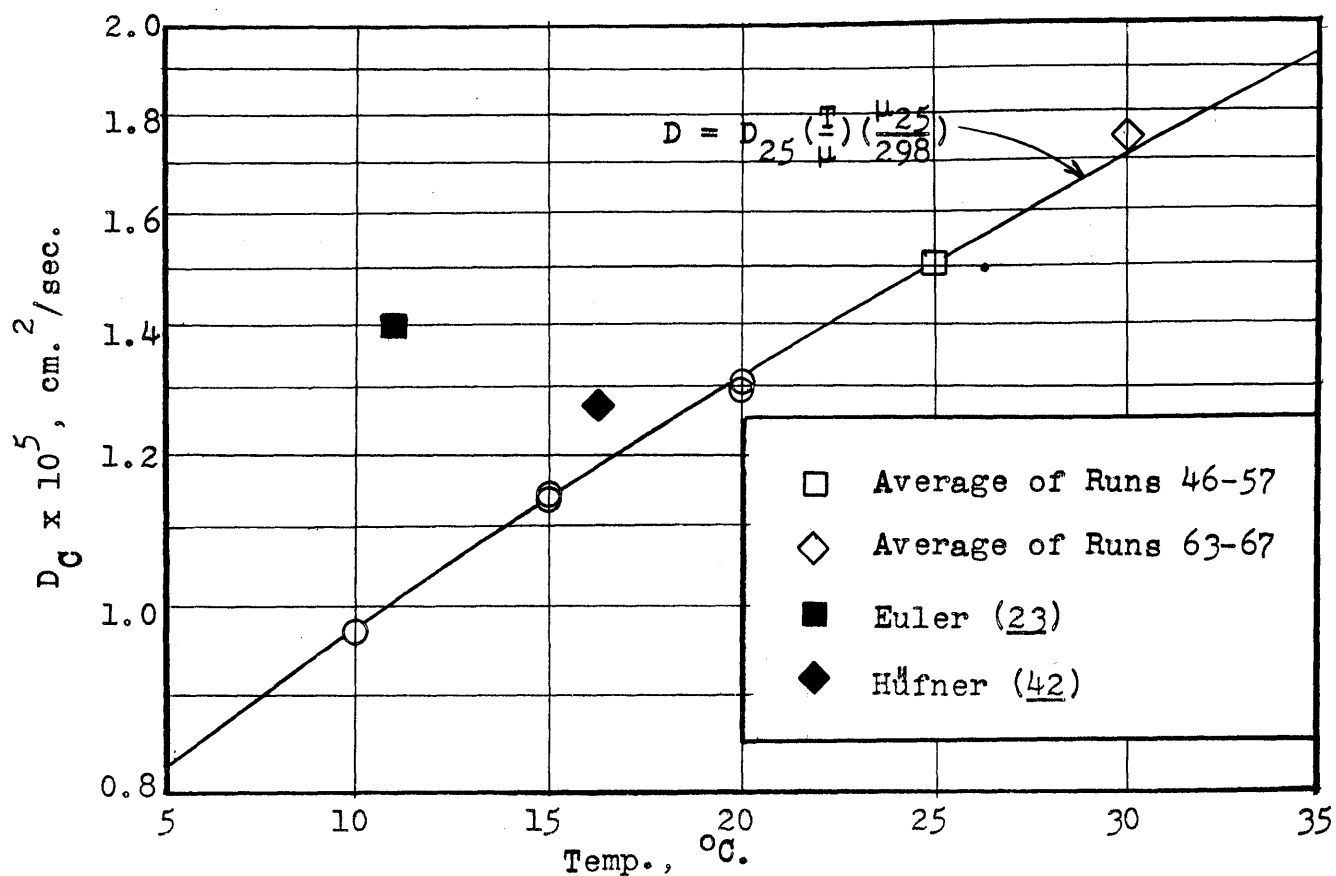
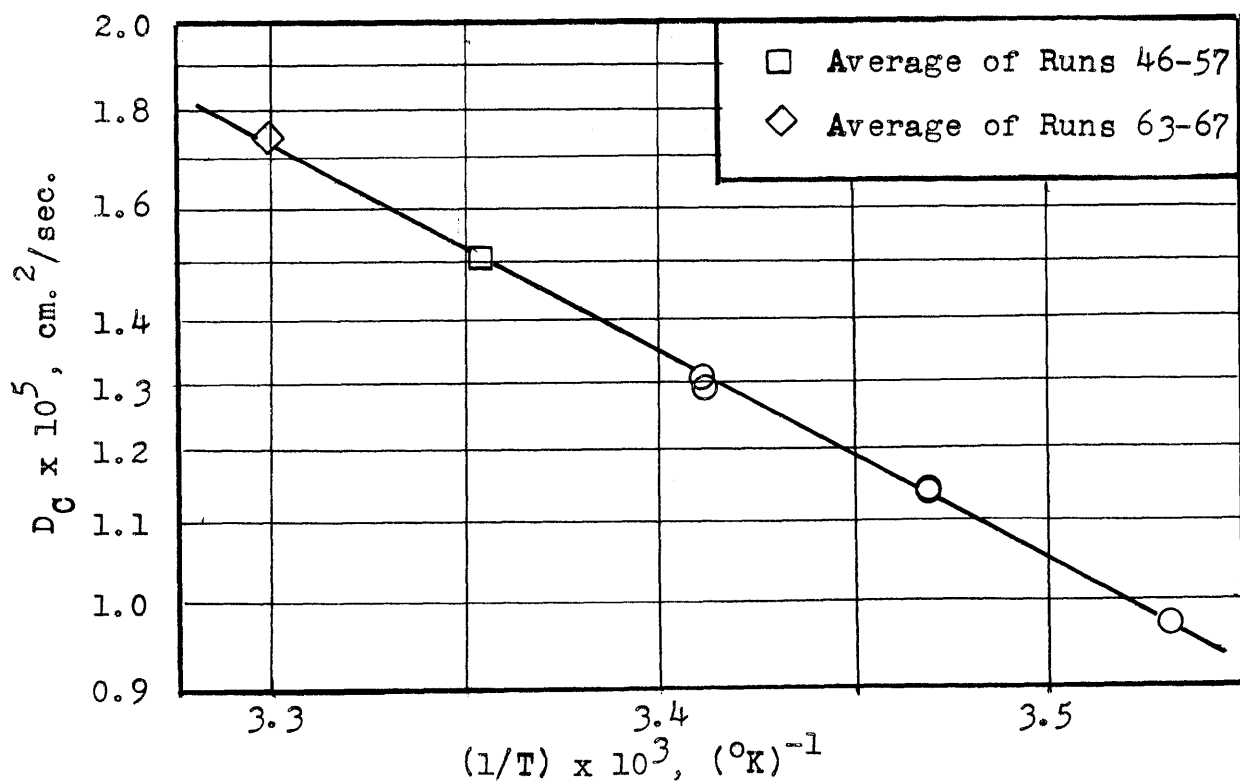


Fig. 11.5

Effect of Temperature on Diffusivity of "Total" Chlorine in Water



In Fig. 11.5, $\log D_G$ has been plotted against the reciprocal of the absolute temperature. The data fall very well on a straight line, indicating that an Arrhenius-type expression may be used

$$D \propto e^{-\Delta E/RT} \quad (11.79)$$

Eq. (11.79) implies that diffusion is an activation process, with ΔE being the activation energy of the process. From the slope of the line, it is calculated that $\Delta E = 4,960 \text{ cal/(g.mole)}$.

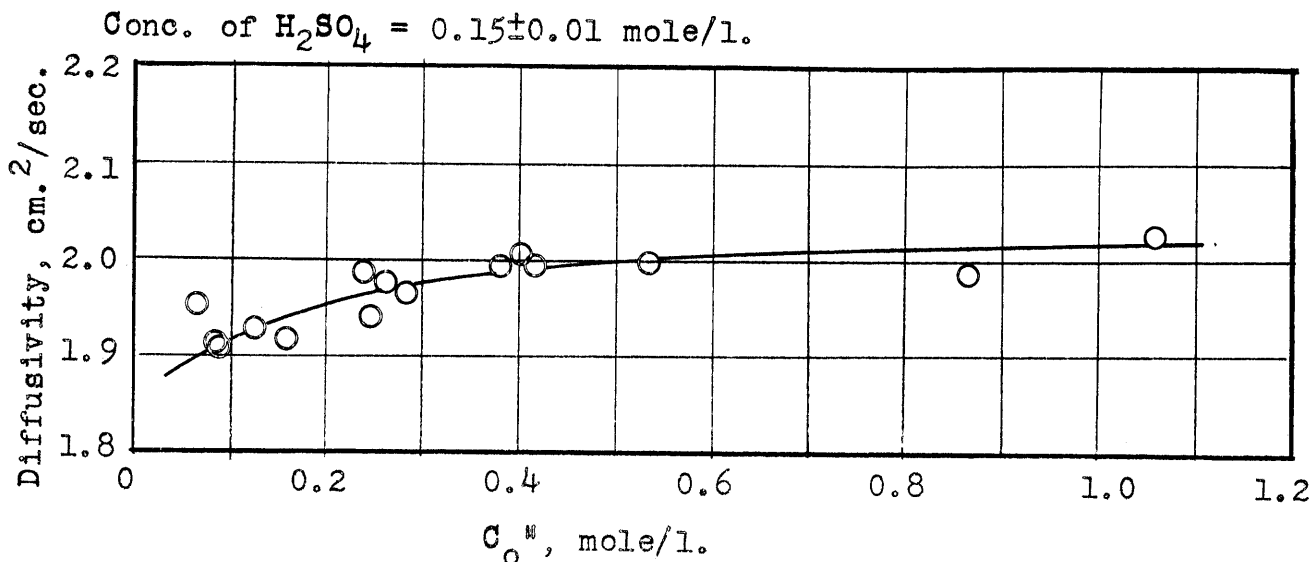
Actually, it must be borne in mind that the range of temperature is too small to establish definitely what type expression best gives the variation of diffusivity with temperature. Both the relationships used here adequately represent the data, as probably do some other expressions, but care should be exercised in using them to extrapolate the data beyond the range investigated here.

11.27. Diffusion of Sulfur Dioxide through Dilute Sulfuric Acid. The measurements on diffusion of sulfur dioxide in sulfuric acid and in water were made, for the most part, during the hot summer months and, even though a cooling coil was placed in the thermostat, the bath could not be maintained at 25°C . because the Cambridge city water came out of the tap at between 25° and 27°C . For this reason, most of the runs were made at 30°C ., and, in studying the effect of temperature, the range investigated was higher than for the chlorine studies. It was not until the end of the summer that the temperature of the tap water dropped sufficiently to permit measurements at 25° and 20°C .

Fifteen runs on sulfur dioxide in dilute sulfuric acid were made at 30°C ., using essentially one concentration of sulfuric acid. The decision to use just one concentration of H_2SO_4 was based on the results with chlorine in dilute hydrochloric acid which showed no effect of acid concentration, as well as on the calculation that less than five per cent of sulfur dioxide exists in the ionized form at the concentration of sulfuric acid used.

Fig. 11.6

Effect of Concentration on Diffusivity of Sulfur Dioxide
in Dilute Sulfuric Acid at 30°C.



The data and calculated results are presented in Table 11.13. As in the case of chlorine in dilute HCl, the diffusivity has been corrected for the viscosity of the sulfuric acid, the ratio of viscosities of sulfuric acid and water being taken from the International Critical Tables (45).

Figure 11.6 shows a plot of D , thus corrected for viscosity, versus C_0'' . There exists a significant dependence of the diffusivity on the concentration up to a value of C_0'' of about 0.4 moles/l., whereupon it levels off to a practically constant value. The observed increase with concentration is quite unusual, as shown by a glance at the tabulation of liquid diffusivities in the International Critical Tables (46). There it may be seen that wherever the effect of concentration has been determined, the diffusivity decreases with concentration, as would be expected from the Stokes-Einstein equation, since viscosity generally increases with concentration. However, no previous data have been reported on the effect of concentration on the diffusivity of dissolved gases, so that it may well be that solutions of gases in liquids behave differently from other solutes in this respect.

Table 11.13

Diffusion of Sulfur Dioxide through Dilute Sulfuric Acid at 30°C.Data and Calculated Results

Run No.	Cell	Concentrations, moles/l.			Volumes, cm. ³		Time hours	C ₀ " moles/l.
		Sulfur Dioxide C _f "	H ₂ SO ₄ C _f '	H ₂ SO ₄	V'	V"		
68	A	0.1355	0.0388	0.16	71.3	125.7	100.15	0.1584
69	C	.0746	.0180	.16	73.1	124.3	95.98	.0854
70	D	.0771	.0169	.16	66.8	127.3	95.53	.0862
71	E	.2331	.0453	.16	69.2	121.2	100.72	.2597
72	F	.3347	.0801	.16	66.1	120.2	100.92	.3796
73	A	0.10447	0.02782	0.15	71.3	125.7	91.97	0.1209
74	C	.2451	.0600	.15	73.1	124.3	94.73	.2809
75	D	.3697	.0854	.15	66.8	127.3	96.52	.4155
76	E	.2127	.0390	.15	69.2	121.2	94.37	.2357
77	F	.06037	.01309	.15	66.1	120.2	92.75	.0677
78	A	0.7378	0.2137	0.14	71.3	125.7	97.82	0.8635
79	C	.2119	.0534	.14	73.1	124.3	98.92	0.2437
80	D	.4705	.1130	.14	66.8	127.3	100.42	0.5311
81	E	.9472	.1899	.14	69.2	121.2	101.60	1.0590
82	F	.3520	.0850	.14	66.1	120.2	101.12	0.3997
Run No.	Cell	ΔC _f moles/l.	log ₁₀ (ΔC _f /ΔC ₀)	β cm. ⁻²	Dx10 ⁵ cm. ² /sec.	Correc- tion Factors for Vis- cosity	Corrected Dx10 ⁵ cm. ² / sec.	
68	A	0.0967	0.2141	0.0729	1.88	1.023	1.92	
69	C	.0566	.1785	.0636	1.87	1.023	1.91	
70	D	.0602	.1560	.0560	1.87	1.023	1.91	
71	E	.1878	.1409	.0463	1.93	1.023	1.98	
72	F	.2546	.1735	.0564	1.95	1.023	1.99	
73	A	0.0767	0.1978	0.0729	1.89	1.023	1.93	
74	C	.1851	.1812	.0636	1.92	1.023	1.97	
75	D	.2843	.1648	.0560	1.95	1.023	1.99	
76	E	.1737	.1326	.0463	1.94	1.023	1.99	
77	F	.0473	.1561	.0564	1.91	1.023	1.95	
78	A	0.5241	0.2169	0.0729	1.94	1.022	1.99	
79	C	.1585	.1868	.0636	1.90	1.022	1.94	
80	D	.3576	.1718	.0560	1.95	1.022	2.00	
81	E	.7573	.1456	.0463	1.98	1.022	2.02	
82	F	.2670	.1751	.0564	1.96	1.022	2.01	

Why, then, was this effect not noticed for the case of chlorine diffusing through water? The answer probably lies in the range of concentrations investigated which, because of the lower solubility, was sufficiently small that the variation of diffusivity was hidden by the scatter of the data.

11.28. Diffusion of Sulfur Dioxide through Water at 30°C. Ten runs were made, using two different initial concentrations of sulfur dioxide. The data obtained are listed in Table 11.14 along with the derived results.

In Fig. 11.7, $\log_{10}(\Delta C_o/\Delta C_f)$ has been plotted against βt , with different symbols used for the two initial concentrations of sulfur dioxide. Just as with chlorine in water, the plot is remarkably straight, showing no effect of either time or concentration on the slope of the line. Thus, just as for "total" chlorine, it is permissible to refer to the diffusivity of "total" sulfur dioxide, which may be calculated in the same way by eq. (11.73). This diffusivity has been calculated for each run in Table 11.14. The average value is 2.08×10^{-5} ; the standard deviation is 1.0%, the standard error of the mean is 0.3%. Thus, $D_C = (2.08 \pm 0.01) \times 10^{-5}$ cm.²/sec.

In order to calculate D_F , eqs. (11.67) and (11.73) are combined to give

$$D_C = D_G + (D_F - D_G)(\Delta F/\Delta C) \quad (11.80)$$

which may be solved for D_F

$$D_F = D_G + (D_C - D_G)/(\Delta F/\Delta C) \quad (11.81)$$

The values of F for each compartment at the beginning and end of every run was calculated, using the equilibrium relationship

$$K_S = \frac{F^2}{G} \quad (11.65)$$

where K_S is the apparent equilibrium constant, determined by Campbell and Maass (8) to be 0.0151 moles/l. at 30°C. Eq. (11.65) may be rewritten

$$K_S = \frac{F^2}{C-F} \quad (11.82)$$

and solved for F by trial and error.

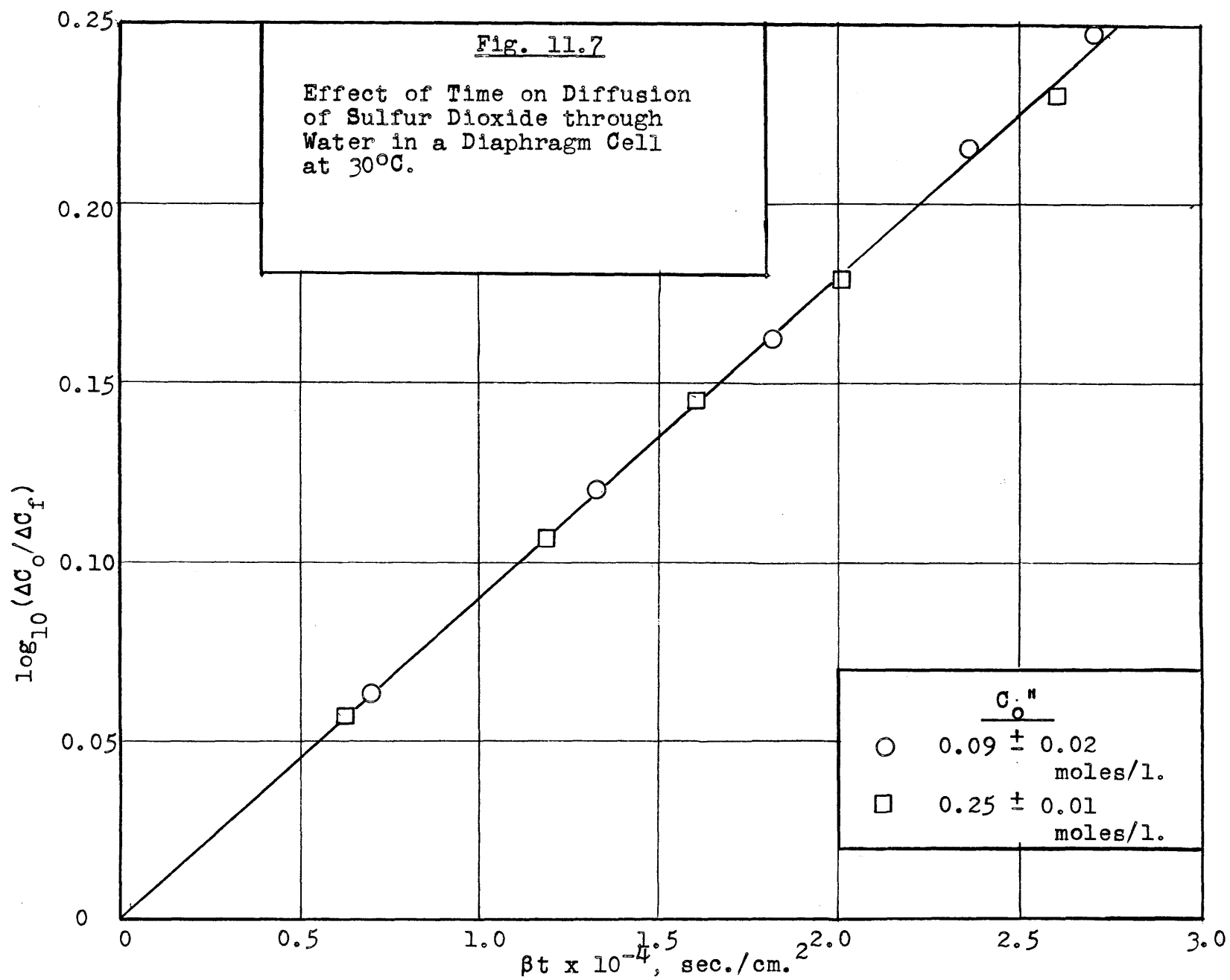
TABLE 11.14

Diffusion of Sulfur Dioxide through Water at 30°C.
Data and Calculated Results

Run No.	Cell	Concn., moles/l.		Volumes, cm. ³		Time, hours	C _o " moles/l.	ΔC _f moles/l.	log ₁₀ ($\frac{\Delta C_o}{\Delta C_f}$)	
		C _f "	C _f '	V _i	V _{ii}					
83	A	0.09318	0.02058	71.3	125.7	69.18	0.10540	0.07260	0.1619	
84	C	.07672	.02493	73.1	124.3	118.23	.09157	.05179	.2475	
85	D	.08023	.01374	66.8	127.3	65.97	.08764	.06649	.1200	
86	E	.08064	.00721	69.2	121.2	42.15	.08502	.07343	.0636	
87	F	.06896	.02011	66.1	120.2	116.13	.08020	.04885	.2153	
88	A	.2193	.06707	71.3	125.7	99.05	.2587	.1522	.2303	
89	C	.2374	.03530	73.1	124.3	51.92	.2587	.2021	.1071	
90	D	.2258	.05637	66.8	127.3	99.55	.2560	.1694	.1792	
91	E	.2296	.04589	69.2	121.2	96.80	.2566	.1837	.1452	
92	F	.2382	.01947	66.1	120.2	30.98	.2495	.2187	.0571	

Run No.	Cell	β cm. ⁻²	βt x 10 ⁻⁵ sec./cm. ²	D _c x 10 ⁵ cm. ² /sec.	Concentrations, moles/l.				ΔF _f ΔC _f	ΔF _o ΔC _o
					F _o "	F _f "	F _f '	ΔF _f		
83	A	0.0729	0.1816	2.05	0.03305	0.03071	0.01163	0.01908	0.263	0.314
84	C	.0636	.2708	2.10	.03039	.02731	.01327	.01404	.272	.332
85	D	.0560	.1329	2.08	.02960	.02807	.00871	.01936	.291	.338
86	E	.0463	.0702	2.09	.02907	.02815	.00533	.02282	.311	.342
87	F	.0564	.2359	2.10	.02806	.02559	.01144	.01415	.290	.350
88	A	.0729	.2601	2.04	.05541	.05049	.02516	.02533	.166	.214
89	C	.0636	.1189	2.07	.05540	.05280	.01674	.03606	.178	.214
90	D	.0560	.2006	2.06	.05508	.05133	.02259	.02874	.170	.215
91	E	.0463	.1612	2.07	.05516	.05181	.01983	.03198	.174	.215
92	F	.0564	.0629	2.09	.05429	.05290	.01118	.04172	.191	.218

Average $D_c = 2.08 \times 10^{-5}$ cm.²/sec.



The values of $\Delta F_f/\Delta C_f$ and $\Delta F_o/\Delta C_o$ are listed in the last two columns of Table 11.14. It can be seen that there is comparatively little variation of $\Delta F/\Delta C$ with time. Thus, for each value of C_o'' , it is possible to assign a value of $\Delta F/\Delta C$; in the following table, for each set of runs, average values of C_o'' and $\Delta F/\Delta C$ were taken.

Runs	C_o''	$\Delta F/\Delta C$
83-87	0.090	0.31
88-92	0.256	0.20

The appropriate value of D_G to use in eq. (11.81) is obtained by calculating G_o'' from C_o'' and using this as the abscissa on Fig. 11.6 to obtain D_G . Then D_F may be calculated by eq. (11.81) for each C_o'' .

C_o''	G_o''	D_G	D_F
0.090	0.06	1.90	1.96
0.256	0.20	1.95	2.01

Although we have observed an increase in D_G with concentration, the accuracy of these data are not sufficient to allow one to ascribe a like trend to D_F . It may only be concluded that at 30°C. over the range investigated, D_F is $1.99 \pm 0.03 \times 10^{-5}$ cm.²/sec.

11.29. Effect of Temperature on Diffusion of Sulfur Dioxide in Water. The effect of temperature on D_j was studied by making eight runs at four different temperatures, in addition to the ten runs made at 30°C. which have been discussed in the previous section. The data and derived results are presented in Table 11.15; the results are plotted on Figs. 11.8 and 11.9.

Fig. 11.8 also includes the value obtained by Kolthoff and Miller, which appears to be significantly higher than the results obtained here.

Fig. 11.8 shows a comparison of the data with the Stokes-Einstein equation, where 30°C. is chosen as the reference temperature. The agreement is good.

On Fig. 11.9 where $\log D$ is plotted against the reciprocal of the absolute temperature, the data fall equally well on a straight line, indicating that eq. (11.79) may be used. From the slope of the line, it is calculated that $\Delta E = 4,360$ cal./(g.mole).

Table 11.15

Effect of Temperature on Diffusion of Sulfur Dioxide Through WaterData and Calculated Results

Run No.	Cell	Temp. °C.	Concn., moles/l.		Volumes, cm. ³		Time hours
			C_f''	C_f'	V'	V''	
93	A	40.0	0.19373	0.07065	71.3	125.7	95.43
94	F	40.0	.20036	.05958	66.1	120.2	96.07
95	A	35.0	0.20177	0.06150	71.3	125.7	87.18
96	F	35.0	.20814	.05198	66.1	120.2	87.92
97	A	25.0	0.20416	0.05145	71.3	125.7	89.97
98	F	25.0	.20907	.04393	66.1	120.2	92.60
99	A	20.0	0.20308	0.04802	71.3	125.7	95.12
100	F	20.0	.20820	.04033	66.1	120.2	95.90

Run No.	Cell	C_o'' moles/l.	ΔC_f moles/l.	$\log_{10}(\Delta C_o/\Delta C_f)$	β cm. ⁻²	Apparent $D \times 10^5$ cm. ² /sec.
93	A	0.23507	0.12308	0.2810	0.0729	2.58
94	F	0.23368	0.14078	0.2201	0.0564	2.60
95	A	0.23791	0.14027	0.2295	0.0729	2.31
96	F	0.23728	0.15616	0.1817	0.0564	2.34
97	A	0.23456	0.15271	0.1864	0.0729	1.82
98	F	0.23377	0.16514	0.1509	0.0564	1.85
99	A	0.23151	0.15506	0.1741	0.0729	1.61
100	F	0.23091	0.16787	0.1385	0.0564	1.64

Fig. 11.8

Effect of Temperature on Diffusivity of "Total" Sulfur Dioxide in Water

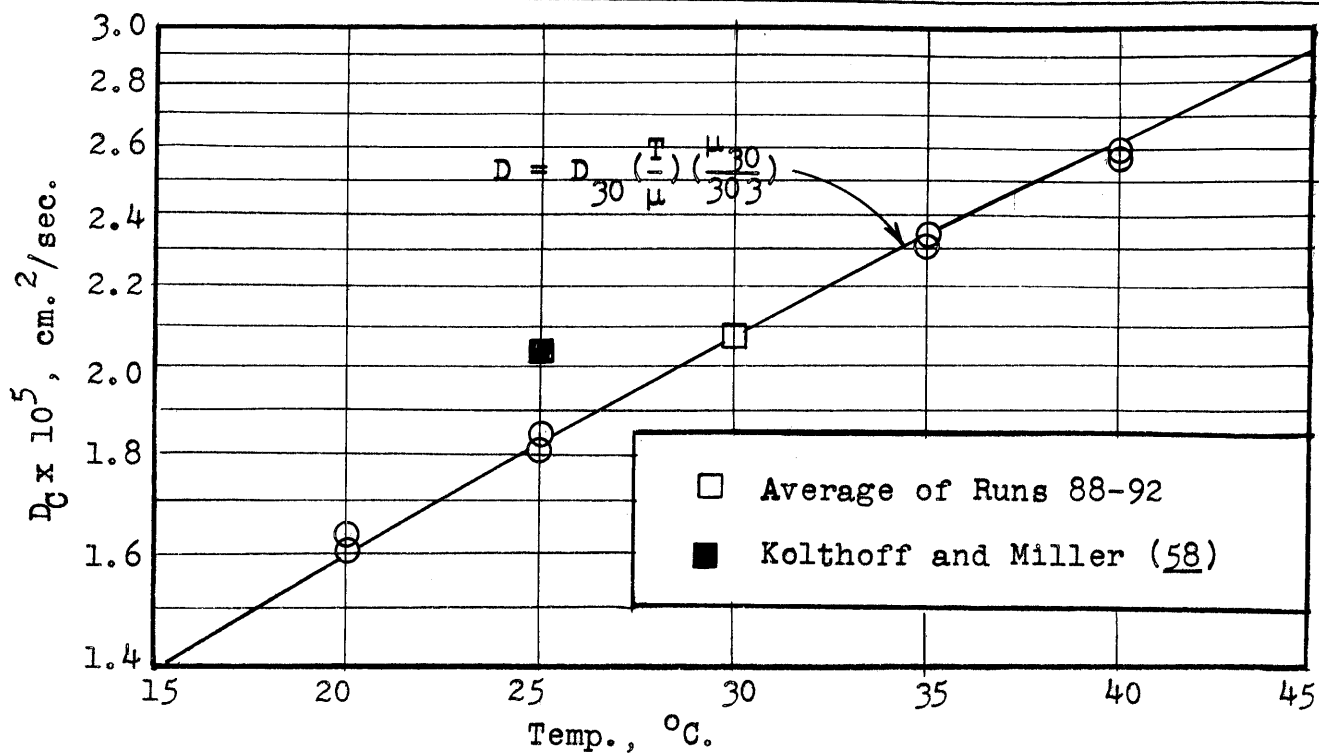
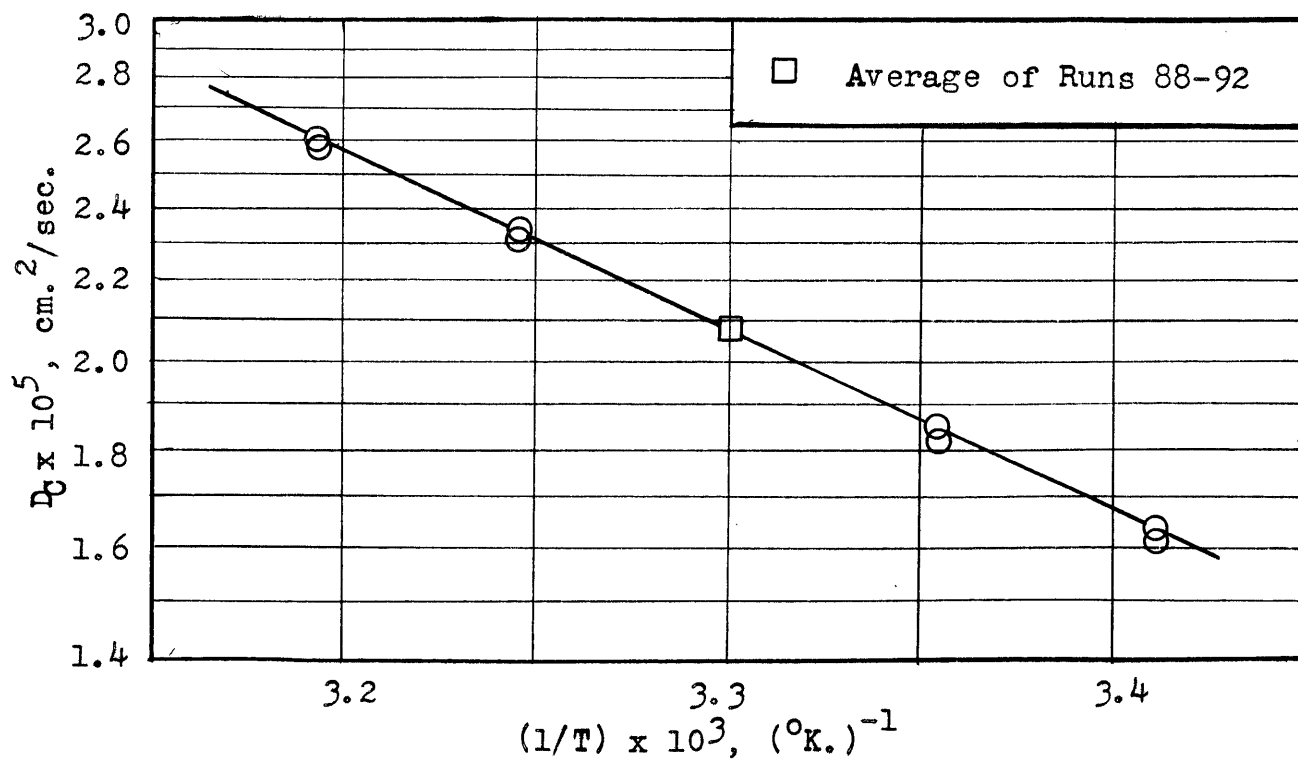


Fig. 11.9

Effect of Temperature on Diffusivity of "Total" Sulfur Dioxide in Water



Again, the range of temperature investigated is too small to establish which expression best gives the variation of diffusivity with temperature. It can only be said that both of the relationships used here adequately represent the data.

11.30. Miscellaneous Measurements. Several measurements were made on two other solutes chiefly for the purpose of comparison with other data in the literature in order to establish confidence in the method used here, rather than to obtain any additional data. However, they are included here for completeness. The data and derived results are listed in Table 11.16.

The results found for HCl at 10°C., 2.03×10^{-5} cm.²/sec., agrees very well with the value of 2.02×10^{-5} found by James and Gordon (see Table 11.2), who also used the diaphragm cell method.

The average of the four runs on CO₂ at 30°C. have been plotted with the previously reported values for CO₂ (see Table 11.5) in Fig. 11.10. The scatter among the points is considerable. The least squares line was calculated and is shown on the plot. Also shown is a curve representing the Stokes-Einstein relationship, with the value of D given by the least squares line at 25°C. used as the reference. It can be seen that the Stokes-Einstein equation does not adequately represent the trend of the value.

In order to round out the picture, the values reported in the literature for oxygen (see Table 11.4) are plotted on Fig. 11.11. The lack of agreement among the various workers is quite apparent. It seems likely that the values of Tammann and Jessen are too high, because their measurements were made using solutions of agar, and it is quite possible that some of the oxygen was consumed by reaction with the agar thus giving high apparent rates of diffusion.

11.31. Sources of Error. One of the most important sources of error lies in the method of sampling. When liquid containing a volatile solute is first drawn into the pipette, desorption takes place at the surface so that the contents of the pipette are at first somewhat lower in concentration than the sample. Because slug flow does not exist within the pipette (as discussed in Sec. 5.3) this lean mixture continues to mix with the liquid that is sucked through afterwards.

Table 11.16

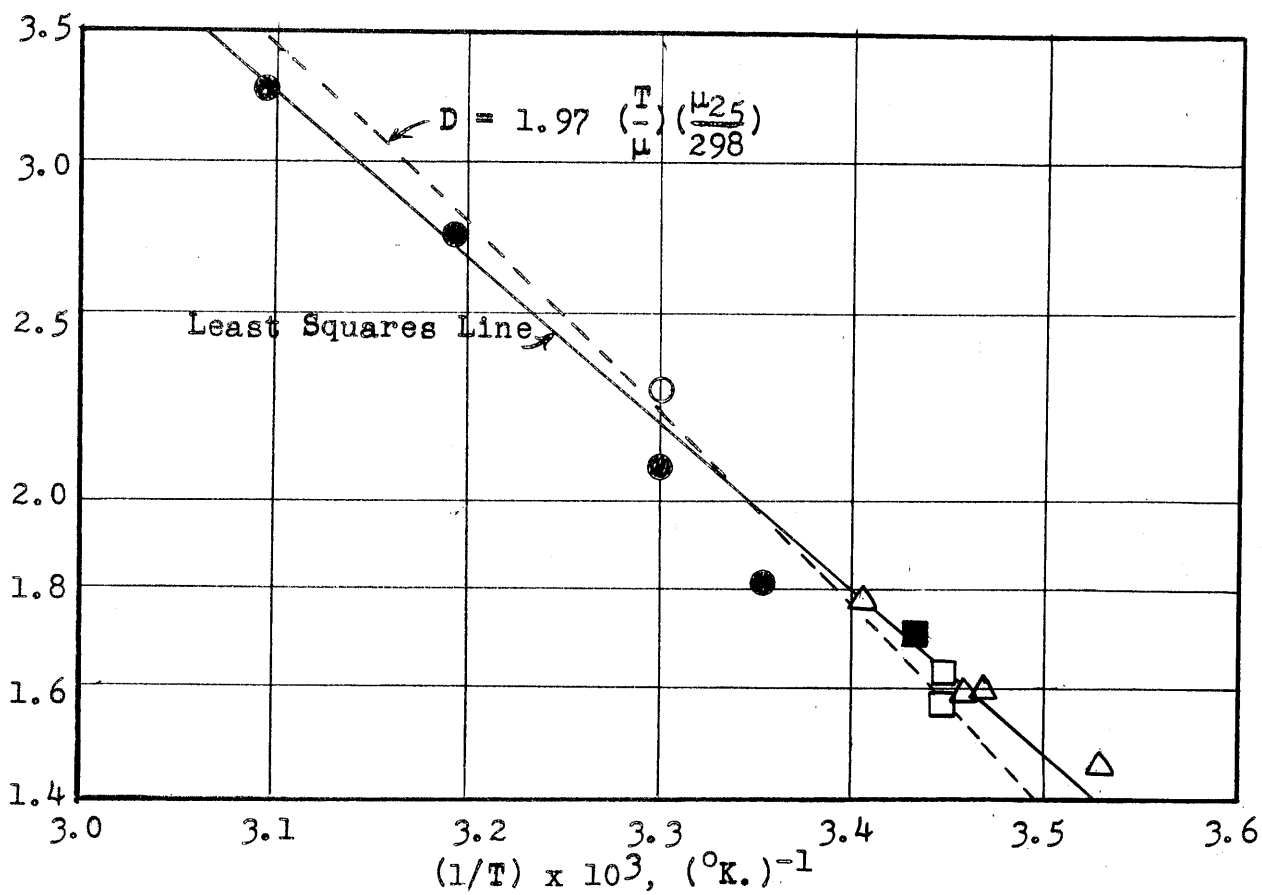
Miscellaneous Diffusion MeasurementsData and Calculated Results

Run No.	System	Cell	Temp. °C.	Concn., moles/l.		Volumes, cm. ³		Time hours
				C _F ^{''}	C _F [']	V [']	V ^{''}	
101	HCl in H ₂ O	A	10.0	0.08947	0.01921	71.3	125.7	67.22
102	CO ₂ in H ₂ O	A	30.0	0.04323	0.02119	71.3	125.7	145.30
103	"	D	30.0	0.04763	0.01991	66.8	127.3	165.13
104	"	E	30.0	0.04622	0.01661	69.2	121.2	165.30
105	"	F	30.0	0.04738	0.01740	66.1	120.2	144.63

Run No.	C ₀ ^{''} moles/l.	ΔC _F moles/l.	log ₁₀ (ΔC ₀ /ΔC _F)	β ₋₂ cm. ⁻²	Dx _{1/2} 10 ⁵ cm./sec.
101	0.10007 ^a 0.10088 ^b	0.07026	0.1536 ^c 0.1571 ^d	0.0729	2.00 ^c 2.05 ^d 2.03 (avg)
102	0.05555	0.02204	0.4015	0.0729	2.42
103	0.05822	0.02772	0.3223	0.0560	2.23
104	0.05589	0.02961	0.2759	0.0463	2.31
105	0.05709	0.02998	0.2797	0.0564	2.19 2.29 (avg)

- a - Measured value of C₀^{''}
b - C₀^{''} calculated by eq. (11.70)
c - Calculated, using ΔC₀ = measured C₀^{''}
d - Calculated, using ΔC₀ = calculated C₀^{''}

Fig. 11.10

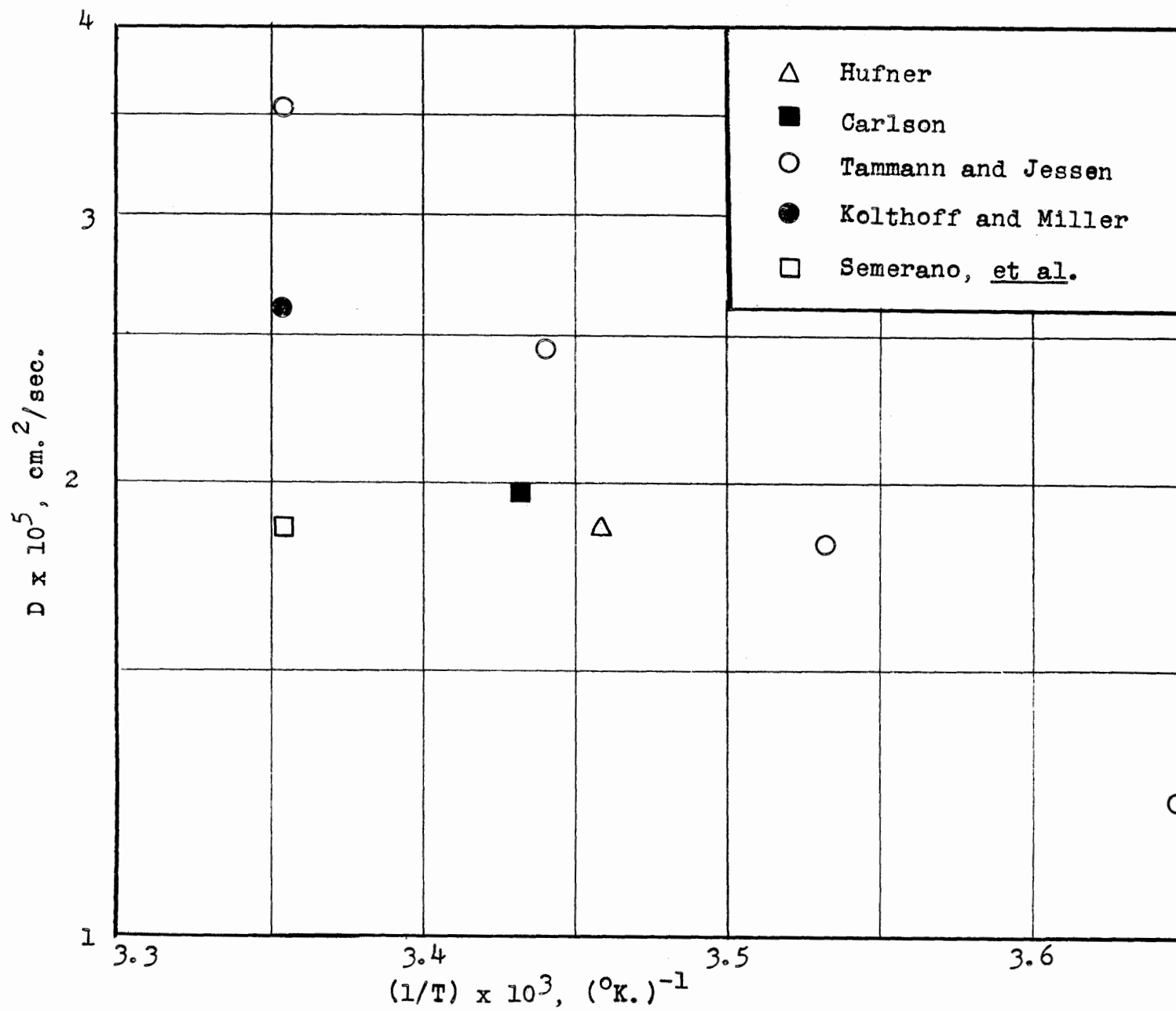
Comparison of Data on Diffusivity of Carbon Dioxide in Water

See Table 11.5

- Stefan
- △ Hüfner
- Carlson (Average of 3 values)
- Ringbom
- This thesis (Average of Runs 102-105)

Fig. 11.11

Comparison of Data on Diffusivity of Oxygen in Water



As only two or three volumes are sucked through the pipette, the resulting sample has too low a concentration. However, samples from both the upper and lower chambers are subject to this error, and since ratios of concentrations are used to calculate the diffusivities, the main effect of this error is to increase the scatter of the results.

Another potential source of error lies in the possibility of surface transport of the solute, a possibility which exists because of the large surface area within the diaphragm. Stokes (96) has shown that anomalously rapid transport of an electrolytic solute takes place in dilute solutions, below 0.05N. Thus, above 0.05N, the integral diffusivities he measured for KCl agreed well with those calculated from Harned and Nuttall's data (calculated as in Sec. 11.19 here), while they became high as the concentration approached zero. He also found the same effect with KBr. Stokes referred to the work of Mysels and McBain (78) as confirming this phenomenon. They made conductivity measurements in a cell with a Pyrex diaphragm placed between the electrodes, and found that 0.1N KCl behaved reproducibly, while 0.0005 N KCl gave erratic values which varied with time and depended on the previous treatment of the diaphragm. They also found that the ratio of the conductivity of 0.0005N solution to that of 0.1N solution is 5-10 per cent higher than the ratio in the absence of the diaphragm. Stokes concludes that the diaphragm-cell technique should be restricted to solutions of concentration greater than 0.05N if accurate results are desired, at least with electrolytes.

There is no information available as to whether there is any surface transport when the solute is a non-electrolyte, but the possibility of such anomalous transport of the dissolved gases investigated here should be borne in mind. Furthermore, dilute solutions of electrolytes are present in the solutions of chlorine and sulfur dioxide in water, so that it is likely that the results are affected somewhat by this phenomenon; it is not yet possible to evaluate the magnitude of this effect, however.

Further uncertainty exists in the use of density stirring rather than mechanical stirring. This problem has been discussed in Sec. 5.2.

The more conventional sources of error which are present in the analytical procedures can be evaluated. As pointed out in Sec. 11.23, the maximum error due to

the analysis is estimated to be about 1.4 per cent. Considering the additional scatter caused by the sampling technique, the values of standard deviations of 1 to 2.5 per cent encountered in this work appear to be quite reasonable.

G. Conclusions and Recommendations

11.32. It is concluded that, in spite of the uncertainties listed above, the diaphragm-cell technique gives results correct to within a few per cent, an accuracy which is entirely satisfactory for engineering purposes.

In view of the discrepancy which exists among various investigators on the diffusivities of other gases and because of the importance of these measurements in mass transfer work, it is recommended that diaphragm cells be used to study the diffusion in water of various gases; in particular, oxygen, carbon dioxide, hydrogen, ammonia and nitrogen. It is also recommended, in further work with dissolved gases, that the diaphragm cells be redesigned so that the sampling may be done, not by using a pipette, but by allowing the sample to flow directly into the solution in the receiving flask, and weighing the flask before and after taking the sample. This method of sampling was used in the work on desorption of chlorine in water, and was found to work very well. If still more precise results are desired, it is recommended that mechanical stirring be used.

CHAPTER 12

EFFECT OF DIFFUSIVITY ON LIQUID-SIDE RESISTANCE
IN PACKED COLUMNS

One of the main arguments supporting the applicability of Higbie's penetration theory (37) to packed columns is the finding of Sherwood and Holloway (93) that k_L^*a varies as the 0.47 power of the liquid diffusivity, in excellent agreement with Higbie's prediction of an exponent of 0.50. A close examination of Holloway's work shows that on the basis of his data, the above conclusion is unjustified and, furthermore, that the data available are not sufficient to pin down definitely the value of the exponent.

Holloway studied the desorption from water into air of carbon dioxide, oxygen and hydrogen. In his first series of runs, which were made with all three gases using 1.5 inch Raschig rings, the measured solute transfer included a rather large end effect at the bottom, estimated by Holloway to be equivalent to six inches of packing, as compared with the actual packed height of eight inches. The coefficients he calculated were based on the actual packed height; consequently, as he pointed out, the results could be used only for purposes of comparison. With these data, he evaluated the effect of temperature and of diffusivity. A second series of runs was then made in which sampling funnels were placed immediately below the packing. By varying the packed height, he showed that his end effect then was negligible. Only oxygen was used in the second series, and the effect of liquor rate and size and type of packing were investigated.

Having determined that, in the first series, the coefficients varied with the 0.75 power of the liquor rate, Holloway (40) plotted the data on two graphs which are reproduced on Figs. 12.1 and 12.2. The values of diffusivity which he used to calculate $(\mu/\rho D)$ are listed in the following table.

TABLE 12.1
Diffusivities of Several Gases in Water

<u>Gas</u>	<u>$D \times 10^5$, cm.²/sec.</u>	<u>Temp. °C.</u>
CO ₂	1.71	18.0
O ₂	1.98	18.0
H ₂	4.7	16

He corrected these values for temperature by use of the Stokes-Einstein equation:

$$D \propto T/\mu \quad (12.1)$$

The slope of the line of Fig. 12.2 is 0.47, from which he concluded that k_L^*a/D varies as the 0.53 power of $(\mu/\rho D)$, and hence that k_L^*a varies as the 0.47 power of D .

Fig. 12.1

Desorption in Packed Column

Data of Holloway (40)

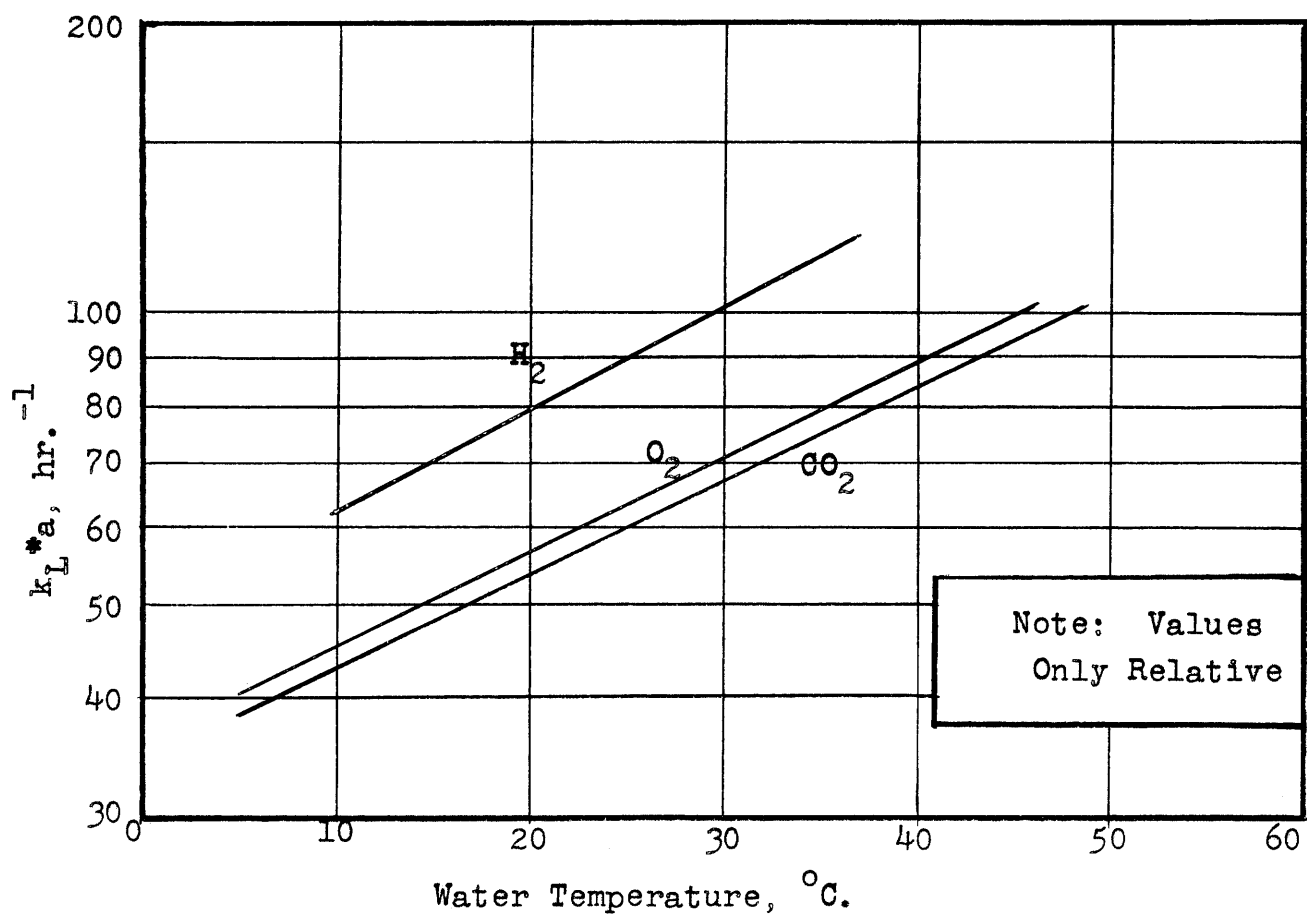
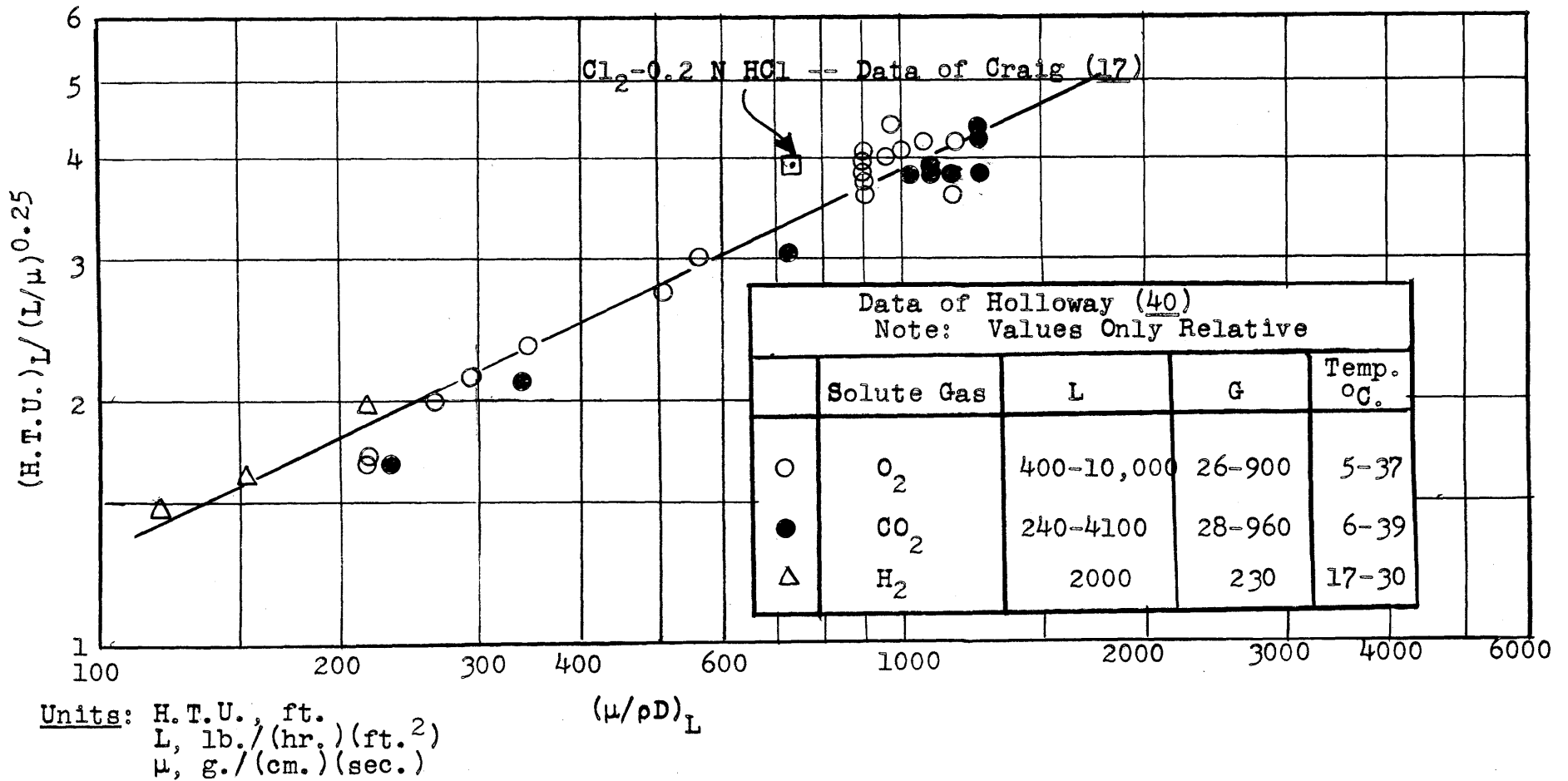
 $L = 2000 \text{ lb.}/(\text{hr.})(\text{ft.}^2)$; $G = 230 \text{ lb.}/(\text{hr.})(\text{ft.}^2)$ 

Fig. 12.2

Effect of Schmidt Number in Packed Columns



Two other sets of data should be described at this point. Vivian and Whitney (101) desorbed oxygen from water in a column packed with one-inch Raschig rings at 70°F. and obtained the results shown on Fig. 12.3. These results are in excellent agreement with those of Sherwood and Holloway. Craig (17) absorbed chlorine in 0.2 N hydrochloric acid, also in one-inch Raschig rings at the same temperature, and his results are also shown on Fig. 12.3.

Now, knowing the diffusivities of chlorine and oxygen, it should be possible to predict from the oxygen coefficients what the chlorine coefficients obtained by Craig should be since, in the presence of hydrochloric acid, the hydrolysis of the chlorine was suppressed and the system is a physical one which should fit the Sherwood and Holloway correlation. The diffusivity of chlorine in dilute hydrochloric acid was measured in this thesis, and is shown in Sec. 11.24 to be 1.48×10^{-5} cm.²/sec. at 25°C., and is shown to vary with temperature according to eq. (12.1). Using this equation, the diffusivity at 70°F. is 1.33×10^{-5} . The diffusivity of oxygen used by Holloway is 1.98×10^{-5} at 18°C.; using eq. (12.1), this becomes 2.16×10^{-5} at 70°F. Using an exponent on D of 0.50, the chlorine coefficients should be $(1.33/2.16)^{0.5}$ or 0.785 times the oxygen coefficients. This predicted line is shown as a dotted line on Fig. 12.3. Craig's data fell about 14% below the predicted line.

Further evidence that Craig's data fail to correlate with the others may be seen on Fig. 12.2. Since Craig's values of k_L^*a vary as $L^{0.75}$, all of his data would plot as a single point on this plot. Two corrections must be made; one for the fact that Holloway and Craig used different size Raschig rings, and the other for Holloway's end effect. Holloway showed that the ratio of H.T.U.'s for 1.0- and 1.5-inch rings is 0.9; he also estimated that his end effect was equivalent to six inches of packing, while his actual packed height was eight inches. Therefore, in order to compare them with Holloway's data, Craig's values of H.T.U.'s must be multiplied by a factor of $(1/0.9)$. $(8/14)$. The point representing all of Craig's data falls 18% higher than Holloway's line.

Before attempting to explain this failure of the chlorine-0.2 N HCl system to fit into the Sherwood and Holloway correlation, it is necessary to examine this correlation more closely, particularly with regard to the effect of diffusivity. To this end, the data of Fig. 12.1 are replotted on Fig. 12.4. Values of D were taken from Table 12.1, and corrected by eq. (12.1) to 70°F.; values of k_L^*a were taken from Fig. 12.1 corresponding to 70°F. For the Cl₂-0.2 N HCl system, the value of k_L^*a corresponding to $L = 2000$ lb./((hr.)(ft.²)) was determined from Craig's data and corrected for the difference in size of packing and the end effect by multiplying by $(0.9)(14/8)$. Again, it can be seen that Craig's data lie well below the line for Holloway's data. But more important, the slope of the line

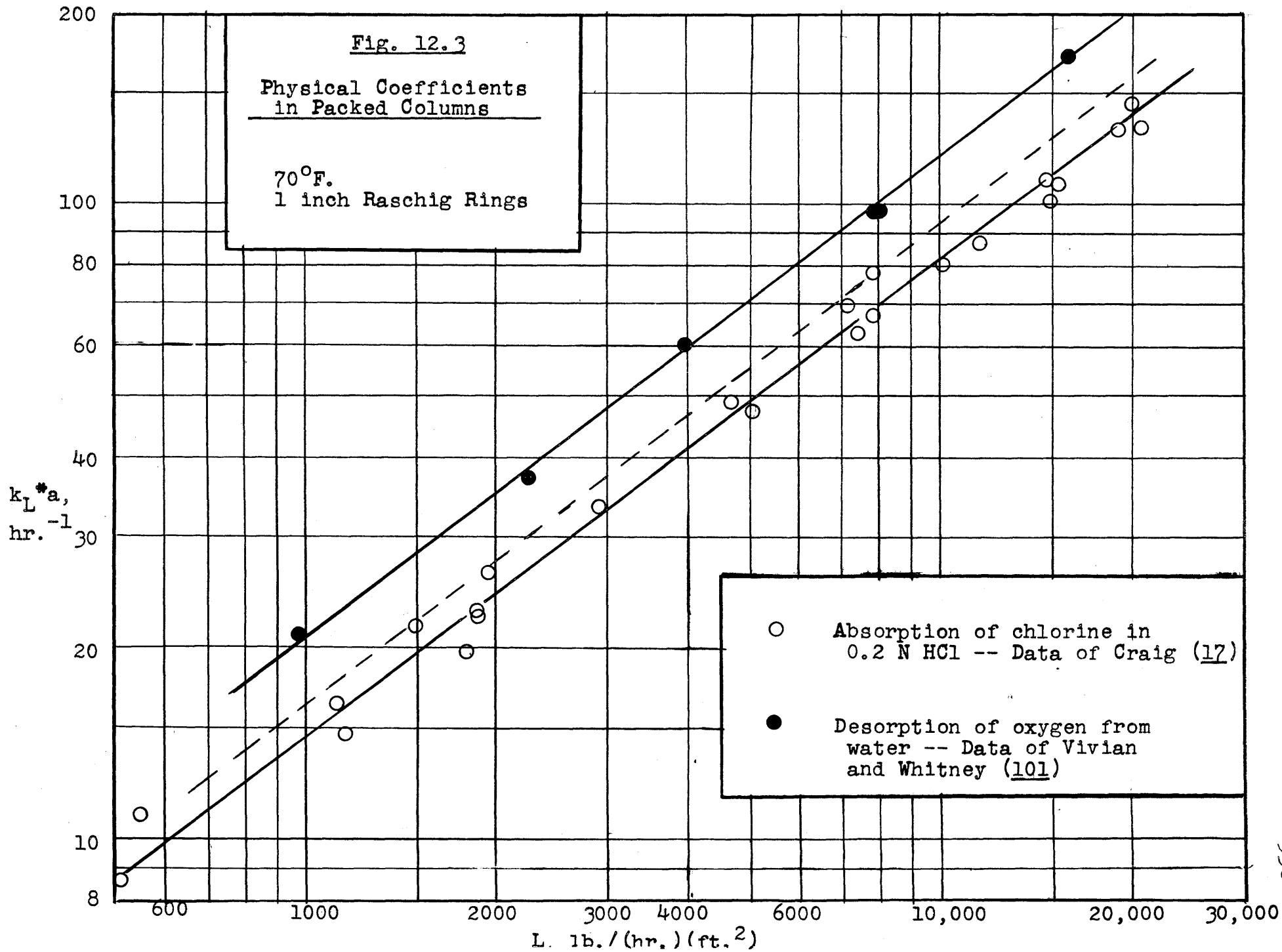
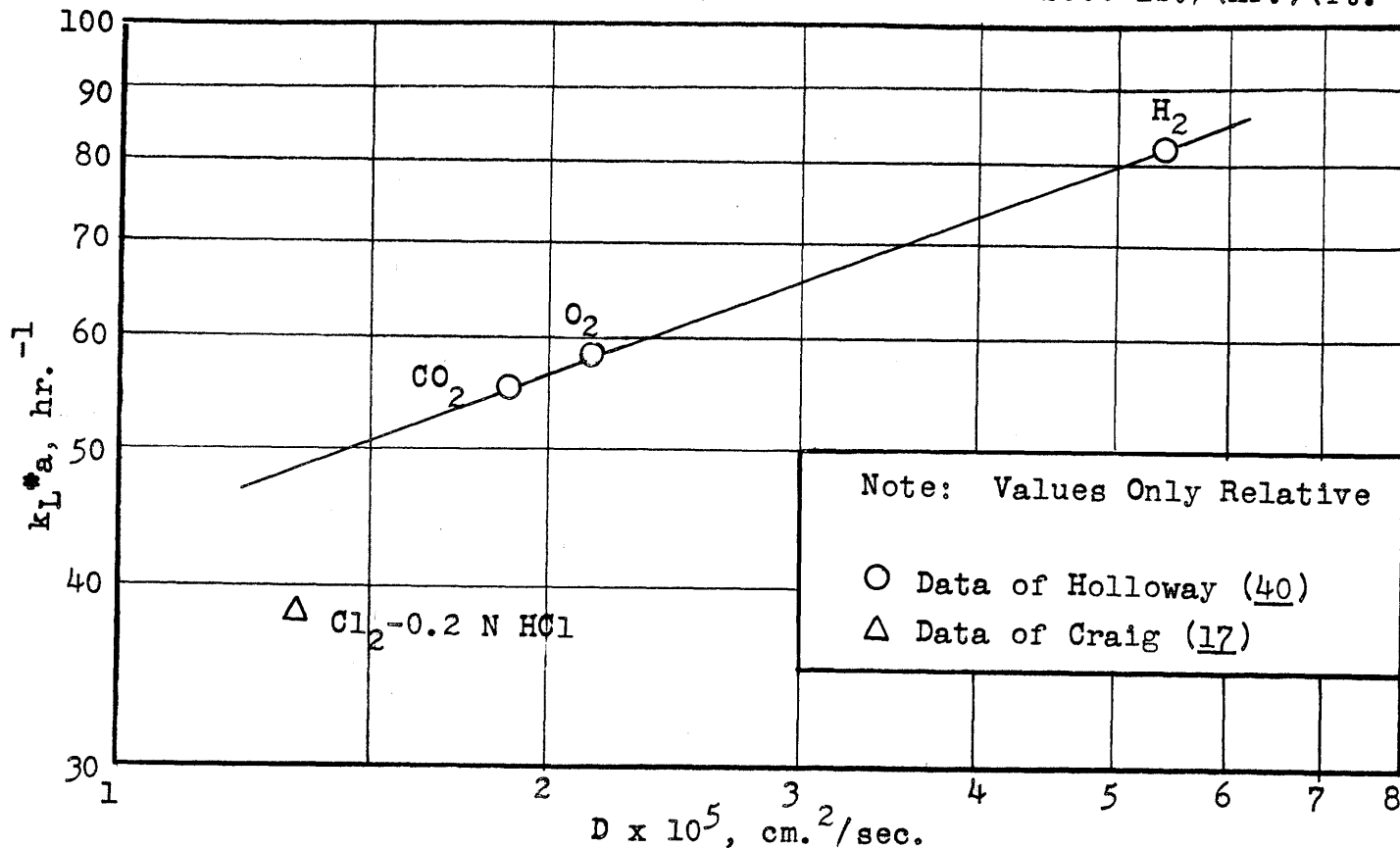


Fig. 12.4

Effect of Diffusivity on Physical Coefficients in Packed Columns1.5 inch Raschig Rings Temp. = 70°F. L = 2000 lb./ (hr.) (ft.²)

for Holloway's data is only 0.37, very much different from Holloway's value of 0.47.

It will be remembered that Holloway obtained the figure of 0.47 from the slope of Fig. 12.2. In determining the effect of $(\mu/\rho D)$ on this plot, he was determining, for the most part, the effect of changing the temperature on H.T.U., and to a lesser extent the effect of changing the diffusivity. Furthermore, the diffusivities at the various temperatures used to calculate the Schmidt number were obtained by the use of the Stokes-Einstein equation. The validity of this equation for solutions of gases has not been established; the data on oxygen and hydrogen are too few to determine the effect of temperature, while, as may be seen from Fig. 11.10, the available data for carbon dioxide show that this equation is not satisfactory.

It is quite clear that Holloway's data do not support the contention of the 0.5 power of the diffusivity, but do they refute it? In view of the fact that in the runs used to evaluate the effect of diffusivity, almost half the mass transfer occurred

in the bottom section below the packing, and in view of the probability that the mechanism of liquid-side resistance in the bottom section is very different from that in the packed section, it would not be surprising if the effect of diffusivity which he actually obtained were different from what would be obtained with no end effect. It is quite possible that in the bottom section, the mechanism of mass transfer might involve chiefly eddy diffusion, wherein the effect of diffusivity would be small, thus causing the overall apparent effect of diffusivity to be low.

What information can be obtained by comparison of Vivian's oxygen data with Craig's chlorine data? From Fig. 12.3, we can see that the ratio of oxygen to chlorine coefficients is 1.45. Using the same values of diffusivity for oxygen and chlorine used so far, we can write

$$k_L \cdot a(\text{oxygen}) / k_L \cdot a(\text{chlorine}) = (D_{O_2} / D_{Cl_2})^n \quad (12.2)$$

$$1.45 = (2.16 / 1.33)^n$$

Solving for n gives $n = 0.77$. This exponent on the diffusivity seems to be too high. However there is a great uncertainty in this calculation, namely, the diffusivity of oxygen. Fig. 11.11 shows that the disagreement among various investigators on the diffusivity of oxygen is very great. The value used by Holloway was that obtained by Carlson, among the lowest of the values.

If we suppose n to be 0.5 in eq. (12.2), and solve for the diffusivity of oxygen, using the same value of diffusivity of chlorine, which was measured in this thesis, we have

$$1.45 = (D_{O_2} / 1.33)^{0.5}$$

which gives $D_{O_2} = 2.8 \times 10^{-5}$ cm.²/sec, (at 70°F.). This value lines up very well with the three values found by Tammann and Jessen.

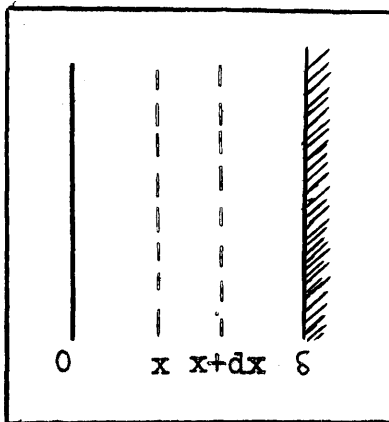
Thus, on the basis of the available data, it is not unreasonable to use an exponent of 0.5 on diffusivity, but it must be emphasized that the available data are too meager to indicate definitely what the exponent should be. In order to pin down this exponent, the diffusivities of oxygen and hydrogen and possibly carbon dioxide in water should be studied, just as chlorine and sulfur dioxide have been studied in this thesis. The available data on the oxygen-water and chlorine-0.2 N HCl systems in packed columns may be sufficient to establish the exponent fairly well; however, it may be necessary to repeat the desorption of hydrogen and oxygen in a packed column, taking due precautions against end effects.

CHAPTER 13

INTERFACIAL LIQUID VELOCITY IN SHORT WETTED-WALL COLUMNS

13.1. Introduction. In using the penetration theory to calculate the liquid-side coefficient of absorption in the short wetted-wall column, it is necessary to know the time of exposure of an element of surface to the gas phase. This time of exposure may be calculated directly from the interfacial velocity of the liquid.

13.2. Flow Down a Plane Surface. The simplest set of assumptions that can be made concerning the flow of fluid down a surface are: the surface is vertical and plane; the velocity of the liquid at the surface is zero; the shearing force on the liquid at the gas-liquid interface is zero; there is no change of velocity with vertical distance.



Using Fig. 13.1, consider a force balance on an element of fluid of unit area and thickness dx . The downward force on the left face is

$$-\mu \frac{dv}{dx}$$

The upward force on the right face is

$$-\mu \left(\frac{dv}{dx} + \frac{d^2v}{dx^2} dx \right)$$

Fig. 13.1
Profile of Liquid Layer

In addition, there is a downward force due to gravity, $\rho g dx$. Equating the upward to the downward forces,

$$-\mu \left(\frac{dv}{dx} + \frac{d^2v}{dx^2} dx \right) = -\mu \frac{dv}{dx} + \rho g dx$$

$$\text{or} \quad \mu \frac{d^2v}{dx^2} + \rho g = 0 \quad (13.1)$$

The boundary conditions are

$$\text{At } x = 0, \quad \frac{dv}{dx} = 0 \quad (13.2)$$

$$\text{At } x = \delta, \quad v = 0 \quad (13.3)$$

Integrating eq. (13.1) once,

$$\mu \frac{dv}{dx} + \rho gx = c_1$$

Using B.C. (13.2), we have $c_1 = 0$

Integrating again,

$$\mu v + \frac{\rho g}{2} x^2 = c_2$$

Using B.C. (13.3) we obtain

$$c_2 = \rho g \delta^2 / 2$$

whence

$$v = \frac{\rho g}{2\mu} (\delta^2 - x^2) \quad (13.4)$$

and

$$v_i = \rho g \delta^2 / 2\mu \quad (13.5)$$

We wish to relate v_i to Γ . Integrating velocity, we have

$$\Gamma / \rho = \int_0^{\delta} v \, dx \quad (13.6)$$

$$\Gamma = \frac{\rho g}{2\mu} \int_0^{\delta} (\delta^2 - x^2) \, dx$$

$$\Gamma = \rho^2 g \delta^3 / 3\mu \quad (13.7)$$

By eliminating δ between eqs. (13.5) and (13.7) we obtain

$$v_i = \left(\frac{2 g \Gamma^2}{8 \mu \rho} \right)^{1/3} \quad (13.8)$$

Eqs. (13.7) and (13.8) may be expressed in terms of two dimensionless parameters, the Reynolds number, Re , and the friction factor, f . The Reynolds number is defined by

$$Re = \frac{4r_h v_{av} \rho}{\mu} \quad (13.9)$$

where r_h is the hydraulic radius, the ratio of the cross-sectional area of the liquid to the wetted perimeter. Since $r_h = \delta$, and $v_{av} \rho = \Gamma / \delta$, we have

$$Re = \frac{4\Gamma}{\mu} \quad (13.10)$$

The friction factor may be defined by the Fanning equation.

$$\frac{dF}{dL} = \frac{f v_{av}^2}{2g_c r_h} \quad (13.11)$$

Since $dF/dL = g$, $g_c = 1$ in the metric system, $v_{av} = \Gamma/(\rho\delta)$, and $r_h = \delta$, we have

$$f = 2g\rho^2 \delta^3 / \Gamma^2 \quad (13.12)$$

By combining eqs. (13.7) and (13.12), we obtain

$$\Gamma = 6\mu/f \quad (13.13)$$

Substitution into eq. (13.10) yields

$$f = 24/Re \quad (13.14)$$

Eqs. (13.8) and (13.10) may be combined to give

$$v_1 = \left(\frac{9}{128} \frac{g\mu Re^2}{\rho} \right)^{1/3}$$

$$\text{or } v_1 \left(\frac{\rho}{g\mu} \right)^{1/3} = \left(\frac{9}{128} \right)^{1/3} Re^{2/3} \quad (13.15)$$

13.3. Effect of Gas Rate. To study the effect of the shearing force of the gas on the liquid, we proceed as follows. Let \mathcal{T} be the shear force upward on the liquid per unit area at the interface. Then, the same differential equation holds, but one boundary condition changes.

$$\text{At } x = 0, \quad \mu dv/dx = \mathcal{T} \quad (13.16)$$

$$\text{At } x = \delta, \quad v = 0 \quad (13.17)$$

Proceeding as before, we get $c_1 = \mathcal{T}$

$$\mu \frac{dv}{dx} + \rho gx = \mathcal{T}$$

$$\mu v + \frac{\rho g}{2} x^2 = \mathcal{T}x + c_2$$

$$c_2 = \rho g \delta^2 / 2 - \mathcal{T} \delta$$

$$v = \frac{\rho g}{2\mu} (\delta^2 - x^2) - \frac{\mathcal{T}}{\mu} (\delta - x) \quad (13.18)$$

$$v_1 = \frac{\rho g \delta^2}{2\mu} - \frac{\mathcal{T} \delta}{\mu} \quad (13.19)$$

Using eq. (13.6) we get

$$\Gamma = \frac{\rho^2 g}{2\mu} \int_0^{\infty} (\delta^2 - x^2) dx - \frac{\mathcal{T} \rho}{\mu} \int_0^{\infty} (\delta - x) dx$$

$$\Gamma = \frac{\rho^2 g \delta^3}{3\mu} - \frac{\mathcal{T} \rho \delta^2}{2\mu} \quad (13.20)$$

The relation of \mathcal{T} to the upward velocity of the gas may be found by use of the equation defining the friction factor, f . See McAdams (66), p. 117.

$$\mathcal{T} = f \rho_G (v_{G,av} - v_1)^2 / 2 \quad (13.21)$$

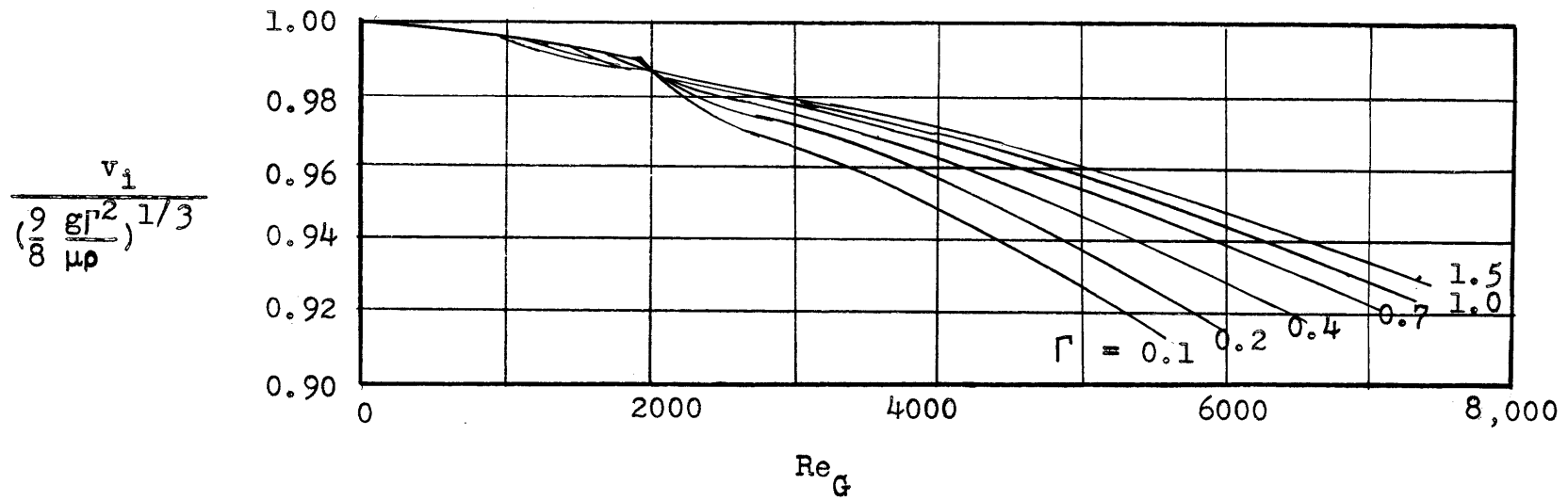
where $v_{G,av}$ is the average velocity of the gas relative to the pipe surface. The friction factor is, of course, related to the relative Reynolds number of the gas, which is computed from $v_{G,av} - v_1$.

Eqs. (13.19), (13.20) and (13.21) constitute a system of equations which must be solved by trial and error to obtain v_1 for given values of Γ and $v_{G,av}$. Fig. 13.2 presents a solution to these equations for the conditions temp. = 25°C., diameter of pipe = 2.54 cm. The abscissa is the Reynolds number of the gas computed from $v_{G,av}$; in other words, relative to the surface of the pipe. The ordinate is the ratio of the interfacial velocity to the value the interfacial velocity would have if the gas exerted no shearing force on the liquid. The breaks in the various curves correspond to the transition between streamline and turbulent flow in the gas.

In this thesis, except when the effect of gas rate was being studied, Re_G was always well below 2100. From the graph, it can be seen that whenever Re_G is below 2100, v_1 may be calculated from eq. (13.8) with less than one percent error.

Fig. 13.2

Effect of Gas Rate on Interfacial Velocity of Liquid



13.4. Effect of Acceleration. If the velocity of the liquid changes with distance down the column, the differential equation must be modified to include a term for acceleration of the element of fluid. Now, instead of equating the upward force to the downward force, we set the net downward force equal to the rate of change of momentum of the element.

$$-\mu \frac{\partial v}{\partial x} + \rho g dx + \mu \left(\frac{\partial v}{\partial x} + \frac{\partial^2 v}{\partial x^2} dx \right) = \frac{\partial}{\partial t} (\rho v dx)$$

Since $\frac{\partial v}{\partial t} = \left(\frac{\partial v}{\partial y} \right) \left(\frac{\partial y}{\partial t} \right) = v \frac{\partial v}{\partial y}$, where y is the vertical distance downward, we get

$$\mu \frac{\partial^2 v}{\partial x^2} + \rho g = \rho v \frac{\partial v}{\partial y}$$

This equation is non-linear. To add further to the difficulty of solving the problem, the boundary conditions are not simple. Again, we may write

$$\begin{aligned} \text{At } x=0, & \quad \frac{\partial v}{\partial x} = 0 \\ \text{At } x=\delta, & \quad v = 0 \end{aligned}$$

For the initial condition on y , we might assume that the liquid enters at some uniform velocity, v_0 .

$$\text{At } y = 0, \quad v = v_0$$

What makes the problem difficult is that δ is not constant, but varies with y in such a manner that the total amount of liquid flowing past any point is constant, and it can be seen that δ decreases as the liquid accelerates with increasing y . To be able to solve eq. (13.22) numerically, one would have to know δ as a function of y , but to obtain this function, one would have to know the average velocity as a function of y . Because of the non-linearity and the variable layer thickness, no attempt is made to solve the problem, since the results probably would not have enough utility to justify the labor involved.

13.5 Previous Work in Long Wetted-Wall Columns. Previous workers studying the dynamics of liquid layer flow down a wall have not concerned themselves with the behavior of the liquid during the first few inches below the entrance of the liquid, but rather have been more interested in studying the flow sufficiently far down that the layer undergoes no appreciable change with distance. Both Cooper, Drew and McAdams (15) and Friedman and Miller (27) present good reviews of these investigations. The following is quoted from Friedman and Miller.

"Considerable work has been done by investigators on the film thickness of liquids in film flow bounded on one side by a liquid-solid interface and on the other by a liquid-gas interface. Hopf and Schoklitsch studied the flow of water along an inclined plane; Chwang investigated the flow of water and oil on a flat glass plate; Claassen examined the flow of water down the outside of a steel tube; Willey and Cooper studied the flow of dilute sulfuric acid solutions inside of glass tubes; and Warden investigated the flow of water down glass and brass tubes. The data of Warden and Willey and Cooper are perhaps best of those cited. These data were well correlated by Cooper, Drew, and McAdams (15) in a plot of Reynolds number vs. friction factor. Fallah, Hunter and Nash (26) recorrelated these data together with measurements of their own for the flow of water inside glass tubes in somewhat the same manner. In all of the above cases, with the exception of Hopf, Schoklitsch and Chwang who studied the flow on flat surfaces, the average film thickness was measured by stopping the flow of the liquid and measuring the amount of liquid on the tube when the flow was stopped. From these investigations, it was concluded that the change from viscous to turbulent flow occurred at about Re 1500 since for all values of Re below 1500 the plot of f vs. Re fell along the line $f = 24/Re$. This result, in the light of the preceding theory, would tend to indicate that a parabolic velocity gradient existed through the film when viscous flow existed and that the velocity at the liquid-gas interface was a maximum at a value of $v_i = 1.5 v_{av}$.

"However, when Kirkbride (55) measured the film thickness with a micrometer arrangement of water and hydrocarbon oils flowing down the outside of a vertical tube, he found that ripples which started to occur at Re 8 tended to make his results deviate positively from the theoretical film thickness. These same waves were noted by Fallah, Hunter, and Nash (26) in their investigation at even their lowest flow rates (Re about 200). No attempt has been made to explain these apparently anomalous results of Kirkbride (55) which seemed to indicate a change in the type of flow at Re 8 when film thickness was actually measured."

Friedman and Miller (27) also determined the average layer thickness by stopping the liquid flow and measuring the amount of liquid on the tube when the flow was stopped. Using water, kerosene, oil and toluene, they found the data were very well correlated by

$$\delta = \left(\frac{3\mu \Gamma}{\rho^2 g} \right)^{1/3}$$

or, equivalently, by $f = 24/Re$, up to a Reynolds number of 500, in agreement with the previous investigators.

In addition, Friedman and Miller (27) measured the maximum velocity by inserting a small drop of colored fluid into the moving layer, and clocking the velocity of the color downward between two markers. Their results for water, oil, kerosene and toluene are shown in Fig. 13.3 where, as suggested by eq. (13.15) the dimensionless group $v_1(\rho/g\mu)^{1/3}$ is plotted vs. Re . Below $Re = 20-30$, the agreement with theory is good, but above that value of Re , the interfacial velocity deviates positively from theoretical. They noted also the occurrence of waves or ripples in the liquid above $Re = 20-30$. Based on these results, Friedman and Miller postulated that a change of some sort occurs in the flow mechanism at $Re = 20-30$, and proposed that the region between $Re = 25$ and $Re = 1500$ should be called a "pseudo-streamline" region, characterized by the appearance of waves in the liquid layer, a much higher interfacial velocity than that predicted by the true streamline flow equations, and an average film thickness agreeing with the predicted value.

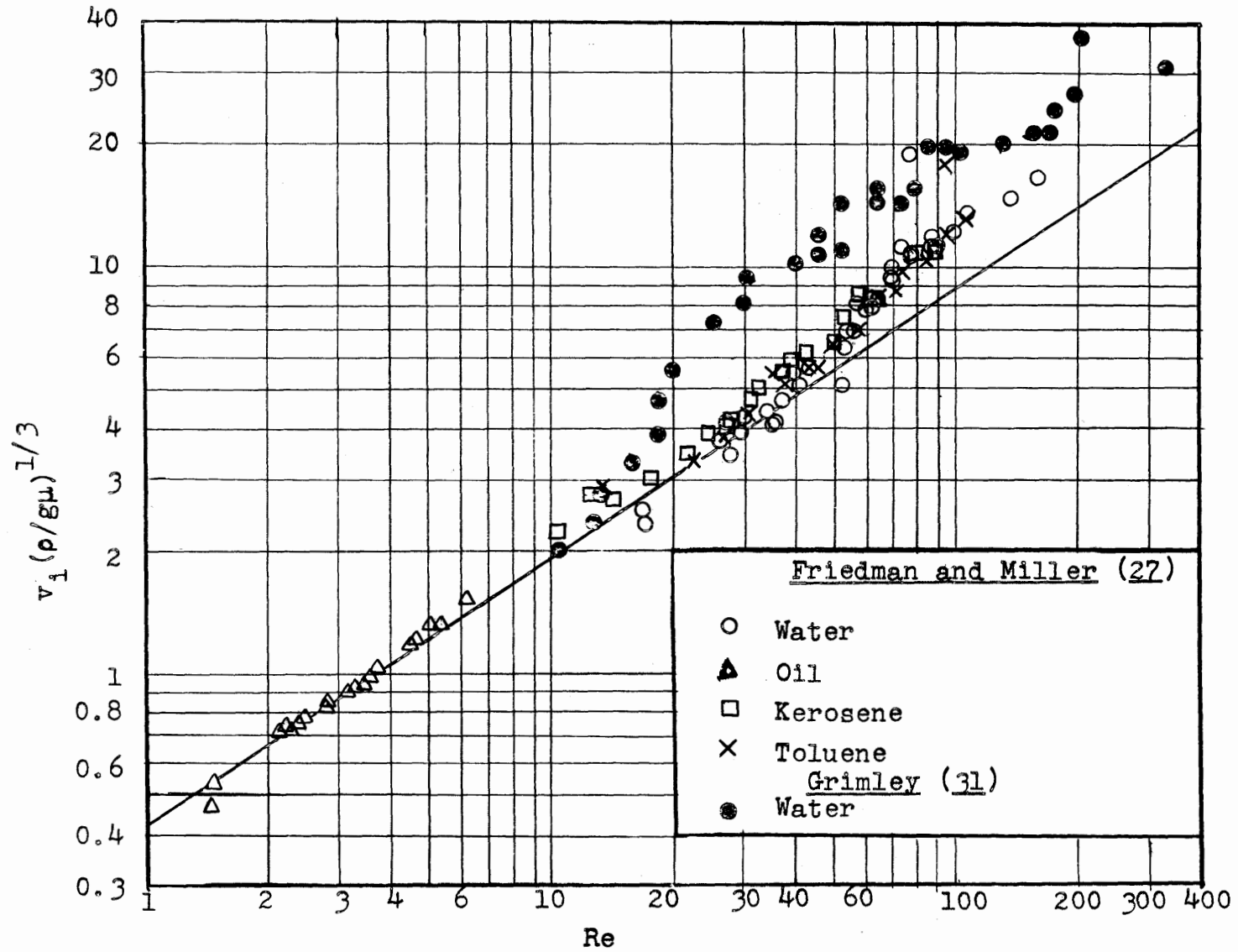
Grimley (31) also studied the maximum velocity in the layer by timing the fall of a drop of dye added to the surface. His results are also shown in Fig. 13.3. He too observed interfacial velocity greater than theoretical, but his departure from theoretical starts at a lower Reynolds number, and the deviation is considerably larger.

In view of this uncertainty regarding the interfacial velocity, and because of the need for information concerning the velocity in the first few inches of travel of the liquid, some experiments on liquid velocity were made on the short wetted-wall columns used in this thesis.

13.6. Procedure. Because of the short distances involved, it was not feasible to attempt to measure the velocity of the liquid by timing the rate of fall of a drop of dye inserted into the layer with a stopwatch. Two indirect procedures were tried, a conductivity method and a stroboscopic method.

Fig. 13.3

Interfacial Velocity in Long Wetted-Wall Columns



Preliminary studies were made on a brass wetted-wall column using a conductivity method. The brass column was one-inch inside diameter, and eight inches long. The liquid, which was water, flowed from an open pan onto the inside surface of the tube as shown in Fig. 13.4. Instead of a drop of dye, a drop of

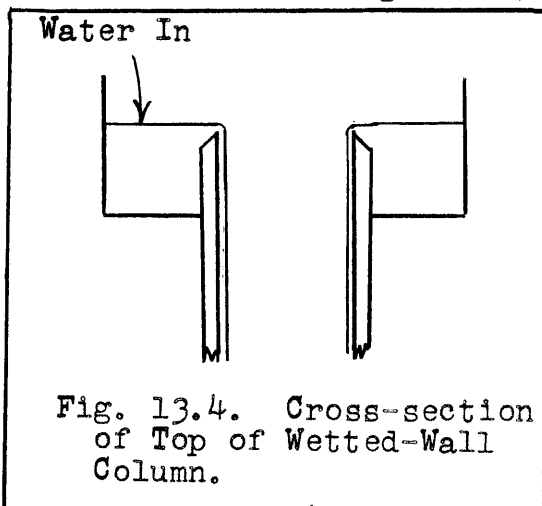


Fig. 13.4. Cross-section of Top of Wetted-Wall Column.

concentrated hydrochloric acid was added to the surface of the liquid just before flowing over the top of the tube. Two conductivity probes were inserted into the liquid layer at different heights, and the conductivity of the water as measured by the two probes were recorded on the rapidly moving tape of a Brush recording oscillograph. The acid flowed down with the water and when it reached the first probe, the resistance between its two platinum wires inserted in the layer suddenly underwent a decrease, and when the acid reached the second probe, its resistance suddenly decreased. The time interval between these two sudden decreases in resistance gave the time required to flow from the upper probe to the lower probe.

The precision of this method was extremely poor, duplicate determinations sometimes giving variations as great as 100%. The lower the probes from the top, the greater the discrepancy in duplicate measurements, indicating that probably the drops of acid were not traveling in a direct line with the probes. No definite conclusions could be drawn from these studies, but they did seem to indicate that the liquid undergoes an acceleration in the first inch or two of the column, reaching a limiting velocity that agreed with those found by Grimley.

With the use of the short wetted-wall column made of glass, it was possible to devise an optical method which had much greater precision. The method consisted of inserting small drops of dye into the liquid layer at about thirty times per second and illuminating the column with a stroboscopic tachometer to make the drops appear to stand still. The distance between drops multiplied by the number of flashes of the stroboscope per second gave the velocity of the liquid.

The system used to create intermittent pulses of dye is shown schematically in Fig. 13.5. A cam mounted on an induction motor rotating 1783 r.p.m. struck a metal plate on each revolution, pressing in the rubber diaphragm and compressing the air inside the "bellows." The bellows was connected to the bottle containing the dye and the successive compressions of the air caused the dye to flow through the hyperdermic tube (inside diameter = 0.015 inch) in intermittent pulses at a rate of 29.7 pulses per second.

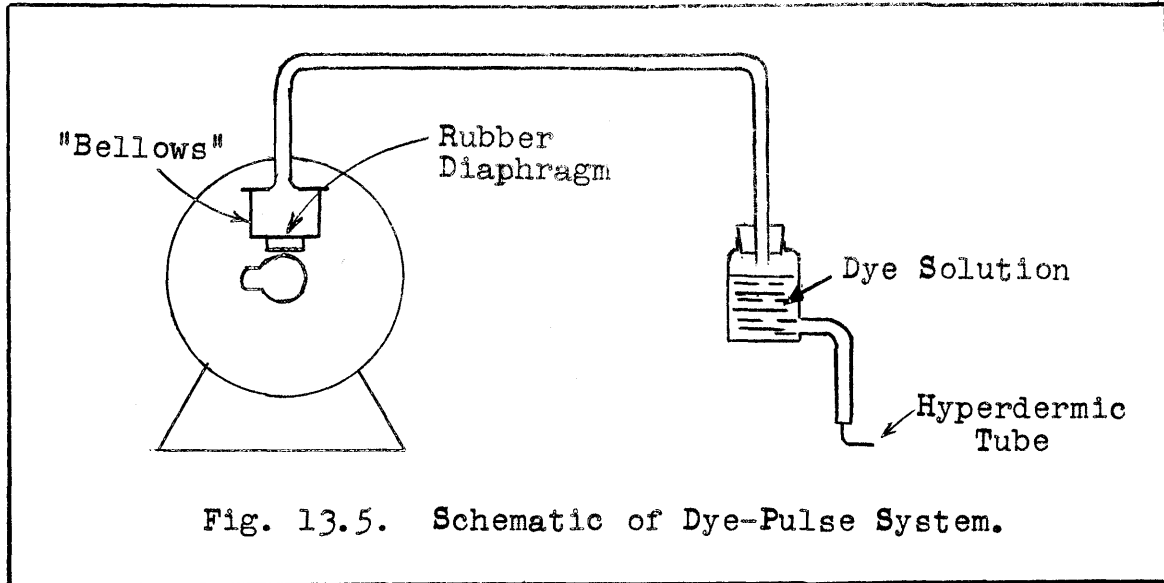


Fig. 13.5. Schematic of Dye-Pulse System.

The stroboscope (Strobotac) was set at twice this speed, i.e., 3565 flashes per minute, in order to reduce the apparent distance between the drops, which appeared to be standing still. Actually what were visible were not discrete drops but rather, somewhat wierd patterns which repeated themselves down the column. These patterns generally varied quite a bit with time as the hyperdermic tube was not fastened in position but was held by hand in that position which gave a pattern that could be measured. It was found that the best place to hold the hyperdermic tube was just at the top of the column. The method required quite a bit of imagination on the part of the operator in order to discern the repeating patterns.

The question may be raised as to whether the method actually gives the maximum velocity of the liquid layer. Where just one drop of dye is put in and the rate of descent of the color is timed, it is quite clear that the maximum velocity would be obtained, since only the front edge of the dye spot would be watched. In this experiment, however, all parts of the successive dye spots are being watched, and since the injection tube is well below the surface of the liquid, one would expect that the effect of variation of velocity with distance perpendicular to the interface would show up, so that some of the dye would be traveling faster than other parts, thus giving a continuous array of distances between the patterns. The fact remains that it was possible, by holding the injection tube just right, to get a single repeating pattern, and the results which were obtained are sufficiently reasonable to indicate that the above difficulty was not serious.

13.7. Results and Discussion. Two of the glass short wetted-wall columns used for the absorption and desorption studies described in this thesis were used here. Both were

an inch and a half long; one had an upflow bevel, the other had a downflow bevel. Two series of runs were made. In the first series, the set-up was the same as that shown in Figs. 3.1 and 3.2, except that the upper Teflon piece was removed. Thus the water, instead of flowing onto the inside of the tube by means of an entrance slot, simply flowed from an open channel and over the top of the tube. The results are shown as the open circles and squares on Fig. 13.6, where $v_1(\rho/g\mu)^{1/3}$ is plotted versus Reynolds number. For comparison, the lines representing the theoretical equation (13.15) and the data of Friedman and Miller and of Grimley are also presented.

At the lower flow rates, the data agree well with Grimley's results, while at the higher flow rates they fall substantially below Grimley's. They also fall somewhat below the extension of the line representing the results of Friedman and Miller.

These results are not consistent with the results of the study of carbon dioxide from water. Because the coefficients of desorption fall somewhat below the theoretical coefficients, it was indicated that the interfacial velocity was lower than theoretical, rather than higher. Since, in the desorption runs, the liquid always entered the column through an entrance slot, the possibility was raised that the presence of entrance slot would influence the interfacial velocity. To investigate this, runs were made with the upper Teflon section in place, exactly as shown in Fig. 3.2. The results are shown in Fig. 13.6 as solid circles and squares for the two different slot widths. No appreciable acceleration of the liquid could be detected.

There appears to be no effect of slot width and, more important, the results agree with the theoretical equation within the experimental error.

These results are in much better agreement with the velocities which are indicated by the desorption runs, and thus make more valid the conclusion of the desorption studies that the penetration theory is applicable to the short wetted-wall column.

The fact that entrance slot width has no effect on interfacial velocity is in agreement with the finding that desorption coefficients of carbon dioxide from water are also independent of slot width.

Apparently the method whereby the liquid enters the column has a great effect on the interfacial velocity. It may well be that in the "psuedo-streamline" region described by Friedman and Miller (27) there exists an instability of some sort in the liquid flow, analagous to the instability which causes turbulence in turbulent flow, and that when the liquid enters through a thin slot this instability is suppressed. It might be mentioned that except at the highest flow rates no rippling

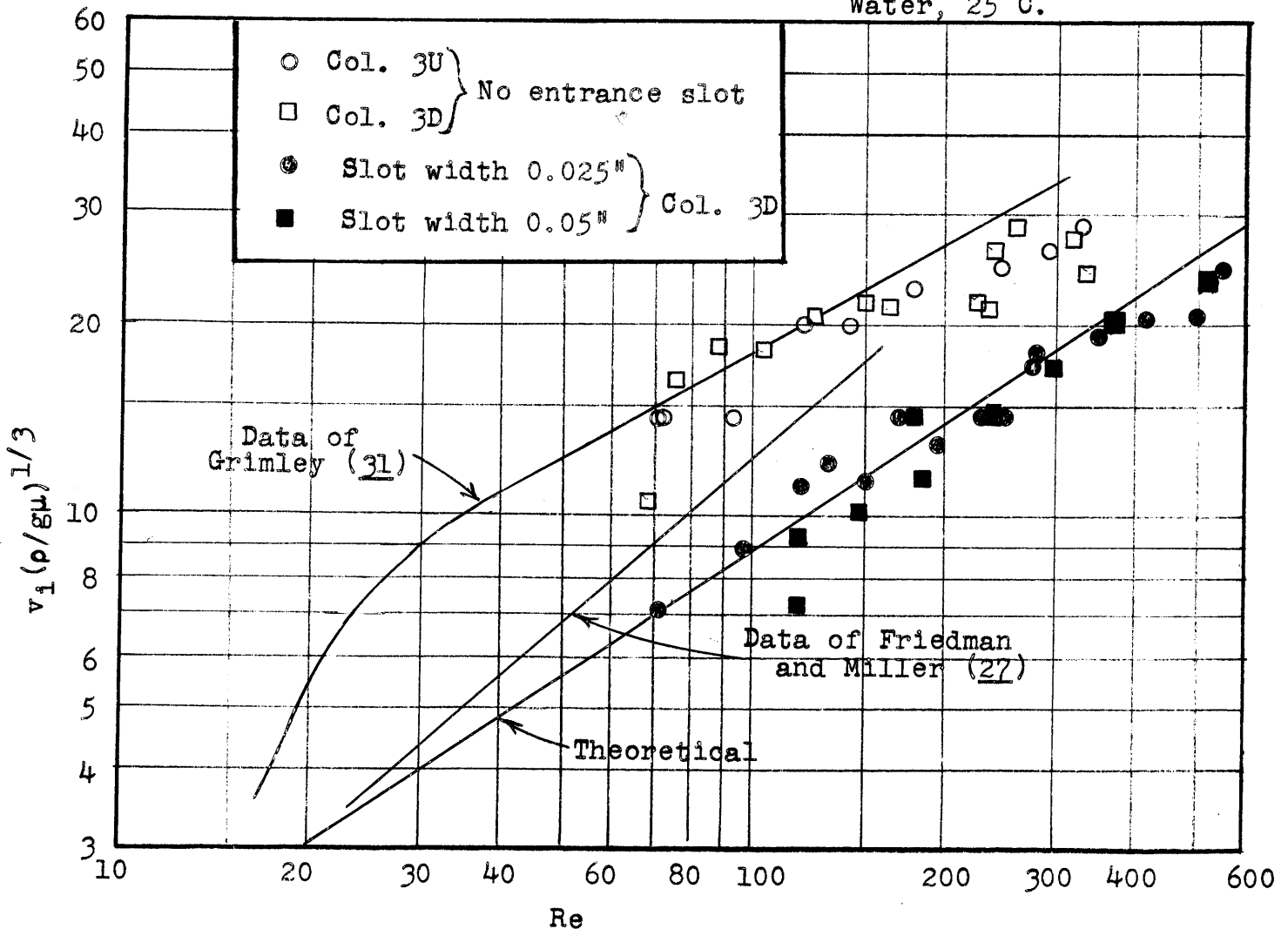
occurs in this short column, and rippling is supposed to be one of the characteristics of "pseudo-streamline" flow. Since Grimley and Friedman and Miller had different entrance conditions in their columns, one might explain the difference between their results, as shown on Fig. 13.3, as due to differences in instability of flow caused by different entrance conditions.

13.8. Conclusions. It is concluded that in the absorption and desorption runs in the short wetted-wall columns, the interfacial velocity is equal to that predicted by streamline flow theory.

Fig. 13.6

Interfacial Velocity in Short Wetted-Wall Column

Water, 25°C.



CHAPTER 14

APPLICATION OF ELECTRONIC ANALOG COMPUTER

The film theory of absorption with second order irreversible chemical reaction gives rise to the differential equations

$$D_A(d^2A/dx^2) = D_B(d^2B/dx^2) = k_1AB \quad (14.1)$$

with the boundary conditions

$$\text{At } x = 0, \quad A = A_1, \quad dB/dx = 0$$

$$\text{At } x = x_f, \quad A = 0, \quad B = B_0 \quad (14.2)$$

In addition to the two approximate solutions discussed in Secs. 8.25-8.28, a set of solutions was obtained by the use of an electronic analog computer. Chronologically, the work on the computer preceded the mathematical work which led to the two approximate solutions, but it turned out that the results obtained from the computer were less useful than the approximations. However, the work on the electronic differential analyzer will be presented here for completeness, and also because of the possible future application of machine computation to the theory of absorption with chemical reaction. This work has already been described briefly in a published article (100).

Eqs. (14.1) and (14.2) may be reduced to dimensionless form by making the substitutions

$$\alpha = A/A_1 \quad (14.3)$$

$$\beta = B/B_0 \quad (14.4)$$

$$\eta = x/x_f \quad (14.5)$$

$$q = D_A A_1 / D_B B_0 \quad (8.195)$$

$$M = k_1 B_0 x_f^2 / D_A \quad (8.202)$$

Then

$$d^2\alpha/d\eta^2 = M\alpha\beta \quad (14.6)$$

$$d^2\beta/d\eta^2 = Mq\alpha\beta \quad (14.7)$$

with the boundary conditions

$$\text{At } \eta = 0, \quad \alpha = 1, \quad d\beta/d\eta = 0$$

$$\text{At } \eta = 1, \quad \alpha = 0, \quad \beta = 1 \quad (14.8)$$

We desire to find ϕ . From eq. (8.194)

$$\phi = \frac{N_A x_f}{D_A A_1} \quad (8.194)$$

and $N_A = -D_A (dA/dx)_{x=0}$

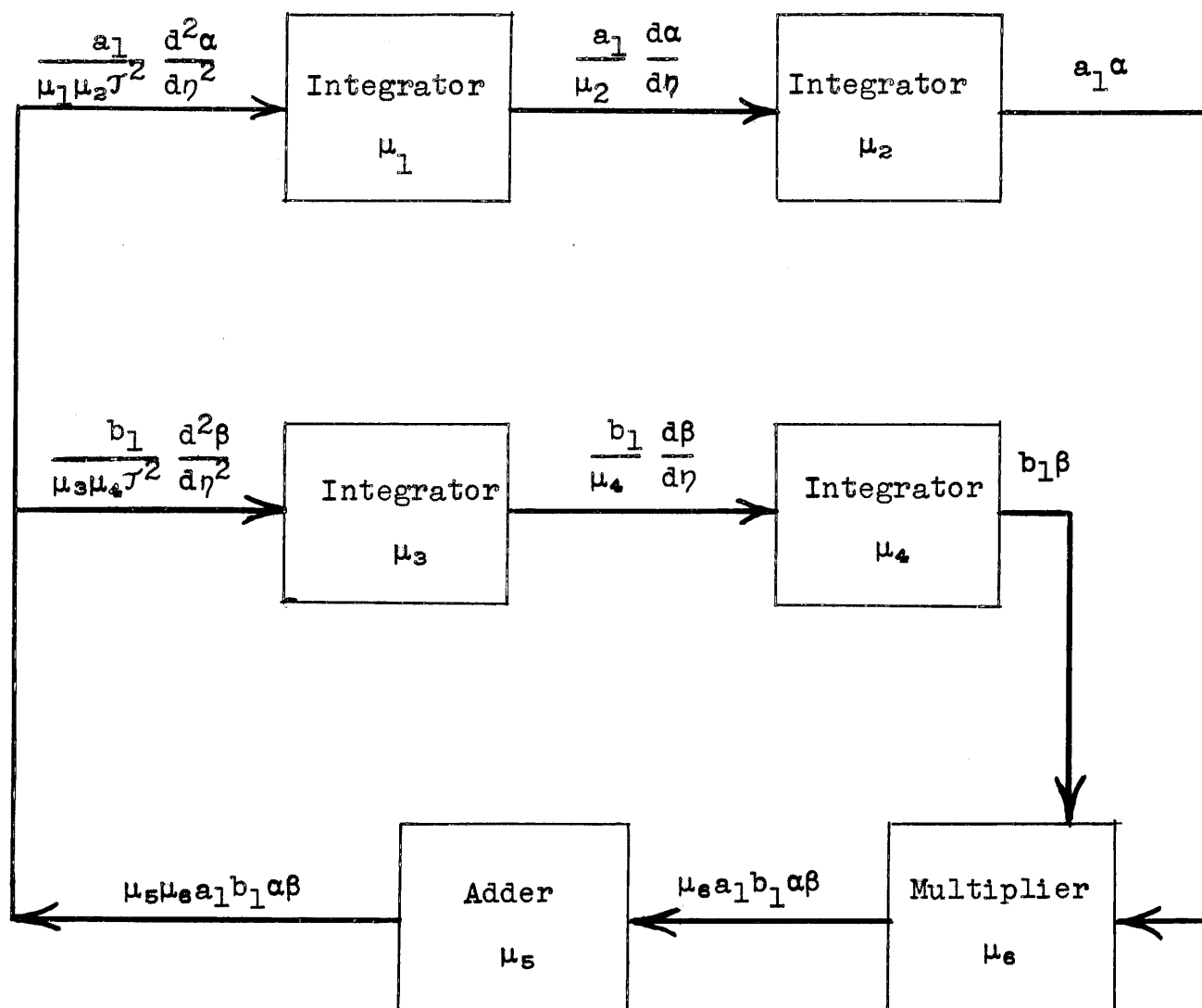
we have $\phi = -(x_f/A_1)(dA/dx)_{x=0}$

or $\phi = -(d\alpha/d\eta)_{\eta=0} \quad (14.9)$

The machine used to solve eqs. (14.6) and (14.7) is an electronic differential analyzer described by Macnee (69), (70). An electronic analog computer, it was built by Macnee and is located in the Research Laboratory of Electronics at M.I.T. It consists of a number of electronic components which may be connected together as required by the differential equation to be solved. The integrating component is a high-gain amplifier connected with a resistor and a condenser in such a way that the output voltage is the time integral of the input voltage multiplied by a gain constant. The adders are units whose output voltage is the sum of two input voltages multiplied by a gain constant. A third component is the multiplier, whose output voltage is the product of two input voltages multiplied by its gain constant. For the purposes of this problem, the components were connected as shown in Fig. 14.1. The gain constant for each component is designated on the figure by a " μ " with a subscript. The voltages are also designated on the wires connecting the components. Why this particular hook-up satisfies the differential equations (14.6) and (14.7) may be shown as follows: Let the output voltage from integrator number 2 be $a_1\alpha$, where a_1 is a scale factor relating the voltage to the quantity α , and similarly let the output of integrator number 4 be $b_1\beta$. The voltage from the multiplier will then be $\mu_5(a_1\alpha)(b_1\beta)$. The adder is here used not for adding two voltages, but for multiplying the voltage from the multiplier by a constant, μ_5 .

Thus, its output will be $\mu_5\mu_6 a_1 b_1 \alpha \beta$. Now, since $a_1\alpha$ is μ_2 times the integral of the input voltage to integrator number 2, that input voltage must be $(1/\mu_2)(d[a_1\alpha]/dt)$, where t is time. If we let $t = \mathcal{T}\eta$, where \mathcal{T} is a scale factor relating time to the quantity η , the input voltage may be written $(1/\mu_2)(a_1/\mathcal{T})(d\alpha/d\eta)$. Similarly, the input to integrator number 1 must be $(1/\mu_1\mu_2)(a_1/\mathcal{T}^2)(d^2\alpha/d\eta^2)$. Likewise, the input to integrator number 3 must be $(1/\mu_3\mu_4)(b_1/\mathcal{T}^2)(d^2\beta/d\eta^2)$. Now, since the output from the adder is directly connected to the input of integrators number 1 and 3, the voltages at that point must be the same; i.e.,

Fig. 14.1

Hook-up of Electronic Analog Computer

$$\mu_5 \mu_6 a_1 b_1 \alpha \beta = \frac{a_1}{\mu_1 \mu_2 \mathcal{T}^2} = \frac{d^2 \alpha}{d\eta^2} = \frac{b_1}{\mu_3 \mu_4 \mathcal{T}^2} \frac{d^2 \beta}{d\eta^2}$$

or

$$\frac{d^2 \alpha}{d\eta^2} = \mu_1 \mu_2 \mu_5 \mu_6 \mathcal{T}^2 b_1 \alpha \beta \quad (14.10)$$

$$\frac{d^2 \beta}{d\eta^2} = \mu_3 \mu_4 \mu_5 \mu_6 \mathcal{T}^2 a_1 \alpha \beta \quad (14.11)$$

Comparison with eqs. (14.6) and (14.7) shows that

$$M = \mu_1 \mu_2 \mu_5 \mu_6 \mathcal{T}^2 b_1 \quad (14.12)$$

$$Mq = \mu_3 \mu_4 \mu_5 \mu_6 \mathcal{T}^2 a_1$$

whence

$$q = \frac{\mu_3 \mu_4}{\mu_1 \mu_2} \frac{a_1}{b_1} \quad (14.13)$$

The differential analyzer solves the differential equation sixty times per second. At the beginning of the cycle, a fixed voltage is applied to each integrator, which corresponds to the constant of integration. Then the solution of the equation takes place for a period of about 0.01 seconds, followed by an off-period, and then the initial voltage is reapplied and the cycle is repeated. At each point in the circuit, an oscilloscope can be connected. The horizontal sweep of the oscilloscope is set at 60 cps., so that the image on the screen is a plot of the voltage as a function of time, and if connected at the output of integrator number 2, gives $a_1 \alpha$ vs. t , if at the output of integrator number 1 gives $(a_1 / \mu_2 \mathcal{T}^2) (d\alpha / d\eta)$, and so forth. The initial voltage, or constant of integration, may be adjusted for each integrator by the setting of a dial on that integrator. Also, every component has a dial with which to adjust the gain constant.

The procedure used will now be outlined. The gain constants were measured as follows. A square wave of some definite voltage which was arbitrarily chosen as one unit was used as the input of the adder. The output voltage, measured on the scope, divided by the input voltage, directly gave the gain of the adder. Where the square wave is used as the input of the integrator, the output voltage is a triangular wave, whose slope, equal to the vertical distance (measured in terms of the input square wave voltage) divide by the horizontal distance (which represents time) is the gain constant of the integrator. Naturally, the units of time would

affect the value of the gain constant, and the length of the solution period time was arbitrarily chosen as one unit. The value of μ_2 for the multiplier was measured by putting in two known square waves and reading the size of the square wave output.

In the actual carrying out of the solution, definite values were assigned to a_1 and b_1 at the start. Because the length of the solution period was arbitrarily chosen as one unit, \mathcal{T} was equal to one. Then, the gain constants were set to give the desired values of q and M . The initial condition for integrator number 3 was set at zero, since at $\eta = 0$, $d\beta/d\eta = 0$. The initial condition for integrator number 2 was set at a_1 , since $\alpha = 1$ and, therefore, $a_1\alpha = a_1$ at $\eta = 0$. Then the initial conditions for integrators number 1 and 4 were adjusted by trial and error until at the end of the solution period ($\eta = 1$), $a_1\alpha = 0$ and $b_1\beta = b_1$ since at $\eta = 1$, $\alpha = 0$ and $\beta = 1$. Then the initial conditions for integrators number 1 and 4 were read off, these being equal respectively to $-a_1\phi/\mu_2$ and $b_1\beta_1$. The values of ϕ and β_1 thus obtained were compared by means of eq. (8.196).

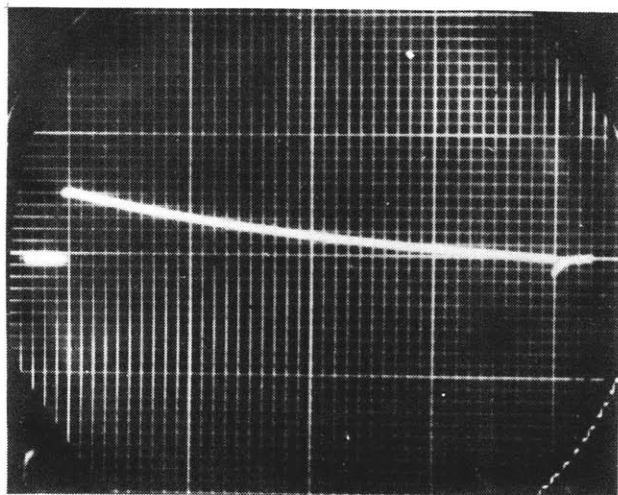
$$\beta_1 = B_1/B_0 = 1 - q(\phi - 1) \quad (8.196)$$

and if they satisfied that equation, the run was considered a good one.

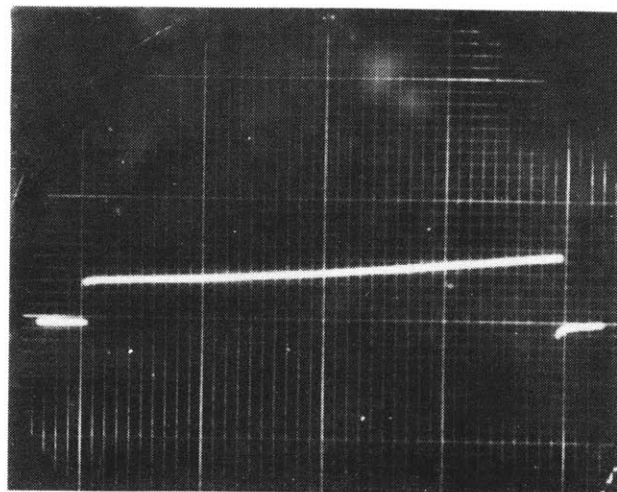
A typical run is shown in Fig. 14.2 which is a photograph of the screen of the oscilloscope. $q = 0.5$ and $M = 3.86$.

There were two chief sources of error. One was that the initial value voltages were not absolutely constant, so that in certain regions of the problem, namely low q or high M , where the initial conditions are very critical and any small change in them will cause a large change in the final conditions, the solution on the oscilloscope tended to flicker and jump around quite a bit. A second source of error lay in the multiplier which is not at all perfect, and has quite a large error especially when the input voltages are small. Now, again for low q or high M , the values of α and β are rarely large at the same time; i.e., one or both is quite small. (Physically, this means that for high rate of reaction, components A and B cannot exist together at high concentrations.) Thus, in this region of q and M , the differential analyzer can be expected to give the poorest results. Another source of error due to the multiplier lay in the fact that when α was made equal to zero at $\eta = 1$, the product $\alpha\beta$ at $\eta = 1$ would be different from zero, and hence $d^2\alpha/d\eta^2$ and $d^2\beta/d\eta^2$ were not equal to zero. It was decided, then, in setting the initial conditions, to make $\alpha\beta = 0$, at $\eta = 1$ and let α be whatever it wanted to be. The effect of flicker was to make it impossible sometimes to set $b_1\beta = b_1$ at $\eta = 1$. This difficulty was somewhat overcome by use of a trial and error technique. When the initial

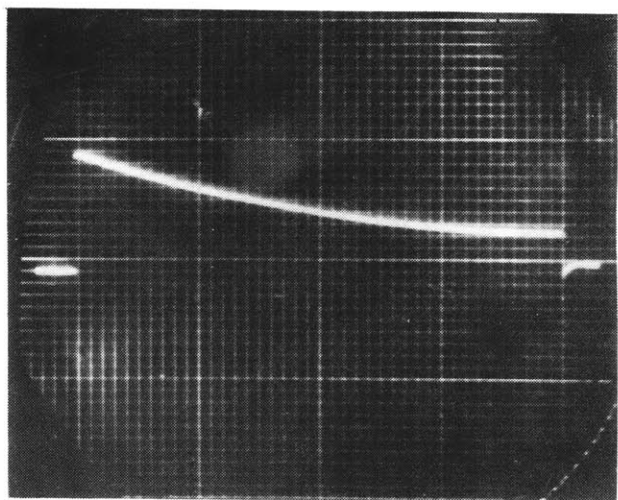
Fig. 14.2. Screen of Oscilloscope Showing Solutions Obtained on Electronic Computer



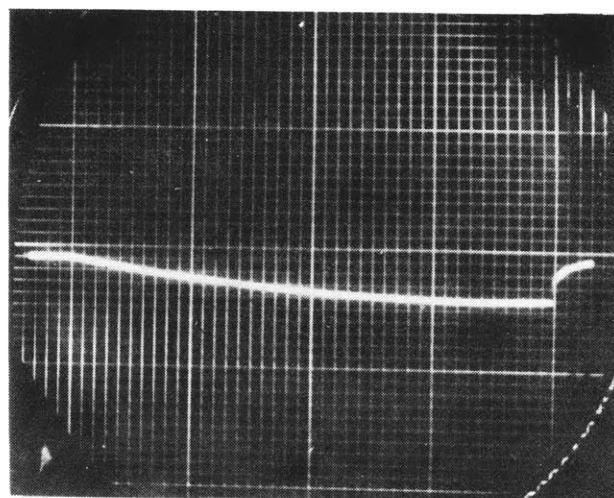
$a_1 \alpha$ vs t



$b_1 \beta$ vs t



$-(a_1/\mu_2)(d\alpha/dt)$ vs t



$-(b_1/\mu_4)(d\beta/dt)$ vs t

conditions for integrators number 1 and 4 were approximately right, $b_1\beta_1$ and $a_1\phi/\mu_2$ were recorded. Then $b_1\beta_1$ was changed just a little bit. This would usually stop the flicker, but then $\alpha\beta$ would no longer be zero at $\eta=1$. Then $a_1\phi/\mu_2$ was adjusted so that $\alpha\beta$ would be zero, and the flicker of course would start again. Then these values of $b_1\beta_1$ and $a_1\phi/\mu_2$ were recorded. This process would be repeated several times. Then, of this series of values of β_1 and ϕ , that pair would be chosen which satisfied eq. (8.196).

The results are shown in Fig. (14.3). Different diagrams are used for each value of q in order to avoid confusion between overlapping points. The solid and dotted curves are the same as those on Fig. 8.11, and between these two sets of curves, the true solution is bracketed. It is seen that the machine solutions are no better than those obtained by using either approximate solution.

The purpose of using the differential analyzer was to check the accuracy of eq. (8.203). If eqs. (8.214)-(8.216) had been derived sooner, it is unlikely that the computer would have been used. However, it is not felt that the work on the differential analyzer was a waste of time. This work does have two chief values. One, it illustrates that the analyzer can be used on this type of problem, i.e., absorption with chemical reaction (using the film theory), and it may be worthwhile to use it for other variations of this problem, where different types of chemical reaction occur, and where mathematics does not yield such satisfactory results. Secondly, these results are of value to the people on the differential analyzer project, who are interested in learning of the types of problems which the analyzer can handle, and of the accuracy which can be expected from it over various ranges of the parameters. Fig. 14.3, with the points compared with the minimum and maximum possible values of ϕ , is an excellent indication of the accuracy which can be obtained on this problem. In general, we can say that the results obtained from the differential analyzer are correct to within 10% of the correct answer. Furthermore, in the regions of q and R where the analyzer gives the poorest results, the approximate solutions are found to be the most accurate.

Although the design of the computer sacrifices accuracy for speed of operation, the accuracy should be satisfactory for most engineering purposes. Because once the analyzer is set up a solution is obtained immediately, and because the constants associated with the differential equations may be changed quite easily and rapidly on the analyzer by a mere twist of the knobs, it is possible to explore a wide variety of conditions with a comparatively small expenditure of time. This feature is particularly valuable where not all the initial conditions are known, but must be found by trial and error as was done in this problem.

Fig. 14.3

Theoretical Values of ϕ for Absorption with Second Order Irreversible Chemical Reaction. Solution by Electronic Analog Computer

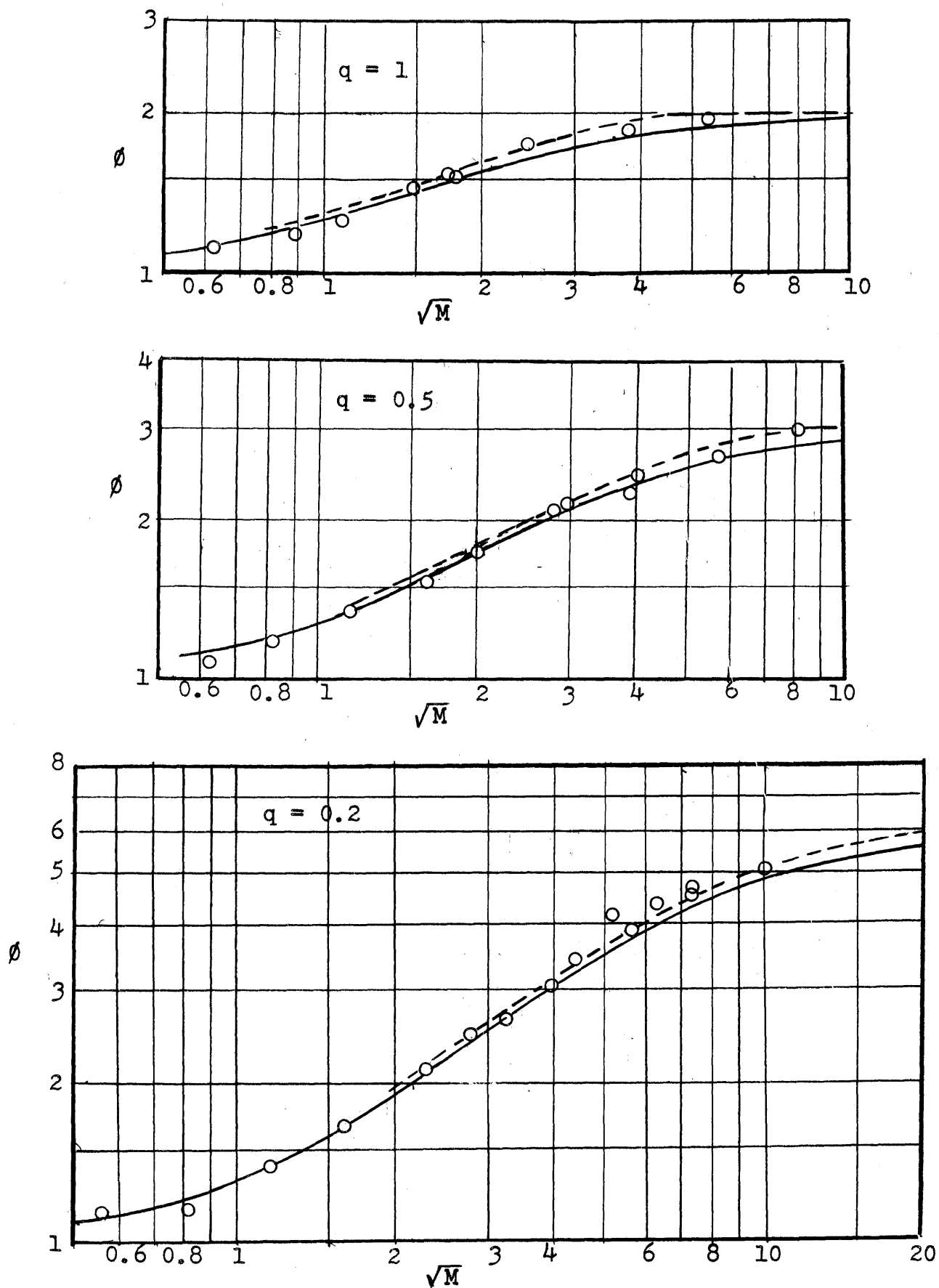
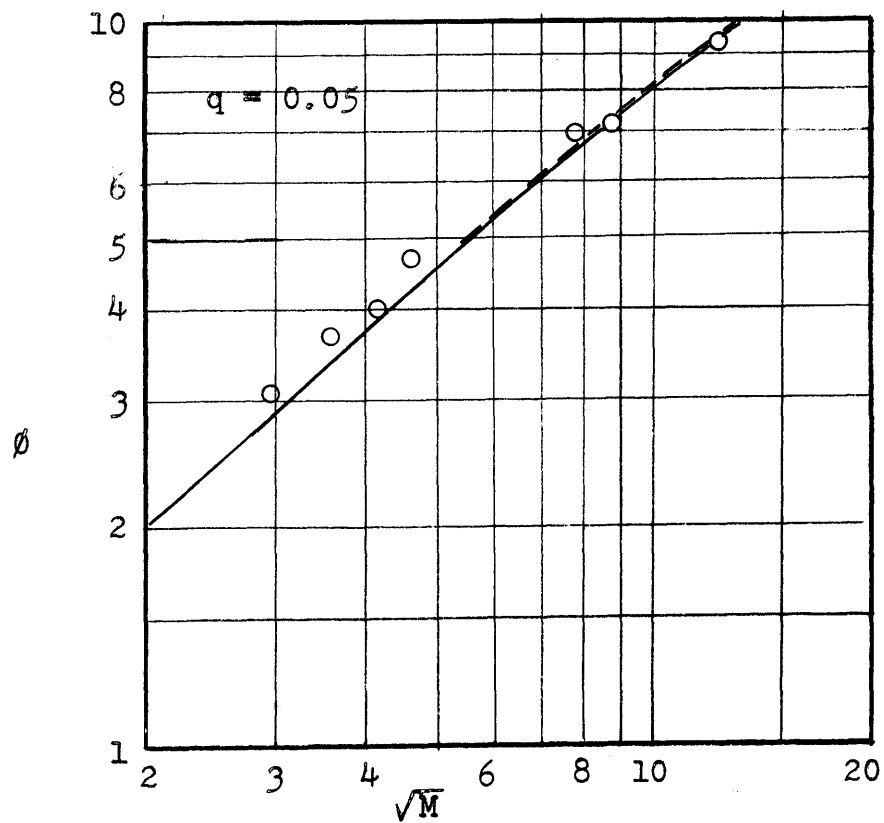
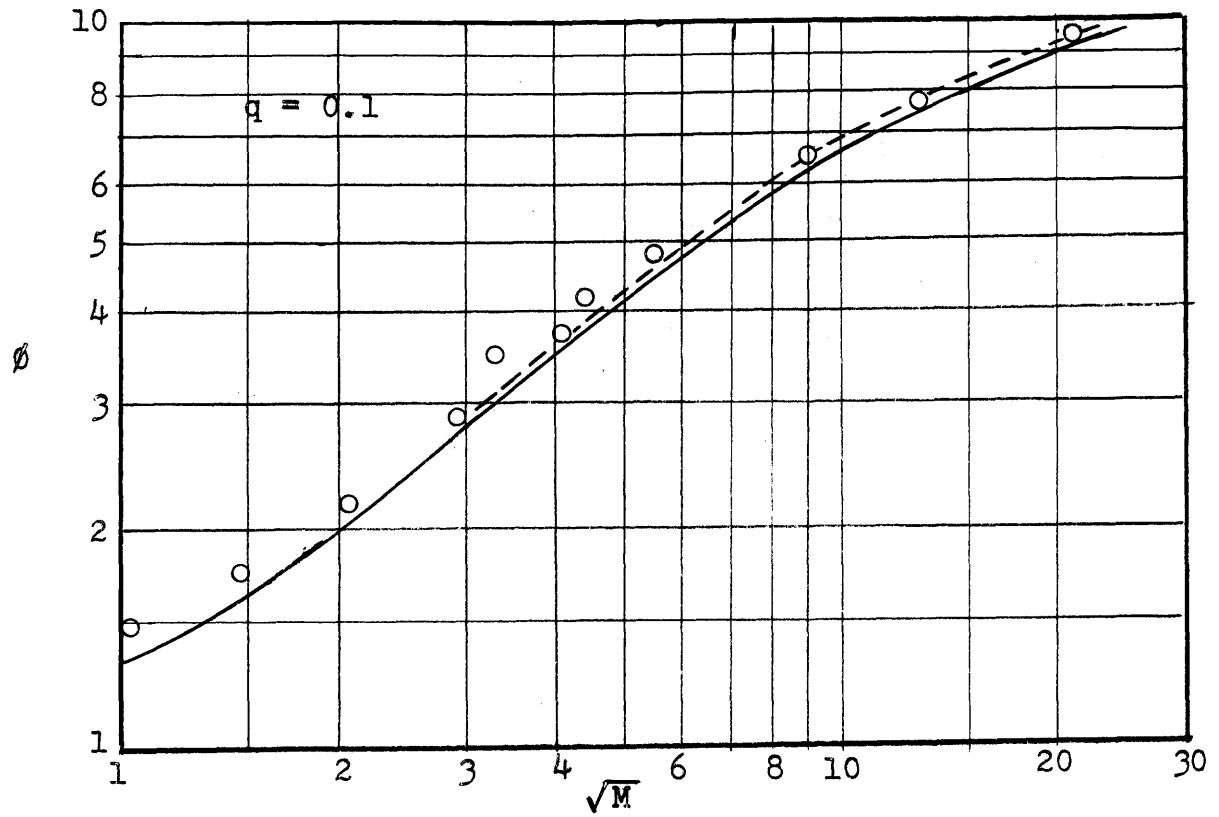


Fig. 14.3 (continued)

— Calculated by Eq. (8.203)
 - - - Calculated by Eqs. (8.214)-(8.216)



It is suggested that this machine be used to study the film theory of second order reversible reactions for the purpose of checking the results obtained in Secs. 8.32-8.33.

Unfortunately, analog computers are of very little use for solving non-linear unsteady-state diffusion problems. According it is proposed that digital computers be used to study the penetration theory of absorption with second order reactions for the purpose of checking the results obtained by using the film theory.

CHAPTER 15SAMPLE CALCULATIONS

15.1. Desorption of Carbon Dioxide from Water in the Short Wetted-Wall Column. The data are presented from Run No. 85.

Column 2D; downflow slot

Water Rate	458 g./min
Diameter of Column	2.86 cm.
Slot Width	0.05 in.
Length of Column	2.99 cm. + slot width
Water Temperature	24.3°C.
Volume of liquid sample	25.00 ml.
Volume Ba(OH) ₂ added to samples	50.00 ml.
Resistance of samples	
Blank	48.4 ohms
Inlet liquid	1475 ohms
Outlet liquid	490 ohms
Cell Constant (spec. conductance divided by resistance)	0.2287

Determination of Concentrations

- a) Blank (50 ml. Ba(OH)₂ + 25 ml. distilled water)
 Spec. Cond. = $0.2287/48.4 = 4.73 \times 10^{-3} \text{ ohm.}^{-1} \text{ cm.}^{-1}$

The I.C.T. (47) gives a table of equivalent conductance vs. concentration for Ba(OH)₂ solutions. For each concentration, the specific conductance was calculated, and the equivalent conductance was plotted against specific conductance. Using this plot:

$$\begin{aligned} \text{Equiv. Cond.} &= 0.2262 \text{ (ohm)(cm.)(equiv.)}/1. \\ \text{Normality of Ba(OH)}_2 &= 4.73/0.2262 = 20.91 \text{ meq./l.} \end{aligned}$$

- b) Inlet Sample
 Spec. Cond. = $0.2287/1475 = 0.1551 \times 10^{-3}$
 Equiv. Cond. = 0.2487
 Normality of Ba(OH)₂ = $0.1551/0.2487 = 0.624 \text{ meq./l.}$

- c) Outlet Sample
 Spec. Cond. = $0.2287/490 = 0.467 \times 10^{-3}$
 Equiv. Cond. = 0.2452
 Normality of Ba(OH)₂ = $0.467/0.2452 = 1.903 \text{ meq./l.}$

d) $(C_1 - C_2)/C_1$
 $C_1 = (20.91 - 0.624)75/25 = 60.9 \text{ meq./l.}$
 $C_2 = (20.91 - 1.903)75/25$

$$\frac{C_1 - C_2}{C_1} = \frac{1.903 - 0.624}{20.91 - 0.624} = \frac{1.279}{20.29} = 0.0630$$

Flow Rate per Unit Perimeter -- Based on inside diameter of glass column.

$$\Gamma = \frac{458}{\pi(2.86)} = 50.9 \text{ g./}(cm.)(min.)$$

Interfacial Area

a) Length = $2.99 + 2.54(0.05) = 3.117 \text{ cm.}$

b) Perimeter of Interface = $\pi(\text{Diam. of Col.} - \text{Twice Layer Thickness})$

$$\delta^3 = \frac{3\mu\Gamma}{\rho^2g} \quad \text{from eq. (13.7)}$$

$$\delta^3 = \frac{3(0.00908)(50.9/60)}{(1)^2(980)}$$

$$\delta = 0.0286 \text{ cm.}$$

Perimeter = $\pi(2.86 - 2 \times 0.0286) = 8.81 \text{ cm.}$
 Interfacial Area = $3.117(8.81) = 27.4 \text{ cm.}$

Physical Coefficient

$$k_L^* = (V/a)(C_1 - C_2)/C_1$$

$$k_L^* = (458/27.4)(0.0630) = 1.052 \text{ cm./min.}$$

Temperature Correction to 25°C. (See Sec. 5.6)

$$\begin{aligned} k_{L,25^\circ}^* &= k_L^* \exp(0.011 [25.0 - t^\circ\text{C.}]) \\ &= 1.052 \exp(0.011 [25.0 - 24.3]) \\ &= 1.052(1.008) = 1.060 \text{ cm./min.} \end{aligned}$$

15.2. Desorption of Chlorine from Dilute Hydrochloric Acid in the Short Wetted-Wall Column. The data are presented from Run No. 104

Column 3D; downflow slot

Water Rate	111 g./min.
Diameter of Column	2.87 cm.
Slot Width	0.025 in.

Length of Column	4.08 cm. + slot width
Water Temperature	25.2°C.
Concentration of chlorine in inlet liquid, C_1	25.49 mmole/l.
Total chlorine desorbed during run	4.104 mmoles
Time of Run	10.00 min.

Flow Rate per Unit Perimeter

$$\Gamma = \frac{111}{\pi(2.87)} = 12.3 \text{ g./}(cm.)(min.)$$

Interfacial Area

$$\text{Length} = 4.08 + 2.54(0.025) = 4.140 \text{ cm.}$$

$$\delta^3 = \frac{3(0.00889)(12.3/60)}{(1)^2(980)}$$

$$\delta = 0.018 \text{ cm.}$$

$$\text{Perimeter of interface} = \pi(2.87 - 2 \times 0.018) = 8.91 \text{ cm.}$$

$$\text{Interfacial Area} = 4.140(8.90) = 36.9 \text{ cm.}^2$$

Physical Coefficient

$$k_L^* = -N_A/C_1$$

$$k_L^* = \frac{4.104/(10.0)(36.9)}{25.49 \times 10^{-3}} = 0.437 \text{ cm./min.}$$

Temperature Correction to 25°C. (See Sec. 5.6)

$$\begin{aligned} k_{L^*}, 25^\circ &= k_L^* \exp(0.019 [25.0 - t^\circ C.]) \\ &= 0.437 \exp(0.019 [25.0 - 25.2]) \\ &= 0.437(0.996) = 0.435 \text{ cm./min.} \end{aligned}$$

15.3. Desorption of Chlorine from Water in the Short Wetted-Wall Column. The data are presented from Run No. 173.

Column 3D; downflow slot

Water Rate	380 g./min.
Diameter of Column	2.87 cm.
Slot Width	0.025 in.
Length of Column	4.08 cm.+slot width
Water Temperature	24.9°C.
Concentration of chlorine in inlet liquid, C_1	39.29 mmole/l.

Concentration of chlorine in outlet liquid, C_2 37.72 mmole/l.
 Total chlorine desorbed during run 5.800 mmoles
 Time of run 10.00 min.

Flow Rate per Unit Perimeter

$$\Gamma = \frac{380}{\pi(2.87)} = 42.1 \text{ g./}(\text{cm.})(\text{min.})$$

Interfacial Area

$$\text{Length} = 4.08 + 2.54(0.025) = 4.140 \text{ cm.}$$

$$\delta^3 = \frac{3(0.00894)(42.1/60)}{(1)^2(980)}$$

$$\delta = 0.027 \text{ cm.}$$

$$\begin{aligned} \text{Perimeter of interface} &= \pi(2.87 - 2 \times 0.027) = 8.85 \text{ cm.} \\ \text{Interfacial Area} &= 4.140(8.85) = 36.6 \text{ cm.}^2 \end{aligned}$$

"Total" Coefficient

$$k_L = -N_A/C_1 \quad \text{Eq. (5.21)}$$

$$k_L = \frac{5.800/(10.0)(36.6)}{39.29 \times 10^{-3}} = 0.403 \text{ cm./min.}$$

Temperature Correction to 25°C. (See Sec. 5.14)

$$\begin{aligned} k_{L,25^\circ} &= k_L \exp(0.019 [25.0 - 24.9]) \\ &= 0.403(1.002) = 0.404 \text{ cm./min.} \end{aligned}$$

Pseudo-Coefficient

$$K_c = (C_1 - A_1)^3 / A_1 \quad \text{Eq. (5.24)}$$

$$3.29 \times 10^{-4} = (0.03929 - A_1)^3 / A_1$$

By trial and error, $A_1 = 0.02042 \text{ mole/l.}$

$$A_1/C_1 = 0.02042/0.03929 = 0.5196$$

$$k_{L^\circ,25^\circ} = k_{L,25^\circ} C_1 / A_1 \quad \text{Eq. (5.23)}$$

$$k_{L^\circ,25^\circ} = 0.404/0.5196 = 0.777 \text{ cm./min.}$$

Experimental Value of ϕ

$$k_L^* \sqrt{h/D} = 83.2^{0.40} \quad \text{Eq. (5.4a)}$$

$$k_L^* \sqrt{4.140/(1.48 \times 10^{-5})} = 83.2(42.1)^{0.40}$$

$$k_L^* = 0.701 \text{ cm./min.}$$

$$\phi = k_L^0/k_L^*$$

$$\phi = 0.777/0.701 = 1.11$$

Material Balance

$$\begin{aligned} \text{Chlorine in} &= VC_1 \\ &= 380(39.29 \times 10^{-3}) \\ &= 14.93 \text{ mmoles/min.} \end{aligned}$$

$$\begin{aligned} \text{Chlorine out} &= VC_2 + \text{rate of desorption} \\ &= 380(37.72 \times 10^{-3}) + 5.800/10.0 \\ &= 14.33 + 0.58 = 14.91 \text{ mmoles/min.} \end{aligned}$$

$$\begin{aligned} \text{Error in closure} &= (14.93 - 14.91)/14.93 \\ &= 0.1\% \end{aligned}$$

CHAPTER 16SUMMARY OF DATA AND CALCULATED RESULTS FOR
DESORPTION IN SHORT WETTED-WALL COLUMNTable 16.1Column Dimensions

<u>Column No.</u>	<u>Slot Type</u>	<u>Total Length cm.</u>	<u>Inside Diameter cm.</u>
1U	Upflow	1.88	2.88
2U	Upflow	2.72	2.87
2D	Downflow	2.95 + slot width (Runs 79-84) 2.99 + slot width (Runs 85-91)	2.86
3U	Upflow	4.25	2.88
3D	Downflow	4.08 + slot width	2.87

Table 16.2

Desorption of Carbon Dioxide from WaterEffect of TemperatureColumn 3U

Run	Temp. Water	°C Air	C_1 meq./l.	$\frac{C_1 - C_2}{C_1}$	k_L^* cm./min.
1	22.2	21.5	66.0	0.1151	0.603
2	25.1	25.0	60.0	0.1220	0.639
3	31.0	30.0	48.9	0.1275	0.668
4	25.2	24.9	59.7	0.1195	0.625
5	26.5	26.0	57.9	0.1270	0.665
6	27.9	27.0	55.1	0.1228	0.641
7	29.0	28.8	54.8	0.1218	0.636
8	30.0	29.0	51.6	0.0825	0.431

Slot width = 0.05 in.

$V = 197$ g./min.

$Re_G = 2350$

Interfacial Area = 37.9 cm.²

$\Gamma = 21.8$ g./ (cm.) (min.)

length = 4.25 cm.

TABLE 16.3

Desorption of Carbon Dioxide from Water
Effect of Air Rate

Column 3U

Run	Re _G	Temp. °C		C ₁ meq./l.	$\frac{C_1 - C_2}{C_1}$	k _L * cm./min.	k _L * 25° cm./min.
		Water	Air				
9	3800	26.0	25.3	57.1	0.1401	0.732	0.725
10	3120	26.0	25.6	58.4	0.1432	0.748	0.740
11	2170	26.2	25.9	56.7	0.1175	0.615	0.607
12	950	27.5	26.7	54.6	0.1182	0.618	0.607
13	0	27.5	----	58.6	0.1182	0.618	0.607
14	0	27.9	----	58.4	0.1142	0.598	0.586
15	950	29.9	28.9	55.4	0.1191	0.623	0.592

Slot width = 0.05 in.

V = 198 g./min.

Interfacial Area = 37.9 cm.²

Γ = 21.9 g./ (cm.) (min.)

length = 4.25 cm.

TABLE 16.4
Desorption of Carbon Dioxide from Water
Effect of Slot Width
Column 3U

Run	Slot Width in.	Water Temp. °C	C_1 meq./l.	$\frac{C_1 - C_2}{C_1}$	k_L^* cm./min.	$k_L^*_{250}$ cm./min.
16	0.0125	23.0	64.3	0.1150	0.605	0.617
17	0.025	25.5	60.4	0.0978	0.514	0.511
18	0.075	25.2	60.8	0.1150	0.605	0.604
19	0.100	25.0	61.3	0.1155	0.607	0.607
20	0.125	25.0	59.3	0.1200	0.630	0.630
21	0.150	25.1	59.2	0.1150	0.605	0.605
22	0.0375	25.5	56.2	0.1195	0.625	0.622

$$V = 199 \text{ g./min.}$$

$$Re_G = 0$$

$$\text{Interfacial Area} = 37.9 \text{ cm.}^2$$

$$\Gamma = 22.0 \text{ g./}(\text{cm.})(\text{min.})$$

$$\text{length} = 4.25 \text{ cm.}$$

TABLE 16.5
Desorption of Carbon Dioxide from Water
Effect of Water Rate

Run	V g./min.	Temp. °C Water	<u>Column 3U</u>		$\frac{C_1 - C_2}{C_1}$	Interfac. area cm. ²
			Air	C ₁ meq./l.		
23	730	23.9	----	55.4	0.0316	37.5
24	592	23.9	----	56.9	0.0590	37.5
25	592	24.1	----	56.1	0.0606	37.6
26	510	23.9	----	58.6	0.0701	37.6
27	401	25.0	----	56.0	0.0686	37.6
28	308	25.0	----	58.6	0.0735	37.8
29	140	25.0	----	58.7	0.1205	37.9
30	71.4	25.0	----	59.0	0.1841	38.0
31	71.4	25.0	----	59.8	0.1790	38.0
32	601	32.5	----	44.9	0.0670	37.6
33	601	32.4	----	43.5	0.0690	37.6
34	520	33.2	----	43.2	0.0709	37.6
35	400	33.8	----	43.2	0.0820	37.6
36	305	32.8	----	47.7	0.1095	37.8
37	305	31.2	----	45.2	0.0876	37.8
38	134	26.5	----	57.1	0.0883	37.9
39	78.2	29.9	----	50.1	0.2035	37.9
40	359	24.5	23.8	56.3	0.0800	37.8
41	255	25.0	24.0	59.9	0.1050	37.8
42	200	25.0	24.0	59.9	0.1010	37.9
43	179	25.0	24.0	59.9	0.1225	37.9
44	147	25.0	24.0	59.9	0.1539	37.9
45	100.5	25.0	24.0	59.9	0.1670	37.9

(continued on next page)

TABLE 16.5 (Contd.)

Run	Γ g./cm. ² (min.)	k_L^* cm./min.	$k_L^*_{25^\circ C}$ cm./min.
23	80.3	0.615	0.624
24	65.0	0.932	0.945
25	65.0	0.959	0.968
26	56.1	0.951	0.966
27	44.1	0.732	0.732
28	33.9	0.599	0.599
29	15.4	0.447	0.447
30	7.85	0.346	0.346
31	7.85	0.336	0.336
32	66.1	1.073	0.995
33	66.1	1.107	1.021
34	57.1	0.981	0.900
35	44.0	0.874	0.799
36	33.6	0.885	0.815
37	33.6	0.706	0.662
38	14.75	0.313	0.308
39	8.60	0.420	0.399
40	39.5	0.760	0.760
41	28.0	0.709	0.709
42	22.0	0.580	0.580
43	19.70	0.579	0.579
44	16.19	0.596	0.596
45	11.07	0.442	0.442

Slot width = 0.05 Runs 23, 24, 26 - 30, 32-45

 = 0.025 Runs 25, 31

$Re_G = 0$ Runs 23-39

 = 870 Runs 40-45

length = 4.25 cm.

TABLE 16.6

Desorption of Carbon Dioxide from Water
Effect of Water Rate

Column 2U

Run	V g./min.	Water Temp. °C	C ₁ meq./l.	$\frac{C_1 - C_2}{C_1}$	Interfac. Area cm. ²
46	706	25.0	55.5	0.0341	23.9
47	546	24.9	57.0	0.0464	24.0
48	450	24.8	59.6	0.0575	24.0
49	300	24.6	59.7	0.0568	24.1
50	200	25.0	59.9	0.0716	24.2
51	151	25.0	59.8	0.1160	24.2
52	97.0	25.0	59.7	0.1431	24.2
53	70.1	25.0	60.0	0.1735	24.3
54	375	25.0	50.0	0.0583	24.1
55	245	23.5	55.4	0.0721	24.1
56	180	25.0	52.1	0.0836	24.2
57	102	25.0	54.5	0.1560	24.2
58	83.8	25.0	52.1	0.1281	24.3
59	300	25.2	55.9	0.0762	24.1
60	131	25.0	59.8	0.1279	24.2
61	66	25.0	60.2	0.1715	24.3
62	718	25.0	54.0	0.0445	23.9
63	582	24.2	56.9	0.0575	24.0
64	453	25.0	55.5	0.0486	24.0

(continued on next page)

TABLE 16.6 (Contd)

Run	Γ g./((cm.)(min.))	k_L^* cm./min.	$k_L^*_{250C}$ cm./min.
46	78.5	1.010	1.010
47	60.7	1.057	1.057
48	50.0	1.079	1.079
49	33.4	0.706	0.706
50	22.2	0.592	0.592
51	16.8	0.723	0.723
52	10.80	0.579	0.579
53	7.80	0.502	0.502
54	41.6	0.906	0.906
55	27.25	0.733	0.745
56	20.0	0.621	0.621
57	11.33	0.656	0.656
58	9.32	0.444	0.444
59	33.3	0.949	0.947
60	14.56	0.692	0.692
61	7.34	0.466	0.466
62	79.9	1.332	1.332
63	64.7	1.392	1.400
64	50.4	0.916	0.916

slot width = 0.05 in.

$Re_G = 0$

length = 2.72 cm.

TABLE 16.7

Description of Carbon Dioxide from Water
Effect of Water Rate

Column 3D

Run	V g./min.	Water temp. °C	C ₁ meq./l.	$\frac{C_1 - C_2}{C_1}$	Interfac. Area, cm. ²
65	730	25.0	54.1	0.0582	37.1
66	652	25.0	53.6	0.0577	37.1
67	526	25.4	53.6	0.0599	37.1
68	457	25.5	53.8	0.0681	37.1
69	322	25.2	57.0	0.0939	37.2
70	243	25.2	57.8	0.1315	37.2
71	150	25.0	57.9	0.1408	37.4
72	98.0	25.5	57.0	0.1781	37.4
73	70.1	26.0	56.5	0.1985	37.5

Run	Γ g./((cm.)(min.))	k _L * cm./min.	k _L *25°C cm./min.
65	81.1	1.148	1.148
66	72.5	1.016	1.016
67	58.5	0.851	0.849
68	50.9	0.841	0.839
69	35.8	0.812	0.811
70	27.0	0.859	0.858
71	16.69	0.565	0.565
72	10.90	0.466	0.464
73	7.80	0.372	0.368

slot width = 0.05

Reg = 0

length = 4.21 cm.

TABLE 16.8

Desorption of Carbon Dioxide from Water
Effect of Slot Width

Column 3D

Run	Slot Width in.	Water Temp. °C	C_1 meq./l.	$\frac{C_1 - C_2}{C_1}$	length Z, cm.	Interfac. Area, cm.
74	0.0125	25.0	58.2	0.1112	4.12	36.5
75	0.025	25.0	58.4	0.1072	4.15	36.7
76	0.0375	25.0	58.1	0.1221	4.18	37.1
77	0.050	25.0	57.7	0.1108	4.21	37.4
78	0.075	25.0	57.5	0.1252	4.27	37.9

Run	k_L^* cm./min.	$k_L^*_{250}$ cm./min.	$k_L^*_{250} \sqrt{Z/Z_0}$ cm./min.
74	0.608	0.608	0.601
75	0.585	0.585	0.581
76	0.658	0.658	0.655
77	0.591	0.591	0.591
78	0.661	0.661	0.666

$$Z_0 = (\text{length when slot width} = 0.05 \text{ in.}) = 4.21 \text{ cm.}$$

$$V = 200 \text{ g./min.}$$

$$Re_G = 0$$

$$\Gamma = 22.2 \text{ g./}(\text{cm.})(\text{min.})$$

TABLE 16.9

Desorption of Carbon Dioxide from Water
Effect of Water Rate

Run	V g./min.	Temp. °C		Re _G	C ₁ meq./l.	$\frac{C_1 - C_2}{C_1}$	Interfac. Area, cm. ²
		Water	Air				
79	74.5	25.2	25.3	1200	61.1	0.1833	27.3
80	269	25.9	25.7	1200	60.1	0.0938	27.2
81	118	25.5	25.2	1200	60.7	0.1563	27.3
82	187	25.6	25.5	1200	59.1	0.1073	27.2
83	232	25.6	25.5	1200	58.3	0.0958	27.2
84	349	26.5	25.7	1200	55.8	0.0692	27.1
85	458	24.3	24.3	1250	60.9	0.0630	27.4
86	725	24.6	24.3	1200	57.1	0.0415	27.4
87	183	24.7	24.6	1250	62.1	0.0979	27.6
88	613	24.7	25.0	1200	57.1	0.0515	27.4
89	790	24.2	24.7	1200	57.0	0.0412	27.3
90	545	24.7	24.7	1200	60.4	0.0668	27.4
91	395	24.7	24.8	1200	60.6	0.0724	27.5

Run	Γ g./ (cm.) (min.)	k _L * cm./min.	k _L *250 cm./min.
79	8.28	0.499	0.498
80	29.9	0.929	0.919
81	13.12	0.676	0.672
82	20.7	0.735	0.730
83	25.8	0.817	0.812
84	38.8	0.890	0.876
85	50.9	1.052	1.060
86	80.6	1.100	1.105
87	20.4	0.649	0.651
88	68.2	1.153	1.156
89	87.8	1.191	1.201
90	60.6	1.328	1.332
91	43.9	1.041	1.044

Slot width = 0.05 in.

length = 3.07 cm. (Runs 79-84)

= 3.11 cm. (Runs 85-91)

TABLE 16.10

Desorption of Carbon Dioxide from Water
Effect of Water Rate
Column 1U

Run	V g./min.	Temp. °C.		Re _G	C ₁ meq./l.	$\frac{C_1 - C_2}{C_1}$	Interfac. Area, cm. ²
		Water	Air				
92	390	25.5	25.1	1250	59.5	0.0442	16.66
93	303	25.5	24.7	1250	59.4	0.0546	16.69
94	478	25.6	24.7	1250	59.3	0.0471	16.64
95	228	25.9	24.8	1250	53.6	0.0703	16.72
96	165	25.1	25.0	1120	61.4	0.0824	16.74
97	115	25.0	24.0	1200	61.3	0.1091	16.77
98*	88.5	26.1	25.1	1250	38.0	0.0285	16.79
99*	76.5	26.2	25.1	1250	35.1	0.0874	16.80

Run	\int g./ (cm.) (min.)	k _L * cm./min.	k _L * ₂₅₀ cm./min.
92	43.4	1.035	1.029
93	33.7	0.992	0.986
94	53.2	1.353	1.344
95	25.4	0.959	0.949
96	18.35	0.812	0.811
97	12.79	0.748	0.748
98*	9.84	0.150	0.149
99*	8.51	0.398	0.393

Runs 98 and 99 were rejected because the inlet concentrations were considerably lower than saturation and decreasing comparatively rapidly with time, thus making the measured values of k_L too low.

slot width = 0.05 in. (Runs 92-96)

= 0.025 in. (Runs 97-99)

length = 1.88 cm.

TABLE 16.11

Desorption of Chlorine from Dilute Hydrochloric Acid

Run	V g./min.	Temp. °C		Reg	Cl mmole/l.	Rate of De- sorption mmole/min.	Concen. of HCl mole/l.
		Water	Air				
100	380	25.0	25.0	400	11.80	0.279	0.182
101	213	25.0	25.0	400	11.63	0.233	0.175
102	128	25.0	25.0	400	11.49	0.1959	0.169
103	91	25.0	24.7	400	11.37	0.1729	0.167
104	111	25.2	25.5	400	25.5	0.410	0.160
105	165	25.0	24.9	390	25.0	0.460	0.158
106	283	25.1	25.0	370	25.2	0.573	0.159
107	463	25.0	25.0	370	25.2	0.696	0.159
108	594	25.0	25.0	390	25.3	0.707	0.157
109	213	25.0	25.0	370	40.2	0.801	0.158

Run	Interfac. Area cm.	Γ g./((cm.)(min.))	k_L^* cm./min.	$k_L^*25^\circ$ cm./min.
100	36.6	42.1	0.645	0.645
101	36.8	23.6	0.545	0.545
102	36.9	14.1	0.463	0.463
103	36.9	10.1	0.412	0.412
104	36.9	12.3	0.437	0.435
105	36.8	18.3	0.500	0.500
106	36.7	31.4	0.619	0.618
107	36.6	51.3	0.756	0.756
108	36.5	65.9	0.767	0.767
109	36.8	23.6	0.543	0.543

slot width = 0.025 in.

length = 4.14 cm.

TABLE 16.12

Desorption of Chlorine from Water
Column 3D

Run	V g./min.	Temp. °C.		Reg	C ₁ mmole/l.	Rate of De- sorption mmole/min.	Interfac. Area cm. ²
		Water	Air				
110*	213	26.8	28.7	900	40.4	0.980	36.8
111	380	26.4	26.8	480	12.40	0.0840	37.2
112	213	26.2	26.9	480	11.93	0.0673	37.3
113	127.5	26.1	26.7	430	11.63	0.0569	36.9
114	66.8	26.0	26.7	430	11.67	0.0499	36.9
115	58.9	25.9	26.5	430	11.57	0.0468	37.0
116	94.0	25.5	26.7	430	11.78	0.0550	36.9
117	165	25.2	26.5	430	11.67	0.0610	36.8
118*	283	25.0	26.2	430	11.71	0.0902	36.7
119	380	25.0	24.5	430	28.8	0.329	36.6
120	213	24.9	24.5	430	28.1	0.319	36.8
121	128	25.0	24.5	440	29.5	0.319	36.9
122	66	24.9	24.7	430	29.0	0.243	36.9
123	53	24.9	24.8	430	29.1	0.222	37.0
124	91	24.9	24.8	430	29.4	0.276	36.9
125	165	25.0	24.9	430	29.6	0.327	36.8
126	283	25.0	25.0	430	29.6	0.361	36.7
127	435	25.0	25.0	430	29.6	0.399	36.6
128	380	25.1	25.8	480	21.0	0.221	36.6
129	213	25.1	25.5	470	20.1	0.178	36.8
130	128	25.0	25.2	460	21.0	0.155	36.9
131*	66	25.2	25.2	460	21.0	0.122	36.9
132	66	25.2	25.2	460	21.8	0.153	36.7
133	53	25.2	25.1	460	21.6	0.145	36.7
134	91	25.0	25.0	470	21.5	0.168	36.6
135	165	25.0	25.0	480	21.6	0.186	36.5
136	283	25.0	25.0	480	21.6	0.207	36.7
137	473	25.0	25.0	480	21.5	0.235	36.6
138	380	24.7	25.0	530	48.9	0.955	36.6
139	213	24.9	24.8	510	50.3	0.862	36.8
140	128	25.0	24.7	510	49.5	0.736	36.9

slot width = 0.025 in. (except runs 111 and 112 where = 0.05 in.)
length = 4.14 cm. (except runs 111 and 112 where = 4.20 cm.)

*Run 110 rejected because of poor wetting and temperature control. This run was made only to check material balance.

*Run 118 rejected because of liquid overflowing from bottom slot into calming section.

*Run 131 rejected because of incomplete wetting.

TABLE 16.12 (Contd)

Run	V g./min.	Temp. °C.		Reg	C ₁ mmole/l.	Rate of Desorption mmole/min.	Interfac. area cm. ²
		Water	Air				
141	91	25.0	24.8	530	49.5	0.655	36.9
142	91	25.1	24.7	500	49.9	0.628	36.6
143	128	25.1	24.7	480	50.1	0.821	36.6
144	165	25.1	24.5	480	50.0	0.851	36.5
145	165	25.3	24.7	510	49.9	0.833	36.8
146	283	25.2	24.9	480	49.7	0.951	36.7
147	424	25.0	25.0	510	49.7	0.964	36.6
148	380	25.0	25.0	510	7.75	0.0284	36.6
149	213	25.0	24.9	530	7.32	0.0231	36.8
150	128	25.0	24.8	510	8.28	0.0266	36.9
151	91	24.9	24.9	510	8.16	0.0237	36.9
152	111	24.9	25.1	510	8.37	0.0260	36.9
153	165	25.0	25.0	530	8.33	0.0282	36.8
154	283	25.0	25.0	530	8.35	0.0316	36.7
155	463	25.0	24.9	530	8.31	0.0350	36.6
156	558	25.0	24.9	530	8.26	0.0351	36.5
157	380	25.0	24.7	300	6.31	0.0167	36.6
158	213	25.0	25.0	510	6.05	0.0134	36.8
159	128	25.0	25.0	510	6.07	0.0128	36.9
160	91	24.9	24.6	500	5.94	0.0116	36.9
161	111	25.1	24.7	510	6.07	0.0130	36.9
162	165	25.0	25.1	500	6.40	0.0154	36.8
163	283	25.0	25.0	500	6.25	0.0155	36.7
164	463	25.0	25.0	510	6.16	0.0166	36.6
165	594	25.0	25.0	510	6.09	0.0169	36.5
166	380	25.0	25.0	530	3.78	0.00430	36.6
167	380	25.0	24.9	510	5.02	0.00945	36.6
168	380	25.1	24.9	520	7.49	0.0247	36.6
169	380	24.9	24.9	520	10.72	0.0538	36.6
170	380	25.0	25.0	530	14.82	0.1044	36.6

slot width = 0.025 in. (except runs 142 and 143
where = 0.0125 in.).

length = 4.14 cm. (except runs 142 and 143
where = 4.11 cm.)

TABLE 16.12 (contd.)

Run	V g./min.	Temp. °C		Reg	C ₁ mmole/l.	Rate of Desorption mmole/min.	Interfac. Area Cm. ²
		Water	Air				
171	380	25.0	25.0	540	18.12	0.1626	36.6
172	380	24.9	25.0	510	25.8	0.295	36.6
173	380	24.9	24.9	530	39.3	0.580	36.6
174	380	25.1	24.9	510	70.5	1.880	36.6
175	380	25.0	24.7	500	77.8	2.00	36.6
176	594	25.0	25.1	520	7.46	0.0276	36.5
177	594	25.0	24.8	510	13.05	0.0997	36.5
178	594	25.5	25.3	520	20.1	0.225	36.5
179	594	25.7	24.9	530	29.2	0.408	36.5
180	594	25.7	25.0	510	48.4	0.910	36.5
181	594	25.3	24.7	530	67.7	1.526	36.5
182	91	25.0	25.0	370	6.30	0.0128	36.9
183	165	25.0	25.0	370	6.27	0.0143	36.8
184	165	25.0	25.0	370	4.04	0.00458	36.8
185	165	25.0	25.0	390	12.34	0.0678	36.8
186	91	25.0	24.9	370	12.16	0.0573	36.9
187	91	25.0	24.9	390	19.75	0.1420	36.9
188	165	25.0	24.8	390	19.76	0.1665	36.8
189	165	25.0	24.9	390	28.2	0.332	36.8
190	91	25.0	24.8	390	27.7	0.288	36.9
191	91	25.1	25.0	390	73.1	1.356	36.9
192	165	25.3	25.1	390	72.9	1.745	36.8
193	487	25.3	25.1	400	74.2	2.44	36.6
194	283	25.2	25.0	400	71.3	1.972	36.7
195	128	25.1	25.3	400	67.7	1.464	36.9
196	229	25.1	25.2	400	66.5	1.534	36.7
197	424	25.0	25.3	400	75.4	2.48	36.6
198	594	25.1	25.0	400	72.8	2.28	36.5

slot width = 0.025 in.
length = 4.14 cm.

Outlet liquid concentrations measured for three runs.

Run 110, C₂ = 40.4 mmole/l.

Run 121, C₂ = 26.9 mmole/l.

Run 173, C₂ = 37.7 mmole/l.

TABLE 16.12(Contd)

Run	Γ g./ (cm.) (min.)	k_L cm./min.	$k_{L,250}$ cm./min.	$k_{L,250}^o$ cm./min.	ϕ
110*	23.6	0.659	0.638	1.211	2.18
111	42.1	0.182	0.178	0.804	1.15
112	23.6	0.151	0.148	0.698	1.26
113	14.14	0.133	0.130	0.632	1.40
114	7.41	0.116	0.114	0.551	1.58
115	6.53	0.109	0.108	0.526	1.59
116	10.42	0.127	0.126	0.601	1.50
117	18.3	0.142	0.142	0.685	1.37
118*	31.4	0.210	0.210	1.012	1.62
119	42.1	0.312	0.312	0.708	1.01
120	23.6	0.309	0.310	0.714	1.29
121	14.1	0.294	0.294	0.657	1.46
122	7.32	0.227	0.227	0.514	1.48
123	5.88	0.206	0.207	0.465	1.47
124	10.1	0.254	0.255	0.571	1.45
125	18.3	0.300	0.300	0.670	1.34
126	31.4	0.332	0.332	0.741	1.19
127	48.2	0.368	0.368	0.821	1.11
128	42.1	0.287	0.287	0.804	1.15
129	23.6	0.241	0.240	0.698	1.26
130	14.1	0.201	0.201	0.562	1.25
131*	7.32	0.157	0.157	0.440	1.27
132	7.32	0.192	0.191	0.521	1.50
133	5.88	0.183	0.183	0.501	1.58
134	10.1	0.214	0.214	0.590	1.50
135	18.3	0.235	0.235	0.644	1.29
136	31.4	0.262	0.262	0.718	1.15
137	52.5	0.298	0.298	0.822	1.07
138	42.1	0.534	0.537	0.939	1.34
139	23.6	0.466	0.466	0.807	1.45
140	14.1	0.403	0.403	0.701	1.55

*Run 110 rejected because of poor wetting and temperature control.
This run was made only to check material balance.

*Run 118 rejected because of liquid overflowing from bottom slot into
calming section.

*Run 131 rejected because of incomplete wetting.

TABLE 16.12 (Contd)

Run	Γ g./((cm.)(min.))	k_L cm./min.	$k_{L,25^\circ}$ cm./min.	$k_{L,25^\circ}^o$ cm./min.	ϕ
141	10.1	0.359	0.359	0.624	1.58
142	10.1	0.343	0.343	0.595	1.51
143	14.1	0.448	0.447	0.774	1.72
144	18.3	0.466	0.465	0.806	1.61
145	18.3	0.454	0.451	0.784	1.56
146	31.4	0.522	0.520	0.903	1.45
147	47.0	0.530	0.530	0.902	1.23
148	42.1	0.100	0.100	0.813	1.16
149	23.6	0.0859	0.0859	0.757	1.36
150	14.1	0.0873	0.0873	0.647	1.43
151	10.1	0.0787	0.0788	0.596	1.51
152	12.3	0.0843	0.0845	0.617	1.45
153	18.3	0.0921	0.0921	0.678	1.35
154	31.4	0.103	0.103	0.755	1.21
155	51.3	0.115	0.115	0.849	1.12
156	61.9	0.116	0.116	0.864	1.06
157	42.1	0.0724	0.0724	0.796	1.14
158	23.6	0.0603	0.0603	0.709	1.28
159	14.1	0.0570	0.0570	0.666	1.48
160	10.1	0.0531	0.0532	0.642	1.63
161	12.3	0.0580	0.0579	0.677	1.59
162	18.3	0.0652	0.0652	0.702	1.40
163	31.4	0.0674	0.0674	0.752	1.21
164	51.3	0.0737	0.0737	0.841	1.11
165	65.9	0.0760	0.0760	0.883	1.05
166	42.1	0.0311	0.0311	0.805	1.15
167	42.1	0.0514	0.0514	0.816	1.16
168	42.1	0.0901	0.0900	0.767	1.09
169	42.1	0.137	0.137	0.732	1.04
170	42.1	0.192	0.192	0.726	1.04

TABLE 16.12 (contd)

Run	$\sqrt{\text{g.}/(\text{cm.})(\text{min.})}$	k_L cm./min.	$k_{L,25^\circ}$ cm./min.	$k_{L,25^\circ}^o$ cm./min.	ϕ
171	42.1	0.245	0.245	0.772	1.10
172	42.1	0.312	0.313	0.760	1.08
173	42.1	0.403	0.404	0.777	1.11
174	42.1	0.728	0.727	1.118	1.59
175	42.1	0.703	0.703	1.051	1.50
176	65.9	0.101	0.101	0.868	1.03
177	65.9	0.209	0.209	0.897	1.07
178	65.9	0.306	0.303	0.878	1.05
179	65.9	0.383	0.378	0.851	1.01
180	65.9	0.514	0.509	0.895	1.07
181	65.9	0.617	0.614	0.957	1.14
182	10.1	0.0552	0.0552	0.608	1.54
183	18.3	0.0619	0.0619	0.687	1.37
184	18.3	0.0308	0.0308	0.710	1.42
185	18.3	0.149	0.149	0.680	1.36
186	10.1	0.128	0.128	0.590	1.50
187	10.1	0.195	0.195	0.572	1.45
188	18.3	0.229	0.229	0.672	1.34
189	18.3	0.320	0.320	0.734	1.46
190	10.1	0.282	0.282	0.655	1.66
191	10.1	0.503	0.502	0.764	1.94
192	18.3	0.651	0.647	0.987	1.97
193	54.0	0.901	0.896	1.358	1.75
194	31.4	0.753	0.751	1.151	1.85
195	14.1	0.587	0.586	0.914	2.03
196	25.4	0.628	0.627	0.982	1.72
197	47.0	0.892	0.892	1.345	1.84
198	65.9	0.859	0.858	1.308	1.56

CHAPTER 17

Recalculation of Pseudo-Coefficient from
Data of Vivian and Whitney

It was found by de Nicolas (79), in studying the data of Vivian and Whitney (101), that they used a logarithmic mean "pseudo-driving force" to calculate their pseudo-coefficients. De Nicolas recalculated some pseudo-coefficients using graphical integration, and found considerable differences, especially at the lower flow rates. For this reason, all of Vivian and Whitney's runs are recalculated in this chapter.

It is possible to calculate the pseudo-coefficient without using a "pseudo-operating line" as was suggested by Vivian and Whitney (101). This may be done by using partial pressure driving forces rather than molecular chlorine driving forces, as follows.

The pseudo coefficient is usually found by application of eq. (17.1),

$$k_L^{\circ} a = \int_1^2 \frac{L \, dC}{\rho Z (A_1 - A_0)} \quad (17.1)$$

where 1 and 2 refer to the bottom and the top of the column, respectively. If P is the partial pressure of chlorine in the gas, and P_0 is the partial pressure of chlorine which would be in equilibrium with the bulk of the liquid, we have

$$A_1 = HP \quad (17.2)$$

and

$$A_0 = HP_0 \quad (17.3)$$

whence

$$k_L^{\circ} a = \int_1^2 \frac{L \, dC}{\rho Z H (P - P_0)} \quad (17.4)$$

The trapezoidal rule was used to carry out the integration. A sample calculation follows.

Run No. 62

$$\begin{aligned}
 \text{Temp.} &= 70^{\circ}\text{F} \\
 L &= 9,200 \text{ lbs.}/(\text{hr.})(\text{ft.}^2) \\
 Z &= 2.25 \text{ ft.} \\
 C_1 &= 9.0 \times 10^{-4} \text{ lb. moles}/\text{ft.}^3 \\
 P_1 &= 0.197 \text{ atm.} \\
 P_2 &= 0.168 \text{ atm.}
 \end{aligned}$$

Then, from material balance,

$$P = 0.168 + \frac{0.197 - 0.168}{9.0 \times 10^{-4}} C_0 \quad (17.5)$$

At 70 F, $H = 0.00447 \text{ lb. moles}/(\text{ft.}^3)(\text{atm.})$

$$K_c = 11.2 \times 10^{-7} (\text{lb. moles}/\text{ft.}^3)^2$$

(Found by interpolation of Vivian and Whitney's values (101))

Then, a plot of P_0 vs. C_0 was made, using

$$C_0 = HP_0 + (KHP_0)^{1/3} \quad (17.6)$$

Next, a table was constructed. P was calculated from eq. (17.5), while P_0 was obtained from the plot.

$C_0 \times 10^4$	P	P_0	$P - P_0$	$1/(P - P_0)$
0.0	0.168	0.000	0.168	5.95
1.0	0.171	0.000	0.171	5.85
2.0	0.174	0.002	0.172	5.81
3.0	0.178	0.004	0.174	5.75
4.0	0.181	0.009	0.172	5.81
5.0	0.184	0.016	0.168	5.95
6.0	0.187	0.024	0.163	6.13
7.0	0.191	0.033	0.158	6.33
8.0	0.194	0.044	0.150	6.67
9.0	0.197	0.056	0.141	7.09

The trapezoidal rule gives

$$\begin{aligned}
 \int_1^2 \frac{dC}{P - P_0} &= 10^{-4} \left[\begin{aligned} &1/2(5.95) + 5.85 + 5.81 + 5.75 \\ &+ 5.81 + 5.95 + 6.13 + 6.33 \\ &+ 6.67 + 1/2(7.09) \end{aligned} \right] \\
 &= 54.82 \times 10^{-4}
 \end{aligned}$$

Using the logarithmic mean gives

$$\int_1^2 \frac{dC}{P-P_0} = 58.1 \times 10^{-4}$$

$$\frac{L}{\rho ZH} = \frac{9200}{(62.4)(2.25)(0.00447)} = 1.467 \times 10^4$$

From eq. (17.4),

$$k_L^0 a = 1.467 (54.82) = 80$$

Using the logarithmic mean gives $1.467 (58.1) = 85$

Table 17.1 summarizes the calculations for all the runs made at 70°F. The run numbers correspond to the numbers used by Vivian and Whitney.

TABLE 17.1

Absorption of Chlorine in Water in Packed Column --
Recalculation of Pseudo-Coefficient

Data of Vivian and Whitney (101).

Temp. = 70°F.

Packing = 1" Raschig rings.

Run	L lb./hr (ft ²)	C ₁ × 10 ⁴ lb. moles/ft ³	P ₁ atm.	P ₂ atm.	$\int \frac{dc}{P-P_0}$	k _L a
1*	3,160	13.4	0.197	0.183	94.6	54
2*	3,130	10.7	.196	.184	66.4	37
3*	1,890	11.2	.171	.164	83.5	28
4*	1,010	12.5	.163	.159	107.5	19
5*	1,400	15.7	.232	.226	97.5	24
6*	2,390	11.3	.171	.161	85.4	37
7*	3,950	9.3	.161	.147	69.7	49
8*	5,800	8.6	.161	.143	63.7	66
9*	7,600	7.9	.156	.134	60.2	82
10*	2,420	9.4	.118	.109	103.4	45
11*	10,100	7.8	.194	.166	46.7	85
12*	13,600	8.6	.220	.178	47.1	115
13*	19,000	6.9	.209	.156	40.1	141
14*	25,200	4.8	.156	.112	37.1	167
15*	21,300	6.2	.191	.142	39.1	150
16*	18,000	7.8	.203	.153	47.3	154
17*	15,400	7.5	.194	.148	47.2	130
18*	12,300	8.1	.193	.156	50.5	111
19*	1,960	11.5	.162	.155	94.0	33
20*	3,450	9.3	.154	.142	73.3	45
21*	5,400	8.8	.160	.142	66.2	64
22*	8,700	6.9	.146	.124	55.2	86
23	5,000	11.2	.182	.141	85.3	68
24	5,000	10.7	.168	.140	85.2	68
25	5,000	10.6	.168	.148	81.7	65

(continued on next page)

*Runs 1-22, C₁ refers to the analysis of sample taken at the base plate. Z was taken as 2.00 ft. For all other runs, C₁ refers to analysis of trap sample and includes end effect, so Z was taken as 2.25 ft.

TABLE 17.1
(Contd.)

Run	L lb./hr (ft ²)	C ₁ x 10 ⁴ lb.moles/ft ³	P ₁ atm.	P ₂ atm.	$\int \frac{dC}{P-P_0}$	k _L ^o a
26	5,000	9.4	.139	.126	82.9	66
27	5,000	11.2	.166	.154	94.7	76
28	5,000	11.7	.168	.167	90.2	72
29	5,000	11.2	.160	.156	90.4	72
30	9,000	8.8	.150	.144	68.6	98
31	9,000	9.5	.177	.163	64.1	92
32	1,960	13.3	.165	.161	119.9	37
33	2,000	13.4	.160	.158	128.5	41
34	5,000	11.9	.203	.197	73.1	58
35	9,000	10.0	.199	.177	60.9	87
36	2,000	13.6	.178	.170	112.2	36
37	2,000	16.7	.236	.211	111.9	36
38	9,000	9.9	.221	.158	59.1	85
39	2,700	13.7	.190	.177	99.0	43
40	3,700	12.7	.194	.177	88.8	52
41	6,700	11.7	.216	.188	69.5	74
42	1,450	15.4	.188	.180	136.7	32
43	1,300	15.5	.185	.176	144.3	30
44	910	15.8	.185	.180	152.1	22
45	12,200	9.3	.210	.170	54.5	106
46	15,600	8.2	.206	.161	48.6	121
47	18,300	8.4	.220	.166	47.3	138
48	22,500	7.4	.227	.171	39.5	142
49	28,000	6.7	.232	.169	35.2	157
50	28,000	6.9	.229	.163	37.2	166
62	9,200	9.0	.197	.168	54.8	80
64	9,300	6.3	.119	.096	63.4	94
65	9,300	10.3	.213	.180	60.1	89
66	9,300	14.5	.342	.300	53.4	79
67	9,300	10.1	.237	.204	51.4	76
68	9,300	13.4	.290	.248	59.3	88
69	9,300	8.5	.181	.152	56.6	84
70	9,300	5.9	.128	.107	53.3	79

CHAPTER 18Location of Original Data

The original data upon which this thesis is based may be found in the office of Professor J. E. Vivian, Department of Chemical Engineering, Massachusetts Institute of Technology, Cambridge 39, Massachusetts.

CHAPTER 19NOMENCLATURE

- A concentration of A (component being absorbed), moles/cm.³
- A_i Airy integral
- a interfacial area per unit of packed volume, ft.⁻¹
- a₁ scale factor relating voltage to α (electronic computer)
- a area for mass transfer, cm.²
- B concentration of B, moles/cm.³
- B.C. Boundary Condition
- B_i Airy integral
- b B₁/B₀
- b₁ scale factor relating voltage to β (electronic computer)
- C "total" concentration, A + E, moles/cm.³
- c constant of integration
- cosh hyperbolic cosine
- D diffusivity in the liquid, cm.²/sec.
- D₀ diffusivity at zero concentration, cm.²/sec.
- E concentration of E, moles/cm.³
- erf error function. $\text{erf}(x) = \int_0^x \exp(-u^2) du$
- erfc complement of the error function. $\text{erfc}(x) = 1 - \text{erf}(x)$
- exp exponential function. $\exp(x) = e^x$
- F concentration of F, moles/cm.³
- f friction factor
- G concentration of SO₂ + concentration of H₂SO₃, moles/cm.³
- g acceleration due to gravity, cm./sec.²

- H Henry's law constant, = A/P (or C/P when chemical reaction is absent), moles/(cm.³)(atm.)
- h height of wetted-wall column, cm.
- I $\sqrt{\frac{m}{D_A} + \frac{nF_1^2}{D_E}}$
- i $\sqrt{-1}$
- J $(K+1)/(D_A+KD_E)$
- K equilibrium constant, = k_1/k_2
- K_c equilibrium constant for chlorine-water system, $[\text{HOCl}][\text{H}^+][\text{Cl}^-]/[\text{Cl}_2]$
- K_s equilibrium constant for sulfur dioxide-water system, $[\text{H}^+][\text{HSO}_3^-]/[\text{SO}_2]$. (Neglects existence of H_2SO_3 .)
- K_w equilibrium constant for dissociation of water, $[\text{H}^+][\text{OH}^-]$
- k $M^{1/3}/(1-b)^{2/3}$
- k_L "total" coefficient (see Sec. 8.19), cm./sec. (Sometimes called normal coefficient.)
- k_L^o pseudo-coefficient (see Sec. 8.19), cm./sec.
- k_L^* physical coefficient (see Sec. 8.19), cm./sec.
- k_1 forward rate constant, units of moles, cm., and sec.
- k_2 reverse rate constant, units of moles, cm., and sec.
- L effective length of diffusion path in diaphragm, cm. Also, liquid flow rate in packed column, lb./(hr.)(ft.²)
- \mathcal{L} Laplace transform
- \mathcal{L}^{-1} inverse Laplace transform
- M $B_0 R^2 x_f^2 = k_1 B_0 x_f^2 / D_A$
- m forward rate constant for the reaction $\text{Cl}_2 + \text{H}_2\text{O} \rightleftharpoons \text{HOCl} + \text{H}^+ + \text{Cl}^-$
- N_A rate of absorption of A, moles/(cm.²)(sec.)
- $N_{x,A}$ rate of transfer of A across a plane parallel to the interface, and at a distance x from it, moles/(cm.²)(sec.)
- n reverse rate constant for the reaction $\text{Cl}_2 + \text{H}_2\text{O} \rightleftharpoons \text{HOCl} + \text{H}^+ + \text{Cl}^-$

- P partial pressure of component being absorbed, atm.
- P* partial pressure of component being absorbed in equilibrium with bulk of liquid, atm.
- p transform variable corresponding to t, sec.⁻¹
- Q $(d\bar{\alpha}/dx)_{x=0} = \int_0^L (\partial\alpha/\partial x)_{x=0}$
- q $(D_A A_1)/(D_B B_0)$
- q' $2(D_A A_1)/(D_B B_0)$
- R $\sqrt{\frac{k_1}{D_A} + \frac{k_2}{D_B}}$ used for first order reactions, cm.⁻¹
- Re Reynolds number, $4r_h v_{av} \rho/\mu$
- r ratio of volume of pores of diaphragm to the volume of the lower compartment of the diaphragm cell.
- r_h hydraulic radius, ratio of cross-sectional area of fluid to wetted perimeter, cm.
- S $\sqrt{(k_1+k_2+p)/D}$
- s effective area for diffusion through pores in diaphragm, cm.²
- sinh hyperbolic sine
- T $\sqrt{p/D}$
- t time, sec. (also, time of exposure) (Also, temperature)
- tanh hyperbolic tangent
- U $\sqrt{\frac{k_1 B_1}{D_A} + \frac{k_2 F_1}{D_E}}$
- V volumetric rate of flow, cm.³/sec.
- V' volume in lower compartment of diaphragm cell, cm.³
- V'' volume in upper compartment of diaphragm cell, cm.³
- v downward velocity of liquid, cm./sec.
- W
$$\frac{k_2 F_1 \left(\frac{A_0 - A_1}{D_E} + \frac{E_0 - E_1}{D_A} \right)}{\frac{k_1 B_1}{D_A} + \frac{k_2 F_1}{D_E}}$$

- $$W' = \frac{nF_i^2 \left(\frac{A_0 - A_i}{D_E} + \frac{E_0 - E_i}{D_A} \right)}{\frac{m}{D_A} + \frac{nF_i^2}{D_E}}$$
- w temperature coefficient of absorption or desorption rate, $(^{\circ}\text{C})^{-1}$
- x distance in the liquid from the interface, cm.
- x_f film thickness, cm.
- $$Y = \sqrt{\frac{k_1 B_i}{D_A} + \frac{k_2}{D_E}}$$
- y vertical distance in downward direction, cm.
- $$Z = \frac{k_2 F_i \left(\frac{A_i}{D_E} + \frac{E_i}{D_A} \right)}{\frac{k_1 B_i}{D_A} + \frac{k_2 F_i}{D_E}}$$
- $$Z' = \frac{nF_i^2 \left(\frac{A_i}{D_E} + \frac{E_i}{D_A} \right)}{\frac{m}{D_A} + \frac{nF_i^2}{D_E}}$$
- z height of packing in packed column, ft.
- $\alpha = (A - A_0) / (A_i - A_0)$
- β diaphragm cell constant, $[(1/V') + (1/V'')] (s/L)$, cm.^{-2}
 Also, B/B_0 (Chap. 14)
- Γ mass flow rate per unit perimeter, $\text{g.}/(\text{cm.})(\text{sec.})$
- $\gamma = \left[D_0 \Delta C / \int_{C'}^{C''} D \, dC \right] - 1$ (see eq. (11.23))
- Δ difference between lower compartment and upper compartment in diaphragm cell.
- δ volume of holdup per unit interfacial area, also thickness of liquid layer, cm.
- $\epsilon = (E - E_0) / (A_i - A_0)$
- $\eta = x/x_f$
- $\theta = Dh / (\delta^2 v_i)$
- $\lambda = k [b + (1-b)x/x_f]$

- μ viscosity, g./cm.(sec.)
- $\mu_1, \mu_2, \dots, \mu_n$ gain constants of components of electronic computer
- π 3.1415926...
- ρ density of liquid, g./cm.³
- γ scale factor relating time to η (electronic computer).
Also, shear force per unit area at the interface (Chap. 13).
- ϕ k_L°/k_L^*
- ω quantity defined by eq. (8.227)

Subscripts

- A, B, E, F refers to components A, B, E or F.
- f refers to final conditions in the diaphragm cell
(exception, x_f)
- H refers to homogeneous solution of an ordinary linear differential equation
- i refers to interface
- inst instantaneous
- int refers to integral or average value
- o
1. Film Theory of Absorption: refers to bulk of liquid
 2. Penetration Theory of Absorption: refers to conditions at beginning of time of exposure.
 3. Diffusion Studies in Diaphragm Cell: refers to initial conditions. (Exception: D_o)
- P refers to a particular solution of an ordinary linear differential equation
- 1 refers to inlet liquid stream
- 2 refers to outlet liquid stream

Superscripts

- o refers to lower chamber of diaphragm cell
- u refers to upper chamber of diaphragm cell

CHAPTER 20LITERATURE CITATIONS

- (1) Abbanat, R. F. and Lobo, P. A., "The Absorption of Carbon Dioxide by Sodium Hydroxide in a Short Wetted-Wall Column", S.M. Thesis, Chem. Eng., M.I.T. (1951).
- (2) Adair, G. S., Biochem. J. 14, 762-79 (1920).
- (3) Arnold, J.H., "The Theory of Diffusional Processes", Sc.D. Thesis, Chem. Eng., M.I.T. (1932).
- (4) van Arsdel, W.B., Chem. Met. Eng. 23, 1115-6 (1920).
- (5) van Arsdel, W.B., Chem. Met. Eng. 28, 889-92 (1923).
- (6) Brinkhan, R., Margarita, R., and Roughton, F.J. W., Phil. Trans. Roy. Soc., London, A232, 65-97 (1933).
- (7) Campbell, G.A., and Foster, R.M., "Fourier Integrals for Practical Applications", D. Van Nostrand Company, Inc., New York, 1948.
- (8) Campbell, W.B., and Maass, O., Can. J. Research 2, 42-64 (1930).
- (9) Carlson, T., J. Am. Chem. Soc., 33, 1027-32 (1911).
- (10) Carlson, T., J. Chim. Phys. 9, 228-44 (1911).
- (11) Chang, S.Y., "Determination of Diffusion Coefficient in Aqueous Solutions", S.M. Thesis, Chem. Eng., M.I.T. (1949).
- (12) Childress, H.L., B.S. Thesis, Chem. Eng., Univ. of Illinois, (1941).
- (13) Chou, C.H., "Mathematical Analysis of Absorption and Rate of Reaction of Chlorine in Water", S.B. Thesis, Chem. Eng., M.I.T. (1947).
- (14) Cole, A.F.W., and Gordon, A.R., J. Phys. Chem. 40, 733-37 (1936).
- (15) Cooper, C.M., Drew, T.B., and McAdams, W.H., Ind. Eng. Chem. 26, 428-31 (1934).
- (16) Coste, J.H., J. Soc. Chem. Ind. 36, 846-53 (1917).
- (17) Craig, E.T., "The Absorption of Chlorine in Hydrochloric Acid Solutions", S.M. Thesis, Chem. Eng., M.I.T. (1946).

- (18) Danckwerts, P.V., Trans. Faraday Soc. 46, 300-4 (1950).
- (19) Danckwerts, P.V., Trans. Faraday Soc. 46, 701-712 (1950).
- (20) Dawson, C.R., J.Am.Chem.Soc. 55, 432-3 (1933).
- (21) Donnan, F.G., and Masson, I., J.Soc.Chem.Ind. 39, 236-41T (1920).
- (22) Erdey-Grúz, T., Hunyár, A., Pogány, E., and V'ali, A., Hung. Acta Chim. 1, No. 3, 7-26 (1948). Chem.Abst. 43, 8773f (1949).
- (23) Euler, H., Ann.Physik und Chem. 63, 273-77 (1897).
- (24) Falinski, M., Compt. rend. 218, 745-5 (1944).
- (25) Falinski, M., Compt. rend. 218, 938-9 (1944).
- (26) Fallah, R., Hunter, T.G., and Nash, A.W., J.Soc.Chem.Ind. 53, 369-79T (1934).
- (27) Friedman, S.J., and Miller, C.O., Ind.Eng.Chem. 33, 885-91 (1941).
- (28) Gilliland, E.R., and Sherwood, T.K., Ind.Eng.Chem. 26, 516-23 (1934).
- (29) Gordon, A.R., Ann. N.Y. Acad. Sci. 46, 285-308 (1945).
- (30) Gordon, A.R., J.Chem.Phys. 5, 522-26 (1937).
- (31) Grimley, S.S., Trans. Inst. Chem. Engrs. 23, 228-35 (1945).
- (32) Harned, H.S., Chem.Rev. 40, 461-522 (1947).
- (33) Harned, H.S., and Geary, C.G., J.Am.Chem.Soc. 59, 2032-5 (1937).
- (34) Harned, H.S., and Nuttall, R.L., J.Am.Chem.Soc. 69, 736-40 (1947).
- (35) Harned, H.S., and Nuttall, R.L., J.Am.Chem.Soc. 71, 1460-3 (1949).
- (36) Hartley, G.S., and Runnicles, D.F., Proc.Roy.Soc. (London) A168, 401-19 (1938).
- (37) Higbie, R., Trans.Am.Inst.Chem.Engrs. 31, 365-89 (1935).
- (38) Hildebrand, F.B., "Advanced Calculus for Engineers", 1st ed., pgs. 52-94, Prentice-Hall, Inc., New York, 1949.

- (39) Hodson, J.R., "Desorption of Oxygen from an Aqueous Solution in a Wetted-Wall Tower", S.M. Thesis, Chem.Eng., M.I.T. (1949).
- (40) Holloway, F.A.L., "Performance of Commercial Absorption Tower Packings", Sc.D. Thesis, Chem.Eng., M.I.T. (1939).
- (41) Høye, J., Kgl. Norske Videnskab. Selskabs, Forh. 14, 1-4 (1941). Chem.Abst. 40, 6321⁵ (1946).
- (42) Hüfner, G., Ann. Physik und Chem. 60, 134-68 (1897).
- (43) Hüfner, G., Wien Ann. 60, 134 (1897). (Not read; referred to by Tammann and Jessen (97)).
- (44) Hurlburt, H.Z., "Mass Transfer in a Wetted-Wall Column", Sc.D. Thesis, Chem.Eng., M.I.T. (1949).
- (45) International Critical Tables, Vol. 5, 1st. ed., p. 12, National Research Council, McGraw-Hill Book Company, New York, 1929.
- (46) *ibid.*, Vol. 5, pp. 63-66.
- (47) *ibid.*, Vol. 6, p. 246.
- (48) Jahnke, E., and Emde, F., "Tables of Functions", 4th ed., Dover Publications, New York (1945).
- (49) James, W.A., and Gordon, A.R., J. Chem. Phys. 7, 963-5 (1939).
- (50) James, W.A., Hollingshead, E.A., and Gordon, A.R., J. Chem. Phys. 7, 89-92 (1939).
- (51) Jenny, F.J., "Gas Absorption Followed by Chemical Reaction in the Liquid Phase", Sc.D. Thesis, Chem.Eng., M.I.T., (1936).
- (52) Jesser, B.W., and Elgin, J.C., Trans.Am.Inst.Chem.Engrs., 39, 277-98 (1943).
- (53) Johnstone, H.F., and Pigford, R.L., Trans. Am.Inst.Chem. Engrs., 38, 25-51 (1942).
- (54) Jütner, F., Z. Elektrochem. 15, 169-70 (1909).
- (55) Kirkbride, C.G., Trans.Am.Inst.Chem.Engrs., 30, 170-86 (1933-34).
- (56) Kniel, K., "Desorption of Hydrogen Sulfide from Water", S.B. Thesis, Chem.Eng., M.I.T., (1951).

- (57) Kolthoff, I.M., and Miller, C.S., J.Am.Chem.Soc. 63, 1013-17 (1941).
- (58) Kolthoff, I.M., and Miller, C.S., J.Am.Chem.Soc. 63, 2818-21 (1941).
- (59) van Krevelen, D.W., and Hoftijzer, P.J., Chem.Eng. Progress 44, 529-36 (1948).
- (60) van Krevelen, D.W., and Hoftijzer, P.J., Rec. trav. chim. 67, 563-86 (1948).
- (61) van Krevelen, D.W., and Hoftijzer, P.J., Rec. trav. chim. 68, 221-33 (1949).
- (62) van Krevelen, D.W., Hoftijzer, P.J., and van Hooren, C.J., Rec. trav. chim. 66, 513-32 (1947).
- (63) Lambe, H.W., "Desorption of Carbon Dioxide from Water in a Short Wetted-Wall Column", S.M. Thesis, Chem.Eng., M.I.T. (1950).
- (64) Lewis, W.K., Ind.Eng.Chem. 8, 825-33 (1916).
- (65) Lewis, W.K., and Whitman, W.G., Ind.Eng.Chem. 16, 1215-20 (1924).
- (66) McAdams, W.H., "Heat Transmission", 2nd ed., McGraw-Hill, New York (1942).
- (67) McBain, J.W., and Dawson, C.R., Proc.Roy.Soc. (London) All8, 32-39 (1935).
- (68) McBain, J.W., and Liu, T.H., J.Am.Chem.Soc. 53, 59-74 (1931).
- (69) Macnee, A.B., "An Electronic Differential Analyzer", Technical Report No. 90, Research Laboratory of Electronics, M.I.T., Dec. 16, 1948.
- (70) Macnee, A.B., Proceedings of the I.R.E. 37, 1315-24 (1949).
- (71) Marshall, W.R., and Pigford, R.L., "Applications of Differential Equations to Chemical Engineering Problems", pp. 114-122, Univ. of Delaware, Newark, Del., 1947.
- (72) Mayo, F., Hunter, T.G., and Nash, A.W., J.Soc.Chem. Ind. (London), 54, 375-85T (1935).
- (73) Miller, E.G., S.B. Thesis, Chem.Eng., Univ. of Delaware (1948).

- (74) Miller, J.A., "Correlation of Data on the Desorption of Chlorine in a Packed Tower", S.M. Thesis, Chem.Eng., M.I.T. (1951).
- (75) Miller, J.C.P., British Association for the Advancement of Science, Mathematical Tables, Part-Volume B, "The Airy Integral", University Press, Cambridge (1946).
- (76) Morris, J.C., J.Am.Chem.Soc. 68, 1692-4 (1946).
- (77) Mouquin, H., and Cathcart, W.H., J.Am.Chem.Soc. 57, 1791-94 (1935).
- (78) Mysels, K.J., and McBain, J.W., J. Colloid Sci. 3, 45-51 (1948).
- (79) de Nicolas y Garcia, A.M., "Determination of Liquid-Film Coefficient and Interfacial Area for the Absorption of Chlorine in Water in a Packed Tower", S.M. Thesis, Chem. Eng., M.I.T. (1950).
- (80) Northrup, J.H., and Anson, M.L., J.Gen.Physiol. 12, 543-54 (1929).
- (81) Noyes, W.A. and Wilson, T.A., J.Am.Chem.Soc. 44, 1630-7 (1922). Chem. Abst. 16, 3420⁷ (1922).
- (82) Philoon, W.C., "Mass Transfer in a System of Small Dissolving Particles", Sc.D. Thesis, Chem.Eng., M.I.T. (1950).
- (83) Phipps, R.L., "The Rate of Hydrolysis of Sulfur Dioxide", S.B. Thesis, Chem.Eng., M.I.T. (1947).
- (84) Pierce, B.O., "A Short Table of Integrals", 3rd ed., Ginn and Company, Boston (1929).
- (85) Pigford, R.L., Sc.D. Thesis, Chem.Eng., Univ. of Illinois (1941).
- (86) Quincy, R.R., "The Mechanism of the Absorption of Chlorine in Water", S.M. Thesis, Chem. Eng., M.I.T. (1951).
- (87) Ringbom, A., Z. anorg. allgem. Chem. 238, 94-102 (1938).
- (88) Saal, R.N.J., Rec. trav. chim. 47, 73-93 (1928).
- (89) Scott, W.S., "Standard Methods of Chemical Analysis", 5th ed., D. Van Nostrand Company, Inc., New York, 1939.

- (90) Semerano, G., Riccoboni, L., and Foffani, A., *Gazz. chim. ital.* 79, 395-417 (1949). *Chem. Abst.* 43, 8823h (1949).
- (91) Sherrill, M.S., and Izard, E.F., *J. Am. Chem. Soc.* 53, 1667-74 (1931).
- (92) Sherwood, T.K., "Absorption and Extraction", 1st ed., p. 24, McGraw-Hill Book Company, New York (1937).
- (93) Sherwood, T.K., and Holloway, F.A.L., *Trans. Am. Inst. Chem. Engrs.*, 36, 39-70 (1940).
- (94) Shilov, E., and Solodushenkov, S., *Acta Physicochimica, URSS*, 20, 667-82 (1945).
- (95) Shilov, E.A., and Solodushenkov, S.M., *Compt. rend. acad. sci. (U.S.S.R.) (N.S.)*, 3, 15-19 (1936).
- (96) Stokes, R.H., *J. Am. Chem. Soc.* 72, 763-67 (1950).
- (97) Tammann, A., and Jessen, V., *Z. anorg. allgem. Chem.* 179, 125-44 (1929).
- (98) Terill, H.M., and Sweeny, L., *J. Franklin Inst.* 238, 220-22 (1944).
- (99) Vivian, J.E., "Absorption of Chlorine in Water and Caustic", Sc.D. Thesis, Chem. Eng., M.I.T. (1945).
- (100) Vivian, J.E., and Peaceman, D.W., *Chem. Eng.*, 57, No. 8, 106-7 (1950).
- (101) Vivian, J.E., and Whitney, R.P., *Chem. Eng. Progress* 43, 691-702 (1947).
- (102) Voorhees, H.R., "Desorption of Chlorine from Water Solution", S.M. Thesis, Chem. Eng., M.I.T. (1947).
- (103) Weisman, J., and Bonilla, C.F., *Ind. Eng. Chem.* 42, 1099-1105 (1950).
- (104) Whitman, W.G., *Chem. Met. Eng.* 29, 146-8 (1923).
- (105) Whitman, W.G., and Keats, J.L., *J. Ind. Eng. Chem.* 14, 186-91 (1922).
- (106) Whitney, R.P., "The Absorption of Sulfur Dioxide in Water", Sc.D. Thesis, Chem. Eng., M.I.T. (1945).
- (107) Whitney, R.P., and Vivian, J.E., *Chem. Eng. Progress* 45, 323-37 (1949).

- (108) Willard, H.H., and Furman, N.H., "Elementary Quantitative Analysis", 3rd Ed., D. Van Nostrand Company, Inc., New York, 1940.
- (109) Yakovkin, A., J.Russ.Phys.Chem.Soc., 32, 673 (1900).

CHAPTER 21Biographical Note

The author was born in Miami, Florida, on June 1, 1926. His elementary school education was obtained in Elmont, New York, and New York City. High school education was obtained in Brooklyn Technical High School.

He attended the College of The City of New York from 1943 to 1947 and received the B.Ch.E. degree magna cum laude in June, 1947. He was awarded the City College Club Award and the Eliza Ford Memorial Prize, and won honorable mention in the 1947 A.I.Ch.E. Student Problem Contest.

He entered the Graduate School of M.I.T. in September, 1947. The doctorate research program was initiated February of 1949. He served as a teaching assistant in the Department of Chemical Engineering from September 1947 to January 1949, and as an instructor in Chemical Engineering during the summer of 1950. He held the Kimberly-Clark Corporation Fellowship from February 1949 to June, 1951.

The author is now employed by the Production Research Division of the Humble Oil and Refining Company.